POLYMER SCIENCE & TECHNOLOGY

second edition

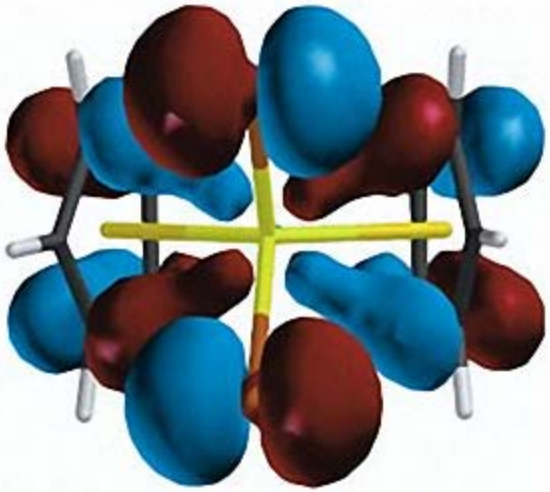

JOEL R. FRIED

468

POLYMER SCİENCE AND TECHNOLOGY

Polymer Science and Technology

Joel R. Fried
University of Cincinnati

PRENTICE HALL PTR
Upper Saddle River, New Jersey 07458

Fried, Joel R.
Polymer science and technology / Joel R. Fried.
p. cm.
Includes bibliographical references and index.
ISBN 0-13-685561-X
1. Polymers: 2. Polymerization. I. Title
QD381.F73 1995 94-22209
668.9--dc20 CIP

314409

QD381
F73
c.4

Editorial/production supervision: *Ann Sullivan*
Cover design: *Wanda Lubelska*
Manufacturing manager: *Alexis R. Heydt*

Printed in the United States of Ame

10 9 8 7 6 5 4

ISBN 0-13-685561-X

Prentice-Hall International (UK) Limited, *London*
Prentice-Hall of Australia Pty. Limited, *Sydney*
Prentice-Hall Canada Inc., *Toronto*
Prentice-Hall Hispanoamericana, S.A., *Mexico*
Prentice-Hall of India Private Limited, *New Delhi*
Prentice-Hall of Japan, Inc., *Tokyo*
Simon & Schuster Asia Pte. Ltd., *Singapore*
Editora Prentice-Hall do Brasil, Ltda., *Rio de Janeiro*

To my parents who provided the opportunities and to Ava, Marc, and Aaron for their love, patience, and understanding.

Contents

At least dozens of good introductory textbooks on polymer science and engineering are now available. Why then has yet another book been written? The decision was based on my belief that none of the available texts fully addresses the needs of students in chemical engineering. It is not that chemical engineers are a rare breed, but rather that they have special training in areas of thermodynamics and transport phenomena that is seldom challenged by texts designed primarily for students of chemistry or materials science. This has been a frustration of mine and of many of my students for the past 15 years during which I have taught an introductory course, *Polymer Technology*, to some 350 chemical engineering seniors. In response to this perceived need, I had written nine review articles that appeared in the SPE publication *Plastics Engineering* from 1982 to 1984. These served as hard copy for my students to supplement their classroom notes but fell short of a complete solution.

In writing this text, it was my objective to first provide the basic building blocks of polymer science and engineering by coverage of fundamental polymer chemistry and materials topics given in Chapters 1 through 7. As a supplement to the traditional coverage of polymer thermodynamics, extensive discussion of phase equilibria, equation-of-state theories, and UNIFAC has been included in Chapter 3. Coverage of rheology, including the use of constitutive equations and the modeling of simple flow geometries, and the fundamentals of polymer processing operations are given in Chapter 11. Finally, I wanted to provide information on the exciting new materials now available and the emerging areas of technological growth that could motivate a new generation of scientists and engineers. For this reason, engineering and specialty polymers are surveyed in Chapter 10 and important new applications for polymers in separations (membrane separations), electronics (conducting polymers), biotechnology (controlled drug release), and other specialized areas of engineering are given in Chapter 12. In all, this has been an ambitious undertaking and I hope that I have succeeded in at least some of these goals.

Although the intended audience for this text is advanced undergraduates and graduate students in chemical engineering, the coverage of polymer science fundamentals (Chapters 1 through 7) should be suitable for a semester course in a materials science or chemistry curriculum. Chapters 8 through 10 intended as survey chapters of the principal categories of polymers — commodity thermoplastics and fibers, network polymers (elastomers and thermosets), and engineering and specialty polymers — may be included to supplement and reinforce the material presented in the chapters on fundamentals and should serve as a useful reference source for the practicing scientist or engineer in the plastics industry.

Joel R. Fried
Cincinnati, Ohio

Acknowledgments

This text could not have been completed without the help of many colleagu who provided figures and photographs and offered important advice duri the course of its preparation. I am particularly indebted to those colleagu who read all or sections of the draft of this text and offered very helpful advi These include Professor James E. Mark of the University of Cincinnati, Profes Otto Vogl of the Polytechnic University, Professor Erdogan Kiran of University of Maine, Professor Paul Han of the University of Akron, Profes Donald R. Paul of the University of Texas, and Professor R. P. Danner of Pe State.

I wish to also thank those colleagues who kindly provided some key illust tions and photos. These are Dr. Roger Kambour of General Electric, Professor E Koros of the University of Texas, Professor Paul Han of the University of Akr Professor John Gilham of Princeton University, Professor Paul Philips of University of Tennessee, Dr. Marty Matsuo of Nippon Zeon (Japan), Dr. Rob Cieslinski of The Dow Chemical Company, Dr. Richard Baker of Membra Technology & Research, Inc., and Dr. Mostafa Aboulfaraj of Pechiney Centre Recherches de Voreppe (France). Appreciation is also extended to my student, Jian-Shen Jiang, who spent many hours preparing high-quality computer graph when she had much more interesting things to do.

1

Introduction to Polymer Science

The word *polymer* is derived from the classical Greek words *poly* meaning "many" and *meres* meaning "parts." Simply stated, a polymer is a long-chain molecule that is composed of a large number of *repeating units* of identical structure. Certain polymers, such as proteins, cellulose, and silk, are found in nature, while many others, including polystyrene, polyethylene, and nylon, are produced only by synthetic routes. In some cases, naturally occurring polymers can also be produced synthetically. An important example is natural rubber (i.e., Hevea), which is known as polyisoprene in its synthetic form.

Polymers that are capable of high extension under ambient conditions find important applications as elastomers. In addition to natural rubber, there are synthetic elastomers such as nitrile and butyl rubber. Other polymers may have characteristics that permit their formation into long fibers suitable for textile applications. The synthetic fibers, principally nylon and polyester, are good substitutes for the naturally occurring fibers such as cotton, wool, and silk.

In contrast to the usage of the word *polymer*, those commercial materials, other than elastomers and fibers, that are derived from synthetic polymers are called *plastics*. A typical commercial plastic resin may contain two or more polymers in addition to various additives and fillers. These are added to improve some property such as the processability, thermal or environmental stability, and mechanical properties of the final product.

The birth of polymer science may be traced back to the mid-nineteenth century. In the 1830s, Charles Goodyear developed the vulcanization process that transformed the sticky latex of natural rubber to a useful elastomer for tire use. In 1847, Christian F. Schönbein reacted cellulose with nitric acid to produce cellulose nitrate. This was used in the 1860s as the first man-made thermoplastic, celluloid. In 1907, Leo Backeland produced Bakelite (phenol-formaldehyde resin), and glyptal (unsaturated-polyester resin) was developed as a protective coating resin by General Electric in 1912.[1]

By the 1930s, researchers at Du Pont in the United States had produced a variety of new polymers including synthetic rubber and more exotic materials such as nylon and Teflon™. In 1938, Dow had produced several tons of polystyrene and, in 1939, polyethylene (low-density) was made for the first time by scientists at ICI in England. Efforts to develop new polymeric materials, particularly synthetic rubber, were intensified during World War II when many naturally occurring materials such as Hevea rubber were in short supply. In the 1950s, Ziegler and Natta independently developed a family of stereospecific transition-metal catalysts that lead to the commercialization of polypropylene as a major commodity plastic. The 1960s and 1970s witnessed the development of a number of high-performance polymers that could compete favorably with more traditional materials, such as metals, for automotive and aerospace applications.

Today, polymeric materials are used in nearly all areas of daily life and their production and fabrication are major worldwide industries. As indicated by data given in Table 1.1, the annual U.S. production of plastics, rubber, and fibers reached a record 67.35 billion pounds in 1993. As a group, plastics accounted for over 78% of this production, while synthetic fibers (14%) and elastomers (7.4%) made up the rest.

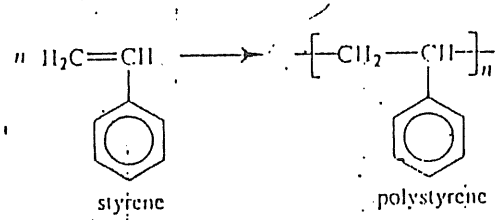

Figure 1.1. Polymerization of styrene.

The repeating unit of a common polymer, polystyrene, is illustrated in Figure 1.1. In this example, the repeating unit has the same chemical composition (i.e., C_8H_8) as the low-molecular-weight *monomer*, styrene, from which polystyrene is synthesized. The number of repeating units is indicated by the index n. In the case

TABLE 1.1 U.S. POLYMER PRODUCTION
(billions of pounds)

	1993	1992
PLASTICS		
Thermosetting Resins	6.87	6.34
Phenol resins	3.08	2.92
Urea resins	1.74	1.55
Polyesters (unsaturated)	1.26	1.18
Epoxies	0.51	0.46
Melamine resins	0.27	0.23
Thermoplastic Resins	46.19	45.23
Low-density polyethylene (LDPE)	12.04	11.92
PVC and copolymers	10.26	9.99
High-density polyethylene (HDPE)	9.91	9.81
Polystyrene	5.37	5.10
Polypropylene	8.61	8.42
TOTAL	53.06	51.57
FIBERS		
Cellulosics	0.51	0.50
Rayon	0.28	0.28
Acetate	0.23	0.22
Noncellulosics	8.79	8.57
Polyester	3.56	3.58
Nylon	2.66	2.56
Olefin	2.14	2.00
Acrylic	0.43	0.44
TOTAL	9.30	9.07
SYNTHETIC RUBBER		
Styrene–butadiene rubber (SBR)	1.89	1.92
Polybutadiene	1.03	1.02
Ethylene–propylene rubber	0.58	0.58
Nitrile rubber (NBR)	0.14	0.13
Other	1.37	1.42
TOTAL	5.00	5.07
TOTAL PRODUCTION	67.35	65.71

Source: *Chemical and Engineering News*, April 11, 1994.

of commercial grades of polystyrene, the average value of n may be 1000 or more. Given that the molecular weight of a polystyrene repeating unit is 104, a value of 1000 for n represents an average molecular weight of 104,000. Molecules with fewer than 10 repeating units are termed *oligomers* and exhibit quite different thermal and mechanical properties compared to the corresponding high-molecular-weight polymer. For example, oligomeric styrene having only seven repeating units (i.e., $n = 7$) is a viscous liquid at room temperature while commercial-grade, high-molecular-weight polystyrene is a brittle solid that does not soften until it is heated to above approximately 100°C.

1.1 CLASSIFICATION OF POLYMERS

Thousands of polymers have been synthesized and more are likely to be produced in the future. Fortunately, all polymers can be assigned to one of two groups based upon their processing characteristics or type of polymerization mechanism. More specific classification can be made on the basis of polymer structure. Such groupings are useful because they facilitate the discussion of properties.

1.1.1 Thermoplastics and Thermosets

All polymers can be divided into two major groups based on their thermal processing behavior. Those polymers that can be heat-softened in order to process into a desired form are called *thermoplastics*. Waste thermoplastics can be recovered and refabricated by application of heat and pressure. Polystyrene is an important example of a commercial thermoplastic. Other major examples are the polyolefins (e.g., polyethylene and polypropylene) and poly(vinyl chloride). In comparison, *thermosets* are polymers whose individual chains have been chemically linked by covalent bonds during polymerization or by subsequent chemical or thermal treatment during fabrication. Once formed, these crosslinked networks resist heat softening, creep, and solvent attack, but cannot be thermally processed. Such properties make thermosets suitable materials for composites, coatings, and adhesive applications. Principal examples of thermosets include epoxy, phenol–formaldehyde resins, and unsaturated polyesters.

1.1.2 Classification Based upon Polymerization Mechanism

In addition to classifying polymers on the basis of their processing characteristics, polymers may also be classified according to the mechanism of polymerization. One approach is to classify polymers as either *addition* or *condensation* — a scheme attributed to Wallace Carothers,[1] a pioneer of the polymer industry working at Du Pont during the 1920s and 1930s. Polystyrene, which is polymerized by a sequential addition of styrene monomers (see Figure 1.1), is an important example of addition polymer. Most important addition polymers are polymerized from ethylene-based monomers. A few other polymers that are traditionally recognized as belonging to the addition class are polymerized, not by addition to an ethylene double bond, but through a ring-opening polymerization of a sterically strained cyclic monomer. An example is the ring-opening polymerization of trioxane to give polyoxymethylene (an engineering thermoplastic), which is illustrated in Figure 1.2. The chemical structure of the repeating units and the commonly used nomenclature for some of the most important addition-type polymers that are derived from substituted ethylene

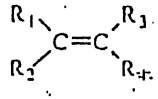

are given in Table 1.2.

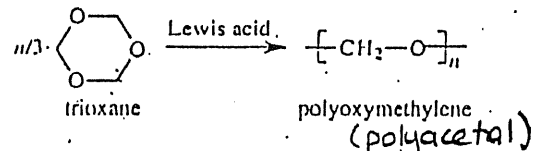

Figure 1.2. Ring-opening polymerization of trioxane.

Condensation polymers are obtained by the random reaction of two molecules. A molecule participating in a polycondensation reaction may be a monomer, oligomer, or higher-molecular-weight intermediate each having complementary functional end units, such as carboxylic acid or hydroxyl groups. Typically, condensation polymerizations occur by the liberation of a small molecule in the form of a gas, water, or salt. Any high-yield condensation reaction such as esterification or amidation can be used to obtain a high-molecular-weight polymer. An example of a condensation polymerization is the synthesis of nylon-6,6 by condensation of adipic acid and hexamethylene diamine, as shown in Figure 1.3A. This polymerization is accompanied by the liberation of two molecules of water for each repeating unit. Another important example of a polycondensation, illustrated in Figure 1.3B, is the preparation of polycarbonate from bisphenol-A and phosgene. In this case, two molecules of hydrogen chloride are formed for each repeating unit. Alternately, if the *sodium salt* of bisphenol-A was used in the polymerization, the by-product of the condensation would be sodium chloride rather than hydrogen chloride. The salt will precipitate out of the organic solvent used for the

TABLE 1.2 EXAMPLES OF SOME IMPORTANT ADDITION POLYMERS DERIVED FROM ETHYLENE DERIVATIVES

Polymer	R_1	R_2	R_3	R_4	Repeating Unit
Polyethylene	H	H	H	H	$-[CH_2-CH_2]-$
Polypropylene	H	H	H	CH_3	$-[CH_2-CH(CH_3)]-$
Poly(vinyl chloride)	H	H	H	Cl	$-[CH_2-CH(Cl)]-$
Poly(vinyl alcohol)	H	H	H	OH	$-[CH_2-CH(OH)]-$
Polyacrylonitrile	H	H	H	$C\equiv N$	$-[CH_2-CH(C\equiv N)]-$
Poly(vinyl acetate)	H	H	H	$O-C(=O)-CH_3$	$-[CH_2-CH(O-C(=O)-CH_3)]-$
Polystyrene	H	H	H	C_6H_5	$-[CH_2-CH(C_6H_5)]-$
Poly(methyl methacrylate)	H	H	CH_3	$C(=O)-O-CH_3$	$-[CH_2-C(CH_3)(C(=O)-O-CH_3)]-$
Poly(vinylidene chloride)	H	H	Cl	Cl	$-[CH_2-C(Cl)_2]-$

polymerization and, therefore, can be easily and safely removed. Some other examples of condensation polymers are given in Table 1.3.

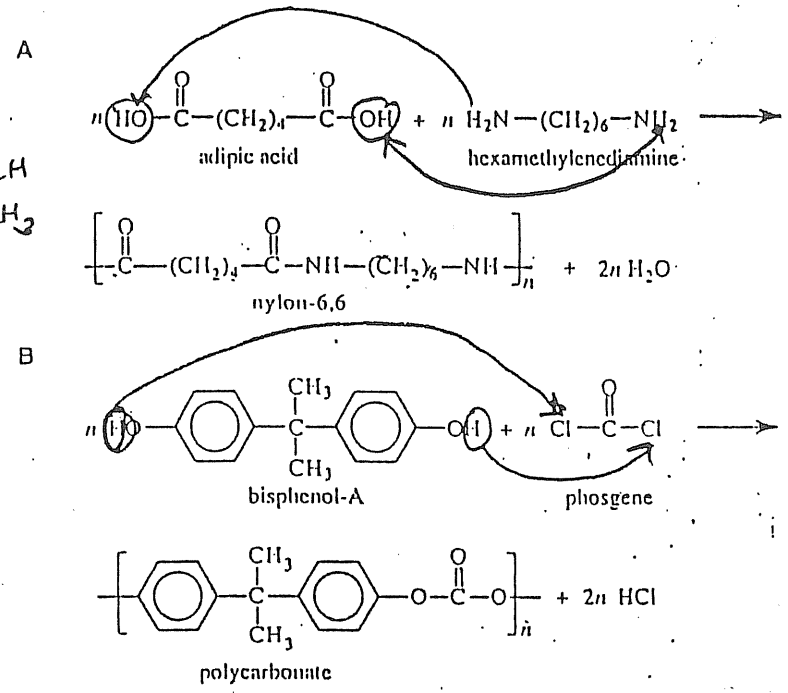

Figure 1.3. Two examples of a condensation polymerization. A. Polyamidation of nylon-6,6. B. Polymerization of bisphenol-A polycarbonate.

More recently, another classification scheme based on polymerization kinetics has been adopted over the more traditional addition and condensation categories. According to this scheme, all polymerization mechanisms are classified as either *step* growth or *chain* growth. Most condensation polymers are step growth, while most addition polymers are chain growth, but a number of important exceptions exist as will be discussed in Chapter 2. During chain-growth polymerization, high-molecular-weight polymer is formed early during the polymerization, and the polymerization yield, or the percent of monomer converted to polymer, gradually increases with time. In step-growth polymerization, high-molecular-weight polymer is formed only near the end of the polymerization (i.e., at high monomer conversion, typically >98%). Details of the mechanisms for chain-growth and step-growth polymerizations are discussed in Chapter 2.

TABLE 1.3 EXAMPLES OF SOME CONDENSATION THERMOPLASTICS

Polymer	Repeating Unit
Polysulfone	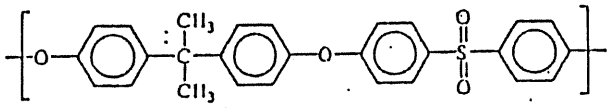
Poly(ethylene terephthalate)	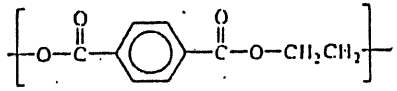 PET
Poly(hexamethylene sebacamide)	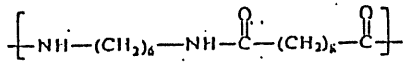
Poly(ethylene pyromellitimide)	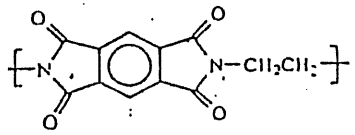

1.1.3 Classification Based upon Polymer Structure

In addition to classification based upon processing and polymerization characteristics, polymers may also be grouped based upon the chemical structure of their backbones. For example, polymers having all carbon atoms along their backbone are important examples of *homochain* polymers. They may be further classified depending upon whether there are single, double, or triple bonds along their backbone. Carbon-chain polymers with only single bonds along the backbone

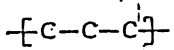

are known as *polyalkylenes* (or polyalkylidenes). Examples of polyalkylenes include the addition-type polymers polystyrene, polyolefins (e.g., polyethylene and polypropylene), and poly(vinyl chloride).

Carbon-chain polymers with double bonds along the chain

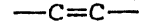

such as the diene elastomers — polyisoprene and polybutadiene — are called *polyalkenylenes*. Another example of a polyalkenylene is polyacetylene, an electrically conducting polymer (see Section 10.2.7). Carbon-chain polymers with triple bonds

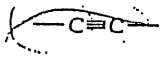

are *polyalkynylenes*.

Heterochain polymers that contain more than one atom type in their backbone are grouped according to the types of atoms and chemical groups (e.g., carbonyl, amide, or ester) located along the backbone. The most important classes of heterochain polymers are listed in Table 1.4.

TABLE 1.4 BACKBONE STRUCTURES OF SOME IMPORTANT ORGANIC HETEROCHAIN POLYMERS

Carbon–Oxygen Polymers	
Polyethers	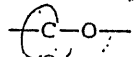
Polyesters of carboxylic acids	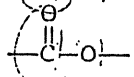
Polyanhydrides of carboxylic acids	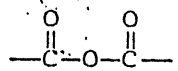
Polycarbonates	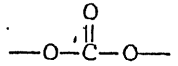
Carbon–Sulfur Polymers	
Polythioethers	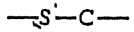
Polysulfones	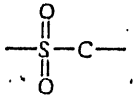
Carbon–Nitrogen Polymers	
Polyamines	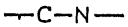
Polyimines	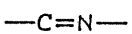
Polyamides	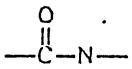
Polyureas	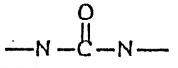

1.2 POLYMER STRUCTURE

The properties of polymers are strongly influenced by details of the chain structure. These details include the overall chemical composition and the sequence of monomer units in the case of copolymers, the stereochemistry or tacticity of the chain, and geometric isomerization in the case of diene-type polymers for which several synthesis routes may be possible.

1.2.1 Copolymers

Often, it is possible to obtain polymers with new and desirable properties by linking two or three different monomers or repeating units during the polymerization. Polymers with two different repeating units in their chains are called *copolymers*. In the less frequent case when there are three chemically-different repeating units, the resulting polymer is termed a *terpolymer*. Commercially, the most important copolymers are derived from vinyl monomers such as styrene, ethylene, acrylonitrile, and vinyl chloride.

The exact sequence of monomer units along the chain can vary widely depending upon the relative reactivities of each monomer during the polymerization process. At the extremes, monomer placement may be totally random or may be perfectly alternating, as illustrated in Figure 1.4. The actual sequence of monomer units is determined by the relative reactivities of the monomers as will be described in Section 2.2.1. Under special circumstances, it is possible to prepare copolymers that contain a long block of one monomer (A) followed by a block of the other monomer (B). These are called AB-block copolymers. Triblock copolymers have a central B block joined by A blocks at the end. A commercially important ABA-triblock copolymer is polystyrene-*block*-polybutadiene-*block*-polystyrene (SBS), a thermoplastic elastomer (see Section 9.1.3). In addition to these copolymer structures, *graft* copolymers can be prepared by polymerizing a monomer in the presence of a fully-formed polymer of another monomer. Graft copolymers are important as elastomeric (e.g., SBR) and high-impact polymers (e.g., high-impact polystyrene and ABS).

1.2.2 Tacticity

In addition to the type, number, and sequential arrangement of monomers along the chain, the *spatial* arrangement of substituent groups is also important in determining properties. The possible steric configurations of an asymmetric vinyl-polymer chain can be best represented by drawing the chain in its extended-chain or planar zigzag conformation, as illustrated in Figure 1.5. A *conformation* describes the *geometrical* arrangement of atoms in the polymer chain while *configuration* denotes the *stereochemical* arrangement of atoms. Unlike the conformation, the configuration of a polymer chain cannot be altered without breaking chemical bonds. For long, flexible polymer-chains, the total number of conformations is nearly infinite. The extended-chain conformation for vinyl polymers is often the lowest-energy conformation.

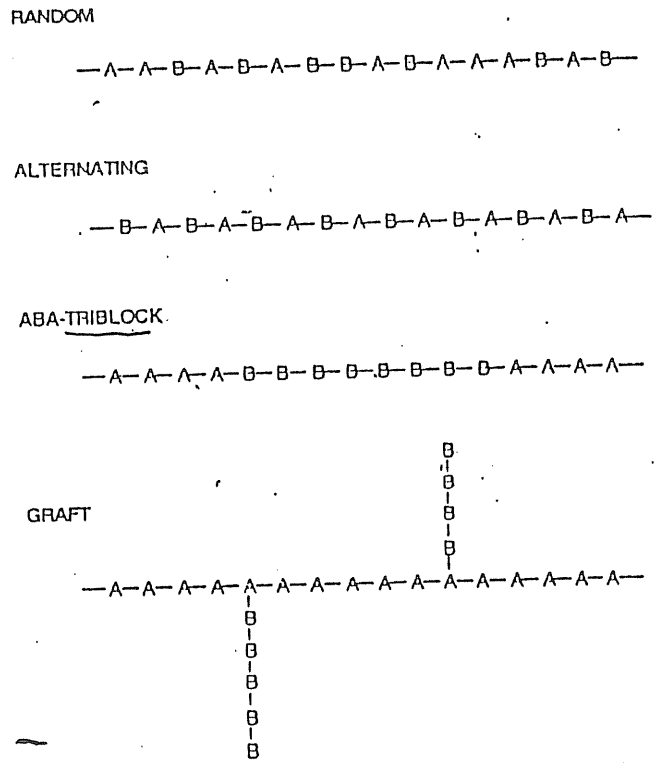

Figure 1.4. Possible structures of copolymers containing A and B repeating units.

As illustrated in Figure 1.5, several different placements of the asymmetric substituent group, R, are possible. As examples, a substituent group may be a methyl group as in polypropylene, a chlorine atom as in poly(vinyl chloride), or a phenyl ring as in polystyrene. In one configuration, all the R groups may lie on the same side of the plane formed by the extended-chain backbone. Such polymers are termed *isotactic*. If the substituent groups regularly alternate from one side of the plane to the other, the polymer is termed *syndiotactic*. Polymers with no preferred placement are *atactic*. More complicated arrangements of substituent groups

are possible in the case of 1,2-disubstituted polymers; however, these are commercially less important and will not be discussed here.

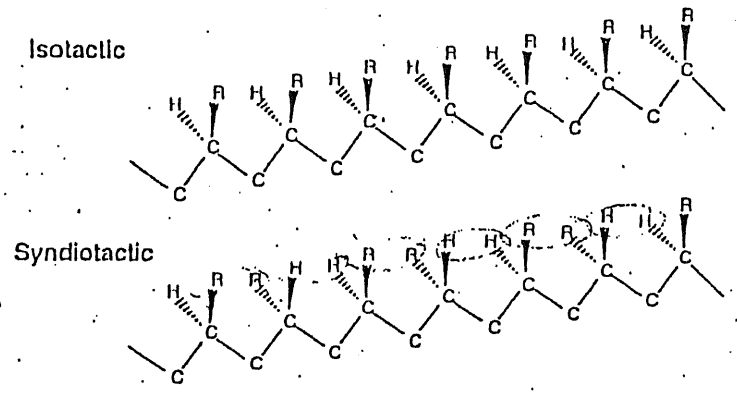

Figure 1.5. Two forms of stereochemical configuration of an extended-chain vinyl polymer having a substituent group R other than hydrogen.

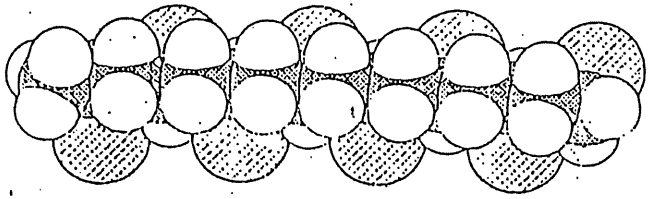

Figure 1.6. A computer-optimized view of eight repeating units of a PVC chain having *syndiotactic* placement of the chlorine atoms (large lightly shaded spheres). The view is looking down on the chain with the chlorine atoms at the base. Hydrogen atoms are represented by small unfilled spheres. Carbon atoms are represented by heavily shaded spheres.

In general, tactic polymers (i.e., isotactic or syndiotactic) are partially crystalline, while atactic polymers are *amorphous* indicating the absence of all crystalline order. In addition to crystallinity, other polymer properties, such as thermal and mechanical behavior, can be significantly affected by the tacticity of the polymer as later examples will show. Whether a specific polymer will be atactic, isotactic, or syndiotactic depends upon the specific conditions of the polymerization, such as temperature and choice of solvent, as will be discussed in Chapter 2. Commercial polypropylene is an important example of an isotactic polymer, although atactic and syndiotactic forms of this polymer also can be prepared. Commercial poly(vinyl chloride) (PVC) is an example of a polymer with imperfect tactic structure. Although the overall structure of commercial-grade PVC reasonably can be characterized as atactic, there are populations of repeating units whose sequences are highly syndiotactic and that impart a small degree of crystallinity to the commercial resin. A space-filling model for a short PVC chain having eight repeating units with syndiotactic placement of the chlorine atoms is shown in Figure 1.6. Using special polymerization methods, highly syndiotactic as well as isotactic PVC can be made (see Chapter 8), although these isomers have no attractive commercial value.

1.2.3 Geometric Isomerism

When there are unsaturated sites along a polymer chain, several different isomeric forms are possible. As Figure 1.7 illustrates, 1,3-butadiene (structure A) can be polymerized to give 1,2-poly(1,3-butadiene) (B) or as either of two *geometric isomers* of 1,4-poly(1,3-butadiene) (C and D). The numbers preceding the *poly* prefix designate the first and last carbon-atoms of the backbone repeating-unit. 1,2-Poly(1,3-butadiene) has a vinyl-type structure, where the substituent group (ethene) contains an unsaturated site; therefore, this geometric isomer can be atactic, syndiotactic, or isotactic. In the case of the commercially more important 1,4-poly(1,3-butadiene), all four carbons in the repeating unit lie along the chain. Carbons 1 and 4 can lie either on the same side of the central double bond (i.e., *cis*-configuration, C) or on the opposite side (i.e., *trans*-configuration, D). The structure of polybutadiene used in SBR rubber (i.e., a copolymer of styrene and butadiene) is principally the *trans*-1,4 isomer with some *cis*-1,4- and 1,2-poly(1,3-butadiene) content.

1.2.4 Nomenclature

As the preceding examples illustrate, a very large number of different polymer structures are possible. In order to identify these as unambiguously as possible, it is important to establish a reasonable system of nomenclature. As already evident, simple vinyl polymers are designated by attaching the prefix *poly* to the monomer name (e.g., polystyrene, polyethylene, and polypropylene); however, when the monomer name consists of more than one word or is preceded by a letter or number, the monomer is enclosed by parentheses preceded by the prefix *poly*. For example, the polymer obtained from the polymerization of 4-chlorostyrene is poly(4-chlorostyrene) and that from vinyl acetate is poly(vinyl acetate). Tacticity may be noted by prefixing the letters *i* (isotactic) or *s* (syndiotactic) before *poly* as in *i*-polystyrene. Geometric and structural isomers may be indicated by using the appropriate prefixes, *cis* or *trans* and 1,2- or 1,4-, before *poly*, as in *trans*-1,4-poly(1,3-butadiene).

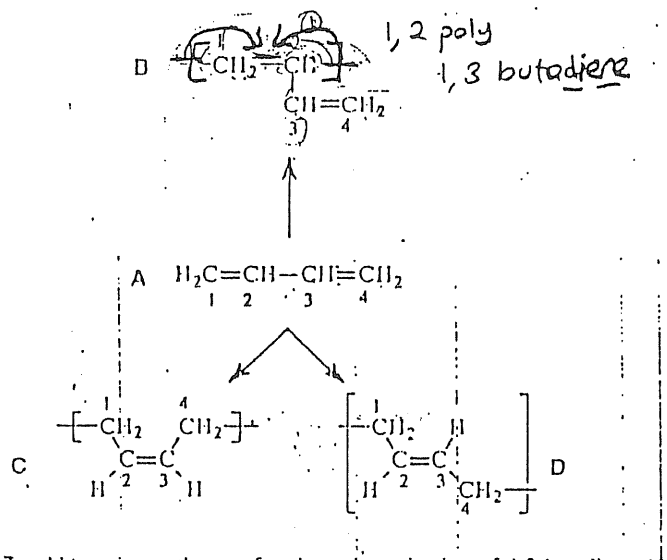

Figure 1.7. Alternative pathways for the polymerization of 1,3-butadiene (A) to give 1,2-poly(1,3-butadiene) (B), *cis*-1,4-poly(1,3-butadiene) (C), or *trans*-1,4-poly(1,3-butadiene) (D).

Nomenclature rules for nonvinyl polymers such as condensation polymers are generally more complicated than for vinyl monomers. These polymers are usually named according to the initial monomer or the functional group of the repeating unit. For example, the most important commercial nylon, commonly called nylon-6,6 (66 or 6/6), is more descriptively called poly(hexamethylene adipamide) denoting the polyamidation of hexamethylenediamine (alternately called 1,6-hexane diamine) with adipic acid (see Figure 1.3A). Similarly, the aliphatic nylon obtained by the polyamidation of hexamethylenediamine with a 10-carbon dicarboxylic acid, sebasic acid, is nylon-6,10 or poly(hexamethylene sebacamide) (see Table 1.3).

In some cases, the common names are used almost exclusively in place of the more chemically-correct nomenclature. For example, the polycondensation of phosgene and bisphenol-A — the common name for 2,2-bis(4-hydroxyphenyl) propane — produces the engineering thermoplastic, polycarbonate (Figure 1.3B). Often, the prefix bisphenol-A is placed before polycarbonate to distinguish it from other polycarbonates that can be polymerized by using bisphenol monomers other than bisphenol-A, such as tetramethylbisphenol-A.

Over the past 25 years, the International Union of Pure and Applied Chemistry (IUPAC) and the American Chemical Society (ACS) have developed a detailed, structure-based nomenclature for polymers. In addition, an industrial standard (ASTM D-4000) for specifying specific commercial grades of reinforced and

nonreinforced plastics has been offered by the American Society for Testing and Materials (ASTM).

The IUPAC structure-based rules for naming organic, inorganic, and coordination polymers have been compiled in a recent publication.[2] Although such nomenclature provides an unambiguous method for identifying the large number of known polymers (over 60,000 polymers are listed in the CAS Chemical Registry System), semisystematic or trivial names and sometimes even principal trade names (much to the displeasure of the manufacturer) continue to be used in place of the frequently unwieldy IUPAC names. As examples, the IUPAC name for polystyrene is poly(1-phenylethylene) and that for polytetrafluoroethylene

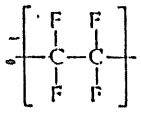

is poly(difluoromethylene) — a polymer more typically recognized by its trademark, Teflon™.

TABLE 1.5 SCHEME FOR NAMING COPOLYMERS

Type	Connective	Example
Unspecified	*-co-*	Poly[styrene-*co*-(methyl methacrylate)]
Statistical[a]	*-stat-*	Poly(styrene-*stat*-butadiene)
Random	*-ran-*	Poly[ethylene-*ran*-(vinyl acetate)]
Alternating	*-alt-*	Poly[styrene-*alt*-(maleic anhydride)]
Block	*-block-*	Polystyrene-*block*-polybutadiene
Graft	*-graft-*	Polybutadiene-*graft*-polystyrene

[a] A statistical polymer is one in which the sequential distribution of the monomeric units obeys statistical laws. In the case of a random copolymer, the probability of finding a given monomeric unit at any site in the chain is independent of the neighboring units in that position.

For convenience, several societies have developed a very useful set of two-, three-, and four-letter abbreviations for the names of many common thermoplastics, thermosets, fibers, elastomers, and additives. Sometimes, abbreviations adopted by different societies for the same polymer may vary, but there is widespread agreement on the abbreviations for a large number of important polymers. These abbreviations are quite convenient and widely used. As examples, PS is generally

recognized as the abbreviation for polystyrene, PVC for poly(vinyl chloride), PMMA for poly(methyl methacrylate), and PTFE for polytetrafluoroethylene. A listing of commonly accepted abbreviations is given in Appendix A at the end of this book.

Following IUPAC recommendations, copolymers are named by incorporating an italicized connective term between the names of monomers contained within parentheses or brackets or between two or more polymer names. The connective term designates the type of copolymer as indicated for six important classes of copolymers in Table 1.5.

1.3 MOLECULAR WEIGHT

1.3.1 Molecular-Weight Distribution

A typical synthetic polymer sample contains chains with a wide distribution of chain lengths. This distribution is seldom symmetric and contains some molecules of very high molecular weight. An illustration of a representative distribution is shown in Figure 1.8. The exact breadth of the molecular-weight distribution depends upon the specific conditions of polymerization, as will be described in Chapter 2. For example, the polymerization of some polyolefins results in a molecular-weight distribution that is extremely broad, while it is possible to polymerize some polymers, such as polystyrene, with nearly monodisperse distributions under laboratory conditions. Therefore, it is necessary to define an *average* molecular weight to characterize an individual polymer sample as detailed in the following section.

1.3.2 Molecular-Weight Averages

For a discrete distribution of molecular weights, an average molecular weight, $\overline{M}$, may be defined as

$$\overline{M} = \frac{\sum_i N_i M_i^{\alpha}}{\sum_i N_i M_i^{\alpha-1}} \tag{1.1}$$

where N_i indicates the number of moles of molecules with a molecular weight of M_i and the parameter α is a weighting factor that defines a particular average of the molecular-weight distribution. The weight, W_i, of molecules with molecular weight M_i is then

$$W_i = N_i M_i. \tag{1.2}$$

are the number average, $\overline{M}_n$ ($\alpha = 1$), the weight average, $\overline{M}_w$ ($\alpha = 2$), and the z average, $\overline{M}_z$ ($\alpha = 3$).

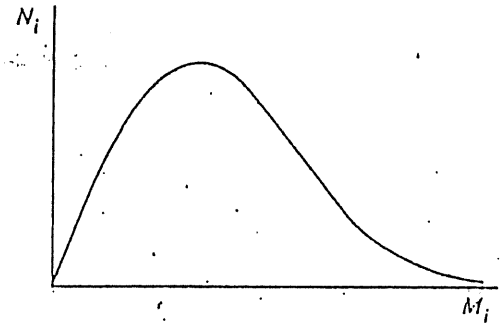

Figure 1.8. A typical distribution of molecular weights shown as a plot of the number of moles of chains, N_i, having molecular weight M_i, against M_i.

Since the molecular-weight distribution of commercial polymers is normally a continuous function, the molecular-weight averages can be determined by integration if the mathematical form of the molecular-weight distribution (i.e., N as a function of M) is known. For example, the number-average molecular weight would be given for discrete and continuous distributions, respectively, as

$$\overline{M}_n = \frac{\sum_{i=1}^{N} N_i M_i}{\sum_{i=1}^{N} N_i}, \tag{1.3a}$$

where N is the total number of polymer species in the distribution, and

$$\overline{M}_n = \frac{\int_0^M NM\,dM}{\int_0^M N\,dM}. \tag{1.3b}$$

The corresponding relationships for the weight-average molecular weight are given as

$$\overline{M}_w = \frac{\sum_{i=1}^{N} N_i M_i^2}{\sum_{i=1}^{N} N_i M_i} \tag{1.4a}$$

and

$$\overline{M}_w = \frac{\int_0^M NM^2 dM}{\int_0^M NM dM}. \tag{1.4b}$$

In the case of high-molecular-weight polymers, the number-average molecular weight is directly determined by membrane osmometry, while the weight-average molecular weight is determined by light scattering and other scattering techniques as will be discussed in Chapter 3.

A measure of the breadth of the molecular-weight distribution is given by the ratios of molecular-weight averages. For this purpose, the most commonly used ratio is $\overline{M}_w/\overline{M}_n$, which is called the *polydispersity index* or PDI. The PDIs of commercial polymers vary widely. For example, commercial grades of polystyrene with a $\overline{M}_n$ of over 100,000 have polydispersities indices between 2 and 5, while polyethylene synthesized in the presence of a stereospecific catalyst may have a PDI as high as 30. In contrast, the PDI of some vinyl polymers prepared by "living" polymerization (see Chapter 2) can be as low as 1.06. Such polymers with nearly monodisperse molecular-weight distributions are useful as molecular-weight standards for the determination of molecular weights and molecular-weight distributions of commercial polymers (see Section 3.3).

1.4 CHEMICAL STRUCTURE AND THERMAL TRANSITIONS

As the previous discussion has shown, many important synthetic polymers such as polystyrene and poly(methyl methacrylate) consist of long, flexible chains of very high molecular weight. In many cases, individual chains are randomly coiled and intertwined with no molecular order or structure. Such a physical state is termed *amorphous*. Commercial-grade (atactic) polystyrene and poly(methyl methacrylate) are examples of polymers that are amorphous in the solid state. Below a certain temperature called the glass-transition temperature (T_g), long-range, cooperative motions of individual chains cannot occur; however, short-range motions involving several contiguous groups along the chain backbone or substituent group are possible. Such motions are called *secondary-relaxation* processes and can occur at temperatures as low as 70 K. By comparison, glass-transition temperatures vary from 150 K for polymers with very flexible chains such as polydimethylsiloxane

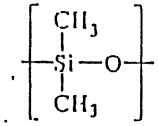

to well over 600 K for those with highly rigid aromatic backbones such as the high-modulus fiber, poly[2,2'-(*m*-phenylene)-5,5'-bibenzimidazole] (PBI)

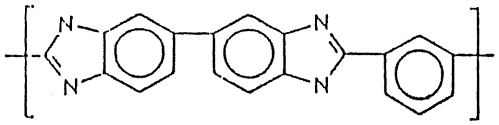

with a T_g reported in the range from 700 to 773 K.

Polymer chains with very regular structures, such as linear polyethylene and isotactic polypropylene, can be arranged in highly-regular structures called crystallites. Each crystallite consists of rows of folded chains. Since sufficient thermal energy is needed to provide the necessary molecular mobility for the chain-folding process, crystallization can occur only at temperatures above T_g. If the temperature is too high, chain folds become unstable and high thermal energy disorders the crystallites — a crystalline–amorphous transition occurs. The temperature that marks this transition is called the *crystalline-melting temperature* or T_m. Crystalline melting temperatures can vary from 334 K for simple, flexible-chain polyesters such as polycaprolactone

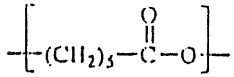

to over 675 K for aromatic polyamides such as poly(*m*-phenylene isophthalamide) (Nomex™).

468
POLYMER SCİENCE AND TECHNOLOGY

Polymer Science and Technology

Joel R. Fried
University of Cincinnati

PRENTICE HALL PTR
Upper Saddle River, New Jersey 07458

Fried, Joel R.
Polymer science and technology / Joel R. Fried.
p. cm.
Includes bibliographical references and index.
ISBN 0-13-685561-X
1. Polymers; 2. Polymerization. I. Title
QD381.F73 1995 94-22289
668.9--dc20 CIP

Editorial/production supervision: *Ann Sullivan*
Cover design: *Wanda Lubelska*
Manufacturing manager: *Alexis R. Heydt*

10 9 8 7 6 5 4

ISBN 0-13-685561-X

Prentice-Hall International (UK) Limited, *London*
Prentice-Hall of Australia Pty. Limited, *Sydney*
Prentice-Hall Canada Inc., *Toronto*
Prentice-Hall Hispanoamericana, S.A., *Mexico*
Prentice-Hall of India Private Limited, *New Delhi*
Prentice-Hall of Japan, Inc., *Tokyo*
Simon & Schuster Asia Pte. Ltd., *Singapore*
Editora Prentice-Hall do Brasil, Ltda., *Rio de Janeiro*

To my parents who provided the opportunities and to Ava, Marc, and Aaron for their love, patience, and understanding.

Contents

At least dozens of good introductory textbooks on polymer science and engineering are now available. Why then has yet another book been written? The decision was based on my belief that none of the available texts fully addresses the needs of students in chemical engineering. It is not that chemical engineers are a rare breed, but rather that they have special training in areas of thermodynamics and transport phenomena that is seldom challenged by texts designed primarily for students of chemistry or materials science. This has been a frustration of mine and of many of my students for the past 15 years during which I have taught an introductory course, *Polymer Technology*, to some 350 chemical engineering seniors. In response to this perceived need, I had written nine review articles that appeared in the SPE publication *Plastics Engineering* from 1982 to 1984. These served as hard copy for my students to supplement their classroom notes but fell short of a complete solution.

In writing this text, it was my objective to first provide the basic building blocks of polymer science and engineering by coverage of fundamental polymer chemistry and materials topics given in Chapters 1 through 7. As a supplement to the traditional coverage of polymer thermodynamics, extensive discussion of phase equilibria, equation-of-state theories, and UNIFAC has been included in Chapter 3. Coverage of rheology, including the use of constitutive equations and the modeling of simple flow geometries, and the fundamentals of polymer processing operations are given in Chapter 11. Finally, I wanted to provide information on the exciting new materials now available and the emerging areas of technological growth that could motivate a new generation of scientists and engineers. For this reason, engineering and specialty polymers are surveyed in Chapter 10 and important new applications for polymers in separations (membrane separations), electronics (conducting polymers), biotechnology (controlled drug release), and other specialized areas of engineering are given in Chapter 12. In all, this has been an ambitious undertaking and I hope that I have succeeded in at least some of these goals.

Although the intended audience for this text is advanced undergraduates and graduate students in chemical engineering, the coverage of polymer science fundamentals (Chapters 1 through 7) should be suitable for a semester course in a materials science or chemistry curriculum. Chapters 8 through 10 intended as survey chapters of the principal categories of polymers — commodity thermoplastics and fibers, network polymers (elastomers and thermosets), and engineering and specialty polymers — may be included to supplement and reinforce the material presented in the chapters on fundamentals and should serve as a useful reference source for the practicing scientist or engineer in the plastics industry.

Joel R. Fried
Cincinnati, Ohio

Acknowledgments

This text could not have been completed without the help of many colleagu who provided figures and photographs and offered important advice duri the course of its preparation. I am particularly indebted to those colleagu who read all or sections of the draft of this text and offered very helpful advi These include Professor James E. Mark of the University of Cincinnati, Profes Otto Vogl of the Polytechnic University, Professor Erdogan Kiran of t University of Maine, Professor Paul Han of the University of Akron, Profes Donald R. Paul of the University of Texas, and Professor R. P. Danner of Pe State.

I wish to also thank those colleagues who kindly provided some key illust tions and photos. These are Dr. Roger Kambour of General Electric, Professor E Koros of the University of Texas, Professor Paul Han of the University of Akr Professor John Gilham of Princeton University, Professor Paul Philips of t University of Tennessee, Dr. Marty Matsuo of Nippon Zeon (Japan), Dr. Rob Cieslinski of The Dow Chemical Company, Dr. Richard Baker of Membra Technology & Research, Inc., and Dr. Mostafa Aboulfaraj of Pechiney Centre Recherches de Voreppe (France). Appreciation is also extended to my student, J Jian-Shen Jiang, who spent many hours preparing high-quality computer graph when she had much more interesting things to do.

1

Introduction to Polymer Science

The word *polymer* is derived from the classical Greek words *poly* meaning "many" and *meres* meaning "parts." Simply stated, a polymer is a long-chain molecule that is composed of a large number of *repeating units* of identical structure. Certain polymers, such as proteins, cellulose, and silk, are found in nature, while many others, including polystyrene, polyethylene, and nylon, are produced only by synthetic routes. In some cases, naturally occurring polymers can also be produced synthetically. An important example is natural rubber (i.e., Hevea), which is known as polyisoprene in its synthetic form.

Polymers that are capable of high extension under ambient conditions find important applications as elastomers. In addition to natural rubber, there are synthetic elastomers such as nitrile and butyl rubber. Other polymers may have characteristics that permit their formation into long fibers suitable for textile applications. The synthetic fibers, principally nylon and polyester, are good substitutes for the naturally occurring fibers such as cotton, wool, and silk.

In contrast to the usage of the word *polymer*, those commercial materials, other than elastomers and fibers, that are derived from synthetic polymers are called *plastics*. A typical commercial plastic resin may contain two or more polymers in addition to various additives and fillers. These are added to improve some property such as the processability, thermal or environmental stability, and mechanical properties of the final product.

The birth of polymer science may be traced back to the mid-nineteenth century. In the 1830s, Charles Goodyear developed the vulcanization process that transformed the sticky latex of natural rubber to a useful elastomer for tire use. In 1847, Christian F. Schönbein reacted cellulose with nitric acid to produce cellulose nitrate. This was used in the 1860s as the first man-made thermoplastic, celluloid. In 1907, Leo Backeland produced Bakelite (phenol-formaldehyde resin), and glyptal (unsaturated-polyester resin) was developed as a protective coating resin by General Electric in 1912.

By the 1930s, researchers at Du Pont in the United States had produced a variety of new polymers including synthetic rubber and more exotic materials such as nylon and Teflon™. In 1938, Dow had produced several tons of polystyrene and, in 1939, polyethylene (low-density) was made for the first time by scientists at ICI in England. Efforts to develop new polymeric materials, particularly synthetic rubber, were intensified during World War II when many naturally occurring materials such as Hevea rubber were in short supply. In the 1950s, Ziegler and Natta independently developed a family of stereospecific transition-metal catalysts that lead to the commercialization of polypropylene as a major commodity plastic. The 1960s and 1970s witnessed the development of a number of high-performance polymers that could compete favorably with more traditional materials, such as metals, for automotive and aerospace applications.

Today, polymeric materials are used in nearly all areas of daily life and their production and fabrication are major worldwide industries. As indicated by data given in Table 1.1, the annual U.S. production of plastics, rubber, and fibers reached a record 67.35 billion pounds in 1993. As a group, plastics accounted for over 78% of this production, while synthetic fibers (14%) and elastomers (7.4%) made up the rest.

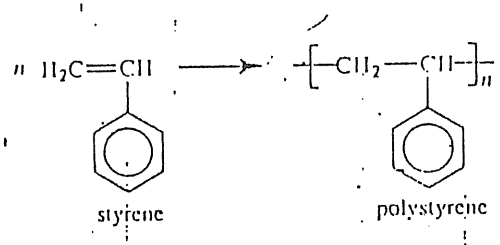

Figure 1.1. Polymerization of styrene.

The repeating unit of a common polymer, polystyrene, is illustrated in Figure 1.1. In this example, the repeating unit has the same chemical composition (i.e., C_8H_8) as the low-molecular-weight *monomer*, styrene, from which polystyrene is synthesized. The number of repeating units is indicated by the index *n*. In the case

TABLE 1.1 U.S. POLYMER PRODUCTION
(billions of pounds)

	1993	1992
PLASTICS		
Thermosetting Resins	6.87	6.34
Phenol resins	3.08	2.92
Urea resins	1.74	1.55
Polyesters (unsaturated)	1.26	1.18
Epoxies	0.51	0.46
Melamine resins	0.27	0.23
Thermoplastic Resins	46.19	45.23
Low-density polyethylene (LDPE)	12.04	11.92
PVC and copolymers	10.26	9.99
High-density polyethylene (HDPE)	9.91	9.81
Polystyrene	5.37	5.10
Polypropylene	8.61	8.42
TOTAL	53.06	51.57
FIBERS		
Cellulosics	0.51	0.50
Rayon	0.28	0.28
Acetate	0.23	0.22
Noncellulosics	8.79	8.57
Polyester	3.56	3.58
Nylon	2.66	2.56
Olefin	2.14	2.00
Acrylic	0.43	0.44
TOTAL	9.30	9.07
SYNTHETIC RUBBER		
Styrene–butadiene rubber (SBR)	1.89	1.92
Polybutadiene	1.03	1.02
Ethylene–propylene rubber	0.58	0.58
Nitrile rubber (NBR)	0.14	0.13
Other	1.37	1.42
TOTAL	5.00	5.07
TOTAL PRODUCTION	67.35	65.71

Source: *Chemical and Engineering News*, April 11, 1994.

of commercial grades of polystyrene, the average value of n may be 1000 or more. Given that the molecular weight of a polystyrene repeating unit is 104, a value of 1000 for n represents an average molecular weight of 104,000. Molecules with fewer than 10 repeating units are termed *oligomers* and exhibit quite different thermal and mechanical properties compared to the corresponding high-molecular-weight polymer. For example, oligomeric styrene having only seven repeating units (i.e., $n = 7$) is a viscous liquid at room temperature while commercial-grade, high-molecular-weight polystyrene is a brittle solid that does not soften until it is heated to above approximately 100°C.

1.1 CLASSIFICATION OF POLYMERS

Thousands of polymers have been synthesized and more are likely to be produced in the future. Fortunately, all polymers can be assigned to one of two groups based upon their processing characteristics or type of polymerization mechanism. More specific classification can be made on the basis of polymer structure. Such groupings are useful because they facilitate the discussion of properties.

1.1.1 Thermoplastics and Thermosets

All polymers can be divided into two major groups based on their thermal processing behavior. Those polymers that can be heat-softened in order to process into a desired form are called *thermoplastics*. Waste thermoplastics can be recovered and refabricated by application of heat and pressure. Polystyrene is an important example of a commercial thermoplastic. Other major examples are the polyolefins (e.g., polyethylene and polypropylene) and poly(vinyl chloride). In comparison, *thermosets* are polymers whose individual chains have been chemically linked by covalent bonds during polymerization or by subsequent chemical or thermal treatment during fabrication. Once formed, these crosslinked networks resist heat softening, creep, and solvent attack, but cannot be thermally processed. Such properties make thermosets suitable materials for composites, coatings, and adhesive applications. Principal examples of thermosets include epoxy, phenol–formaldehyde resins, and unsaturated polyesters.

1.1.2 Classification Based upon Polymerization Mechanism

In addition to classifying polymers on the basis of their processing characteristics, polymers may also be classified according to the mechanism of polymerization. One approach is to classify polymers as either *addition* or *condensation* — a scheme attributed to Wallace Carothers,[1] a pioneer of the polymer industry working at Du Pont during the 1920s and 1930s. Polystyrene, which is polymerized by a sequential addition of styrene monomers (see Figure 1.1), is an important example of addition polymer. Most important addition polymers are polymerized from ethylene-based monomers. A few other polymers that are traditionally recognized as belonging to the addition class are polymerized, not by addition to an ethylene double bond, but through a ring-opening polymerization of a sterically strained cyclic monomer. An example is the ring-opening polymerization of trioxane to give polyoxymethylene (an engineering thermoplastic), which is illustrated in Figure 1.2. The chemical structure of the repeating units and the commonly used nomenclature for some of the most important addition-type polymers that are derived from substituted ethylene

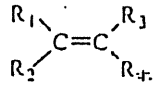

are given in Table 1.2.

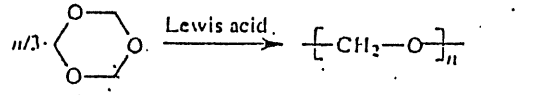

Figure 1.2. Ring-opening polymerization of trioxane.

Condensation polymers are obtained by the random reaction of two molecules. A molecule participating in a polycondensation reaction may be a monomer, oligomer, or higher-molecular-weight intermediate each having complementary functional end units, such as carboxylic acid or hydroxyl groups. Typically, condensation polymerizations occur by the liberation of a small molecule in the form of a gas, water, or salt. Any high-yield condensation reaction such as esterification or amidation can be used to obtain a high-molecular-weight polymer. An example of a condensation polymerization is the synthesis of nylon-6,6 by condensation of adipic acid and hexamethylene diamine, as shown in Figure 1.3A. This polymerization is accompanied by the liberation of two molecules of water for each repeating unit. Another important example of a polycondensation, illustrated in Figure 1.3B, is the preparation of polycarbonate from bisphenol-A and phosgene. In this case, two molecules of hydrogen chloride are formed for each repeating unit. Alternately, if the *sodium salt* of bisphenol-A was used in the polymerization, the by-product of the condensation would be sodium chloride rather than hydrogen chloride. The salt will precipitate out of the organic solvent used for the

TABLE 1.2 EXAMPLES OF SOME IMPORTANT ADDITION POLYMERS DERIVED FROM ETHYLENE DERIVATIVES

Polymer	R_1	R_2	R_3	R_4	Repeating Unit
Polyethylene	H	H	H	H	$-[CH_2-CH_2]-$
Polypropylene	H	H	H	CH_3	$-[CH_2-CH(CH_3)]-$
Poly(vinyl chloride)	H	H	H	Cl	$-[CH_2-CH(Cl)]-$
Poly(vinyl alcohol)	H	H	H	OH	$-[CH_2-CH(OH)]-$
Polyacrylonitrile	H	H	H	C≡N	$-[CH_2-CH(C\equiv N)]-$
Poly(vinyl acetate)	H	H	H	$-O-C(=O)-CH_3$	$-[CH_2-CH(O-C(=O)-CH_3)]-$
Polystyrene	H	H	H	C_6H_5	$-[CH_2-CH(C_6H_5)]-$
Poly(methyl methacrylate)	H	H	CH_3	$-C(=O)-O-CH_3$	$-[CH_2-C(CH_3)(C(=O)-O-CH_3)]-$
Poly(vinylidene chloride)	H	H	Cl	Cl	$-[CH_2-C(Cl)_2]-$

polymerization and, therefore, can be easily and safely removed. Some other examples of condensation polymers are given in Table 1.3.

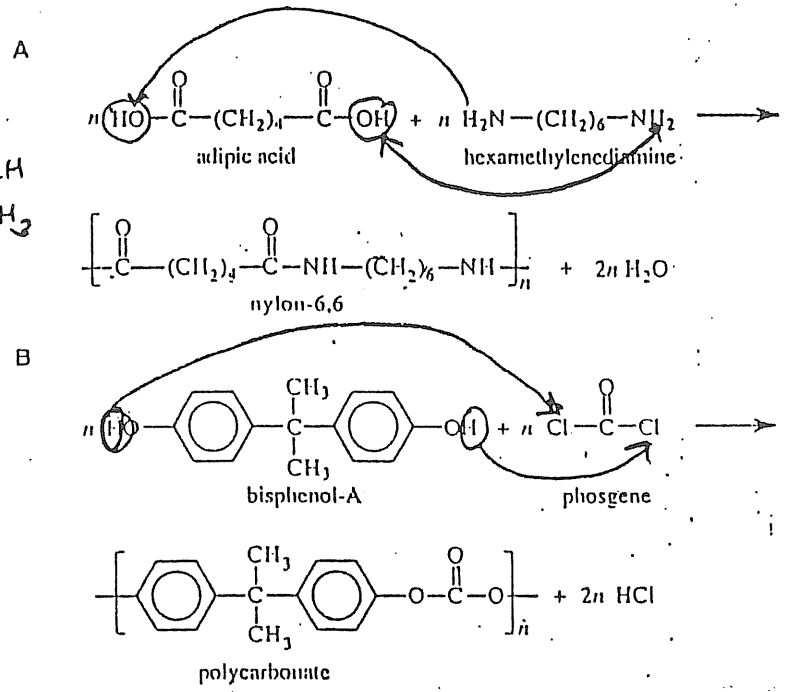

Figure 1.3. Two examples of a condensation polymerization. A. Polyamidation of nylon-6,6. B. Polymerization of bisphenol-A polycarbonate.

More recently, another classification scheme based on polymerization kinetics has been adopted over the more traditional addition and condensation categories. According to this scheme, all polymerization mechanisms are classified as either *step* growth or *chain* growth. Most condensation polymers are step growth, while most addition polymers are chain growth, but a number of important exceptions exist as will be discussed in Chapter 2. During chain-growth polymerization, high-molecular-weight polymer is formed early during the polymerization, and the polymerization yield, or the percent of monomer converted to polymer, gradually increases with time. In step-growth polymerization, high-molecular-weight polymer is formed only near the end of the polymerization (i.e., at high monomer conversion, typically >98%). Details of the mechanisms for chain-growth and step-growth polymerizations are discussed in Chapter 2.

TABLE 1.3 EXAMPLES OF SOME CONDENSATION THERMOPLASTICS

Polymer	Repeating Unit
Polysulfone	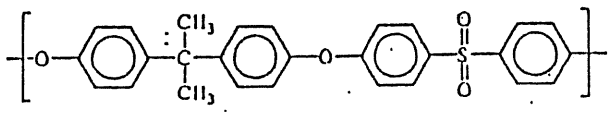
Poly(ethylene terephthalate)	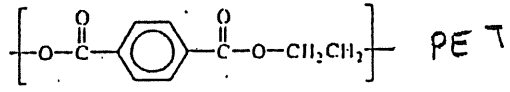
Poly(hexamethylene sebacamide)	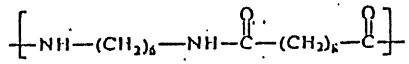
Poly(ethylene pyromellitimide)	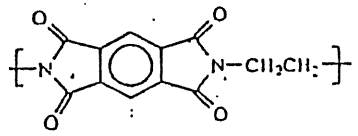

1.1.3 Classification Based upon Polymer Structure

In addition to classification based upon processing and polymerization characteristics, polymers may also be grouped based upon the chemical structure of their backbones. For example, polymers having all carbon atoms along their backbone are important examples of *homochain* polymers. They may be further classified depending upon whether there are single, double, or triple bonds along their backbone. Carbon-chain polymers with only single bonds along the backbone

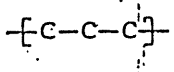

are known as *polyalkylenes* (or polyalkylidenes). Examples of polyalkylenes include the addition-type polymers polystyrene, polyolefins (e.g., polyethylene and polypropylene), and poly(vinyl chloride).

Carbon-chain polymers with double bonds along the chain

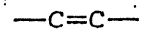

such as the diene elastomers — polyisoprene and polybutadiene — are called *polyalkenylenes*. Another example of a polyalkenylene is polyacetylene, an electrically conducting polymer (see Section 10.2.7). Carbon-chain polymers with triple bonds

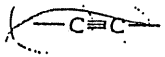

are *polyalkynylenes*.

Heterochain polymers that contain more than one atom type in their backbone are grouped according to the types of atoms and chemical groups (e.g., carbonyl, amide, or ester) located along the backbone. The most important classes of heterochain polymers are listed in Table 1.4.

TABLE 1.4 BACKBONE STRUCTURES OF SOME IMPORTANT ORGANIC HETEROCHAIN POLYMERS

Carbon–Oxygen Polymers	
Polyethers	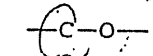
Polyesters of carboxylic acids	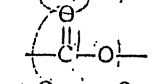
Polyanhydrides of carboxylic acids	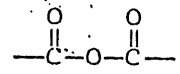
Polycarbonates	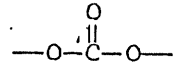
Carbon–Sulfur Polymers	
Polythioethers	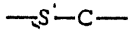
Polysulfones	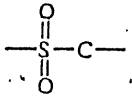
Carbon–Nitrogen Polymers	
Polyamines	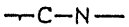
Polyimines	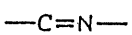
Polyamides	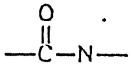
Polyureas	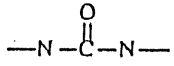

1.2 POLYMER STRUCTURE

The properties of polymers are strongly influenced by details of the chain structure. These details include the overall chemical composition and the sequence of monomer units in the case of copolymers, the stereochemistry or tacticity of the chain, and geometric isomerization in the case of diene-type polymers for which several synthesis routes may be possible.

1.2.1 Copolymers

Often, it is possible to obtain polymers with new and desirable properties by linking two or three different monomers or repeating units during the polymerization. Polymers with two different repeating units in their chains are called *copolymers*. In the less frequent case when there are three chemically-different repeating units, the resulting polymer is termed a *terpolymer*. Commercially, the most important copolymers are derived from vinyl monomers such as styrene, ethylene, acrylonitrile, and vinyl chloride.

The exact sequence of monomer units along the chain can vary widely depending upon the relative reactivities of each monomer during the polymerization process. At the extremes, monomer placement may be totally random or may be perfectly alternating, as illustrated in Figure 1.4. The actual sequence of monomer units is determined by the relative reactivities of the monomers as will be described in Section 2.2.1. Under special circumstances, it is possible to prepare copolymers that contain a long block of one monomer (A) followed by a block of the other monomer (B). These are called AB-block copolymers. Triblock copolymers have a central B block joined by A blocks at the end. A commercially important ABA-triblock copolymer is polystyrene-*block*-polybutadiene-*block*-polystyrene (SBS), a thermoplastic elastomer (see Section 9.1.3). In addition to these copolymer structures, *graft* copolymers can be prepared by polymerizing a monomer in the presence of a fully-formed polymer of another monomer. Graft copolymers are important as elastomeric (e.g., SBR) and high-impact polymers (e.g., high-impact polystyrene and ABS).

1.2.2 Tacticity

In addition to the type, number, and sequential arrangement of monomers along the chain, the *spatial* arrangement of substituent groups is also important in determining properties. The possible steric configurations of an asymmetric vinyl-polymer chain can be best represented by drawing the chain in its extended-chain or planar zigzag conformation, as illustrated in Figure 1.5. A *conformation* describes the *geometrical* arrangement of atoms in the polymer chain while *configuration* denotes the *stereochemical* arrangement of atoms. Unlike the conformation, the configuration of a polymer chain cannot be altered without breaking chemical bonds. For long, flexible polymer-chains, the total number of conformations is nearly in-

finite. The extended-chain conformation for vinyl polymers is often the lowest-energy conformation.

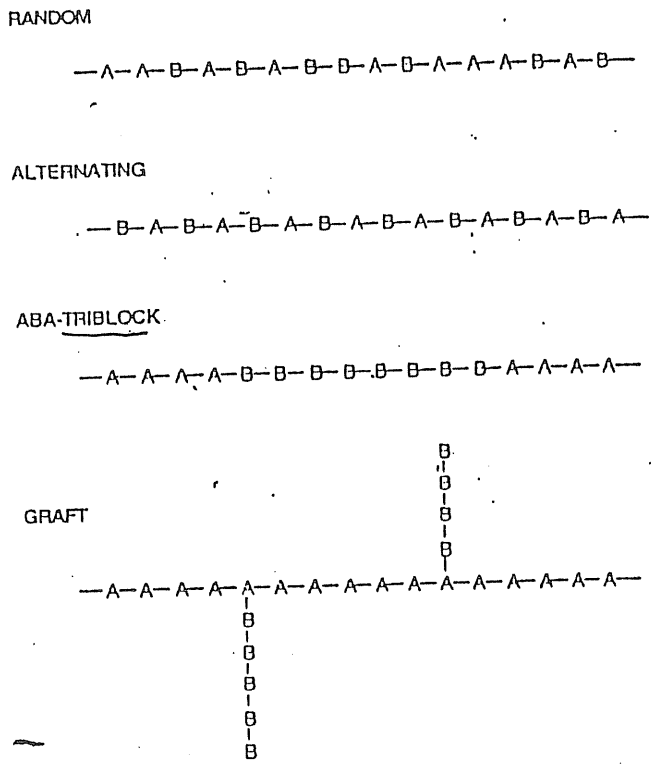

Figure 1.4. Possible structures of copolymers containing A and B repeating units.

As illustrated in Figure 1.5, several different placements of the asymmetric substituent group, R, are possible. As examples, a substituent group may be a methyl group as in polypropylene, a chlorine atom as in poly(vinyl chloride), or a phenyl ring as in polystyrene. In one configuration, all the R groups may lie on the same side of the plane formed by the extended-chain backbone. Such polymers are termed *isotactic*. If the substituent groups regularly alternate from one side of the plane to the other, the polymer is termed *syndiotactic*. Polymers with no preferred placement are *atactic*. More complicated arrangements of substituent groups

are possible in the case of 1,2-disubstituted polymers; however, these are commercially less important and will not be discussed here.

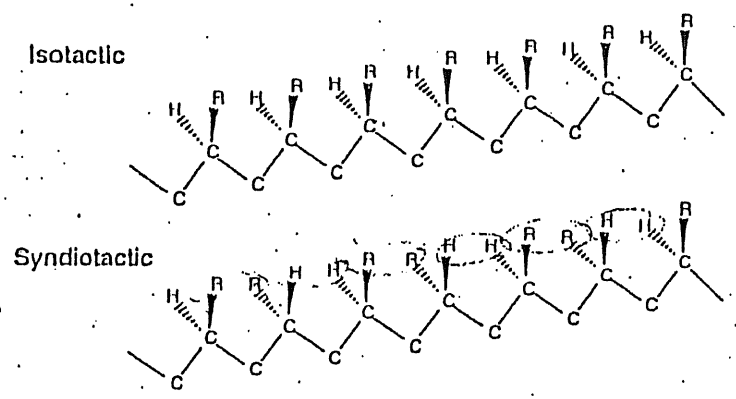

Figure 1.5. Two forms of stereochemical configuration of an extended-chain vinyl polymer having a substituent group R other than hydrogen.

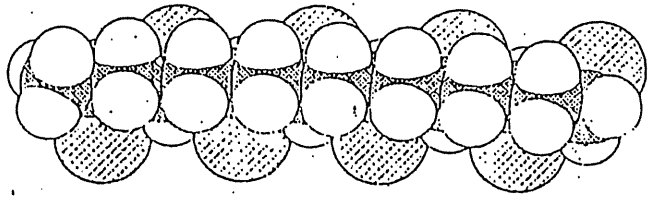

Figure 1.6. A computer-optimized view of eight repeating units of a PVC chain having *syndiotactic* placement of the chlorine atoms (large lightly shaded spheres). The view is looking down on the chain with the chlorine atoms at the base. Hydrogen atoms are represented by small unfilled spheres. Carbon atoms are represented by heavily shaded spheres.

In general, tactic polymers (i.e., isotactic or syndiotactic) are partially crystalline, while atactic polymers are *amorphous* indicating the absence of all crystalline order. In addition to crystallinity, other polymer properties, such as thermal and mechanical behavior, can be significantly affected by the tacticity of the polymer as later examples will show. Whether a specific polymer will be atactic, isotactic, or syndiotactic depends upon the specific conditions of the polymerization, such as temperature and choice of solvent, as will be discussed in Chapter 2. Commercial polypropylene is an important example of an isotactic polymer, although atactic and syndiotactic forms of this polymer also can be prepared. Commercial poly(vinyl chloride) (PVC) is an example of a polymer with imperfect tactic structure. Although the overall structure of commercial-grade PVC reasonably can be characterized as atactic, there are populations of repeating units whose sequences are highly syndiotactic and that impart a small degree of crystallinity to the commercial resin. A space-filling model for a short PVC chain having eight repeating units with syndiotactic placement of the chlorine atoms is shown in Figure 1.6. Using special polymerization methods, highly syndiotactic as well as isotactic PVC can be made (see Chapter 8), although these isomers have no attractive commercial value.

1.2.3 Geometric Isomerism

When there are unsaturated sites along a polymer chain, several different isomeric forms are possible. As Figure 1.7 illustrates, 1,3-butadiene (structure A) can be polymerized to give 1,2-poly(1,3-butadiene) (B) or as either of two *geometric isomers* of 1,4-poly(1,3-butadiene) (C and D). The numbers preceding the *poly* prefix designate the first and last carbon-atoms of the backbone repeating-unit. 1,2-Poly(1,3-butadiene) has a vinyl-type structure, where the substituent group (ethene) contains an unsaturated site; therefore, this geometric isomer can be atactic, syndiotactic, or isotactic. In the case of the commercially more important 1,4-poly(1,3-butadiene), all four carbons in the repeating unit lie along the chain. Carbons 1 and 4 can lie either on the same side of the central double bond (i.e., *cis*-configuration, C) or on the opposite side (i.e., *trans*-configuration, D). The structure of polybutadiene used in SBR rubber (i.e., a copolymer of styrene and butadiene) is principally the *trans*-1,4 isomer with some *cis*-1,4- and 1,2-poly(1,3-butadiene) content.

1.2.4 Nomenclature

As the preceding examples illustrate, a very large number of different polymer structures are possible. In order to identify these as unambiguously as possible, it is important to establish a reasonable system of nomenclature. As already evident, simple vinyl polymers are designated by attaching the prefix *poly* to the monomer name (e.g., polystyrene, polyethylene, and polypropylene); however, when the monomer name consists of more than one word or is preceded by a letter or number, the monomer is enclosed by parentheses preceded by the prefix *poly*. For example, the polymer obtained from the polymerization of 4-chlorostyrene is poly(4-chlorostyrene) and that from vinyl acetate is poly(vinyl acetate). Tacticity may be noted by prefixing the letters *i* (isotactic) or *s* (syndiotactic) before *poly* as in *i*-polystyrene. Geometric and structural isomers may be indicated by using the appropriate prefixes, *cis* or *trans* and 1,2- or 1,4-, before *poly*, as in *trans*-1,4-poly(1,3-butadiene).

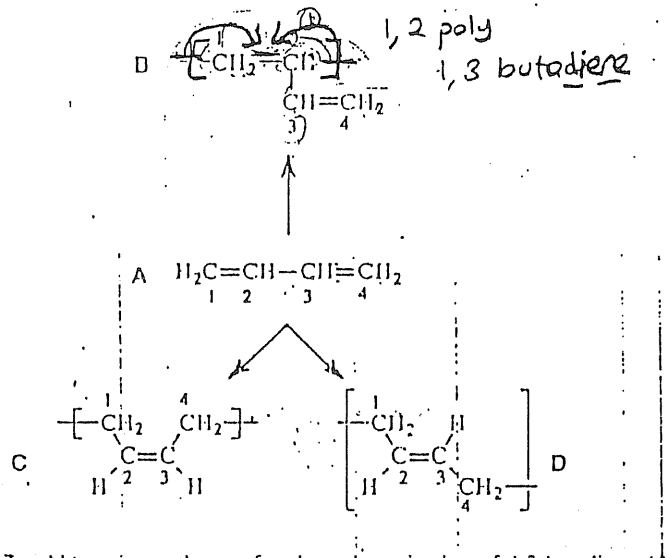

Figure 1.7. Alternative pathways for the polymerization of 1,3-butadiene (A) to give 1,2-poly(1,3-butadiene) (B), *cis*-1,4-poly(1,3-buladiene) (C), or *trans*-1,4-poly(1,3-butadiene) (D).

Nomenclature rules for nonvinyl polymers such as condensation polymers are generally more complicated than for vinyl monomers. These polymers are usually named according to the initial monomer or the functional group of the repeating unit. For example, the most important commercial nylon, commonly called nylon-6,6 (66 or 6/6), is more descriptively called poly(hexamethylene adipamide) denoting the polyamidation of hexamethylenediamine (alternately called 1,6-hexane diamine) with adipic acid (see Figure 1.3A). Similarly, the aliphatic nylon obtained by the polyamidation of hexamethylenediamine with a 10-carbon dicarboxylic acid, sebasic acid, is nylon-6,10 or poly(hexamethylene sebacamide) (see Table 1.3).

In some cases, the common names are used almost exclusively in place of the more chemically-correct nomenclature. For example, the polycondensation of phosgene and bisphenol-A — the common name for 2,2-bis(4-hydroxyphenyl) propane — produces the engineering thermoplastic, polycarbonate (Figure 1.3B). Often, the prefix bisphenol-A is placed before polycarbonate to distinguish it from other polycarbonates that can be polymerized by using bisphenol monomers other than bisphenol-A, such as tetramethylbisphenol-A.

Over the past 25 years, the International Union of Pure and Applied Chemistry (IUPAC) and the American Chemical Society (ACS) have developed a detailed, structure-based nomenclature for polymers. In addition, an industrial standard (ASTM D-4000) for specifying specific commercial grades of reinforced and

nonreinforced plastics has been offered by the American Society for Testing and Materials (ASTM).

The IUPAC structure-based rules for naming organic, inorganic, and coordination polymers have been compiled in a recent publication.[2] Although such nomenclature provides an unambiguous method for identifying the large number of known polymers (over 60,000 polymers are listed in the CAS Chemical Registry System), semisystematic or trivial names and sometimes even principal trade names (much to the displeasure of the manufacturer) continue to be used in place of the frequently unwieldy IUPAC names. As examples, the IUPAC name for polystyrene is poly(1-phenylethylene) and that for polytetrafluoroethylene

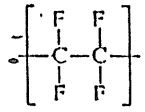

is poly(difluoromethylene) — a polymer more typically recognized by its trademark, Teflon™.

TABLE 1.5 SCHEME FOR NAMING COPOLYMERS

Type	Connective	Example
Unspecified	*-co-*	Poly[styrene-*co*-(methyl methacrylate)]
Statistical[a]	*-stat-*	Poly(styrene-*stat*-butadiene)
Random	*-ran-*	Poly[ethylene-*ran*-(vinyl acetate)]
Alternating	*-alt-*	Poly[styrene-*alt*-(maleic anhydride)]
Block	*-block-*	Polystyrene-*block*-polybutadiene
Graft	*-graft-*	Polybutadiene-*graft*-polystyrene

[a] A statistical polymer is one in which the sequential distribution of the monomeric units obeys statistical laws. In the case of a random copolymer, the probability of finding a given monomeric unit at any site in the chain is independent of the neighboring units in that position.

For convenience, several societies have developed a very useful set of two-, three-, and four-letter abbreviations for the names of many common thermoplastics, thermosets, fibers, elastomers, and additives. Sometimes, abbreviations adopted by different societies for the same polymer may vary, but there is widespread agreement on the abbreviations for a large number of important polymers. These abbreviations are quite convenient and widely used. As examples, PS is generally

recognized as the abbreviation for polystyrene, PVC for poly(vinyl chloride), PMMA for poly(methyl methacrylate), and PTFE for polytetrafluoroethylene. A listing of commonly accepted abbreviations is given in Appendix A at the end of this book.

Following IUPAC recommendations, copolymers are named by incorporating an italicized connective term between the names of monomers contained within parentheses or brackets or between two or more polymer names. The connective term designates the type of copolymer as indicated for six important classes of copolymers in Table 1.5.

1.3 MOLECULAR WEIGHT

1.3.1 Molecular-Weight Distribution

A typical synthetic polymer sample contains chains with a wide distribution of chain lengths. This distribution is seldom symmetric and contains some molecules of very high molecular weight. An illustration of a representative distribution is shown in Figure 1.8. The exact breadth of the molecular-weight distribution depends upon the specific conditions of polymerization, as will be described in Chapter 2. For example, the polymerization of some polyolefins results in a molecular-weight distribution that is extremely broad, while it is possible to polymerize some polymers, such as polystyrene, with nearly monodisperse distributions under laboratory conditions. Therefore, it is necessary to define an *average* molecular weight to characterize an individual polymer sample as detailed in the following section.

1.3.2 Molecular-Weight Averages

For a discrete distribution of molecular weights, an average molecular weight, $\overline{M}$, may be defined as

$$\overline{M} = \frac{\sum_i N_i M_i^{\alpha}}{\sum_i N_i M_i^{\alpha-1}} \tag{1.1}$$

where N_i indicates the number of moles of molecules with a molecular weight of M_i and the parameter α is a weighting factor that defines a particular average of the molecular-weight distribution. The weight, W_i, of molecules with molecular weight M_i is then

$$W_i = N_i M_i. \tag{1.2}$$

are the number average, $\overline{M}_n$ ($\alpha = 1$), the weight average, $\overline{M}_w$ ($\alpha = 2$), and the z average, $\overline{M}_z$ ($\alpha = 3$).

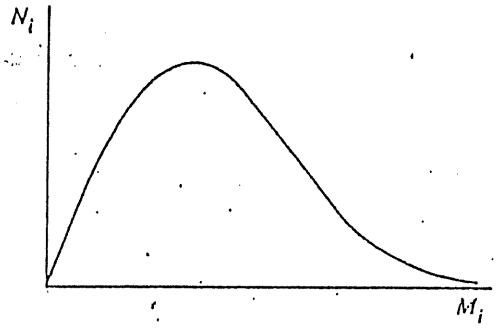

Figure 1.8. A typical distribution of molecular weights shown as a plot of the number of moles of chains, N_i, having molecular weight M_i, against M_i.

Since the molecular-weight distribution of commercial polymers is normally a continuous function, the molecular-weight averages can be determined by integration if the mathematical form of the molecular-weight distribution (i.e., N as a function of M) is known. For example, the number-average molecular weight would be given for discrete and continuous distributions, respectively, as

$$\overline{M}_n = \frac{\sum_{i=1}^{N} N_i M_i}{\sum_{i=1}^{N} N_i}, \tag{1.3a}$$

where N is the total number of polymer species in the distribution, and

$$\overline{M}_n = \frac{\int_0^M NM\,dM}{\int_0^M N\,dM}. \tag{1.3b}$$

The corresponding relationships for the weight-average molecular weight are given as

$$\overline{M}_w = \frac{\sum_{i=1}^{N} N_i M_i^2}{\sum_{i=1}^{N} N_i M_i} \tag{1.4a}$$

and

$$\overline{M}_w = \frac{\int_0^M NM^2 dM}{\int_0^M NM dM}. \tag{1.4b}$$

In the case of high-molecular-weight polymers, the number-average molecular weight is directly determined by membrane osmometry, while the weight-average molecular weight is determined by light scattering and other scattering techniques as will be discussed in Chapter 3.

A measure of the breadth of the molecular-weight distribution is given by the ratios of molecular-weight averages. For this purpose, the most commonly used ratio is $\overline{M}_w/\overline{M}_n$, which is called the *polydispersity index* or PDI. The PDIs of commercial polymers vary widely. For example, commercial grades of polystyrene with a $\overline{M}_n$ of over 100,000 have polydispersities indices between 2 and 5, while polyethylene synthesized in the presence of a stereospecific catalyst may have a PDI as high as 30. In contrast, the PDI of some vinyl polymers prepared by "living" polymerization (see Chapter 2) can be as low as 1.06. Such polymers with nearly monodisperse molecular-weight distributions are useful as molecular-weight standards for the determination of molecular weights and molecular-weight distributions of commercial polymers (see Section 3.3).

1.4 CHEMICAL STRUCTURE AND THERMAL TRANSITIONS

As the previous discussion has shown, many important synthetic polymers such as polystyrene and poly(methyl methacrylate) consist of long, flexible chains of very high molecular weight. In many cases, individual chains are randomly coiled and intertwined with no molecular order or structure. Such a physical state is termed *amorphous*. Commercial-grade (atactic) polystyrene and poly(methyl methacrylate) are examples of polymers that are amorphous in the solid state. Below a certain temperature called the glass-transition temperature (T_g), long-range, cooperative motions of individual chains cannot occur; however, short-range motions involving several contiguous groups along the chain backbone or substituent group are possible. Such motions are called *secondary-relaxation* processes and can occur at temperatures as low as 70 K. By comparison, glass-transition temperatures vary from 150 K for polymers with very flexible chains such as polydimethylsiloxane

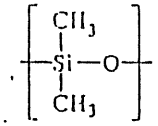

to well over 600 K for those with highly rigid aromatic backbones such as the high-modulus fiber, poly[2,2'-(*m*-phenylene)-5,5'-bibenzimidazole] (PBI)

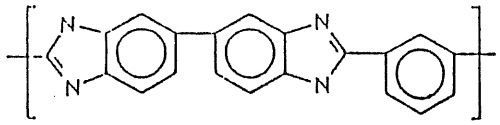

with a T_g reported in the range from 700 to 773 K.

Polymer chains with very regular structures, such as linear polyethylene and isotactic polypropylene, can be arranged in highly-regular structures called crystallites. Each crystallite consists of rows of folded chains. Since sufficient thermal energy is needed to provide the necessary molecular mobility for the chain-folding process, crystallization can occur only at temperatures above T_g. If the temperature is too high, chain folds become unstable and high thermal energy disorders the crystallites — a crystalline–amorphous transition occurs. The temperature that marks this transition is called the *crystalline-melting temperature* or T_m. Crystalline melting temperatures can vary from 334 K for simple, flexible-chain polyesters such as polycaprolactone

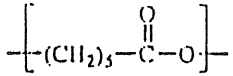

to over 675 K for aromatic polyamides such as poly(*m*-phenylene isophthalamide) (Nomex™).

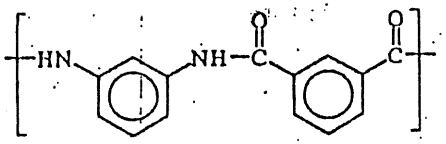

As an approximate rule-of-thumb, T_g is one-half to two-thirds of T_m expressed in absolute temperature (Kelvin). The glass-transition and crystalline-melting temperatures can be determined by a wide range of techniques including measurement of volume (dilatometry), specific heat (calorimetry), and mechanical properties, particularly modulus (dynamic mechanical analysis), as discussed in Chapter 4.

REFERENCES

1. W. H. Carothers, *Chem. Rev.*, 8, 353 (1931).
2. W. V. Metanomski, *Compendium of Macromolecular Nomenclature*, Blackwell Scientific Publications, Oxford, 1991.

GENERAL READING

F. W. Harris, "Introduction to Polymer Chemistry," *J. Chem. Educ.*, 58, 837–843 (1981).

L. Mandelkern, *An Introduction to Macromolecules*, Springer–Verlag, New York, 1983.

H. Morawetz, *Polymers: The Origins and Growth of a Science*, John Wiley & Sons, New York, 1985.

R. B. Seymour, "Polymer Science Before and After 1899: Notable Developments During the Lifetime of Maurits Dekker," *J. Macromol. Sci.–Chem.*, A26, 1023–1032 (1989).

R. B. Seymour and C. E. Carraher, *Giant Molecules*, John Wiley & Sons, New York, 1990.

Problems

1-1. A polydisperse sample of polystyrene is prepared by mixing three *monodisperse* samples in the following proportions:

2 g 50,000 molecular weight
2 g 100,000 molecular weight

Using this information, determine the following: (a) number-average; (b) weight-average; and (c) z-average molecular weight of the mixture.

1-2. A polymer is fractionated and is found to have the molecular-weight distribution shown below. For this continuous distribution, calculate the following: (a) the number-average; (b) the weight-average; and (c) the z-average molecular weight.

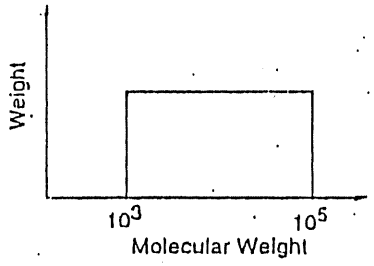

2

The Synthesis of High Polymers

As discussed in Chapter 1, a useful classification of all polymers is based upon the kinetics of the polymerization. In this classification scheme, a *step-growth* polymerization is defined as one that involves a *random* reaction of two molecules that may be any combination of a monomer, oligomer, or a longer-chain molecule. High molecular-weight polymer is formed only near the end of the polymerization when most of the monomer has been depleted. In *chain-growth* polymerization, the only chain-extension reaction is that of attachment of a monomer with an "active" chain. The active end may be a free-radical or ionic site (i.e., anion or cation). In contrast to step-growth polymerization, some high-molecular-weight polymer is formed in the early stages of the chain-growth polymerization.

2.1 STEP-GROWTH POLYMERIZATION

The major classifications of step-growth polymers are given in Table 2.1. Of these, the most important in terms of the size of the commercial market are the aliphatic polyamides or nylons (e.g., nylon-6, nylon-6,6, and nylon-6,10) and polyester [e.g., poly(ethylene terephthalate)]. Specialty or engineering-grade step-growth polymers include polycarbonate (e.g., Lexan™), aromatic polyamides (e.g., Nomex™ and Kevlar™), polyimides (e.g., Kapton™), polysulfones (e.g., Udel™), polyurethanes, and poly(2,6-dimethyl-1,4-phenylene oxide) (PPO™), as discussed in Chapter 10.

TABLE 2.1 CLASSIFICATION OF STEP-GROWTH POLYMERS

Classification	Monomer 1	Monomer 2
Condensation		
Polyamide	Dicarboxylic acid	Diamine
Polycarbonate	Bisphenol	Phosgene
Polyester	Dicarboxylic acid	Diol or polyol
Polyimide	Tetracarboxylic acid	Diamine
Polysulfone	Bisphenol	Dichlorophenylsulfone
Noncondensation		
Polyurethane	Diisocyanate	Diol or polyol
Poly(phenylene oxide)	2,6-Disubstituted phenol	Oxygen

Some examples of commercially-important step-growth polymerizations are illustrated in Figure 2.1. Most step-growth polymerizations involve a classical condensation reaction such as esterification (Figure 2.1A), ester interchange (Figure 2.1B), or amidation (Figure 2.1C). Note that two routes exist for the preparation of the aromatic polyester, poly(ethylene terephthalate) (PET) — polyesterification of terephthalic acid and ethylene glycol (Figure 2.1A) and an ester interchange involving dimethyl terephthalate and ethylene glycol (Figure 2.1B). These polymerizations and the preparation of the aliphatic polyamide, nylon-6,6 (Figure 2.1C), are examples of A–A/B–B step-growth condensation-polymerizations. Each of the two monomers is bifunctional and contains the same functionality at each end (i.e., A or B functional group). For example, PET may be formed (Figure 2.1A) by the polycondensation of a dicarboxylic acid (terephthalic acid) and a diol (ethylene glycol). Alternately, an aliphatic polyester, polycaprolactone, can be formed by the *self-condensation* of ω-hydroxycaproic acid (Figure 2.1D). Since the functional end groups of this acid are different (i.e., a carboxylic acid and a hydroxyl group at opposite ends), this polyesterification is an example of an A–B step-growth polycondensation.

Two *noncondensation*-type step-growth polymerizations are illustrated in Figure 2.2. Figure 2.2A shows the polymerization of a polyurethane prepared by the ionic *addition* of a diol (1,4-butanediol) to a diisocyanate (1,6-hexane diisocyanate). Note that, unlike a condensation polymerization, liberation of a small molecule is not a by-product of this polymerization. Shown in Figure 2.2B is the polymerization of a high-temperature thermoplastic, poly(2,6-dimethyl-1,4-pheny-

A

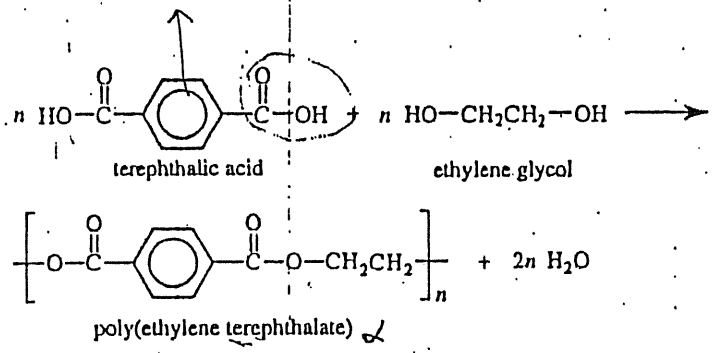

B

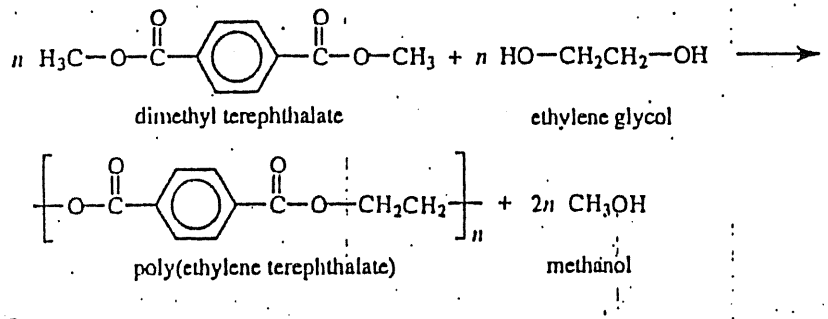

C

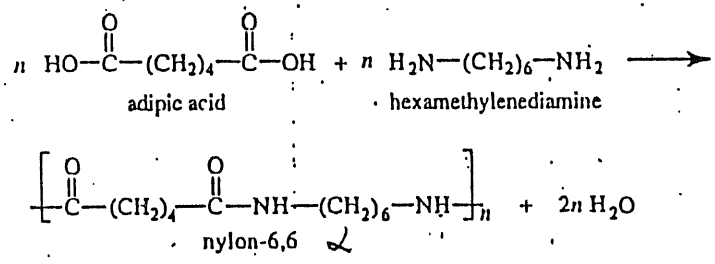

D

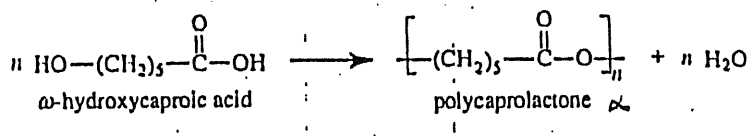

Figure 2.1. Examples of important polycondensations having a step-growth mechanism. A. Polyesterification. B. Ester-interchange polymerization. C. Polyamidation. D. Self-condensation of an A–B monomer.

nism of this polymerization is *free radical*, but the kinetics of this and the previous polymerization are distinctly step growth, which means that high-molecular-weight polymer is obtained only at the end of the polymerization. Normally, the kinetics of a free-radical polymerization are chain growth, as will be described in Section 2.2.

A

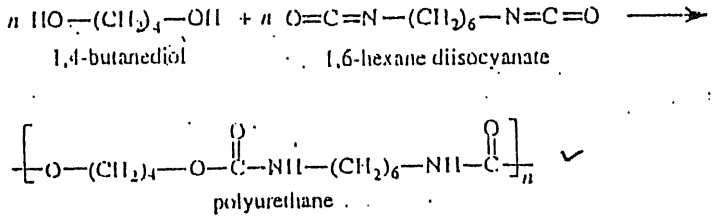

B

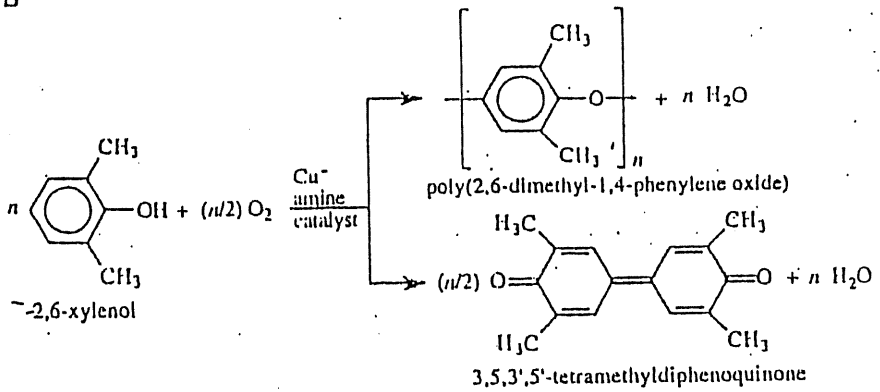

Figure 2.2. Two noncondensation step-growth polymerizations. A. Addition polymerization of a polyurethane. B. Oxidative-coupling polymerization of 2,6-xylenol to yield a high-molecular-weight polymer or a low-molecular-weight quinone as a byproduct.

2.1.1 Molecular Weight in a Step-Growth Polymerization

Polymer molecular-weight in a step-growth polymerization is determined by the fractional conversion, p, of the monomer during the polymerization. One way to express molecular weight is through the *degree of polymerization*, which normally represents the number of repeating units in the polymer chain. Since any polymerization mechanism yields a distribution of molecular weights, it is neces-

sary to define an average degree of polymerization in the same way as average molecular weight was defined earlier (see Section 1.3.2). The average degree of polymerization is designated as $\overline{X}$ or $\overline{DP}$. The most important averages are the number-average ($\overline{X}_n$) and weight-average ($\overline{X}_w$) degrees of polymerization. An equation attributed to Carothers relates the number-average degree of polymerization to fractional monomer-conversion, p, in a step-growth polymerization as[1]

$$\boxed{\overline{X}_n = \frac{1}{1-p}}, \tag{2.1}$$

Similarly, the weight-average degree of polymerization is given as

$$\overline{X}_w = \frac{1+p}{1-p}. \tag{2.2}$$

These equations do not apply to interfacial polycondensations or to the step-growth polymerization of monomers with a functionality greater than 2. Use of eq. 2.1 indicates that, in order to achieve a typical commercial $\overline{X}_n$ of 50, a monomer conversion of 98% ($p = 0.98$) must be obtained; for a $\overline{X}_n$ of 100, the monomer conversion must be 99%. This requirement for high conversion also indicates that a nearly exact stoichiometric-equivalence of monomers is required to obtain high monomer conversion in an A–A/B–B polycondensation. Often, this can be achieved by preparing an intermediate low-molecular-weight salt. Sometimes, a slight excess of one monomer may be used to control molecular weight.

In addition to high conversion, a step-growth polymerization requires high *yield*. High yield means the absence of any side reactions that could deactivate the polymerization process. For example, a carbon–carbon coupling to give a low-molecular-weight quinone derivative is competitive to the carbon–oxygen coupling polymerization of 2,6-xylenol, as was shown in Figure 2.2B. In this case, the yield of the high polymer is determined by the nature of the catalyst system and other polymerization conditions.

High monomer *purity* is also very important in order to obtain high molecular-weight polymer. In A–A/B–B polycondensation, the incorporation of any monomer that is monofunctional (i.e., having a single A or B group) in the growing polymer chain will terminate the polymerization. An example is the use of a monofunctional amine in place of the diamine in the preparation of nylon-6,6

[1] The number-average molecular weight is given as

$$\overline{M}_n = \frac{M_0}{1-p}$$

where M_0 is the molecular weight of a repeating unit.

(Figure 2.1C). Sometimes, a monofunctional monomer may be added during the polymerization process to control molecular weight. Trifunctional monomers can be used to create crosslinked polymers (i.e., thermosets), as will be discussed in Section 9.2.

In summary, high-molecular-weight polymer can be obtained in a step-growth polymerization only if the following conditions are achieved:

- High monomer conversion
- High monomer purity
- High reaction yield
- Stoichiometric equivalence of functional groups (in A–A/B–B polymerization)

2.1.2 Step-Growth Polymerization Kinetics

A step-growth polymerization may be first, second, or third order depending on whether it is an A–B or A–A/B–B type and whether a catalyst is involved. The polymerization rate, R_p, may be expressed as the time rate of change of monomer concentration. For a noncatalyzed A–A/B–B polymerization, this polymerization rate, as defined by the rate of *disappearance* of monomer, is second order in monomer concentration, as given by the expression

$$R_p = -\frac{d[\text{A}-\text{A}]}{dt} = k[\text{A}-\text{A}][\text{B}-\text{B}] \tag{2.3}$$

where k is the polymerization rate constant and the brackets indicate monomer (e.g., A–A or B–B) concentration. Assuming a stoichiometric balance of monomer concentration, eq. 2.3 can be simplified as

$$R_p = -\frac{d[\text{A}-\text{A}]}{dt} = k[\text{A}-\text{A}]^2. \tag{2.4}$$

Integration of eq. 2.4 then gives the relation

$$\frac{1}{[\text{A}-\text{A}]} - \frac{1}{[\text{A}-\text{A}]_0} = kt \tag{2.5}$$

where $[\text{A}-\text{A}]_0$ represents the initial monomer-concentration (i.e., at $t = 0$). The nonpolymerized monomer concentration at any time t is related to the fractional conversion and initial monomer-concentration by

$$[\text{A}-\text{A}] = (1-p)[\text{A}-\text{A}]_0. \tag{2.6}$$

Equation 2.6 can be rearranged for $(1-p)$ and then substituted into the Carothers equation (eq. 2.1). Subsequent rearrangement and substitution of eq. 2.5 gives an

expression for the number-average degree of polymerization as a function of time and initial monomer concentration as

$$\overline{X}_n = [A-A]_o kt + 1. \tag{2.7}$$

2.2 CHAIN-GROWTH POLYMERIZATION

Chain-growth polymerizations require the presence of an initiating molecule that can be used to attach a monomer molecule at the start of the polymerization. The initiating species may be a radical, anion, or cation, as discussed in the following sections. Free-radical, anionic, and cationic chain-growth polymerizations share three common steps — *initiation*, *propagation*, and *termination*. Whether the polymerization of a particular monomer can occur by one or more mechanisms (i.e., free radical, anionic, or cationic) depends, in part, on the chemical nature of the substituent group. Monomers with an *electron-withdrawing* group can polymerize by an anionic pathway, while those with an *electron-donating* group follow a cationic pathway. Some polymers with a resonance-stabilized substituent-group such as a phenyl ring may be polymerized by more than one pathway. For example, polystyrene can be polymerized by both free-radical and anionic methods.

2.2.1 Free-Radical Polymerization and Copolymerization

Like other chain-growth polymerizations, a free-radical polymerization has three principal steps:

- Initiation of the active monomer
- Propagation or growth of the active (free-radical) chain by sequential addition of monomers
- Termination of the active chain to give the final polymer product

These steps and their associated kinetics are described next in general terms for free-radical polymerizations, with the polymerization of styrene given as an example.

Initiation. Initiation in a free-radical polymerization consists of two steps — a *dissociation* of the initiator to form two radical species, followed by addition of a single monomer molecule to the initiating radical (the *association* step). The dissociation of the initiator (I–I) to form two free-radical initiator species (I•) can be represented as

$$\text{I–I} \xrightarrow{k_d} 2\,\text{I}\bullet \tag{2.8}$$

where k_d is the *dissociation rate-constant*. The dissociation rate-constant follows an Arrhenius dependence on temperature given as

$$k_d = A\exp(-E_a/RT) \tag{2.9}$$

where E_a is the *activation energy* for dissociation. In addition to a strong dependence on temperature, dissociation rate-constants for different initiators vary with the nature of the solvent used in solution polymerization, as shown by data given in Table 2.2.

TABLE 2.2 DISSOCIATION RATE-CONSTANTS FOR SOME COMMON INITIATORS IN SOLUTION

Initiator	Solvent	T (°C)	k_d (s^{-1})	E_a (kJ mol^{-1})
Benzoyl peroxide	Benzene	30	4.80×10^{-8}	116
		70	1.38×10^{-5}	
	Toluene	30	4.94×10^{-8}	121
		70	1.10×10^{-5}	
AIBN	Benzene	40	5.44×10^{-7}	128
		70	3.17×10^{-5}	
	Toluene	70	4.0×10^{-5}	121

Initiators for free-radical polymerizations include any organic compound with a labile group, such as an azo (–N=N–), disulfide (–S–S–), or peroxide (–O–O–) compound. The labile bond of the initiator can be broken by heat or irradiation, such as ultraviolet or gamma irradiation. An important example of a free-radical initiator is benzoyl peroxide whose dissociation is

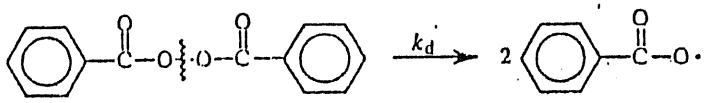

Another important group of free-radical initiators are the azo (R–N=N–R) compounds such as 2,2'-azobis(isobutyronitrile) (AIBN), which thermally decomposes to yield nitrogen and two cyanoisopropyl radicals (R•) as

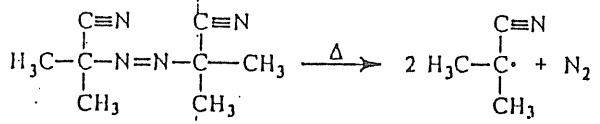

In the second step of initiation (i.e., *association*), a monomer molecule (M) is attached to the initiator radical. This addition step may be represented as

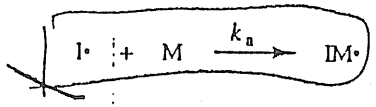

(2.10)

where k_a is the rate constant for monomer association. In the specific case of the polymerization of styrene initiated by benzoyl peroxide, the addition occurs as

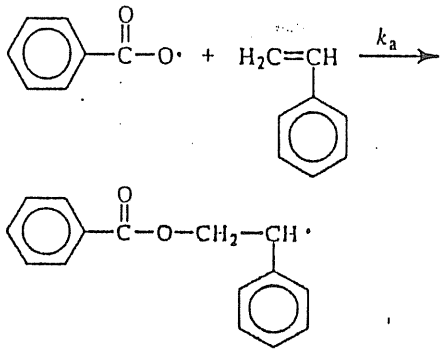

Propagation. In the next step, called *propagation*, additional monomer units are added to the initiated monomer species as

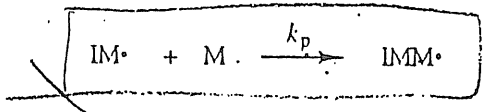

(2.11a)

where k_p is the *propagation rate constant*. For styrene addition with benzoyl peroxide initiation, the first propagation step is

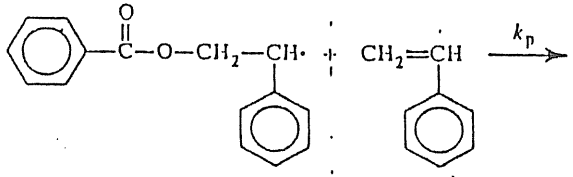

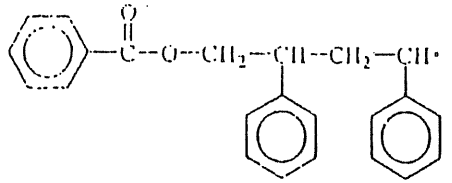

Additional monomers are added sequentially during subsequent propagation steps, as represented in a general way by the equation

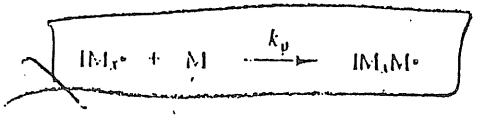

(2.11b)

Termination. Propagation will continue until some termination process occurs. One obvious termination mechanism occurs when two propagating radical chains of arbitrary degrees of polymerization of x and y meet at their free-radical ends. Termination in this manner occurs by *combination* to give a single terminated chain of degree of polymerization $x + y$ through the formation of a covalent bond between the two combining radical chains, as illustrated by the following reaction:

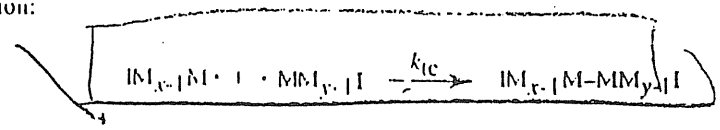

(2.12)

For the example of styrene polymerization, termination by combination gives the following chemical structure:

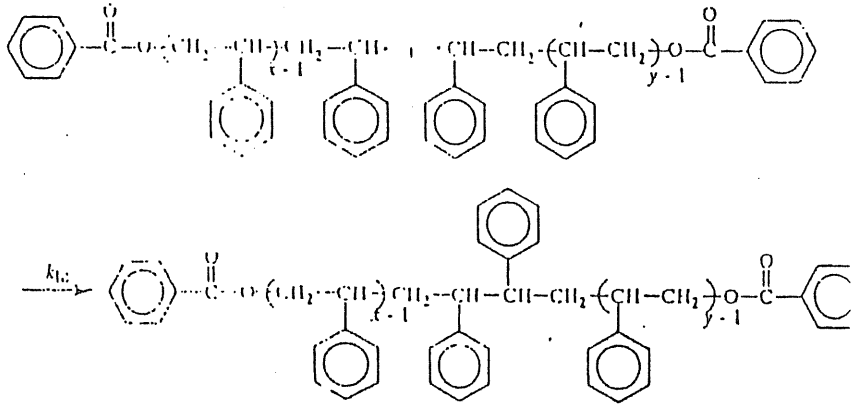

Termination also can occur by a *disproportionation* reaction to give two terminated chains, as illustrated below. In this case, one terminated chain will have an unsaturated carbon group while the other terminated end is fully saturated. In both

cases of termination, one end (i.e., in termination by disproportionation) or both ends (i.e., in termination by combination) contain the initiating free-radical group of the initiator molecule. In the case of termination by combination, the benzoyl peroxide group caps *both* ends of the chain. This indicates the important difference between a true initiator, which becomes incorporated in the terminated chain, and a polymerization *catalyst*, which promotes the polymerization but is fully recovered at the end of the polymerization. Catalysts are used in cationic and coordination polymerizations as discussed in Section 2.2.2.

$$\mathrm{IM}_{x-1}\mathrm{M}\cdot + \cdot\mathrm{M}\mathrm{M}_{y-1}\mathrm{I} \xrightarrow{k_{td}} \mathrm{IM}_x + \mathrm{IM}_y \qquad (2.13)$$

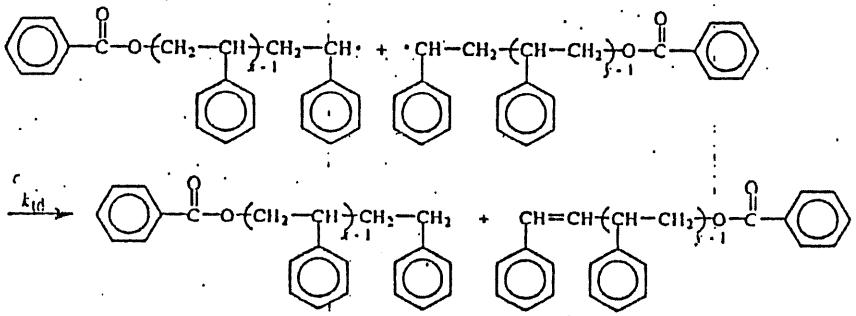

In addition to termination by combination and disproportionation, another mechanism of termination is *chain transfer* by hydrogen abstraction from an initiator, monomer, polymer, or solvent molecule. In general terms, this process may be represented as

$$\mathrm{IM}_{x-1}\mathrm{M}\cdot + \mathrm{SH} \xrightarrow{k_{tr}} \mathrm{IM}_{x-1}\mathrm{MH} + \mathrm{S}\cdot \qquad (2.14)$$

where SH represents a solvent or any other molecule with an abstractable hydrogen atom. In the specific case of the benzoyl peroxide-initiated polymerization of styrene, termination by chain transfer occurs as

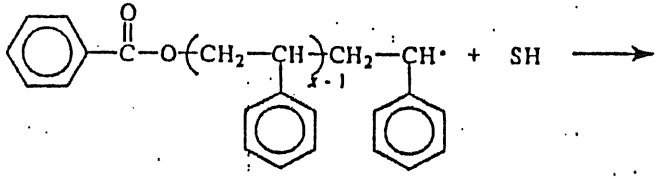

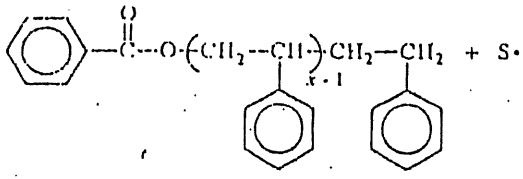

As illustrated, the radical site is transferred to the chain-transfer agent (S•), which can then add monomer units to continue the polymerization process. The terminated chain resulting from chain transfer then will have one (i.e., termination by disproportionation) or two (i.e., termination by combination) chain-transfer moieties at the polymer ends.

Examples of propagation and termination rate constants are given in Table 2.3. Both k_p and k_t show a strong (Arrhenius) dependence upon temperature, as illustrated by data for styrene. Rate constants can vary by several orders of magnitude depending on monomer type (i.e., vary with the chemical nature of the substituent group in vinyl polymerization).

TABLE 2.3 REPRESENTATIVE VALUES OF PROPAGATION (k_p) AND TERMINATION (k_t) RATE CONSTANTS

Monomer	T (°C)	k_p, L (mol·s)$^{-1}$	k_t, L (mol·s)$^{-1}$ × 10^{-6}
Styrene	25	44	48
	30	55	51
	60	176	72
Vinyl acetate	25	1012	59
Vinyl chloride	25	3130	2300
Vinylidene chloride	25	8.6	0.175
Acrylonitrile	25	52	5
Ethylene[a]	83	470	1050
Methyl methacrylate	40	513	47

[a] Polymerization in benzene.

Free-Radical Polymerization Kinetics. The overall rate of polymerization (R_o) in a free-radical polymerization is simply the rate of chain propagation (R_p), which is obtained from eq. 2.11b as

$$R_o \equiv R_p = k_p[\mathrm{IM}_x\cdot][\mathrm{M}]. \qquad (2.15)$$

This statement makes the assumption that all steps, including the first, in the propagation step have equal reactivity. Compared to step-growth polymerization, the propagation rate for free-radical polymerization is very rapid. Under typical conditions, a polymer having molecular weight of 10 million can be formed in only 0.1 s.

One problem with the use of eq. 2.15 to determine the polymerization rate is that the radical concentration, $[IM_x^\bullet]$, normally is not known. To overcome this difficulty, the radical concentration can be related to more easily-determined concentrations (i.e., monomer and initiator concentrations) by assuming that the total radical population obtains a *steady-state* concentration over most of the polymerization process. Since radicals are formed in the initiation step and consumed in the termination step, the steady-state condition can be expressed as

$$R_i \equiv R_t \,. \tag{2.16}$$

As described previously, the initiation process involves two separate steps — initiator dissociation and monomer association. *The overall rate of initiation is, therefore, controlled by the slower step, which is the dissociation of the initiator.* The rate of initiation, expressed as the time rate of increase in radical-initiator concentration, is then obtained from the dissociation expression (eq. 2.8) as

$$R_i = \frac{d[I^\bullet]}{dt} = 2k_d[I] \tag{2.17a}$$

where [I] is used to represent the initiator (I–I) concentration. The factor of 2 appearing on the RHS of eq. 2.17a is due to the fact that *two* radicals are produced in each dissociation step. In order to obtain an expression for the rate of polymerization, it is necessary to consider only those initiator radicals that add monomer and, therefore, contribute to chain propagation. Some initiator radicals may recombine with other radicals (e.g., initiator and monomer radical groups) or partially decompose into noninitiating products. For these reasons, only some fraction, f, of the original initiator concentration is effective in contributing to the polymerization process. Typical initiator efficiencies fall in the range from 0.3 to 0.8 (e.g., $f \sim 0.6$ for AIBN over a wide range of monomer concentration). The fraction of effective initiator-radicals can then be introduced in the rate expression (eq. 2.17a) to give

$$R_i = \frac{d[I^\bullet]}{dt} = 2fk_d[I]. \tag{2.17b}$$

In a similar fashion, the rate of termination is the time-rate of decrease in radical concentration (i.e., the propagating radical-chain) resulting from all operative termination steps — combination (eq. 2.12), dissociation (eq. 2.13), and/or chain transfer (eq. 2.14). For the moment, it is convenient to consider only termination

by combination and disproportionation and leave termination by chain transfer for later treatment. Without any loss in generality, termination by both combination and disproportionation can be expressed as

$$IM_x^\bullet + IM_x^\bullet \xrightarrow{k_t} P \tag{2.18}$$

where P represents the *deactivated* polymer and the termination rate constant, k_t, is the sum of the individual termination rate-constants of combination and disproportionation (i.e., $k_t = k_{tc} + k_{td}$). Therefore, the termination rate equation can be written for the reaction given in eq. 2.18 as

$$R_t = -\frac{d[IM_x^\bullet]}{dt} = 2k_t[IM_x^\bullet]^2. \tag{2.19}$$

The factor of 2 arises because two radicals are consumed in each termination step.

Applying the steady-state assumption (eq. 2.16) by equating eqs. 2.17b and 2.19 gives the expression for the radical concentration as

$$[IM_x^\bullet] = \left(\frac{fk_d}{k_t}\right)^{1/2}[I]^{1/2}. \tag{2.20}$$

Finally, substitution of eq. 2.20 into the polymerization rate equation (eq. 2.15) gives the final important result:

$$\boxed{R_p = k_p\left(\frac{fk_d}{k_t}\right)^{1/2}[I]^{1/2}[M]}. \tag{2.21}$$

Equation 2.21 shows that the polymerization rate in free-radical polymerization is proportional to monomer concentration and to the square-root of initiator concentration.†

† It is important to recognize that eq. 2.21 gives the polymerization rate at some arbitrary time t when the initiator and monomer concentrations are [I] and [M] at that time. These concentrations differ from their initial concentrations, $[I]_0$ and $[M]_0$, which are known at the beginning of the polymerization. The relationships between [I] and $[I]_0$ and between [M] and $[M]_0$ are obtained from the appropriate rate-equations. For example, the initiator concentration is obtained from the rate of dissociation obtained from eq. 2.8 as

$$-\frac{d[I]}{dt} = k_d[I].$$

The number-average degree of polymerization at any time can be obtained from the ratio of the rate of propagation to the rate of termination as†

$$\overline{X}_n = \frac{R_p}{R_t} \tag{2.22}$$

which at steady state is given as

$$\overline{X}_n = \frac{k_p[M]}{2(k_t f k_d[I])^{1/2}} \tag{2.23}$$

In the above derivations, we have considered only termination by combination and disproportionation. If termination by chain transfer can also occur, the degree of polymerization equation (eq. 2.22) must be modified to include this contribution to the termination rate. As the chain-transfer process increases the overall rate of termination, it is clear from eq. 2.22 that the degree of polymerization, therefore, should decrease. We can write the number-average degree of polymerization in the case of termination by all three termination mechanisms as

$$\overline{X}_n = \frac{R_p}{R_{tc} + R_{td} + R_{tr}} \tag{2.24}$$

where R_{tr} is the rate of termination by chain transfer obtained from eq. 2.14 as

$$R_{tr} = k_{tr}[\mathrm{IM}_x\cdot][\mathrm{SH}]. \tag{2.25}$$

Rearrangement and integration of the above equation from $t = 0$ to time t gives

$$[I] = [I]_0 \exp(-k_d t).$$

Similarly, monomer concentration is obtained from the propagation step (eq 2.11b) as

$$-\frac{d[M]}{dt} = k_p[\mathrm{IM}_x\cdot][M]$$

which upon integration gives

$$[M] = [M]_0 \exp\left(-k_p[\mathrm{IM}_x\cdot]t\right).$$

† Alternately, a *kinetic chain length*, ν, may be defined as the average number of steps of growth per effective radical given as the ratios of the propagation and initiation rates as $\nu = R_p/R_i$.

Rearrangement of eq. 2.24 and substitution of the rate equation for R_{tr} (eq. 2.25) and that for R_p (eq. 2.15) gives

$$\frac{1}{\overline{X}_n} = \frac{1}{(\overline{X}_n)_0} + C\left(\frac{[\mathrm{SH}]}{[M]}\right) \tag{2.26}$$

where $(\overline{X}_n)_0$ is the degree of polymerization in the absence of chain transfer (i.e., eq. 2.22) and C is the *chain-transfer coefficient* given as

$$C = \frac{k_{tr}}{k_p}. \tag{2.27}$$

Representative values of chain-transfer constants for several common monomers and chain-transfer agents (i.e., initiator, monomer, polymer, solvent, or additive) are given in Table 2.4.

TABLE 2.4 REPRESENTATIVE VALUES OF CHAIN-TRANSFER CONSTANTS

Monomer	Chain-Transfer Agent	T (°C)	$C \times 10^4$
Styrene	Styrene	25	0.279
		50	0.35–0.78
	Polystyrene	50	1.9–16.6
	Benzoyl peroxide	50	0.13
	Toluene	60	0.125
Methyl methacrylate	Methyl methacrylate	30	0.117
		70	0.2
	Poly(methyl methacrylate)	50	0.22–1000
	Benzoyl peroxide	50	0.01
	Toluene	60	0.170

Thermodynamics of Free-Radical Polymerization. The (Gibbs) free energy of polymerization, ΔG_p, is given by the first and second laws of thermodynamics for a reversible process as

$$\Delta G_p = \Delta H_p - T\Delta S_p \tag{2.28}$$

where ΔH_p is called the *heat of polymerization* defined as

$$\Delta H_p = E_p - E_{dp} \tag{2.29}$$

and E_p and E_{dp} are the activation energies for propagation (i.e., polymerization)[1] and depolymerization, respectively. Both ΔH_p and ΔS_p are negative and, therefore, ΔG_p also will be negative (i.e., polymerization is favored) at low temperatures. As temperature increases, ΔG_p becomes less negative (i.e., less favorable). At some temperature, called the *ceiling temperature* (T_c), the polymerization reaches equilibrium. In other words, the rates of polymerization and depolymerization become equal and

$$\Delta G_p = 0. \tag{2.30}$$

The ceiling temperature is then defined as

$$\boxed{T_c = \frac{\Delta H_p}{\Delta S_p}}. \tag{2.31}$$

Representative values of ΔH_p and T_c for some common monomers are given in Table 2.5.

TABLE 2.5 HEATS OF POLYMERIZATION AND CEILING TEMPERATURES FOR SOME COMMON MONOMERS

Monomer	ΔH_p kJ mol^{-1}	T_c (°C)
α-Methylstyrene	-35.2	61
Methyl methacrylate	-54.5	220
Propylene	-69.1	300
Styrene	-68.7	310
Ethylene	-93.8	400

Free-Radical Copolymerization. In a free-radical copolymerization involving two monomers, four separate propagation steps are possible, as illustrated in Figure 2.3. Each propagation step has its own rate constant k_{ij}, where the first subscript, i, identifies the monomer at the end of the propagating chain (i.e., $\sim\!\sim M_i \cdot$) prior to addition of monomer j. The rates of disappearance of monomers M_1 and M_2 can be obtained by considering the individual steps by which M_1 (see propagation steps A and C) and M_2 (see propagation steps B and D) are consumed. The rate equations are, therefore, given as

$$\frac{-d[M_1]}{dt} = k_{11}[\sim\!\sim M_1 \cdot][M_1] + k_{21}[\sim\!\sim M_2 \cdot][M_1] \tag{2.32}$$

and

$$\frac{-d[M_2]}{dt} = k_{12}[\sim\!\sim M_1 \cdot][M_2] + k_{22}[\sim\!\sim M_2 \cdot][M_2]. \tag{2.33}$$

In the case of a terpolymerization (three monomers), the number of propagation steps would increase from four to nine and there would be *three* rate-equations to consider.

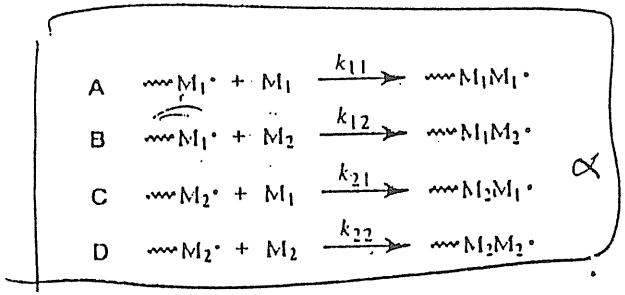

Figure 2.3. The four propagation steps that can occur during a free-radical copolymerization.

During a copolymerization, it is important to be able to predict how copolymer composition varies as a function of comonomer reactivity and concentration at any time. The approach used relies on the realization that monomer consumed during the copolymerization becomes incorporated into the copolymer structure and, therefore, any relative change in the composition of the comonomer mixture reflects the composition of the copolymer formed at that instance of time. The relative change in the comonomer composition is given by the *instantaneous copolymerization equation*, which is obtained by dividing eq. 2.32 by eq. 2.33 to give

$$\frac{d[M_1]}{d[M_2]} = \frac{[M_1]}{[M_2]} \frac{k_{11}[\sim\!\sim M_1 \cdot] + k_{21}[\sim\!\sim M_2 \cdot]}{k_{12}[\sim\!\sim M_1 \cdot] + k_{22}[\sim\!\sim M_2 \cdot]} \tag{2.34}$$

[1] $k_p = A\exp(-E_p/RT)$.

Equation 2.34 can be expressed in a more concise and useful form by defining a monomer *reactivity ratio*. The reactivity ratios for monomers 1 and 2 are defined as

$$r_1 = \frac{k_{11}}{k_{12}} \tag{2.35a}$$

and

$$r_2 = \frac{k_{22}}{k_{21}}. \tag{2.35b}$$

These expressions indicate that the reactivity ratio for monomer 1 (r_1) is simply the ratio of propagation rate-constants for the addition of M_1 (i.e., homopolymerization) and addition of M_2 (i.e., copolymerization) to a propagating radical-chain with monomer 1 at the radical end ($\sim\sim M_1\cdot$). Similarly, the reactivity ratio for monomer 2 is the ratio of propagation rate-constants for the addition of M_2 (i.e., homopolymerization) and addition of M_1 (i.e., copolymerization) to a propagating radical-chain with monomer 2 at the radical end ($\sim\sim M_2\cdot$). From the definitions of reactivity ratios (eqs. 2.35a and 2.35b), it should be clear that, when both reactivity ratios equal unity, there is no preferential monomer incorporation into the propagating chain (i.e., $k_{11} = k_{12}$ and $k_{22} = k_{21}$). This means that the monomer sequence in the resulting copolymer is completely *random*. An example of a nearly random or "ideal" copolymerization is that of styrene and 4-chlorostyrene (see Problem 2–4). When both reactivity ratios are zero (i.e., $k_{11} = k_{22} = 0$), the monomer sequence will be perfectly *alternating*, as is nearly the case for the copolymerization of styrene and maleic anhydride. If both reactivity ratios are small but not exactly zero, the comonomer sequence will be highly alternating with some random placement, as in the case of the commercially-important copolymers of styrene and acrylonitrile. On the other hand, when *both* reactivity ratios are very much larger than unity (i.e., $k_{ii} >> k_{ij}$), only homopolymers or block copolymers will form.

Reactivity ratios have been determined for many important combinations of monomers and have been tabulated in several reference sources, such as the *Polymer Handbook*.[1] Some representative values are given in Table 2.6. Reactivity ratios for less common monomer-pairs can be calculated by means of the Q-e scheme proposed by Alfrey and Price.[2] In this approach, the propagation rate-constant, k_{ij}, is defined as

$$k_{ij} = P_i Q_j \exp\left(-e_i e_j\right) \tag{2.36}$$

where P_i is a proportionality constant, Q_j is a measure of the monomer reactivity, and e is the polarity of the radical $M_1\cdot$ or $M_2\cdot$. It then follows from the definition of the reactivity ratios (eqs. 2.35a and 2.35b) that

$$r_1 = \frac{k_{11}}{k_{12}} = \left(\frac{Q_1}{Q_2}\right)\exp\left[-e_1\left(e_1 - e_2\right)\right] \tag{2.37a}$$

and

$$r_2 = \frac{k_{22}}{k_{21}} = \left(\frac{Q_2}{Q_1}\right)\exp\left[-e_2\left(e_2 - e_1\right)\right]. \tag{2.37b}$$

TABLE 2.6 EXAMPLES OF REACTIVITY RATIOS FOR FREE-RADICAL COPOLYMERIZATION

Monomer 1	Monomer 2	r_1	r_2
Ethylene	Vinyl acetate	0.130	1.230
	Carbon monoxide	0.025	0.004
	Propylene	3.200	0.620
Styrene	Acrylonitrile	0.290	0.020
	Butadiene	0.820	1.380
	Divinylbenzene	0.260	1.180
	Maleic anhydride	0.097	0.001
	Methyl methacrylate	0.585	0.478
	4-Chlorostyrene	0.816	1.062
	Vinylidene chloride	1.700	0.110
Vinyl chloride	Vinylidene chloride	0.205	3.068

Values of Q and e also have been tabulated for many monomers.[1] Table 2.7 gives values for some commercially-important monomers. In the case of styrene, the most common comonomer, the values of Q and e are 1.0 and -0.8, respectively. In general, the value of a reactivity ratio is independent of the nature of the initiator and solvent in a free-radical copolymerization; however, there is a weak temperature dependence.

TABLE 2.7 Q-e VALUES FOR FREE-RADICAL COPOLYMERIZATION

Monomer	Q	e
Acrylamide	0.23	0.54
Acrylonitrile	0.48	1.23
Butadiene	1.70	-0.50
Ethylene	0.016	0.05
Isobutylene	0.023	-1.20
Isoprene	1.99	-0.55
Maleic anhydride	0.86	3.69
Methacrylic acid	0.98	0.62
Methyl methacrylate	0.78	0.40
N-Vinyl pyrrolidone	0.088	-1.62
Styrene	1.00	-0.80
Vinyl acetate	0.026	-0.88
Vinyl chloride	0.056	0.16
Vinylidene chloride	0.31	0.34

A limitation of the copolymerization equation as written in eq. 2.34 is the use of radical-chain concentrations, which are usually not known or easily measured. By using the definitions of reactivity ratios and by assuming a steady-state radical-concentration for either $\sim\sim M_1\cdot$ and $\sim\sim M_2\cdot$ during propagation, the instantaneous copolymerization equation (eq. 2.33), as first derived by Mayo and Lewis,[3] becomes

$$\boxed{\frac{d[M_1]}{d[M_2]} = \frac{[M_1]}{[M_2]}\left(\frac{r_1[M_1]+[M_2]}{[M_1]+r_2[M_2]}\right)} \qquad (2.38)$$

Since the relative rate of monomer disappearance is equal to the relative rate of monomer incorporation, eq. 2.38 can be used to estimate copolymer composition when the reactivity ratios are known. Conversely, knowledge of monomer concentration and determination of the copolymer composition can be used to obtain experimental values for the reactivity ratios.

The copolymerization equation (eq. 2.38) may be recast in an alternative form that is useful for calculating the instantaneous copolymer composition for a given monomer concentration. For this purpose, the mole fraction of monomer 1 in the monomer mixture is defined as

$$f_1 = \frac{[M_1]}{[M_1]+[M_2]} \qquad (2.39)$$

where $f_1 + f_2 = 1$. In a similar fashion, the mole fraction of monomer 1, F_1, in the copolymer is given by the relative differential change in monomer concentration as

$$F_1 = \frac{d[M_1]}{d[M_1]+d[M_2]} \qquad (2.40)$$

where $F_1 + F_2 = 1$. If the numerator and denominator of eq. 2.40 are each divided by $d[M_2]$, use of eqs. 2.38 and 2.39 give the following useful relationship:

$$\boxed{F_1 = \frac{r_1 f_1^2 + f_1 f_2}{r_1 f_1^2 + 2 f_1 f_2 + r_2 f_2^2}} \qquad (2.41)$$

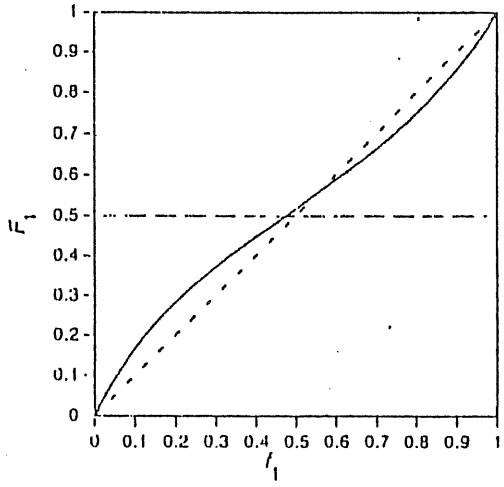

Figure 2.4. Plot of mole fraction of monomer 1 in copolymer, F_1, versus mole fraction of monomer 1 in the feed, f_1, for (---) ideal ($r_1 = r_2 = 1$), (–·–) alternating ($r_1 = r_2 = 0$), and (—) partially alternating copolymerization (copolymerization of styrene and methyl methacrylate, where $r_1 = 0.585$ and $r_2 = 0.478$).

An illustration of several possible relationships between f_1 and F_1 is given by Figure 2.4. Use of eq. 2.41 indicates that $F_1 = f_1$ when $r_1 = r_2 = 1$. This is the

iting case of *ideal* or random copolymerization illustrated by the dashed line in Figure 2.4. Inspection of eq. 2.41 also indicates that $F_1 = 0.5$ when $r_1 = r_2 = 0$. This indicates that the copolymer sequence is always *alternating* and is, therefore, *independent of the comonomer concentration of the feed*, as indicated by the broken line in Figure 2.4. An example of a copolymerization that is preferentially, but not perfectly, alternating — the copolymerization of styrene and methyl methacrylate — is represented by the curve in Figure 2.4. In such cases, which are neither ideal (i.e., random) or perfectly alternating, the most reactive monomer will be preferentially consumed. This means that the monomer feed composition will change (i.e., drift) with time. If this drift is appreciable, the product copolymer obtained at high monomer conversion will be a heterogeneous mixture of individual copolymers having different compositions. This heterogeneity can lead to undesirable properties such as low mechanical strength due to phase separation in the solid state. To avoid significant drift, copolymerization conversion can be kept low. Unfortunately, low conversion results in high costs for copolymer recovery. In commercial practice, the more rapidly depleted monomer is continuously added to the copolymerization mixture to maintain constant feed-composition.

2.2.2 Ionic Polymerization and Copolymerization

Ionic polymerizations follow the same basic steps as free-radical chain-growth polymerization (i.e., initiation, propagation, and termination); however, there are some important differences, as will be discussed in the following sections. Either a carbanion ($C^{\ominus}$) or carbonium ($C^{\oplus}$) ionic site can be formed in the initiation process. Polymerization of vinyl monomers with an electron-withdrawing group can proceed by an anionic pathway, while monomers with an electron-donating group (e.g., methyl) can polymerize by a cationic mechanism.

Anionic Polymerization. The initiator in an anionic polymerization may be any strong nucleophile, including Grignard reagents[†] and other organometallic compounds like *n*-butyl (n-C_4H_9) lithium. As an example, the anionic initiation of styrene is illustrated next:

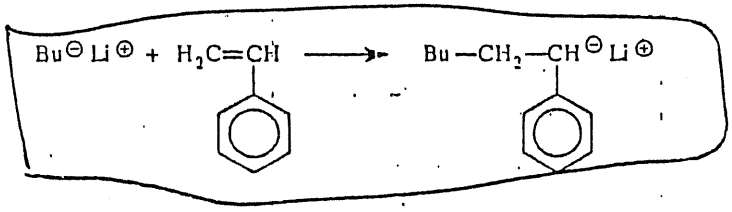

During the initiation process, the addition of the butyl anion to styrene produces a carbanion at the head end in association with the positively-charged lithium *counter-ion*. The chain propagates by insertion of additional styrene monomers between the carbanion and counterion.

If the starting reagents are pure and if the polymerization reactor is purged of all oxygen and traces of water, propagation can proceed indefinitely or until all monomer is consumed. For this reason, anionic polymerization is sometimes called "living" polymerization. In this case, termination occurs only by the deliberate introduction of oxygen, carbon dioxide, methanol, or water as follows:

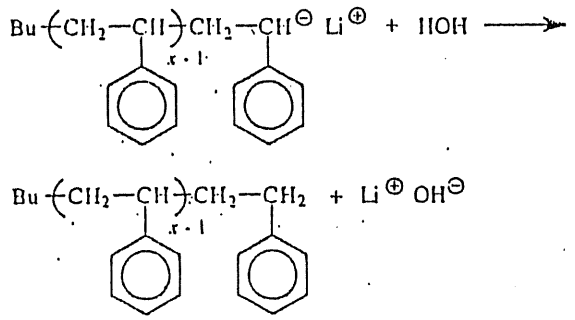

Note that the initiating species in this example (n-C_4H_9) has been incorporated as an end group of the terminated polymer-chain. This illustrates the role of butyllithium as a true initiator — rather than a catalyst — as was also the case for benzoyl peroxide in the free-radical polymerization of styrene.

In the absence of a termination mechanism, each monomer in an anionic polymerization has an equal probability of attaching to an anion site. Therefore, the number-average degree of polymerization, $\overline{X}_n$, is simply equal to the ratio of initial monomer to initial initiator concentration as

$$\boxed{\overline{X}_n = \frac{[M]_o}{[I]_o}} \qquad (2.42)$$

The absence of termination during a living polymerization leads to a very narrow molecular-weight distribution with polydispersities (see Section 1.3.2) as low as 1.06. By comparison, polydispersities above 2 and as high as 20 are typical in free-radical polymerization.

Cationic Polymerization. Unlike free-radical and anionic polymerizations, initiation in cationic polymerization employs a true catalyst that is restored at the end of the polymerization and does not become incorporated into the terminated polymer-chain. Any strong Lewis acid[†] like boron trifluoride (BF_3) can be

[†] The chemical formula of a Grignard reagent can be given as RMgX, where R is an alkyl, aryl, or other organic group and X is a halogen, especially Cl, Br, or I.

[†] A Lewis acid is formally defined as an electron acceptor such as H^+, BF_3, or $AlCl_3$.

used as a catalyst. In this case, a *cocatalyst* (e.g., water) is required to provide the actual proton source. Cationic initiation is illustrated next for the commercially important example of isobutylene polymerization.

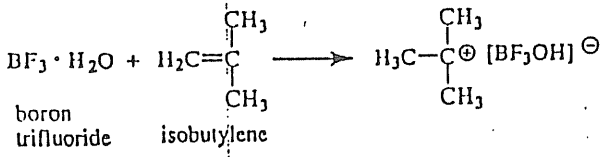

In the above case, proton addition yields an isobutylene *carbonium* ion that forms an association with a $BF_3 \cdot OH$ counterion or *gegen* ion. The carbonium ion can then add to the double bond of another isobutylene molecule during propagation, as follows:

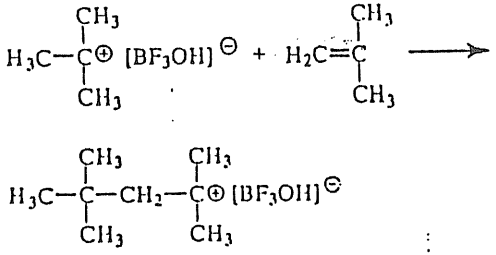

Unlike the case of free-radical polymerization, termination by combination of two cationic polymer chains cannot occur. In certain cationic polymerizations, a distinct termination step may not take place (i.e., "living" cationic polymerization); however, *chain transfer* to a monomer, polymer, solvent, or counterion can occur. The process of chain transfer to the counterion is

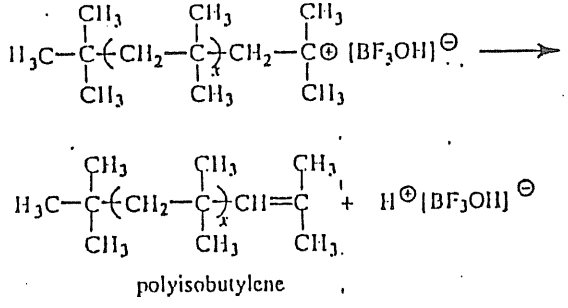

Cationic polymerizations are usually conducted in solution and often at low temperature, typically -80° to -100°C, which provides satisfactory polymerization rates. The choice of solvent for cationic polymerizations is important because of the relation of solvent to the intimate association between cation and counterion. A "tight" association will prevent monomer insertion during propagation. Typically, there is a linear increase in polymer chain-length and an exponential increase in polymerization rate as the dielectric strength of the solvent increases.

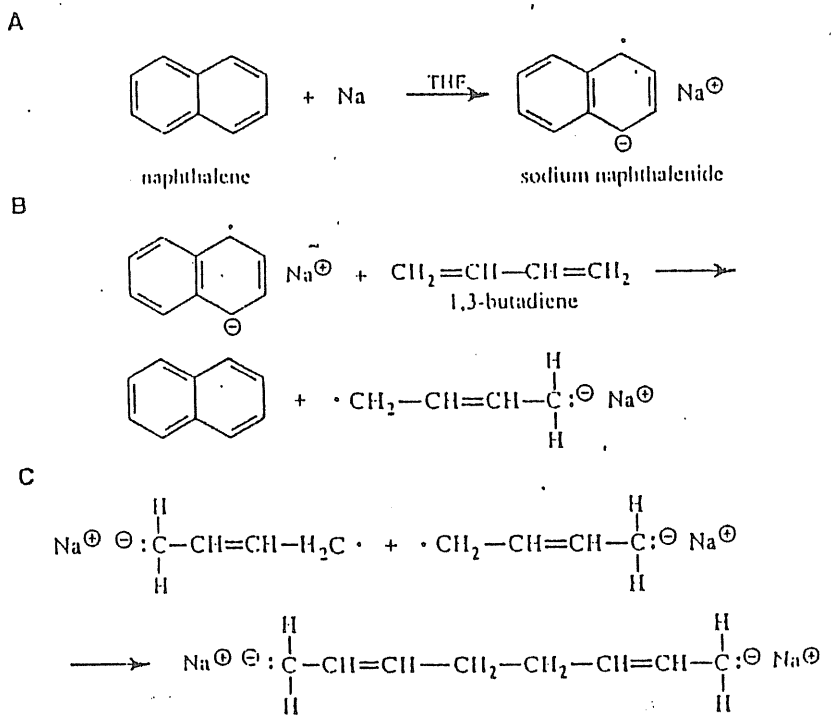

Figure 2.5. Use of sodium naphthalenide in the synthesis of a SBS triblock copolymer. A. Formation of sodium naphthalenide from napthalene and sodium. B. Reaction of sodium naphthalenide with butadiene monomer. C. Combination of radicals to give the dianion available for anionic polymerization at both ends.

Ionic Copolymerization. As in the case of free-radical copolymeriz tion, two or more monomers can be copolymerized by an ionic mechanism. F example, the commercial elastomer of polyisobutylene (butyl rubber) is a copol mer obtained by the cationic copolymerization of isobutylene with 0.5% to 2% isoprene. The comonomer, isoprene, provides unsaturated sites for vulcanizati (see Section 9.1.1).

Another important example of an ionic copolymerization is the triblock copolymer SBS, which has a central block of butadiene with a block of styrene at each end of the chain. This triblock copolymer is an example of a thermoplastic elastomer that is elastic at ambient temperature but can be molded like other thermoplastics at higher temperatures. It can be prepared by adding styrene monomer to an active butadiene chain having anionic sites at both ends (i.e., a butadiene dianion). The dianion is obtained by using an electron-transfer initiator such as sodium naphthalenide prepared by reacting naphthalene with sodium as shown in Figure 2.5A. The naphthalene radical-anion can transfer an electron to the monomer (butadiene) to form a monomer radical-anion, as illustrated in Figure 2.5B. Two radical anions can then combine to give a dimer with carbanion sites at opposite ends, as illustrated in Figure 2.5C. The carbanion sites are then available for addition of more butadiene monomers to obtain a predetermined degree of polymerization. At that point, styrene monomer can be added to form the SBS triblock copolymer.

2.2.3 Coordination Polymerization

One of the earliest and most important groups of thermoplastics is the polyolefins — polyethylene and polypropylene. In 1939, a high-pressure, free-radical process was developed at ICI in England to polymerize ethylene. This polymer had a $-CH_2-CH_2-$ backbone with some short and long alkane branches. Crystallinity was moderate and both thermal and mechanical properties were suitable for film and bottle applications. Today, this particular grade of polyethylene is called low-density polyethylene (LDPE) and is the largest-volume commodity thermoplastic (see Table 1.1). In contrast, free-radical polymerization of propylene yields an amorphous polymer that is a tacky gum at room temperature and has no important commercial use. It was not until the 1954, through the work of Giulio Natta in Italy, that a stereochemical process was developed to polymerize *isotactic* polypropylene (*i*-PP). This form of polypropylene had a level of crystallinity comparable to LDPE and exhibited good mechanical properties over a wide range of temperatures. A process similar to that used in the production of *i*-PP was developed by Karl Ziegler in Germany to polymerize ethylene at substantially lower temperature and pressure than required for free-radical polymerization. This polyethylene — high-density polyethylene (HDPE) — had fewer branches and, therefore, could obtain a higher degree of crystallinity than LDPE. For their work in developing these processes, Ziegler and Natta were awarded the Nobel prize in 1963.

The processes used in the polymerization of both *i*-PP and HDPE employ a novel class of transition-metal catalysts, called Ziegler–Natta catalysts, which utilize a coordination- or insertion-type mechanism during polymerization. In general, a Ziegler–Natta catalyst is a metal–organic complex of a metal cation from groups I–III in the periodic table, such as triethyl aluminum, $Al(C_2H_5)_3$, and a transition metal compound from groups IV–VIII, such as titanium tetrachloride ($TiCl_4$). As an example, linear (i.e., high-density) polyethylene can be prepared by bubbling ethylene into a suspension of $Al(C_2H_5)_3$ and $TiCl_4$ in hexane at room temperature. Polypropylene of nearly 90% isotacticity can be prepared by the polymerization of propylene in the presence of titanium trichloride ($TiCl_3$) and diethylaluminum chloride, $Al(C_2H_5)_2Cl$, at 50°C. Similar catalysts systems can be used to polymerize other α-olefins such as 1-butene ($H_2C=CH-CH_2-CH_3$), geometric isomers of diolefins (e.g., isoprene), and acetylene ($HC\equiv CH$).

Although the exact mechanism of coordination polymerization is still unclear, it is believed that the growing polymer-chain is bound to the metal atom of the catalyst and that monomer insertion involves a coordination of the monomer with the atom. It is this coordination of the monomer that results in the stereospecificity of the polymerization. Coordination polymerizations can be terminated (poisoned) by introduction of water, hydrogen, aromatic alcohol, or metals like zinc.

2.3 POLYMERIZATION TECHNIQUES

2.3.1 Bulk Polymerization

The simplest technique and the one that gives the highest-purity polymer is bulk polymerization. Only monomer, a monomer-soluble initiator, and perhaps a chain-transfer agent to control molecular weight are used. Advantages of this technique include high yield per reactor volume, easy polymer recovery, and the option of casting the polymerization mixture into final product form (i.e., cast polymerization). Among the limitations of bulk polymerization are the difficulty of removing the last traces of monomer and the problem of dissipating heat produced during the polymerization. Free-radical polymerizations are typically highly exothermic (typically 42 to 88 kJ mol^{-1}, see Table 2.5), while the specific heat and coefficient of thermal conductivity of polymers are low. An increase in temperature will increase the polymerization rate and, therefore, generate additional heat to dissipate. Heat removal becomes particularly difficult near the end of the polymerization when viscosity is high. This is because high viscosity limits the diffusion of long-chain radicals as required for termination. This means that radical concentration will increase and, therefore, the rate of polymerization also will increase, as indicated by eq. 2.15. By comparison, the diffusion of small monomer molecules to the propagation sites is less restricted. This means that the termination rate decreases more rapidly than the propagation rate, and the overall polymerization rate, therefore, increases with accompanying additional heat production. This autoacceleration process is called the *Trommsdorff* or *gel* effect. In practice, heat dissipation during bulk polymerization can be improved by providing special baffles for improved heat transfer or by performing the bulk polymerization in separate steps of low-to-moderate conversion.

Bulk-polymerization processes can be used for many free-radical polymerizations and some step-growth (condensation) polymerization. Important examples of polymers usually polymerized by free-radical bulk polymerization include

polystyrene and poly(methyl methacrylate) for which cast polymerization accounts for about half of the total production. Low-density (i.e., high-pressure) polyethylene as well as some ethylene copolymers, is also sometimes produced by free-radical bulk-polymerizations.

2.3.2 Solution Polymerization

Heat removal during polymerization can be facilitated by conducting the polymerization in an organic solvent or water. The requirements for selection of the solvent are that both the initiator and monomer be soluble in it and that the solvent have acceptable chain-transfer characteristics and suitable melting and boiling points for the conditions of the polymerization and subsequent solvent-removal step. Solvent choice may be influenced by other factors such as flash point, cost, and toxicity. Examples of suitable organic solvents include aliphatic and aromatic hydrocarbons, esters, ethers, and alcohols. Often, the polymerization can be conducted under conditions of solvent reflux to maximize heat removal. Reactors are usually stainless steel or glass lined. The obvious disadvantages of solution polymerization are the small yield per reactor volume and the requirement for a separate solvent-recovery step.

Many free-radical and ionic polymerizations are conducted in solution. Important water-soluble polymers that can be prepared in aqueous solution include poly(acrylic acid), polyacrylamide, poly(vinyl alcohol), and poly(*N*-vinylpyrrolidinone). Poly(methyl methacrylate), polystyrene, polybutadiene, poly(vinyl chloride), and poly(vinylidene fluoride) can be polymerized in organic solvents.

2.3.3 Suspension Polymerization

Improved heat transfer can be obtained by using the excellent thermal properties of water through either suspension or emulsion polymerization. In suspension ("bead" or "pearl") polymerization, a batch reactor fitted with a mechanical agitator is charged with a water-*in*soluble monomer and initiator. Sometimes, a chain-transfer agent may be added to control molecular weight in a free-radical polymerization. Droplets of monomer containing the initiator and chain-transfer agent are formed. These are typically between 50 and 200 μm in diameter and serve as miniature reactors for the polymerization. Coalescence of these "sticky" droplets is prevented by the addition of a protective colloid, typically poly(vinyl alcohol), and by constant agitation of the polymerization mixture. Near the end of the polymerization, the particles harden and then can be recovered by filtration, which is followed by a final washing step. Although solvent cost and recovery operations are minimal in comparison with solution polymerization, polymer purity is low due to the presence of suspending and other stabilizing additives that are difficult to completely remove. In addition, reactor capital costs are typically higher than for solution polymerization.

Polymers commonly produced by free-radical suspension polymerization include styrenic ion-exchange resins (Section 2.4.1), extrusion and injection-molding grades of poly(vinyl chloride), poly(styrene-*co*-acrylonitrile) (SAN), and extrusion-grade poly(vinylidene chloride-*co*-vinyl chloride).

2.3.4 Emulsion Polymerization

Another technique that utilizes water as a heat-transfer agent is emulsion polymerization. In addition to water and monomer, a typical reactor-charge for an emulsion polymerization consists of a *water-soluble* initiator, a chain-transfer agent, and a surfactant such as the sodium salt of a long-chain fatty acid. The (hydrophobic) monomer molecules form large droplets (typically 0.5 to 10 μm in diameter), which are stabilized by the surfactant molecules whose hydrophilic ends point outward and whose hydrophobic (aliphatic) ends point inward toward the monomer droplet, as illustrated in Figure 2.6. The size of monomer droplets depends upon the polymerization temperature and the rate of agitation. Above a certain surfactant concentration, the *critical micelle concentration*, residual surfactant molecules can align to form *micelles*, which are small rodlike structures (~50 Å in length) that contain between 50 and 100 surfactant molecules.

An important difference between suspension and emulsion polymerization is that the initiator used in an emulsion polymerization must be soluble in water. An example of a commonly-used water-soluble initiator is the redox persulfate–ferrous initiator, which yields a radical sulfate anion through the reaction

$$S_2O_8^{-2} + Fe^{+2} \longrightarrow Fe^{+3} + SO_4^{-2} + SO_4^{\cdot-}$$

During the emulsion-polymerization process, monomer molecules that have a small but significant water solubility can migrate from the monomer droplets through the water medium to the center of the micelles. Polymerization is initiated when the water-soluble initiating radical enters a monomer-containing micelle. Due to the very high concentration of micelles, typically 10^{18} per mL, compared to that of the monomer droplets (10^{10} to 10^{11} per mL), the initiator is statistically more likely to enter a micelle than a monomer droplet. As the polymerization proceeds, additional monomer molecules are transferred from the droplets to the growing micelles. At 50% to 80% monomer conversion, the monomer droplets are depleted and the swollen micelles are transformed to relatively large polymer particles, typically between 0.05 and 0.2 μm in diameter. The suspension of polymer particles in water is called a *latex*. The latex is very stable and can be used as is (e.g., latex paints) or the polymer can be recovered by coagulation of the latex with acids or salts.

The free-radical kinetics of emulsion polymerization are different from the usual free-radical kinetics of bulk, solution, or suspension polymerization as described in Section 2.2.1. Smith and Ewart[4] have analyzed the kinetics of free-radical emulsion polymerization. They assumed that the micelles are sufficiently small that, on the average, only *one* propagating chain or *one* terminated chain can exist inside the micelle at any time. This means that the radical concentration, $[M_x^{\cdot}]$, is

simply equal to one-half of the number of micelles, N, which in turn is determined by the surfactant and initiator concentrations, among other factors. Therefore, the polymerization rate (see eq. 2.15) is given as

$$R_0 = k_p(N/2)[M]. \tag{2.43}$$

This expression should be compared to the usual steady-state rate expression for free-radical polymerization given by eq. 2.21. While both rates are proportional to monomer concentration, the rate of emulsion polymerization is no longer proportional to the square root of initiator concentration but follows a more complicated dependence on initiator concentration through its dependence on N.

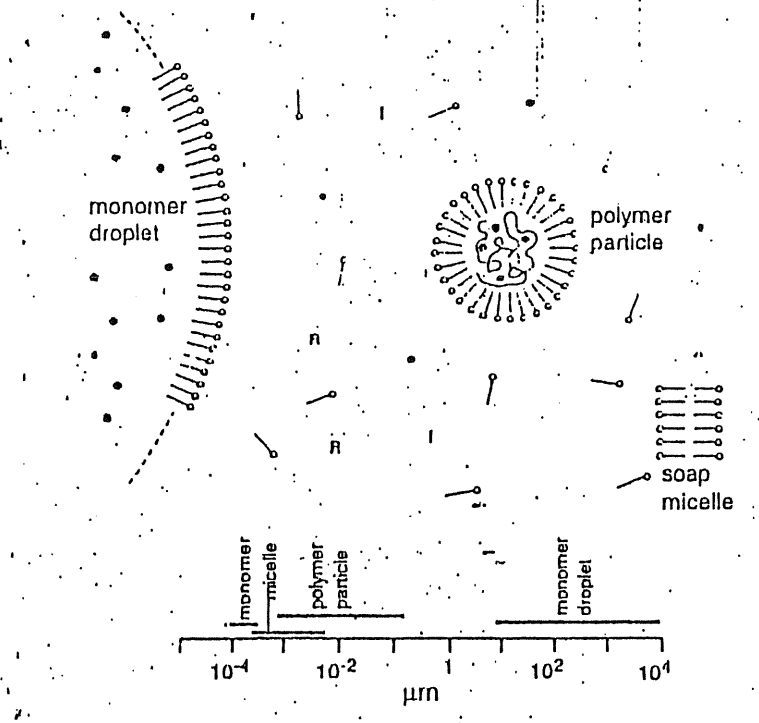

Figure 2.6. Representation of the composition of an emulsion polymerization and relative particle size. Symbols: ●, monomer molecule; I, initiator molecule; and R, primary radical. (Adapted from P. Rempp and E. W. Merrill, *Polymer Synthesis*, Hüthig & Wepf, Basel, 1986, with permission of the publisher).

When the monomer is hydrophilic, emulsion polymerization may proceed through what's called an *inverse* emulsion process. In this case, the monomer (usually in aqueous solution) is dispersed in an organic solvent using a water-in-oil emulsifier. The initiator may be either water soluble or oil soluble. The final product in an inverse emulsion polymerization is a colloidal dispersion of a water-swollen polymer in the organic phase.

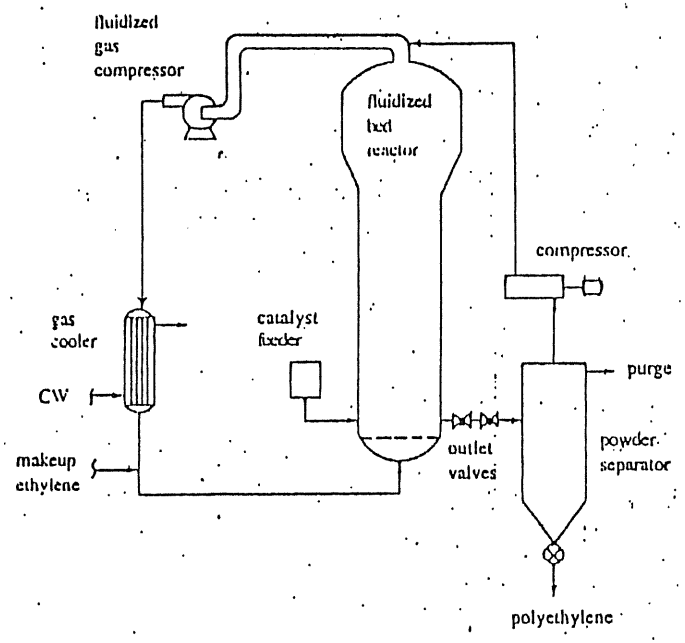

Figure 2.7. Unipol process for the polymerization of ethylene. (Adapted from N. F. Brockmeier, in the *Concise Encyclopedia of Polymer Science and Engineering*, J. I. Kroschwitz, ed. Copyright ©1990 by John Wiley & Sons. Reprinted by permission of John Wiley & Sons, Inc.)

2.3.5 Solid-State, Gas-Phase, and Plasma Polymerization

In addition to the usual methods of polymerization such as bulk and solution, polymers can be prepared in the gas or vapor phase. This is especially the case for the polymerization of olefins such as HDPE. In the Unipol process for PE, which is illustrated in Figure 2.7, gaseous ethylene and solid catalyst (chromium or other complexes) are combined in a continuous fluidized-bed reactor. Since the polymer-

ization is highly exothermic, proper management of heat transfer is critical to prevent agglomeration of the particles and a shutdown of the process. Variations of this process have been used for the polymerization of propylene and the copolymerization of ethylene and propylene.

In addition to gas-phase polymerizations, more exotic routes may be followed for specialty applications. For example, some monomers in their crystalline state can be polymerized to give extended-chain polymers oriented along crystallographic directions. The result is a polymer single-crystal with interesting optical properties.

A wide variety of monomers can also be polymerized in a plasma environment, which may consist of a low-pressure glow discharge of positively and negatively charged species, electrons, excited and neutral species, and electromagnetic radiation. Plasma polymerization can be used to prepare graft copolymers or to deposit a thin polymer film on a metal or other substrate (e.g., a photoresist on a silicon wafer or a corrosion-resistant coating on a metal).

2.4 REACTIONS OF SYNTHETIC POLYMERS

In many cases, a polymer can be chemically modified to improve some property, such as biocompatibility, fire retardancy, or adhesion, or to provide specific functional groups for ion-exchange or other applications. For example, bromination is sometimes used to impart fire retardancy to some polymers. As another example, poly(vinyl chloride) can be chlorinated after polymerization to increase its softening temperature or to improve its ability to blend with other polymers. In some cases, important commercial polymers can be produced only by the chemical modification of a precursor polymer. Examples include poly(vinyl alcohol), poly(vinyl butyral), cellulose derivatives such as cellulose acetate and cellulose nitrate, and polyphosphazenes — an interesting group of inorganic polymers.

2.4.1 Chemical Modification

Chloromethylation. Chloromethylation of polystyrene (see Figure 2.8), by reacting with a chloromethyl ether in the presence of a Friedel-Crafts catalyst like aluminum chloride, $AlCl_3$, can be used to introduce functionality such as aldehyde or carboxylic acid groups in polystyrene. In the Merrifield synthesis of proteins, crosslinked polystyrene (PS) beads that have been lightly chloromethylated provide the anchor sites for the sequential addition of amino acids. Highly chloromethylated PS can be quaternized with tertiary amines to yield water-soluble polymers, ionomers, and ion-exchange resins, as described in the following section. Chloromethylated PS also can be reacted with a phosphide to introduce phosphinic ligands for binding metal coordination complexes in the preparation of polymer-bound catalysts.

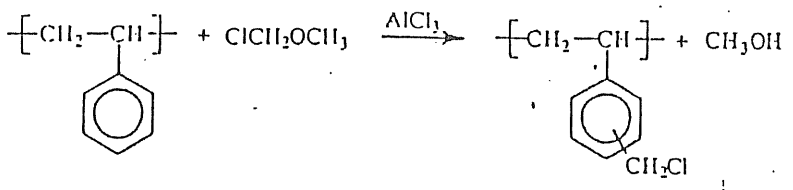

Figure 2.8. Chloromethylation of polystyrene.

Surface Modification. In many cases, it may be desirable to modify the surface of a polymer to provide sites for immobilization of enzymes or other biopolymers or to improve the solvent resistance or biocompatibility of a polymer. For example, the surface of a hydrocarbon polymer such as polyethylene or polypropylene can be fluorinated by exposure to 5% to 10% fluorine gas diluted in nitrogen for 1 to 15 min. The fluorinated surface provides hydrophobicity, oxidation resistance, and solvent resistance for applications such as plastic fuel tanks and rubber gloves. Surface-modification reactions include oxidation, nitration, and sulfonation.

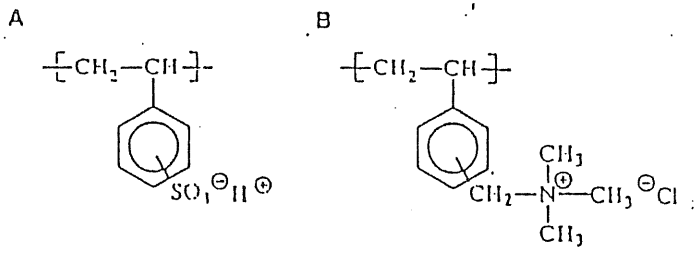

Figure 2.9. Example of a strongly acidic cation-exchange resin (A) and a strongly basic anion-exchange resin (B) prepared from polystyrene.

Ion-Exchange Resins. Another need for chemical modification is the preparation of ion-exchange resins. Cation-exchange resins possess a fixed negative charge and exchange cations such as Ca^{2+}, Na^+, and H^+. Anion-exchange resins possess a positive charge on the functional group or are positively charged during the ion-exchange reaction during which anions such as HCO_3^-, SO_4^-, and OH^- are exchanged. Most ion-exchange resins are prepared by suspension polymerization of monomers such as styrene, which can be crosslinked by incorporation of a few percent of a difunctional comonomer such as divinylbenzene. The resulting beads are macroporous and can be used as a column packing. Functionalization can be obtained by different chemical routes, such as sulfonation, phosphonation,

phosphination, chloromethylation, amino-methylation, aminolysis, and hydrolysis. For example, a cation-exchange resin can be prepared by sulfonation of a crosslinked polystyrene bead in concentrated sulfuric acid or in a molecular complex of SO_3 with an organic solvent, such as dioxane. Sulfonation primarily occurs at the *para*-position with some *ortho*-substitution. A styrenic anion-exchange resin can be prepared by reacting the benzyl chloride of chloromethylated polystyrene (see Figure 2.8) with a tertiary amine, $N(CH_3)_3$. Examples of styrenic ion-exchange resins are illustrated in Figure 2.9.

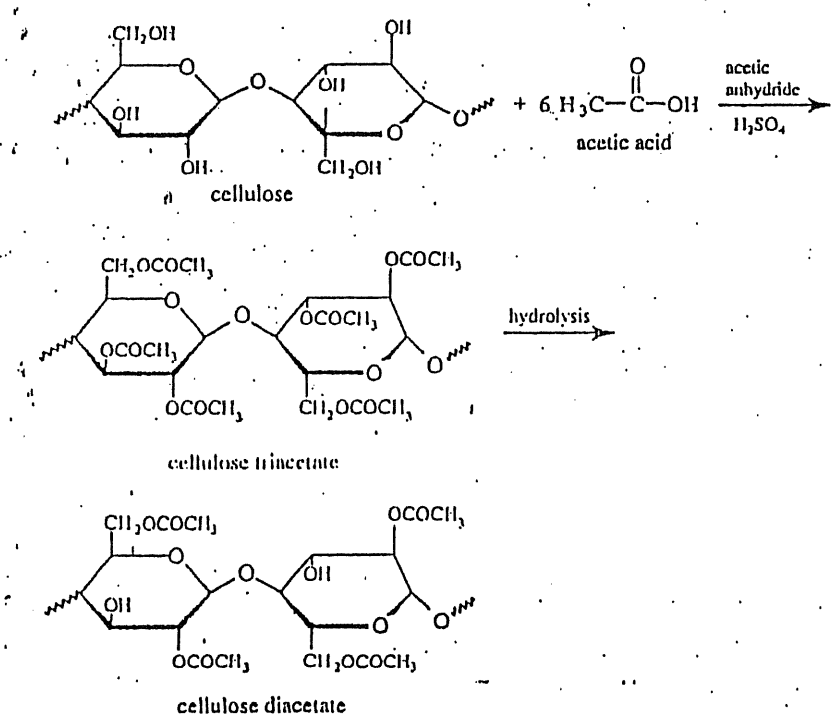

Figure 2.10. Preparation of cellulose acetate from cellulose.

2.4.2 Preparation of Polymer Derivatives

Cellulose. Cellulose, which can be obtained from wood pulp and short fibers left from cotton recovery, is one of nature's most abundant biopolymers. A typical chain is composed of 2000 to 6000 anhydroglucose units (typical molecular weight of 300,000 to 1,000,000) each of which contains three hydroxyl groups and is linked by an acetal bridge, as shown in Figure 2.10. The rigid chain of cellulose is strongly hydrogen bonded and highly crystalline. For these reasons, cellulose is essentially insoluble and infusible (degrades before melting), and therefore fibers and films can be obtained only by chemically modifying cellulose. As described in Section 8.2.2, cellulose fiber (rayon) or film (cellophane) is obtained by the *viscose* process. In this regeneration process, cellulose pulp is first reacted with carbon disulfide to form cellulose xanthate, which is soluble in caustic solution. The xanthate form is then converted back to cellulose (regeneration) by treatment with aqueous sulfuric acid.

Various soluble cellulose derivatives can be obtained by chemical modification of the hydroxyl groups. One of the most important of these is cellulose acetate, which is obtained by reacting cellulose with glacial acetic acid in the presence of acetic anhydride and traces of sulfuric acid in refluxing methylene chloride (Figure 2.10). If all the hydroxyl groups are reacted, the polymer is known as cellulose triacetate (CTA), which can be wet spun into fiber (acetate) from a methylene chloride–alcohol solvent mixture. Cellulose triacetate can be partially hydrolyzed to give cellulose diacetate in which two (secondary) of the three hydroxyl groups in each anhydroglucose unit remain acetylated. In the case of commercial cellulose acetate, about 65% to 75% of all available hydroxyl groups remain acetylated. This polymer is amorphous and highly soluble in many solvents including acetone, from which it can be dry spun (see Section 8.2.4).

Poly(vinyl alcohol) and Poly(vinyl butyral). Poly(vinyl alcohol) (PVAL) is obtained by the direct hydrolysis (or catalyzed alcoholysis) of poly(vinyl acetate) (PVAC) as shown by the following reaction:

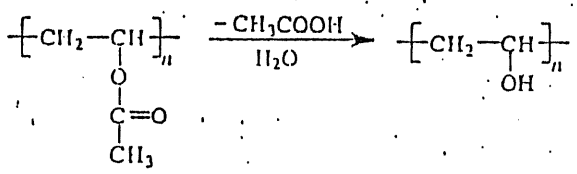

Poly(vinyl acetate) is produced by free-radical emulsion or suspension polymerization. It has a low glass-transition temperature (ca. 29°C) and finds some applications as an adhesive. Poly(vinyl alcohol), which is used as a stabilizing agent in emulsion polymerizations and as a thickening and gelling agent, cannot be polymerized directly because its monomer, vinyl alcohol, is isomeric with acetaldehyde:

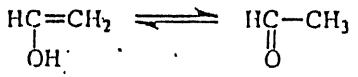

Another important polymer, poly(vinyl butyral) (PVB), which is used as the film between the layers of glass in safety windshields, is obtained by partially react-

ing PVAL with butyraldehyde as shown in Figure 2.11. For safety-glass applications, approximately 25% of the repeating units of PVAL are left unreacted to promote adhesion to the glass through interaction of the hydroxyl group with the surface (i.e., silanol) groups of the glass.

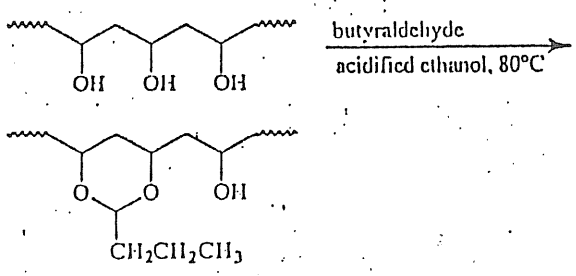

Figure 2.11. Production of poly(vinyl butyral) from poly(vinyl alcohol) precursor.

Poly(organophosphazenes). Another class of polymers that are obtained by chemical modification of a precursor polymer is the poly(organophosphazenes). These are inorganic polymers having an alternating nitrogen–phosphorus backbone, as follows:

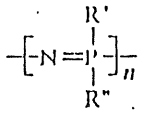

A very large number of different substituent groups (R', R") can be linked to the phosphorous atom. These include alkoxy, aryloxy, amino, alkyl, aryl, or even an inorganic or organometallic unit. At present, more than 300 different poly(organophosphazenes) have been prepared of which several have been commercialized. Properties vary from elastomeric ($T_g \approx -80°C$) to microcrystalline. Potential applications of poly(organophosphazenes) include those in which good chemical stability is required, such as O-rings, gaskets, and fuel lines, and in areas where good biostability and biocompatibility are necessary, such as in the encapsulation of pancreatic cells. Poly(organophosphazenes) also exhibit extremely high permeability for fixed gases and organic liquids and may find use in membrane applications (see Section 12.1).

The precursor polymer for all poly(organophosphazenes) is poly(dichlorophosphazene), which is obtained from the radiation- or plasma-polymerization of hexachlorocyclotriphosphazene. Poly(dichlorophosphazene) is unstable due to its high susceptibility to hydrolysis, producing phosphoric acid, hydrogen chloride, and ammonia as by-products. Fortunately, the active chlorine sites are readily substituted by nucleophiles such as alkoxides, aryloxides, and amines to yield a wide variety of high-molecular-weight poly(organophosphazenes) that are chemically and thermally stable. Various substituent pathways are illustrated in Figure 2.12.

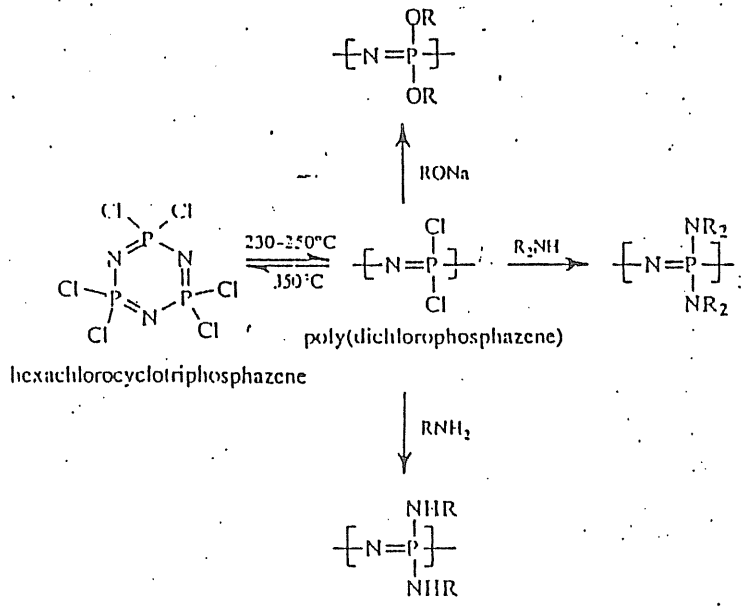

Figure 2.12. Ring-opening polymerization of hexachlorocyclotriphosphazene to poly(dichlorophosphazene) and representative substitution reactions to give poly(organophosphazenes).

2.5 SPECIAL TOPICS IN POLYMER SYNTHESIS

Sections 2.1 and 2.2 described the traditional step-growth and chain-growth polymerization methods that have been developed over the past 75 years and are widely used in today's commercial plastics industry. During the past few years, there has been renewed interest in several specialized polymerization methods as well as the development of new approaches. These range from metathesis ring-opening polymerization, first developed in the early 1960s, to more recent techniques, such as group-transfer polymerization and the use of macromers for the preparation of graft copolymers.

2.5.1 Metathesis

Cyclic olefins, like cyclobutene and cyclopentene, can undergo a ring-opening polymerization called *metathesis* to yield elastomers (polyalkenamers) having attractive properties for specialty applications. Polyalkenamers obtained from the metathesis polymerization of cyclooctene and norbornene (bicylco[2.2.1]hept-2-ene) are now marketed as specialty elastomers. Polymerizations proceed with good rates at room temperature, and polymer stereochemistry can be controlled by the choice of catalyst. Typical catalysts for olefin metathesis include Ziegler types such as prepared from the reaction product of tungsten hexachloride with ethanol and ethylaluminum dichloride, $WCl_6/(C_2H_5)_3Al$. Other important examples of catalysts include MoO_3/Al_2O_3 and $TiCl_4/LiAlR_4$. As an example, routes in the production of *cis*- and *trans*-isomers of polypentenamer by the metathesis polymerization of cyclopentene are illustrated in Figure 2.13.

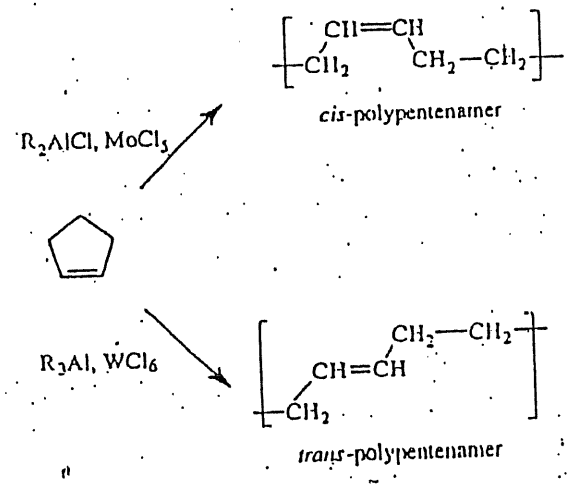

Figure 2.13. Metathesis of cyclopentene to polypentenamer.

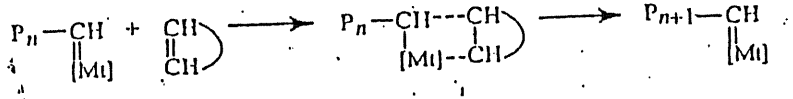

Figure 2.14. A propagation step in the metathesis polymerization of a cycloalkene where P represents a repeat unit, *n* is the degree of polymerization, and Mt represents a metal complex.

The mechanism of methathesis polymerization is a typical coordination type involving the propagation of a metal–carbene complex via a metallacyclobutane intermediate, as illustrated in Figure 2.14. Metathesis polymerization of highly strained cycloalkanes such as norbornene and cyclobutene proceed much more rapidly than less strained structures such as cyclopentene (Figure 2.13).

2.5.2 Group-Transfer Polymerization

Group-transfer polymerization (GTP), first patented by Du Pont in 1983, is the "living" polymerization of α,β-unsaturated esters (principally acrylates and methacrylates), ketones, nitriles, or amides with initiation by silyl ketene acetals. Examples of monomers that can be polymerized in this manner include methyl methacrylate, ethyl acrylate, butyl acrylate, and 2-methacryloxyethyl acrylate. Typical initiators are 1-alkoxy-1-(trimethylsiloxy)-2-methyl-1-alkenes such as 1-methoxy-1-(trimethylsiloxy)-2-methyl-1-propene used in the polymerization of methyl methacrylate. The initiator is activated by nucleophilic catalysts such as soluble fluorides, bifluorides [e.g., tris(dimethylamino)sulfonium bifluoride], azides, and cyanides.

A

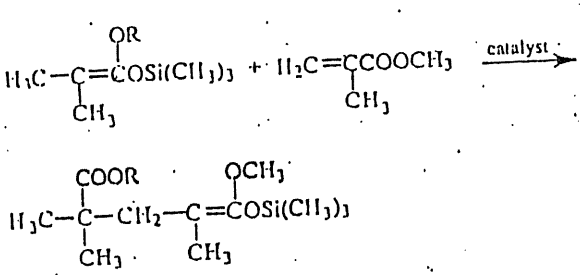

B

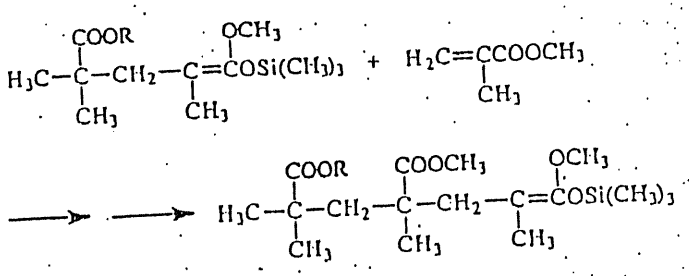

Figure 2.15. Group-transfer polymerization of methyl methacrylate. A. Initiation of monomer. B. Propagation step.

During the polymerization, the reactive ketene silyl acetal group is transferred to the head of each new monomer molecule as it adds to the chain, hence the name group-transfer polymerization. As in anionic polymerization, the ratio of monomer to initiator concentration determines the molecular weight. An important example is the GTP of methyl methacrylate shown in Figure 2.15.

Group-transfer polymerizations are typically conducted in solution using an organic solvent such as toluene and THF at low temperatures (ca. 0° to 50°C). Active hydrogen compounds like some protonic solvents will stop the polymerization. For this reason, the polymerization environment must be completely free of water. Under these conditions, the polymerization will proceed until all monomer is exhausted as in other "living" polymerizations; however, high-molecular-weight polymers with molecular weights in excess of 100,000 are difficult to achieve unless the monomer, solvent, initiator, and catalyst are extremely pure. The high cost of GTP relative to more traditional free-radical polymerizations and the use of toxic catalysts such as azides and cyanides have limited widespread commercial utilization. Potential applications include high-performance automotive finishes, the fabrication of silicon chips, and coatings for optical fibers.

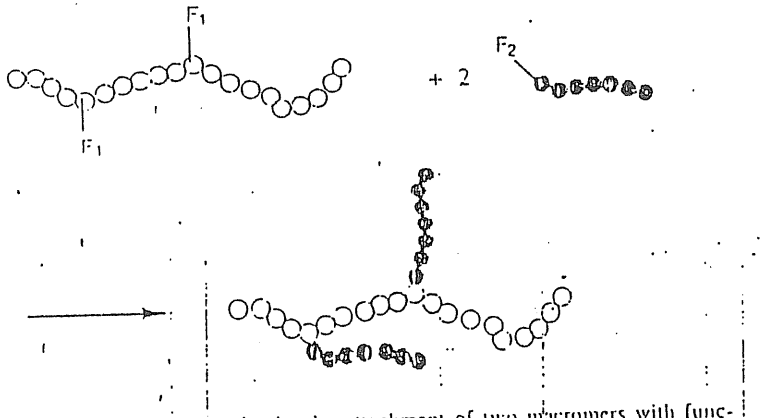

Figure 2.16. Graft polymerization by attachment of two macromers with functional group F_2 to a prepolymer with two complementary functional groups F_1.

2.5.3 Macromers in Polymer Synthesis

A macromer or macromonomer is an abbreviation of the term *macromolecular monomer*. As the name suggests, a macromer is a low-molecular-weight oligomer or polymer with a functional group (F) at the chain end. This functional group can further polymerize to yield a higher-molecular-weight polymer. Examples of functional moieties include a vinyl group as well as a variety of difunctional chemical groups such as a dicarboxylic acid, diol, or diamine that can be used in a step-growth (or condensation) polymerization step. One use for macromers is controlled graft copolymerization. In this case, suitable comonomer units are contained in a prepolymer. The macromer then attaches to the comonomer sites and forms branches, as illustrated in Figure 2.16. These graft copolymers can be used as compatibilizers for polymer blends (see Chapter 7) and as surface-modifying agents.

2.6 CHEMICAL STRUCTURE DETERMINATION

This chapter has described a variety of techniques used to synthesize polymers and copolymers. Once the polymer has been made, several analytical methods are available to confirm that the polymer made is actually the one desired and to identify various specific features of the polymer microstructure, such as comonomer composition and sequence, stereoregularity, branching, crystallinity, orientation, and oxidation sites if thermooxidative degradation has occurred (see Chapter 6). In addition, the presence of various additives, such as stabilizers and lubricating agents, or contaminants that may have been introduced during polymerization or in processing can be readily identified. The most important of these techniques include the common spectroscopic methods such as infrared, nuclear magnetic resonance (NMR), and Raman spectroscopy. Applications of spectroscopic methods to polymer characterization are briefly described in this section. In this, a general understanding of the basic principles of spectroscopy is assumed.

2.6.1 Vibrational Spectroscopy

Perhaps the most widely used method to characterize polymer structure is infrared spectrosocopy, particularly Fourier transform infrared (FTIR) spectroscopy.[5] Polymer samples for IR analysis can have a variety of forms including thin film, solution, or a pellet containing a mixture of the granulated polymer and an IR-transparent powder such as potassium bromide. Bulk samples can be analyzed by reflection or attenuated total reflectance (ATR).

The IR spectra of a polymer is unique, and a large number of spectra libraries are available to assist identification.[6] Several atomic groups, such as –CH, –CO, and $-CH_3$, are readily identified by the presence of a single absorption band. As an example, the –CH– stretching vibration can be found in the narrow frequency range from 2880 to 2900 cm^{-1}. The exact location of the principal absorption band or bands of other chemical groups depends on the local chemical environment, especially the occurrence of intra- or intermolecular hydrogen bonding. In the case of the carbonyl group which can easily bond with hydrogen, absorption may occur over the broad range from 1700 to 1900 cm^{-1}. The presence of stereoisomers (i.e., tacticity and geometry isomers) may be identified by the appearance of new absorption frequencies, shifting of absolute frequencies, and band broadening in the infrared spectrum.

A good example of a typical FTIR spectrum is that shown in Figure 2.17 for the engineering thermoplastic, polycarbonate

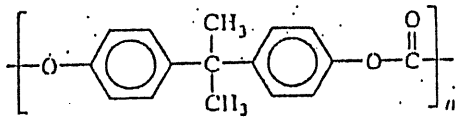

The IR-spectrum of this polymer is very distinctive. Principal absorption bands include those at 823 cm^{-1} (ring C-H bending), 1164 and 1231 cm^{-1} (C-O stretching), 1506 cm^{-1} (skeletal ring vibrations), and 1776 (C=O stretching).

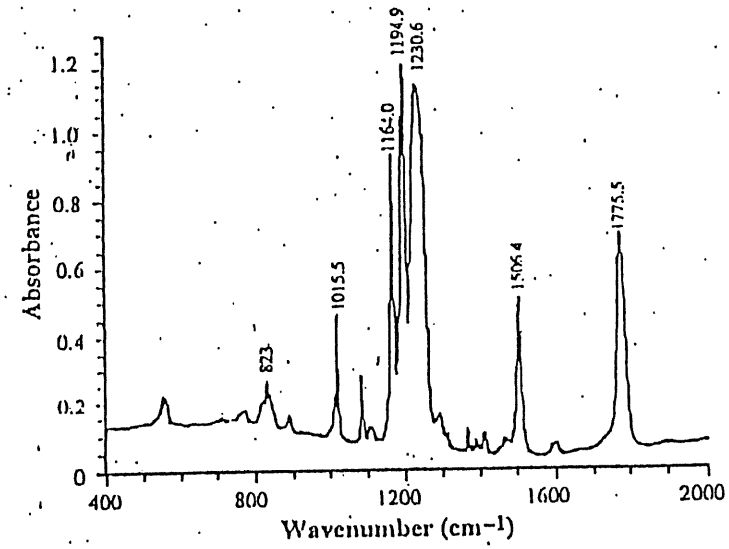

Figure 2.17. FTIR spectrum of a polycarbonate film.

The locations of IR absorbance peak maxima can also be sensitive to whether the chemical groups lie in crystalline lamellae (see Chapter 4) or in amorphous regions and, therefore, FTIR measurements can be used as a means to determine the degree of crystallinity of a sample. For example, FTIR-measurements can be used to follow the development of crystallinity of poly(vinyl chloride)

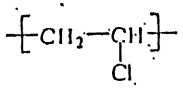

as a function of heat treatment. Commercial-grade PVC is a polymer of low crystalline order (ca. 7 to 10 % crystallinity). When heated above its glass transition temperature (87°C) and below its crystalline-melting temperature (212°C), the degree of crystallinity can be increased. One way of determining the percent of crystallinity is by density measurements (see Section 4.2.4). Another method is by quantitative measurements of the intensity of certain IR-absorbance peaks.

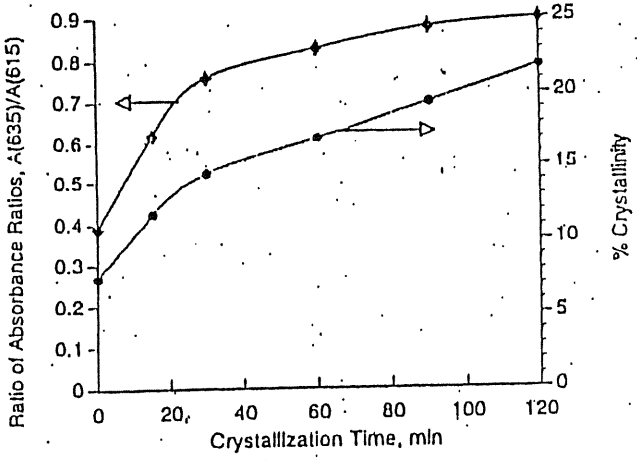

Figure 2.18. Plot of the ratio of the amplitudes of the FTIR absorbance peaks of poly(vinyl chloride) at 635 and 615 cm^{-1} as a function of crystallization time at 110° to 115°C.[7] Comparison is made to the percent crystallinity determined from density measurements.

In the case of PVC, there are two principal overlapping absorbance peaks lying between 550 and 665 cm^{-1} and attributed to C-Cl stretching vibrations. One peak that appears to be crystalline sensitive is located at 635 cm^{-1}, while the other is crystalline insensitive and is located at 615 cm^{-1}. The ratio of the amplitude of the 635- and 615-cm^{-1} peaks can, therefore, be used as a quantitative measure of the degree of crystallinity. This ratio is plotted as a function of crystallization time in Figure 2.18. As shown, the increase in the absorbance ratio closely follows the percent crystallinity determined from density measurements of the same samples.

Raman Spectroscopy. A technique related to infrared spectroscopy is Raman scattering, which results from a change in induced dipole moment or polarization of a molecule upon irradiation. In the case of Rayleigh scattering, there is no exchange of energy between the incident light and the molecule and therefore the scattered light has the same frequency, υ_R, as the incident light, υ_o. In Raman scat-

tering, the molecule returns inelastically to an energy level different from the original state, and therefore the frequency of the scattered light will be different (i.e., $\upsilon_R = \upsilon_0 + \Delta\upsilon$). The strongest bands are those appearing at lower frequencies (i.e., the Stokes bands) and are the ones normally recorded. Perhaps the greatest advantage of Raman scattering in polymer characterization is that no special sample preparation is required, and therefore liquids and solids can be studied nondestructively. For this reason, Raman spectroscopy particularly lends itself to the study of polymer morphology, especially the study of crystalline structure and orientation effects.

TABLE 2.8 Nuclei Used in Polymer NMR

Nuclei	Spin	Natural Abundance (%)	Shift Range (ppm)
^{1}H	1/2	99.985	15
^{2}H	1	0.0156	15
^{13}C	1/2	1.108	220
^{14}N	1	99.634	900
^{15}N	1/2	0.365	900
^{17}O	5/2	0.037	800
^{19}F	1/2	100	800
^{29}Si	1/2	4.70	250
^{31}P	1/2	100	700

2.6.2 Nuclear Magnetic Resonance Spectroscopy

Nuclear magnetic resonance (NMR) spectroscopy is a very powerful technique for polymer characterization that can be used to determine tacticity, branching, structural defects such as the occurrence of head-to-head placement of monomers in vinyl polymers, the sequence of comonomer units in a copolymer chain, and chemical changes such as oxidation states, which can be detected at levels as low as one site per 500 repeat units. Although ^{13}C NMR is commonly used in polymer characterization, NMR measurements employing other NMR-active nuclei such as ^{1}H, ^{13}C, ^{17}O, and ^{19}F having magnetic moments may have an advantage in the study of some polymers.[1] For example, ^{29}Si NMR may be used in the characterization of polysiloxanes, ^{19}F NMR for fluoropolymers, ^{15}N NMR for polyamides, and ^{31}P NMR for polyphosphazenes. A complete listing of important NMR-active nuclei and their natural abundance is given in Table 2.8.

[1] Any atomic nuclei having a *nonzero* spin quantum number, I, possess a magnetic moment. When placed in a magnetic field, these nuclei occupy $2I + 1$ quantized magnetic energy levels, called Zeeman levels. Transitions (resonance) between energy levels can occur by application of a resonant rf field of frequency υ_0 (equal to the Larmor precession frequency). Resonance for a particular nucleus will occur at slightly different frequencies depending upon its chemical environment (i.e., its chemical bonding and position in the molecule) due to the shielding effect of electron clouds on a nucleus, which reduces the Larmor frequency. These frequency changes are termed *chemical shifts* and are given in reference to tetramethylsilane (TMS) as a standard. The range of chemical shifts is about 100 ppm for ^{1}H but >200 ppm for ^{13}C and other nuclei.

Two techniques of NMR measurements have been used in polymer studies. Broad-line NMR methods, usually proton relaxation, can be used to determine amorphous content and chain orientation in semicrystalline polymers. High-resolution NMR measurements can be used to obtain information concerning the sequence of repeating units in the chain. This enables the determination of tacticity and comonomer distribution, as described next.

Chemical Structure Determination by NMR Measurements. NMR measurements can provide a very detailed description of the chemical microstructure of a polymer chain, such as branching, head-to-head or head-to-tail addition, comonomer sequence, and tacticity, by measuring chemical shifts that are sensitive to the local environment (electron shielding) of a particular nucleus. For example, NMR measurements can be used to determine the isotactic content of a particular polymer. To understand NMR analysis of tacticity, it is useful to look at the spatial arrangement of several monomer units having an asymmetric substituent group, R. For a sequence of five monomer units, called a pentad, two extreme cases are possible, as discussed in Chapter 1. In an isotactic sequence, all the R groups lie on the same side of the chain:

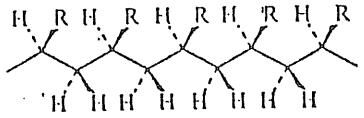

In this case, the four sequential pairs of monomer units (diads) are called *meso* (m) and, therefore, this particular pentad can be described as mmmm. For four repeating units (quartet), the sequence is represented as mmm and for three repeating units (triad), the sequence is represented as mm. In the case of syndiotactic chain structure, the substituent groups alternates from side to side:

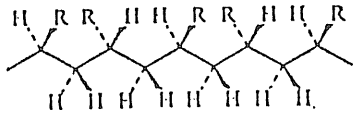

The sequence is all *racemic* (r) and the pentad can be described as rrrr. Correspondingly, the quartet is rrr and the triad is rr. The surrounding molecular environment can affect the chemical shift of the proton on a β-methylene (CH_2) group or a proton on the α-carbon substituent group. Whether the resolution can extend to triad, quartet, or pentad sequence identification depends upon the frequency of the applied rf field.

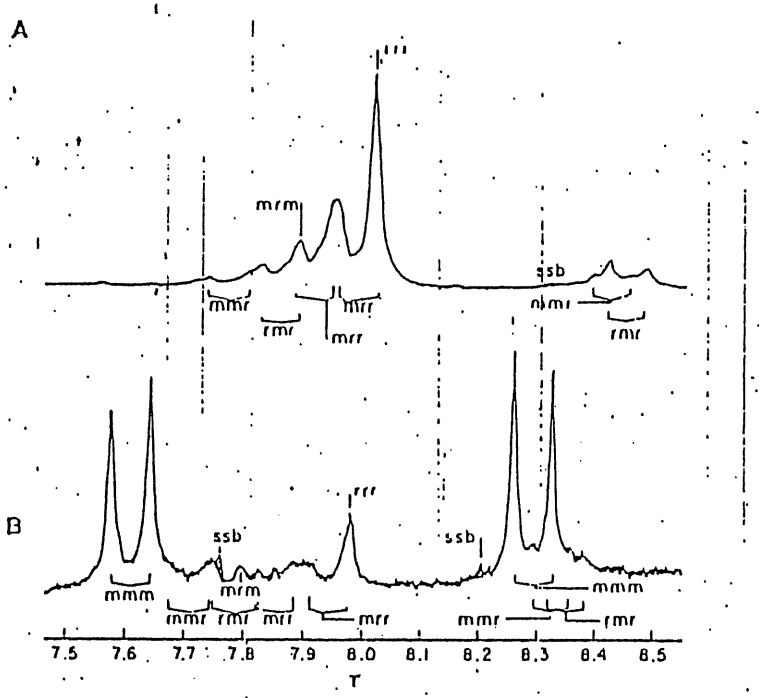

Figure 2.19. NMR spectra of the β-methylene proton for two samples of poly(methyl methacrylate) (PMMA) obtained in solution at 220 MHz. A. Predominantly syndiotactic PMMA. B. Predominantly isotactic PMMA. (Reproduced from F. A. Bovey, *High Resolution NMR of Macromolecules*, Academic Press, New York, 1972, with permission of the publisher.)

A good illustration of the use of NMR measurements to determine polymer structure is poly(methyl methacrylate) (PMMA). Two repeating units (a diad) of an isotactic sample of PMMA are

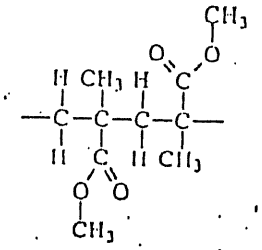

If the polymer chain is syndiotactic, the two protons on the β-methylene groups are equivalent and, therefore, there should be a single resonance; however, if the chain is isotactic, the local environments (due to electron-cloud shielding) of the two protons are different, and four principal resonances (due to spin–spin interactions) result. NMR spectra for predominately syndiotactic and predoininatly isotactic PMMA samples in 10% chlorobenzene at 135°C and observed at high frequency (220 MHz) are shown in Figure 2.19. The major peak intensity is assigned to the rrr quartet of the predominantly syndiotactic sample (Figure 2.19A) and four major peaks are assigned to the mmm quartet of the predominantly isotactic sample (Figure 2.19B).

Solid-State NMR. The spectral linewidth of solid samples is broad relative to that of liquids (0.2 to 5.0 Hz). This is because the relative immobility of molecules in the solid state results in stronger interactions compared to highly mobile molecules in the liquid state for which intramolecular interactions are averaged out. A technique that allows high-resolution NMR measurements of polymers in the solid state is called magic-angle spinning (MAS) NMR.[8] In this procedure, a cylindrical sample is rotated at high speed (>2 kHz) at an angle of 54.7° relative to the static field. Under these circumstances, linewidths decrease to those comparable to solution samples (~1 ppm). Solid-state NMR can be used to investigate the segmental mobility of polymer chains, the diffusion of small molecules in polymers, and polymer annealing and aging processes.

REFERENCES

1. J. Brandrup and E. H. Immergut, eds., *Polymer Handbook*, 3rd ed., John Wiley & Sons, New York, 1989.
2. T. Alfrey, Jr., and C. C. Price, *J. Polym. Sci.*, 2, 101 (1947).
3. F. R. Mayo and F. M. Lewis, *J. Am. Chem. Soc.*, 66, 1594 (1944).
4. W. V. Smith and R. H. Ewart, *J. Chem. Phys.*, 16, 592 (1948).
5. J. L. Koenig, *Adv. Polym. Sci.*, 54, 87 (1983).
6. D. O. Hummel, *Atlas of Polymer and Plastics Analysis*, Carl Hanser Verlag, Munich, 1978.

7. R. L. Ballard, Ph.D. Dissertation, University of Cincinnati, 1992.
8. J. Schaefer, E. O. Stejskal, and R. Buchdahl, *Macromolecules*, 8, 291 (1975).

GENERAL READING

T. Altares, Jr., and E. L. Clark, "Pilot Plant Preparation of Polystyrene of Very Narrow Molecular Weight Distribution," *Ind. Eng. Chem.*, 9, 168 (1970).

J. L. Koenig, "Molecular Spectroscopy," in *Physical Properties of Polymers*, 2nd ed., J. E. Mark, A. Eisenberg, W. W. Graessley, L. Mandelkern, E. T. Samulski, J. L. Koenig, and G. D. Wignal, American Chemical Society, Washington, DC, 1993, pp. 263–312.

J. E. McGrath, "Chain Reaction Polymerization," *J. Chem. Educ.*, 58, 844 (1981).

J. E. McGrath, "Block and Graft Copolymers," *J. Chem. Educ.*, 58, 914 (1981).

J. K. Stille, "Step-Growth Polymerization," *J. Chem. Educ.*, 58, 862 (1981).

SPECIALIZED READING

A. Akelah and A. Moet, *Functionalized Polymers and Their Applications*, Chapman and Hall, London, 1990.

D. C. Allport and W. H. Janes, eds., *Block Copolymers*, Halsted Press, New York, 1973.

H. G. Barth and J. W. Mays, *Modern Methods of Polymer Characterization*, John Wiley & Sons, New York, 1991.

D. S. Breslow, "Metathesis Polymerization," *Prog. Polym. Sci.*, 18, 1141–1195 (1993).

F. A. Bovey, *High Resolution NMR of Macromolecules*, Academic Press, New York, 1972.

G. Bodor, *Structural Investigation of Polymers*, Ellis Horwood, London, 1991.

S. Bywater, "Structure and Mechanism in Anionic Polymerization," *Prog. Polym. Sci.*, 19, 287–316 (1994).

J. R. Ebdon, ed., *New Methods of Polymer Synthesis*, Chapman and Hall, New York, 1991.

J. L. Koenig, *Chemical Microstructure of Polymer Chains*, John Wiley & Sons, New York, 1980.

J. L. Koenig, *Spectroscopy of Polymers*, American Chemical Society, Washington, DC, 1992.

R. W. Lenz, *Organic Chemistry of Synthetic High Polymers*, Interscience Publishers, New York, 1967.

A. Noshey and J. E. McGrath, *Block Copolymers*, Academic Press, New York, 1977.

C. C. Price and E. J. Vandenberg, eds., *Coordination Polymerization*, Plenum Publishing Corp., New York, 1983.

P. Reinpp and E. W. Merrill, *Polymer Synthesis*, Hüthig & Wepf Verlag, Heidelberg, 1986.

C. E. Schildknecht, ed., *Polymerization Processes*, John Wiley & Sons, New York, 1977.

Problems

2–1. What would be the number-average molecular weight of polystyrene obtained at the completion of an anionic (i.e., "living") polymerization in which 0.01 g of *n*-butyllithium and 10 g of styrene monomer are used? The molecular weights of butyllithium and styrene are 64.06 and 104.12, respectively.

2–2. Styrene is polymerized by free-radical mechanism in solution. The initial monomer and initiator concentrations are 1 *M* (molar) and 0.001 *M*, respectively. At the polymerization temperature of 60°C, the initiator efficiency is 0.30. The rate constants at the polymerization temperature are as follows:

$$k_d = 1.2 \times 10^{-5}\ s^{-1}$$
$$k_p = 176\ M^{-1}\ s^{-1}$$
$$k_t = 7.2 \times 10^{7}\ M^{-1}\ s^{-1}$$

Given this information, determine the following:

(a) Rate of initiation at 1 min and at 16.6 h

(b) Steady-state free-radical concentration at 1 min

(c) Rate of polymerization at 1 min

(d) Average free-radical lifetime, τ, at 1 min, where τ is defined as the radical concentration divided by the rate of termination

(e) Number-average degree of polymerization at 1 min

2–3. It has been reported that the rate of a batch *photopolymerization* of an aqueous acrylamide solution using a light-sensitive dye is proportional to the square of the monomer concentration, $[M]^2$, and the square root of the absorbed light-intensity, $I^{1/2}$. Note that, although this polymerization is free radical, the apparent kinetics appear not to be typical of usual free-radical polymerization for which the rate of polymerization is proportional to the first power of monomer concentration and to the square root of the initiator concentration (eq. 2.21). The following polymerization mechanism has been proposed to explain the observed kinetics:

Initiation

$$M + D \xrightarrow{k_1, h\nu} R\bullet$$

$$R\bullet + M \xrightarrow{k_2} RM_1\bullet$$

Propagation

$$RM_1\bullet + M \xrightarrow{k_3} RM_2\bullet$$

$$\vdots$$

$$RM_n\bullet + M \xrightarrow{k_3} RM_{n+1}\bullet$$

Termination

$$RM_n\bullet + RM_n\bullet \xrightarrow{k_4} P$$

$$R\bullet \xrightarrow{k_5} S$$

where

M, monomer
D, dye
P, terminated polymer
S, deactivated initiator

Show that this mechanism appears to be correct by deriving an equation for the rate of propagation in terms of [M], I, and the appropriate rate constants. The following assumptions may be made:

1. Equal reactivity in the propagation steps
2. Steady-state concentration of $R\bullet$ and $RM_n\bullet$
3. $k_2 << k_5$
4. The concentration of dye, [D], that has been activated by light and thereby contributes to the first initiation step is proportional to the absorbed light intensity.

2–4. Given the Q-e values for styrene ($Q = 1.00$, $e = -0.8$) and 4-chlorostyrene ($Q = 1.03$, $e = -0.33$):

(a) Calculate the reactivity ratios for styrene and 4-chlorostyrene.

(b) Plot the instantaneous copolymer composition as a function of monomer concentration in the copolymerization mixture.

(c) Comment on the expected monomer sequence distribution in the resulting copolymer.

2–5. If the number-average degree of polymerization for polystyrene obtained by the bulk polymerization of styrene at 60°C is 1000, what would be the number-average degree of polymerization if the polymerization were conducted in a 10% solution in toluene (900 g of toluene per 100 g of styrene) under otherwise identical conditions? The molecular weights of styrene and toluene are 104.12 and 92.15, respectively.

2–6. Assume that a polyesterification is conducted in the absence of solvent or catalyst and that the monomers are present in stoichiometric ratios. Calculate the time (min) required to obtain a number-average degree of polymerization of 50 given that the dicarboxylic acid concentration is 3 mol L^{-1} and that the polymerization rate constant is 10^{-2} L mol^{-1} s^{-1}.

3

Solution Properties, Thermodynamics, and Molecular-Weight Determination

Solvents are frequently used during the polymerization process (Chapter 2), during fabrication (i.e., film casting, fiber formation, and coatings), and for the determination of molecular weight and molecular-weight distribution. Interactions between a polymer and solvent influence chain dimensions (i.e., conformations) and, more importantly, determine solvent activities. The measurement of osmotic pressure and scattered-light intensity from dilute polymer solutions — techniques based upon the principles of polymer-solution thermodynamics — are the primary methods used to determine number-average and weight-average molecular weights, respectively. Other solution-property techniques, such as the determination of intrinsic viscosity and gel-permeation chromatography (GPC), are widely used as rapid and convenient methods to determine polymer molecular weight and, in the case of GPC, molecular-weight distribution as described in this chapter.

3.1 POLYMER CONFORMATION AND CHAIN DIMENSIONS

As briefly discussed in Chapter 1, the *configuration* of a polymer chain refers to the stereochemical arrangement of atoms along that chain. Examples include tactic and geometric isomers, which are determined by the mechanism of the polymerization and, therefore, cannot be altered without breaking primary valence bonds. In contrast, polymer chains in solution are free to rotate around individual bonds, and almost a limitless number of *conformations* or chain orientations in three-dimensional space are possible for long, flexible macromolecules.

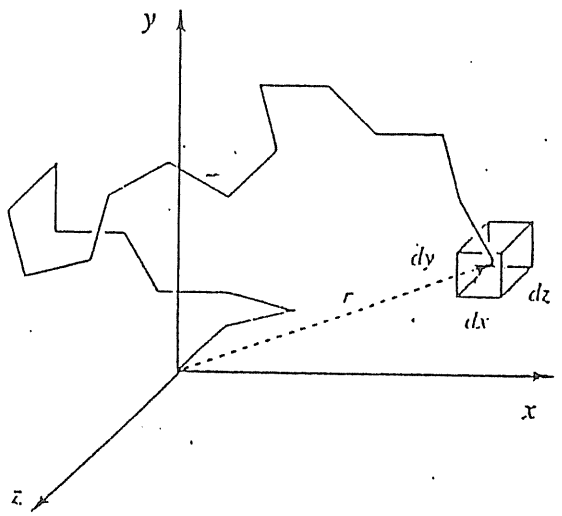

Figure 3.1. Illustration of a random conformation of an idealized freely jointed polymer chain having 20 segments of equal length. The end-to-end distance of this conformation is indicated as r. With one end of the chain fixed at the origin of the Cartesian coordinate-system, the probability of finding the other end in some infinitesimal volume element ($dV = dx \cdot dy \cdot dz$) is expressed by the Gaussian distribution-function given by eq 3.2.

To describe the conformation of polymer molecules, a model of a *random-flight* or *freely jointed* and *volumeless* chain is often used as the starting point. Such a hypothetical chain is assigned n freely jointed links of equal length, ℓ. If one end of this hypothetical chain is fixed at the origin of a Cartesian coordinate-system, the other end of the chain has some finite probability of being at any other coordinate position, as illustrated by Figure 3.1. One of the many possible conformations, and the simplest, for this idealized chain is the fully extended (linear) chain where the end-to-end distance, r, is

$$r = n\ell. \tag{3.1}$$

Flory[1] was the first to derive an expression for the probability of finding one end of the freely jointed polymer chain in some infinitesimal volume ($dV = dx\,dy\,dz$) around a particular coordinate (x, y, z) point when one end of the chain is fixed at the origin of a Cartesian coordinate-system, as illustrated in Figure 3.1. The probability is given as a *Gaussian distribution function* in the form

$$\omega(x,y,z) = \left(\frac{b}{\pi^{1/2}}\right)^3 \exp\left(-b^2 r^2\right) \tag{3.2}$$

where r is the radius of a spherical shell centered at the origin

$$r^2 = x^2 + y^2 + z^2 \tag{3.3}$$

and

$$b^2 = \frac{3}{2n\ell^2} \tag{3.4}$$

Alternately, a *radial-distribution function* is obtained by multiplying $\omega(x,y,z)$ by the volume of a spherical shell of thickness dr (i.e., by $4\pi r^2 dr$):

$$\omega(r) = \left(\frac{b}{\pi^{1/2}}\right)^3 \exp\left(-b^2 r^2\right) 4\pi r^2. \tag{3.5}$$

The radial-distribution function for a freely jointed polymer chain consisting of 10^4 freely jointed links each of length 2.5 Å is plotted as a function of the radial distance, r, in Figure 3.2.

A mean-square end-to-end distance can be obtained from the second moment of the radial-distribution function:

$$\left\langle r^2 \right\rangle = \frac{\int_0^\infty r^2 \omega(r)\,dr}{\int_0^\infty \omega(r)\,dr}. \tag{3.6}$$

Substitution of the radial distribution function (eq. 3.5) into eq. 3.6 and evaluating the integral gives the mean-square end-to-end distance of the freely jointed and volumeless chain as

$$\boxed{\left\langle r^2 \right\rangle = n\ell^2}. \tag{3.7}$$

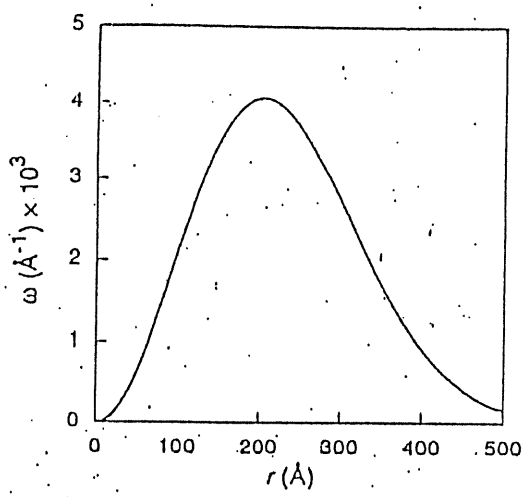

Figure 3.2. The radial-distribution function calculated (eq. 3.5) for a hypothetical polymer chain consisting of 10^4 freely jointed segments of length 2.5 Å.

Alternately, the *root*-mean-square end-to-end distance, $\langle r^2 \rangle^{1/2}$, of the freely rotating chain is given as

$$\left\langle r^2 \right\rangle^{1/2} = n^{1/2}\ell. \tag{3.8}$$

Real polymer chains differ from the above idealized, freely jointed model in the following three significant ways:

- *Valence angles of real bonds are fixed.* For example, the tetrahedrally bonded C–C bond angle is 109.5°. Introducing fixed bond angles results in an expansion of the chain expressed by the mean-square end-to-end distance as

$$\left\langle r^2 \right\rangle = n\ell^2 \frac{1-\cos\theta}{1+\cos\theta} \tag{3.9}$$

where θ is the valence bond angle, as illustrated for an extended chain conformation in Figure 3.3. For the tetrahedral angle, $\theta = 109.5°$, $\cos\theta = -1/3$, and therefore

$$\left\langle r^2 \right\rangle = 2n\ell^2. \tag{3.10}$$

Comparison of this result with that of eq. 3.7 indicates that the fixed valence angle restriction results in a doubling of the mean-square end-to-end distance over that of a freely rotating chain.

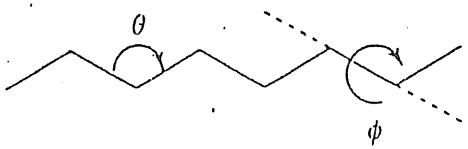

Figure 3.3. Illustration of an extended polymer chain showing the valence bond angle, θ, and bond-rotation angle, ϕ.

Rotations of polymer chains may be restricted due to interference from bulky substituent groups, as illustrated by the potential-energy diagram shown in Figure 3.4. The result of steric interference is to further expand chain dimensions over the random-flight model. Equation 3.7 may be further modified to include the effects of both fixed bond angles and hindered rotations as

$$\langle r^2 \rangle = n\ell^2 \frac{1-\cos\theta}{1+\cos\theta} \frac{1+\langle\cos\phi\rangle}{1-\langle\cos\phi\rangle} \qquad (3.11)$$

where $\langle\cos\phi\rangle$ represents the average cosine of the bond-rotation angle, ϕ, identified in Figure 3.3. This second contribution is a much more difficult one to evaluate but can be obtained by statistical-weighting methods, as discussed by Flory.[2]

Real chain bonds have a finite (van der Waals) volume and therefore some volume is *excluded*. This means that a real bond cannot occupy the same space of any other bond — a condition not imposed in the random-flight model. As in the case of restricted rotation, the effect of excluded volume is to increase the spatial dimensions of the polymer chain over that of the random-flight model.

Beyond the calculation of mean-square end-to-end distances, the conformations of realistic polymer models can be simulated by computer. For example, Figure 3.5 shows the results of a Monte Carlo simulation of the conformation of a small polyethylene chain having 200 skeletal bonds using values of actual bond lengths, bond angles, and the known preference for *trans*-rotational states for this polymer.[3]

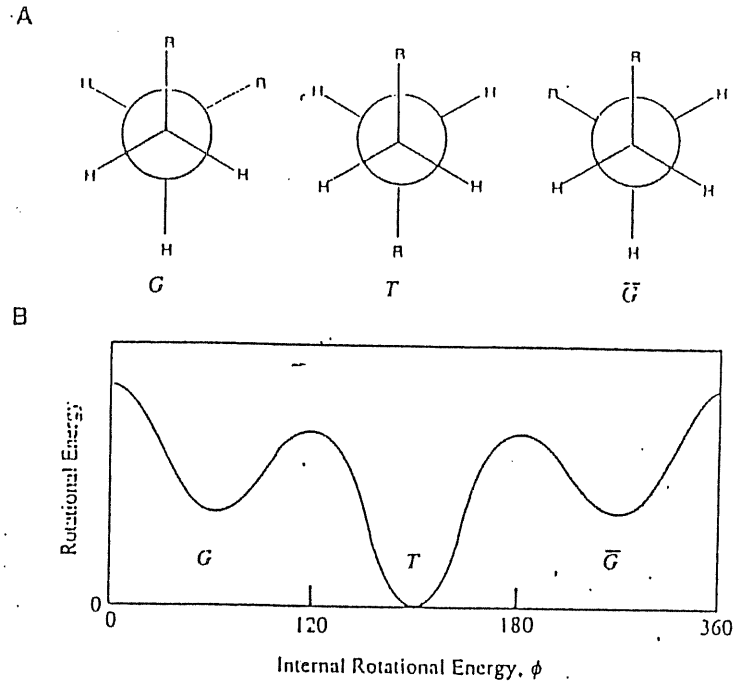

Figure 3.4. A. Three low-energy projections of two adjacent bond atoms with substituent group, R. In the case of a polymer chain, R represents all chain segments before and after the bond in question. B. Potential-energy diagram illustrating the three lowest energy rotational states — *trans* (T) and the two *gauche* forms, G and $\bar{G}$.

As a convenient way to express the size of a real polymer chain in terms of parameters that can be readily measured, the freely rotating chain model (eq. 3.7) may be modified to include the effects of fixed bond angles, restricted rotation, and excluded volume on the root-mean-square end-to-end distance in the following way:

$$\langle r^2 \rangle^{1/2} = \alpha (nC_N)^{1/2} \ell. \qquad (3.12)$$

In this expression, α is called the *chain expansion factor* which is a measure of the effect of excluded volume, and C_N is called the *characteristic ratio*, which contains the contributions from both fixed valence angles and restricted chain rotation. For large polymer chains, typical values of C_N range from about 5 to 10. Another way to represent eq. 3.12 is by use of an *unperturbed* root-mean-square end-to-end distance, $\langle r^2 \rangle_o^{1/2}$, as

$$\langle r^2 \rangle^{1/2} = \alpha \langle r^2 \rangle_0^{1/2} \tag{3.13}$$

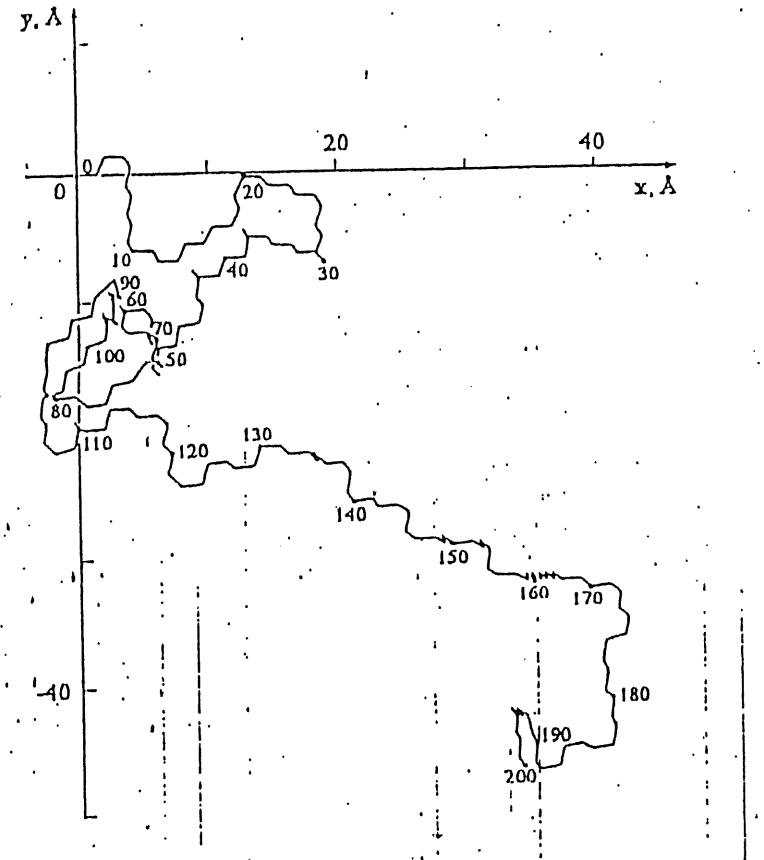

Figure 3.5. A three-dimensional computer simulation of a conformation of a small polyethylene chain (200 bonds) projected on the plane of the graph. (Reprinted with permission of the publisher from "Rubber Elasticity" by J. E. Mark. *Journal of Chemical Education*, 1981, 58, pp. 2898–2903.)

Comparison of eqs. 3.12 and 3.13 indicates that *unperturbed* dimensions are those of a real polymer chain in the absence of excluded-volume effects (i.e., for $\alpha = 1$). By equating eqs. 3.12 and 3.13, the characteristic ratio[†] is obtained as the ratio of the unperturbed mean-square end-to-end distance to the mean-square end-to-end distance of the freely jointed model (eq. 3.7)

$$C_N = \frac{\langle r^2 \rangle_0}{nl^2}. \tag{3.14}$$

Unperturbed dimensions are realized in the case of a polymer in solution with a thermodynamically-poor solvent at a temperature near incipient precipitation. This temperature is called the *theta* (θ) temperature. Experiments, using small-angle neutron scattering, have indicated that the dimensions of polymer chains in the amorphous solid-state are also unperturbed. In solution with a good solvent (i.e., $\alpha > 1$), where polymer–solvent interactions are stronger than polymer–polymer or solvent–solvent interactions, dimensions of the polymer chain are expanded over those in the unperturbed state ($\alpha = 1$).

3.2 THERMODYNAMICS OF POLYMER SOLUTIONS

In 1942, Gee and Treloar[4] reported that even dilute polymer solutions deviated strongly from ideal-solution behavior. In these early experiments, a high molecular-weight rubber was equilibrated with benzene vapor in a closed system and the partial pressure of the benzene (the solvent), p_1, was measured. The solvent activity, a_1, was calculated as the ratio of p_1 to the saturated vapor pressure of pure benzene, p_1°, at the system temperature as[†]

---

[1] The characteristic ratio can be calculated from a knowledge of actual valence angles, θ, and the statistical weighting of torsional angles ϕ (see eq. 3.11), as[2]

$$C_N = \frac{1-\cos\theta}{1+\cos\theta}\,\frac{1+\langle\cos\phi\rangle}{1-\langle\cos\phi\rangle}.$$

[†] By definition, the activity of the ith component in a mixture is defined as

$$a_i = \frac{\hat{f}_i}{f_i^\circ}$$

where $\hat{f}_i$ is the fugacity of that component in the mixture and f_i° is the standard-state fugacity, usually the fugacity of the pure liquid component at the system temperature. In the limit of low pressure at which the vapor mixture becomes ideal, the two fugacities may be replaced by the corresponding pressure terms (i.e., $\hat{f}_i = p_i = x_i p$ and $f_i^\circ = p_i^\circ$). If the vapor phase is nonideal, the solvent activity can be obtained from the relationship[5]

$$a_1 = \frac{p_1}{p_1^\circ}\exp\left[-\frac{B}{RT}\left(p_1^\circ - p_1\right)\right]$$

where B is the second virial coefficient of the pure vapor at the system temperature.

$$a_1 = \frac{p_1}{p_1^0}. \tag{3.15}$$

Experimental benzene activity is plotted as a function of the volume fraction of rubber, ϕ_2, in Figure 3.6. These data are compared with predictions of *Raoult's law* for an ideal solution given as

$$p_1 = x_1 p_1^0, \tag{3.16}$$

where x_1 is the mole fraction of the solvent. Substitution of eq. 3.16 into eq. 3.15 yields the result that $a_1 \equiv x_1$ for an ideal solution. As the experimental data (Figure 3.6) show, polymer-solution behavior follows a strong *negative* deviation from Raoult's ideal-solution law.

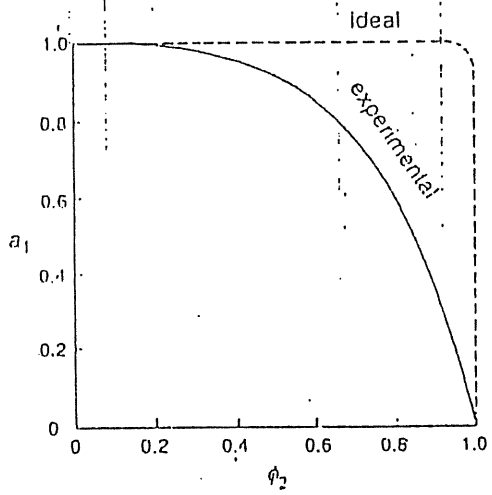

Figure 3.6. Plot of benzene activity, a_1, versus volume fraction of rubber, ϕ_2. Dashed line represents ideal-solution behavior. (Adapted from ref 1 by permission of the publisher.)

3.2.1 The Flory–Huggins Theory

In the early 1940s, Paul Flory[6] and Maurice Huggins,[7] working independently, developed a theory based upon a simple lattice model that could be used to understand the nonideal nature of polymer solutions. In the *Flory–Huggins model*, the lattice sites, or holes, are chosen to be the size of the solvent molecule. As the simplest example, consider the mixing of a low-molecular-weight solvent (component 1) with a low-molecular-weight solute (component 2). The solute molecule is assumed to have the same size as a solvent molecule, and therefore only one solute or one solvent molecule can occupy a single lattice site at a given time. A representation of the lattice model for this case is illustrated in Figure 3.7.

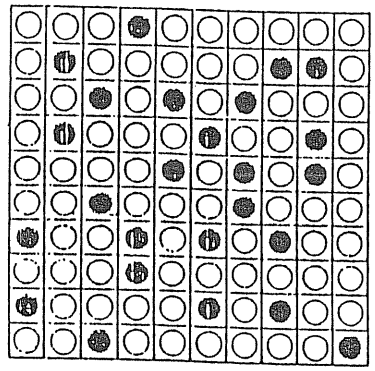

Figure 3.7. Representation of two-dimensional Flory–Huggins lattice containing solvent molecules (○) and a low-molecular-weight solute (●).

The increase in entropy due to mixing of a solvent and solute, ΔS_m, may be obtained from the *Boltzmann relation*

$$\Delta S_m = k \ln \Omega \tag{3.17}$$

where k is Boltzmann's constant (1.38×10^{-23} J K^{-1}) and Ω gives the total number of ways of arranging n_1 solvent molecules and n_2 solute molecules, where $N = n_1 + n_2$ is the total number of lattice sites. The probability function is given as

$$\Omega = \frac{N!}{n_1! n_2!}. \tag{3.18}$$

Use of Stirling's approximation

$$\ln n! = n \ln n - n \tag{3.19}$$

leads to the expression for the entropy of mixing as

$$\Delta S_m = -k(n_1 \ln x_1 + n_2 \ln x_2). \tag{3.20a}$$

Alternately, the *molar* entropy of mixing can be written as

$$\boxed{\Delta S_m = -R(x_1 \ln x_1 + x_2 \ln x_2)} \tag{3.20b}$$

where R is the ideal gas constant[†] and x_1 is the mole fraction of the solvent given as

$$x_1 = \frac{n_1}{n_1 + n_2}. \tag{3.21}$$

Equation 3.20 is the well-known relation for the entropy change due to mixing of an *ideal* mixture, which can also be obtained from classical thermodynamics of an ideal solution following the Lewis–Randall law.[‡] Equation 3.20 can be written for a multicomponent system having N components as

$$\Delta S_m^{id} = -R \sum_{i=1}^{N} x_i \ln x_i. \tag{3.22}$$

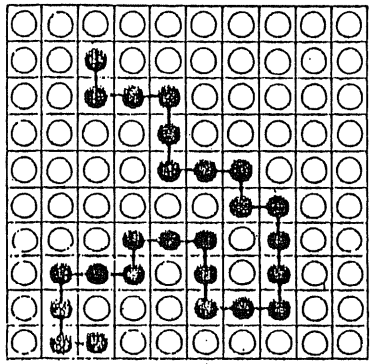

Figure 3.8. Lattice model for a polymer chain in solution. Symbols represent solvent molecules (○) and polymer-chain segments (●).

The entropy of mixing a low-molecular-weight solvent with a *high*-molecular-weight *polymer* is smaller than given by eq. 3.20 for a low-molecular-weight mixture. This is due to the loss in conformational entropy resulting from the linkage of individual repeating units along a polymer chain compared to the less ordered case of unassociated low-molecular-weight solute-molecules dispersed in a low-molecular-weight solvent. In the development of an expression for ΔS_m for a high-molecular-weight polymer in a solvent, the lattice is established by dividing the polymer chain into r segments, each the size of a solvent molecule, where r is the

---

[†] $R = N_A k$ where N_A is Avogadro's number.

[‡] The relationship between the partial-molar Gibbs free-energy and fugacity is given as

$$d\overline{G}_i = d\mu_i = RT d \ln \hat{f}_i.$$

Integration from the standard state to some arbitary state gives

$$\overline{G}_i - \overline{G}_i^{\circ} = \overline{\Delta G}_i = RT \ln \frac{\hat{f}_i}{f_i^{\circ}}$$

where $\hat{f}_i$ is the fugacity of component i in a mixture and f_i° is the standard-state fugacity. Substitution of the Lewis–Randall law

$$\hat{f}_i^{id} = x_i f_i^{\circ}$$

gives

$$\overline{\Delta G}_i^{id} = RT \ln x_i.$$

Since the thermodynamic properties of a solution are the sum of the product of the mole fraction and the partial-molar property of each of m components in the mixture, it follows that the molar change in Gibbs free energy of an ideal solution is then expressed as

$$\boxed{\Delta G^{id} = RT \sum_{i=1}^{m} x_i \ln x_i}.$$

Since

$$\overline{\Delta G}_i^{id} = \overline{\Delta H}_i^{id} - T\overline{\Delta S}_i^{id}$$

and $\overline{\Delta H}_i^{id} = 0$ for an ideal solution, we have

$$\overline{\Delta S}_i^{id} = -\frac{1}{T}\overline{\Delta G}_i^{id} = -R \ln x_i$$

and

$$\boxed{\Delta S^{id} = -R \sum_{i=1}^{m} x_i \ln x_i}.$$

ratio of polymer volume to solvent volume. For n_2 polymer molecules, the total number of lattice sites is then $N = n_1 + rn_2$. A lattice containing low-molecular-weight solvent molecules and a single polymer-chain is illustrated in Figure 3.8.

Without going into details of the derivations,[1] the expression for the entropy change due to mixing obtained by Flory and Huggins is given as

$$\Delta S_m = -k(n_1 \ln \phi_1 + n_2 \ln \phi_2) \tag{3.23}$$

where ϕ_1 and ϕ_2 are the lattice *volume* fractions of solute (component 1) or polymer (component 2), respectively. These are given as

$$\phi_1 = \frac{n_1}{n_1 + rn_2} \tag{3.24a}$$

and

$$\phi_2 = \frac{rn_2}{n_1 + rn_2}. \tag{3.24b}$$

For a polydisperse polymer, eq. 3.23 may be modified as

$$\Delta S_m = -k\left(n_1 \ln \phi_1 + \sum_{i=2}^{N} n_i \ln \phi_i\right) \tag{3.25}$$

where the summation is over all polymer chains (N) in the molecular-weight distribution. For simplicity, the most commonly used form of the entropy expression, eq. 3.23, will be used in further discussion. Equation 3.23 provides the entropy term in the expression for the Gibbs free energy of mixing, ΔG_m, of a polymer solution given as

$$\Delta G_m = \Delta H_m - T\Delta S_m. \tag{3.26}$$

Once an expression for the enthalpy of mixing, ΔH_m, is known, expressions for the chemical potential and activity of the solvent can be obtained as

$$\Delta\mu_1 = \mu_1 - \mu_1^\circ = \overline{\Delta G}_m = \left(\frac{\partial \Delta G_m}{\partial n_1}\right)_{T,P} \tag{3.27}$$

[1] An excellent review of the development of the lattice model is given by Flory.[8]

where $\overline{\Delta G}_m$ is the partial-molar Gibbs free energy of mixing and the activity is related to the chemical potential as

$$\ln a_1 = \frac{\Delta\mu_1}{kT}. \tag{3.28}$$

For an ideal solutions, $\Delta H_m = 0$. Solutions for which $\Delta H_m \neq 0$ but for which ΔS_m is given by eq. 3.20 are termed *regular* solutions and are the subject of most thermodynamic models for polymer mixtures. The expression that Flory and Huggins gave for the enthalpy of mixing is

$$\Delta H_m = z n_1 r_1 \phi_2 \Delta\omega_{12} \tag{3.29}$$

where z is the lattice coordination number or number of cells that are first neighbors to a given cell, r_1 represents the number of "segments" in a solvent molecule for consideration of the most general case, and $\Delta\omega_{12}$ is the change in internal energy for formation of an unlike molecular pair (solvent–polymer or 1–2) contacts given by the *mean-field expression* as

$$\Delta\omega_{12} = \omega_{12} - \frac{1}{2}(\omega_{11} + \omega_{22}) \tag{3.30}$$

where ω_{ij} is the energy of i–j contacts. It is clear from eqs. 3.29 and 3.30 that an ideal solution ($\Delta H_m = 0$) is one for which the energies of 1–1, 1–2, and 2–2 molecular interactions are equal.

Since z and ω_{12} have the character of empirical parameters, it is convenient to define a single energy parameter called the Flory *interaction parameter*, χ_{12}, given as

$$\chi_{12} = \frac{z r_1 \Delta\omega_{12}}{kT}. \tag{3.31}$$

The interaction parameter is a dimensionless quantity that characterizes the interaction energy per solvent molecule (having r_1 segments) divided by kT. As eq. 3.31 indicates, χ_{12} is inversely related to temperature but is independent of concentration.

The expression for the enthalpy of mixing may then be written by combining eqs. 3.29 and 3.31 as

$$\Delta H_m = kT\chi_{12} n_1 \phi_2. \tag{3.32}$$

Combining the expression for the entropy (eq. 3.23) and enthalpy (eq. 3.32) of mixing gives the well-known Flory–Huggins expression for the Gibbs free energy of mixing

$$\boxed{\Delta G_m = kT\left(n_1 \ln \phi_1 + n_2 \ln \phi_2 + \chi_{12} n_1 \phi_2\right)} \quad (3.33)$$

From this relationship, the activity of the solvent (eq. 3.28) can be obtained from eq. 3.33 as

$$\ln a_1 = \ln\left(1-\phi_2\right) + \left(1-\frac{1}{r}\right)\phi_2 + \chi_{12}\phi_2^2. \quad (3.34)$$

In the case of high-molecular-weight polymers for which the number of solvent-equivalent segments, r,[†] is large, the $1/r$ term within parentheses on the right-hand side of eq. 3.34 can be neglected to give

$$\boxed{\ln a_1 = \ln\left(1-\phi_2\right) + \phi_2 + \chi_{12}\phi_2^2} \quad (3.35)$$

The Flory–Huggins equation is still widely used and has been largely successful in describing the thermodynamics of polymer solutions; however, there are a number of important limitations of the original expression that should be emphasized. The most important are the following:

- Applicability only to solutions that are sufficiently concentrated that they have uniform segment-density.
- There is no volume change of mixing (whereas favorable interactions between polymer and solvent molecules should result in a *negative* volume change).
- There are no energetically-preferred arrangements of polymer segments and solvent molecules in the lattice.

There have been a number of subsequent developments to extend the applicability of the original Flory–Huggins theory and to improve agreement between theoretical and experimental results. For example, Flory and Krigbaum have developed a thermodynamic theory for dilute polymer solutions, which was given in Flory's original text.[1] Koningsveld[9] and others have improved the agreement of the original Flory–Huggins theory with experimental data by an empirical modification of χ_{12} to include a composition dependence and to account for polymer polydispersity. Both of these approaches are presented briefly in the following section. More recent approaches employ equation-of-state theories such as those developed by Flory[8] and others for which a volume change of mixing can be incorporated. These are developed later in Section 3.2.3.

[†] For a polymer sample with a distribution of molecular weights, r may be taken to be the number-average degree of polymerization, $\overline{X}_n$.

3.2.2 Flory–Krigbaum and Modified Flory–Huggins Theory

Flory–Krigbaum Theory. Flory and Krigbaum[10] have provided a model to describe the thermodynamics of a dilute polymer solution in which individual polymer chains are isolated and surrounded by regions of solvent molecules. In contrast to the case of a semidilute solution addressed by the Flory–Higgins theory, segmental density can no longer be considered to be uniform. In their development, Flory and Krigbaum viewed the dilute solution as a dispersion of clouds consisting of polymer segments surrounded by regions of pure solvent. For a dilute solution, the expression for solvent activity was given as

$$\ln a_1 = \left(\kappa_1 - \psi_1\right)\phi_2^2 \quad (3.36)$$

where κ_1 and ψ_1 are heat and entropy parameters,[†] respectively. They defined an "ideal" or *theta* (θ) temperature as

$$\theta = \frac{\kappa_1 T}{\psi_1} \quad (3.37)$$

from which eq. 3.36 can be written as

$$\ln a_1 = -\psi_1\left(1-\frac{\theta}{T}\right)\phi_2^2. \quad (3.38)$$

It follows from eq. 3.38 that solvent activity approaches unity as temperature approaches the θ temperature. At the θ temperature, the dimensions of a polymer chain collapse to unperturbed dimensions (i.e., in the absence of excluded-volume effects), as described in Section 3.1.

Modified Flory–Huggins. In the original lattice theory, χ_{12} was given an inverse dependence upon temperature (eq. 3.31) but there was no provision for a concentration dependence which experimental studies has shown to be important. Koningsveld[9] and others have introduced an empirical dependence to improve the agreement with experimental data by casting the Flory–Huggins expression in the general form

$$\Delta G_m = RT\left(\phi_1 \ln \phi_1 + \phi_2 \ln \phi_2 + g\phi_1\phi_2\right). \quad (3.39)$$

In eq. 3.39, g is an interaction energy term for which the concentration dependence can be given as a power series in ϕ_2 as

[†] $\overline{\Delta H}_1 = RT\kappa_1\phi_2^2$; $\overline{\Delta S}_1 = R\psi_1\phi_2^2$.

$$g = g_0 + g_1\phi_2 + g_2\phi_2^2 + \cdots \tag{3.40}$$

where each g term, g_k ($k = 0, 1, 2...$), has a temperature dependence that can be expressed in the form

$$g_k = g_{k,1} + \frac{g_{k,2}}{T}. \tag{3.41}$$

3.2.3 Equation-of-State Theories

Although the Flory–Huggins theory is still useful as a starting point for describing polymer thermodynamics, there are a number of weaknesses. For example, the simple lattice model does not accommodate a volume change of mixing, which can be significant in the case of a thermodynamically-good solution. Such an inability to incorporate a volume change of mixing can lead to particular weakness in the prediction of phase equilibria. Substantial improvement in the theoretical treatment of polymer thermodynamics has been obtained by adopting a statistical-thermodynamics approach based upon an equation of state (EOS) as first proposed by Flory.[11] Other successful EOS theories have been proposed by Sanchez[12] and by Simha.[13] For the purpose of providing an introduction to the use of EOS theories in the treatment of polymer thermodynamics, only the Flory EOS-theory, which was the first and is still widely used, is described in this section.

Flory Equation of State. Thermodynamic variables in statistical thermodynamics are obtained from a suitable partition function which can be simple or complex function depending upon the size and physical state of the molecule being considered. The simplest partition functions are obtained for monatomic and diatomic gases such as helium and nitrogen. The partition function chosen by Flory for the polymer was obtained from contributions by internal (i.e., intramolecular chemical-bond forces) and external (i.e., intermolecular forces) degrees of freedom. The internal contribution is dependent upon temperature, while the external contribution is dependent upon both temperature and volume. The Flory partition function can be given in reduced form as[7]

$$Z = Z_{comb}\left(g\upsilon^*\right)^{rnc}\left(\tilde{\upsilon}^{1/3} - 1\right)^{3nc} \exp\left(rnc / \tilde{\upsilon}\tilde{T}\right). \tag{3.42}$$

Here, Z_{comb} is a combinatory factor, g is an inconsequential geometric factor, υ^* is a characteristic (specific) volume per segment (usually called the hard-core or closed-packed volume), $\tilde{\upsilon}$ is a reduced volume per segment defined in terms of the characteristic volume, r is the mean number of segments per molecule, n is the number of molecules (or mers), c is the mean number of external degrees of freedom per segment,[†] and $\tilde{T}$ is a reduced temperature as defined later. The exponential

[†] The total number of degrees of freedom in the system is $3rnc$.

term in eq. 3.42 is related to the configurational or mean potential energy (in van der Waals form), which is inversely proportional to volume.

Statistical thermodynamics provides the following equation to obtain an EOS from the partition function:

$$p = kT\left(\frac{\partial \ln Z}{\partial V}\right)_T. \tag{3.43}$$

The resulting EOS obtained from the partition function given by eq. 3.42 is given in reduced form as

$$\boxed{\frac{\tilde{p}\tilde{\upsilon}}{\tilde{T}} = \frac{\tilde{\upsilon}^{1/3}}{\tilde{\upsilon}^{1/3} - 1} - \frac{1}{\tilde{T}\tilde{\upsilon}}} \tag{3.44}$$

where $\tilde{p}$ is the reduced pressure. The reduced parameters are defined in terms of the characteristic parameters (three EOS parameters, υ^*, T^*, and p^*, for each of the pure components) as

$$\tilde{\upsilon} = \frac{\upsilon}{\upsilon^*} \tag{3.45}$$

$$\tilde{T} = \frac{T}{T^*} = \frac{2\upsilon^* cRT}{s\eta} \tag{3.46}$$

and

$$\tilde{p} = \frac{p}{p^*} = \frac{2p\upsilon^{*2}}{s\eta}. \tag{3.47}$$

where c represents the mean number of external degrees of freedom per segment, s is the number of contact sites per segment, and η is an energy parameter characterizing a pair of sites in contact. The characteristic parameters can be obtained from experimental PVT data.[‡] Representative values for Flory EOS-parameters evaluated

[‡] Differentiation of the EOS (eq. 3.44) with respect to temperature at constant pressure yields at zero pressure the characteristic hard-core volume as

$$\upsilon^* = \upsilon\left[\frac{3+3\alpha T}{3+4\alpha T}\right]^3.$$

Differentiation of the EOS with respect to temperature at constant volume yields at zero pressure the characteristic pressure

at 25°C for four low-molecular-weight organic compounds and for four polymers are given in Table 3.1. In general, v^* and T^* increase with increasing temperature while p^* decreases.

TABLE 3.1 REPRESENTATIVE VALUES OF FLORY EQUATION-OF-STATE PARAMETERS AT 25°C

Polymer	v^* (cm^3 g^{-1})	T^* (K)	p^* (J cm^{-3})
Toluene	0.9275	5197	547
Cyclohexane	1.0012	4721	530
Benzene	0.8860	4709	628
Methyl ethyl ketone	0.9561	4555	582
Polystyrene	0.8098	7420	547
Polydimethylsiloxane	0.8395	5530	341
Natural rubber	0.9432	6775	519
Polyisobutylene	0.9493	7580	448

Adaptation of the Flory EOS to *mixtures* is based upon the following two premises:

$$p_i^* = \gamma T \tilde{v}^2 = (\alpha/\beta) T \tilde{v}^2$$

where α is the *thermal-expansion coefficient*

$$\alpha = \frac{1}{V}\left(\frac{\partial V}{\partial T}\right)_p.$$

β is the *compressibility coefficient*

$$\beta = -\frac{1}{V}\left(\frac{\partial V}{\partial p}\right)_T.$$

and γ is the *thermal-pressure coefficient*

$$\gamma = \left(\frac{\partial p}{\partial T}\right)_V.$$

Finally, the characteristic temperature is obtained from the EOS by letting $\tilde{p} = 0$:

$$T^* = \frac{T\tilde{v}^{4/3}}{\tilde{v}^{1/3} - 1}.$$

1. Core volumes of the solution components are additive.

$$v^* = \frac{n_1 v_1^* + n_2 v_2^*}{n_1 + n_2} \tag{3.48}$$

2. The intermolecular energy depends on the *surface* area of contact between molecules and/or segments.

Since a segment is an arbitrary unit, the segment size can be chosen such that $v_1^* = v_2^* = v^*$. This gives the following mixing rules for the mixture:

$$\frac{1}{r} = \frac{\phi_1}{r_1} + \frac{\phi_2}{r_2} \tag{3.49}$$

where ϕ_1 and ϕ_2 are *segment* (or *core-volume*) *fractions*:

$$\phi_1 = 1 - \phi_2 = \frac{n_1 v_1^*}{n_1 v_1^* + n_2 v_2^*}. \tag{3.50}$$

The *number of contact sites*, s, for the mixture is given as

$$s = \phi_1 s_1 + \phi_2 s_2 \tag{3.51}$$

where s_i is the *surface area* of a segment of component i. In a similar manner, the mean number of external degrees of freedom for the mixture can be written as

$$c = \phi_1 c_1 + \phi_2 c_2. \tag{3.52}$$

The *site fraction* is defined as

$$\theta_2 = 1 - \theta_1 = \frac{\phi_2 s_2}{s}. \tag{3.53}$$

The *characteristic pressure* for the mixture is given as

$$p^* = \phi_1 p_1^* + \phi_2 p_2^* - \phi_1 \theta_2 X_{12} \tag{3.54}$$

where X_{12} is called the *exchange interaction-parameter*, defined as

$$X_{12} = \frac{s_1(\eta_{11} + \eta_{22} - 2\eta_{12})}{2v^{*2}} = \frac{s_1 \Delta\eta}{2v^{*2}} \tag{3.55}$$

where the η_{ij} terms are energy parameters for the i–j segment pairs and $\Delta\eta = \eta_{11} + \eta_{22} - 2\eta_{12}$. The exchange interaction-parameter is analogous to $\Delta\omega_{12}$ in the Flory–Huggins theory (eq. 3.30) but has the dimensions of energy density. Finally, the *characteristic temperature* for the mixture is given as

$$T^* = \frac{\phi_1 p_1^* + \phi_2 p_2^* - \phi_1 \theta_2 X_{12}}{\dfrac{\phi_1 p_1^*}{T_1^*} + \dfrac{\phi_2 p_2^*}{T_2^*}}. \tag{3.56}$$

The EOS of the mixture is given in the same form as that of the pure component (eq. 3.44) except that the reduced parameters refer to those of the mixture. The reduced volume of the mixture, $\tilde{v}$, may be obtained from the EOS with $\tilde{p}$ set to zero for low pressures and $\tilde{T}$ defined by use of the characteristic temperature given by eq. 3.56 for the mixture. Subsequently, other important quantities can be calculated. For example, the molar enthalpy of mixing is given as

$$\Delta H_m = \frac{\theta_2 x_1 v_1^* X_{12}}{\tilde{v}} + x_1 v_1^* p_1^* \left(\frac{1}{\tilde{v}_1} - \frac{1}{\tilde{v}}\right) + x_2 v_2^* p_2^* \left(\frac{1}{\tilde{v}_2} - \frac{1}{\tilde{v}}\right) \tag{3.57}$$

where

$$x_1 = \frac{n_1}{n_1 + n_2}. \tag{3.58}$$

An important relationship is the Flory-EOS expression for $\Delta\mu_1$ given as

$$\Delta\mu_1 = RT\left[\ln\phi_1 + \left(1 - \frac{v_1^*}{v_2^*}\right)\phi_2\right] + \frac{\theta_2^2 v_1^* X_{12}}{\tilde{v}} + v_1^* p^* \left[3\tilde{T}_1 \ln\left(\frac{\tilde{v}_1^{1/3} - 1}{\tilde{v}^{1/3} - 1}\right) + \frac{1}{\tilde{v}_1} - \frac{1}{\tilde{v}}\right]. \tag{3.59}$$

Alternately, eq. 3.59 has been given in the form

$$\Delta\mu_1 = RT\left(\ln\phi_1 + \frac{1 - r_1}{r_2}\phi_2\right) + p^* v_1^* \left[3\tilde{T}_1 \ln\left(\frac{\tilde{v}_1^{1/3} - 1}{\tilde{v}^{1/3} - 1}\right) + \tilde{v}_1^{-1} - \tilde{v}^{-1} + \tilde{p}_1\left(\tilde{v} - \tilde{v}_1\right)\right] + \left(\chi_{12} - TQ_{12}\tilde{v}\right) v_1^* \frac{\theta_2^2}{\tilde{v}}. \tag{3.60}$$

The principal difference between eqs. 3.59 and 3.60 is the appearance of Q_{12} in the last term of eq. 3.60. This parameter is called the *noncombinational entropy correction* and generally is used as an adjustable parameter. Comparison of the standard Flory–Huggins relationship (eq. 3.34, where $\Delta\mu_1 = RT\ln a_1$ and $\phi_1 = 1 - \phi_2$) with the Flory EOS (eq. 3.59) shows that the first term within brackets in eq. 3.59 is simply a combinatory term. Despite its cumbersome form, the Flory-EOS theory provides substantial improvement over the earlier lattice theory. For example, the theory reasonably predicts an excess volume of mixing as

$$\frac{V^E}{V} = \frac{v^E}{\tilde{v}} = 1 - \frac{\phi_1 \tilde{v}_1 + \phi_2 \tilde{v}_2}{\tilde{v}}. \tag{3.61}$$

Furthermore, it is capable of modeling the complete range of the observed phase-behavior of polymer solutions, as discussed in the next section.

3.2.4 Phase Equilibria

Whether or not a polymer and solvent are mutually soluble, or *miscible*, is governed by the sign of the Gibbs free energy of mixing, ΔG_m, which is related to the enthalpy and entropy of mixing by eq. 3.26. Three different dependencies of ΔG_m on solution composition (i.e., volume fraction of polymer) at constant temperature are illustrated in Figure 3.9. If ΔG_m is positive over the entire composition range, as illustrated by curve I, the polymer and solvent are totally immiscible over the complete composition range and will coexist at equilibrium as two distinct phases. Two other possibilities are those of partial and total miscibility, as illustrated by curves II and III, respectively. For total miscibility, it is *necessary* that both

$$\Delta G_m < 0 \tag{3.62}$$

and that the second derivative of ΔG_m with respect to the volume fraction of solvent (component 1) or polymer (component 2) be greater than zero

$$\left(\frac{\partial^2 \Delta G_m}{\partial \phi_2^2}\right)_{p,T} > 0 \tag{3.63}$$

over the entire composition range. Both conditions for miscibility are satisfied by curve III but not curve II, which exhibits two minima in ΔG_m, and therefore the derivative criterion expressed by eq. 3.63 is not satisfied at all points along the ΔG_m–composition curve. A solution that exhibits such minima will phase-separate at equilibrium into two phases containing different compositions of both components. The compositions of the two phases are given by the points of common tangent as illustrated in Figure 3.9 where the composition of the solvent-rich phase is identified as ϕ_2^A and that of the polymer-rich phase as ϕ_2^B.

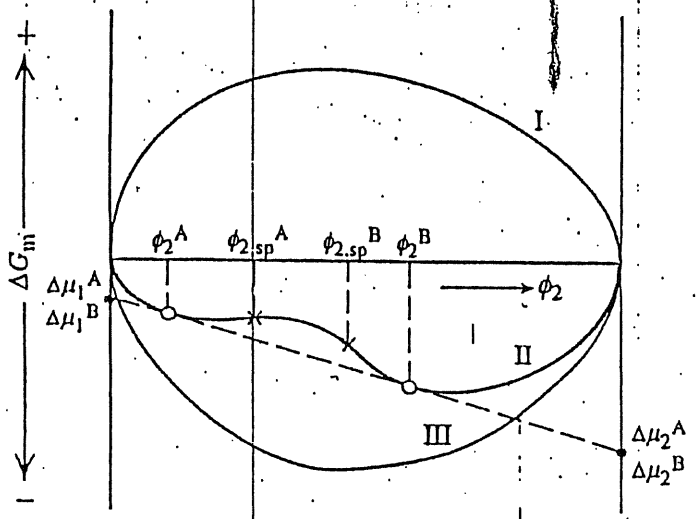

Figure 3.9. Idealized representation of three generalized possibilities for the dependence of the Gibbs free energy of mixing, ΔG_m, of a binary mixture on composition (volume fraction of polymer, ϕ_2) at constant pressure and temperature. I. Total immiscibility; II. partial miscibility; and III. total miscibility. Curve II represents the intermediate case of partial miscibility whereby the mixture will separate into two phases whose compositions (○) are marked by the volume-fraction coordinates, ϕ_2^A and ϕ_2^B, corresponding to points of common tangent to the free-energy curve. Spinodal points, compositions $\phi_{2,sp}^A$ and $\phi_{2,sp}^A$, occur at the points of inflection (×).

Phase equilibrium is strongly affected by solution temperature. In fact, any of three types of phase behavior illustrated in Figure 3.9 may result by a change in the temperature (or pressure) of the system. Our usual experience with solutions of low-molecular-weight compounds is that solubility increases with an increase in temperature as illustrated by the phase diagram shown in Figure 3.10. In this example, the solution is homogeneous (i.e., the two components are totally miscible) at temperatures above the point identified as UCST which stands for the *upper critical solution temperature* as described below. At lower temperatures (i.e., below the UCST), phase separation may occur depending upon the overall composition of the mixture. At a given temperature below the UCST (e.g., T_1), compositions lying *outside* the curves are those constituting a homogeneous phase, while those lying inside the curves are thermodynamically unstable and therefore the solution will phase-separate at equilibrium. The compositions of the two phases, identified as phases A and B, are given by points lying along the curve called the *binodal*. The binodal is the loci of points that satisfy the conditions for thermodynamic equilibrium of a binary mixture given as

$$\mu_1^A = \mu_1^B \tag{3.64a}$$

and

$$\mu_2^A = \mu_2^B. \tag{3.64b}$$

As the chemical potential is given by the derivative of the Gibbs free energy with respect to composition (eq. 3.27), the chemical potentials are obtained graphically from the intercepts of the common tangent drawn to curve II with the free energy axes as illustrated in Figure 3.9.

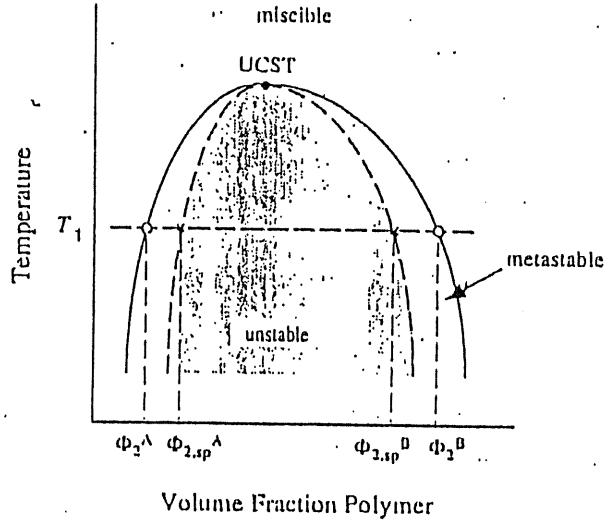

Figure 3.10. Representative phase diagrams for a polymer solution showing an upper critical solution temperature (UCST) (•), spinodal curve (– – – –), and binodal curve (———).

Between the binodal and the unstable region lies the *metastable* region, which is bounded by the *spinodal*. In the metastable region, the system can resist small concentration fluctuations but will eventually equilibrate to the stable two-phase state given by the binodal. Points lying along the spinodal correspond to the points of inflection identified in curve II of the free-energy diagram (Figure 3.9) and satisfy the relationship

$$\left(\frac{\partial^2 \Delta G_m}{\partial \phi_2^2}\right)_{p,T} = 0. \tag{3.65}$$

The binodal and spinodal coincide at the *critical point*, which satisfies the following equality for the third derivative of the Gibbs free energy with respect to composition:

$$\left(\frac{\partial^3 \Delta G_m}{\partial \phi_2^3}\right)_{p,T} = 0. \tag{3.66}$$

In the case of the upper critical solution temperature (UCST), the critical point lies at the top of the phase diagram as shown in Figure 3.10.

Although the UCST behavior of dilute polymer solutions had been observed for many years, it was not until 1961 that phase separation of polymer solutions was first reported to occur with an *increase* in temperature.[14] In this case, the binodal and spinodal curves coincide at a temperature and composition called the *lower critical solution temperature* or LCST. One serious limitation of the Flory–Huggins theory (Section 3.2.1) is that it fails to predict LCST behavior. The more recent equation-of-state theories (Section 3.2.3) are much more successful in predicting the entire range of phase behavior, as will be discussed in Section 7.2.1.

3.2.5 Determination of the Interaction Parameter

Experimentally, χ_{12} as well as the exchange interaction parameter, X_{12}, in the Flory EOS-theory can be determined by a variety of techniques, including several scattering methods as discussed in the next section and from the melting-point depression of semicrystalline polymers (Section 4.2.2). By far the most commonly used method to determine polymer–solvent as well as polymer–polymer interaction parameters (Chapter 7) has been inverse gas-chromatography or IGC.[15]

Inverse Gas-Chromatography. The term "inverse" is used to indicate that the substance being characterized constitutes the stationary phase (i.e., the bed packing) rather than the mobile phase, as is the case in traditional gas chromatography. The stationary phase is prepared by coating a thin layer of a polymer or polymer blend from a dilute solution onto a commercial packing material in the form of small beads. A fluidized bed sometimes is used in the coating process. The coated packing is vacuum dried to remove all residual solvent and then packed into a GC column which is heated to approximately 50°C above the glass-transition temperature (T_g). A solvent probe is then injected into the carrier gas (He or H_2), and the time for the probe to be eluted from the column is measured. During its passage, the probe is free to be sorbed into the liquid polymer coating of the packed bed. The extent of solubility (i.e., activity) is directly related to the retention time from which a *specific retention volume*, V_g, can be calculated. From this value, the infinite-dilution volume-fraction activity coefficient is then obtained as[16]

$$\ln \gamma_1^{\infty} = \ln\left(\frac{a_1}{\phi_1}\right)^{\infty} = \lim_{\phi_1 \to 0}\left(\frac{a_1}{\phi_1}\right) = \ln\left(\frac{273.16 R v_2}{V_g p_1^{\circ}}\right) - \frac{p_1^{\circ}(B_{11} - V_1)}{RT} \tag{3.67}$$

where ϕ_1 is the volume fraction of solvent (probe), p_1° is the vapor pressure of the probe (solvent) in the carrier gas, v_2 is the specific volume of the polymer, V_1 is the molar volume of the probe, and B_{11} is the second virial coefficient of the pure probe vapor at the measurement temperature. From measurement of γ_1^{∞} at different temperatures, the heat of mixing can be determined as

$$\Delta H_m = R\left[\frac{\partial \ln \gamma_1^{\infty}}{\partial (1/T)}\right]. \tag{3.68}$$

From eq. 3.67 and the Flory–Huggins equation (eq. 3.35), it is easily shown that the Flory interaction-parameter is obtained directly as

$$\chi_{12} = \ln\left(\frac{273.16 R v_2}{V_g p_1^{\circ} V_1}\right) - \frac{p_1^{\circ}(B_{11} - V_1)}{RT} - 1. \tag{3.69}$$

In a similar manner, the interaction energy, X_{12}, in the Flory equation of state also can be obtained.

3.2.6 Predictions of Solubilities

Solubility Parameters. As discussed in the previous section, there are a number of experimental methods by which approximate values of χ_{12} can be obtained; however, there is no theory by which values of χ_{12} can be *predicted* at the present time. One approach that can be used to estimate χ_{12}, and to predict solubility, in general is based upon the concept of the *solubility parameter*, δ, which was originally developed to guide solvent selection in the paint and coatings industry. The solubility parameter is related to the cohesive energy-density, E^{coh}, or the molar energy of vaporization of a pure liquid, ΔE^v, as

$$\boxed{\delta_i = \sqrt{E_i^{coh}} = \sqrt{\frac{\Delta E_i^v}{V_i}}} \tag{3.70}$$

where ΔE^v is defined as the energy change upon isothermal vaporization of the saturated liquid to the ideal gas state at infinite dilution[†] and V_i is the molar vol-

[†] The energy of vaporization is approximately related to the enthalpy of vaporization as

$$\Delta E_i^v = \Delta H_i^v - RT.$$

ume of the liquid. Units of δ are $(cal/cm^3)^{1/2}$ or $(MPa)^{1/2}$. Equation 3.70 can be used to calculate the solubility parameter of a pure solvent given values of ΔE^v and V_l. Since it is not reasonable to talk about an energy of vaporization for solid polymers, the solubility parameter of a polymer has to be indirectly determined or calculated by group-contribution methods. Experimentally, the solubility parameter of a polymer can be estimated by comparing the swelling of a crosslinked polymer sample immersed in different solvents. The solubility parameter of the polymer is taken to be that of the solvent resulting in the maximum swelling.

TABLE 3.2 REPRESENTATIVE MOLAR ATTRACTION CONSTANTS AT 25°C

	Molar Attraction Constant, F $(MPa)^{1/2}$ cm^3 mol^{-1}		
Group	Small[17]	Hoy[18]	van Krevelen[19]
$-CH_3$	438	303	420
$-CH_2-$	272	269	280
>CH–	57	176	140
>C<	-190	65.5	0
$-CH(CH_3)-$	495	(479)	560
$-C(CH_3)_2-$	686	(672)	840
–CH=CH–	454	497	444
>C=CH–	266	422	304
Phenyl	1504	1398	1517
p-Phenylene	1346	1442	1377
–O– (ether)	143	235	256
–OH	—	462	754
–CO– (ketones)	563	538	685
–COO– (esters)	634	668	512
–OCOO– (carbonate)	—	(904)	767
–CN	839	726	982
–N=C=O	—	734	—
–NH–	—	368	—
–S– (sulfides)	460	428	460
–F	(250)	84.5	164
–Cl (primary)	552	420	471
–Br (primary)	696	528	614
$-CF_3$ (*n*-fluorocarbons)	561	—	—
–Si–	-77	—	—

Alternately, the solubility parameter of a polymer can be estimated by use of one of several group-contribution methods, such as those given by Small[17] and by Hoy.[18] An extensive presentation of group-contribution methods for estimating polymer properties, including those for solubility parameters, is given by van Krevelen.[19] Calculation of δ by a group-contribution method requires the value of a molar attraction constant, F_i, for each chemical group in the polymer repeating-unit. Values of F_i have been obtained by regression analysis of physical property data for a large number of organic compounds (640 compounds in the case of Hoy[18]). In the case of Small, all compounds (e.g., hydroxyl compounds, amines, and carboxylic acids) in which hydrogen bonding occurs were excluded. A listing of some important molar attraction constants is given in Table 3.2.

TABLE 3.3 SOLUBILITY PARAMETERS OF SOME COMMON SOLVENTS AND POLYMERS[a]

	Solubility Parameter, δ	
	$(MPa)^{1/2}$	$(cal\ cm^{-3})^{1/2}$
Solvents		
n-Hexane	14.9	7.28
Carbon tetrachloride	17.8	8.70
Toluene	18.2	8.90
Benzene	18.6	9.09
Chloroform	19.0	9.29
Tetrahydrofuran	19.4	9.48
Chlorobenzene	19.6	9.58
Acetone	20.1	9.82
Methylene chloride	20.3	9.92
1,4-Dioxane	20.5	10.0
N-Methyl-2-pyrrolidone	22.9	11.2
Dimethylformamide	24.8	12.1
Methanol	29.7	14.5
Water	47.9	23.4
Polymers		
Polysulfone	20.3	9.92
Poly(vinyl chloride)	21.5	10.5
Polystyrene	22.5	11.0
Poly(methyl methacrylate)	22.7	11.1
Polyacrylonitrile	25.3	12.4

[a] Hansen solubility parameters (eq. 3.77) at 25°C.

The solubility parameter of a polymer is then calculated from these molar attraction constants and molar volume V_i (units of $cm^3\ mol^{-1}$), as

$$\delta_i = \frac{\sum_{i=1} F_i}{V_i} \tag{3.71}$$

where the summation is taken over all groups in the repeating unit. For this purpose, chemical groups are chosen to be the smallest uniquely identifiable groups in the polymer repeating unit such as methyl, methylene, phenyl, and halogen corresponding to those in Table 3.2. Calculated values of solubility parameters for some common solvents and polymers have been tabulated in a number of publications.[19–21] Some of these values are collected in Table 3.3. An example calculation is given next.

Example Problem 3.1

Estimate the solubility parameters, in units of $(MPa)^{1/2}$, for poly(methyl methacrylate) (PMMA) by the method of Small. The density of PMMA is reported to be 1.188 g cm^{-3} at 25°C.

Solution

The structure of PMMA is

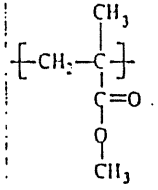

Review of the available chemical groups listed in Table 3.2 indicates that molar-attraction constants contributions for the repeating unit of PMMA can be given as follows:

Group	F	Number of Groups	$\sum F_i$
$-CH_3$	438	2	876
$-CH_2-$	272	1	272
>C<	-190	1	-190
-COO- (ester)	634	1	634
		$\sum F_i =$	1592

The formula weight of a PMMA repeating unit is calculated from atomic weights (Appendix F) as follows:

C:	$5 \times 12.01115 =$	60.06
O:	$2 \times 15.9994 =$	32.00
H:	$8 \times 1.00797 =$	8.06
		100.12

The molar volume, V, is then $100.12/1.188 = 84.28\ cm^3\ mol^{-1}$. The solubility parameter is then calculated as

$$\delta_i = \frac{\sum F_i}{V_i} = \frac{1592}{84.28} = 18.9\ (MPa)^{1/2}$$

Another approach that can be used to calculate δ is based upon knowledge of the equation of state, $V(p,T)$, for the polymer:[22]

$$\delta \equiv \sqrt{\frac{T\alpha}{\beta}} \tag{3.72}$$

where α is the (isobaric) *thermal-expansion coefficient*,

$$\alpha = \left(\frac{1}{V}\right)\left(\frac{\partial V}{\partial T}\right)_p \tag{3.73}$$

and β is the (isothermal) *compressibility coefficient*,[†]

$$\beta = -\left(\frac{1}{V}\right)\left(\frac{\partial V}{\partial P}\right)_T \tag{3.74}$$

Equations of state are now available for most commercial polymers.[21]

From values of the solubility parameters for the solvent and polymer, the heat of mixing can be *estimated* by the Scatchard[23]–Hildebrand[24] equation as

$$\Delta H_m = V(\delta_1 - \delta_2)^2 \phi_1 \phi_2 \tag{3.75}$$

[†] Since volume *decreases* with increasing pressure, the negative sign in eq 3.74 provides a positive value for β.

where V is the volume of the mixture. Making use of eq. 3.32, the interaction parameter can be estimated from this value of ΔH_m as†

$$\boxed{\chi_{12} \cong \frac{V_1}{RT}(\delta_1 - \delta_2)^2} \quad (3.76)$$

As the form of eq. 3.75 indicates, the solubility parameter approach can be used to estimate the heat of mixing when $\Delta H_m \geq 0$ but not when $\Delta H_m < 0$ (i.e., for exothermic heat of mixing).

The matching of polymer and solvent solubility parameters to minimize ΔH_m is a useful approach for solvent selection in many cases but often fails when specific interactions such as hydrogen bonding occur. To improve the prediction, two- and three-dimensional solubility parameters, which give individual contributions for dispersive (i.e., van der Waals), polar, and hydrogen bonding interactions, are sometimes used. In the case of the three-dimensional model proposed by Hansen,[25] the overall solubility parameter can be obtained as

$$\delta = \sqrt{\delta_d^2 + \delta_p^2 + \delta_h^2} \quad (3.77)$$

where δ_d, δ_p, and δ_h are the dispersive, polar, and hydrogen-bonding solubility parameters, respectively. Values of δ calculated from eq. 3.77 for common solvents and polymers were given in Table 3.3.

Activity Predictions. Once a value for the interaction parameter is known or can be estimated, the activity of a solvent in a polymer solution can be estimated by means of the Flory–Huggins equation (eq. 3.35). It is also possible to predict activity through a variety of chemical group-contribution methods, which have been reviewed recently.[26] The most fully developed of these methods is UNIFAC-FV.[27] The acronym UNIFAC stands for *UNI*QUAC *F*unctional-group *A*ctivity *C*oefficients, which had been widely used for the prediction of vapor–liquid equilibria (VLE) for mixtures of low-molecular-weight components,[28] and FV represents a free-volume contribution originating from the Flory EOS-theory. UNIQUAC, itself, is an acronym for *Uni*versal *Qua*si-*C*hemical equations, which provides good representation of both vapor–liquid equilibria (VLE) and liquid–liquid equilibria (LLE) for binary and multicomponent mixtures of nonelectrolytes using one or two adjustable (energy) parameters per binary pair.[29] The difference between UNIQUAC and UNIFAC or UNIFAC-FV is that UNIFAC uses the solution-of-functional groups (SOG) concept[30] to obtain group-contribution parameters (the adjustable parameters in UNIQUAC) from knowledge of the chemical groups comprising the mixture components in a manner similar to the way that solubility parameters are calculated by the methods of Small or Hoy as discussed in the previous section.

According to UNIFAC-FV, solvent activities may be calculated as contributions from three sources — a combinatorial (entropy) term, a residual (enthalpic term), and a (Flory EOS) free-volume term as

$$\ln a_i = \ln a_i^C + \ln a_i^R + \ln a_i^{FV}. \quad (3.78)$$

The combinatorial term is given as

$$\ln a_1^C = \ln \phi_1' + \phi_2' + \frac{z}{2} M_1 q_1' \ln\left(\frac{\theta_1'}{\theta_1'}\right) - \frac{z}{2} M_1 q_1' \left(1 - \frac{\phi_1'}{\theta_1'}\right) \quad (3.79)$$

where ϕ_1' is the segment volume fraction, θ_1' is the surface area fraction, z is the coordination number of the lattice (taken to be 10), and M_1 is the molecular weight of component 1 (i.e., the solvent).

The parameter q_1' is related to the van der Waals surface area as

$$q_i' = \frac{1}{M_i} \sum_{i=1}^{N} \upsilon_i^{(i)} Q_k \quad (3.80)$$

where $\upsilon_i^{(i)}$ is the number of type i groups in molecule i and Q_k is a group area parameter obtained from the (Bondi) van der Waals group surface area, A_{wk}, and normalized to a methylene unit of polyethylene as

$$Q_k = \frac{A_{wk}}{2.5 \times 10^9}. \quad (3.81)$$

The surface area fraction, θ_i', is calculated from q_i', and the weight fraction, w_i, as

$$\theta_i' = \frac{q_i' w_i}{\sum_{j=1}^{N} q_j' w_j}. \quad (3.82)$$

Similarly, the segment volume fraction, ϕ_i', is calculated from the weight fraction, w_i, and a group volume parameter, r_i', as

† Sometimes, the Flory interaction parameter is considered to have both an enthalpic component, χ_H, and entropic (or residual) component, χ_S. In this case, we can write

$$\chi_{12} = \chi_S + \chi_H = \chi_S + \frac{V_1}{RT}(\delta_1 - \delta_2)^2 \approx 0.34 + \frac{V_1}{RT}(\delta_1 - \delta_2)^2.$$

$$\phi_i' = \frac{r_i' w_i}{\sum_{j=1}^{N} r_j' w_j} \tag{3.83}$$

where the relative van der Waals volume is given as

$$r_i' = \frac{1}{M_i} \sum_{k=1}^{N} \upsilon_k^{(i)} R_k \tag{3.84}$$

and $\upsilon_k^{(i)}$ is the number of groups (an integer) of type k in molecule i and R_k is the normalized van der Waals group volume, V_{wk}, evaluated as

$$R_k = \frac{V_{wk}}{15.17}. \tag{3.85}$$

The molar group area parameter, Q_k (eq. 3.81), and the molar group volume parameter, R_k, are available for most structural groups as well as for some common solvents, such as water, carbon disulfide, and dimethylformamide. These group parameters are continuously updated and new ones added in the literature.[31] Some representative values of Q_k and R_k are given in Table 3.4.

It is noted that the first two terms on the RHS of eq. 3.79 are essentially the combinatorial terms of the Flory–Huggins (F–H) equation (eq. 3.35) with the exception that segment rather than volume fractions are used. The remaining two terms serve to correct for the effect of molecular shape. The difference between the combinatorial activity given by eq. 3.79 and that of the F–H expression is usually small when segment fractions are used in place of volume fractions in the F–H expression.

The residual contribution in UNIQUAC is given as

$$\ln a_1^{R} = M_1 q_1' \left[1 - \ln \left(\sum_{i=1}^{N} \theta_i' \tau_{i1} \right) - \sum_{i=1}^{N} \left(\theta_i' \tau_{1i} \Big/ \sum_{j=1}^{N} \theta_j' \tau_{ji} \right) \right] \tag{3.86}$$

where the two *adjustable* parameters, τ_{ij} and τ_{ji}, are given as

$$\tau_{ij} = \exp\left[-\left(\frac{u_{ij} - u_{jj}}{RT} \right) \right] \tag{3.87}$$

and

$$\tau_{ji} = \exp\left[-\left(\frac{u_{ji} - u_{ii}}{RT} \right) \right]. \tag{3.88}$$

The parameter u_{ij} is the potential energy of an i–j pair.

TABLE 3.4 REPRESENTATIVE VALUES OF THE MOLAR GROUP AREA (Q_k) AND VOLUME (R_k) PARAMETERS[a]

Main Group	Subgroup	R_k	Q_k	Sample Group Assignment
CH_2	CH_3	0.9011	0.848	Hexane
	CH_2	0.6744	0.540	*n*-Butane
	CH	0.4469	0.228	2-Methylpropane
	C	0.2195	0.000	Neopentane
C=C	CH_2=CH	1.3454	1.176	Hexene-1
	CH=CH	1.1167	0.867	Hexene-2
	CH_2=C	1.1173	0.988	2-Methyl-1-butene
	CH=C	0.8886	0.676	2-Methyl-2-butene
	C=C	0.6605	0.485	2,3-Dimethylbutene
CH_2CO	CH_3CO	1.6724	1.448	Butanone
	CH_2CO	1.4457	1.180	Pentanone-3
ACH[b]	ACH	0.5313	0.400	Naphthalene
	AC	0.3652	0.120	Styrene
$ACCH_2$	$ACCH_3$	1.2663	0.968	Toluene
	$ACCH_2$	1.0396	0.660	Ethylbenzene
	ACCH	0.8121	0.348	Cumene
OH		1.0000	1.200	Propanol-2
CH_3OH		1.4311	1.432	Methanol
H_2O		0.9200	1.400	Water
$CHCl_3$		2.8700	2.410	Chloroform
$HCON(CH_3)_2$		3.0856	2.736	*N,N*-Dimethylformamide

[a] Supplementary material to ref. 31.
[b] The prefix A indicates that the group is contained in an *aromatic* structure.

In UNIFAC, the *residual* term is replaced by the SOG concept as

$$\ln a_i^{R} = \sum_{\text{all groups}} \upsilon_k^{(i)} \left[\ln \Gamma_k - \ln \Gamma_k^{(i)} \right] \tag{3.89}$$

where Γ_k is the group residual-activity (or activity coefficient) and $\Gamma_k^{(i)}$ is the group residual-activity (or activity coefficient) of group k in a reference solution containing only molecules of type i (for normalization so that $a_i \rightarrow 1$ as $w_i \rightarrow 1$). The group activation term, Γ_k or $\Gamma_k^{(i)}$, is obtained from the expression

$$\ln \Gamma_k = M_k Q_k' \left[1 - \ln \left(\sum_{\text{all groups}} \Theta_m' \Psi'_{mk} \right) - \sum_{\text{all groups}} \frac{\Theta_m' \Psi'_{km}}{\sum_{\text{all groups}} \Theta_n' \Psi_{nm}} \right] \tag{3.90}$$

where Θ_m' is the *area fraction* of group m, calculated in a similar way to that of θ_j':

$$\Theta_m' = \frac{Q_m' W'_m}{\sum_{n=1}^{N} Q_n' W'_n} \tag{3.91}$$

In the above equations, M_k is the molecular weight of the functional group k, Q_m' is the group-area parameter per gram such that $Q_m' = Q_k/M_k$, and W'_m is the weight fraction of group m in the mixture. The *group interaction parameter*, Ψ'_{mn}, is given by

$$\Psi'_{mn} = \exp\left[-\left(\frac{U_{mn} - U_{nn}}{RT} \right) \right] = \exp\left(-\frac{a_{mn}}{T} \right) \tag{3.92}$$

where U_{mn} is a measure of the energy of interaction between groups m and n. The group-interaction parameters, a_{mn} and a_{nm} ($a_{mn} \neq a_{nm}$), for each pair of groups have been compiled and continuously revised, principally by fitting experimental VLE or LLE data for low-molecular-weight compounds. Representative values of the group-interaction parameters derived from VLE data are given in Table 3.5. In tables of group-interaction parameters, each major group contains several subgroups with their own R_k and Q_k values (Table 3.4), but all subgroups are assumed to have identical group-interaction parameters.

TABLE 3.5 REPRESENTATIVE VALUES OF GROUP-INTERACTION PARAMETERS (a_{nm} and a_{mn})[a]

	CH_2	C=C	ACH	$ACCH_2$	OH	CH_2CO	CH_3OH
CH_2	0.0	86.02	61.13	76.50	986.5	476.4	697.2
C=C	-35.36	0.0	38.81	74.15	524.1	182.6	787.6
ACH	-11.12	3.446	0.0	167.0	636.1	25.77	637.4
$ACCH_2$	-69.70	-113.6	-146.8	0.0	803.2	-52.10	603.3
OH	156.4	457.0	89.60	25.82	0.0	84.00	-137.1
CH_2CO	26.76	42.92	140.1	365.8	164.5	0.0	108.7
CH_3OH	16.51	-12.52	-50.00	-44.50	249.1	23.39	0.0

[a] Supplementary material to ref. 31; values applicable to vapor–liquid equilibria.

For polymer–solvent systems, Oishi and Prausnitz[27] have shown that the *free-volume* contribution appearing in eq. 3.78 can be a significant *positive* contribution to the total activity and used the Flory EOS (where $X_{12} = 0$) to obtain

$$\ln a_1^{FV} = 3c_1 \ln \left[\frac{\left(\tilde{\upsilon}_1^{1/3} - 1 \right)}{\left(\tilde{\upsilon}_M^{1/3} - 1 \right)} \right] - c_1 \left[\left(\frac{\tilde{\upsilon}_1}{\tilde{\upsilon}_M} - 1 \right) \left(1 - \frac{1}{\tilde{\upsilon}_1^{1/3}} \right)^{-1} \right] \tag{3.93}$$

In this equation, $3c_1$ represents the number of external degrees of freedom per solvent (i.e., component 1) molecule (c_1 is usually set to 1.1), subscript M refers to the mixture, and $\tilde{\upsilon}$ is the reduced volume as defined earlier (eq. 3.45). Oishi and Prausnitz have suggested calculating the reduced volume for the solvent as

$$\tilde{\upsilon}_1 = \frac{\upsilon_1}{15.17 b r_1'} \tag{3.94}$$

where b is a proportionality factor of order unity (often taken as 1.28). The reduced volume of the mixture, $\tilde{\upsilon}_M$, is calculated by assuming that the volume of the liquid mixture is additive. For a binary mixture of solvent and polymer (component 2), $\tilde{\upsilon}_M$ is given as

$$\tilde{\upsilon}_M = \frac{\upsilon_1 w_1 + \upsilon_2 w_2}{15.17 b \left(r_1' w_1 + r_2' w_2 \right)} \tag{3.95}$$

UNIFAC-FV has been very successful in the prediction of solvent activities for polymer solutions,[26] as illustrated for polyisobutylene/benzene in Figure 3.11. Although the UNIFAC-FV approach was developed to improve predictions of activ-

ities or activity coefficients for polymeric systems, it has also been used for mixtures of low-molecular-weight compounds with reasonable success. It was noted that free-volume contributions can be important even for mixtures of low-molecular-weight components when their characteristic temperatures (T^*) differ significantly, as in the case of gas/hydrocarbon mixtures for example.

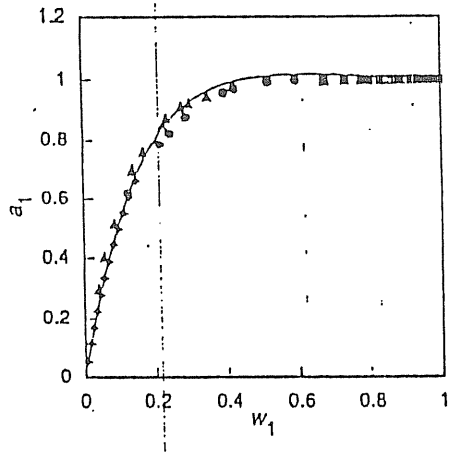

Figure 3.11. Comparison of experimental data (◆,▲,●,■) for the activity of benzene (a_1) as a function of its weight fraction (w_1) in polyisobutylene at 25°C with predictions (—) of UNIFAC-FV.[26]

3.3 MEASUREMENT OF MOLECULAR WEIGHT

As discussed in Section 1.3, commercial synthetic polymers have broad distributions of molecular weight, and it is therefore necessary to report an average molecular weight when characterizing a sample. There are three important molecular-weight averages — number average ($\overline{M}_n$), weight average ($\overline{M}_w$), and z average ($\overline{M}_z$). Absolute values of $\overline{M}_n$, $\overline{M}_w$ and $\overline{M}_z$ can be obtained by the *primary* characterization methods of osmometry, scattering, and sedimentation, respectively. In addition to these accurate but time-consuming techniques, there are a number of *secondary* methods by which average molecular weights can be determined provided that polymer samples with narrow molecular-weight distributions are available for reference and calibration. The most important of these secondary methods is gel-permeation chromatography (GPC), sometimes called size-exclusion chromatography (SEC). This method is capable of determining the entire molecular-weight distribution of a polymer sample from which all molecular-weight averages can be determined. Another widely-used secondary method is the determination of intrinsic viscosity from which the viscosity-average molecular weight can be determined. The viscosity-average molecular weight ($\overline{M}_v$) normally lies between $\overline{M}_n$ and $\overline{M}_w$. The principles behind both primary and secondary methods for molecular-weight determination are discussed next.

3.3.1 Osmometry

Membrane Osmometry. The osmotic pressure, Π, of a polymer solution may be obtained from the chemical potential, $\Delta\mu_1$, or equivalently from the activity, a_1, of the solvent through the basic relationship

$$\Delta\mu_1 = RT \ln a_1 = -\Pi V_1 \tag{3.96}$$

where V_1 is the molar volume of the solvent. Substitution of the Flory–Huggins expression for solvent activity (eq. 3.35) into eq. 3.96 and subsequent rearrangement gives

$$\Pi = -\frac{RT}{V_1}\left[\ln\left(1-\phi_2\right) + \phi_2 + \chi_{12}\phi_2^{\,2}\right]. \tag{3.97}$$

Simplification of this relation can be achieved by expansion of the logarithmic term in a Taylor series (see Appendix E) and the substitution of polymer concentration, c, for volume fraction, ϕ_2, through the relationship

$$\phi_2 = c\nu \tag{3.98}$$

where ν is the specific volume of the polymer. Substitution and rearrangement give the expression

$$\frac{\Pi}{c} = \frac{RT}{M}\left[1 + \left(\frac{M\nu^2}{V_1}\right)\left(\frac{1}{2} - \chi_{12}\right)c + \frac{1}{3}\left(\frac{M\nu^3}{V_1}\right)c^2 + \ldots\right]. \tag{3.99}$$

The classical *van't Hoff equation* for the osmotic pressure of an ideal, dilute solution

$$\frac{\Pi}{c} = \frac{RT}{M}, \tag{3.100}$$

may be seen as a special or limiting case of eq. 3.99 obtained when $\chi_{12} = 1/2$ and second- and higher-order terms in c can be neglected (i.e., for dilute solution). For high-molecular-weight, polydisperse polymers, the appropriate molecular weight to use in eq. 3.99 is the number-average molecular weight, $\overline{M}_n$. Equation 3.99 then can be rearranged to give the widely used relation

$$\Pi = RTc\left(\frac{1}{\overline{M}_n} + A_2c + A_3c^2 + \cdots\right) \tag{3.101}$$

where A_2 and A_3 are the second and third virial coefficients, respectively. Comparison of eqs. 3.99 and 3.101 reveals the following relations for the virial coefficients:

$$A_2 = \frac{v^2}{V_1}\left(\frac{1}{2} - \chi_{12}\right) \tag{3.102}$$

and

$$A_3 = \frac{1}{3}\left(\frac{v^3}{V_1}\right). \tag{3.103}$$

In the limit of dilute solution (typically less than 1 g dL^{-1}), terms containing second- and higher-order powers of c can be neglected, and therefore a plot of Π/RTc versus c yields a straight line with an intercept, $1/\overline{M}_n$, and slope, A_2.

As shown by the relation between A_2 and χ_{12} given by eq. 3.102, the second virial coefficient is a convenient measure of the *quality* of polymer–solvent interactions. In good solvents in which the polymer chains are expanded (i.e., $\alpha > 1$, eq. 3.13), A_2 is large and, therefore, χ_{12} is small (e.g., <0.5). At θ conditions (i.e., $\alpha = 1$), $A_2 = 0$ and $\chi_{12} = 0.5$.

Experimental procedures to determine osmotic pressure are relatively simple although often very time consuming. A basic osmometer design is illustrated in Figure 3.12. In operation, pure solvent and a dilute solution of the polymer in the same solvent are placed on opposite sides of a semipermeable membrane, typically cellulose or a cellulose derivative. Regenerated cellulose is an especially good membrane polymer because it is insoluble in most organic solvents. Normally, the membrane is first preconditioned in the solvent used in the measurements. An ideal membrane will allow the solvent to pass through the membrane but will retain the polymer molecules in solution. The resulting difference in chemical potential between solvent and the polymer solution causes solvent to pass through the membrane and raise the liquid head of the solution reservoir. The osmotic pressure is calculated from the height, h, of the equilibrium head representing the difference between the height of solvent in the solvent capillary and the height of solution in the opposite capillary at equilibrium as

$$\Pi = \rho g h \tag{3.104}$$

where ρ is the solvent density.

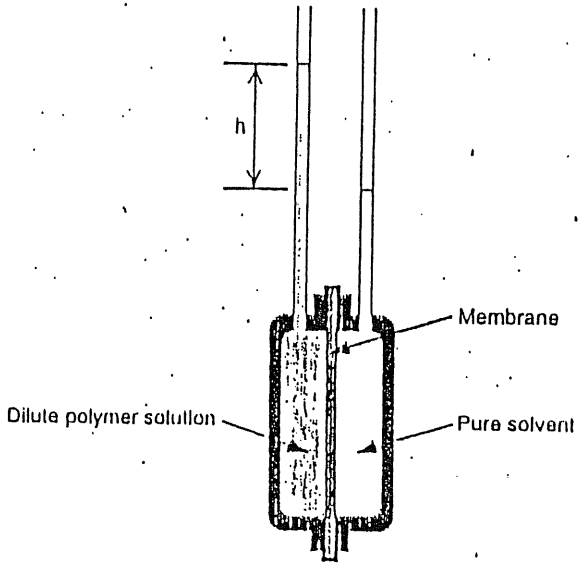

Figure 3.12. Schematic of a simple membrane osmometer. A dilute polymer solution is located on the left-hand side of the membrane and pure solvent on the right-hand side.

One intrinsic problem with membrane osmometry is the performance of the membrane. No membrane is completely impervious to passage of small molecules, and any migration of smaller polymer molecules across the membrane during measurement will not contribute to the osmotic pressure and, therefore, an artificially high value of $\overline{M}_n$ will be obtained. For this reason, membrane osmometry is considered to be accurate only for polymer samples with molecular weights above about 20,000. The upper limit for molecular weight is approximately 500,000 due to inaccuracy in measuring small osmotic pressures. For the characterization of low molecular-weight (i.e., <20,000) oligomers and polymers, an alternative technique called vapor-pressure osmometry (VPO) is preferred, particularly when molecular weight is less than about 10,000. The basic principles of this technique are described next.

Vapor-Pressure Osmometry. When a polymer is added to a solvent, the vapor pressure of the solvent will be lowered due to the decrease in solvent activity. The relation between the difference in vapor pressure between solvent and solution, $\Delta p \left(= p_1 - p_1^\circ\right)$, and the number-average molecular weight, $\overline{M}_n$, of the polymer is given as

$$\lim_{c\to 0}\left(\frac{\Delta p}{c}\right) = -\frac{p_1^{\circ}V_1^{\circ}}{\overline{M}_n} \tag{3.105}$$

where p_1° and V_1° are, respectively, the vapor pressure and molar volume of the pure solvent. Due to the inverse dependence of Δp on $\overline{M}_n$ given by eq. 3.105, the effect of even a low-molecular-weight polymer on the lowering of vapor pressure will be very small and, therefore, direct measurement of the vapor pressure is a very imprecise method of molecular-weight determination. For this reason, an indirect approach, based upon thermoelectric measurements, is used in commercial instrumentation as described below.

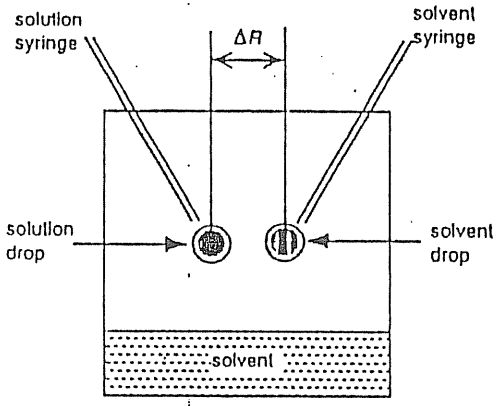

Figure 3.13. Representation of basic instrumentation for vapor-pressure osmometry.

As shown by Figure 3.13, a commercial vapor-pressure osmometer uses two matched thermistors that are placed in a closed, constant-temperature (± 0.001°C) chamber containing saturated solvent vapor. A drop of solvent is placed by syringe on one thermistor and a drop of dilute polymer-solution on the other. As a result of condensation of solvent vapor onto the solution, the temperature of the solution thermistor increases until the vapor pressure of the solution equals that of the solvent. The difference in temperature between the two thermistors is recorded in terms of a difference in resistance (ΔR), which is calibrated by use of a standard low-molecular-weight sample. Extrapolation of $\Delta R/c$ over a range of dilute-solution concentrations to zero concentration yields $\overline{M}_n$ through

$$\left(\frac{\Delta R}{c}\right)_{c\to 0} = \frac{K_{VPO}}{\overline{M}_n} \tag{3.106}$$

where K_{VPO} is the calibration constant obtained by measuring ΔR for a low molecular-weight standard whose molecular weight is precisely known. As in membrane osmometry, the slope of the plot of $\Delta R/c$ versus c is related to the second virial coefficient. Criteria for the selection of calibrants for VPO include high purity (>99.9%) and low vapor pressure (<0.1% of p_1°). Examples of calibrant include mannitol and sucrose for aqueous solution measurements and pentaerythrityl tetrastearate, and low-polydispersity, low-molecular-weight polystyrene and polyisobutylene standards for organic-solution determinations. Since calibration by a low-molecular-weight standard is required to obtain K_{VPO}, VPO is considered a secondary method of molecular-weight determination, in contrast to membrane osmometry for which no calibrants are necessary.

3.3.2 Light-Scattering Methods

The weight-average molecular weight can be obtained directly only by scattering experiments. The most commonly used technique is light scattering from dilute polymer solution. It is also possible to determine $\overline{M}_w$ by small-angle neutron scattering of specially-prepared solid samples. Although this technique has great current importance in polymer research, it is not routinely used for molecular-weight determination because of the difficulty and expense of sample preparation and the specialized facilities required. The basic principles of light-scattering measurements of dilute polymer solutions are described next.

The fundamental relationship for light scattering is given as[1]

$$\boxed{\frac{Kc}{R(\theta)} = \frac{1}{\overline{M}_w P(\theta)} + 2A_2c + \cdots} \tag{3.107}$$

In this equation, K is a function of the refractive index, n_o, of the pure solvent, the specific refractive increment, dn/dc, of the dilute polymer solution, and the wavelength, λ, of the incident light according to the relationship

$$K = \frac{2\pi^2 n_o^2}{N_A \lambda^4}\left(\frac{dn}{dc}\right)^2 \tag{3.108}$$

where N_A is Avogadro's number (6.023×10^{23} molecules mol^{-1}). The specific refractive increment is the change in refraction index, n, of dilute polymer solutions

[1] It can be shown[1] from the thermodynamic theory of fluctuations that the relationship between scattered light intensity and chemical potential is given as

$$R(\theta) = \frac{KcRTV_1\left(1+\cos^2\theta\right)}{-\partial\mu_1/\partial c} = \frac{KcRTV_1\left(1+\cos^2\theta\right)}{\partial\Pi/\partial c}.$$

with increasing polymer concentration. The term $R(\theta)$ appearing in eq. 3.107 is called the *Rayleigh ratio*, which is defined as

$$R(\theta) = \frac{i(\theta)r^2}{I_o V} \tag{3.109}$$

In this equation, I_o is the intensity of the incident light beam and $i(\theta)$ is the intensity of the *scattered* light measured at a distance of r from the scattering volume, V, and at an angle θ with respect to the incident beam. The parameter $P(\theta)$ appearing in eq. 3.107 is called the *particle scattering function*, which incorporates the effect of chain size and conformation on the angular dependence of scattered light intensity, as illustrated in Figure 3.14. Spherical particles smaller than the wavelength of light act as independent scattering centers generating a symmetrical envelope of scattered light intensity. In this case of small particles, $P(\theta)$ is unity, but in the case of polymer chains whose dimensions are $>\lambda/20$, scattering may occur from different points along the same chain. For this reason, diminution of scattered light intensity can occur due to interference, and the scattering envelope is no longer spherically symmetrical, as illustrated in Figure 3.14. In this case, the angular dependence of scattered light intensity is given by the particle scattering function, which, for a *monodisperse* system of randomly-coiling molecules in dilute solution, is given by the expression

$$P(\theta) = \frac{2}{\upsilon^2}\left[e^{-\upsilon} - (1-\upsilon)\right] \tag{3.110}$$

where

$$\upsilon = 16\left(\frac{\pi n}{\lambda}\right)^2 \langle s^2 \rangle \sin^2\left(\frac{\theta}{2}\right) \tag{3.111}$$

and $\langle s^2 \rangle$ is called the mean-square radius of gyration. For linear-chain polymers, $\langle s^2 \rangle$ is related to the mean-square end-to-end distance as

$$\langle s^2 \rangle = \frac{\langle r^2 \rangle}{6} \tag{3.112}$$

Basic instrumentation for light-scattering measurements is illustrated in Figure 3.15. Light from a high-intensity mercury lamp (or laser as described later) is polarized and filtered before passing through a glass sample cell that contains a filtered, dilute polymer solution. Scattered light intensity at an angle θ is recorded as a signal from a movable high-voltage photomultiplier tube. Alternately, multiple detectors can be located at several fixed positions.

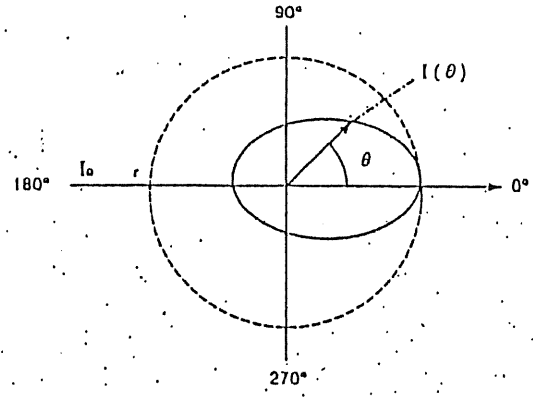

Figure 3.14. Intensity distribution of light scattering at various angles for a small particle (dashed line), symmetric distribution, and a large polymer molecule (solid line), asymmetric distribution.

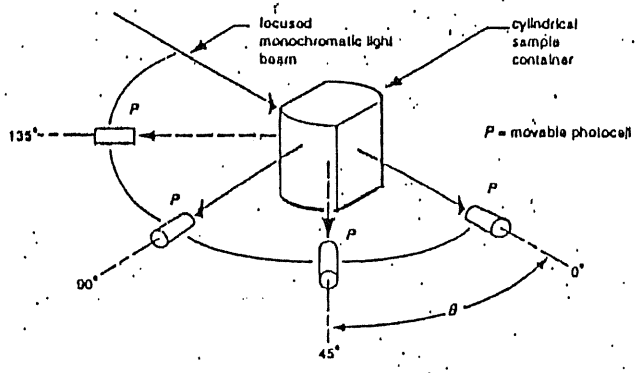

Figure 3.15. Conventional light-scattering instrumentation showing incident and scattered light, sample cell, and photomultiplier. (Adapted from *Principles of Polymer Systems*, p. 166, F. Rodriguez, Hemisphere Publishing Corporation, New York, 1989. Reproduced with permission. All rights reserved.)

To determine $\overline{M}_w$ from eq. 3.107, it is necessary to know the value of $P(\theta)$ at each angle for which $R(\theta)$ has been measured. When the molecular-weight distribution of a polymer is polydisperse, as it usually is, $P(\theta)$ is not precisely given by eq. 3.110, but by a summation of similar equations for polymer chains of

different sizes weighted by the amount of variously sized chains present in the polymer sample. Since this information is generally not known, it is customary to treat the data in a way that does not require explicit knowledge of $P(\theta)$. In practice, two approaches can be used. These are called the *dissymmetry* and *Zimm* methods, which are discussed in the following sections.

Dissymmetry Methods. Molecular-weight determination by the *dissymmetry* method requires measurement of the scattered intensity at three angles — typically 45°, 90°, and 135° (see Figure 3.15) — and at several different (dilute) polymer concentrations. A dissymmetry ratio, z, is defined as

$$z = \frac{i(45°)}{i(135°)}. \tag{3.113}$$

Since z is normally concentration dependent, a value at zero concentration is determined by plotting $(z-1)^{-1}$ versus concentration. This value then can be used to obtain $P(90°)$ and also $\langle r^2\rangle^{1/2}$ from published values if the conformational state (e.g., rods, disks, spheres, or random coils) of the polymer in solution is known. In the absence of information to the contrary, a random-coil conformation, typical of flexible-chain polymers, is assumed. Once $P(90°)$ is known, $\overline{M}_w$ can be obtained from the intercept and A_2 obtained from the slope of a plot of $Kc/R(90°)$ versus concentration extrapolated to zero concentration.

Zimm Method. Another approach to determine $\overline{M}_w$ from light-scattering data is by means of a *Zimm plot*. This procedure has the advantage that chain conformation need not be known in advance; however, Zimm plots require tedious measurements of scattered light-intensity at many more angles than needed by the dissymmetry technique. A double extrapolation to both zero concentration *and* zero angle is used to obtain information concerning molecular weight, second-virial coefficient, and chain dimensions, as discussed next.

In the limit of small angles where $P(\theta)$ approaches unity, it can be shown by means of a series expansion of $1/P(\theta)$ that eq. 3.107 becomes

$$\frac{Kc}{R(\theta)} = \frac{1}{\overline{M}_w}\left[1 + \frac{16}{3}\left(\frac{\pi n}{\lambda}\right)^2 \langle s^2\rangle \sin^2\left(\frac{\theta}{2}\right)\right] + 2A_2 c. \tag{3.114}$$

As illustrated in Figure 3.16, data is plotted in the form of $Kc/R(\theta)$ versus $\sin^2(\theta/2) + kc$ for different angles and concentrations (where k is an arbitrary constant added to provide spacing between curves). A *double* extrapolation to $\theta = 0°$ and $c = 0$, for which the second and third terms on the right of eq. 3.114 become zero, yields $\overline{M}_w$ as the reciprocal of the intercept. As inspection of eq. 3.114 indicates, A_2 is then obtained as one-half of the slope of the extrapolated line at $\theta = 0$;

the mean-square radius of gyration is obtained from the initial slope of the extrapolated line at $c = 0$ as

$$\langle s^2\rangle = \frac{3\overline{M}_w}{16}\left(\frac{\lambda}{\pi n}\right)^2 \times \text{slope (at } \theta = 0). \tag{3.115}$$

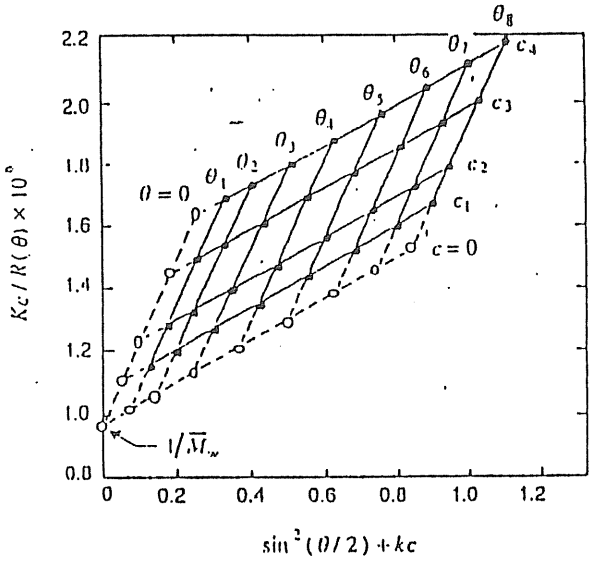

Figure 3.16. Idealized Zimm plot of light-scattering data (●) taken at different angles (θ) and solution concentrations (c). Double extrapolations to zero concentration and zero scattering-angle are represented by broken lines.

Low-Angle Laser Light-Scattering (LALLS). In recent years, helium–neon (He–Ne) lasers ($\lambda = 6328$ Å) have replaced conventional light-sources in some commercial light-scattering instruments. The high intensity of these light sources permits scattering measurements at much smaller angles (2° to 10°) than possible with conventional light sources and for smaller samples at lower concentrations. Since at low angles, the particle scattering-function, $P(\theta)$, approaches unity, eq. 3.114 effectively reduces to the classical *Debye equation* for scattering by small spherical particles as

$$\boxed{\frac{Kc}{R(\theta)} = \frac{1}{\overline{M}_w} + 2A_2 c}. \tag{3.116}$$

Therefore, a plot of $Kc/R(0)$ versus c at a single angle gives $\overline{M}_w$ as the inverse of the intercept and A_2 as one-half of the slope.

A representative LALLS plot of $Kc/R(\theta)$ versus c is shown for cellulose acetate (CA) in acetone at 25°C in Figure 3.17. From the intercept, a value of 150,000 is obtained for $\overline{M}_w$ of the CA sample; the second virial coefficient, A_2, is obtained from the slope as 7.53×10^{-3} mL mol g^{-2}. One limitation of the LALLS method is that chain dimensions cannot be obtained since scattering is measured only at a single angle.

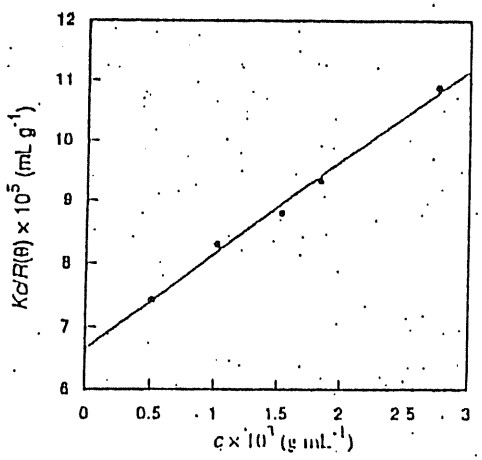

Figure 3.17. Plot of low-angle laser light-scattering data for cellulose acetate in acetone.[32]

3.3.3 Intrinsic-Viscosity Measurements

A method widely used for routine molecular-weight determination is based upon the determination of the intrinsic viscosity, $[\eta]$, of a polymer in solution through measurements of solution viscosity. Molecular weight is related to $[\eta]$ by the *Mark–Houwink–Sakurada equation* given as

$$\boxed{[\eta] = K\overline{M}_v^{\,a}} \tag{3.117}$$

where $\overline{M}_v$ is the viscosity-average molecular weight defined for a discrete distribution of molecular weights (see Section 1.3) as

$$\overline{M}_v = \left[\sum_{i=1}^{N} N_i M_i^{1+a} \Big/ \sum_{i=1}^{N} N_i M_i\right]^{1/a} \tag{3.118}$$

Both K and a are empirical (Mark–Houwink) constants that are specific for a given polymer, solvent, and temperature. The exponent a normally lies between the values of 0.5 for a θ solvent and 1.0 for a thermodynamically-good solvent. Extensive tables of Mark–Houwink parameters for most commercially important polymers are available.[21] Some typical values for representative polymers are given in Table 3.6. The value of $\overline{M}_v$ normally lies between the values of $\overline{M}_n$ and $\overline{M}_w$ obtained by osmometry and light-scattering measurements, respectively. As indicated by eq. 3.118, $\overline{M}_v \cong \overline{M}_w$ in the case of a thermodynamically good solvent when $a \cong 1$.

TABLE 3.6 TYPICAL VALUES OF THE MARK–HOUWINK PARAMETERS FOR SOME REPRESENTATIVE POLYMERS AT 25°C[a]

Polymer	Solvent	$K \times 10^3$ mL g^{-1}	a
Polystyrene	Tetrahydrofuran	14	0.70
	Toluene	7.5	0.75
	Benzene	9.2	0.74
Poly(methyl methacrylate)	Benzene	5.5	0.76
Cellulose acetate[b]	Tetrahydrofuran	51.3	0.69
Polycarbonate	Tetrahydrofuran	38.9	0.70
Polydimethylsiloxane	Toluene	2.4	0.84
Poly(2,6-dimethyl-1,4-phenylene oxide)	Toluene	28.5	0.68

[a] Values obtained from light-scattering data.
[b] 55.5 wt % acetal content.

Intrinsic viscosity is implicitly expressed by the *Huggins equation*

$$\boxed{\frac{\eta_i}{c} = [\eta] + k_H[\eta]^2 c} \tag{3.119}$$

where k_H is a dimensionless parameter (the Huggins coefficient) whose value depends upon temperature as well as the specific polymer/solvent combination. The parameter η_i is called the *relative viscosity-increment*, which is defined as

$$\eta_i = \frac{\eta - \eta_s}{\eta_s} \tag{3.120}$$

where η and η_s are the viscosities of the dilute polymer solution and pure solvent, respectively. The ratio η_i/c is commonly called the reduced viscosity, η_{red}, or viscosity-number according to recommended IUPAC[1] nomenclature.

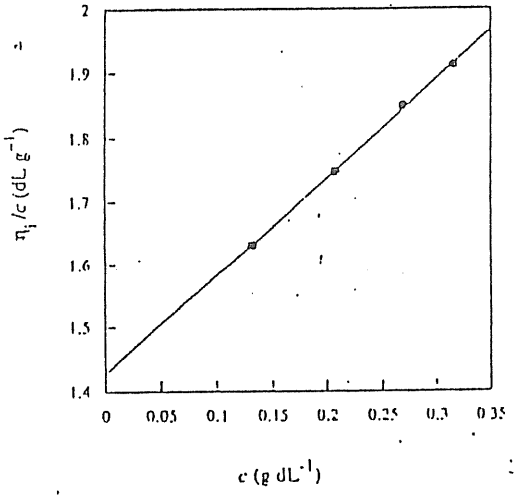

Figure 3.18. Plot of reduced viscosity of a cellulose acetate (intrinsic viscosity of 1.43 dL g^{-1}) in acetone at 25°C.[32]

As indicated by the form of eq. 3.119, $[\eta]$ can be obtained from the intercept of a plot of reduced viscosity versus c as shown for cellulose acetate in acetone at 25°C in Figure 3.18. In actual practice, reduced viscosity is obtained at different concentrations not by direct measurement of solution and solvent viscosities but by measurement of the time required for a dilute solution (t) and pure solvent (t_s) to

[1] International Union of Pure and Applied Chemistry.

fall from one fiducial mark to another in a small glass capillary. If these efflux times are sufficiently long (e.g., >100 s), the relative viscosity increment can be obtained as

$$\eta_i = \frac{t - t_s}{t_s}. \tag{3.121}$$

Efflux times may be noted visually or more precisely by means of commercially available photocell devices.

Capillary viscometers may be either Ostwald–Fenske or Ubbelohde types as illustrated in Figure 3.19. The latter have the advantage that different solution concentrations can be made directly in the viscometer by successive dilutions with pure solvent. During measurement, the viscometer is immersed in a constant temperature bath controlled to within 0.02°C of the set temperature, typically 25° or 30°C.

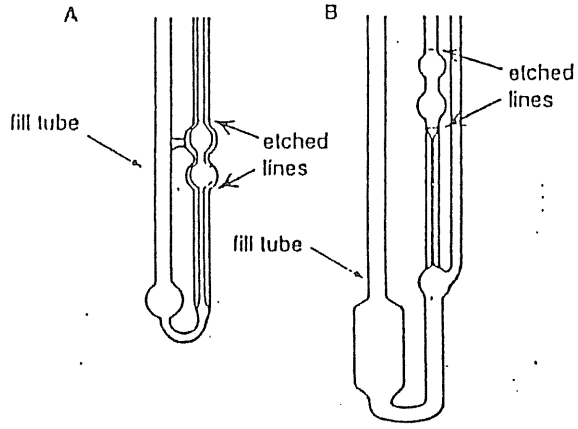

Figure 3.19. Ostwald–Fenske (A) and Ubbelohde (B) capillary viscometers.

In addition to determination of molecular weight, measurement of intrinsic viscosity can also be used to estimate chain dimensions in solution. The mean-square end-to-end distance is related to intrinsic viscosity through the relationship

$$\langle r^2 \rangle = \left(\frac{M[\eta]}{\Phi} \right)^{2/3} \tag{3.122}$$

where Φ is considered to be a universal constant ($\Phi \approx 2.1 \times 10^{21}$ dL g^{-1} cm^{-3}) known as the *Flory constant*.

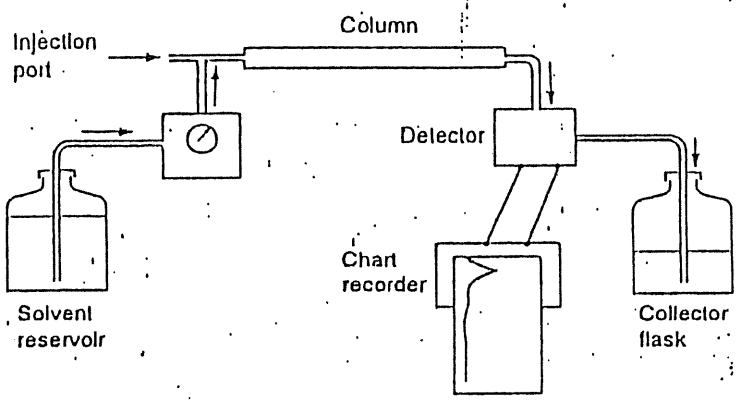

Figure 3.20. Basic instrumentation for gel-permeation chromatography (GPC). (Harry Allcock and Frederick W. Lampe, *Contemporary Polymer Chemistry*, 2nd ed., ©1990, p. 396. Reprinted by permission of Prentice-Hall, Englewood Cliffs, NJ.)

3.3.4 Gel-Permeation Chromatography

One of the most widely used methods for the routine determination of molecular weight and molecular-weight distribution is gel-permeation chromatography (GPC), which employs the principle of size-exclusion chromatography (sometimes referred to as SEC) to separate samples of polydisperse polymers into fractions of narrower molecular-weight distribution. Basic instrumentation for GPC analysis is shown in Figure 3.20. Several small-diameter columns, typically 30 to 50 cm in length, are packed with small, highly porous beads. These are usually fabricated from polystyrene (crosslinked with a small fraction of divinylbenzene as a comonomer) or the packing may be porous glass-beads that are usually modified with an ether- or diol linkage. Pore diameters of the beads may range from 10 to 10^7 Å, which approximate the dimensions of polymer molecules in solution. During GPC operation, pure prefiltered solvent is continuously pumped through the columns at a constant flow rate, usually 1 to 2 mL min^{-1}. Then, a small amount (1 to 5 mL) of a dilute polymer solution (<0.2 g dL^{-1}) is injected by syringe into the solvent stream and carried through the columns. Polymer molecules can then diffuse from this mobile phase into the stationary phase composed of solvent molecules occupying the pore volumes. The smallest polymer molecules are able to penetrate deeply into the interior of the bead pores, but the largest molecules may be completely excluded by the smaller pores or only

partially penetrate the larger ones. As pure solvent elutes the columns after injection, the largest polymer molecules pass through and finally out of the packed columns. These are followed by the next largest molecules, then the next largest, and so on, until all the polymer molecules have been eluted out of the column in descending order of molecular weight. Total sample elution in high-resolution columns may require several hours.

The concentration of polymer molecules in each eluting fraction can be monitored by means of a polymer-sensitive detector, such as an infrared or ultraviolet device. Usually, the detector is a differential refractometer, which can detect small differences in refractive index between pure solvent and polymer solution. A signal from the detector is recorded (either by a chart recorder or digitally) as a function of time, which for a fixed flow-rate is directly proportional to the elution volume, V_r. A representative GPC chromatogram for a commercial polystyrene sample is shown in Figure 3.21.

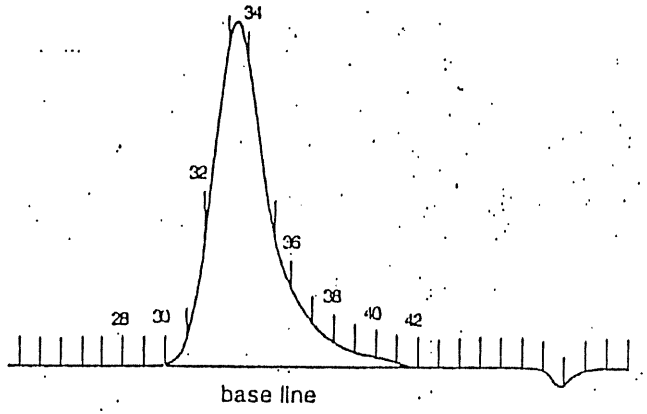

Figure 3.21. GPC chromatogram of a polystyrene sample using tetrahydrofuran as the solvent at a flow rate of 2.0 mL min^{-1}. Vertical marks represent elution counts. The highest-molecular-weight polymer molecules elute at the lowest elution counts (above ca. 29). The negative peak at high elution-volume is usually due to a low-molecular-weight impurity or impurities, such as traces of solvent, stabilizer, water, or dissolved air. (Adapted from L. H. Sperling, *Introduction to Physical Polymer Science*. Copyright ©1986. Reprinted by permission of John Wiley & Sons, Inc.)

For a given polymer, solvent, temperature, pumping rate, and column packing and size, V_r is related to molecular weight. The form of this relation can be found only by comparing elution volumes with those of known molecular weight

and narrow molecular-weight distribution, under identical conditions. Usually, only polymer standards of polystyrene and a few other polymers such as poly(methyl methacrylate) that can be prepared by anionic "living" polymerization (see Section 2.2.2) are available commercially for this purpose. Such standards are available with molecular weights ranging from about 500 to over 2 million with polydispersities as low as 1.06. Since different polymer molecules in the same solvent can have different dimensions, care must be exercised when using polystyrene standards to calibrate elution volumes of other polymers for which standards are not available. The most exact but demanding procedure is to use a universal calibration curve, as illustrated in Figure 3.22.

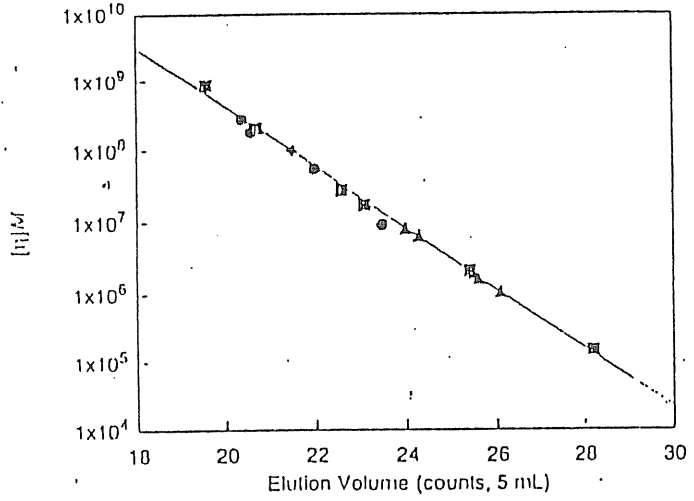

Figure 3.22. Universal GPC calibration-curve showing data points for polystyrene (▣), poly(vinyl chloride) (▲), polybutadiene (◆), and poly(methyl methacrylate) (●) standards in tetrahydrofuran solution. Line gives best fit of polystyrene data.[33]

The universal calibration approach is based on the fact that the product $[\eta]M$ is proportional to the hydrodynamic volume of a polymer molecule in solution (see eq 3.122). This hydrodynamic volume is the effective molecular volume as seen by the pore sites. Universal calibration can be used if the Mark–Houwink constants (see eq. 3.117) are known for both the standard and unknown polymer samples in the same solvent and at the same temperature.

In the calculation of molecular-weight averages, the signal strength (i.e., peak height in Figure 3.21) is proportional to W_i (eq 1.2). Once a proper calibration curve is available to relate V_i to the molecular weight (M_i) of the calibration stand-

ard, direct calculation of all molecular weights — $\overline{M}_n$, $\overline{M}_w$, $\overline{M}_z$, and even $\overline{M}_{z+1}$ — and, therefore, polydispersities ($\overline{M}_w/\overline{M}_n$ or $\overline{M}_z/\overline{M}_n$) is possible, typically by commercially available software. Recently, on-line coupling of GPC with low-angle light-scattering instrumentation (Section 3.3.2) has enabled rapid on-line computation of molecular weight without the need for separation calibration of the elution curve.

REFERENCES

1. P. J. Flory, *Principles of Polymer Chemistry*, Cornell University Press, Ithaca, New York, 1953.
2. P. J. Flory, *Statistical Mechanics of Chain Molecules*, Oxford University Press, New York, 1989.
3. J. E. Mark, *J. Chem. Ed.*, 58, 898 (1981).
4. G. Gee and L. R. G. Treloar, *Trans. Far. Soc.*, 38, 147 (1942).
5. C. Booth and C. J. Devoy, *Polymer*, 12, 320 (1971).
6. P. J. Flory, *J. Chem. Phys.*, 9, 660 (1941); 10, 51 (1942).
7. M. L. Huggins, *J. Chem. Phys.*, 9, 440 (1941); *J. Am. Chem. Soc.*, 64, 1712 (1942).
8. P. J. Flory, *Disc. Far. Soc.*, 49, 7 (1970).
9. R. Koningsveld, L. A. Kleintjens, and H. M. Schoffeleers, *Pure Appl. Chem.*, 39, 1 (1974).
10. P. J. Flory and W. R. Krigbaum, *J. Chem. Phys.*, 18, 1086 (1950).
11. P. J. Flory, *J. Am. Chem. Soc.*, 87, 1833 (1965).
12. I. C. Sanchez and R. H. Lacombe, *Macromolecules*, 11, 1145 (1978).
13. R. K. Jain and R. Simha, *Macromolecules*, 3, 1501 (1980).
14. P. I. Freeman and J. S. Rowlinson, *Polymer*, 1, 20 (1961).
15. J. E. G. Lipson and J. E. Guillet, in *Developments in Polymer Characterisation-3*, J. V. Dawkins, ed., Applied Science Publishers, London, 1982, pp. 33–74.
16. D. H. Everett, *Trans. Faraday Soc.*, 61, 1637 (1965).
17. P. A. Small, *J. Appl. Chem.*, 3, 71 (1953).
18. K. L. Hoy, *J. Paint Technol.*, 42, 76 (1970).
19. D. W. van Krevelen, *Properties of Polymers*, 3rd edition, Elsevier, Amsterdam, 1990.
20. A. F. M. Barton, *CRC Handbook of Polymer–Liquid Parameters and Solubility Parameters*, CRC Press, Boca Raton, FL, 1990.
21. J. Brandrup and E. H. Immergut, eds., *Polymer Handbook*, 3rd ed., John Wiley & Sons, New York, 1989.
22. J. Biros, L. Zeman, and D. Patterson, *Macromolecules*, 4, 30 (1971).
23. G. Scatchard, *Chem. Rev.*, 8, 321 (1931).
24. J. H. Hildebrand and R. L. Scott, *The Solubility of Non-Electrolytes*, 3rd ed., Reinhold, New York, 1959.

. C. M. Hansen, *J. Paint Technol.*, 39, 104 (1967).
. J. R. Fried, J. S. Jiang, and E. Yeh, *Comput. Polym. Sci.*, 2, 95 (1992).
. T. Oishi and J. M. Prausnitz, *Ind. Eng. Chem. Process Des. Dev.*, 17, 333 (1978).
. Aa. Fredenslund, R. L. Jones, and J. M. Prausnitz, *AIChE J.*, 21, 1086 (1975).
. D. S. Abrams and J. M. Prausnitz, *AIChE J.*, 21, 116 (1975).
. E. L. Derr and C. H. Deal, *Adv. Chem. Ser.*, 124, 11 (1973).
. H. K. Hansen, P. Rasmussen, Aa. Fredenslund, M. Schiller, and J. Gmehling, *Ind. Eng. Chem. Res.*, 30, 2355 (1991).
. C.-S. Wang, Ph. D. Dissertation, University of Cincinnati, 1983.
. Z. Grubisic, P. Rempp, and H. Benoit, *J. Polym. Sci., Polym. Lett. Ed.*, 5, 753 (1967).

BIBLIOGRAPHY

G. Barth and J. W. Mays, *Modern Methods of Polymer Characterization*, John iley & Sons, New York, 1991.

. J. R. Cantow, ed., *Polymer Fractionation*, Academic Press, New York, 1967.

P. Danner and M. S. High, *Handbook of Polymer Solution Thermodynamics*, nerican Institute of Chemical Engineers, New York, 1993.

. Einaga, "Thermodynamics of Polymer Solutions and Mixtures," *Prog. Polym.* i., 19, 1–28 (1994).

. C. Forsman, ed., *Polymers in Solution: Theoretical Considerations and Newer ethods of Characterization*, Plenum Press, New York, 1986.

. J. Hunt and S. R. Holding, eds., *Size Exclusion Chromatography*, Chapman and all, New York, 1989.

. Morawetz, *Macromolecules in Solution*, John Wiley & Sons, New York, 1975.

. C. Ward, "Molecular Weight and Molecular Weight Distributions in Synthetic olymers," *J. Chem. Educ.*, 58, 867–879 (1981).

. W. Yau, J. J. Kirkland, and D. D. Bly, *Modern Size-Exclusion hromatography*, John Wiley & Sons, New York, 1979.

Problems

3-1. Polyisobutylene (PIB) is equilibrated in propane vapor at 35°C. At this temperature, the saturated vapor pressure (p_1°) of propane is 9050 mm Hg and its density is 0.490 g cm^{-3}. Polyisobutylene has a molecular weight of approximately 1 million and its density is 0.915 g cm^{-3}. The concentration of propane, c, sorbed by PIB at different partial pressures of propane (p_1) is given in the following table. Using this information, determine an average value of the Flory interaction-parameter, χ_{12}, for the PIB–propane system.

p_1 (mm Hg)	c (g propane/g PIB)
496	0.0061
941	0.0116
1452	0.0183
1446	0.0185

3-2. The following osmotic-pressure data are available for a polymer in solution:

c (g dL^{-1})	h (cm of solvent)
0.32	0.70
0.66	1.82
1.00	3.10
1.40	5.44
1.90	9.30

Given this information and assuming that the temperature is 25°C and the solvent density is 0.85 g cm^{-3}

(a) Plot Π/RTc versus concentration, c.

(b) Determine the molecular weight of the polymer and the second virial coefficient, A_2, for the polymer solution.

3-3. The following viscosity data were obtained for solutions of polystyrene (PS) in toluene at 30°C:

c (g dL^{-1})	t (s)
0	65.8
0.54	101.2
1.08	144.3
1.62	194.6
2.16	257.0

Using this information:

(a) Plot the reduced viscosity as a function of concentration.

(b) Determine the intrinsic viscosity of this PS sample and the value of the Huggins constant, k_H.

(c) Calculate the molecular weight of PS using Mark–Houwink parameters of $a = 0.725$ and $K = 1.1 \times 10^{-4}$ dL g^{-1}.

3-4. Given that the molecular weight of a polystyrene (PS) repeating unit is 104 and that the carbon–carbon distance is 1.54 Å, calculate the following:

(a) The mean-square end-to-end distance for a PS molecule of 1 million molecular weight assuming that the molecule behaves as a freely rotating, freely jointed, volumeless chain. Assume that each link is equivalent to a single repeating unit of polystyrene.

(b) The unperturbed root-mean-square end-to-end distance, $\langle r^2 \rangle_0^{1/2}$, given the relationship for intrinsic viscosity, $[\eta]$, of PS in a θ solvent at 35°C as

$$[\eta] = 8 \times 10^{-4} M^{0.5}$$

where $[\eta]$ is in units of dL g^{-1} and the Flory–Fox constant (Φ) is 2.1×10^{21} dL g^{-1} cm^{-3}.

(c) The characteristic ratio, C_N, for PS.

3-5. The use of universal calibration curves in GPC is based upon the principle that the product $[\eta] M$, the hydrodynamic volume, is the same for all polymers at equal elution volumes. If the retention volume for a monodisperse polystyrene (PS) sample of 50,000 molecular weight is 100 mL in toluene at 25°C, what is the molecular weight of a fraction of poly(methyl methacrylate) (PMMA) at the same elution volume in toluene at 25°C? The Mark–Houwink parameters, K and a, for PS are given as 7.54×10^{-3} mL g^{-1} and 0.783, respectively; the corresponding values for PMMA are 8.12×10^{-3} mL g^{-1} and 0.71.

3-6. Using the values of molar attraction constants given by van Krevelen in Table 3.2, calculate the solubility parameters, (MPa)$^{1/2}$ at 25°C, for the following polymers:

(a) Polyisobutylene ($\rho = 0.924$ g cm^{-3})
(b) Polystyrene ($\rho = 1.04$ g cm^{-3})
(c) Polycarbonate ($\rho = 1.20$ g cm^{-3})

3-7. Show that the most probable end-to-end distance of a freely jointed polymer chain is given as $\left(2n\ell^2/3\right)^{1/2}$.

3-8. The (reduced or excess) Rayleigh ratio (R_θ) of cellulose acetate (CA) in dioxane was determined as a function of concentration by low-angle laser light-scattering measurements. Data are given in the following table. If the refractive index (n_0) of dioxane is 1.4199, the refractive-index increment (dn/dc) for CA in dioxane is 6.297×10^{-2} cm^3 g^{-1}, and the wavelength (λ) of the light is 6328 Å, calculate the weight-average molecular weight of CA and the second virial coefficient (A_2).

$c \times 10^3$ (g mL^{-1})	$R(0) \times 10^5$ (cm^{-1})
0.5034	0.239
1.0068	0.440
1.5102	0.606
2.0136	0.790
2.517	0.902

4

The Solid-State Properties of Polymers

Some commercial polymers, particularly the polyolefins, are highly crystalline materials with well-defined crystalline morphology consisting of chain-folded lamella joined in supramolecular structures called spherulites. Although single crystals of some polymers such as polyethylene can be grown under laboratory conditions, no bulk polymer is completely crystalline. In the case of semicrystalline polymers, regular crystalline units are linked by unoriented, random-conformation chains that constitute amorphous regions. Other polymers may have very low crystallinity characterized by poorly defined crystalline microstructure in an amorphous matrix. An important example of commercial polymer with low crystallinity is poly(vinyl chloride). Many other polymers, such as atactic polystyrene and poly(methyl methacrylate), are totally amorphous. In all cases, morphological aspects such as the presence of crystalline structure have a significant influence on the physical, thermal, and mechanical properties of the polymer. Issues concerning polymer-chain microstructure and the relationship between morphology, bulk properties, and chain conformation and interchain effects are addressed in this chapter. Methods by which bulk properties are measured are also discussed.

4.1 THE AMORPHOUS STATE

Completely amorphous polymers like atactic polystyrene exist as long, randomly coiled, interpenetrating chains that are capable of forming stable, flow-restricting *entanglements* at sufficiently high molecular weight. In the amorphous

solid state, chains assume their unperturbed dimensions as they do in solution under θ conditions (see Section 3.1). In the melt, thermal energy is sufficiently high for long segments of each polymer-chain to move in random micro-Brownian motions. As the melt is cooled, a temperature is reached at which all long-range segmental motions cease. This characteristic temperature is called the *glass-transition temperature*, or T_g, which varies widely with polymer structure. In the glassy state, at temperatures below T_g the only molecular motions that can occur are short-range motions of several contiguous chain segments and motions of substituent groups. These processes are called *secondary* relaxations. The concepts of chain entanglements, the glass transition, and secondary-relaxation processes are developed in the following sections.

4.1.1 Chain Entanglements and Reptation

As illustrated by Figure 4.1, polymer chains that are sufficiently long can form stable, flow-restricting entanglements. A good analogy can be made to a bowl of spaghetti. When the individual strands of spaghetti are long, it is very difficult to separate one from the others with a fork; however, when the strands are short, they can be removed easily. Entanglements have significant importance in relation to viscoelastic properties (see Chapter 5), melt viscosity (see Chapter 11), and mechanical properties such as stress relaxation, creep, and craze formation, as will be discussed in this chapter.

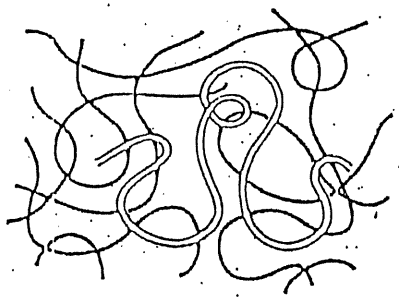

Figure 4.1. Representation of polymer chain intertwined in a network of entangled chains. (Adapted from P.-G. de Gennes, *Scaling Concepts in Polymer Physics*, Cornell University Press, Ithaca, New York, 1979, with permission of the publisher.)

Critical Molecular Weight. The minimum polymer chain-length or *critical molecular weight* M_c for the formation of stable entanglements depends upon the flexibility of a polymer chain and may be directly related to the characteristic ratio, a measure of intramolecular steric hindrance (see Section 3.1).[1]

Relatively flexible polymer chains, such as polystyrene, have a high M_e, while more rigid-chain polymers, such as those with aromatic backbones (e.g., polycarbonate), have a relatively low M_e. A related parameter is M_e, which is the *molecular weight between entanglements*. Representative values of M_e and M_e are given in Table 4.1. As a rough rule of thumb, $M_e \approx 2M_e$. Typically, the molecular weight of most commercial polymers is significantly greater than M_e in order to achieve maximum thermal and mechanical properties. For example, the molecular weight of commercial polystyrene typically falls in the range of 100,000 to 400,000, while the critical molecular weight for entanglements is only about 31,200.

TABLE 4.1 ENTANGLEMENT MOLECULAR-WEIGHTS FOR LINEAR POLYMERS[a]

Polymer	M_e	M_e
1,4-Polybutadiene	5,900	1,900
cis-Polyisoprene	10,000	5,800
Polyisobutylene	15,200	8,900
Polydimethylsiloxane	24,400	8,100
Poly(vinyl acetate)	24,500	12,000
Poly(methyl methacrylate)	27,500	5,900
Poly(α-methylstyrene)	28,000	13,500
Polystyrene	31,200	18,100

[a] From Graessley.[2]

Reptation. If individual chains are entangled in the solid state, the question arises as to how long-range movement of chains can occur as the polymer is heated through its glass-transition temperature and passes from the solid to the melt state. A reasonable explanation has been provided on the basis of the theory of reptation, as originally developed by de Gennes[3] for fixed networks such as a polymer gel and later extended to include melts[4] and concentrated polymer solutions. In the melt state, individual polymer chains can move by local Brownian motion restricted by the topological constraint of neighboring chains. Movement can be visualized as snakelike motion (i.e., reptation) of the chain within a virtual tube, which is defined by the locus of its entanglements with neighboring molecules as illustrated in the top view of Figure 4.2. The theory of reptation has been largely successful toward developing a qualitative and quantitative molecular theory for the dynamics and viscoelastic properties of entangled polymers.

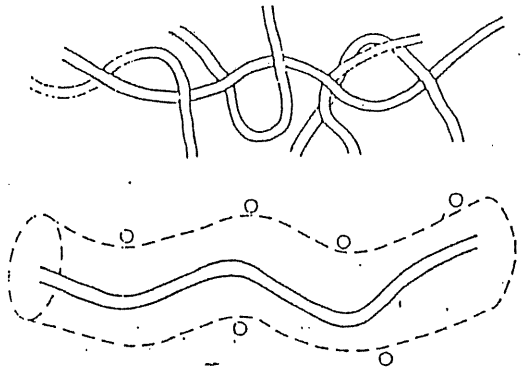

Figure 4.2. Reptation model of a polymer chain constrained in entangled network. A particular chain can be viewed as constrained to move within a virtual tube defined by neighboring entanglement sites. Circles pictured in the lower view represent cross sections of chains constituting the tube constraints. [Adapted with permission from J. Klein, *Nature*, 271, 143 (1978). Copyright ©1978 by Macmillan Magazines Limited.]

4.1.2 The Glass Transition

As mentioned earlier, the temperature that marks the transition from the amorphous solid state to the melt state is called the glass-transition temperature, T_g. Several phenomenological models have been used to provide an understanding of the glass transition. One is that the glass transition marks an *isoviscous* state. This means that, as a polymer is cooled from its melt state, viscosity increases rapidly to a common (maximum) value, ca. 10^{12} Pa-s (10^{13} poise) at T_g, for all glassy materials — both low-molecular-weight and polymeric.

A second view is that the glass transition represents a state of *isofree volume*. Free volume, V_f, may be defined as the difference between the actual volume (or specific volume), V, of the polymer at a given temperature and its equilibrium volume at absolute zero, V_0,

$$V_f = V - V_0 \tag{4.1}$$

The volume at absolute zero can be approximated by the sum of the van der Waals volumes of each chain segment, which can be easily obtained by group-contribution methods.[5] The concept of free volume has significant importance for a number of other related subjects in polymer science, including time–temperature superposition of viscoelastic properties (Chapter 5), melt viscosity (Chapter 11), and permeability (Chapter 12).

A third view of the glass transition is that it represents an *isoentropic* state. This is the foundation of the important Gibbs–DiMarzio theory.[6] Gibbs and

DiMarzio have suggested that there is a temperature, T_2, at which the conformational entropy, S_c (a measure of the total number of ways of arranging a polymer molecule or collection of chains), goes to zero. It can be shown (see Section 5.1.5) that this equilibrium-state temperature lies approximately 52°C below the experimentally-measured T_g, which depends upon the *rate* at which the polymer sample is heated or cooled during measurement. As discussed in Chapter 3, polymeric chains can exist in a large number of possible spatial conformations in solution or in the melt state. Each of these conformations corresponds to a different energy state. As the melt is cooled, fewer high-energy conformations are accessible. If the melt is cooled infinitely slowly to assure the attainment of equilibrium, eventually a temperature will be reached (i.e., T_2) at which only the lowest-energy conformation is available. At this point, the conformational entropy will be zero.

The glass-transition temperature of amorphous polymers can vary widely with the chemical structure of the polymer chain. As illustrated by representative values of T_g for several important polymers given in Table 4.2, T_g can vary over a range of 300°C or more. In general, polymers with flexible backbones and small substituent groups (e.g., polyethylene and polydimethylsiloxane) have low T_g, while those with rigid backbones, such as polymers containing main-chain aromatic groups (e.g., polysulfone), have high T_g. A more detailed discussion of structure–property relationships for the thermal transitions of polymers is given in Section 4.3.3.

TABLE 4.2 REPRESENTATIVE VALUES OF THE GLASS-TRANSITION TEMPERATURE OF SOME AMORPHOUS POLYMERS

Polymer	T_g (°C)
Polydimethylsiloxane	-123
Poly(vinyl acetate)	28
Polystyrene	100
Poly(methyl methacrylate)	105
Polycarbonate	150
Polysulfone	190
Poly(2,6-dimethyl-1,4-phenylene oxide)	220

4.1.3 Secondary-Relaxation Processes

As previously discussed, secondary-relaxation processes are small-scale molecular motions that can occur in the amorphous glassy state. These can involve limited motions of the main chain or rotations, vibrations, or flips of substituent groups. An example of a main-chain secondary-relaxation that has been proposed is the Schatzki *crankshaft* rotation model illustrated in Figure 4.3. According to this model, several contiguous bonds can rotate around the main-chain consisting of C–C bonds. Such limited, or noncooperative, motions can occur at very low temperatures, near -120°C. Other examples of main-chain secondary-relaxations include rotations or flips of aromatic rings in the backbone of some high-temperature polymers, such as polycarbonate. In addition to these main-chain secondary-relaxation motions, substituent groups can rotate or wag at extremely low temperatures in the glassy state. For example, the phenyl ring of polystyrene may rotate at temperatures as low as 70 K. All these motions can occur in the glassy state, below T_g, as a precursor to the onset of long-range, main-chain cooperative-motions that mark the glass transition. The magnitude and temperature assignment of secondary-relaxation processes can have significant influence on glassy-state properties. For example, the presence of main-chain secondary-relaxation processes has been correlated with impact strength and even with the gas permeability (see Chapter 12) of amorphous polymers.

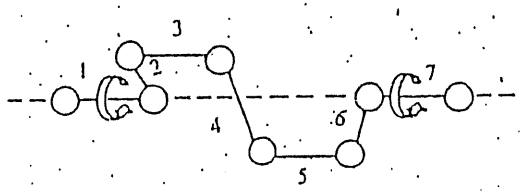

Figure 4.3. Schatzki model of crankshaft motion of a carbon–carbon backbone. The dashed line represents the virtual axis around which bonds 2–6 rotate.

4.2 THE CRYSTALLINE STATE

4.2.1 Ordering of Polymer Chains

Under favorable conditions, some polymers cooled from the melt can organize into regular crystalline structures. Such crystalline polymers have less perfect organization than crystals of low-molecular-weight compounds or low-molecular weight polymers crystallized from the solution. The basic units of crystalline polymer morphology are crystalline *lamellae* consisting of arrays of folded chains. Reentry of each chain in the folded structure can be adjacent or nonadjacent as illustrated by Figure 4.4. A chain participating in adjacent reentry can form a tight (or regular) loop (Figure 4.4B) or form a loose (irregular) loop (Figure 4.4C). The thickness of a typical crystallite may be only 100 to 200 Å (10 to 20 nm), indicating that only a portion of the complete chain (e.g., 40 to 80 repeating units in the case of polyethylene) is involved in each fold.

As mentioned earlier, high thermal energy favors a large number of conformations in the melt state. As the melt is cooled, the lower-energy conformations are favored, and chains are free to organize into lamellar structure. For many polymers, the lowest-energy conformation is the extended chain or planar zigzag conformation. Such polymers include polyethylene, syndiotactic vinyl polymers, and polymers capable of hydrogen bonding between chains, such as poly(vinyl alcohol) and nylons. In cases of polymers with larger substituent groups, such as the methyl group in polypropylene, for most isotactic polymers, and for polymers of some 1,1-disubstituted ethylenes like polyisobutylene, the lowest-energy conformation is a helix of some preferred geometry. For the example of polypropylene, three monomer units form a single turn in the helix (i.e., a 3_1 helix). A discussion of the concept of chain conformation and dimension was given in Chapter 3.

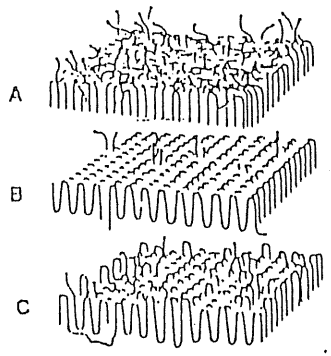

Figure 4.4. Three idealized models for chain folding in polymer crystallites. A, nonadjacent reentry; B, regular adjacent reentry; C, irregular adjacent reentry. (Reprinted from J. R. Fried, *Plast. Eng.*, June, 1982, p. 52. with permission of the publisher.)

For some polymers crystallized from the melt or from concentrated solution, crystallites can organize into larger spherical structures called *spherulites*, as illustrated in Figure 4.5. Each spherulite contains arrays of lamellar crystallites that are typically oriented with the chain axis perpendicular to the radial (growth) direction of the spherulite. In a few cases, such as occurs in the crystallization of polypropylene, chain folding will occur with the chain oriented along the radial direction. The anisotropic morphology of a spherulite results in the appearance of a characteristic extinction cross, or Maltese cross, when viewed under polarized light. During the early stages of crystallization, these supramolecular structures are spherical, but as the level of crystallinity increases, the growing spherulites will eventually meet.

Impingement ceases primary crystalline growth and the spherical boundaries are lost.

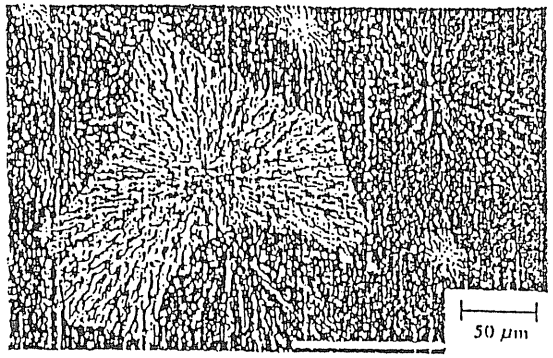

Figure 4.5. Scanning electron micrograph showing the spherulitic structure of polypropylene. The sample was cut using a carborundum-impregnated wire, polished with very fine (0.1 μm) alumina powder, and finally etched using a permanganic acid solution which acts on the amorphous regions of the spherulites to reveal the structure of the lamellae. Polypropylene exists in a number of crystalline forms including a monoclinic α-form (dark areas) and a hexagonal β-form (light areas). The radial structure of the spherulites and impingement of neighboring spherulites are clearly evident in this electron micrograph. (Courtesy of M. Aboulfaraj, Pechiney Centre de Recherches de Voreppe, France.)

Since no polymer is completely crystalline, even the most crystalline polymers like high-density polyethylene have lattice defect regions that contain unordered, amorphous material. Crystalline polymers may exhibit, therefore, both a T_g corresponding to long-range segmental motions in the amorphous regions and a *crystalline-melting temperature*, or T_m, at which crystallites are destroyed and an amorphous, disordered melt is formed. For many polymers, T_g is approximately one-half to two-thirds of T_m (expressed in Kelvins). Representative values of T_g and T_m for some semicrystalline polymers are given in Table 4.3.

The chemical structure of a polymer determines whether it will be crystalline or amorphous in the solid state. In general, symmetrical chain structures, which allow close packing of polymer molecules into crystalline lamellae and specific interactions between chains that favor molecular orientation, favor crystallinity. For example, linear polyethylene and polytetrafluoroethylene, which have symmetrically substituted repeating units, are highly crystalline. Atactic poly(vinyl chloride) (PVC) with its asymmetrically placed chlorine is highly amorphous. When two chlorine atoms are symmetrically located on the same carbon atom, as they are in poly(vinylidene chloride), crystallinity is again favored.

TABLE 4.3 REPRESENTATIVE VALUES OF THERMAL TRANSITIONS FOR SEMICRYSTALLINE POLYMERS

Polymer	T_g, °C	T_m, °C
Polyethylene (high-density)	-120	135
Polycaprolactone	-60	61
Poly(vinylidene fluoride)	-45	172
Polyoxymethylene	-85	195
Poly(vinyl alcohol)	85	258
Poly(hexamethylene adipamide) (nylon-6,6)	49	265
Poly(ethylene terephthalate)	69	265

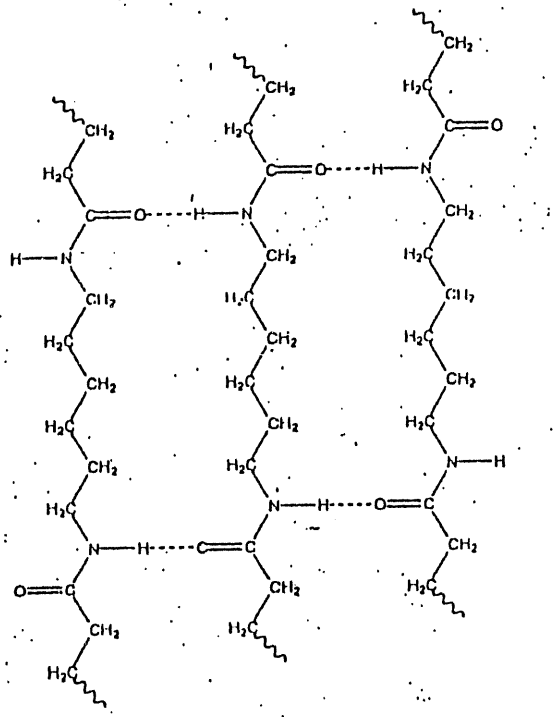

Figure 4.6. Illustration of hydrogen bonding between the amide groups in nylon-6,6.

Although atactic-PVC is amorphous, atactic-poly(vinyl alcohol) is partly crystalline because of the occurrence of specific interchain interactions (i.e., hydrogen bonding). Specific interactions are particularly important in enhancing crystallinity in the case of nylons, for which hydrogen bonds can form between an amide carbonyl group on one chain and the hydrogen atom of an amide group on an adjacent chain. Such bonding is illustrated in Figure 4.6 for nylon-6,6, poly(hexamethylene adipamide). The T_m of nylon-6,6 is 265°C compared to 135°C for polyethylene, which, due to the absence of polar groups, is incapable of participating in interchain interactions.

Both tacticity and geometric isomerism (i.e., *trans* configuration) favor crystallinity. For example, *cis*-polyisoprene is amorphous, while more easily packed *trans*-polyisoprene is crystalline. Although *cis*-1,4-poly(1,3-butadiene) is partly crystalline, its crystalline form is less stable than the preferred *trans* configuration, as indicated by its lower T_m (2°C) compared to *trans*-1,4-poly(1,3-butadiene) (145°C). In general, tactic polymers with their more stereoregular chain structure are more likely to be crystalline than their atactic counterparts. For example, isotactic polystyrene is crystalline, while commercial-grade atactic polystyrene is amorphous. Commercial-grade suspension-polymerized PVC has a portion of its repeating units in syndiotactic placement and, therefore, has some crystallinity (about 11%). By lowering the temperature of PVC polymerization, syndiotactic placement is favored and the crystalline content will be increased.

4.2.2 Crystalline-Melting Temperature

From the first law of thermodynamics, the free energy of fusion per repeating unit of the polymer, ΔG_u, can be expressed as

$$\Delta G_u = \Delta H_u - T\Delta S_u \tag{4.2}$$

where ΔH_u and ΔS_u are the enthalpy and entropy of fusion per repeating unit, respectively. At the *equilibrium* melting temperature ($T = T_m°$), $\Delta G_u = 0$ and, therefore,

$$T_m° = \frac{\Delta H_u}{\Delta S_u}. \tag{4.3}$$

Some representative values of $T_m°$, ΔH_u, and ΔS_u are given in Table 4.4.

In general, the observed crystalline-melting temperature, T_m, is always lower than the equilibrium value, $T_m°$. A number of factors can contribute to this melting-point depression. One is due to the kinetic effect of a finite heating or cooling rate. Another is due to crystallite size, which can be influenced by conditions of the crystallization process or by the presence of impurities. The surface free energy increases with decreasing crystallite size and, therefore, T_m decreases with decreasing size. In addition, the presence of a diluent such as residual solvent or plasticizer can reduce T_m on the basis of thermodynamic considerations. Using the Flory–Huggins

theory (see Section 3.2.1), the approximate relation for the melting-point depression of a high-molecular-weight polymer by a diluent is

$$\frac{1}{T_m} - \frac{1}{T_m^\circ} = \left(\frac{R}{\Delta H_u}\right)\left(\frac{V_u}{V_1}\right)\left(\phi_1 - \chi_{12}\phi_1^2\right) \tag{4.4}$$

where R is the ideal gas constant, V_u is molar volume per repeating unit of polymer, V_1 is the molar volume of the diluent, ϕ_1 is the volume fraction of the diluent, and χ_{12} is the Flory interaction parameter between the diluent (component 1) and polymer (component 2). Equation 4.4 indicates that melting-point depression is one way to determine the interaction parameter of a crystallizable polymer in a homogeneous mixture with a solvent, a plasticizer, or second polymer. Since the presence of a diluent can also decrease T_m by reducing crystallite size, care must be exercised in separating out crystalline size effects from thermodynamic effects.[7]

TABLE 4.4 REPRESENTATIVE VALUES OF THE THERMODYNAMIC PARAMETERS FOR SOME SEMICRYSTALLINE AND CRYSTALLIZABLE POLYMERS

Polymer	T_m° °C	ΔH_u cal mol^{-1}	ΔS_u cal K^{-1} mol^{-1}
Polyethylene	146	960	2.3
Polyoxymethylene	180	1590	3.5
Polypropylene	200	1386	2.9
Poly(ethylene terephthalate)	280	6431	11.6
Polycarbonate[a]	335	6348	10.4

[a] Solvent-induced crystallization.

4.2.3 Crystallization Kinetics

For a given polymer, the extent of crystallization attained during melt processing depends upon the rate of crystallization and the time during which melt temperatures are maintained. Above T_m, some polymers that have low rates of crystallization, such as poly(ethylene terephthalate) and polycaprolactone, can be quenched rapidly enough to achieve an amorphous state. Other polymers having much higher rates of crystallization, such as polyethylene, cannot be quenched quickly enough to prevent crystallization. For a given polymer, the rate of crystallization depends upon the crystallization temperature, as illustrated by Figure 4.7, which shows the effect of temperature on the rate of spherulite growth in poly(ethylene terephthalate) (PET).

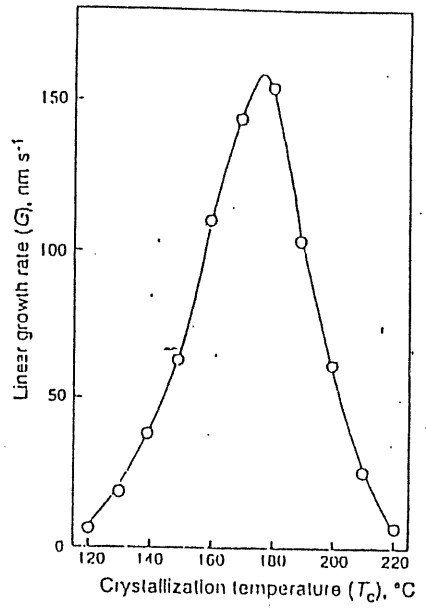

Figure 4.7. Plot of linear growth rate of spherulites in poly(ethylene terephthalate) (PET) as a function of temperature and at a pressure of 1 bar.[8] The maximum growth rate is observed near 178°C. Values of T_g and T_m for PET are approximately 69° and 265°C, respectively.

At T_m, the crystalline lamellae are destroyed as fast as they are formed from the melt and, therefore, the net rate of crystallization is zero. Since the large-scale segmental mobility required for chain folding ceases at T_g, the crystallization rate is again zero. At some intermediate temperature, T_{max}, an optimum balance is reached between chain mobility and lamellae growth. The temperature at which the crystallization rate is maximum is independent of molecular weight; however, the maximum crystallization rate decreases as the molecular weight increases.

The rate of crystallization can be followed by a variety of techniques, such as dilatometric measurement of volume changes, infrared spectroscopy, and optical-microscopic measurement of the growth of spherulite radii with time (e.g., Figure 4.7). During the crystallization process, the fractional crystallinity, ϕ, at time t may be approximated by the *Avrami equation*[9]

$$\phi = 1 - \exp\left(-kt^n\right) \tag{4.5}$$

where k is a temperature-dependent growth-rate parameter and n is a temperature-independent nucleation index. Typically, n varies between 1 and 4 depending on the nature of nucleation and growth processes. For example, in the case of sporadically nucleating spherulites, as may result during quiescent melt crystallization near T_m, the nucleation index is approximately 4. The fractional crystallinity of a polymer can be determined by a variety of techniques, including infrared spectroscopy as discussed in Section 2.6.1, density and X-ray diffraction measurements as described in the next section of this chapter, and by calorimetric methods, which will be described in Section 4.3.2.

TABLE 4.5 AMORPHOUS AND CRYSTALLINE DENSITIES

Polymer	ρ_a g cm^{-3}	ρ_c g cm^{-3}
Nylon-6	1.09	1.12–1.14
Nylon-6,6	1.09	1.13-1.145
Poly(ethylene terephthalate)	1.335	1.515
Poly(vinyl chloride)	1.385	1.44–1.53
Polycarbonate	1.196	1.316
Poly(*p*-phenylene sulfide)	1.32	1.43
Poly(2,6-dimethyl-1,4-phenylene oxide)	1.06	1.31

4.2.4 Techniques to Determine Crystallinity

Density Measurements. Densities can be easily measured at some standard temperature (e.g., 23°C) by means of a calibrated density-gradient column (ASTM[1] D 792). Once the density (ρ) of the semicrystalline sample has been measured, the fractional crystallinity, ϕ, can be determined as

$$\phi = \frac{\rho - \rho_a}{\rho_c - \rho_a} \tag{4.6}$$

if the densities of a totally amorphous (ρ_a) and totally crystalline sample (ρ_c) are known or can be estimated. Generally, values of amorphous densities are available only for semicrystalline polymers with low crystallization rates that enable rapid quenching from the melt to a totally amorphous state. The crystalline densities of polymers can be obtained from density measurements of single crystals or crystalline low-molecular-weight analogs or may be determined from X-ray determination of crystal densities. Densities for some semicrystalline polymers are given in Table 4.5.

[1] American Society for Testing and Materials (ASTM) standard.

X-Ray Diffraction. X-ray diffraction is a widely used technique of polymer characterization that can provide information concerning both the crystalline and amorphous states. X-rays are high-energy photons having short wavelengths ($\lambda \approx 0.5$ to 2.5 Å) that interact with electrons. When a X-ray beam is focused on a material, some electrons will be absorbed, some will be transmitted unmodified, while others will be scattered due to interaction with electrons. This interaction results in a scattering pattern that is a function of the scattering angle, usually designated as 2θ for convenience. The scattering pattern provides information on the electron-density distribution and, therefore, the positions of atoms in a polymer. The relationship between the intensity of an (unpolarized) X-ray beam, I_0, the scattered intensity, I, and the scattering angle is given by the *Thomson formula*

$$I = I_0 \frac{K}{r^2} \frac{1+\cos^2 2\theta}{2} \tag{4.7}$$

In eq. 4.7, r is the distance between the electron and the detector at which the scattered-beam intensity is measured and K is a constant given as

$$K = \frac{e^4}{m^2 c^4} \tag{4.8}$$

where e ($\approx 1.6022 \times 10^{-19}$ C) and m ($\approx 9.1095 \times 10^{-35}$ kg) are the charge and mass of an electron, respectively, and c is the speed of light ($\approx 3.00 \times 10^8$ m s^{-1}).

Terms often used in X-ray scattering are wide-angle X-ray scattering (WAXS) and small-angle X-ray scattering (SAXS). WAXS is used for the investigation of small-scale structures (<10 Å) while SAXS is used to study large-scale morphological features (10 to 10^4 Å). The need to measure the scattered-beam intensity at very small angles (e.g., 0.022 to 2.2°) in relation to the transmitted electron beam in the case of SAXS requires collimators for sharply focusing the incident beam and more specialized detectors than required for WAXS.

WAXS is used for the determination of fractional crystallinity as well as crystalline dimensions. An example of a WAXS diffraction pattern of a highly crystalline polymer is shown in Figure 4.8. In this case, there is an appearance of several large, narrow peaks positioned upon a broad background pattern. The background pattern is due to scattering from amorphous regions (the amorphous halo), while the peaks, called *Bragg peaks*, represent scattering from well-defined crystalline regions having regular spacing. In many cases, the fractional crystallinity can be estimated by comparing the intensity or height of the amorphous halo (I_{am})

of the crystalline sample with the intensity (I_{am}^{0}) of a totally amorphous polymer as sometimes can be obtained by rapid quenching from the melt as

$$w_c = 1 - \frac{I_{am}}{I_{am}^{0}} \tag{4.9}$$

where w_c is the *weight* fraction of the crystalline phase.

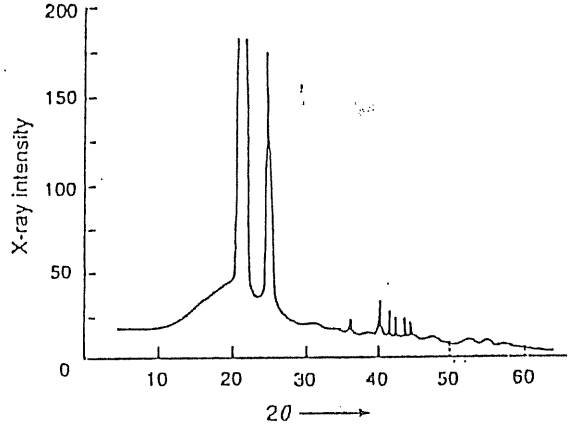

Figure 4.8. X-ray diffraction pattern (WAXS) of high-density polyethylene showing the superposition of crystalline Bragg diffusion peaks on an amorphous background. (Adapted from R.-J. Roe, in the *Concise Encyclopedia of Polymer Science and Engineering*, J. I. Kroschwitz, ed. Copyright ©1990 by John Wiley & Sons.)

4.3 THERMAL TRANSITIONS AND PROPERTIES

4.3.1 Fundamental Thermodynamic Relationships

Many of the commonly used techniques to determine T_g and T_m can be understood on the basis of the thermodynamic definition of a phase transition originally proposed by Paul Ehrenfest[10] in 1933. A *first*-order transition is defined as one for which a discontinuity occurs in the first derivative of the Gibbs free energy (G). According to the first law of thermodynamics for a reversible, closed system, the Gibbs free energy can be expressed in differential form as a function of temperature and pressure, $G(T, p)$, as

$$dG = -S\,dT + V\,dp \tag{4.10}$$

where S is entropy and V is the system volume.

The free energy may be differentiated with respect to temperature (at constant pressure) as

$$\left(\frac{\partial G}{\partial T}\right)_p = -S \tag{4.11}$$

and with respect to pressure (at constant temperature) as

$$\left(\frac{\partial G}{\partial p}\right)_T = V. \tag{4.12}$$

In terms of describing transitions in polymer systems, the most useful of the preceding relationships is the first derivative with respect to p (eq. 4.12), which indicates that a *first-order transition should occur as a discontinuity in volume*, as illustrated in Figure 4.9. Volume is easily measured as a function of temperature by a technique called *dilatometry*, which is described in the next section. The dependence of volume on temperature in the region about the crystalline-melting temperature approximates such a transition (see Figure 4.12).

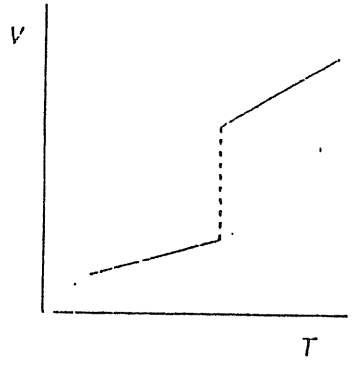

Figure 4.9. Thermodynamic first-order transition in volume at constant pressure.

Second-Order Transition. The glass transition approximates an Ehrenfest *second*-order transition, which means that a discontinuity should be observed in the *second* derivatives of the Gibbs free energy. Three possible second derivatives can be used to provide a basis for the experimental measurement of T_g. From eqs. 4.11 and 4.12, the corresponding second derivatives are

$$-\left(\frac{\partial^2 G}{\partial T^2}\right)_p = \left(\frac{\partial S}{\partial T}\right)_p, \tag{4.13}$$

$$\left(\frac{\partial^2 G}{\partial p^2}\right)_T = \left(\frac{\partial V}{\partial p}\right)_T, \tag{4.14}$$

and

$$\left[\frac{\partial}{\partial T}\left(\frac{\partial G}{\partial p}\right)_T\right]_p = \left(\frac{\partial V}{\partial T}\right)_p. \tag{4.15}$$

Since entropy is not an experimentally measurable quantity, eq. 4.13 may be recast into a more useful form in terms of the specific heat at constant pressure, C_p, which is defined as

$$C_p = \left(\frac{\partial H}{\partial T}\right)_p. \tag{4.16}$$

From the first law of thermodynamics, a relation between C_p and entropy can be obtained as[1]

$$C_p = T\left(\frac{\partial S}{\partial T}\right)_p. \tag{4.17}$$

Substitution of eq. 4.17 into eq. 4.13 indicates that *a second-order transition should occur as a discontinuity in specific heat*, as illustrated in Figure 4.10. Specific heat is easily measured by calorimetric techniques such as differential scanning calorimetry, as described in the next section.

The other two second derivatives indicate that second-order transitions should occur as discontinuities in the slope of volume as a function of pressure (eq. 4.14) or volume as a function of temperature (eq. 4.15). These slopes define two useful parameters — the isothermal *compressibility* coefficient, β, and the (isobaric) *thermal-expansion* coefficient, α. As defined earlier, (eqs. 3.73 and 3.74), these are

$$\beta = -\left(\frac{1}{V}\right)\left(\frac{\partial V}{\partial p}\right)_T \tag{4.18}$$

and

$$\alpha = \left(\frac{1}{V}\right)\left(\frac{\partial V}{\partial T}\right)_p. \tag{4.19}$$

This means that a discontinuity in a plot of α or β versus temperature, or alternately a change in slope of a plot of volume versus temperature (at constant pressure) or a plot of volume versus pressure (at constant temperature), marks the occurrence of a second-order transition as illustrated in Figures 4.11A and 4.11B, respectively. Both coefficients may be obtained by dilatometric measurements, although the constant-pressure experiment is the easier experiment and, therefore, the more commonly used.

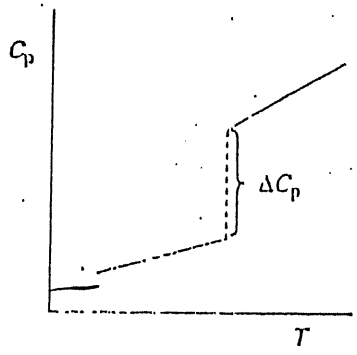

Figure 4.10. Thermodynamic second-order transition in specific heat at constant pressure.

The magnitudes of the discontinuities in C_p, α, and β at the second-order transition may be expressed as

$$\Delta C_p = C_{p,2} - C_{p,1}, \tag{4.20}$$

$$\Delta\alpha = \alpha_2 - \alpha_1, \tag{4.21}$$

[1] The first law of thermodynamics for a reversible, closed system may be written as

$$dH = T\,dS + V\,dp$$

for which a Legendre transformation gives

$$\left(\frac{\partial H}{\partial T}\right)_p = T\left(\frac{\partial S}{\partial T}\right)_p.$$

and

$$\Delta\beta = \beta_2 - \beta_1 \tag{4.22}$$

where the subscripts, 1 and 2, represent values at temperatures below and above the transition, respectively. These discontinuities are indicated in the illustrations of Figures 4.10 and 4.11.

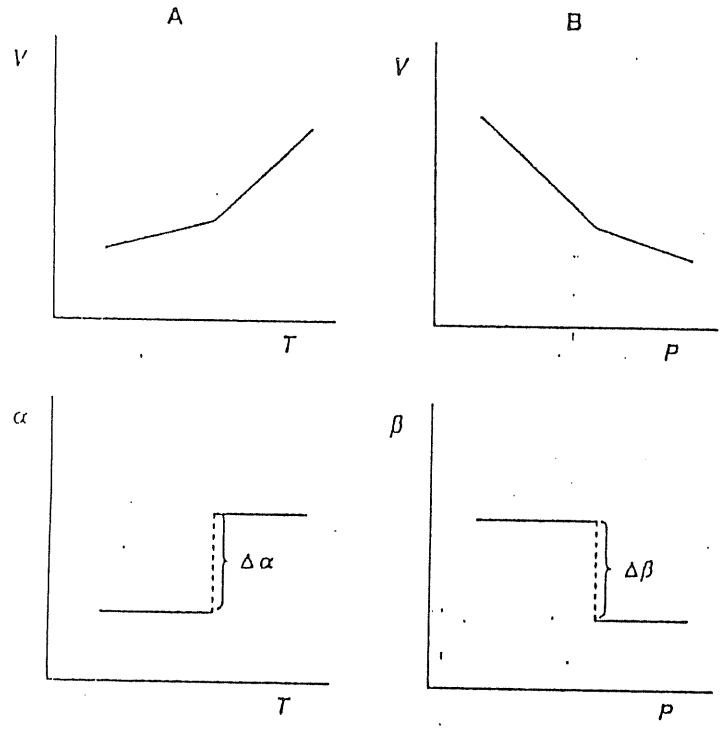

Figure 4.11. A. Thermodynamic second-order transition in volume as a function of temperature at constant pressure. B. Thermodynamic second-order transition in volume as a function of pressure at constant temperature.

As illustrated in the next section, the glass transition is not a *true* thermodynamic transition but, rather, it is considered to be a *pseudo*-second-order transition that is influenced by the kinetics of glass formation (i.e., the rate of heating or cooling). Both volume and specific-heat data for polymers closely approximate second-order transition behavior, but the discontinuities or changes in slope are more gradual and are affected by the heating rate.

4.3.2 Measurement Techniques

A wide variety of experimental methods can be used to determine the glass-transition and crystalline melting temperatures in polymers. For example, thermal transitions may be detected by a changes in refractive index, NMR line width, and birefringence as a function of temperature; however, the most commonly used techniques are dilatometry and, especially, differential scanning calorimetry (DSC), which are described in this section. Another important method of detecting thermal transitions is by recording the response to a cyclical strain (dynamic-mechanical analysis) or electric voltage (dielectric spectroscopy), as will be discussed in Chapter 5. An additional bonus in the case of dynamic-mechanical and dielectric measurements is the capability of detecting different low-temperature secondary relaxations. By contrast, dilatometric or calorimetric methods are insensitive to the occurrence of secondary-relaxation processes. The glass and melt transitions can also be detected by measurement of modulus as a function of temperature in tensile, stress relaxation, and other mechanical tests, as will be discussed in Section 4.4.2.

Dilatometry. One of the earliest methods used to determine thermal transitions is dilatometry. In this procedure, a small sample of polymer is sealed in a glass bulb to which a precision-bored, calibrated glass capillary is attached. Mercury, whose coefficient of thermal expansion is accurately known, is used to fill the bulb and part of the capillary. The dilatometer is then immersed in a controlled-temperature bath and the height of the mercury in the capillary is recorded at different temperatures. Heating rate is normally kept very small (1° to 2° min^{-1}) to assure thermal equilibrium, especially near T_g. From this information, the specific volume of the polymer sample can be obtained as a function of temperature. As illustrated in Figure 4.12, the glass-transition temperature is determined as that temperature at which the volume–temperature curve changes slope (i.e., a discontinuity in α), while at the crystalline-melting temperature (a first-order transition temperature), there is a discontinuity, or step change, in specific volume. Some representative dilatometric data for T_g and thermal-expansion coefficients are given in Table 4.6.

As an approximation, the change in thermal-expansion coefficient going from the liquid (i.e., $T > T_g$) to the glassy state (i.e., $T < T_g$),

$$\Delta\alpha = \alpha^l - \alpha^g, \tag{4.23}$$

is sometimes taken to be 4.8×10^{-4} K^{-1}; however, extensive data have shown that $\Delta\alpha$ increases with decreasing temperature, as the data given in Table 4.6 serve to illustrate. As a better approximation, Simha and Boyer[12] have suggested that

$$\Delta\alpha \approx \frac{0.113}{T_g} \qquad (4.24)$$

where T_g is in Kelvins.

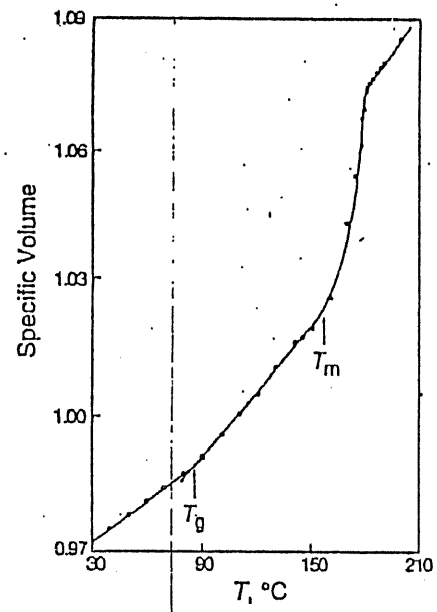

Figure 4.12. Dilatometric data of specific volume of a semicrystalline polymer, poly(*N*,*N*'-sebacoyl piperazine), plotted against temperature.[11] Results indicate a glass transition near 90°C and a crystalline-melting transition above 160°C.

Calorimetry. One of the most widely used techniques to measure T_g and T_m is differential scanning-calorimetry (DSC). This method uses individual heaters to maintain identical temperatures for two small platinum holders — one contains a small (10 to 30 mg) polymer sample mechanically sealed in a small aluminum pan and the other contains an empty (reference) pan, as illustrated in Figure 4.13. Temperatures are measured by use of identical platinum-resistance thermisters. The differential power needed to maintain both the reference and sample pans at equal temperatures during a programmed heating cycle (range of 0.3125° to 320°C min^{-1}) is then recorded as a function of temperature.

TABLE 4.6 REPRESENTATIVE DILATOMETRIC DATA FOR POLYMERS[12]

Polymer	T_g (K)	α' ($\times 10^4$) (K^{-1})	$\Delta\alpha$ ($\times 10^4$) (K^{-1})
Polydimethylsiloxane	150	8.12–12	5.4–9.3
Poly(vinyl acetate)	302	5.98	3.9
Poly(vinyl chloride)	355	5.2	3.1
Polystyrene	373	5.5	3.0
Poly(methyl methacrylate)	378	4.6–5.0	2.45–3.05

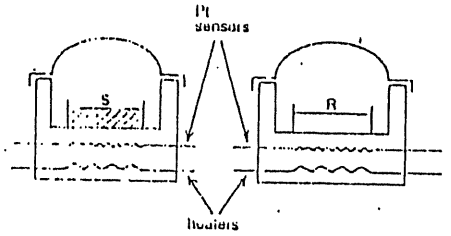

Figure 4.13. Schematic representation of a typical DSC sample cell showing the sample (S) and reference (R) pans, as well as the heating and temperature sensing elements.

In place of differential power, values of specific heat, C_p, may be obtained from the recorded heat-flow rate by calibration with a pure compound such as sapphire for which C_p is known precisely at different temperatures from calorimetry measurements. As illustrated in Figure 4.14, a discontinuity in C_p (i.e., $\Delta C_p = C_p^{\ell} - C_p^{g}$) characteristic of a second-order transition (see preceding discussion) is observed at the polymer T_g, which is often identified as the temperature at the midpoint of the step change in C_p (i.e., at $\Delta C_p/2$). For many amorphous polymers, T_g (K) and ΔC_p (J g^{-1} K^{-1}) are related by the approximate relationship[12] that $\Delta C_p \times T_g \approx 115$ J g^{-1} (27.5 cal g^{-1}).

During heating of a semicrystalline polymer, additional crystallization may occur at temperatures between T_g and T_m, as illustrated by the crystallization exotherm of poly(ethylene terephthalate) shown in Figure 4.14. At T_m, which may be defined as the extrapolated temperature of the initial slope of the melt endotherm, the crystallites begin to melt over a wide range of temperatures. The breadth of the endotherm is much larger than typically observed for pure low-molecular-weight compounds as a consequence of the lower order of perfection of polymer crystallites. By calibration with a low-molecular-weight standard such as benzoic acid, the heat

of fusion (ΔQ) of a semicrystalline polymer can be determined from measurement of the area under the melt endotherm recorded by DSC. The heat of fusion of the same polymer at 100% crystallinity (ΔH_f) can be estimated from a comparison of the heats of fusion of a homologous series of low-molecular-weight crystals, or from measurement of the melting-point depression of the semicrystalline polymer by diluents (see eq. 4.4). With this information, the fractional crystallinity (ϕ) of the polymer sample can be obtained by the equation

$$\phi = \frac{\Delta Q}{\Delta H_f}. \tag{4.25}$$

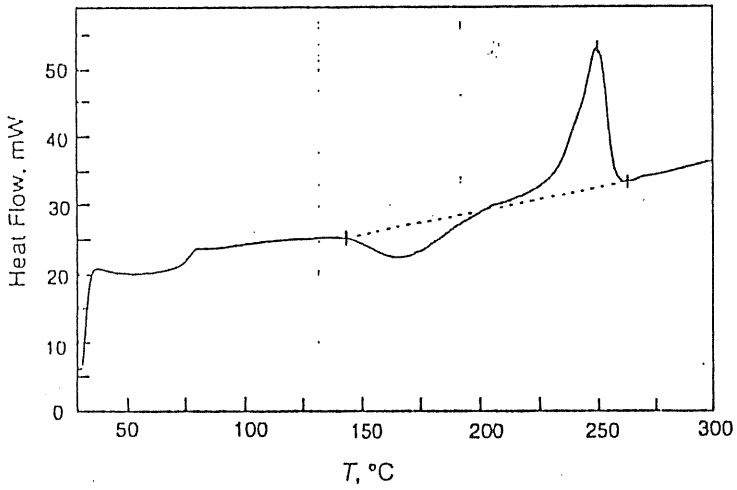

Figure 4.14. DSC thermogram of poly(ethylene terephthalate) crystallized at 200°C for 90 s showing a glass transition near 75°C, an excess crystallization peak above 143°C, and a crystalline-melting endotherm with a peak maximum near 250°C.

In the case of some polymers, such as isotactic polystyrene with high crystalline order, it is also possible to estimate ϕ from measurement of the specific-heat increment of the semicrystalline polymer at T_g and that of the same polymer in the amorphous state, $(\Delta C_p)_{am}$, obtained by rapid thermal quenching from above T_m, where

$$\phi = 1 - \frac{\Delta C_p}{(\Delta C_p)_{am}}. \tag{4.26}$$

Fractional crystallinity of polymers with low rates of crystallization, such as is the case for polycaprolactone, can be obtained in this manner. For many polymers with low crystalline order, eq. 4.26 will significantly overestimate ϕ because the specific-heat increment of the amorphous phase of the semicrystalline state may be depressed by the presence of small disorganized crystallites that are dispersed in the amorphous matrix.

TABLE 4.7 THERMAL-TRANSITION TEMPERATURES

Polymer	HDT[a] (°C)	T_g (°C)	T_m (°C)
Polyethylene	29 to 126	-120 to -125	137
Polypropylene	40 to 152	-10 to -18	176
Nylon-6,6	62 to 261	49	265
Poly(vinyl chloride)	60 to 76	87	Low crystallinity
Polystyrene	63 to 112	100	Amorphous
Polycarbonate	39 to 148	150	Amorphous
Polysulfone	146 to 273	190	Amorphous

[a] At 1.82 MPa (264 psi); HDT range indicates values reported for all commercial grades, including reinforced resins.

Heat-Distortion Temperature. An alternate, and more applications-oriented, measure of T_g or T_m is called the *heat-distortion* (or heat-deflection) temperature (HDT). The HDT is defined by ASTM Standard D 648[†] as the temperature at which a sample bar of standard dimensions (e.g., 127 × 13 × 3 mm) deflects by 0.25 mm (0.01 in.) under a standard flexural load of 455 kPa (66 psi)[‡] placed at its center. The sample is heated in an immersion bath at a rate of 2°C min^{-1}. In the case of an amorphous polymer, HDT is slightly (10° to 20°C) lower than the T_g as determined by thermal techniques, while in the case of semicrystalline polymers, HDT is more closely identified with T_m, as shown by the values given in Table 4.7. Heat-deflection temperature is, therefore, a useful indicator of the temperature limit above which polymers (or commercial grades of plastics) cannot be used for structural (load-supporting) applications. It is widely used to report the thermal properties of different grades of commercial plastics, including reinforced or filled

[†] Specification for *tensile* heat distortion temperature for plastic sheet (0.025 to 1.5 mm in thickness) is given by ASTM D 1637.
[‡] A load of 1820 kPa (264 psi) may be specified for a thicker sample.

resins. A listing of other important ASTM standards is given in Appendix C at the end of this text.

4.3.3 Structure–Property Relationships

As suggested by data that were given in Tables 4.2 and 4.3, both T_g and T_m are strongly influenced by the chemical structure of the repeating unit. In general, both T_g and T_m increase with decreasing flexibility of the polymer chain. Flexibility decreases with increasing aromatic composition of the main chain or by incorporation of bulky substituent groups or nonrotational (e.g., unsaturated) groups in the main chain. This is illustrated by the relation of T_m to repeating-unit structure for an analogous series of polyesters in Table 4.8. Replacement of the aliphatic sequence $(CH_2)_4$ of compound A with an aromatic ring (compound B) increases T_m by 220°C. Replacement by two coupled aromatic rings (compound C) further increases T_m by 85°C, but incorporation of a flexible $(CH_2)_2$ group between aromatic rings lowers T_m by 135°C (compound D). By contrast, incorporation of a nonrotational, unsaturated –CH=CH– linkage between aromatic rings (compound E) results in the highest-T_m polyester.

TABLE 4.8 EFFECT OF BACKBONE STRUCTURE ON THE CRYSTALLINE-MELTING TEMPERATURE OF POLYESTERS DERIVED FROM ETHYLENE GLYCOL ($HOCH_2CH_2OH$)

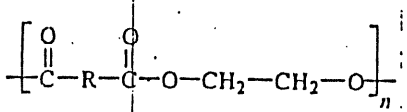

Compound	Main-Chain Unit, R	T_m (°C)
A	$-(CH_2)_4-$	50
B	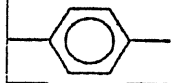	270
C	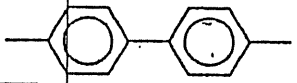	355
D	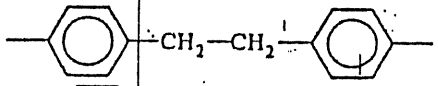	220
E	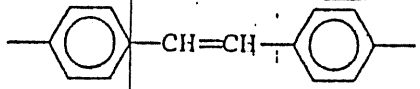	420

Chain flexibility is particularly important in determining T_g. Flexible chains, as may be obtained by incorporating an oxygen atom into the main chain (e.g., polydimethylsiloxane), are capable of large-scale molecular motions at very low temperatures and, therefore, have low T_g. Bulky substituent groups hinder chain rotation and therefore raise T_g as shown by structure–T_g comparisons for several vinyl polymers in Table 4.9.

TABLE 4.9 GLASS-TRANSITION TEMPERATURES OF SELECTED VINYL POLYMERS

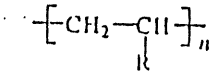

Polymer	Substituent Group, R	T_g (°C)
Polyethylene	H	-125
Polypropylene (atactic)	CH_3	-20
Poly(vinyl chloride)	Cl	89
polyacrylonitrile	C≡N	100
Polystyrene		100
Poly(α-vinyl naphalene)	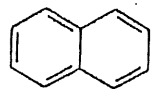	135

For comparably sized substituent groups, increasing polarity, which may enhance intermolecular interactions, can elevate T_g. This is illustrated by T_g data for the vinyl polymers — polypropylene (T_g = -20°C), poly(vinyl chloride) (T_g = 89°C), and polyacrylonitrile (T_g = 100°C) — given in Table 4.9. As illustrated in Table 4.10, increasing flexibility of the side group can lower T_g, as is evident by comparison of the chemical structures of poly(methyl methacrylate), poly(ethyl methacrylate), and poly(propyl methacrylate). Syndiotactity increases T_g as illustrated by data for poly(methyl methacrylate) (PMMA) prepared with different tacticities: *i*-PMMA (T_g = 45°C), *a*-PMMA (T_g =105°C), and *s*-PMMA (T_g = 115°C). *Trans* geometric isomers have higher T_g than *cis*-isomers, as for example in the case of *cis*-polybutadiene (T_g = -108°C) compared to *trans*-polybutadiene (T_g = -18°C) or

in the case of *cis*-polyisoprene (T_g = -73°C) compared to *trans*-polyisoprene (T_g = -53°C).

TABLE 4.10 EFFECT OF INCREASING SIZE OF THE SUBSTITUENT GROUP ON THE GLASS-TRANSITION TEMPERATURE OF POLYMETHACRYLATES

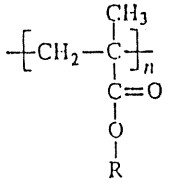

Polymethacrylate	Substituent Group, R	T_g (°C)
Poly(methyl methacrylate)	CH_3	105
Poly(ethyl methacrylate)	CH_2CH_3	65
Poly(propyl methacrylate)	$CH_2CH_2CH_3$	35

4.3.4 Effect of Molecular Weight, Composition, and Pressure on T_g

Molecular-Weight Dependence. The glass-transition temperature increases with molecular weight at low molecular weight but reaches a point at moderate molecular weight where further increase in molecular weight has very little effect on T_g. This is an example of a *limiting-property relationship*. The crystalline-melting temperature, T_m, follows a similar dependence on molecular weight. The particular molecular-weight average most relevant to T_g is the number-average, $\overline{M}_n$. This dependence can be rationalized on the basis of the free-volume theory of the glass transition. Since larger free volume is associated with the ends of long polymer chains than with other chain segments, free volume increases with an increasing *number* of chain ends (i.e., decreasing molecular weight).

The form of dependence of T_g on molecular weight is approximated by the *Fox-Flory equation*[13]

$$T_g = T_g^{\infty} - \frac{K}{\overline{M}_n} \tag{4.27}$$

where T_g^{∞} is the limiting value of T_g at high molecular weight (obtained from the intercept of a plot of T_g versus reciprocal number-average molecular weight) and K is a constant for a given polymer. Equation 4.27 has been found to give a good fit of experimental data for many polymers; however, there is evidence that K may not be constant for molecular weights below about 10,000.[14] Representative values of the Fox–Flory parameters, T_g^{∞} and K, for some well-characterized polymers are given in Table 4.11.

TABLE 4.11 FOX–FLORY PARAMETERS

Polymer	T_g^{∞} (K)	K (K)
Polydimethylsiloxane	148	5.9×10^3
Poly(vinyl chloride)	351	8.1×10^4
Polystyrene	373	1.2×10^5
Poly(methyl methacrylate)	387	2.1×10^5
Poly(α-methylstyrene)	446	3.6×10^5

Composition Dependence. When a second component, either a low-molecular-weight additive or a second polymer, is blended to form a *homogeneous* mixture, the T_g of the mixture will depend upon the amount of each component and upon the T_g of the second component. The form of the T_g–composition dependence may be approximated by several theoretical or semiempirical models.

An approximate relationship between the T_g of a miscible mixture and composition is given by the *simple rule of mixtures*, which for a binary mixture is given as

$$T_g = W_1 T_{g,1} + W_2 T_{g,2} \tag{4.28a}$$

where W_1 is the weight fraction and $T_{g,1}$ (in Kelvins) is the glass-transition temperature of the ith component (i.e., component 1 or 2 in a binary mixture). For a multicomponent mixtures, we can write

$$T_g = \sum_{i=1}^{N} W_i T_{g,i} \tag{4.28b}$$

The simple rule of mixtures is a good approximation for blends of two or more polymers but overpredicts the T_g of polymers plasticized with a low-molecular-weight organic compound such as an ester or phthalate (see Section 7.1.1).

Improved predictive capability is available through a number of other empirical or theoretical relationships. One of the earliest theoretical expressions is the *Kelley–Bueche equation*,[15] which is derived from the isofree volume model of the glass transition. At constant pressure and at a temperature, T, above the glass transition, the fractional free volume, f, is given as

$$f = f_g + \alpha_p\left(T - T_{g,p}\right)\phi_p + \alpha_d\left(T - T_{g,d}\right)\phi_d \tag{4.29}$$

where f_g is the fractional free volume at T_g ($f_g \approx 0.025$), α is the (isobaric) thermal-expansion coefficient (eq. 4.19) of the melt, and ϕ is the volume fraction of the polymer (p) or diluent (d), where $\phi_p + \phi_d = 1$. By equating T with the T_g of the mixture (whereby $f = f_g$), eq. 4.29 reduces to

$$\alpha_p\left(T_g - T_{g,p}\right)\phi_p + \alpha_d\left(T_g - T_{g,d}\right)\phi_d = 0 \tag{4.30}$$

which upon rearrangement gives the frequently used Kelley–Bueche expression

$$\boxed{T_g = \frac{\alpha_p\phi_p T_{g,p} + \alpha_d\left(1-\phi_p\right)T_{g,d}}{\alpha_p\phi_p + \alpha_d\left(1-\phi_p\right)}} \tag{4.31}$$

A more recent relation[16] is based upon a classical thermodynamic treatment of the glass-transition temperature at which the entropies of the glass and liquid phases are equal. The resulting equation for a binary system is given as

$$\ln\left(\frac{T_g}{T_{g,1}}\right) = \frac{W_2\Delta C_{p,2}\ln\left(T_{g,2}/T_{g,1}\right)}{W_1\Delta C_{p,1} + W_2\Delta C_{p,2}} \tag{4.32}$$

where ΔC_p is the change in specific heat at T_g (see eq. 4.20). Assuming that the product $T_g\,\Delta C_p$ is constant for all polymers,[12] eq. 4.32 reduces to the simpler form[17]

$$\ln\left(\frac{T_g}{T_{g,1}}\right) = \frac{W_2\ln\left(T_{g,2}/T_{g,1}\right)}{W_1\left(T_{g,2}/T_{g,1}\right) + W_2} \tag{4.33}$$

If the T_gs of the polymer and diluent are not too different, a truncated Taylor series expansion of the log terms and rearrangement gives the commonly used *inverse rule of mixtures*

$$\boxed{\frac{1}{T_g} = \frac{W_1}{T_{g,1}} + \frac{W_2}{T_{g,2}}} \tag{4.34}$$

which is known as the *Fox equation* when applied to T_g. The Fox equation has been considered to be an empirical relation; however, the preceding derivation shows that it may be viewed as representing a limiting case of the more general theoretical relationship. Another commonly used empirical relation that can be derived from eq. 4.32 is the *logarithmic rule of mixtures* given as

$$\boxed{\ln T_g = W_1 \ln T_{g,1} + W_2 \ln T_{g,2}} \tag{4.35}$$

Pressure Dependence. Compared to effects of molecular weight and plasticization, T_g is relatively insensitive to pressure. The glass-transition temperature will increase with increasing pressure at a rate of approximately 25 K per kbar of pressure. The pressure dependence can be estimated from the compressibility and thermal expansion coefficients as

$$\frac{dT_g}{dp} = \frac{\Delta\beta}{\Delta\alpha} \tag{4.36}$$

4.4 MECHANICAL PROPERTIES

4.4.1 Mechanisms of Deformation

At low strain (i.e., <1%), the deformation of most polymers is elastic meaning that the deformation is homogeneous and full recovery can occur over a finite time. At higher strains, the deformation of glassy polymers occur by either *crazing* characteristic of brittle polymers or by a process called *shear banding* which is the dominant mechanism for ductile polymers. Such deformations are not reversible unless the polymer is heated above its glass-transition temperature.

Crazing. The term, *crazing*, owes it origin to the Middle English word "crasen," which means to break. It was originally applied to describe a network of fine cracks appearing on the surface of ceramics and glasses. When some polymers such as polystyrene are deformed to a certain level, the critical strain (ε_c), what appears to be small cracks develop in a direction *perpendicular* to the principal direction of deformation. Some typical values of critical strains are given in Table 4.12. These crazes reflect light and result in visual cloudiness or whitening of the sample. Crazes developed in a polycarbonate tensile bar are shown in Figure 4.15.

A craze is a unique morphological feature of polymers and is morphologically different from a true crack. A craze, which can be nanometers to a few micrometers in thickness, consists of polymer microfibrils (0.6 to 30 nm in diameter) stretched in the direction of tensile deformation. The microfibrils are surrounded by void space, which can represent as much as 90% of the total volume of the craze. This anisotropic morphology of a craze results in the scattering of light. An electron micrograph of typical craze structures is shown in Figure 4.16.

TABLE 4.12 CRITICAL STRAINS FOR CRAZE INITIATION IN GLASSY POLYMERS

Polymer	Critical Strain (%)
Polystyrene	0.35
Styrene–acrylonitrile copolymer (SAN)	0.49
Poly(methyl methacrylate)	0.8–1.30
Poly(2,6-dimethyl-1,4-phenylene oxide)	1.5
Polycarbonate	1.8
Polysulfone	2.5

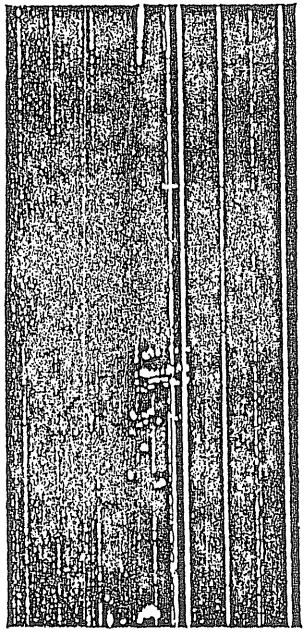

Figure 4.15. Macroscopic view of crazes developed perpendicular to the tensile direction in a polycarbonate dogbone. (Courtesy of R. P. Kambour.)

The time for the initiation of a craze depends upon many factors, including the magnitude of the applied stress, temperature, and the presence of low-molecular-weight liquids which may act to promote craze development (see Section 6.1.3). Although the reasons for craze initiation are still uncertain and several different theories have been proposed, it is recognized that crazes constitute the defects from

which brittle cracks initiate. Mechanical fracture of a sample that has begun crazing is initiated by the breakdown of the fibrillar microstructure to form additional voids that grow slowly until some critical size has been reached. Beyond this point, the craze will rapidly propagate as a crack. As the crack propagates, crazes are formed at the crack tip and act to retard its advance.

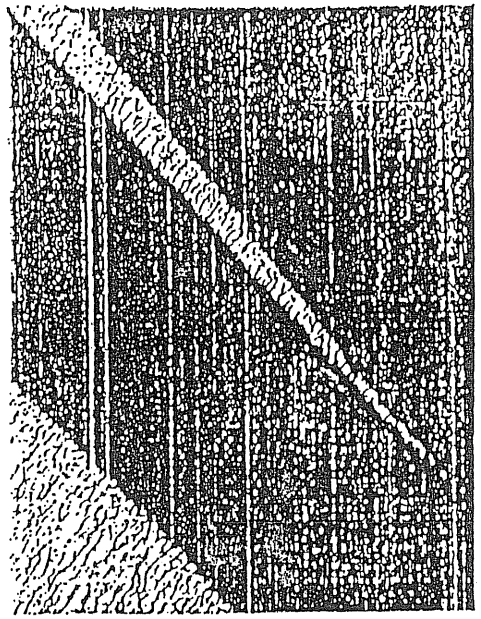

Figure 4.16. Micrograph of craze structures in poly(2,6-dimethyl-1,4-phenylene oxide).[13] (Courtesy of R. P. Kambour.)

Shear Banding. While some polymers such as polystyrene will readily craze when strained in tension, crazes may not develop in other polymers such as polycarbonate under identical conditions. Instead, these polymers will form regions of localized shear deformation. These regions are called shear bands, which develop at angles of 45° to the stretch direction. Other polymers such as SAN can exhibit both modes of deformation. In general, shear-band formation is a dominant mode of deformation during tensile yielding of ductile polymers.

4.4.2 Methods of Testing

As the HDT indicates the temperature limits within which a plastic may be used, a variety of methods are used to determine mechanical performance under a variety of loading conditions. These may be classified as static (i.e., tensile and shear), transient (i.e., creep and stress relaxation), impact (Izod and Charpy), and cyclic (i.e., fatigue tests). Static tests are used to measure the force response when a sample is strained, compressed, or sheared at a constant rate. These provide a means to characterize the mechanical properties of a polymer in terms of modulus, strength, and elongation to failure. Transient tests measure the time response of the force (or stress) on a polymer sample when it is rapidly stretched to a given length (*stress relaxation*) or the time response of strain when a load (stress) is rapidly applied (*creep*). Impact tests measure the energy required for a sample to fail under different loading histories, while fatigue tests determine the number of cycles of applied stress required for failure.

Static Testing. Static tests refer to those for which the deformation rate is steady in time. While tensile, compressive, or shear modes may be employed, tensile testing is the most common. In a typical tensile test, a polymer sample, in the form of a dogbone (e.g., Figure 4.17), is clamped at one end and pulled at a constant rate of elongation at the other clamped end.† The thinner portion of the tensile specimen encourages the sample to fail at the center of the bar and not at the grip sites, where stress concentration may result in premature failure.

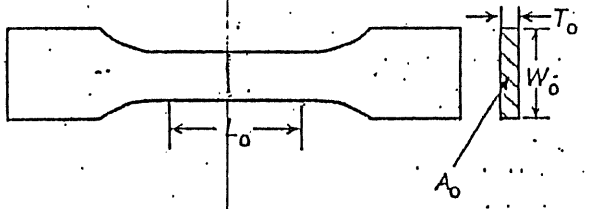

Figure 4.17. Illustration of a typical tensile-dogbone sample. The overall length of the specimens may vary from 63.5 to 246 mm. During tensile measurement, the sample is gripped at the wide ends. Specimen parameters include L_0, gage length (distance between test marks or extensometer span, ca. 50 mm); W_0, initial width (19 or 29 mm); T_0, initial thickness (4 to 14 mm); and A_0, initial cross-sectional area.

† Conditions and sample dimensions for tensile tests are specified by ASTM D 638, "Tensile Properties of Plastics." For specimens of thickness up to 3.2 mm (1/8 in.), conditions and sample dimensions are given by ASTM D 1708, "Tensile Properties of Plastics by Use of Microtensile Specimens."

As indicated in Figure 4.17, the initial length of a central section contained within the narrow region of the tensile specimen is called the initial *gage length*, L_0. During deformation, force, F, is measured as a function of elongation at the fixed end by means of a transducer. Usually, the tensile response is plotted as *engineering* (nominal) *stress*, σ, versus *engineering* (nominal) *strain*, ε, where

$$\sigma = \frac{F}{A_0} \tag{4.37}$$

and

$$\varepsilon = \frac{\Delta L}{L_0}. \tag{4.38}$$

In eq. 4.37, A_0 is the original (undeformed) cross-sectional area of the gage region and ΔL in eq. 4.38 is the change in sample gage length $(L - L_0)$ due to the deformation. Sample length can be determined from instrumental settings of the mechanical-testing instrument or by an extensometer which is a strain gage that is attached to the gage-length region of the tensile specimen.

Alternately, the stress–strain response of a sample may be reported in terms of true stress and true strain. The *true stress* is defined as the ratio of measured force to the *actual* cross-sectional area, A, at a given elongation

$$\sigma^T = \frac{F}{A}. \tag{4.39}$$

Since the actual cross-sectional area decreases as the sample is elongated, the true stress will always be larger than the engineering stress. Assuming that the volume of the sample remains constant during deformation, it can be shown (see Problem 4–1) that the true stress is simply related to the engineering stress as

$$\sigma^T = \sigma \frac{L}{L_0}. \tag{4.40}$$

The *true strain*, ε^T, is defined as

$$\varepsilon^T = \int_{L_0}^{L} \left(\frac{1}{\ell}\right) d\ell = \ln\left(\frac{L}{L_0}\right). \tag{4.41}$$

With the exception of elastomers, the assumption of a constant volume during deformation is not strictly correct, because the volume of glassy polymers increases, or dilates, during extension. This change in volume, ΔV, at a given strain may be calculated from the relation

$$\Delta V = V - V_0 = (1 - 2\upsilon)\varepsilon V_0 \tag{4.42}$$

where V_0 is the initial (unstrained) volume and υ is called *Poisson's ratio* which is defined as the ratio of *true* strain in the transverse direction, ε_T, to the *true* strain in the longitudinal direction, ε_L, and is calculated as

$$\upsilon = -\frac{\varepsilon_T}{\varepsilon_L} = \frac{1}{2}\left[1 - \frac{1}{V}\left(\frac{\partial V}{\partial \varepsilon}\right)\right]. \tag{4.43}$$

For the majority of glassy polymers, $\upsilon = 0.4$, as shown by data for polystyrene, poly(methyl methacrylate), and poly(vinyl chloride) in Table 4.13. For completely incompressible materials, for which the term $(\partial V/\partial \varepsilon)$ within brackets in eq. 4.43 is zero, υ obtains its maximum value of 0.5 as approached by natural rubber and low-density polyethylene ($\upsilon = 0.49$).

TABLE 4.13 POISSON'S RATIO OF SOME IMPORTANT POLYMERS

Polymer	Poisson's Ratio
Polyethylene (LD)	0.49
Poly(methyl methacrylate)	0.40
Polystyrene	0.38
Natural rubber	0.49
Poly(vinyl chloride)	0.4

Hooke's law for an ideal elastic solid provides a relationship between stress and strain for tensile deformation as

$$\sigma = E\varepsilon \tag{4.44}$$

where the proportionality factor, E, is called the tensile (or Young's) modulus. Conversely, the strain and stress are related by the tensile *compliance*, D, defined by

$$\varepsilon = D\sigma. \tag{4.45}$$

For tensile deformation, the compliance is therefore the reciprocal of the modulus

$$D = \frac{1}{E}. \tag{4.46}$$

As shown by the representative stress–strain plot for a typical brittle polymer in Figure 4.18, only the initial portion of the plot follows Hookean behavior. The point at which stress begins to deviate from a linear stress–strain relation is called the *proportional limit*. This normally occurs before 1% strain. Therefore, to designate a value for the modulus, a convenient procedural definition must be adopted. Consequently, the initial slope of the stress–strain curve is called the *initial* modulus. Alternately, a line may be drawn from the origin to some convenient point along the stress–strain curve, for example, at 1% strain. This line defines a secant and the slope defines the *secant modulus*, the 1% secant modulus in this case. The modulus, or the compliance, is a *material property* that is a function of both temperature and the time scale of the deformation.

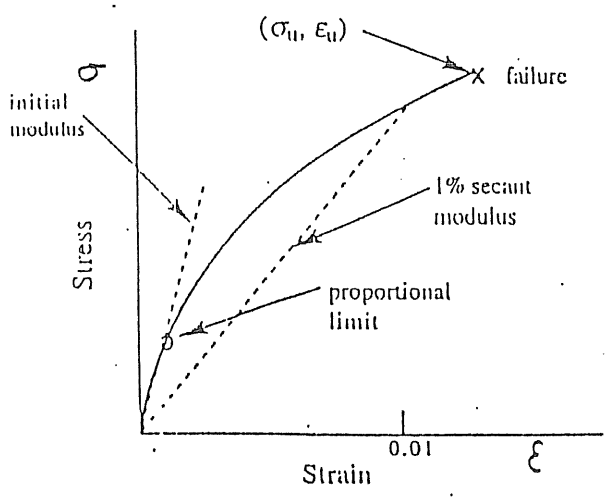

Figure 4.18. Representative stress–strain curve for a polymer undergoing brittle failure.

Figure 4.19 shows a representative plot of modulus versus temperature. At temperatures below T_g, all glassy materials, polymeric as well as low-molecular-weight substances, have approximately the same value of modulus (ca. 10^9 GPa). At first, this modulus slowly decreases with increasing temperature and then rapidly decreases in the region of T_g. For low-molecular-weight materials, modulus continues to fall rapidly with increasing temperature. For high-molecular-weight amorphous polymers, modulus drops to a secondary plateau region (approximately

10^6 GPa) called the *rubbery plateau*. With further increase in temperature, the modulus again rapidly drops. This point marks the *viscous flow* region. Polymers are typically melt-processed in this temperature range in which the viscosity is also low.

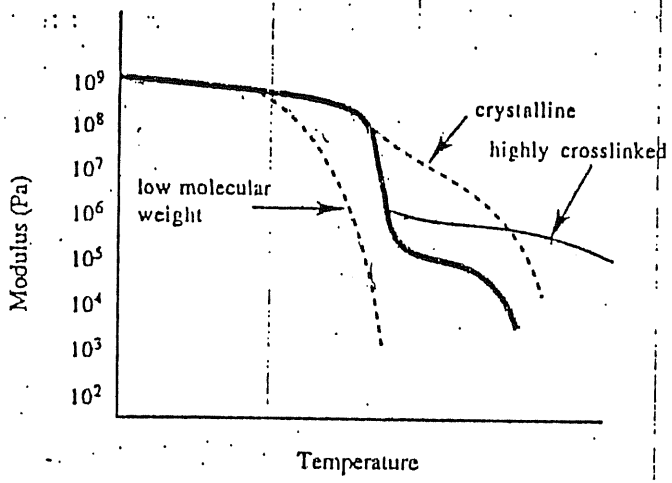

Figure 4.19. Plot of modulus versus temperature for a high-molecular-weight, amorphous polymers with variations for low-molecular-weight ($M < M_e$), crosslinked, and semicrystalline polymers.

The appearance of a rubbery plateau for high-molecular-weight polymers is the result of the formation of entanglements as described earlier in this chapter. Entanglements prevent slippage at temperatures immediately above T_g and, therefore, modulus remains relatively high. Above T_g, the entanglements are easily disassociated due to high kinetic energy and the modulus drops. The rubbery plateau modulus, E_p, is inversely proportional to the molecular weight between entanglements, M_e (see Section 4.1.1), as

$$E_p \propto \frac{\rho RT}{M_e} \tag{4.47}$$

where ρ is density.

The temperature behavior of the modulus of semicrystalline polymers is qualitatively similar to that of high-molecular-weight amorphous polymers except that the modulus is typically higher in the secondary plateau (see Figure 4.19) due to the reinforcing effect of crystallites dispersed in an amorphous rubbery phase at temperature above T_g but below T_m. At T_m, the crystallites melt and the modulus drops in the viscous-flow region.

In addition to tensile deformation, samples may be *compressed* (ASTM D 695) or *sheared*. In the case of compression, the sample is typically prepared in the form of a disk. The measured parameters are the bulk modulus, K, and compliance, B... A simple-shear deformation of a solid is illustrated in Figure 4.20. The engineering *shear* stress, τ, is defined as

$$\tau = \frac{F}{A_o} \tag{4.48}$$

where A_o is the area of the *surface* on which the shear force acts. The shear strain, γ, is given by the angle of deformation, θ, as

$$\gamma = \tan\theta = \frac{\Delta X}{C}. \tag{4.49}$$

Hooke's law for shear deformation is given as

$$\tau = G\gamma \tag{4.50}$$

where G is the shear modulus, while the shear compliance is normally designated as J ($\equiv 1/G$).

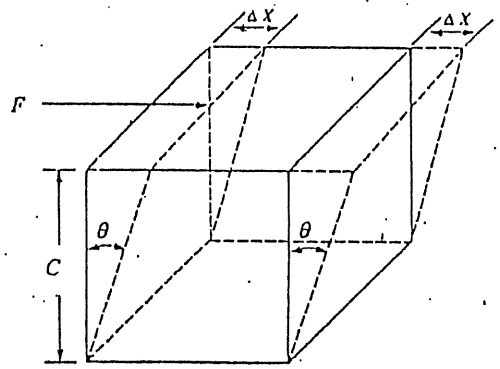

Figure 4.20. Illustration of the shear deformation of a solid with the shear force (F) acting on the top surface of the cube.

Moduli obtained in different deformation modes (tensile, compression, and shear) may be interrelated through Poisson's ratio, υ. For *isotropic* materials, the following relationships hold:

$$E = 2(1+\upsilon)G, \tag{4.51}$$

$$J = 2(1+\upsilon)D, \tag{4.52}$$

and

$$K = \frac{E}{3(1-2\upsilon)}. \tag{4.53}$$

In the limit of incompressibility (i.e., $\upsilon = 0.5$), eqs. 4.51 to 4.53 reduce to

$$E = 3G, \tag{4.54}$$

$$J = 3D, \tag{4.55}$$

and

$$K \to \infty, \tag{4.56}$$

respectively. The limiting behavior for bulk modulus expressed by eq. 4.56 simply means that *incompressible* materials cannot be compressed.

Polymers exhibit a wide range of mechanical behavior depending upon temperature and rate of deformation. Typical stress–strain curves covering this range of behavior are illustrated in Figure 4.21. At normal use temperatures, brittle polymers (e.g., polystyrene) exhibit a rapid increase in stress with increasing strain (i.e., high modulus) up to the point of sample failure (curve 1). The stress at failure is called the *ultimate stress* (σ_u) or stress-at-break (σ_b). Unlike modulus, ultimate stress, resulting from large and irreversible deformation, is a *sample*, rather than material, property and is strongly influenced by sample defects and processing history. For this reason, a sufficiently large number of samples must be evaluated and their values averaged in order to get a statistically meaningful value.

Ductile polymers, including many engineering thermoplastics, polyamides, and toughened (rubber-modified) plastics, exhibit stress–strain behavior represented by curves 2 and 3 in Figure 4.21. As shown, the stress reaches a maximum value, which is called its *yield stress*, σ_y, at a certain strain, ϵ_y. As strain is further increased, stress at first decreases. This process is called *strain softening*, which usually occurs at strains between 5% and 50%. A minimum in stress reached during strain softening is called the *draw stress*. At this point, the sample may either fail (curve 2) or experience *orientation hardening* (curve 3) prior to failure. During orientation hardening, polymer chains are stretched locally in the tensile direction. Chain extension causes a resistance to further deformation; stress is, therefore, observed to increase. Accompanying the molecular processes that are occurring during orientation are macroscopic changes in the shape of the tensile specimen. Above the yield point, a portion of the tensile dogbone begins to locally decrease in width or *neck* within the gage region. If orientation hardening occurs before sample failure, the neck is said to stabilize. This means that no further reduction in cross-sectional area occurs and the neck propagates along the length of the gage region until the sample finally breaks. This process of neck propagation is called *cold drawing*.

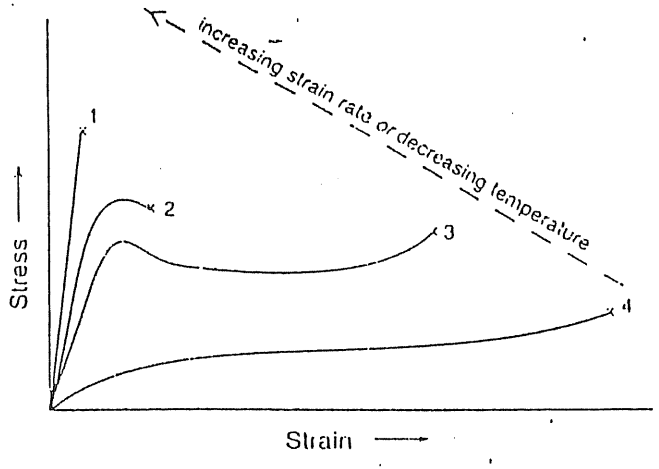

Figure 4.21. Typical stress–strain curves for samples exhibiting brittle failure (curve 1), ductile failure with neck formation (curve 2), ductile failure with cold drawing and orientational hardening (curve 3), and rubbery behavior with evidence of strain-induced crystallization (curve 4). Point of failure is indicated by the symbol ×.

The initial slope of the stress–strain plot for ductile polymers (curves 2 and 3 in Figure 4.21) is smaller than that observed for polymers that fail in a brittle mode (curve 1). In other words, the modulus of ductile polymers is lower. On the other hand, the energy required to deform the sample to the point of failure is much higher for ductile polymers, as indicated by comparison of the areas under the stress–strain curves for a brittle (curve 1) and for a ductile polymer (curve 3). This means that ductile polymers are able to absorb more energy upon impact.

Rubbery polymers follow stress–strain behavior similar to that of curve 4. Modulus is low, but ultimate extension can be very high, on the order of several hundred percent. Before failure, the rubber may experience an increase in stress as a

consequence of strain-induced crystallization caused by molecular orientation in the stretch direction, as discussed in Chapter 5.

Typical values of modulus, yield strength (stress-at-yield), ultimate strength (stress-at-break), and elongation-to-break for a variety of important thermoplastics are given in Table 4.14. The exact nature of the tensile response of a polymeric material depends upon the chemical structure of the polymer, conditions of sample preparation, molecular weight, molecular-weight distribution, crystallinity, and the extent of any crosslinking or branching. The mechanical response also depends in a very significant way on temperature and the rate of deformation. As illustrated by Figure 4.21, any amorphous polymer can exhibit the entire range of tensile behavior, from brittle to rubbery response, by increasing the testing temperature from room temperature to above the T_g of the polymer or (to a lesser extent) by decreasing the rate of deformation.[†]

TABLE 4.14 MECHANICAL PROPERTIES OF REPRESENTATIVE POLYMERS

Polymer	Elastic Modulus GPa[a]	Yield Strength MPa	Ultimate Strength MPa	Elongation to Break %
Polypropylene	1.0–1.6	23	24–38	200–600
Polystyrene	2.8–3.5	—	38–55	1–2.5
Poly(methyl methacrylate)	2.4–2.8	48–62	48–69	2–10
Polyethylene (low-density)	0.14–0.28	6.9–14	10–17	400–700
Polycarbonate	2.4	55–69	55–69	60–120
Poly(vinyl chloride) (rigid)	2.1–4.1	55–69	41–76	5–60
Polytetrafluoroethylene	0.41	10–14	14–28	100–350

[a] To convert GPa to psi, multiply by 1.45×10^5; to convert MPa to psi, multiply by 145.

The combined effect of temperature and strain rate on the stress–strain curve of an elastomer can be represented by a *failure envelope*, as shown in Figure 4.22. The ordinate is nominal stress-to-break normalized to an arbitrary reference temperature. All values of ultimate strength obtained over a wide range of temperatures and strain rates comprise points on the outer failure envelope (heavy curve). The curves originating at the origin are selected stress–strain curves at different temperatures and strain rates. As the failure envelope shows, either increasing the strain rate or decreasing the testing temperature causes the ultimate strength of the sample to decrease.

[†] It should be noted that polymers that appear brittle in tensile tests can appear to yield when tested in compression at the same temperature.

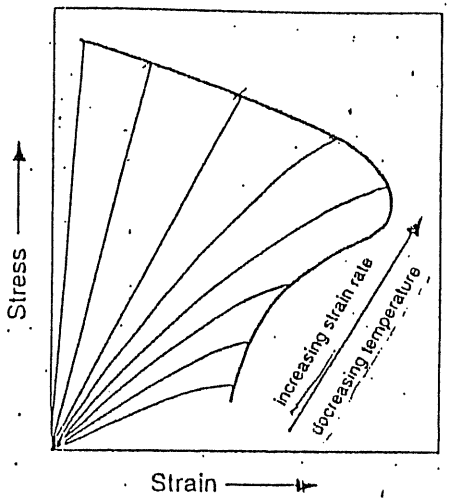

Figure 4.22. Effect of temperature and strain rate on the stress–strain curve.

Transient Testing. As mentioned earlier, two types of transient mechanical tests are creep and stress–relaxation measurements, which can be used to characterize the dimensional stability of a material. A creep test measures the elongation of a specimen subjected to a rapid application of a constant load, σ_0, at constant temperature. By contrast, a stress–relaxation test records the stress required to hold a specimen at a fixed elongation, ε_0, at constant temperature.

Creep tests can be made in shear, torsion, flexure, or compression modes, as well as in tension. Results of these tests are particularly important for selecting a polymer that must sustain loads for long periods. Usually, the parameter of interest is the tensile *compliance*, D, which is the ratio of strain to stress. While the stress, σ_0, is held constant during a creep test, the strain depends upon the time during which the load has been applied and, therefore, the compliance also becomes a function of time as

$$D(t) = \frac{\varepsilon(t)}{\sigma_0}. \tag{4.57}$$

The response of different materials — ideal elastic, ideal viscous, and viscoelastic — to a step change in stress (or load) is illustrated in Figure 4.23. For an ideal (Hookean) elastic material, the resulting strain is instantaneous and constant during the duration of the applied stress. When the load is removed at $t = t'$, the

strain instantaneously drops to zero (Figure 4.23A). This follows from Hooke's law applied to the case of a constant stress:

$$\varepsilon = D\sigma_0 = \varepsilon_0. \tag{4.58}$$

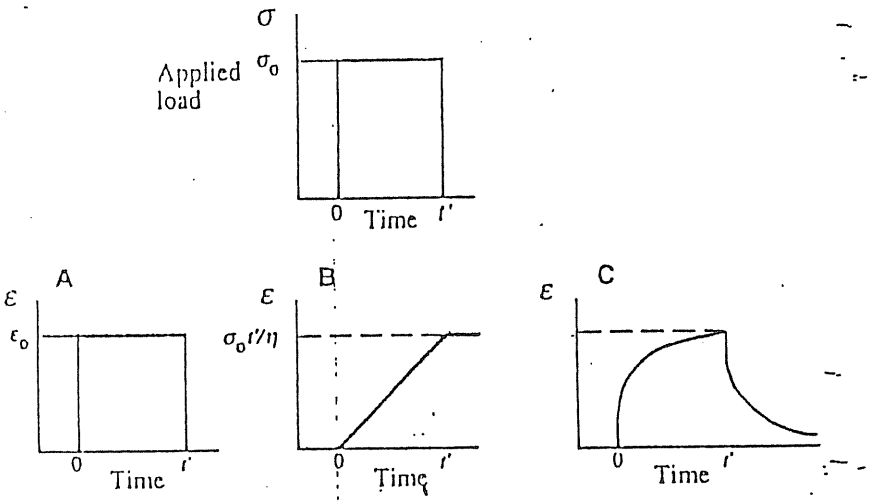

Figure 4.23. Response of different idealized materials to an instantaneous application of a stress at time $t = 0$. A, elastic; B, viscous; and C, viscoelastic.

In the case of an ideal (Newtonian) viscous fluid, the strain response is obtained by integration of Newton's law of viscosity ($\sigma = \eta\dot{\varepsilon}$) arranged as

$$\varepsilon = \int_0^{t'} \left(\frac{\sigma_0}{\eta}\right) dt = \frac{\sigma_0 t'}{\eta}. \tag{4.59}$$

Here, the strain increases linearly with increasing time until the load is removed at $t = t'$ at which time the strain remains constant ($\sigma_0 t'/\eta$) in time (Figure 4.23B) unless an additional load is applied. The deformation is said to be permanent since no elastic recovery is possible.

In the case of a viscoelastic material, recovery can occur due to the elastic contribution of the material. For viscoelastic materials, the strain response will have some of the character of both elastic and viscous materials, as shown in Figure 4.23C. The initial portion of the strain recovery is elastic (i.e., instantaneous) while full recovery is delayed to longer times due to the viscous contribution. The actual viscoelastic response can be reasonably modeled by analyzing the strain response of series or parallel combinations of ideal elastic springs and ideal viscous dashpots (shock absorber) as discussed in Section 5.1.2.

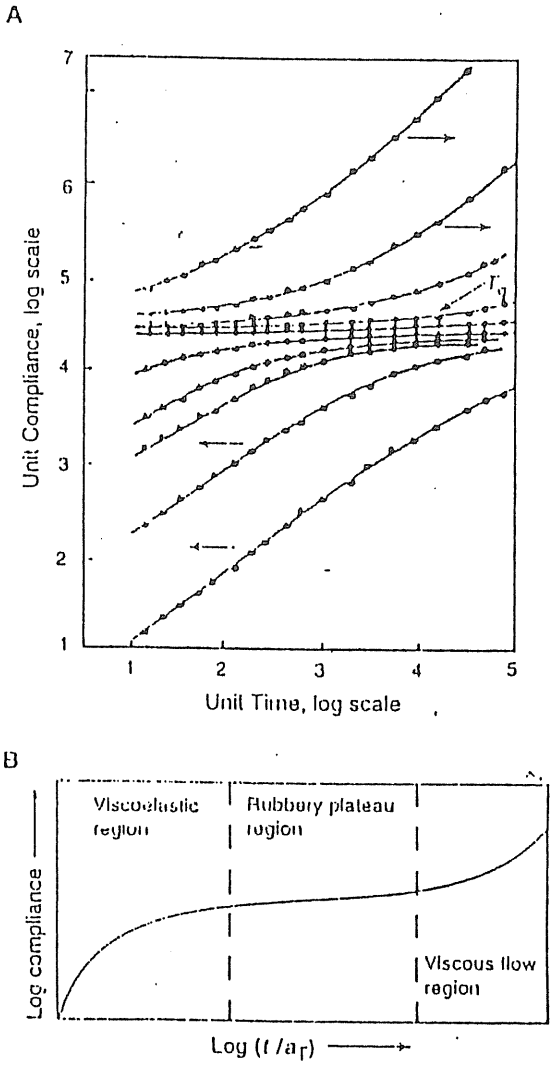

Figure 4.24. A. Representative plots of creep compliance as a function of time at different temperatures. Arrows show direction of the horizontal shift of data to obtain a master curve at a reference temperature taken as the T_g of the polymer. B. Creep master curve obtained by time–temperature superposition.

Instrumentation for creep testing can be a simple laboratory setup whereby a plastic film or bar is clamped at one end to a rigid support (normally enclosed in a temperature-controlled chamber) and a weight is added to the opposite end. The deformation of the loaded specimen is then measured by following the relative movement of two marks, inscribed on the sample, by means of a cathetometer, or traveling microscope.

Typical creep curves of a low-T_g polymer measured over four decades of time and at several temperatures are shown in Figure 4.24A. As illustrated, the creep compliance increases with increasing temperature. This means that the sample softens as temperature is increased, as experience would indicate.

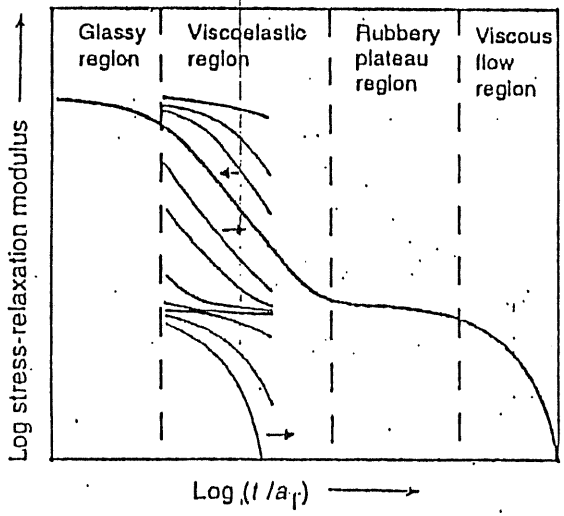

Figure 4.25. Stress-relaxation modulus as a function of time. Arrows show directions of shift to obtain master curve at reference temperature.

Stress-relaxation experiments can be conveniently performed with the same commercial instruments used in tensile tests. Since deformation must be as close as possible to being instantaneous, the preferred instrumentation is hydraulically driven, rather than screw-driven, tensile testing machines. A rapid extension is applied to the sample and the stress on the sample is measured as a function of time by means of a force transducer. In a stress-relaxation experiment, stress is a function of time and, therefore, the stress-relaxation modulus, E_r,

$$E_r(t) = \frac{\sigma(t)}{\varepsilon_0}. \tag{4.60}$$

is also time dependent. Typical stress-relaxation curves are shown in Figure 4.25.

The measurement of a full range of stress-relaxation (or creep-compliance) behavior at a given temperature can take years. Fortunately, it is possible to shift data taken over shorter time periods but at different temperatures to construct a master curve covering a longer time scale. The principle that allows horizontal shifting of data is called *time–temperature superposition*, which is discussed in Section 5.1.5. The result of this shifting of data over a limited time span to form a master curve is shown for creep compliance in Figure 4.24B and for stress-relaxation modulus in Figure 4.25.

Impact Testing. Impact tests measure the energy expended up to failure under conditions of rapid loading. There are a number of different types of impact tests. These include the widely used Izod and Charpy tests in which a hammerlike weight strikes a specimen and the energy-to-break is determined from the loss in the kinetic energy of the hammer. Other variations include the falling-ball or dart test, whereby the energy-to-break is determined from the weight of the ball and the height from which it is dropped. Values of impact strength may also be calculated from the area under the stress–strain curve in high-speed tensile tests. Information obtained from impact tests may be used to determine whether a given plastic has sufficient energy-absorbing properties to be useful for a particular application, such as plastics for beverage bottles or window replacement. In such cases, it is important that the material be tested at temperatures and impact conditions close to those of actual use because impact strength will decrease with decreasing temperature and with increasing rate of deformation. The presence of defects that act as stress concentrators will also reduce impact strength. In order to standardize impact results or to study the effect of cracks and other defects on impact properties, samples with inscribed notches of specified dimensions are often used. Typical values of notched-Izod impact strengths for several important polymers are given in Table 4.15. Brittle polymers, such as polystyrene, have very low impact strengths, while many engineering thermoplastics (e.g., polycarbonate) are very impact resistant.

Generally, amorphous polymers with large bulky substituent groups and nonlinear backbones are brittle. Unoriented crystalline structure also contributes to brittleness in polymers whose T_g is above the testing temperature. Some correlation may exist between the presence of pronounced low-temperature secondary relaxations corresponding to small-scale motions of the chain backbone and the impact properties of many ductile polymers. Brittle polymers can be made to be more impact resistant by dispersing small (<0.1-μm diameter) rubber particles within the polymer matrix, as in the case of high-impact polystyrene (HIPS) and ABS resins (see Section 7.2.2). Good adhesion between the rubbery inclusions and brittle

matrix polymers is important for high impact resistance and is typically achieved by grafting the rubber and matrix (glassy) polymers.

TABLE 4.15 VALUES OF NOTCHED-IZOD IMPACT STRENGTH FOR SOME REPRESENTATIVE THERMOPLASTICS

Polymer	Impact Strength[a] J m^{-1}
Polystyrene	13–21
Poly(vinyl chloride)	21–160
Polypropylene	27–107
Polystyrene (high-impact)	27–427
Polyethylene (high-density)	27–1068
ABS	53–534
Polysulfone	69–267
Polycarbonate	641–961
Polyethylene (low-density)	854

[a] To convert J m^{-1} to ft-lb$_f$ in.$^{-1}$, divide by 53.38.

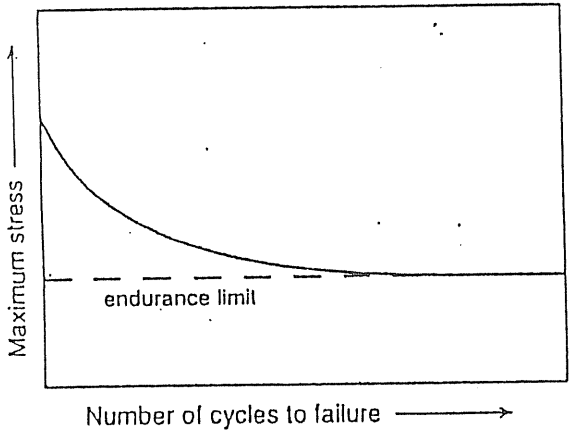

Figure 4.26. Representative fatigue curve.

Fatigue Testing. Fatigue tests are used to determine the number of cycles (N) of applied strain at a given level of stress that a sample can sustain before complete failure. This number of cycles to failure is called the *fatigue life*. The *endurance limit* is the maximum value of applied stress for which failure will not occur no matter for how many cycles the stress is applied. Typically, the value of stress leading to failure at a given N is 20% to 40% of the static tensile-strength. The fatigue life decreases with increasing frequency of oscillation and as temperature is decreased. Information obtained by means of fatigue tests is extremely important in evaluating engineering and composite materials considered for load-bearing applications or when frequent periodic stress loading may be encountered, as, for example, in a plastic hinge joint. A representative fatigue curve is illustrated in Figure 4.26.

REFERENCES

1. R. P. Wool, *Macromolecules*, 26, 1564 (1993).
2. W. W. Graessley, *Adv. Polym. Sci.*, 16, 1 (1974).
3. P.-G. de Gennes, *J. Chem. Phys.*, 55, 572 (1971).
4. J. Klein, *Nature*, 271, 143 (1978).
5. D. W. van Krevelen, *Properties of Polymers*, 3rd ed., Elsevier, Amsterdam, 1990.
6. J. H. Gibbs and E. A. DiMarzio, *J. Chem. Phys.*, 28, 373 (1958).
7. R. S. Stein, *J. Polym. Sci., Polym. Phys. Ed.*, 19, 1281 (1981).
8. P. J. Philips and H. T. Tseng, *Macromolecules*, 22, 1649 (1989).
9. M. Avrami, *J. Chem. Phys.*, 7, 1103 (1939); 8, 212 (1940).
10. P. Ehrenfest, *Leiden Comm. Suppl.*, 756 (1933).
11. P. J. Flory, L. Mandelkern, and H. K. Hall, *J. Am. Chem. Soc.*, 73, 2532 (1951).
12. R. Simha and R. F. Boyer, *J. Chem. Phys.*, 37, 1003 (1962).
13. T. G. Fox and P. J. Flory, *J. Appl. Phys.*, 21, 581 (1950).
14. R. F. Boyer, *Macromolecules*, 7, 142 (1974).
15. F. N. Kelley and F. Bueche, *J. Polym. Sci.*, 50, 549 (1961).
16. P. R. Couchman and F. E. Karasz, *Macromolecules*, 11, 117 (1978).
17. J. R. Fried, S.-Y. Lai, L. W. Kleiner, and M. E. Wheeler, *J. Appl. Polym. Sci.*, 27, 2869 (1982).
18. R. P. Kambour and A. S. Holik, *J. Polym. Sci., Part A-2*, 7, 1393 (1969).

GENERAL READING

J. J. Aklonis, "Mechanical Properties of Polymers," *J. Chem. Ed.*, 58, 892–897 (1981).

P.-G. de Gennes, "Entangled Polymers," *Physics Today*, June 1983, p. 33.

A. Eisenberg, "The Glassy State and the Glass Transition," in *Physical Properties of Polymers*, 2nd ed., J. E. Mark, A. Eisenberg, W. W. Graessley, L. Mandelkern, E. T. Samulski, J. L. Koenig, and G. D. Wignall, American Chemical Society, Washington, DC, 1993, pp. 61–95.

L. Mandelkern, "The Crystalline State," in *Physical Properties of Polymers*, 2nd ed., J. E. Mark, A. Eisenberg, W. W. Graessley, L. Mandelkern, E. T. Samulski, J. L. Koenig, and G. D. Wignall, American Chemical Society, Washington, DC, 1993, pp. 145–200.

P. J. Philips, "Polymer Crystals," *Rep. Prog. Phys.*, 53, 549–604 (1990).

R. S. Stein and M. Srinivasarao, "Fifty Years of Light Scattering: A Perspective," *J. Polym. Sci.: Part B: Polym. Phys.*, 31, 2003–2010 (1993).

I. M. Ward and D. W. Hadley, *An Introduction to the Mechanical Properties of Solid Polymers*, John Wiley & Sons, Chichester, England, 1993.

ADVANCED READING

V. A. Bershtein and V. M. Egorov, *Differential Scanning Calorimetry of Polymers*, Ellis Horwood, Chichester, England, 1994.

R. N. Haward, ed., *The Physics of Glassy Polymers*, John Wiley & Sons, New York, 1973.

R. J. Samuels, *Structured Polymer Properties*, John Wiley & Sons, New York, 1974.

E. A. Turi, ed., *Thermal Characterization of Polymeric Materials*, Academic Press, New York, 1981.

Problems

4-1. Show that $\sigma^T = \sigma(1+\varepsilon)$ for an incompressible material.

4-2. A tensile strip of polystyrene that is 10 cm in length, 5 cm in width, and 2 cm in thickness is stretched to a length of 10.5 cm. Assuming that the sample is isotropic and deforms uniformly, calculate the resulting width and the % volume change after deformation.

4-3. A polymer has a crystalline growth parameter (n) of 2 and a rate constant (k) of 10^{-2} s^{-2} at 100°C. The polymer is melted and then quenched to 100°C and allowed to crystallize isothermally. After 10 s, what is the percent crystallinity of the sample?

4-4. What is the % volume change that is expected at 100% elongation of natural rubber, assuming that no crystallization occurs during deformation?

4-5. Give your best estimate for the weight fraction of plasticizer required to lower the T_g of poly(vinyl chloride) (PVC) to 30°C. Assume that the T_g of PVC is 356 K and that of the plasticizer is 188 K. No other information is available.

5

Viscoelasticity and Rubber Elasticity

At the extremes, a polymer may exhibit mechanical behavior characteristic of either an elastic solid or a viscous liquid. The actual response depends upon temperature, in relation to the glass-transition temperature (T_g) of the polymer, and to the time scale of the deformation. Under usual circumstances, the mechanical response of polymeric materials will be intermediate between that of an ideal elastic or viscous liquid. In other words, polymers are *viscoelastic*. This behavior is readily illustrated by Silly Putty®, which is a silicone rubber having a low T_g. If rolled up into a ball and dropped to the floor, it will bounce with the resilience of a rubber ball. This is a manifestation of elastic behavior resulting from rapid deformation. If left on a desk for several days, the ball will flatten — it will flow like a viscous liquid over long time. If pulled at a moderate rate of strain, the ball will elongate with high extension and eventually fail. This chapter seeks to develop the fundamental concepts of polymer viscoelasticity and rubber elasticity and to describe the basic experimental methods used to measure these properties.

5.1 INTRODUCTION TO VISCOELASTICITY

Viscoelastic behavior may be characterized by a variety of techniques that record the time-dependent response of a polymeric solid, melt, or solution to a periodic perturbation such as the application of a sinusoidal strain or an electrical voltage. The most commonly used method to measure viscoelastic properties as a function of temperature and time (frequency) is dynamic-mechanical analysis, which records the stress response to an application of a sinusoidal strain. In comparison,

dielectric methods record the temperature and frequency dependence of the dielectric constant to an oscillatory voltage applied to a sample pressed between two electrodes. The basic principles of dynamic-mechanical and dielectric analysis and the experimental methods used to measure dynamic-mechanical and dielectric properties of polymers are presented in the following sections.

5.1.1 Dynamic-Mechanical Analysis

In dynamic testing, the stress is measured as a function of strain that is some periodic function of time, usually a sine wave. Unlike fatigue tests (see Section 4.4.2), dynamic-mechanical properties are measured at low strain such that deformation is not permanent. Commercial dynamic-testing instruments are available for operation in several modes of deformation (e.g., tensile, torsion, compression, flexure, and shear) and over a several decades of frequencies. The principles of dynamic-mechanical analysis are described next.

Theory. For a tensile strain that is a sinusoidal function of time, t, the strain function may be expressed as

$$\varepsilon(\omega) = \varepsilon^{\circ} \sin(\omega t). \tag{5.1}$$

In this expression, ε° is the amplitude of the applied strain and ω is the angular frequency of oscillation (units of radians per second). The *angular* frequency is related to frequency, f, measured in cycles per second (Hz), as $\omega = 2\pi f$. The usual range of frequencies for dynamic-mechanical experiments are 0.1 to 110 Hz (0.628 to 691 rad s^{-1}).

The stress resulting from the applied sinusoidal strain will also be a sinusoidal function, which may be written in the most general form as

$$\sigma(\omega) = \sigma^{\circ} \sin(\omega t + \delta) \tag{5.2}$$

where σ° is the amplitude of the stress response and δ is the *phase angle* between the stress and the strain, as illustrated by Figure 5.1. The phase angle is a measure of the viscous response of the material to dynamic strain as discussed later.

In the case of an ideal elastic solid, it follows from Hooke's law (eq. 4.44) that the stress is always in phase with strain (i.e., $\delta = 0$ in eq. 5.2) and, therefore,

$$\sigma = E\varepsilon = E\varepsilon^{\circ} \sin(\omega t) = \sigma^{\circ} \sin(\omega t) \tag{5.3}$$

where σ° is the magnitude (i.e., $\sigma^{\circ} = E\varepsilon^{\circ}$) of the resulting stress function.

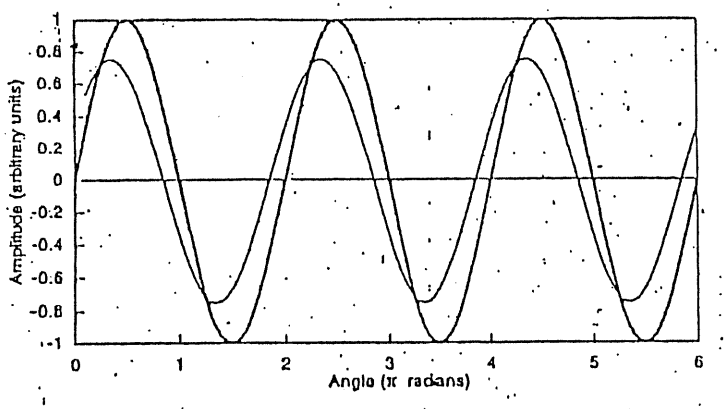

Figure 5.1. Representation of an arbitrary strain function (—) and resulting stress response (—) of a viscoelastic material. In this example, the stress is out of phase with the strain by 45° (i.e., $\delta = \pi/4$ radians), and its amplitude is arbitrarily set at 75% of the strain amplitude (i.e., $\sigma^\circ/\varepsilon^\circ = 0.75$).

In contrast, the stress of an ideal viscous fluid is always 90° out of phase (i.e., $\delta = \pi/2$) with the strain. This can be shown to result from *Newton's law of viscosity*, given as

$$\boxed{\sigma = \eta\left(\frac{d\varepsilon}{dt}\right)} \tag{5.4}$$

The derivative of ε given by eq. 5.1 with respect to time is

$$\frac{d\varepsilon}{dt} = \omega\varepsilon^\circ \cos(\omega t). \tag{5.5}$$

Substitution of this expression into eq. 5.4, and noting that the cosine function is 90° out of phase with the sine function, gives

$$\sigma = \eta\omega\varepsilon^\circ \cos(\omega t) = \sigma^\circ \sin\left(\omega t + \frac{\pi}{2}\right) \tag{5.6}$$

where

$$\sigma^\circ = \eta\omega\varepsilon^\circ. \tag{5.7}$$

At temperatures below T_g, polymeric materials behave more as Hookean solids at small deformations, but at higher temperatures (i.e., in the vicinity of T_g) their behavior is distinctly viscoelastic. Over these temperatures, δ will have a (temperature-dependent) value between 0° (totally elastic) and 90° (totally viscous).

An alternative, and perhaps more useful, approach to discuss the dynamic response of a viscoelastic material to an applied cyclical strain is by use of complex number notation by which a complex strain, ε^*, can be represented as

$$\varepsilon^* = \varepsilon^\circ \exp(i\omega t) \tag{5.8}$$

where $i = \sqrt{-1}$. Following the form of eq. 5.2, the resulting complex stress, σ^*, can be written as

$$\sigma^* = \sigma^\circ \exp\left[i(\omega t + \delta)\right]. \tag{5.9}$$

It follows from Hooke's law that a *complex modulus*, E^*, can be defined as the ratio of complex stress to complex strain as

$$E^* = \frac{\sigma^*}{\varepsilon^*} = \left(\frac{\sigma^\circ}{\varepsilon^\circ}\right)\exp(i\delta). \tag{5.10}$$

This complex modulus can be resolved into two components — one that is in phase (i.e., E') and one that is out of phase (i.e., E'') with the applied strain. Substitution of *Euler's identity*

$$\exp(i\delta) = \cos\delta + i\sin\delta \tag{5.11}$$

into eq. 5.10 gives

$$E^* = \left(\frac{\sigma^\circ}{\varepsilon^\circ}\right)\cos\delta + i\left(\frac{\sigma^\circ}{\varepsilon^\circ}\right)\sin\delta. \tag{5.12}$$

Equation 5.12 may be written in the form given as

$$\boxed{E^* = E' + iE''} \tag{5.13}$$

where E' is called the (tensile) *storage modulus* given as

$$E' = \left(\frac{\sigma^\circ}{\varepsilon^\circ}\right)\cos\delta \tag{5.14}$$

and E'' is the (tensile) *loss modulus*:

$$E'' = \left(\frac{\sigma^o}{\varepsilon^o}\right)\sin\delta. \tag{5.15}$$

The ratio of loss and storage moduli defines another useful parameter in dynamic-mechanical analysis called tan δ, where

$$\boxed{\tan\delta = \frac{\sin\delta}{\cos\delta} = \frac{E''}{E'}} \tag{5.16}$$

As in static testing (see Section 4.4.2) where the tensile modulus is the inverse of the compliance, the dynamic tensile-modulus is inversely related to the dynamic tensile-compliance, D^*, as

$$D^* = \frac{1}{E^*} = \frac{\varepsilon^*}{\sigma^*} = \frac{\varepsilon^o \exp(i\omega t)}{\sigma^o \exp[i(\omega t + \delta)]} = \left(\frac{\varepsilon^o}{\sigma^o}\right)\exp(-i\delta). \tag{5.17}$$

Substitution of Euler's identity in the form of $\exp(-i\delta) = \cos\delta - i\sin\delta$ into eq. 5.17 gives

$$D^* = \left(\frac{\varepsilon^o}{\sigma^o}\right)\cos\delta - i\left(\frac{\varepsilon^o}{\sigma^o}\right)\sin\delta. \tag{5.18}$$

Equation 5.18 may be written in the form

$$D^* = D' - iD'', \tag{5.19}$$

where D' is called the *storage compliance*,

$$D' = \left(\frac{\varepsilon^o}{\sigma^o}\right)\cos\delta, \tag{5.20}$$

and D'' is the (tensile) *loss compliance*,

$$D'' = \left(\frac{\varepsilon^o}{\sigma^o}\right)\sin\delta. \tag{5.21}$$

The negative sign of the second term (i.e., $-iD''$) in the RHS of eq. 5.19 contrasts with the corresponding positive term (i.e., $+iE''$) in eq. 5.13. As in the case of dynamic modulus (eq. 5.16), tan δ is related to the components of the complex dynamic-compliance as

$$\tan\delta = \frac{D''}{D'}. \tag{5.22}$$

It is possible to obtain values of dynamic storage and loss moduli from corresponding values of compliance, and vice versa, by manipulation of their complex conjugates. The complex conjugate of the dynamic modulus (eq. 5.13) is

$$\overline{E^*} = E' - iE''. \tag{5.23}$$

The *magnitude* of the dynamic modulus, $|E^*|$, is obtained from its complex conjugate as

$$E^* \times \overline{E^*} = |E^*|^2 = (E')^2 + (E'')^2. \tag{5.24}$$

Then (from eqs. 5.17, 5.23, and 5.24), we can write

$$D^* = \frac{1}{E^*} = \frac{\overline{E^*}}{(E')^2 + (E'')^2} = \frac{E'}{(E')^2 + (E'')^2} - i\left[\frac{E''}{(E')^2 + (E'')^2}\right]. \tag{5.25}$$

Comparison of the form of eq. 5.25 with the expression for D^* (eq. 5.19) gives the interrelationships between the components of dynamic modulus and dynamic compliance:

$$D' = \frac{E'}{(E')^2 + (E'')^2} \tag{5.26}$$

and

$$D'' = \frac{E''}{(E')^2 + (E'')^2}. \tag{5.27}$$

Similar relationships may be written for E' and E'' as functions of D' and D''.

Work in Dynamic Deformation. As is the case for other forms of mechanical deformation, work is expended during dynamic-mechanical testing. The amount of work, or power, consumed depends upon the viscoelastic properties of the polymer. The work *per unit of sample volume*, W, may be expressed in terms of stress and strain as

$$W = \int \left(\frac{f}{V}\right) d\ell = \int \left(\frac{f}{A}\right) \frac{d\ell}{\ell} = \int \sigma \, d\varepsilon \tag{5.28}$$

where f is the force, $d\ell$ is the differential extension of the sample, and V is the sample volume. Per cycle (i.e., 2π radians) of oscillation, the *dynamic* work (now given per unit volume and cycle) is then obtained as

$$W = \int_0^{2\pi} \sigma^* \, d\varepsilon^*. \tag{5.29}$$

Substitution of the appropriate expressions for σ^* (eq. 5.2) and $d\varepsilon^*$ (eq. 5.5) and integration of eq. 5.29 gives the work per cycle per unit volume for dynamic oscillation of a viscoelastic solid (see Problem 5–2) as

$$W = \pi \sigma^\circ \varepsilon^\circ \sin \delta. \tag{5.30a}$$

Rearrangement of eq. 5.15 gives

$$\sin \delta = \left(\frac{\varepsilon^\circ}{\sigma^\circ}\right) E'',$$

which can be substituted into eq. 5.30a to obtain

$$W = \pi (\varepsilon^\circ)^2 E''. \tag{5.30b}$$

From a consideration of the $\sin \delta$ contribution to W in eq. 5.30a, it is obvious that the work of oscillation for an ideal elastic solid (i.e., $\delta = 0$ and $\sin \delta = 0$) is zero, while the maximum work is expended during deformation of an ideal viscous material (i.e., $\delta = \pi/2$, $\sin \delta = 1$, and $W = \pi \sigma^\circ \varepsilon^\circ$). The *power* consumed per unit volume is then obtained by multiplying the work per cycle (per unit volume) given by eq. 5.30a or 5.30b by the number of cycles per unit time (i.e., $f = \omega/2\pi$) as

$$P = \left(\frac{\omega}{2}\right) \sigma^\circ \varepsilon^\circ \sin \delta = \left(\frac{\omega}{2}\right) (\varepsilon^\circ)^2 E''. \tag{5.31}$$

Experimental Techniques. To usual way to report the viscoelastic response of a polymer is by means of a semilog plot of storage modulus and loss modulus (or $\tan \delta$) as a function of temperature at one or more frequencies. The temperature range may be very broad — often extending from liquid-nitrogen temperatures (ca. -150°C) to temperatures in the range of T_g which can be 200°C or more. The dynamic storage modulus behaves much like the tensile (or shear) modulus as a function of temperature (see Figure 4.19). Maxima in loss modulus, or $\tan \delta$, occur both at T_g and at low temperatures, where small-scale molecular motions can occur (i.e., secondary relaxations). In the case of semicrystalline polymers, an additional peak in $\tan \delta$ corresponding to T_m will occur above T_g. Traditionally, the highest-temperature peak is designated the α relaxation (i.e., the glass transition in amorphous polymers and the crystalline-melting transition in semicrystalline polymers), the next highest is the β relaxation, then the γ relaxation, and so on.

A number of different instruments have been used to obtain dynamic-mechanical data. The earliest designs used a *free-vibration* approach (torsion pendulum and torsional braid) in which a polymer sample in the form of a bar or cylinder is set to oscillate and the damping of the oscillation is recorded as a function of time at a controlled temperature. More recent and versatile instrumentation uses a *forced-oscillation* method whereby a sinusoidal strain (tensile, flexure, compression, shear, or torsional) is applied to a sample and the stress response is recorded as a function of temperature at different frequencies. Free- and forced-vibration methods are described in the following sections.

Free-Vibration Methods. The simplest and earliest dynamic-mechanical technique, the *torsion pendulum*, is a free-vibration technique.[1] In this experiment, a polymer film is rigidly clamped at one end, while the other end is attached to an inertia disk that is free to oscillate. Once the disk is set in oscillation, the viscous response of the polymer sample causes the amplitude of the oscillation to decay as illustrated in Figure 5.2. The time required for one complete oscillation is called the *period* of oscillation (P).

The value of $\tan \delta$ can be determined from the ratio of amplitudes (A) of any two consecutive peaks as

$$\Delta = \pi \tan \delta = \ln \left(\frac{A_1}{A_2}\right) \tag{5.32}$$

where Δ is called the *log decrement*. Frequencies of disk oscillation may range from 0.01 to 50 Hz as determined by sample characteristics. Usually, frequency is approximately 1 Hz and will vary slightly with temperature over the course of the experiment.

Since the mode of deformation is actually torsion, it is usual to represent the response in terms of dynamic *shear* moduli, G' and G'' (where $G^* = G' + iG''$). The shear *storage* modulus, G', is obtained from the sample geometry (F_s), moment of inertia (I), and period of oscillation (P) as

$$G' = F_s I \left(\frac{1}{P^2}\right). \tag{5.33}$$

The relationships from which the shape factor may be calculated depend upon whether the sample is cylindrical or rectangular.[2] For a rectangular sample, the geometry parameter is given as

$$F_s = \frac{64\pi^2 L}{nW t^3}$$

where L is the sample length, W is width, t is thickness, and n is a shape factor that depends upon the (aspect) ratio of the samples (W/t). Once G' and $\log \Delta$ have been measured, the shear loss modulus, G'', can be calculated as

$$G'' = G' \tan \delta = \frac{G'\Delta}{\pi}. \tag{5.34}$$

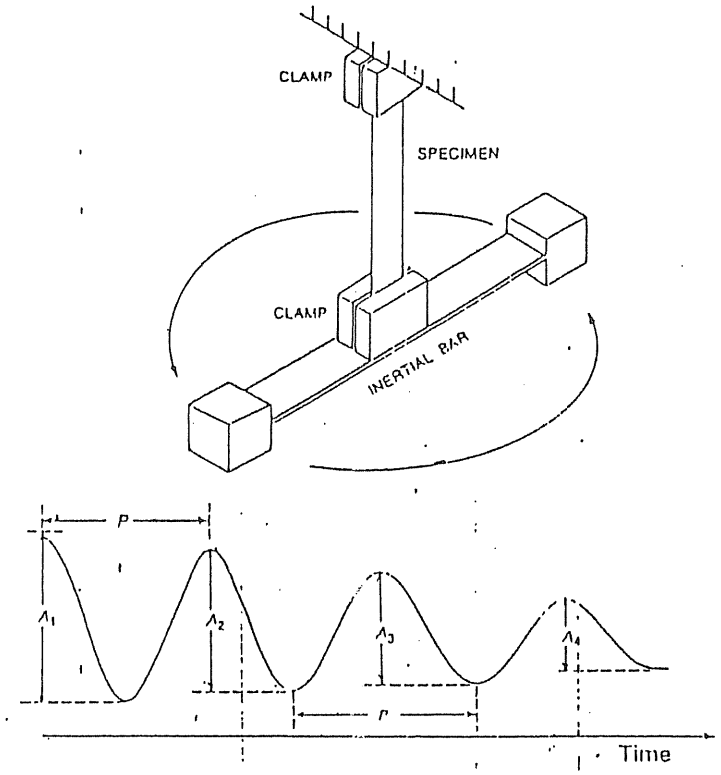

Figure 5.2. Torsion-pendulum apparatus, top view, and plot of amplitude of oscillation, bottom view. (Adapted from Nielsen[1] with permission of the publisher.)

As an example of dynamic-mechanical data, values of the storage modulus and log decrement obtained by early torsion-pendulum measurements[1] of poly(methyl methacrylate) (PMMA) are plotted against temperature in Figure 5.3. The data indicate an α relaxation corresponding to T_g (i.e., maximum in $\log \Delta$ and sharp decrease in G') near 130°C and a (β) secondary-relaxation peak (see Section 4.1.3) near 40°C. A small drop in G' accompanies the broad maximum in $\log \Delta$ at the β relaxation. The β relaxation was attributed in this study to the motion of the large ($-COOCH_3$) pendant group of PMMA whose structure is

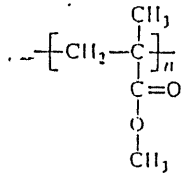

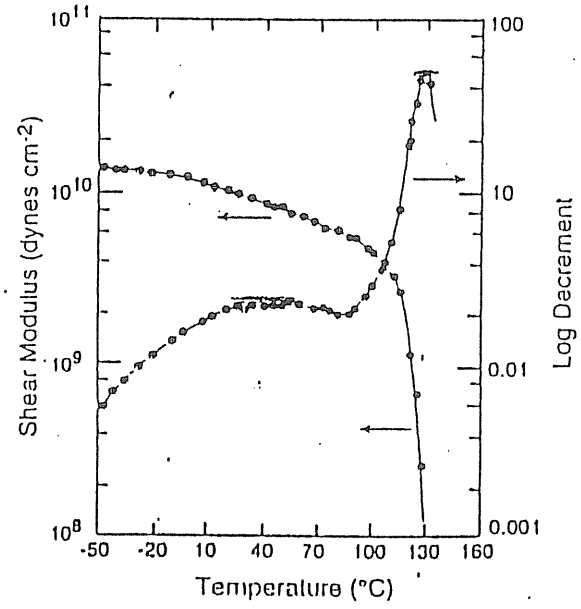

Figure 5.3. Values of shear storage modulus (G') and log decrement (Δ) for poly(methyl methacrylate) plotted as a function of temperature. Data were obtained by torsion-pendulum measurements.[1]

The torsion pendulum is still actively used today and is available commercially as a fully automated instrument. A schematic diagram of a modern torsion-pendulum apparatus is shown in Figure 5.4. Temperature can be controlled to within ±0.05°C isothermally from 25° to 400°C or may be ramped up or down at rates of 0.1 °C h^{-1} to 5°C min^{-1} from -180° to 400°C. The frequency and damping are optically tracked for data acquisition. As shown in Figure 5.4, a light beam passes through a pair of polarizers housed in the optical cage. The upper polarizer oscillates with the specimen, and the intensity of light measured by means of a nondrag optical transducer is a linear function of the angular displacement of the pendulum.

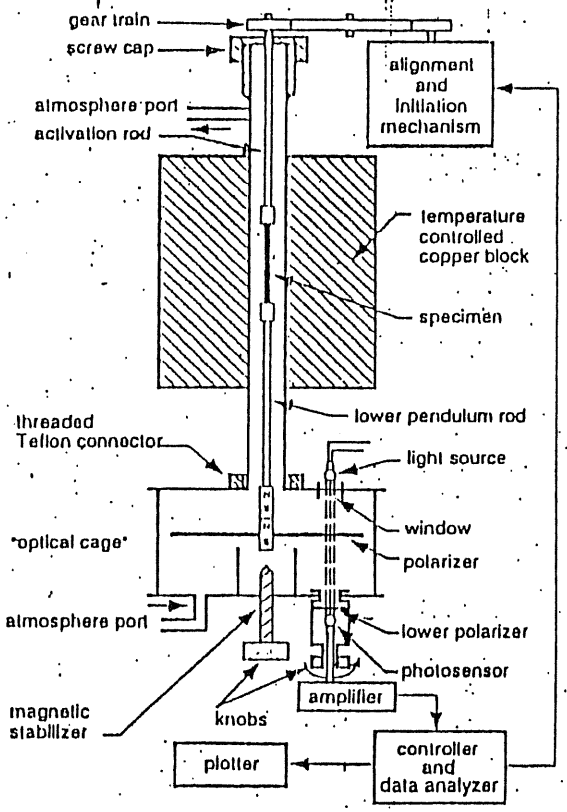

Figure 5.4. Schematic diagram of a commercial torsion-pendulum apparatus. (Courtesy of J. K. Gillham.)

An important variation of the torsion-pendulum technique is called *torsional-braid analysis* (TBA).[3] Instrumentation is the same as used for torsion-pendulum analysis of films, rods, or bars; however, the TBA sample is *supported* on a braid, typically made from glass fibers. The braid is coated with a dilute solution of the sample and dried in vacuum to remove all solvent. Although the quantitative values of dynamic moduli of this composite geometry are *not* the same as the unsupported polymer, the *qualitative* dependence of $\tan\delta$ on temperature is a good representation of the actual polymer response. The advantage of this technique is that the support provided by the braid enables the dynamic-mechanical characterization of low-molecular-weight and *liquid* samples as well as high-molecular-weight polymer samples near and above T_g, where softening would preclude the use of unsupported-sample techniques. For example, the cure of an epoxy resin can be followed by recording the increase in G' with time at a fixed temperature.

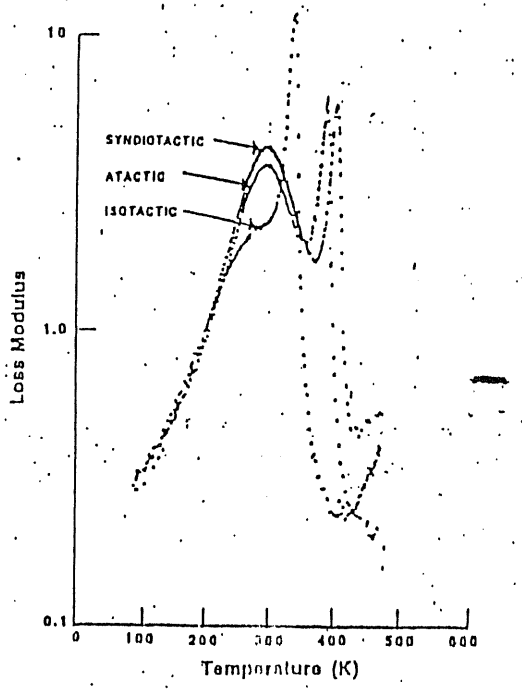

Figure 5.5. Loss-modulus data for PMMA samples with different tacticities as obtained by torsion-braid analysis at a heating rate of 2° min^{-1}. [Redrawn from J. K. Gillham, S. J. Stadnicki, and Y. Hazony, *J. Appl. Polym. Sci.*, 21, 401 (1977). Copyright © 1977 John Wiley & Sons. Reprinted by permission of John Wiley & Sons, Inc.]

As an illustration of TDA data, the loss modulus of PMMA samples[4] with different tacticities is plotted against temperature in Figure 5.5. Results indicate that the lowest T_g (determined as the temperature at the maximum of the high-temperature α peak) is observed for *i*-PMMA (T_g = 334 K), while the T_gs of atactic and syndiotactic PMMA (*s*-PMMA) are higher and approximately equal at 384 K for *a*-PMMA and 399 K for *s*-PMMA.[4] These values compare favorably with T_gs determined by DSC measurements (see Chapter 4, Section 4.3.3) for *a*-PMMA (378 K), *i*-PMMA (318 K), and *s*-PMMA (388 K). In contrast, the temperatures corresponding to the β peaks are nearly invariant with temperature, but the magnitude of the β peak decreases with increasing isotactic content. The decrease in the (β) secondary-relaxation peak for the isotactic form of PMMA is believed to be due to the immobilization of the ester substituent groups in the (5/1) helical conformation[1] of this crystalline isomer.

Forced-Vibration Methods. Today, the most frequently used commercial instruments utilize a *forced-* (rather than free-) vibration method by which a dynamic tensile, compressive, torsional, or flexural strain is applied to the sample, which is cut or molded in the form of a thin film or bar. One important advantage of the forced-vibration mode is that frequency can be controlled precisely over a wider range (0.001 to 100 rad s^{-1}) than is possible for free-vibration methods. As discussed next, comparison of dynamic-mechanical spectra obtained at several frequencies provides useful additional information on the viscoelastic properties of the polymer. Section 5.1.4 outlines the principles of dielectric spectroscopy, which provides viscoelastic information over a much wider range of frequencies (up to 10^{10} Hz).

A representative dynamic-mechanical spectrum of an engineering thermoplastic, polysulfone, whose chemical structure is

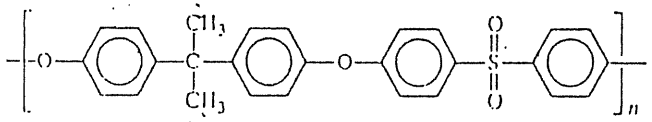

is shown in Figure 5.6. In this example, the dynamic-mechanical data were obtained by forced-vibration instrumentation at 10 rad s^{-1} (ca. 1.6 Hz) in the tensile mode.[6] In addition to the glass transition (α peak), which occurs near 481 K (188°C), there is a major secondary-relaxation process (the γ peak) showing a broad maximum located near 166 K (-107°C). It is believed that this low-temperature transition reflects short-range mobility of the main chain including flips of phenylene rings and possibly coupled rotations of methyl groups.

[1] The first number identifying the conformational form of a helix indicates the number of repeating units participating in a given number of turns of the helix. In the case of a 5/1 or 5_1 helix, five repeating units form one complete turn of the helix.

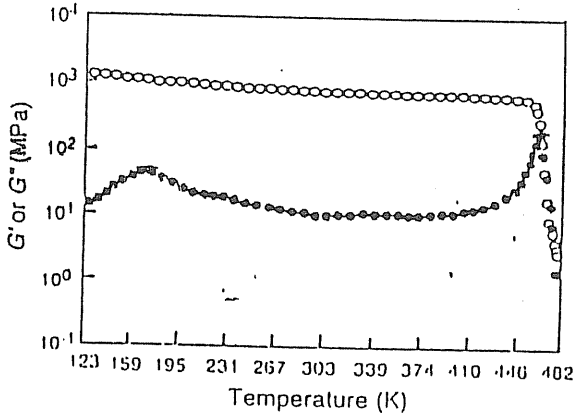

Figure 5.6. Dynamic-mechanical spectrum of polysulfone obtained in forced torsion at 10 rad s^{-1} (~1.6 Hz).[6] Data points indicate (O) shear storage-modulus (G') and (●) shear loss-modulus (G''). A low-temperature, secondary-relaxation (γ) peak with a broad maximum near 166 K (-107°C) appears in the loss-modulus plot. The glass transition (i.e., α peak) occurs at 481 K (188°C).

Activation Energies. Energies required for main-chain and side-group motions can be obtained by determining the effect of frequency on the maximum temperatures of the loss or tan δ peaks. The ability to vary oscillation frequency makes forced-vibration techniques the choice for these studies. The temperature at the peak maxima, T_{max}, increases with increasing frequency, and the activation energy, E_a, of the relaxational process may be determined from the slope of a semilog plot of frequency (f or ω) versus reciprocal peak-temperature ($1/T_{max}$) as

$$\ln f = -\left(\frac{E_a}{R}\right)\frac{1}{T_{max}} + \ln f_0 \qquad (5.35)$$

where f_0 is a constant obtained from the intercept. Typically, activation energies for low-temperature (i.e., secondary) relaxations are low (ca. 10 to 20 kcal mol^{-1}). In the example of the dynamic-mechanical spectra of poly(methyl methacrylate) shown in Figure 5.3, the activation energy of the β peak was reported to be approximately 17 kcal mol^{-1}. The activation energy for the γ relaxation of polysulfone (Figure 5.5) was reported to be 10.7 kcal mol^{-1}, in agreement with predictions of semiempirical molecular-orbital calculations of the energy barriers to rotation for the phenylene rings in the backbone of the polysulfone chain.[6] Corresponding activation energies for the glass transition, reflecting longer-range cooperative motions, are about an order of magnitude greater than those for secondary relaxations.

For example, the activation energy of the α (glass) relaxation of polysulfone is approximately 220 kcal mol^{-1}.[6] High activation energies mean that the temperature location of the α (glass) relaxation is relatively insensitive to a change in frequency compared to secondary-relaxation processes.

5.1.2 Mechanical Models of Viscoelastic Behavior

An insight into the nature of the viscoelastic properties of polymers can be obtained by analyzing the stress or strain response of mechanical models using an ideal spring as the Hookean element and a dashpot as the viscous element. A dashpot may be viewed as a shock absorber consisting of a piston in a cylinder filled with a Newtonian fluid of viscosity η. The elemental models are a series combination of a spring and dashpot, the *Maxwell* element, and a parallel combination of a spring and dashpot, the *Voigt* element, as illustrated in Figure 5.7. In the following sections, relationships for the transient and dynamic responses of Maxwell and Voigt models are developed.

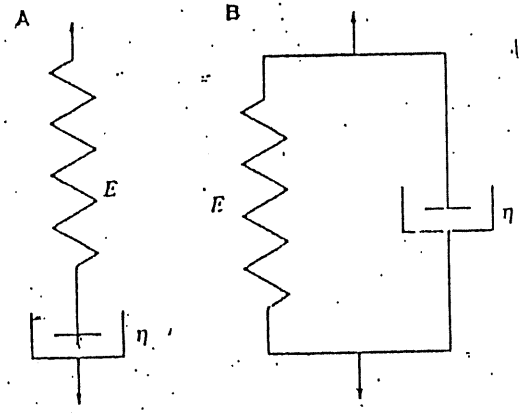

Figure 5.7. Maxwell (A) and Voigt (B) elements.

Maxwell Element. In the case of a series combination of a spring and dashpot, the total strain (or strain rate) is a summation of the individual strains (or strain rates) of the spring and dashpot. From Hooke's law ($\sigma = E\varepsilon$), the strain *rate* of an ideal elastic spring can be written as

$$\frac{d\varepsilon}{dt} = \left(\frac{1}{E}\right)\frac{d\sigma}{dt} \tag{5.36}$$

while the strain rate for the dashpot is obtained by rearranging Newton's law of viscosity (eq. 5.4) as

$$\frac{d\varepsilon}{dt} = \frac{\sigma}{\eta} \tag{5.37}$$

Therefore, the basic equation for strain rate in the Maxwell model is the summation of the strain rates for the spring and dashpot (eqs. 5.36 and 5.37) as

$$\boxed{\frac{d\varepsilon}{dt} = \left(\frac{1}{E}\right)\frac{d\sigma}{dt} + \frac{\sigma}{\eta}} \tag{5.38}$$

This differential equation can be solved for creep, stress relaxation, and dynamic response by applying the appropriate stress or strain function.

In a *creep* experiment (see Section 4.4.2), a *constant* stress, σ_0, is applied instantaneously. Equation 5.38 then reduces to

$$\frac{d\varepsilon}{dt} = \frac{\sigma_0}{\eta} \tag{5.39}$$

Rearrangement and integration of eq. 5.39 gives

$$\varepsilon(t) = \left(\frac{\sigma_0}{\eta}\right)t + \varepsilon_0 \tag{5.40}$$

where ε_0 represents the *instantaneous* (i.e., $t = 0$) strain response of the spring element. The creep compliance function, $D(t)$, is then obtained as

$$D(t) = \frac{\varepsilon(t)}{\sigma_0} = \frac{t}{\eta} + \frac{\varepsilon_0}{\sigma_0} = \frac{t}{\eta} + D \tag{5.41}$$

where $D\ (= \varepsilon_0/\sigma_0)$ is the instantaneous compliance (of the spring). An alternative form of eq. 5.41 may be obtained by defining a *relaxation time*, τ, as

$$\boxed{\tau = \frac{\eta}{E} = \eta D} \tag{5.42}$$

Equation 5.41 can then be represented in normalized form as

$$\frac{D(t)}{D} = \frac{t}{\tau} + 1 \tag{5.43}$$

In a *stress-relaxation* experiment (see Section 4.4.2), the strain (ε_o) is constant and, therefore, the strain rate is zero. Equation 5.38 is then reduced to the first-order ordinary differential equation

$$\left(\frac{1}{E}\right)\frac{d\sigma}{dt}+\frac{\sigma}{\eta}=0. \tag{5.44}$$

Rearrangement of eq. 5.44 and introduction of τ gives

$$\frac{d\sigma}{\sigma}=-\left(\frac{1}{\tau}\right)dt. \tag{5.45}$$

Integration yields the stress response as

$$\sigma=\sigma_o\exp\left(\frac{-t}{\tau}\right) \tag{5.46}$$

where σ_o is the instantaneous stress response of the spring. The stress relaxation modulus, $E_r(t)$, is then obtained as

$$E_r(t)=\frac{\sigma}{\varepsilon_o}=\left(\frac{\sigma_o}{\varepsilon_o}\right)\exp\left(\frac{-t}{\tau}\right)=E\exp\left(\frac{-t}{\tau}\right) \tag{5.47}$$

where $E\,(=\sigma_o/\varepsilon_o)$ is the (Young's) modulus of the spring element.

To obtain an expression for the *dynamic-mechanical* response (i.e., complex compliance or modulus), the expression for complex stress, $\sigma=\sigma^o\exp(i\omega t)$, is substituted into the Maxwell equation (eq. 5.38) to give

$$\frac{d\varepsilon(t)}{dt}=\left(\frac{\sigma^o}{E}\right)i\omega\exp(i\omega t)+\left(\frac{\sigma^o}{\eta}\right)\exp(i\omega t). \tag{5.48}$$

Integration from time t_1 to t_2 gives

$$\varepsilon(t_2)-\varepsilon(t_1)=\left(\frac{\sigma^o}{E}\right)\left[\exp(i\omega t_2)-\exp(i\omega t_1)\right]$$

$$+\left(\frac{\sigma^o}{\eta i\omega}\right)\left[\exp(i\omega t_2)-\exp(i\omega t_1)\right]. \tag{5.49}$$

Since the corresponding stress increment can be written as

$$\sigma(t_2)-\sigma(t_2)=\sigma^o\left[\exp(i\omega t_2)-\exp(i\omega t_1)\right], \tag{5.50}$$

division of both sides of eq. 5.49 by this expression and making use of the definition of relaxation time give the complex compliance as

$$D^*=D-i\left(\frac{D}{\omega\tau}\right). \tag{5.51}$$

Therefore, the storage compliance obtained from the Maxwell model is simply the compliance of the spring

$$D'=D, \tag{5.52}$$

which is independent of time or frequency, while the loss compliance is

$$D''=\frac{D}{\omega\tau}. \tag{5.53}$$

The corresponding expression for complex modulus, E^*, is obtained by recalling that E^* is the reciprocal of D^* and utilizing the complex conjugate of D^* as

$$E^*=\frac{1}{D^*}=\frac{1}{D-i\dfrac{D}{\omega\tau}}\times\frac{D+i\dfrac{D}{\omega\tau}}{D+i\dfrac{D}{\omega\tau}}. \tag{5.54}$$

Performing the multiplication, rearranging, and using the inverse relation $E=1/D$ gives

$$E^*=E'-iE''=\frac{E(\omega\tau)^2}{1+(\omega\tau)^2}+i\left[\frac{E\omega\tau}{1+(\omega\tau)^2}\right] \tag{5.55}$$

where

$$E'=\frac{E(\omega\tau)^2}{1+(\omega\tau)^2} \tag{5.56}$$

and

$$E''=\frac{E\omega\tau}{1+(\omega\tau)^2}. \tag{5.57}$$

It follows from eqs. 5.56 and 5.57 that $\tan\delta$ for a Maxwell model is simply

$$\tan\delta = \frac{E''}{E'} = \frac{1}{\omega\tau}. \tag{5.58}$$

Voigt Element. For a parallel combination of a spring and dashpot, the Voigt model shown in Figure 5.7B, the strain on each element must be equal while the *stress is additive*. The fundamental relation for the Voigt model is, therefore,

$$\boxed{\sigma = E\varepsilon + \eta\frac{d\varepsilon}{dt}}. \tag{5.59}$$

Making use of the relaxation time (eq. 5.42), the Voigt equation for *creep* deformation becomes a linear differential equation:

$$\frac{\sigma_0}{\eta} = \frac{\varepsilon(t)}{\tau} + \frac{d\varepsilon(t)}{dt}, \tag{5.60}$$

which can be solved by using an integrating factor ($e^{t/\tau}$). Solving for $\varepsilon(t)$, gives the compliance function as

$$D(t) = D\left[1 - \exp\left(\frac{-t}{\tau}\right)\right] \tag{5.61}$$

where $D = 1/E$. In contrast to the Maxwell model, *the Voigt equation cannot be solved in any meaningful way for stress relaxation because the dashpot element cannot be deformed instantaneously*.

The response of a Voigt model to *dynamic* strain gives the relationships for the storage and loss compliance as

$$D' = \frac{D}{1+(\omega\tau)^2} \tag{5.62}$$

and

$$D'' = \frac{D\omega\tau}{1+(\omega\tau)^2}. \tag{5.63}$$

The forms of these relationships for compliance are the same as those for dynamic *moduli* (eqs. 5.56 and 5.57) given by the Maxwell model.

Comparison of Simple Models. The two-element (i.e., the Maxwell and Voigt) models approximate some of viscoelastic characteristics of real polymers. Results are summarized in Table 5.1. In general, the modulus (stress relaxation and dynamic mechanical) is best modeled by the Maxwell element, while compliance (creep and dynamic-mechanical) is better represented by the Voigt element. The most significant limitation of these two models is that they utilize a single relaxation time (eq. 5.42). This results in the prediction *single transition* in modulus or compliance, whereas high-molecular-weight polymers (i.e., $M > M_e$) exhibit two major transitions — a glass-to-rubber and rubber-to-liquid transition. As would be expected, improvement in modeling occurs if additional elements are used, as discussed in the following section.

TABLE 5.1 PREDICTIONS OF VISCOELASTIC PROPERTIES BY THE MAXWELL AND VOIGT MODELS

Experiment	Maxwell Model	Voigt Model
Creep	$\frac{D(t)}{D} = 1 + \frac{t}{\tau}$	$\frac{D(t)}{D} = 1 - \exp\left(\frac{-t}{\tau}\right)$
Stress relaxation	$\frac{E(t)}{E} = \exp\left(\frac{-t}{\tau}\right)$	$\frac{E(t)}{E} = 1$
Dynamic mechanical	$\frac{D'}{D} = 1$	$\frac{D'}{D} = \frac{1}{1+(\omega\tau)^2}$
	$\frac{D''}{D} = \frac{1}{\omega\tau}$	$\frac{D''}{D} = \frac{\omega\tau}{1+(\omega\tau)^2}$
	$\frac{E'}{E} = \frac{(\omega\tau)^2}{1+(\omega\tau)^2}$	$E' = E$
	$\frac{E''}{E} = \frac{\omega\tau}{1+(\omega\tau)^2}$	$E'' = \omega\eta$

Multielement Models. A multielement model, particularly suited for modulus, is called the *Maxwell–Wiechert model*, which is a parallel combination of multiple Maxwell elements. In this model, the strains on each Maxwell element are equal and the stresses experienced by each Maxwell element are additive, as they are in the case of the single spring and dashpot in the simple Voigt model. For the two-element Maxwell–Wiechert model illustrated in Figure 5.8, the stress-relaxation modulus is given as

$$E(t) = E_1 \exp\left(\frac{-t}{\tau_1}\right) + E_2 \exp\left(\frac{-t}{\tau_2}\right) \tag{5.64}$$

where $\tau_1 = \eta_1/E_1$ and $\tau_2 = \eta_2/E_2$. By appropriate selection of values for E_i and τ_i, a reasonable representation of the glass and rubber plateau regions of the stress-relaxation modulus is obtained, as illustrated in Figure 5.9.

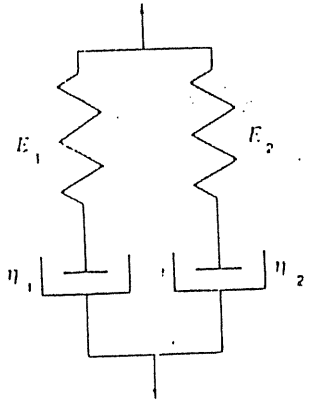

Figure 5.8. Representation of a two-element Maxwell–Wiechert model.

Further improvement in terms of realistic slopes in the transition regions is obtained by adding additional Maxwell elements in the model and, therefore, providing a distribution of relaxation times as would be expected for a high-molecular-weight polymer with a broad distribution of molecular weights. In general, the stress-relaxation modulus of a Maxwell–Wiechert model consisting of N Maxwell elements can be written as the summation

$$E(t) = \sum_{i=0}^{N} E_i \exp\left(\frac{-t}{\tau_i}\right) \tag{5.65}$$

Corresponding equations can be written for dynamic moduli, as shown in Table 5.2.

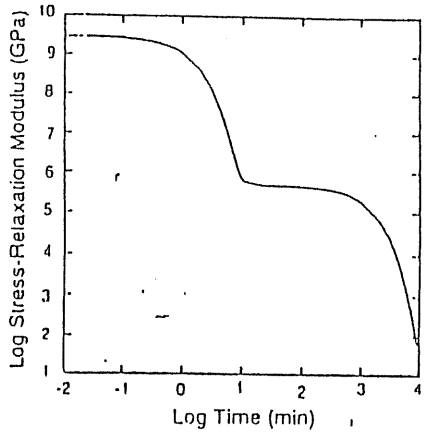

Figure 5.9. Prediction of stress-relaxation modulus, $E(t)$, as a function of dimensionless time (t/τ) for the two-element Maxwell–Wiechert model illustrated in Figure 5.6. Values for model parameters (eq. 5.64) are $E_1 = 3 \times 10^9$ Pa, $E_2 = 5 \times 10^5$ Pa, $\tau_1 = 1$ min, and $\tau_2 = 10^3$ min.

TABLE 5.2 PREDICTIONS OF VISCOELASTIC PROPERTIES BY TWO MULTI-ELEMENT MODELS: MAXWELL–WIECHERT AND VOIGT–KELVIN

Experiment	Maxwell–Wiechert Model	Voigt–Kelvin Model
Creep		$D(t) = \sum_{i=1}^{N} D_i\left[1 - \exp\left(\frac{-t}{\tau_i}\right)\right]$
Stress relaxation	$E(t) = \sum_{i=1}^{N} E_i \exp\left(\frac{-t}{\tau_i}\right)$	
Dynamic mechanical	$E' = \sum_{i=1}^{N} \frac{E_i(\omega\tau_i)^2}{1+(\omega\tau_i)^2}$	$D' = \sum_{i=1}^{N} \frac{D_i}{1+(\omega\tau_i)^2}$
	$E'' = \sum_{i=1}^{N} \frac{E_i\omega\tau_i}{1+(\omega\tau_i)^2}$	$D'' = \sum_{i=1}^{N} \frac{D_i\omega\tau_i}{1+(\omega\tau_i)^2}$

An alternate approach for a multielement model is a *Voigt–Kelvin model* which consists of a *series* arrangement of Voigt elements. A two-element Voigt–Kelvin model is illustrated in Figure 5.10. For N elements, the creep compliance can be written as a summation

$$D(t) = \sum_{i=0}^{N} D_i \left[1 - \exp\left(\frac{-t}{\tau_i}\right)\right]. \tag{5.66}$$

Corresponding equations can be written for dynamic compliance as given in Table 5.2.

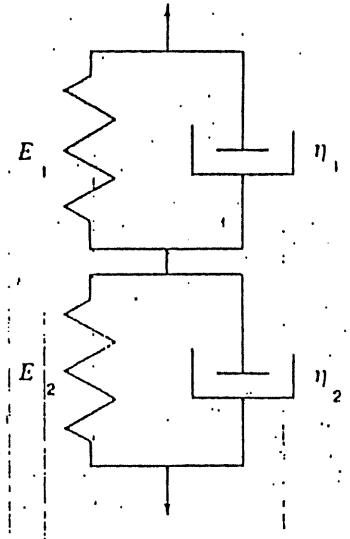

Figure 5.10. Representation of a two-element Voigt–Kelvin model.

Relaxation and Retardation Spectra. In the limit of an infinite number of Maxwell elements in a Maxwell–Wiechert model, the summation given in eq. 5.65 may be replaced by an integral

$$E(t) = \int_0^\infty E(\tau)\exp\left(\frac{-t}{\tau}\right)d\tau. \tag{5.67}$$

In this equation, $E(\tau)$ is a continuous function of the relaxation times. An alternate expression is given as

$$H(\tau) = \tau E(\tau) \tag{5.68}$$

where $H(t)$ is called the *relaxation-time distribution function*. Substitution of this relation into the integral and using $\ln \tau$ in place of τ gives

$$E(t) = \int_{\ln \tau=-\infty}^{\ln \tau=+\infty} H(\tau)\exp\left(\frac{-t}{\tau}\right)d\ln\tau. \tag{5.69}$$

Corresponding expressions can be written for the dynamic moduli.

An expression for compliance is obtained by considering an infinite number of Voigt elements in series (Voigt–Kelvin model)

$$D(t) = \int_{\ln \tau=-\infty}^{\ln \tau=+\infty} L(\tau)\left[1 - \exp\left(\frac{-t}{\tau}\right)\right]d\ln\tau, \tag{5.70}$$

where $L(\tau)$ is called the *retardation* spectrum function. Corresponding expressions can be written for the dynamic moduli.

Relaxation and retardation spectra characterize the viscoelastic properties of a polymer at a particular temperature. They can be calculated from one set of experimental data and then be used to predict the viscoelastic response under different experimental conditions. For example, the relaxation-time spectrum can be calculated from the temperature dependence of the dynamic loss-modulus and then be used to calculate the temperature dependence of the stress-relaxation modulus. Such interrelationships minimize experimental work and provide a basis to test the consistency of experimental data.

5.1.3 Viscoelastic Properties of Polymer Solutions and Melts

Concentrated polymer solutions and melts also exhibit viscoelastic response. It is convenient to characterize this response in terms of a complex viscosity, η^*. This is defined by applying Newton's law of viscosity (eq. 5.4) to the case of an dynamically applied *shear* strain, γ^* ($= \gamma_0 e^{i\omega t}$). The corresponding dynamic shear stress, τ^*, is then written as

$$\tau^* = \eta^* \frac{d\gamma^*}{dt} = i\omega\eta^*\gamma^*. \tag{5.71}$$

The complex viscosity can be written in a form analogous to dynamic compliance;

$$\boxed{\eta^* = \eta' - i\eta''}, \tag{5.72}$$

where η' is called the *dynamic viscosity* and is obtained from the values of the [illegible] G'' and angular [illegible]:

$$\eta' = \frac{G''}{\omega}. \tag{5.73}$$

The imaginary component of the viscosity, η'', is obtained from the shear storage modulus, G', as

$$\eta'' = \frac{G'}{\omega}. \tag{5.74}$$

The *Cox–Merz rule* provides an approximate relationship between the *steady-shear viscosity* in the limit of zero shear rate, η_0 (see Section 11.2.1), and the magnitude of the complex viscosity as

$$\eta_0 = |\eta^*| = \left[(\eta')^2 + (\eta'')^2\right]^{1/2}. \tag{5.75}$$

Experimental Techniques. Commercial instrumentation to determine the stress response of polymeric solutions and melts to small (i.e., linear viscoelastic) static or dynamic shear strains is based on simple-shear geometries such as cone-and-plate, concentric (Couette) cylinder, and rotating parallel plates. The rate of applied strain for these instruments is low (10^{-4} to 10^3 s^{-1}). Two of these rheometers, cone-and-plate and concentric cylinder, are described in detail in Section 11.4 in relation to their importance in determining *apparent viscosity* of polymer melts and concentrated solutions as a function of frequency or shear strain rate at low shear rates. Basic principles of rheometry are described in a variety of sources.[7,8]

The apparent viscosity, as defined by Newton's law of viscosity (eq. 5.4), is obtained from steady-shear measurements as

$$\eta = \frac{\tau}{\dot{\gamma}}. \tag{5.76}$$

Values of complex viscosity or, equivalently, the real and imaginary components of the shear moduli, G' and G'', are obtained by applying an *oscillatory* rather than

[1] Equations 5.73 and 5.74 follow from eq. 5.71 as

$$G^* = G' + iG'' = \frac{\tau^*}{\dot{\gamma}} = i\omega\eta^* = i\omega(\eta' - i\eta'') = \omega(\eta'' + i\eta').$$

steady shear to the cone in a cone-and-plate rheometer or to the cylinder in the case of a Couette rheometer.

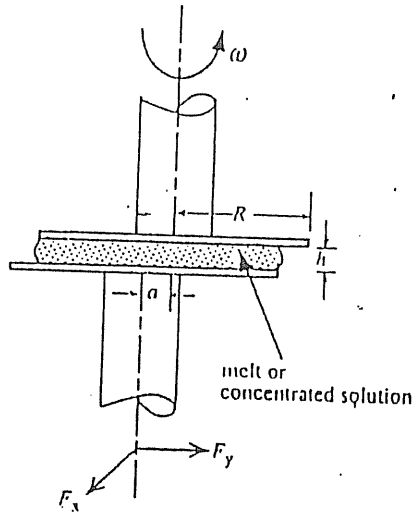

Figure 5.11. Idealized representation of an eccentric rotating-disk (ERD) rheometer. In operation, a concentrated polymer solution or melt is sheared in the gap (h) between the two parallel plates of radii R (e.g., 2.5 cm) and whose axes are offset by the distance a. The top plate is rotated at an angular frequency, ω (rad s^{-1}). Force can be measured in the orthogonal directions by means of transducers mounted in the plane of the bottom plate.

Alternately, the dynamic properties (i.e., G' and G'') of polymer solutions and melts can be obtained directly by using *steady-shear flow* in a rheometer employing an eccentric rotating-disk (ERD) geometry that is illustrated in Figure 5.11. In this rheometer design, the plates are parallel, but the axes perpendicular to the plates are offset by a preset distance, a. This offset results in a flow parallel to the plates that is periodic in time (i.e., dynamic flow), although the top plate is driven at a constant angular frequency, ω. The shear rate is given as

$$\dot{\gamma} = \left(\frac{a}{h}\right)\omega. \tag{5.77}$$

The dynamic moduli are determined from geometric parameters — axes offset (a), plate radius (R), and plate separation (h) — and forces measured in the orthogonal directions (F_x and F_y) as follows:

$$G' = \frac{F_y h}{a\pi R^2} \tag{5.78}$$

and

$$G'' = \frac{F_x h}{a\pi R^2}. \tag{5.79}$$

5.1.4 Dielectric Analysis

In place of a mechanical strain, viscoelastic response may be characterized by applying a time-dependent electric voltage to the sample. The voltage establishes an electrical field in the sample, which becomes electrically polarized. This means that any induced and permanent dipoles become oriented in the electric field. Polarization due to ionic conduction and the induction of a dipole moment of the molecule resulting from the distortion of the electron cloud of individual atoms is nearly instantaneous, while polarization due to the molecular motion and alignment of permanent dipoles in the electric field requires time. The polarization and ionic conduction result in the creation of a current whose amplitude depends upon frequency, temperature, and the dielectric properties of the material. As in the case of the stress response in dynamic-mechanical analysis, the frequency of the current is the same as the applied field but is shifted by the phase angle δ. In dielectric analysis, the most important parameter for characterizing a sample is its *dielectric constant*, ε, which is defined next.

Theory. When a voltage (V) is applied across two electrodes between which a dielectric material is placed, a charge is established across the capacitor. This charge, Q (units of coulombs), is related to V and the capacitance (C) of the material (units of farads) as

$$Q = CV. \tag{5.80}$$

The capacitance may be expressed in terms of the capacitance of vacuum, C_0, as

$$C = \varepsilon C_0 \tag{5.81}$$

where ε (dimensionless) is the dielectric constant which is a function of temperature and time (or frequency). By definition, the dielectric constant for a vacuum is unity. The dielectric constant for air is only slightly higher at 1.0006, while that for water, which is capable of strong polarization, is 81 at room temperature and low frequency. Since polarization is time dependent, there is a *short-time or instantaneous response* for the dielectric constant, ε_U (or ε_∞), which results from ion migration and induced polarization. The *long-time response*, ε_R (or ε_∞), represents the sum of contributions of the instantaneous response and the complete alignment of the permanent dipoles in the electric field.

The *charge density*, σ, is defined as

$$\sigma = \frac{Q}{A} \tag{5.82}$$

where A is the area of the plate electrodes. The charge density in the absence of a dielectric (i.e., a vacuum) between the electrodes is represented as σ_0. This charge density is related to the *electric field*, E, which is defined as the ratio of the voltage across the capacitor and the distance between the electrodes as

$$E = \frac{V}{d}. \tag{5.83}$$

The relation between electric field and charge density is given by *Gauss's flux theorem*

$$E = 4\pi\sigma_0. \tag{5.84}$$

As previously discussed, the polarization that is time dependent, $P(t)$, contains an instantaneous component, P_U, due to dipole induction

$$\lim_{t\to 0} P(t) = P_U. \tag{5.85}$$

The separate time-dependent (dipole-orientation) contribution to polarization is indicated as $P_D(t)$, giving the total polarization as

$$P(t) = P_D(t) + P_U. \tag{5.86}$$

From the limiting conditions at long time

$$\lim_{t\to\infty} P(t) = P_R \tag{5.87}$$

and

$$\lim_{t\to\infty} P_D(t) = P_D, \tag{5.88}$$

it follows that

$$P_R = P_D + P_U. \tag{5.89}$$

The polarization at infinite time, P_R, is related to the charge density as

$$\sigma = \sigma_o + P_R . \tag{5.90}$$

Since

$$\sigma = \varepsilon_R \sigma_o \tag{5.91}$$

and (from eq. 5.84)

$$\sigma_o = \frac{E}{4\pi}, \tag{5.92}$$

it follows that substitution of these equations into eq. 5.90 gives

$$\varepsilon_R - 1 = \left(\frac{4\pi}{E}\right) P_R . \tag{5.93}$$

Substitution of eq. 5.89 into eq. 5.93 then gives

$$\varepsilon_R - 1 = \left(\frac{4\pi}{E}\right)\left(P_D + P_U\right). \tag{5.94}$$

In analogy to the expression for polarization (eq. 5.89), we may write

$$\varepsilon_R = \varepsilon_D + \varepsilon_U \tag{5.95}$$

and (following eq. 5.93)

$$\varepsilon_U - 1 = \left(\frac{4\pi}{E}\right) P_U . \tag{5.96}$$

The objective in the preceding development is to obtain expressions for the time dependency of the transient [i.e., $\varepsilon(t)$] or more commonly the dynamic [i.e., $\varepsilon(\omega,t)$] dielectric constant in response to a steady [i.e., $E(t)$] or oscillatory voltage [i.e., $E^*(\omega,t)$] applied to the electrodes. The approach is to assume that the time rate of change of the polarization is proportional to the magnitude of its displacement from its equilibrium value (P_R) as

$$\frac{dP(t)}{dt} = -\frac{P(t) - P_R}{\tau} \tag{5.97}$$

where τ is a time constant or relaxational time. From eq. 5.86, we may write

$$\frac{dP(t)}{dt} = \frac{dP_D}{dt} .$$

Substitution of the above equation, eq. 5.86 for $P(t)$, and eq. 5.89 for P_R into eq. 5.97 gives

$$\frac{dP_D(t)}{dt} = -\frac{P_D(t) - P_D}{\tau} . \tag{5.98}$$

From eqs. 5.89, 5.93, and 5.96 it can be shown that

$$P_D = \frac{E}{4\pi}\left(\varepsilon_R - \varepsilon_U\right) \tag{5.99}$$

where $(\varepsilon_R - \varepsilon_U)$ is called the *dielectric relaxational strength*. Substitution of eq. 5.99 into eq. 5.98 and rearrangement gives the differential equation for a time-dependent electric field

$$\tau \frac{dP_D(t)}{dt} + P_D(t) = \frac{E(t)}{4\pi}\left(\varepsilon_R - \varepsilon_U\right). \tag{5.100}$$

For a frequency dependent (i.e., sinusoidal) voltage

$$E^*(\omega,t) = E_o \exp(i\omega t), \tag{5.101}$$

the differential equation of eq. 5.100 may be solved assuming that $t >> \tau$, which indicates that steady-state conditions apply. The solution is given as

$$P_D^*(\omega) = \frac{\left(\varepsilon_R - \varepsilon_U\right)}{1 + i\omega\tau}\frac{E^*(\omega)}{4\pi} . \tag{5.102}$$

A complex dielectric constant may be defined in terms of real and imaginary components, in a similar manner to dynamic compliance, as

$$\varepsilon^* = \varepsilon' - i\varepsilon'' \tag{5.103}$$

where

$$\tan\delta_\varepsilon = \frac{\varepsilon''}{\varepsilon'} . \tag{5.104}$$

With analogy to eq. 5.99 and recognizing that ε_R is the only frequency-dependent component of the dielectric constant, we can write

$$\varepsilon^*(\omega) = \frac{4\pi P_D^*(\omega)}{E^*(\omega)} + \varepsilon_U. \tag{5.105}$$

Rearranging this equation for $P_D^*(\omega)$ and substitution of this expression into eq. 5.102 gives

$$\varepsilon^*(\omega) = \varepsilon_U + \frac{\varepsilon_R - \varepsilon_U}{1 + i\omega\tau}. \tag{5.106}$$

Multiplication of the numerator and denominator of the second term on the RHS of eq. 5.106 by its complex conjugate allows the real and imaginary components of ε^* to be resolved as

$$\varepsilon^*(\omega) = \varepsilon_U + \left(\frac{\varepsilon_R - \varepsilon_U}{1 + i\omega\tau}\right) \times \left(\frac{1 - i\omega\tau}{1 - i\omega\tau}\right)$$

$$= \varepsilon_U + \frac{\varepsilon_R - \varepsilon_U}{1 + \omega^2\tau^2} - i\frac{\omega\tau(\varepsilon_R - \varepsilon_U)}{1 + \omega^2\tau^2}. \tag{5.107}$$

Comparison of this equation with eq. 5.103 gives

$$\varepsilon' = \varepsilon_U + \frac{\varepsilon_R - \varepsilon_U}{1 + \omega^2\tau^2} \tag{5.108}$$

and

$$\varepsilon'' = \frac{\omega\tau(\varepsilon_R - \varepsilon_U)}{1 + \omega^2\tau^2}. \tag{5.109}$$

As in the case of dynamic-mechanical oscillation of a Maxwell model (see Problem 5–5b), it is easily shown that ε'' exhibit a maximum at a frequency equal to the reciprocal of the relaxation time, τ, as shown by the plot of ε' (eq. 5.108), ε'' (eq. 5.109), and $\tan\delta_\varepsilon$ versus frequency in Figure 5.12.

Equations 5.108 and 5.109 give a reasonable qualitative behavior of experimental ε' and ε'' with the limitation that the phenomenological model utilizes a single relaxation time, τ, whereas a distribution of relaxation times would be expected for high polymers. From the early work of Peter Debye, there have been a number of attempts to relate macroscopic properties of the dielectric, such as ε and P, with molecular properties such as the dipole moment or molecular polarizability. A full description of these approaches is beyond the scope of this text, and the reader is encouraged to look at other reference sources such as the book by Daniels (see *Specialized Readings*).

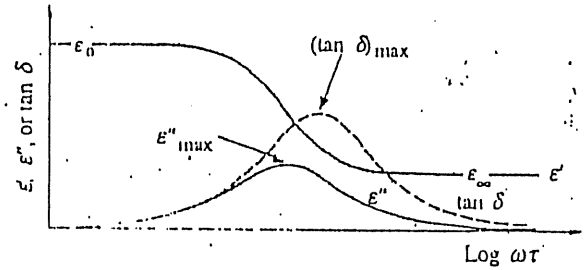

Figure 5.12. Illustration of the frequency dependence of the dielectric constant.

Experimental Methods: Values ε' and ε'' can be readily measured for polymer solutions, melts, and films over a wide range of frequencies (10^{-4} to 10^{10} Hz) by a variety of techniques. As a result of this wide frequency range, dielectric data can be plotted against frequency (i.e., frequency-plane measurements) at constant temperature in comparison with the usual temperature-plane plots typical for dynamic-mechanical measurements.

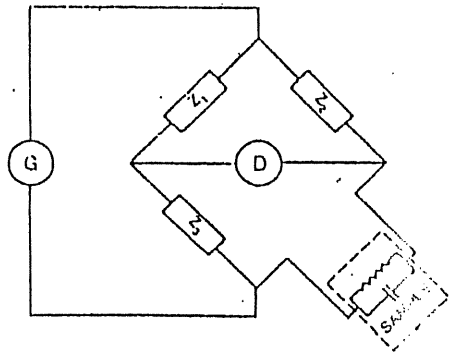

Figure 5.13. Representation of dielectric test facility employing a Schering bridge. During measurement, one or several bridge impedances (i.e., Z_1, Z_2, and Z_3) is adjusted in order that the magnitude and the phase of the voltage drops across Z_1 and Z_2 are zero. Instrumentation includes a frequency generator (G) and null detector (D) or capacitance bridge.

In the case of solid samples, a polymer film may be coated with an electrically conductive layer of gold or other metal to improve contact with the electrodes. The film is then placed in an electrode cell and immersed in a constant-temperature bath. The cell is connected to a frequency generator and typically to an electrical bridge to measure the electrical impedance of the sample. Frequently, a Schering impedance bridge, such as the one illustrated in Figure 5.13, is used over a frequency range from about 1 Hz to 10 MHz (the medium frequency range). A Schering bridge is similar to a Wheatstone bridge except that impedance, rather than resistance, is measured. By balancing the bridge, the equivalent capacitance, C_x, and resistance, R_x, of the sample are determined. The parameters $\tan \delta_e$, ε', and ε'' can then be determined as

$$\tan \delta_e = R_x C_x \omega, \tag{5.110}$$

$$\varepsilon' = \frac{C_x}{C_0\left(1 + \tan^2 \delta_e\right)}, \tag{5.111}$$

$$\varepsilon'' = \varepsilon' \tan \delta_e. \tag{5.112}$$

A plot of dielectric-loss (ε'') data for polycarbonate sample as a function of frequency over a wide range of temperatures is shown in Figures 5.14A and B. In general, the glass transition and secondary-relaxation processes can be investigated by dielectric measurements as long as sufficient polarizability is available by the chemical nature of the side groups or main-chain repeating units. Dielectric measurements have also been used to study the cure process in thermoset composites by measurement of the dielectric constant at fixed frequency and temperature as a function of time.

Thermally Stimulated Current Analysis. Thermally stimulated current (TSC) analysis is a method related to dielectric spectroscopy that can be used to investigated amorphous transitions. In this technique, polymer dipoles are first oriented by applying a high potential across the sample at elevated temperatures (typically above T_g). The orientation is frozen by dropping the temperature below expected transitions while the potential is maintained. Next, the electric field is removed and the sample is heated. As the dipoles reorient, the resulting electric current due to the depolarization is measured as a function of temperature. Maxima appear at each transition due to the increased molecular mobility as temperature is increased. The resulting plot of thermally stimulated current against temperature is very similar to that of the dynamic-mechanical loss data and can be used to identify secondary relaxations and glass transitions.

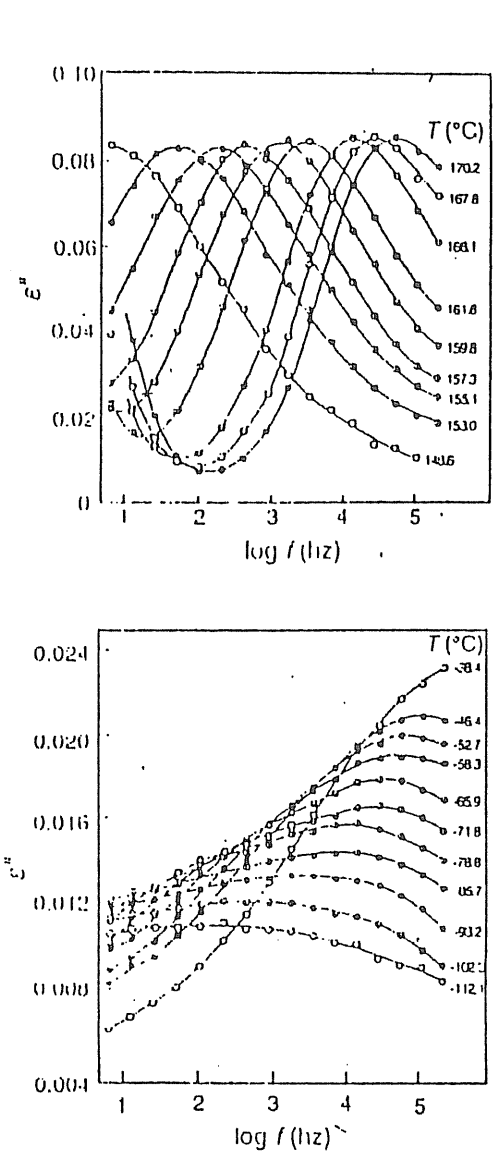

Figure 5.14. Plots of the dielectric loss constant (ε'') of polycarbonate as a function of frequency at different temperatures.[9] A. High-temperature data showing the α (glass transition). B. Low-temperature data showing the secondary γ relaxation. The peak maxima are shown to increase in frequency with increasing temperature.

5.1.5 Time–Temperature Superposition

Often, it is important to know how a material will behave (e.g., creep or stress relaxation) at a fixed temperature but over a long time period (perhaps years) that may not be realistically accessible. Fortunately, long-time behavior can be evaluated by measuring stress-relaxation or creep data over a shorter period of time but at several different temperatures. Information from each of these different temperature curves may then be combined to yield a *master curve* at a single temperature by horizontally shifting each curve along the log time scale. This technique is called *time–temperature superposition* and is a foundation of linear viscoelasticity theory. In this procedure, the master curve is plotted as stress-relaxation modulus or creep compliance versus reduced time, t/a_T. The *shift factor*, a_T, is defined as the ratio of (real) time to reach a particular value of modulus at some temperature to the reference-scale time coordinate, t_r, corresponding to the same value of modulus in the master curve at the reference temperature, T_r.

$$\boxed{a_T = \frac{t}{t_r}}. \tag{5.113}$$

Stated more concisely, the time–temperature superposition principle says that

$$E(T,t) = E(T_r,t_r). \tag{5.114}$$

The procedure of horizontal shifting is illustrated for stress-relaxation and torsional creep data for polycarbonate in Figure 5.15.

The dependence of the shift factor, a_T, on temperature is given by the *Williams–Landel–Ferry (WLF) relationship*

$$\boxed{\log a_T = \frac{-C_1(T-T_r)}{C_2+T-T_r}} \tag{5.115}$$

where C_1 and C_2 are constants for a given polymer and T_r is the reference temperature. When T_r is taken to be the polymer T_g, as it often is, C_1 and C_2 may be approximated by the "universal" values of 17.44 and 51.6, respectively; however, significant deviations from these values may exist for some polymers (see Problem 5-7).

If C_1 and C_2 are not known, each curve may be horizontally shifted to the reference temperature curve until a value of modulus on the shifted curve coincides with one on the reference curve.† The shift factor may then be calculated by use of

† It may be shown that for elastic chains in a network, the shear modulus is proportional to temperature and to density (i.e., chain concentration). Therefore, it may be necessary to introduce a small vertical shift to account for the dependence of modulus on both temperature and density (ρ). This correction may be expressed as

$$E(T_r,t_r) = \frac{\rho(T_r)T_r}{\rho(T)T} E(T,t).$$

Since density decreases with increasing temperature, the *product* of the density and temperature does not increase significantly with temperature, except in the plateau regions.

C_2, may then be determined by plotting $(T-T_r)/\log a_T$ versus $(T-T_r)$, where rearrangement of eq. 5.115 gives

$$\frac{T-T_r}{\log a_T} = -\frac{1}{C_1}(T-T_r) - \frac{C_2}{C_1}. \tag{5.116}$$

Following this procedure, C_1 is obtained directly from the inverse of the slope, and C_2 can be calculated from this value of C_1 and the value of the intercept (C_2/C_1). It can be shown that C_1 and C_2 can be related to the fractional free-volume at T_g (f_g) and the thermal-expansion coefficient of free volume (see Chapter 11, Appendix 1).

As discussed in Section 4.1.2, Gibbs and DiMarzio have suggested that a true second-order transition should occur at a temperature (T_2) where the conformational entropy is zero. This would occur at an *equilibrium* glassy state that conceptionally can be obtained by cooling from the melt at an infinitely slow rate. Therefore, the WLF relation can be used to determine the relationship between the thermodynamic transition-temperature and the kinetic T_g by noting that shifting from a finite to an infinite time-scale requires that the shift factor approach infinity or that the denominator in eq. 5.115 goes to zero, where $T_r = T_g$ and $T = T_2$. This means that

$$T_2 = T_g - C_2 = T_g - 52 \tag{5.117}$$

using the universal value for C_2. In other words, the true second-order transition temperature should lie approximately 52°C *below* the experimentally measured T_g.

The master curve for stress-relaxation modulus, shown in Figure 5.15B, illustrates the four characteristic regions of a high-molecular-weight polymer. At short times, the polymer behaves as a glassy material (glassy plateau), while at longer times the modulus sharply drops to the rubbery-plateau region. At sufficiently long times, the stress-relaxation modulus again rapidly falls. Conceptionally, what is happening is that initially the polymer chains are entangled and unable to fully accommodate the applied strain on the sample. This results in a high apparent modulus. Eventually, sufficient time has elapsed at the experimental temperature for the chains to slip, and the sample adjusts to the load. The form of the master curve for stress relaxation is qualitatively similar to that of Young's modulus (see Figure 4.19) where temperature rather than time is the

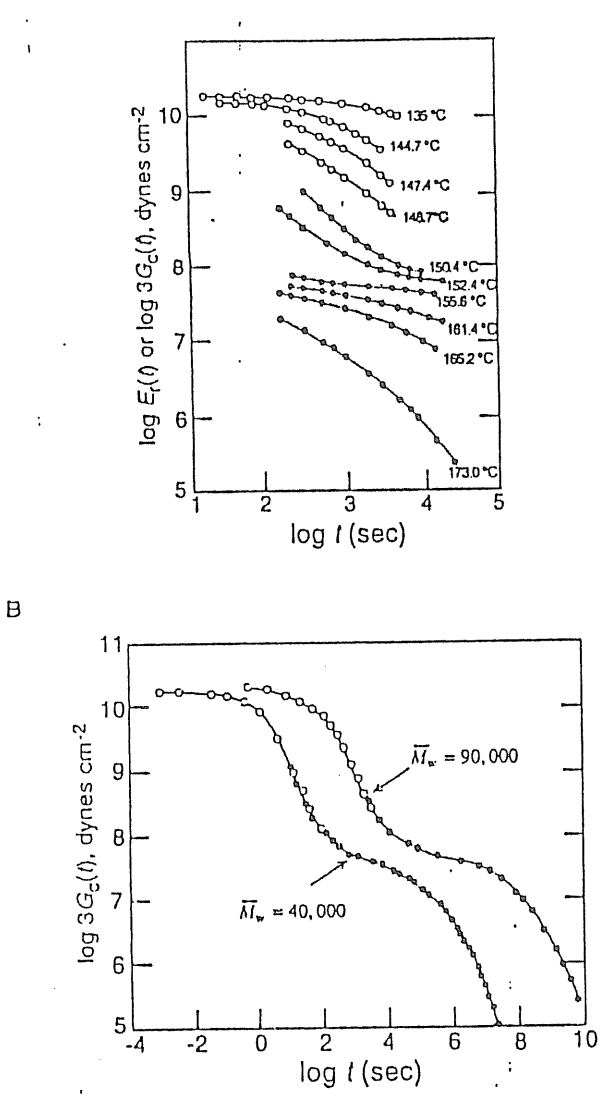

Figure 5.15. A. Modulus of polycarbonate ($\overline{M}_w$ = 40,000) as a function of time and temperature from stress-relaxation (●) and torsional-creep (○) measurements.[10] B. Resulting master curve obtained by shifting both sets of data at a reference temperature of 150°C and for two different molecular-weight samples of polycarbonate ($\overline{M}_w$ = 40,000 and 90,000). The master curve is shown to shift to higher times with increasing molecular weight.

abscissa. The fact that time and temperature can be superimposed means that the change in modulus of the material with increasing time at constant temperature is equivalent to the change in modulus when measured at identical times but at increasing temperature.

5.16 Boltzmann Superposition Principle

For the (ideal) tensile (or shear) compliance are inversely related (see eq. 4.46). The same is true for complex modulus and complex compliance (see eq. 5.17), but creep compliance and stress-relaxation modulus are not as simply related; that is,

$$D(t) \neq \frac{1}{E_r(t)}.$$

This is because creep compliance and stress-relaxation moduli are obtained by distinctly different experimental procedures. As discussed in Chapter 4, a fixed *load* is applied instantly at $t = 0$ in a creep experiment, while a fixed *strain* is applied instantaneously at $t = 0$ for stress-relaxation measurements. Fortunately, a relationship between the creep compliance and stress-relaxation modulus can be established by application of another fundamental statement of linear viscoelasticity, the *Boltzmann superposition principle*.

This Boltzmann superposition principle states that the *total strain is a linear function of total applied stress*. In the case of a creep experiment, the strain is a function of the total load (stress) history in which each load makes an independent contribution to the creep. If a load, σ_0, is instantaneously applied at time $t = 0$ and a second load, σ_1, is applied at time $t = u_1$, as illustrated in Figure 5.16, then the strain at some time t' where $t' > u_1$, is given by the Boltzmann superposition principle as

$$\varepsilon(t') = \sigma_0 D(t') + \sigma_1 D(t' - u_1). \tag{5.118}$$

In the general case of the application of a series of discrete loads, σ_1, σ_2, ... σ_n, applied at times $t = u_1$, u_2, ... u_n, the total resulting strain response in creep deformation is calculated from the tensile compliance function, $D(t)$, as

$$\varepsilon(t) = \sum_{i=1}^{n} \sigma_i D(t - u_i). \tag{5.119}$$

If the applied stress is some *continuous* function of time, $\sigma(t)$, application of the Boltzmann superposition principle gives the creep response in integral form as

$$\varepsilon(t) = \int_{-\infty}^{t} \left[\frac{\partial \sigma(u)}{\partial u}\right] D(t-u)\, du \tag{5.120}$$

where u is the time variable and integration covers the entire stress history ($-\infty < u \leq t$) of the sample. Using a convenient variable change, $a = t - u$, integration of eq. 5.120 by parts (see Appendix E at the end of this text) gives

$$\varepsilon(t) = D(0)\sigma(t) + \int_0^{\infty} \sigma(t-a)\left[\frac{\partial D(a)}{\partial a}\right] da. \tag{5.121}$$

Similar relations may be obtained for stress relaxation as

$$\sigma(t) = \int_{-\infty}^{t} \left[\frac{\partial \varepsilon(u)}{\partial u}\right] E(t-u)\, du \tag{5.122}$$

and

$$\sigma(t) = E(0)\varepsilon(t) + \int_0^{\infty} \varepsilon(t-a)\left[\frac{\partial E(a)}{\partial a}\right] da. \tag{5.123}$$

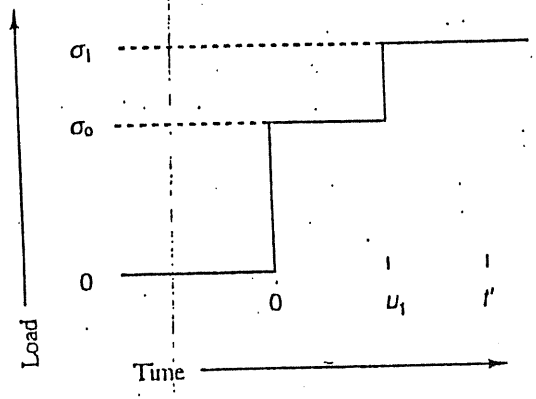

Figure 5.16., Stress history corresponding to the strain response given by eq. 5.118.

5.1.7 Interrelationships between Transient and Dynamic Properties

A basis for relating the creep-compliance and stress-relaxation modulus is obtained by taking the Laplace transform of eqs. 5.120 and 5.122. A summary of the principles and basic relationships of Laplace transforms is included in Appendix E. It can be shown that the transformations of eqs. 5.120 and 5.122 give

$$\mathcal{L}[\varepsilon(t)] = p\,\mathcal{L}[\sigma(t)]\mathcal{L}[D(t)] \tag{5.124}$$

and

$$\mathcal{L}[\sigma(t)] = p\,\mathcal{L}[\varepsilon(t)]\mathcal{L}[E(t)] \tag{5.125}$$

where p is the Laplace variable. Substitution of eq. 5.124 into the RHS of eq. 5.125 gives the relationship between creep-compliance and stress-relaxation modulus in *transform space* (see Problem 5-3) as

$$\boxed{\frac{1}{p^2} = \mathcal{L}[D(t)]\mathcal{L}[E(t)]}. \tag{5.126}$$

The Boltzmann superposition principle also provides a means of interrelating dynamic (moduli) and transient (stress-relaxation) data. Utilizing eq. 5.122 and making a variable change in the form $s = t - u$ gives

$$\sigma(t) = -\int_0^{\infty} \left[\frac{\partial \varepsilon(t-s)}{\partial s}\right] E(s)\, ds. \tag{5.127}$$

In dynamic oscillation,

$$\varepsilon(t-s) = \varepsilon^0 \exp[i\omega(t-s)] \tag{5.128}$$

and

$$\frac{\partial \varepsilon(t-s)}{\partial s} = \varepsilon(t)(-i\omega)\exp(-i\omega s). \tag{5.129}$$

Substitution of these equations into the integral of eq. 5.127, and noting that $\varepsilon(t)$ is not a function of s and, therefore, can be taken outside the integral, gives

$$\sigma(t) = i\varepsilon(t)\int_0^{\infty} \omega \exp(-i\omega s)\, E(s)\, ds. \tag{5.130}$$

Dividing both sides of this equation by $\varepsilon(t)$ and replacing the complex term by Euler's identity [$\exp(-i\omega s) = \cos \omega s - i \sin \omega s$] gives the complex modulus as

$$E^* = \frac{\sigma(t)}{\varepsilon(t)} = \int_0^\infty \omega \sin(\omega s)\, E(s)\, ds + i \int_0^\infty \omega \cos(\omega s)\, E(s)\, ds \qquad (5.131)$$

Relating this equation to the customary form of E^* $(= E' + iE'')$ gives the relationships between the stress-relaxation modulus, $E(s)$, and the storage and loss moduli as

$$\boxed{E' = \omega \int_0^\infty \sin(\omega s)\, E(s)\, ds} \qquad (5.132)$$

and

$$\boxed{E'' = \omega \int_0^\infty \cos(\omega s) E(s) ds}. \qquad (5.133)$$

The preceding equations may be recognized as the Fourier *sine* and *cosine* transforms of the stress-relaxation modulus function. This means that if the form of the stress-relaxation function is known the dynamic moduli can be determined by taking the sine or cosine transforms of the function. Tables of these transforms are available in most handbooks of mathematical tables. For convenience, some important Fourier transforms are listed in Appendix E.

5.2 INTRODUCTION TO RUBBER ELASTICITY

In 1805, John Gough observed that the temperature of a rubber band will increase as it is stretched adiabatically. Also, if a weight is hung from the end of the rubber band and heat is applied, the rubber band will *decrease* in length rather than stretch as observed for other materials such as common metals and gases as illustrated in Figure 5.17. It was not until the 1930s that an explanation for this behavior, known as the Gough–Joule effect, was provided by means of classical thermodynamics as described in the following section.

5.2.1 Thermodynamics

The first and second law of thermodynamics applied to a reversible, equilibrium process provides the relationship between internal energy (U), entropy (S), and work (W) as

$$dU = TdS - dW. \qquad (5.134)$$

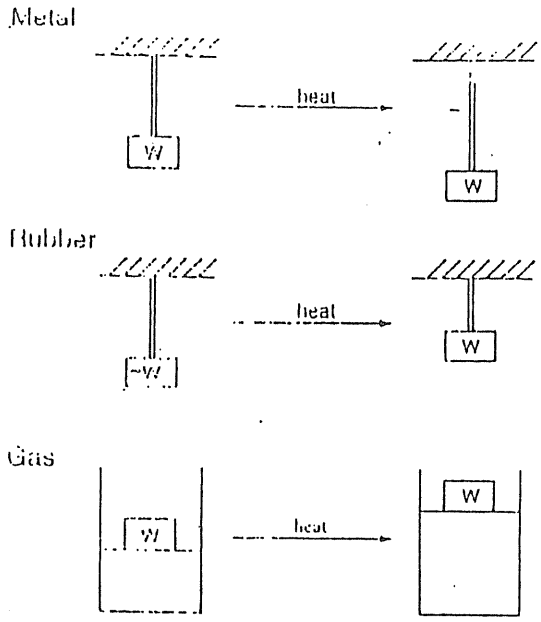

Figure 5.17. Illustration of the effect of heat on metal, rubber, and gas [Adapted from J. E. Mark, *J. Chem. Ed.*, 58, 898 (1981), with permission of the publisher.]

For deformation of a rubber band, the work is a combination of pressure–volu expansion and the work due to the (tensile) force (f) applied to the rubber ba given as

$$dW = pdV - f d\ell \qquad (5.13$$

where the convention is that work done *by* the system (i.e., pressure–volume wo is positive and the work done *on* the system (i.e., force–displacement work) is ne ative. Enthalpy is related to the internal energy as

$$dH = dU + pdV. \qquad (5.13$$

Substitution of eqs. 5.134 and 5.135 into eq. 5.136 gives

$$dH = TdS + f d\ell. \qquad (5.13$$

At constant temperature and pressure, rearrangement of eq. 5.137 in terms of force and taking the (partial) derivative with respect to length at constant temperature and pressure gives

$$f = \left(\frac{\partial H}{\partial \ell}\right)_{T,p} - T\left(\frac{\partial S}{\partial \ell}\right)_{T,p} \tag{5.138}$$

Equation 5.138 shows that elastic force has both an enthalpic and entropic component ($f = f_e + f_s$).

In order to obtain an expression for the temperature dependence of force, we make use of the relation[1]

$$\left(\frac{\partial S}{\partial \ell}\right)_{T,p} = -\left(\frac{\partial f}{\partial T}\right)_{p,L} \tag{5.139}$$

Substitution of eq. 5.139 into eq. 5.138 gives

$$f = \left(\frac{\partial H}{\partial \ell}\right)_{T,p} + T\left(\frac{\partial f}{\partial T}\right)_{p,L} \tag{5.140}$$

Rearrangement of eq. 5.140 gives

$$\left(\frac{\partial f}{\partial T}\right)_{p,L} = \frac{f - (\partial H/\partial \ell)_{T,p}}{T} \tag{5.141}$$

Equation 5.141 indicates that the slope of a force–temperature plot will be positive, as is usually observed for elastomers at moderate or higher extension, if

$$f > \left(\frac{\partial H}{\partial \ell}\right)_{T,p}$$

This condition is satisfied except for very small extensions, as illustrated by Figure 5.18. It can be shown that the change of enthalpy due to deformation at constant temperature and pressure has both internal energy, U, and volume contributions as given by the expression

[1] Obtained from the reciprocity relationship for the exact differential equation for Gibbs free energy:

$$dG = -S\,dT + V\,dp + f\,d\ell$$

$$\left(\frac{\partial H}{\partial \ell}\right)_{T,p} = \left(\frac{\partial U}{\partial \ell}\right)_{T,V} + T\left(\frac{\alpha}{\beta}\right)\left(\frac{\partial V}{\partial \ell}\right)_{T,p} \tag{5.142}$$

Since elastomers are nearly incompressible, it is clear that the second term on the RHS of eq. 5.142 is very small. Furthermore, changes in internal energy due to conformation changes during deformation are also small. For these reasons, enthalpic contributions in rubber elasticity are generally insignificant and rubberlike behavior can be satisfactorily explained on the basis of entropic considerations alone. Conceptionally, we can view polymer chains to be in a entropically favorable, disordered state when undeformed. During deformation, the chains become ordered and, therefore, an entropically driven force develops to restore the more favorable, disordered conformational state.

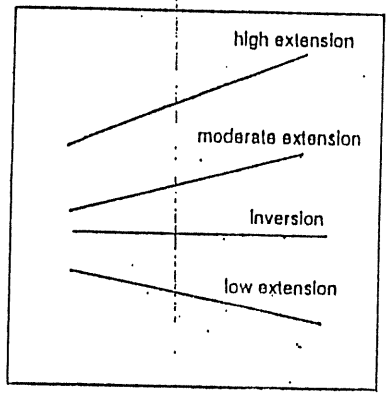

Figure 5.18. Thermoelastic behavior of elastomer at various elongations.

The importance of entropy to the deformation of an ideal elastomer can be compared to that of an ideal gas. Heating a gas increases the driving force toward a state of maximum entropy. This means that an increase in temperature results in an increase in volume at constant pressure as illustrated in Figure 5.17. Since the deformation of a compressed gas can be expressed as the reciprocal volume ($1/V$), we can say that an increase in the temperature of a gas at constant pressure results in a decrease in its deformation. This is analogous to the case of an elastomer whose measure of deformation is its length (ℓ) which decreases with an increase in temperature.

5.2.2 Statistical Theory

In the 1920s, Staudinger developed a thermodynamic expression for elastic force based upon polymer-chain statistics. The elastic force is related to the Helmholtz free energy, A, as

$$f = \left(\frac{\partial \Delta A}{\partial \ell}\right)_{T,V} \tag{5.143}$$

where $A = U - TS$ and ΔA represents the difference in Helmholtz free energy between the deformed and undeformed network ($\Delta A = A_d - A_u$). The entropy contribution is linked to the total number of conformations, Ω, available to the rubber network through the Boltzmann relation $S = k \ln \Omega$. An expression for Ω is obtained from the Gaussian distribution-function $\omega(x_i, y_i, z_i)$ for the ith chain in a network of N chains (see Section 3.1) as

$$\Omega = \prod_{i=1}^{N} \omega(r_i). \tag{5.144}$$

The resulting equation for force is usually given in the form

$$\boxed{f^* = G_0\left(\lambda - \frac{1}{\lambda^2}\right)} \tag{5.145}$$

where f^* is the (nominal) stress, G_0 is the shear modulus (one-third of the tensile modulus for incompressible materials), and λ is the principal *extension ratio*

$$\lambda = \frac{L}{L_0} = 1 + \varepsilon \tag{5.146}$$

where L_0 is the original (undeformed) length of the elastomer.

The shear modulus, G_0, is proportional to temperature and to the number of chains in the elastomeric network (see eq. 4.47). High crosslink density results in an increase in the number of network chains per unit volume and will, therefore, increase modulus. This will become apparent by comparing the stiffness of a lightly crosslinked rubber band with a highly crosslinked ebonite bowling ball.

As shown in Figure 5.19, the theory gives a good representation of the experimental stress–strain curve only for moderate strains ($\lambda < 1.5$). For larger extensions, the theory overpredicts stress because the conformational state is no longer adequately predicted by the Gaussian-distribution model used in the derivation (eq. 5.144). At still higher extensions ($\lambda > 6$), the observed stress rapidly rises due to the development of strain-induced crystallization. The increase in modulus is due to the physical reinforcement effect of the crystallites. In general, the increase in modulus of an elastomer due to the presence of crystallites or the incorporation of fillers such as carbon black can be approximated by the *Guth–Smallwood equation*

$$\boxed{\frac{E_f}{E_0} = 1 + 2.5\phi_f + 14.1\phi_f^2} \tag{5.147}$$

where E_f is the tensile (Young's) modulus of the filled elastomer, E_0 is the modulus of the unreinforced elastomer, and ϕ_f is the volume fraction of the filler.

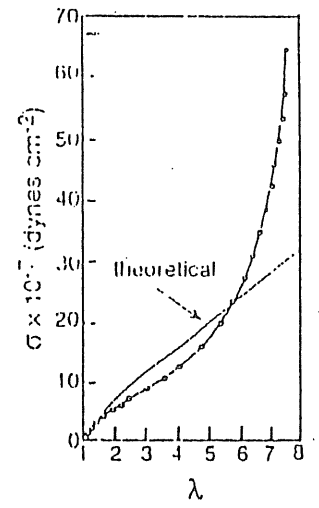

Figure 5.19. Comparison of the statistical-thermodynamic relationship (eq. 5.145 where $G_0 = 1.8 \times 10^6$ dynes cm^{-2}) with the experimental stress–strain data ($\circ$) for natural rubber. [Adapted from L. R. G. Treloar, *Trans. Faraday Soc.*, 40, 59 (1944), with permission of the publisher.]

5.2.3 Phenomenological Model

Another widely used model of rubber elasticity has its origin in continuum mechanisms. It is known as the *Mooney–Rivlin equation*, given as

$$\boxed{f^* = 2\left(C_1 + \frac{C_2}{\lambda}\right)\left(\lambda - \frac{1}{\lambda^2}\right)} \tag{5.148}$$

where C_1 and C_2 are empirical constants (distinct from the WLF constants). Values of C_1 and C_2 are obtained by plotting experimental stress–strain data as

$$[f^*] = \frac{f^*}{\lambda - \lambda^{-1}} \tag{5.149}$$

versus $1/\lambda$. Equation 5.148 is very useful for describing the stress–strain curves of elastomers over a wide range of extensions.

5.2.4 Recent Developments

The statistical theory of rubber elasticity is based upon a number of significant assumptions including that

- crosslinking does not alter the chain dimensions from their unperturbed state
- the end-to-end separation of network chains can be fit by a Gaussian distribution
- crosslink junctions are fixed at their mean positions and these junctions deform in the same ratio as the macroscopic deformation of the sample (i.e., *affine deformation*)

An alternative to the affine model is the "*phantom chain*" approximation whereby chains are permitted to pass through one and another as if they had zero cross-sectional area. While the deformation of the mean position of the crosslink junctions are affine, the junctions are allowed to fluctuate about their mean positions. The phantom theory predicts moduli that are lower than predicted by the affine model. Both models predict that the modulus of a rubber network is independent of the deformation; however, experiments show that modulus actually decreases with an increase in λ as is correctly represented by the Mooney–Rivlin equation (eq. 5.148) which owes its origin to continuum mechanics. Comparison of eq. 5.148 with the form of the statistical-theory result (eq. 5.145) indicates that the λ-dependence of modulus is given as

$$[f^*] = 2C_1 + 2C_2\lambda^{-1} \tag{5.150}$$

where the Mooney–Rivlin constants are themselves independent of λ. More recent theoretical-models which are beyond the scope of this discussion, provide an improved model for the dependence of $[f^*]$ on λ and offer better insight into the molecular theory of rubber elasticity.[11] These include the constrained-junction and, later, the constrained-chain models for which the phantom-model prediction is approached as a limiting case at small deformations.

REFERENCES

1. L. E. Nielsen, *SPE J.*, May, 1960, p. 525.
2. T. Murayama, *Dynamic Mechanical Analysis of Polymeric Material*, Elsevier, Amsterdam, 1978.
3. J. K. Gillham, in *Developments in Polymer Characterisation–3*, J. V. Dawkins, ed., Applied Science Publishers, Ltd., London, 1982, p. 159.
4. J. K. Gillham, S. J. Stadnicki, and Y. Hazony, *J. Appl. Polym. Sci.*, 21, 401 (1977).
5. J. M. O'Reilly, H. E. Bair, and F. E. Karasz, *Macromolecules*, 15, 1083 (1982).
6. J. R. Fried, A. Letton, and W. J. Welsh, *Polymer*, 31, 1032 (1990).
7. K. Walters, *Rheometry*, Chapman and Hall, London, 1975.
8. S. Middleman, *The Flow of High Polymers*, Interscience Publishers, New York, 1968.
9. S. Matsuoka and Y. Ishida, *J. Polym. Sci.: Part C*, 14, 247 (1966).
10. J. P. Mercier, J. J. Aklonis, M. Litt, and A. V. Tobolsky, *J. Appl. Polym. Sci.*, 9, 447 (1965).
11. J. E. Mark, *Kautsch. Gummi, Kunstst.*, 42, 191 (1989).

GENERAL READING

J. J. Aklonis and W. J. MacKnight, *Introduction to Polymer Viscoelasticity*, 2nd ed., John Wiley & Sons, New York, 1983.

R. F. Boyer, "Dependence of Mechanical Properties on Molecular Motion in Polymers," *Polym. Eng. Sci.*, 8, 161–185 (1968).

J. Heijboer, "The Torsion Pendulum in the Investigation of Polymers," *Polym. Eng. Sci.*, 19, 664 (1979).

J. E. Mark, "Rubber Elasticity," *J. Chem. Ed.*, 58, 898–903 (1981).

J. E. Mark and B. Erman, *Rubberlike Elasticity*, John Wiley & Sons, New York, 1988.

L. R. G. Treloar, *The Physics of Rubber Elasticity*, Oxford, 1958.

SPECIALIZED READING

V. V. Daniels, *Dielectric Relaxation*, Academic Press, London, 1967.

J. D. Ferry, *Viscoelastic Properties of Polymers*, 3rd ed., John Wiley & Sons, New York, 1980.

J. E. Mark and B. Erman, *Elastomeric Polymer Networks*, Prentice Hall, Englewood Cliffs, NJ, 1992.

N. G. McCrum, B. E. Read, and G. Williams, *Anelastic and Dielectric Effects in Polymeric Solids*, John Wiley & Sons, New York, 1967.

D. S. Pearson, "Recent Advances in the Molecular Aspects of Polymer Viscoelasticity," *Rubber Chem. Technol.*, 40, 439–496 (1967).

N. W. Tschoegl, *The Phenomenological Theory of Linear Viscoelastic Behavior: An Introduction*, Springer-Verlag, Berlin, 1989.

Problems

5–1. Show that $|E^*| = \sigma^0/\varepsilon^0$ and $|D^*| = 1/|E^*|$.

5–2. Show that the work per cycle per unit volume performed during dynamic tensile oscillation of a viscoelastic solid may be given as $\pi\sigma^0\varepsilon^0 \sin\delta$ (eq. 5.30a).

5–3. Given the expression $G(t) = G_0 \exp(-t/\tau) + G_1$, show that the compliance function, $J(t)$, can be written in the form $J(t) = A - B\exp(-C\,t/\tau)$, where A, B, and C are constants.

5–4. For a Maxwell model, show the following:

(a) The equation for complex modulus E^* (eq. 5.55) can be obtained from the Fourier transform of the stress-relaxation modulus, E_t (eq. 5.47).

(b) A maximum in the loss modulus plotted as a function of frequency occurs at $\omega = 1/\tau$.

5–5. Given the four-element model illustrated, derive an analytical solution for the strain behavior and sketch $\varepsilon(t)$ versus time under the following stress conditions:

$t < 0$	$\sigma = 0$	
$0 \le t < t_1$	$\sigma = \sigma_0$	(creep)
$t_1 \le t < t_2$	$\sigma = 0$	(creep recovery)

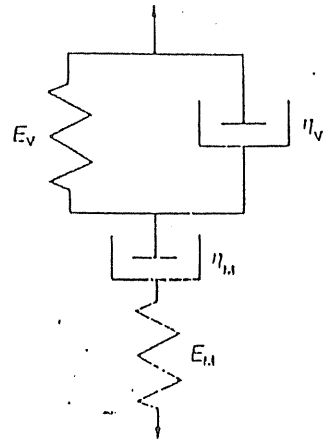

5–6. An expression for the dielectric loss constant is given as

$$\varepsilon' = \frac{(\varepsilon_0 - \varepsilon_\infty)\tau\omega}{1 + (\tau\omega)^2}$$

where $\tau = \tau_0 \exp(H/RT)$ and H is the activation energy. If ε'' assumes its maximum value at that temperature (T_{max}) where $\omega = 1/\tau$, how can the value of H be determined given the data in the form of a plot of ε'' versus T_{max} at different frequencies, f?

5–7. Calculate the WLF shift factor, a_T, for polystyrene (PS) at 150°C given that the reference temperature is taken to be the T_g of PS, 100°C, and using (a) the "universal" values of the WLF parameters, C_1 and C_2, and (b) the reported values of $C_1 = 13.7$ and $C_2 = 50.0$ K for PS.

6

Degradation, Stability, and Environmental Issues

Polymers are susceptible to attack by a wide variety of naturally occurring and man-made agents. Some of these environmental agents and examples of polymers that are particularly susceptible to their action are listed in Table 6.1. In most cases, such environmental action is deleterious. For example, UV-radiation and ozone can seriously degrade the unsaturated elastomers used in rubber tires. This degradation will limit the lifetime of the tire and could cause catastrophic failure. In practice, UV and ozone resistance are provided by adding various fillers and stabilizers to tire formulations (see Chapter 7).

In some cases, degradation may be a desirable goal. For example, it would be advantageous to be able to design plastic bottles and packaging film so that they rapidly degrade into environmentally safe by-products (e.g., carbon dioxide, water, and biomass) that will occupy less volume in a landfill. The trick is to ensure that degradation does not occur during the normal shelf life of the plastic and that cost and mechanical and other properties are not overly compromised to achieve biodegradability.

6.1 POLYMER DEGRADATION AND STABILITY

Polymers can degrade by exposure to high temperature (thermal degradation), oxygen and ozone, ultraviolet light, moisture, radiation, and chemical agents. Often multiple exposures, such as a combination of moisture and heat or oxygen and light, can result in accelerated deterioration. Deterioration of plastics to normal

ing include radiation (ultraviolet, visible, and near-infrared), moisture, temperature cycling, and wind. Factors regulating the effects of temperature, oxygen, moisture, radiation, and chemical agents on the degradation of plastics are discussed in this section.

TABLE 6.1 EFFECTS OF ENVIRONMENTAL AGENTS ON POLYMERS

Agent	Susceptible Polymers	Examples
Organic liquids and vapors	Amorphous polymers	Polystyrene, Poly(methyl methacrylate)
Moisture	Heterochain polymers	Polyesters Polyamides Polyurethanes
Ozone	Unsaturated elastomers	Polyisoprene Polybutadiene
Sunlight	Photosensitive polymers	Polyacetals Polycarbonate
Biodegradation	Short-chain polymers, nitrogen-containing polymers, polyesters	Polyurethanes Polyether–polyurethane
Ionizing radiation	Aliphatic polymers having quaternary carbon atoms	Poly(methyl methacrylate) Polyisobutylene polypropylene

6.1.1 Thermal Degradation

In general, vinyl polymers are particularly susceptible to thermal degradation, which can occur either by chain scission involving the breakage of the backbone bonds to yield free-radical segments or by nonchain scission involving the elimination of a small molecule from a substituent group and double-bond formation. These two routes are illustrated for a vinyl polymer in Figure 6.1.

Chain Scission. Chain scission can occur by one of three mechanisms. These include (1) *random degradation*, where the chain is broken at random sites; (2) *depolymerization*, where monomer units are released at an active chain end; and (3) *weak-link degradation*, where the chain breaks at the lowest-energy bonds. In addi-

tion to thermal energy, degradation may be initiated by photochemical action, irradiation, or mechanical action.

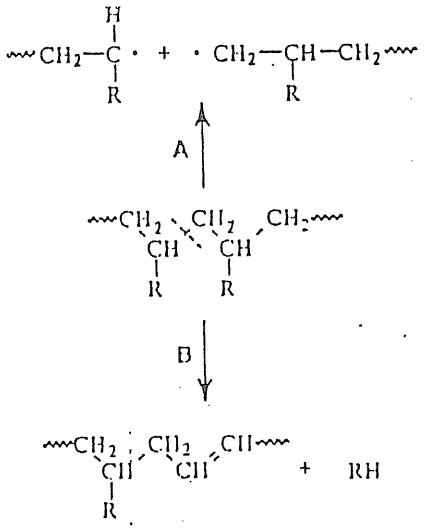

Figure 6.1. Illustration of thermal degradation of a vinyl polymer by random chain scission (A) and by nonchain scission (B) mechanisms.

Random homolytic cleavage of a polymer chain will result in a complex mixture of low-molecular-weight degradation products. Polyethylene and polypropylene degrade in this manner. In the case of 1,1-disubstituted vinyl polymers, the radical segments formed from the initial scission reaction will then depolymerize. This results in a gradual reduction in molecular weight and the production of monomer. Depolymerization may also be preceded by an initial scission at the chain end, as in the case of poly(methyl methacrylate).

The mechanism of *depolymerization* may be represented as

$$M_n^* \underset{k_p}{\overset{k_d}{\rightleftharpoons}} M_{n-1}^* + M$$

where k_d and k_p are the constants for depropagation and propagation, respectively, and M^* represents an active chain. At some temperature, called the *ceiling temperature*, T_c (see Section 2.2.1), the rates of propagation and depolymerization are equal and, therefore,

$$k_d[M_n^*] = k_p[M_{n-1}^*][M]. \tag{6.1}$$

TABLE 6.2 CEILING TEMPERATURES OF SOME COMMON VINYL POLYMERS

Polymer	Structure	T_c (°C)
Poly(α-methylstyrene)	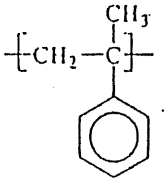	61
Poly(methyl methacrylate)	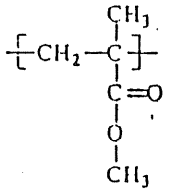	220
Polypropylene	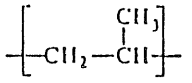	300
Polystyrene	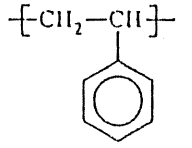	310
Polyethylene	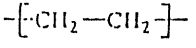	400
Polytetrafluoroethylene	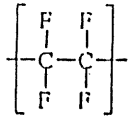	580

If the molecular weight is high (i.e., $n >> 1$), then M_{n-1} and M_n are indistinguishable and, therefore,

$$k_c = k_p[M] \tag{6.2}$$

Expressing the rate constants in Arrhenius form then gives

$$A_d \exp\left(\frac{-E_d}{RT_c}\right) = A_p \exp\left(\frac{-E_p}{RT_c}\right)[M] \tag{6.3}$$

where A_d and A_p are called the collision frequency factors, and E_d and E_p are the activation energies for depolymerization and polymerization, respectively. Rearrangement gives the following relationship for the ceiling temperature:

$$T_c = \frac{E_p - E_d}{R \ln\left(A_p[M]/A_d\right)} \tag{6.4}$$

The ceiling temperature varies widely with polymer structure, as illustrated by values given for several vinyl polymers in Table 6.2. For example, the ceiling temperature of polystyrene is 310°C but only 61°C for the 1,1-disubstituted vinyl polymer, poly(α-methylstyrene), which is much more sterically hindered at the radical site due to the presence of the methyl substituent at the α-carbon site.

Whether or not a polymer will thermally depolymerize to yield monomer is only partly related to its ceiling temperature. Two other factors affecting depolymerization are the reactivity of the polymer-chain radicals in chain-transfer reaction and the activity of the available chain-transfer sites in the polymer. For example, polytetrafluorethylene (PTFE) with a very high T_c (500°C) will produce almost a quantitative yield of monomer upon thermal degradation at temperatures *well below* T_c. The reason for this behavior is that the C–F bond of PTFE is very unreactive to a free-radical chain-transfer reaction and, as a result, the polymer provides no active chain-transfer sites to compete with depolymerization process.

Nonchain Scission Reactions. One example of a common nonchain scission reaction (Figure 6.1A) is *dehydrohalogenation*, which results from the breakage of a carbon–halogen bond and the subsequent liberation of hydrogen halide. The most important example of a polymer that degrades by dehydrohalogenation is poly(vinyl chloride) (PVC). As illustrated in Figure 6.2, PVC undergoes dehydrochlorination at temperatures near and above its T_g (ca. 87°C) to yield hydrogen chloride and ultimately a *polyene* (i.e., conjugated double-bond) structure, which is accompanied by intense color formation. The presence of hydrogen chloride will accelerate the dehydrochlorination process, resulting in further property deterioration. PVC can be stabilized by adding compounds that interfere with the degradation process, neutralize hydrochloric acid as it is formed, trap free radicals, or react with double bonds to prevent subsequent chain scission. Commercial PVC resins usually contain organo-tin or similar thermal stabilizers (see Section 7.1.3).

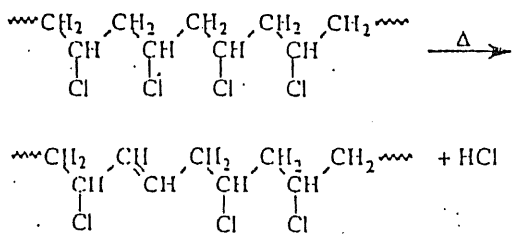

Figure 6.2. Partial dehydrochlorination of a repeating unit of PVC resulting in double-bond formation and the liberation of hydrogen chloride.

Another example of a commercial polymer that undergoes a nonchain scission reaction at high temperatures is poly(vinyl alcohol) (PVA). Thermal degradation liberates acetic acid and results in polyene formation as in the case of PVC.

Polyacrylonitrile (PAN) is an interesting polymer with good gas-barrier properties suitable for packaging film (see Chapter 12). Although PAN can be solution-cast into film or solution-spun into textile (acrylic) fibers from organic solvents such as dimethylformamide (see Section 8.2.4), it cannot be melt-processed like other thermoplastics. This is because the nitrile (-C≡N) groups of PAN undergo a cyclization reaction at elevated temperatures to yield a ladder-type polymer, as shown in Figure 6.3. This thermally modified form is deeply colored and insoluble but is important as the starting material in the production of some carbon and graphite fibers (see Section 7.1.2). Acrylonitrile finds use in thermoplastic and elastomer applications only as a copolymer with other monomers such as styrene and butadiene (e.g., ABS, SAN, NBR).

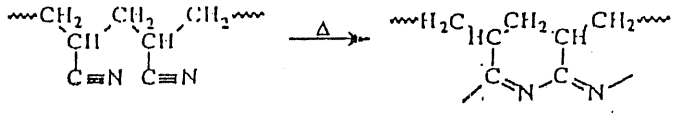

Figure 6.3. Cyclization of polyacrylonitrile at melt temperatures.

Strategies for Thermally Stable Polymers. Many flame-retardant additives as well as comonomers designed to improve the fire resistance of certain polymers are thermally labile and, therefore, the thermal stability of the polymer can be reduced. For use at high temperatures for extended periods of time, the most successful polymers are those with highly aromatic structures, especially

those with [illegible] rings. Resonance stabilization (with energies up to 16.7 kJ mol^{-1}) results in high main-chain bond strength and consequently high thermal stability. Examples of high-temperature polymers and their decomposition temperatures are given in Table 6.3.

TABLE 6.3 EXAMPLES OF THERMALLY STABLE POLYMERS

Polymer	Structure	Decomp. T (°C)[a]
Aromatic polyester	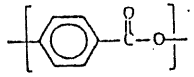	480
Polybenzamide	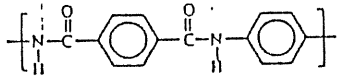	500
Polybenzimidazole	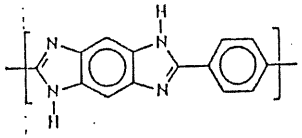	650
Polypyrrole	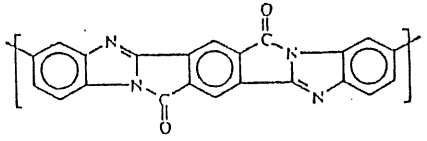	660
Poly(*p*-phenylene)	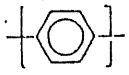	660

[a] Temperature at onset of weight loss in an inert atmosphere as determined by TGA.

Polymers having high-temperature stability as well as other high-performance properties are examples of specialty polymers designed for limited use in aerospace, electronics, and other applications and are discussed in Section 10.2. Unfortunately, the same factors that contribute to high-temperature stability of these polymers also translate to high T_g, high melt-viscosity, and insolubility in common organic solvents, which make these polymers difficult or impossible to process by usual methods, such as extrusion and injection molding. Successful commercialization, therefore, always requires some compromise between thermal properties and processibility.

6.1.2 Oxidative and UV Stability

With the exception of fluoropolymers, most polymers are susceptible to oxidation, particularly at elevated temperature or during exposure to ultraviolet light. Oxidation usually leads to increasing brittleness and deterioration in strength. Generally, the mechanism of oxidative degradation is free radical and is initiated by the thermal or photolytic cleavage of bonds. The free radicals then react with oxygen to yield peroxides and hydroperoxides.

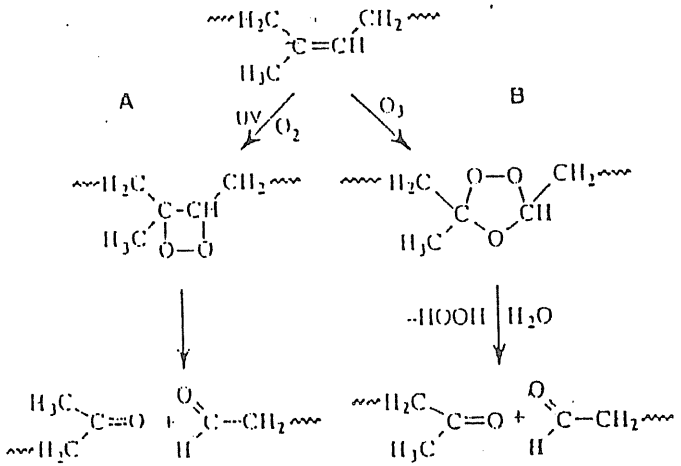

Figure 6.4. Degradation of polyisoprene by photolysis (A) and ozonolysis (B).

In general, unsaturated polyolefins are particularly susceptible to attack by oxygen and by ozone. The combined effect of light and oxygen (photolysis) and the action of ozone (ozonolysis) on the degradation of a common elastomer, polyisoprene, are illustrated in Figure 6.4. In both cases, an intermediate cyclic ozonide structure is formed. Subsequent breakage of the labile O–O bonds leads to chain scission and lower-molecular-weight polymer chains with carbonyl end groups. In the case of ozonolysis (Figure 6.4B), hydrolysis leads to chain scission and liberation of hydrogen peroxide.

Oxidative degradation of saturated polymers can also occur through a complex series of reactions that involve the intermediate formation of peroxy radicals. Polystyrene is especially susceptible to photooxidative degradation. In this case, ultraviolet radiation is absorbed by the phenyl group, which can transfer the energy

to nearby units along the polymer chain. Cleavage of the main chain and phenyl ring can then occur with carbonyl-group formation. The result is yellowing and embrittlement of the plastic.

Commercial antioxidants include organic compounds like hindered phenols and aromatic amines, which act as free-radical scavengers, as well as agents that serve to suppress homolytic breakdown, such as organic phosphites. Effects of UV radiation may be reduced by incorporating additives, such as carbon black widely used in tire manufacture, that screen UV wavelengths (300 to 400 nm). Transparent thermoplastics like polycarbonate can be protected against yellowing and embrittlement from UV light by incorporating compounds, such as benzophenone derivatives, that have a high extinction coefficient in the UV range and are able to convert absorbed radiation into heat without chemical change.

6.1.3 Chemical and Hydrolytic Stability

Solvent Crazing and Cracking. Virtually all thermoplastics in contact with organic liquids and vapors will fail at lower stress or strain even if the interacting chemical is not ordinarily considered to be a solvent for the polymer. The effect of these chemicals is believed to be due to localized plasticization that allows development of crazes or cracks (see Section 4.4.1) at levels of stress lower than otherwise would be required.

As discussed in Chapter 4, crazes consist mostly of voids that can absorb low-molecular-weight stress-cracking or stress-crazing agents. Plasticization reduces the effective T_g in the region of the craze and, therefore, increases the localized mobility of polymer chains and promotes craze and crack development. It is, therefore, not unexpected that the critical strain, ε_c, for solvent craze initiation is often closely related to the solubility parameter (see Section 3.2.6) of the agent in relation to that of the polymer. Minimum critical-strains will be observed for solvents with solubility parameters close to that of the polymer. Under these circumstances, cracks will rapidly develop. The time for initiation of a craze depends on the rate of absorption, with the longest times to reach critical stress or strain observed for fluids of the highest viscosity. Crazes developing in the presence of a solvent grow more rapidly and to larger size that those grown in a solvent-free environment.

The relationship between solubility parameter and ε_c is illustrated for two engineering thermoplastics in Figure 6.5. The two polymers are (bisphenol-A) polysulfone and poly(2,6-dimethyl-1,4-phenylene oxide), whose solubility parameters are approximately 10.7 and 8.6, respectively. As shown, the minimum in ε_c is observed in the case of organic liquids whose solubility parameters approximate those of the two polymers (i.e., cracking agents); however, significant reduction in ε_c is observed for organic liquids whose solubility parameters fall on either side of the minima.

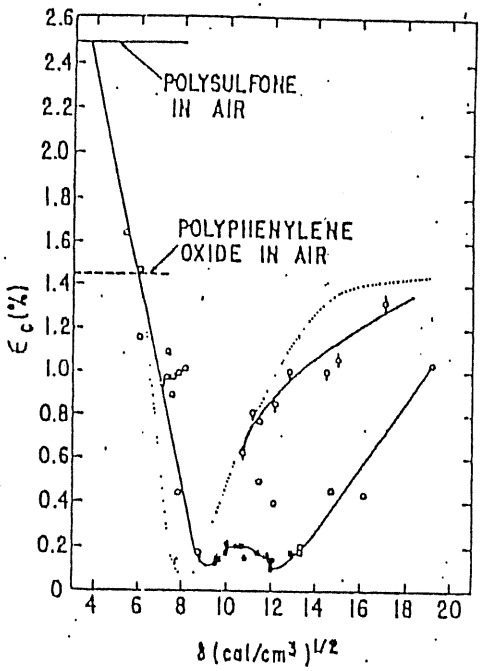

Figure 6.5. Plot of critical strain, ε_c, for crazing and cracking of polysulfone and poly(2,6-dimethyl-1,4-phenylene oxide) as a function of the solubility parameter, δ, of the cracking/crazing agent. Open circles represent crazing agents, while filled circles represent cracking agents. Open circles with single tabs are monohydric alcohols; those with double tabs are dihydric alcohols. Solid curves represent fit of data for polysulfone. Dotted curve represents data for poly(2,6-dimethyl-1,4-phenylene oxide).[1] [Reprinted with permission from R. P. Kambour, E. E. Romagosa, and C. L. Gruner, *Macromolecules*, 5, 335 (1972). Copyright© 1972 American Chemical Company.]

Hydrolysis. Many polymers are susceptible to degradation due to the effect of water, particularly under acidic conditions. These include some naturally occurring polymers, such as polysaccharides and proteins, as well as some synthetic polymers, principally condensation polymers such as polyesters and polyamides. In general, vinyl polymers are not susceptible to hydrolysis. Factors that influence the susceptibility of a given polymer to hydrolysis include water permeability and solubility, which are influenced by the chemical structure of the polymer and its physical state (e.g., crystallinity, glass-transition temperature, etc.). Autocatalysis of hydrolysis is possible if acidic or basic groups are produced by the polymer

breakdown as in the case of polyesters, which yield carboxylic acids upon hydrolysis as follows:

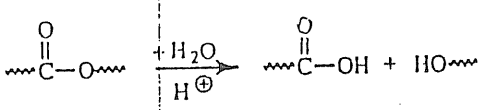

Poly(vinyl esters) and poly(vinyl amides) are hydrolyzed to poly(vinyl carboxylic acids) under basic conditions. In these cases, hydrolysis will be less than complete because the presence of the negatively-charged groups of the poly(carboxylic acid) retards the approach of the reagent (OH^-) to the adjacent ester or amide groups as illustrated for polymethacrylamide.

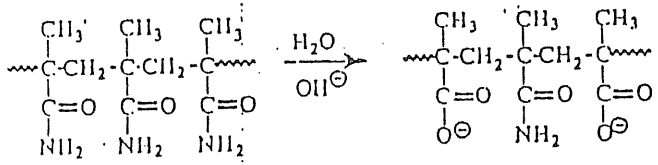

6.1.4 Radiation Effects

Many polymers are susceptible to degradation and crosslinking upon exposure to high-energy ionizing radiation (radiolysis) such as γ-radiation, electron beams, and X-rays. Sometimes, these effects can be used to advantage. For example, integrated circuits can be prepared by microetching a polymer resist coating of a silicon chip by electron-beam irradiation. The exposed silicon can then be doped. Radiation, particularly γ- and electron-beam radiation, can also be used to prepare graft copolymers. Radiation can also be used to polymerize a monomer in the solid state and to modify surfaces for adhesive bonding. In other cases, such as the use of plastics in space vehicles, nuclear power plants, and γ-sterilized medical disposables, polymers and composites selected for these applications must have good resistance to radiation. For example, it has been estimated that the total dosage of radiation for an object spending 30 years in space orbit is on the order of 10 mrad. Sterilizable of medical disposables (e.g., syringes, surgical gowns, and lab ware) by γ-irradiation has become increasingly important due to the limitations of alternative techniques, such as the inefficiency of steam sterilization and the possible carcinogenesis of ethylene oxide used in "cold" sterilization. Some polymers such as polystyrene and polysulfone are very radiation resistant, but others such as polypropylene will readily degrade upon irradiation.

The primary event in radiation damage is the ejection of a high-energy electron:

This primary electron can then ionize additional molecules with the release of additional electrons in a chain reaction. An electronically excited state will result when a positively-charged molecule is recombined with an available electron:

An excited state will also result when the energy transfer associated with interaction of the radiation with the material is insufficient to cause ionization. Excited states in polymers can decay by chemical reactions involving heterolytic bond cleavage producing ionic species or by homolytic bond cleavage of the main chain or substituent groups resulting in the formation of radical species. Radical lifetimes can be hours and even weeks at room temperature. This provides ample opportunity for the radicals to initiate crosslinking or to react with oxygen in the atmosphere. Whether only chain scission or crosslinking will occur depends upon the chemical structure of the polymer chain. In general, polymers having quaternary carbon atoms, such as polyisobutylene or poly(methyl methacrylate), undergo chain scission in an inert atmosphere, while crosslinking is more probable for polymers without quaternary carbon atoms, such as polyethylene and polystyrene. In the presence of oxygen, which can react with the free radicals that are generated upon irradiation, chain scission becomes the predominant mechanism. Antioxidants, which act as radical scavengers, are effective stabilizers for radiation-oxidative degradation.

In general, polymers with aromatic rings such as polystyrene, aromatic polyamides, and polysulfones are extremely radiation resistant, as are thermosets such as epoxies, phenolics, and urethanes. Fibers that have good radiation resistance include poly(ethylene terephthalate) and aromatic polyamides. Among elastomers, polyurethanes have particularly good radiation resistance.

6.1.5 Mechanodegradation

Polymer degradation can also result from the application of stress such as high shear deformation of polymer solutions and melts. In the case of solids, stress-induced degradation may result from comminution (grinding, milling, or crushing), machining, stretching, and fatigue, tearing, abrasion, or wear. Mechanodegradation is particularly severe for high-molecular-weight polymers, which exist in a highly entangled state. The result of stress-induced degradation is the generation of macroradicals originating from random chain rupture. In a process called *mastication*, natural rubber is softened by passing between spiked rollers, which also serve to disperse filler and other additives such as accelerators, vulcanizers, and antioxidants.

6.2 THE MANAGEMENT OF PLASTICS IN THE ENVIRONMENT

At the present, plastics account for roughly a quarter of all solid waste by volume in U.S. landfills versus about 40% for paper. At the present rate, U.S. landfill capacity could be exhausted in a decade or two. To reduce the volume of plastic waste that goes to landfills, there are three alternatives: recycling, incineration, and biodegradation.

6.2.1 Recycling

Recycling of commercial plastics is a significant contemporary issue from many aspects, such as the need to reduce the volume of plastic waste that is sent to landfills and to conserve nonrenewable petroleum resources. In 1990, plastics were the second largest component (21%) of trash, behind only paper and cardboard (32%) in volume. Many commodity plastics are now being recycled in the United States and Europe. These include poly(ethylene terephthalate) (PET) used in beverage containers, as well as polyolefins (i.e., polyethylene and polypropylene), polystyrene, and poly(vinyl chloride) (PVC) used in packaging. For example, approximately 36% of plastic soda bottles are recycled. In 1991, nearly 1 billion pounds of plastics — mostly HDPE and PET — were recycled in the United States, compared to approximately 3 billion pounds in Europe, where the composition of recycled wastes is dominated by the polyethylenes (LDPE and HDPE) and PVC, as illustrated by Figure 6.6.

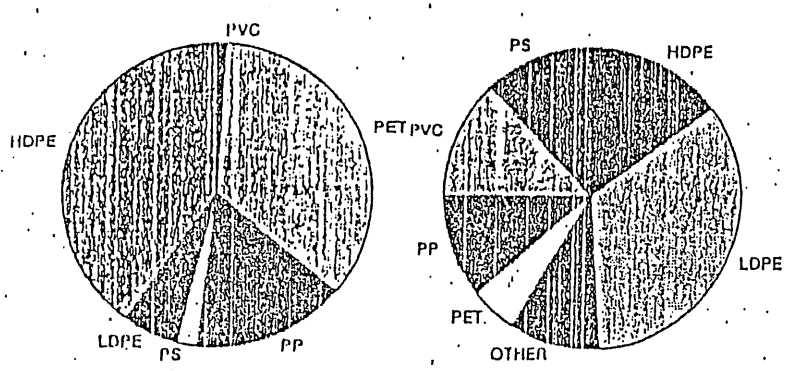

Figure 6.6. Comparison of the compositions of plastic wastes recycled in the United States (left) and Europe (right) during 1991. Source: *Chemical Engineering*, July 1992.

There are two contemporary approaches to recycling. The obvious route is simply the reprocessing of waste plastics, which may take other forms and applications. For example, waste PET has been used recently in the manufacture of insulation boards in competition to the use of expanded polystyrene boards. In this process, waste PET containers is washed, shredded, ground into 5-mm particles, and dried to remove water that would initiate hydrolysis during processing. The particles are then mixed with a nucleating agent and an additive to increase melt viscosity (to facilitate the foaming process) and processed in a standard foam slab extruder unit, where Freon 12 is injected into the molten recycled PET just before it emerges from the extruder. Insulation boards prepared from waste PET have some advantages over expanded polystyrene, including lower smoke emission during burning and suitability for the use of hot-melt adhesives in the preparation of laminates due to the high melting temperature (ca. 260°C) of the semicrystalline PET, compared to the low glass-transition temperature of amorphous polystyrene (ca. 100°C).

The other approach to recycling, which may have more potential is called *tertiary recycling*.† The concept is to use chemical or thermal treatment to transform waste plastics into their monomers that can be used in the polymerization of virgin resins. Condensation polymers such as polyesters, nylons, and polyurethanes can be depolymerized by chemical processes such as glycolysis, methanolysis, and hydrolysis. Addition polymers, such as polyolefins, acrylics, and fluoroplastics, require thermal or catalytic cracking. In the United States, tertiary recycling has focused primarily on PET. Waste polyester resin collected from bottles, fibers, and film is heated with methanol and a catalyst under pressure to cause the depolymerization of PET into its monomers ethylene glycol and dimethyl terephthalate (DMT). DMT can be used as a replacement for *p*-xylene in the synthesis of PET (for details of the commercial production of PET, see Chapter 8). In Europe, attention has been directed toward an acid-catalyzed process that can convert nylon-6 recovered from worn carpets into caprolactam at 536° to 752°F.

The recycling of tires is another major issue for which solutions are needed. In the United States alone, over 234 million tires are discarded annually. The majority of this volume is eventually sent to landfills, but as properly-designed landfill sites become scarce, alternative solutions must be sought. One approach is to extend the service life of tires (source reduction). Recycling of tires includes use of retreads and grinding into crumb for use in pads, mats, carpet backing, moisture barriers, rubber-modified asphalt, and sport tracks. Whole scraped tires can be used in a variety of nontransportation applications, such as erosion control, playgrounds, and artificial reefs. Recently, a process has been developed to use the significant energy content of scrap tires (up to 15,000 Btu per lb) to generate electricity and produce synthesis gas (H_2 and CO) for ammonia and methanol production. In this process, the tires are first mixed with waste oil such as used motor oil at 700°F in a liquefaction reactor. A rotating screw is used to remove steel belts from the melt. During

† "Primary" recycling refers to regrind, while "secondary" recycling is the process of physical or thermal reprocessing into a secondary product.

liquefaction, high-molecular-weight chains, as well as disulfide bridges formed during the vulcanization process, are broken and a liquid hydrocarbon mixture is produced. The liquid mixture is mixed with oxygen (gasification reactor) at 2500°F and 500 to 900 psia to produce synthesis gas and leave an inert slag.

Although the volume of plastics that are recycled is rapidly increasing each year, only less than 3% of all plastics are now recycled, compared to about 20% of glass, 29% of paper, 16% of steel, and 39% of aluminum. Part of the reason for this low recycling rate is that the total cost of producing recycled plastics, including collecting and recycling is typically 20% higher than for the virgin resins. In addition, thermosets, cannot be recycled, account for nearly 11% of the total volume of plastics; however, it has been possible in some cases to granulate glass-reinforced thermosets into 2- or 3-cm particles for use as fillers in other fiber-reinforced composites.

6.2.2 Incineration

Many plastics can be burned as cleanly as natural gas to produce emissions of carbon dioxide, nitrogen oxides, and water vapor. As a pound of plastic produces 16,000 Btu when burned, more than twice the energy in a pound of coal, incineration can be used to generate energy, but not without serious attention to health issues. For example, some significant amounts of toxic compounds such as cadmium and other heavy metals will remain in the incinerator ash or can produce toxic emissions during combustion. Another problem is that the incineration of PVC, a significant component of many plastic wastes, can produces carcinogenic dioxins unless burned at very high temperatures.

6.2.3 Biodegradation

Biodegradable Polymers. Virtually no plastic is totally biodegradable. In fact, most polymers, including polyamides, polyfluorocarbons, polyethylene, polypropylene, and polycarbonate, are highly resistant to microbial attack. Among synthetic polymers, polyurethanes, especially polyether–polyurethanes, are susceptible to biological degradation. In general, naturally occurring polymers are more biodegradable than synthetic polymers. More specifically, polymers containing an ester functionality, particularly aliphatic polyesters, are potentially biodegradable. It is believed that biodegradation of these polymers proceeds by attack of the ester groups by nonspecific esterases produced by ground microflora combined with hydrolytic attack. Products of the degradation can be quickly metabolized by microorganisms.

One commercially important group of biodegradable polymers is the naturally occurring polyesters,[3] the poly(β-hydroxyalkanoates), whose general structure is

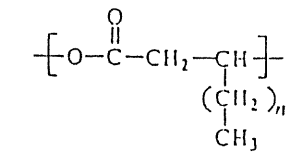

Due to their biodegradability, polyhydroxyalkanoates have commercial potential as biomaterials as well as disposable plastic packaging materials.

Originally identified in 1925, poly(β-hydroxybutyrate) (PHB), $n = 0$, is synthesized by the bacterium *Alcaligenes eutrophus*, which uses globules of PHB as an energy-storage medium analogous to fat in animals or starch in plants. The polymer is accumulated in discrete membrane-bound granules in the cytoplasm of the bacterium. PHB is a brittle polymer that is 100% isotactic and, therefore, highly crystalline (65% to 85%). The glass-transition temperature of PHB is 5° to 10°C while the crystalline-melting temperature is 175°C, which is close to its thermal decomposition temperature of 200°C. Poly(β-hydroxyalkanoates) with longer *n*-alkyl groups, such as poly(β-hydroxyvalerate) (PHV), $n = 1$, can be produced by *A. eutrophus* as well as another bacterium, *P. oleovorans*, depending upon the type of carbon substrates available during the fermentation process.

As shown by data given in Table 6.4, the principal difference in mechanical properties between PHB and the commodity thermoplastic, polypropylene, is the low extension-to-break of PHB. The toughness of PHB can be improved and its T_m lowered with respect to its low thermal decomposition temperature by copolymerization with hydroxyvalerate. This copolymer is produced by *A. eutrophus* when grown in the presence of glucose and either propionic acid or valeric acid. Recently commercialized on a small scale, HB–HV copolymers are totally degradable by soil organisms in landfills or when composted with sewage to yield only carbon dioxide and water. At the moment, this plastic is expensive and may be not suitable for all applications, such as those that require long shelf life and for food-packaging applications where the propensity of PHB for bacterial growth is an obvious problem. One recent commercial use for PHB has been in the manufacture of shampoo bottles. HB–HV copolymers are suitable as matrices for controlled release of drugs due to their favorable biocompatibility and biodegradation properties. The relatively high cost of these biodegradable polymers may be reduced in the future by larger-scale production and advances in biotechnology. For example, the gene that synthesizes PHB has been recently identified, and it should, therefore, be possible to produce these polyesters in higher-productivity bacteria such as *E. coli* or even crop plants such as potatoes or turnips, which would then make PHB instead of starch.

Another important biodegradable polyester is poly(lactic acid) (PLA)

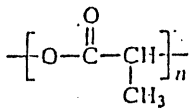

which is polymerized through the self-condensation of lactic acid, which can be produced by the fermentation of potato waste. Since PLA breaks down in the environment back to lactic acid, which can be metabolized, it has found commercial use primarily in medical applications such as sutures, drug-delivery systems, and wound clips. It may also have some agricultural applications, such as timed-release coatings for fertilizers and pesticides and mulch films for moisture and heat retention and to reduce the weed population between rows of crops. Although PLA is relatively expensive compared with most commodity thermoplastics, recent research has shown that the monomer, lactic acid, can be produced from bacterially fermented starch obtained from food wastes such as potato peelings.

TABLE 6.4 TYPICAL PROPERTIES OF POLYHYDROXYBUTYRATE (PHB) COMPARED TO POLYPROPYLENE (PP)

Property	PHB	PP
T_g (°C)	15	-10
T_m (°C)	175	176
Crystallinity (%)	80	70
Density (g cm^{-1})	1.25	0.905
Flexural modulus (GPa)	4.0	1.7
Tensile strength (MPa)	40	38
Extension-to-break (%)	6	400
UV resistance	good	poor
Solvent resistance	poor	good

Other synthetic polymers that can be biodegraded (often with help by adaptation of specific microorganisms or addition of agents to promote chemical degradation) include the polyester polycaprolactone (PCL)

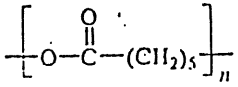

poly(vinyl alcohol)

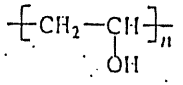

and cellulose and cellulose derivatives (see Section 8.2.2).

Starch Additives. Another approach to biodegradability is to blend or graft a commercial thermoplastic with a naturally degradable material such as starch.[4] For example, starch can be blended with polyethylene during the blow-molding of film for plastic bags. The expectation is that the starch will be eaten by soil microorganisms in a landfill and, therefore, the plastic matrix will be broken down into smaller particles. Starch obtained from corn is a glucose-based biopolymer consisting of linear amylose and highly branched, high-molecular-weight amylopectin. Advantages of starch are that it is inexpensive (ca. $0.10 per lb) and totally biodegradable. Cornstarch granules retain about 6% to 20% moisture but are thermally stable up to 250°C in air. Extruded starch has a tensile strength of 20 to 30 MPa at 10% to 15% elongation. Acrylic and vinyl monomers, such as acrylic acid and styrene, can be grafted onto starch by ceric ion, Ce(IV), initiation.

One problem with this approach is that starch-filled plastics are weak and, therefore, more petroleum-based material may be required to provide adequate strength for such consumer products as grocery bags. Since disposable diapers and trash bags made from blended plastic may contain as little as 5% of starch, the net result could be to introduce more plastic into the environment.

Biodegradation as a Practical Issue. Although biodegradation may have significant potential to alleviate some of the problems associated with plastic waste disposal, there remains some controversy as to whether any significant biodegradation will actually occur in modern, well-designed landfills. In order to store potentially hazardous materials, landfills are built to be free of moisture and airtight. These anaerobic conditions which serve to guard against the release of hazardous chemicals from landfills, also retard biodegradation. Another problem concerns the compatibility of the two major approaches to plastic waste management — biodegradation and recycling — since biodegradable polymers are not suitable candidates in the recycling of commingled plastics.

References

1. G. A. Bernier and R. P. Kambour, *Macromolecules*, 1, 393 (1968).
2. R. P. Kambour, E. E. Romagosa, and C. L. Gruner, *Macromolecules*, 5, 335 (1972).
3. R. W. Lenz, Y. B. Kim, and R. C. Fuller, *J. Bioactive Compatible Polym.*, 6, 382 (1991).
4. Y. Inoue and N. Yoshie, *Prog. Polym. Sci.*, 17, 571 (1992).

Bibliography

A. L. Andrady, "Assessment of Environmental Biodegradation of Synthetic Polymers," *J. Macromol. Sci. — Rev. Macromol. Chem. Phys.*, C34, 25–76 (1994).

R. W. Lenz, "Biodegradable Polymers," *Adv. Polym. Sci.*, 107, 1–40 (1993).

M. M. Nir, J. Miltz, and A. Rain, "Update on Plastics and the Environment: Progress and Trends," *Plast. Eng.*, March 1993, pp. 75–93.

B. Rånby, "Basic Reactions in the Photodegradation of Some Important Polymers," *J. Macromol. Sci. — Pure Appl. Chem.*, A30, 583–594 (1993).

C. L. Swanson, R. L. Shogren, G. F. Fanta, and S. H. Imam, "Starch—Plastic Materials — Preparation, Physical Properties, and Biodegradability (A Review of Recent USDA Research)," *J. Environ. Polym. Degrad.*, 1, 155–166 (1993).

7

Polymer Additives, Blends, and Composites

Typically, commercial plastics are mixtures of one or more polymers along with a variety of *additives* such as plasticizers, flame retardants, processing lubricants, stabilizers, and fillers. The exact formulation will depend upon the specific application or processing requirement. For example, poly(vinyl chloride) (PVC) is a thermally unstable polymer (see Section 6.1.1) having high modulus, or stiffness, typical of other glassy polymers at room temperature. In order to obtain a flexible-grade resin of PVC for use as packaging film or for wire insulation, the polymer must be blended with a plasticizer to reduce its T_g and with a small amount of an additive to improve its thermal stability at processing temperatures.

In many cases, certain properties of a polymer can be enhanced by blending it with another polymer. For example, the engineering thermoplastic, poly(2,6-dimethyl-1,4-phenylene oxide) (PPO®), is a high-T_g polymer that is difficult to process because of its susceptibility to thermal oxidation at high temperatures. Commercial resins of this polymer (Noryl®) are blends of PPO and high-impact polystyrene (HIPS) and may also include different additives, such as lubricants, thermal stabilizers, flame retardants, or fillers. Since the T_g of PS (ca. 100°C) is lower than that of PPO (ca. 214°C), the overall T_g of the PPO/HIPS blend is lower than that of PPO alone and, therefore, the resin can be melt processed at reduced temperatures where the oxidative instability of PPO is not a problem. The incorporation of HIPS also reduces the cost of this engineering resin and improves the impact strength of the blend.

Polymeric composites are physical mixtures of a polymer (the matrix) and a reinforcing filler (the dispersed phase) that serves to improve some mechanical property such as modulus or abrasion resistance. Fillers may be inorganic (e.g., calcium carbonate) or organic (graphite fiber or an aromatic polyamide such as Kevlar®). Virtually any material can be used as the composite matrix, including ceramic, carbon, and polymeric materials. Typically, matrices for polymeric composites are thermosets such as epoxy or (unsaturated) polyester resin; however, some engineering thermoplastics with high T_g and good impact strength, such as thermoplastic polysulfones, have been used for composites. Principal applications for composites are in construction and transportation.

TABLE 7.1 THE U.S. MARKET FOR ADDITIVES[a]

Additive	Millions of lb	%
Fillers	5,750	56.2
Plasticizers	1,770	17.3
Reinforcements	925	9.0
Flame retardants	690	6.7
Colorants	507	5.0
Impact modifiers	140	1.4
Others	448	4.4
Total	10,230	100

[a] 1991 statistics (*Chemical and Engineering News*, August 31, 1992).

7.1 ADDITIVES

Additives are widely used for thermoplastics, thermosets, and elastomers. Examples of common additives include plasticizers, thermal and light stabilizers, flame-retardant agents, fillers, colorants, processing aids, impact modifiers, and biocides. As shown by the data given in Table 7.1, the largest markets for additives are for fillers and plasticizers which are described in the following sections. These may be mixed with the polymer before processing by a variety of techniques, such as dry blending, extrusion, compounding, and other methods discussed in Chapter 11.

7.1.1 Plasticizers

Plasticizers, particularly for PVC, constitute one of the largest segments of the additives market. The principal function of a plasticizer is to reduce the modulus of a polymer at the use temperature by lowering its T_g. The effect of a plasticizer on modulus is illustrated by Figure 7.1. As shown, increasing the concentration of the plasticizer causes the transition from the high-modulus (glassy) plateau region to the low-modulus (rubbery) plateau region to occur at progressively lower temperatures. In addition, the transition of the plasticized polymer occurs over a wider range of temperatures than for the unplasticized polymer. Typically, plasticizers are low-molecular-weight organic compounds having a T_g in the vicinity of -50°C. In some cases, a miscible high-molecular-weight polymer having a low T_g (e.g., polycaprolactone or copolymers of ethylene and vinyl acetate) can be used as a plasticizer.

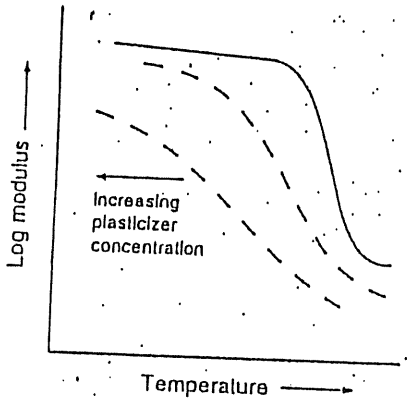

Figure 7.1. Effect of increasing plasticizer concentration on the modulus–temperature plot.

Requirements for an effective plasticizer include partial or complete miscibility with the host polymer and a low T_g. The T_g of the plasticized polymer depends upon the plasticizer concentration and the T_g of each component as estimated by a number of theoretical or empirical equations, such as the Kelley–Bueche equation and others given in Section 4.3.4. Another commonly used relationship first proposed by Wood[1] to predict the T_g of random copolymers has been used to predict the T_g of plasticized polymers. The *Wood equation* has the form

$$T_g = \frac{T_{g,1} + (kT_{g,2} - T_{g,1})W_2}{1 - (1-k)W_2} \tag{7.1}$$

In this equation, k is considered to be an adjustable parameter and W_i is the weight fraction of component i (where component 1 usually designates the diluent).

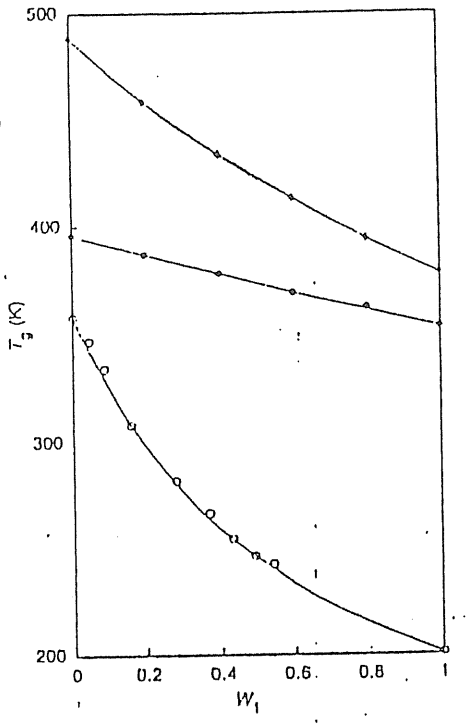

Figure 7.2. DSC-determined values of the glass-transition temperature (T_g) of two polymer blends and plasticized PVC as a function of the weight fraction (W_1) of the low-T_g component (component 1).[2] Data include: (♦) poly(2,6-dimethyl-1,4-phenylene oxide)/polystyrene (1); (●) poly(vinyl chloride)/α-methylstyrene–acrylonitrile–styrene (66/31/3) terpolymer (1); (○) poly(vinyl chloride)/tris-(2-ethylhexyl)trimellitate (TOTM) plasticizer (1). Solid curves represent T_g values predicted by eq. 7.2.

A very convenient equation relating T_g to the composition of a polymer mixture from known parameters (composition and individual polymer T_g) was given in Chapter 4 (eq 4.33) as

$$\ln\left(\frac{T_g}{T_{g,1}}\right) = \frac{W_2 \ln\left(T_{g,2}/T_{g,1}\right)}{W_1\left(T_{g,2}/T_{g,1}\right) + W_2} \tag{7.2}$$

Equation 7.2 has been shown to be useful for a wide variety of polymer mixtures, including polymer blends, for which the T_g of both components are roughly compa-

rable, and plasticized polymers such as PVC, for which the T_g's of the polymer a plasticizer are widely apart. Comparisons between experimental and predicted values are shown for two polymer blends and plasticized PVC in Figure 7.2.

TABLE 7.2 COMMON PLASTICIZERS FOR PVC

Plasticizer Class	Chemical Structure	Examples[a]
Dialkyl phthalate	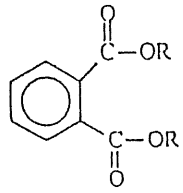	DOP, DIOP
Aliphatic diester	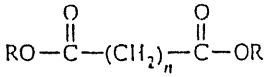	DOA
Trialkyl phosphate	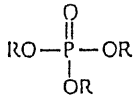	TCP
Trialkyl trimellitate	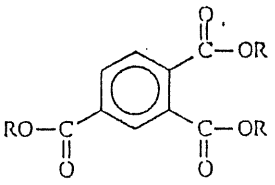	TOTM

[a] Common names for plasticizers: DOP, dioctyl phthalate; DIOP, diisooctyl phthalate; DOA, dioctyl adipate; TCP, tricresyl phosphate; and TOTM, trioctyl trimellitate.

In the case of plasticization, the actual reduction in polymer T_g per uni weight of plasticizer is called the plasticizer *efficiency*. High efficiency indicate that the plasticizer causes the glassy-to-rubbery transition to occur over a very broac temperature range. The problem with high-efficiency plasticizers is that they can diffuse out of the polymer in time due to their low miscibility with the polymer Plasticizers that are susceptible to migration are said to have low *permanence*. Los of plasticizer will lead to a gradual increase in brittleness as the T_g (and, therefore

s modulus) of the plasticized polymer slowly increases to that of the unplasticized e., glassy) polymer. An example of a high-permanence (i.e., low efficiency) asticizer for PVC is tris(2-ethylhexyl)trimellitate or sometimes called trioctyl mellitate (TOTM) (see Table 7.2); T_g data for PVC plasticized with TOTM are otted in Figure 7.2.

When T_g reduction is obtained by compounding a polymer with a low-T_g mpound, the process is called *external plasticization*. In some cases, plasticizer nction can be obtained by copolymerizing the polymer with the monomer of a w-T_g polymer, such as poly(vinyl acetate). This process is called *internal* plasti-zation.

Typical external plasticizers for PVC include the esters of common organic ids such as dialkyl phthalates — examples include diisooctyl phthalate (DIOP) d di-2-ethylhexyl phthalate or dioctyl phthalate (DOP)

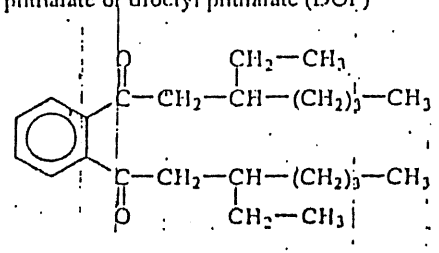

hich has been a widely-used high-efficiency plasticizer for PVC. Other PVC plas-izers include epoxides, such as epoxidized soybean oil; aliphatic diesters, such as -2-ethylhexyl adipate or dioctyl adipate (DOA); phosphates, such as tricresyl iosphate (TCP); and trialkyl trimellitates, such as tris-(2-ethylhexyl trimellitate) trioctyl trimellitate (TOTM). General structures for these classes of PVC plasti-zers are shown in Table 7.2. Examples of polymeric plasticizers include poly-prolactone (PCL)

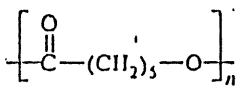

hich has a T_g of -60°C and copolymers (and terpolymers) of ethylene with vinyl etate, carbon monoxide, and sulfur dioxide. Polymeric plasticizers provide high ermanence at the expense of low-temperature flexibility due to their higher T_g and w efficiency.

It has been observed that at low concentrations of plasticizer (e.g., 5% to 0%), modulus and tensile strength may sometimes be greater than that of the un-lasticized polymer, while impact strength and permeability to gases and liquids ay be lower. This behavior is opposite to that usually associated with plasticiza-on and is, therefore, known as *antiplasticization*. If the plasticizer concentration is ncreased to above the antiplasticization range, the modulus and tensile strength will begin to fall, while impact strength and permeability will increase (i.e., plasticization begins).

7.1.2 Fillers and Reinforcements

Fillers for thermoplastics and thermosets may be inert materials that serve to reduce resin cost and (to a lesser extent) improve processability or dissipate heat in exothermic thermosetting reactions. Examples of such fillers include wood flour, clay, talc, fly ash, sand, mica, and glass beads. Mica can also be used to modify the polymer's electrical- and heat-insulating properties. Other particulate fillers may be used to reduce mold shrinkage or to minimize electrostatic charging. These include graphite, carbon black, aluminum flakes, and metal and metal-coated fibers. For example, high loading of carbon fibers can provide electromagnetic interference (EMI) shielding for computer applications.

Reinforcing fillers are used to improve some mechanical property or properties, such as modulus, tensile or tear strength, abrasion resistance, and fatigue strength. For example, particulate fillers such as carbon black or silica are widely used to improve the strength and abrasion resistance of commercial elastomers. Fibers in the form of continuous strands, woven fabrics, and chopped (or discontinuous) fibers are used to reinforce thermoplastics and thermosets.

The typical fiber content of a polymer composite may range from 20% to 80% of the total weight. The most common form of fiber fillers is E-glass, typically used to reinforce thermosets, such as (unsaturated) polyester and epoxy resins. E-glass is a boroaluminosilicate glass having low alkali-metal content and containing small percentages of calcia (CaO) and magnesia (MgO). For special applications, such as in the manufacture of aerospace materials, fibers of boron, Kevlar® (aramid, aromatic polyamide), and especially carbon or graphite, are preferred. Carbon and graphite fibers are obtained by the pyrolysis of organic materials such as polyacrylonitrile (PAN), rayon, or pitch. The highest mechanical properties are obtained by orienting the fibers at temperatures as high as 3000°C (graphite fibers). At the expense of higher cost and increased brittleness, these specialized fibers provide higher composite strength and modulus than obtained by glass-reinforced composites. Recently, there has been interest in using ultrahigh-molecular-weight polyethylene (see Chapter 10), having strength equal to aramid fiber, as a fiber reinforcement for epoxy and other matrices.

In addition to improvement in mechanical properties, composites may also offer weight reduction and improved conductivity, such as provided by carbon or graphite fibers. Properties of typical fiber materials are given in Table 7.3. For highly demanding applications, microfibers or whiskers (synthetically-grown single crystals) of alumina or silicon carbide may be used. Whiskers can have tensile strengths as high as 27.6 GPa (4 million psi) and moduli as high as 690 GPa (100 million psi).

TABLE 7.3 PROPERTIES OF FIBERS USED IN COMPOSITE APPLICATIONS

Fiber	Tensile Modulus GPa[a]	Tensile Strength GPa[a]	Density g cm^{-3}
Boron	386	3.4–3.7	2.38–2.66
Graphite			
high-modulus	483–517	1.86	1.97
high-strength	234–255	2.83	1.77
Kevlar-49	138	2.76	1.44
E-glass	72.4	3.45	2.55
S-glass	85.5	4.83	2.49
Steel	407	4.14	7.81

[a] To convert GPa to psi, multiply by 145,000.

7.1.3 Other Important Additives

In addition to plasticizers and fillers, the other important additives found in commercial plastics include thermal stabilizers, antioxidants, and UV-stabilizers to protect sensitive polymers against degradation due to processing temperatures and environment attack. Other additives are used to improve fire resistance, to meet certain processing requirements (lubricants, curing and blowing agents, and catalysts for polymers prepared by reaction injection-molding), to improve impact strength, to protect against exposure to bacteria and fungi, and to impart color. The specific formulation of a plastics resin is finely tailored to the end use of the resin. Formulations of plastic resins are usually given on the basis of parts per 100 unit weight of resin (phr), where the resin refers to the base polymer in the composition. The methods of action and some examples of these important additives are described in the following sections.

As an important example of the use of plastics additives is PVC resin designed for potable-water pipe. As shown by the data given in Table 7.4, PVC resin designed for this particular application can include eight or more different additives. All the components are blended using a dry blending technique in a specially designed mixer and then continuously extruded through an annular die. For the representative formulation given in Table 7.4, an acrylic-type processing aid may be used to provide a smooth extrudate, while calcium stearate and paraffin wax are present as lubricants. Since it is necessary to provide rigidity for pipe applications, no

plasticizers are used in this formulation. Ultrafine calcium carbonate is used as a reinforcing filler to provide high burst resistance. The choice of a thermal stabilizer depends upon consideration of toxicity levels since it is possible that plasticizer can diffuse out of the pipe into the water supply. For PVC pipe applications, alkyltin or antimony mercaptides are widely used stabilizers in the United States.

TABLE 7.4 TYPICAL FORMULATION OF A PVC RESIN FOR POTABLE-WATER PIPE EXTRUSION

Component	Concentration (phr)
PVC (0.9 to 1.0 IV[a])	100
Processing aids	1–5
Impact modifier	0–10
Calcium carbonate	0–10
Alkyltin or antimony mercaptide	0.3–2.0
Calcium stearate	0.5–1.5
Paraffin wax	0.5–1
Pigment	1–2

[a] Inherent viscosity.

Stabilizers. Short-term stabilizers are those that are used to protect a polymer against the effects of temperature and oxygen during processing. These are typically low-molecular-weight compounds, such as hindered phenols and aromatic amines, which have high diffusivity in the polymer melt and serve as free-radical scavengers. Other antioxidants include those that serve to suppress homolytic breakdown such as organic phosphites. An example of an antioxidant that serves as a free-radical scavenger is 4-methyl-2,6-di-*tert*-butylphenol, which is used to inhibit the thermal oxidation of natural rubber. It functions by terminating free-radical sites formed as a result of thermal oxidation (see Section 6.1.1) by two routes: (1) abstraction of its hydroxyl hydrogen

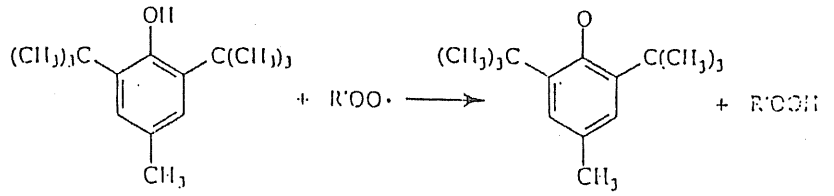

4-methyl-2,6-*tert*-butylphenol

or (2) addition to the *para*-position of the aromatic ring:

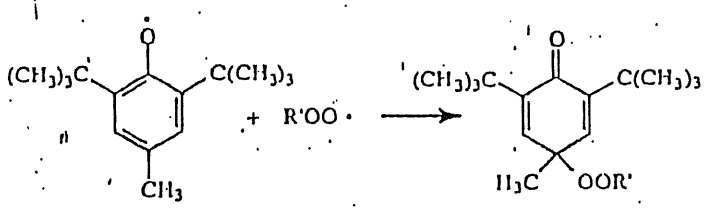

Many polymers will absorb UV radiation in the wavelength from 290 to 400 nm. This absorbed energy can break bonds and initiate free-radical chain reactions that can lead to discoloration, embrittlement, and eventual degradation. UV stabilizers act to either absorb UV radiation or to deactivate free radicals and hydroperoxides as they are formed. As an example, carbon black, widely used in tire manufacture, provides good absorption in the UV range, as well as providing abrasion resistance and serving as a low-cost filler (see Section 9.1). Transparent thermoplastics like polycarbonate can be protected against yellowing and embrittlement from UV irradiation (photolysis) by incorporating compounds like benzophenone derivatives, such as *o*-hydroxybenzophenone:

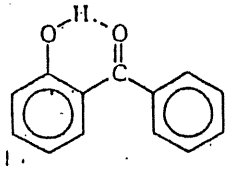

These benzophenones have a high extinction coefficient in the UV range and are able to convert absorbed radiation to heat without chemical change. Benzotriazoles, such as 2-(*o*-hydroxyphenyl)benzotriazole,

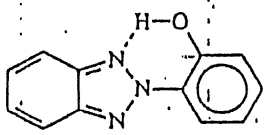

are also widely used as UV absorbers.

Flame Retardants. When subjected to a sufficient heat flux for a sufficiently long time, all organic polymers will thermally degrade. Minimum radiant fluxes vary from about 16 to 34 kilowatts (kW) m^{-2} for polyurethane foam to 43 kW m^{-2} for polytetrafluoroethylene. In the absence of oxygen, thermal degradation is called *pyrolysis*. In the presence of oxygen, thermal degradation is called oxidative pyrolysis or thermal-oxidative degradation.

Flame retardants are added to alter the combustion process in some way. Strategies for effective flame retardants include the following:

1. Inhibition of the vapor-phase combustion of the fuel gases
2. Alteration of the thermal-degradation pathway by providing a low-energy process that promotes solid-state reactions leading to carbonization
3. Formation of a protective coating to insulate against thermal energy

Classes of flame retardants include organochlorine compounds, organobromine compounds, organophosphorus, antimony oxides, boron compounds, and especially alumina trihydrate (ATH).

Biocides. In general, polyolefins and vinyl polymers are particularly resistant to bacterial attack (see Section 6.2.3) while natural rubber, cellulose and cellulose derivatives, and some polyesters are susceptible to microbial attack. A *biocide* is a chemical that controls or destroys bacterial growth. Alternative terminology includes bactericides, bacteristats, mildecides, fungicides, fungistats, germicides, and algicides. Important applications for biocides include latex paints and textiles. The ideal biocide is one that is toxic to the targeted microorganism but otherwise safe to humans and other animal life. For food packaging applications, biocides must be approved by the Federal Food Administration in the United States. All biocides must be registered by the Environmental Protection Agency for use in the United States. Examples of industrial biocides include tributyltin oxide used in latex paints, textiles, and plastics and 10,10'-oxybisphenoxyarsine (OBPA) used in vinyl and urethane–polyolefin formulations.

Processing Additives. Lubricants are added to improve flow during processing by reducing melt viscosity (internal lubricants) or by reducing adhesion between metallic surfaces of the processing equipment and the polymer melt (external lubricants). Principal categories of lubricants include amides, esters, metallic stearates, waxes, and acids. The major market for processing lubricants is PVC, for which stearates are often used. Other lubricants include mineral oil and low-molecular-weight polyolefins. Organofunctional silicone fluids may be used as internal mold-release agents for reaction injection-molding (RIM) of polyurethane (see Section 11.1.2).

Curing Agents. The term *curing* typically refers to the process of applying heat (and pressure) to change the properties of rubber or thermosetting resins. In the curing process, various additives (i.e., curing agents), including a number of sulfur-containing compounds, are used to promote the crosslinking of rubber (i.e., vulcanization) or the formation of a thermoset network (e.g., amines in the cure of epoxies). The process of network formation is discussed in detail in Chapter 9.

Colorants. Plastics can be colored by adding soluble dyes and inorganic and organic pigments that are dispersed in the plastic during processing. In the coloring of thermosets, dye dissolution or pigment dispersion must be completed before the thermoset is fully formed. Classes of dyes that are used for plastics include azo compounds, anthraquinones, xanthenes, and azines. Among the most important inorganic pigments are iron oxides, cadmium, chrome yellow, and especially titanium dioxide (white).

Heat-Distortion and Impact Modifiers. Blends of one polymer with another having greater or lower T_g can be used to modify the T_g or heat-distortion temperature (HDT) of another polymer, as described in Section 7.2.1. Impact modifiers normally include high-impact polystyrene (HIPS), chlorinated polyethylene (CPE), and a variety of copolymers and terpolymers, such as SAN (styrene–acrylonitrile), ABS (acrylonitrile–butadiene–styrene), EVA (ethylene–vinyl acetate), MBS (methyl methacrylate–butadiene–styrene), and MABS (methyl methacrylate–acrylonitrile–butadiene–styrene). The mechanism of toughening is discussed in Section 7.2.1.

Antistatic Agents. Since most polymers are poor electrical conductors (see Section 12.3.1), static electrical charges can form on the surface of plastics. Such static charge buildup can present problems such as dust collection and sparking. Fortunately, hygroscopic additives called *antistats* are effective for dissipating static electrical charges. Antistats belong to either of two categories — external or internal. External, or topical, antistats are applied by spraying, wiping, or dipping the plastic surface, while internal antistats are compounded with the plastic during processing. In the case of internal antistats, the additive diffuses to the surface of the plastic where the hygroscopic additive absorbs moisture and, thereby, provides a conductive layer of water. Examples of antistatic agents include phosphate and fatty acid esters, polyhydric alcohol derivatives, sulfated waxes, ethoxylated and propoxylated aliphatics and aromatics, and especially quaternary ammonium compounds and amines.

Blowing Agents. Many plastics, such as polystyrene (expanded polystyrene) and polyurethanes, are foamed to provide insulating properties (rigid foam) or flexible products (flexible foam) for seat cushions and other applications. Gas production is achieved by adding a gas-producing compound called a *blowing agent* (or foaming agent). *Physical* blowing agents include volatile liquids such as short-chain hydrocarbons (e.g., pentanes, hexanes, and heptanes) and fluorocarbons (e.g., trichloromethane, tetrachloromethane, and trichlorofluoromethane) and gases such as nitrogen, carbon dioxide, and air that are added during processing. Volatilization results in the formation of a cellular structure through a phase change as the gas dissolved in the polymer at high pressure at processing conditions desorbs during depressurization. *Chemical* blowing agents (CBA) such as hydrazine derivatives are solid additives that generate gases when decomposed at processing temperatures. Unsaturated polyester is foamed by the use of a CBA. In some cases, gas production may occur by chemical reaction of the CBA with another component of the polymer system. Concern over emission of volatile organic compounds (VOCs), especially chlorohydrocarbons, during processing has encouraged the development of safer alternatives to many of the physical blowing agents now used.

In the case of polyurethanes, flexible foams are produced by the production of carbon dioxide from the reaction of an isocyanate and water:

$$R{-}N{=}C{=}O + H_2O \longrightarrow RNH_2 + CO_2$$

When the isocyanate is in excess, the resulting amine can react with another molecule of isocyanate to form a urea of the following structure:

$$R'{-}N{=}C{=}O + RNH_2 \longrightarrow R'{-}NH{-}\overset{\displaystyle O}{\overset{\|}{C}}{-}NH{-}R$$

Rigid foams are produced by a physical blowing agent, such as trichlorofluoromethane (refrigerant 11). *Expandable polystyrene* used for disposable drinking cups, cushioned packaging, and thermal insulation is foamed by using a physical blowing agent, usually pentane.

Compatibilizers. As discussed in the following sections, many polymers are immiscible and, therefore, phase separate during processing. The mechanical properties of these immiscible blends are often poor due to inadequate interfacial strength between the dispersed phase and matrix. A variety of additives can be used to promote miscibility by reducing interfacial tension. Reactive compatibilizers chemically react with blend components and are, therefore, effective for many blend compositions. Nonreactive compatibilizers are typically block or graft copolymers of the blend homopolymers and are more specific in their action.

7.2 POLYMER BLENDS AND INTERPENETRATING NETWORKS

7.2.1 Polymer Blends

The blending of two or more polymers has become an increasingly important technique for improving the cost–performance ratio of commercial plastics. For example, blending may be used to reduce the cost of an expensive engineering thermoplastic, to improve the processability of a high-temperature or heat-sensitive thermoplastic, or to improve impact resistant. Commercial blends may be homogeneous, phase separated, or a bit of both.

Thermodynamics. Whether a particular polymer blend will be homogeneous or phase separated will depend upon many factors, such as the kinetics of the mixing process, the processing temperature, and the presence of solvent or other additives; however, the primary consideration for determining miscibility of two polymers is a thermodynamic issue that is governed by the same (Gibbs) free-energy considerations that were discussed in Chapter 3 for polymer–solvent mixtures. The relationship between the change in Gibbs free energy due to mixing (ΔG_m) and the enthalpy (ΔH_m) and entropy (ΔS_m) of mixing for a reversible system was given as

$$\Delta G_m = \Delta H_m - T\Delta S_m. \tag{7.3}$$

If ΔG_m is positive over the entire composition range at a given temperature, the two polymers in the blend will separate into phases that are pure in either component providing that a state of thermodynamic equilibrium has been reached. For complete miscibility, two conditions are necessary: ΔG_m must be negative and the second derivative of ΔG_m with respect to the volume fraction of component 2 (ϕ_2) must be greater than zero

$$\left(\frac{\partial^2 \Delta G_m}{\partial \phi_2^{\,2}}\right)_{T,P} > 0, \tag{7.4}$$

over the whole composition range.

If $\Delta G_m < 0$, but eq. 7.4 is not satisfied (i.e., the appearance of local minima in the free-energy curve as shown in Figure 3.9), the blend will separate at equilibrium into two mixed-composition phases. This means that each phase (i.e., the dispersed and continuous phase) will contain some of each polymer. At a given temperature, equilibrium concentrations are given as a pair of isothermal points along the binodal ($\mu_i^{\alpha} = \mu_i^{\beta}$), which is illustrated for a representative phase diagram in Figure 7.3.

In general, polymer blends can exhibit a wide range of phase behavior, including upper and lower critical solution temperatures (see Section 3.2.4), as illustrated by the liquid–liquid phase diagram given in Figure 7.3. At temperature T_1, which is below the upper critical solution temperature (UCST) for phase separation located at T_2, the equilibrium mixture will separate into two phases whose compositions lie in opposite sides of the binodal at T_1. The *binodal* separates the stable (single phase) from the metastable state, while the *spinodal* marks the transition from the unstable to metastable region. At T_3, which is above the UCST but below the lower critical solution temperature (LCST) located at T_4, the blend is miscible at all compositions. Above the LCST (e.g., at T_5), two phases again coexist with compositions given by the upper binodal.

For polymer blends in the solid state, recent studies have shown that LCST behavior is quite common and needs to be considered during melt processing when

elevated temperatures can cause phase separation and result in deleterious changes in the properties of the blend. An example of LCST phase behavior is a blend of polystyrene with the polycarbonate of tetramethylbisphenol-A.[3] In this case, a phase diagram was obtained by determining the temperature at which a particular blend composition first scatters light due to the incipient phase separation. Data obtained over the entire composition range are used to form a *cloud-point curve*. As shown by the data plotted Figure 7.4, the LCST (assigned to the temperature at the minimum of the cloud-point curve) occurs near 240°C for this blend. This means that if the blend is melt processed above 240°C phase separation will occur. If the blend is heated above the LCST and rapidly cooled, the two-phase morphology will be retained in the solid state. As will be discussed shortly, thermal and mechanical properties will be very different depending on whether the blend forms a homogeneous mixture or a two-phase structure.

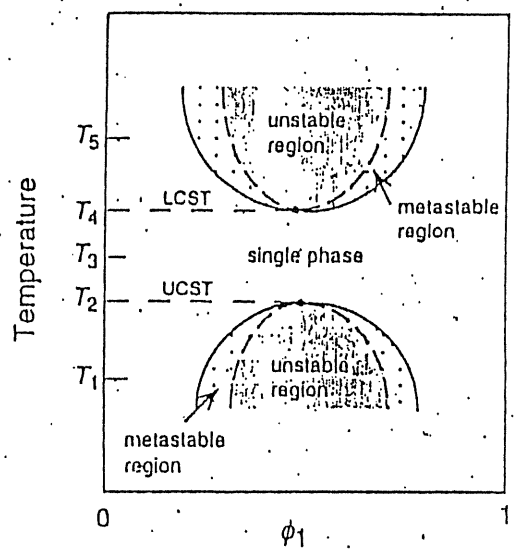

Figure 7.3. Idealized liquid–liquid phase diagram for a polymer blend. The solid curve indicates a binodal, while the broken curve represents a spinodal separating the unstable and metastable regions. The upper critical (UCST) and lower critical solution (LCST) temperatures are located at T_2 and T_4, respectively.

Compared to LCST phase behavior, UCST behavior is much more difficult to observe since an UCST may fall below the blend T_g, at which temperature all long-range (cooperative) segmental motions cease. Such chain mobility is required to achieve phase separation. For this reason, UCST behavior may be observed only

in a solution of the blend in a low-molecular-weight solvent or under other special circumstances.

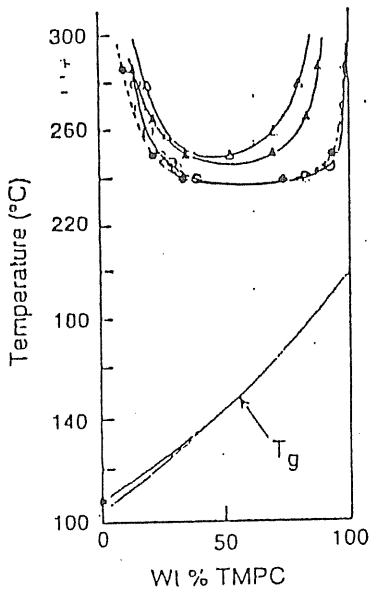

Figure 7.4. Phase behavior of blends of tetramethylbisphenol-A polycarbonate (TMPC) and polystyrene (PS). Bottom curve shows the dependence of T_g on the wt % of TMPC in the homogeneous blend below the lower critical solution temperature (LCST), which is near 240°C for high-molecular-weight PS. The top curves represent the phase diagrams (i.e., cloud-point curves) for TMPC/PS blends illustrating LCST behavior. The LCST shifts upward in temperature with decreasing PS molecular weight, and the cloud-point curve becomes skewed toward the low-molecular-weight component, TMPC ($\overline{M}_w = 41{,}000$)., In contrast, there is only a small effect of PS molecular weight on the T_g–composition curve for the homogeneous blend at temperatures below the LCST. The effect of molecular weight is seen as a divergence of the T_g–composition curve at low TMPC composition due to the small effect of molecular weight on the T_g of the PS component. Molecular weight ($\overline{M}_w$) of PS: (△), 42,000; (▲), 59,000; (○), 180,000; and (●), 320,000. (Adapted from ref. 3 with permission of the publisher.)

The bulk of experimental evidence indicates that most polymer pairs are immiscible. Immiscibility is a consequence of the very small combinatorial entropy change that results when two high-molecular-weight polymers are mixed. Scott[4] has extended the Flory–Huggins (F–H) lattice model (Section 3.2.1) to obtain an expression for ΔS_m for a polymer blend as

$$\Delta S_m = \left(\frac{RV}{V_r}\right)\left[\left(\frac{\phi_1}{x_1}\right)\ln\phi_1 + \left(\frac{\phi_2}{x_2}\right)\ln\phi_2\right] \tag{7.5}$$

where R is the ideal gas constant, V is the volume of the blend, V_r is a reference volume (often taken as the molar volume of the smallest polymer repeating unit), ϕ_i is the volume fraction of polymer 1 or 2, and x_i is the degree of polymerization of polymer 1 or 2 relative to the reference volume. The corresponding equation for the Gibbs free energy of mixing is then

$$\Delta G_m = \left(\frac{RTV}{V_r}\right)\left[\left(\frac{\phi_1}{x_1}\right)\ln\phi_1 + \left(\frac{\phi_2}{x_2}\right)\ln\phi_2 + \chi_{12}\phi_1\phi_2\right] \tag{7.6}$$

where χ_{12} is the (Flory) interaction parameter of the blend of polymers 1 and 2.

Since the degree of polymerization (x_1 and x_2 appearing in the denominators on the RHS of eq. 7.5) of high-molecular-weight polymers is large, ΔS_m is small. In order for ΔG_m (eq. 7.3) to be negative as a necessary condition of miscibility, the enthalpic contribution to mixing, ΔH_m, must be either negative or zero, or have a small positive value. This implies that blend miscibility requires favorable interactions between the two blend polymers. Examples of favorable interactions include dispersive and dipole–dipole interactions, hydrogen bonding, or charge-transfer complexation.

As discussed in Chapter 3, the Flory–Huggins theory, although providing a useful basis for discussion, fails to correctly predict all aspects of polymer-blend behavior. For example, the F–H theory does not predict LCST behavior, which has been shown to occur. Good qualitative predictions of polymer phase behavior are, however, provided through the Flory equation of state (EOS) and other EOS models. For example, the effect of polymer molecular weight on the phase behavior of a binary polymer blend is qualitatively well represented using a modified form of the Flory-EOS theory given by McMaster.[5] As shown in Figure 7.5, the LCST moves down in temperature as the molecular weight of either polymer in the blend decreases. This means that the region of miscibility increases with decreasing molecular weight, as may be expected from the favorable effect of decreasing molecular weight on increasing the combinatory entropy of the blend. Also evident is the skewness of the binodal and spinodal curves when chain lengths of the molecular weight of the two polymers considerably differ. Specifically, the critical composition moves to the left as the ratio of chain lengths r_1/r_2 decreases. Figure 7.6 shows the effect of changes in the value of the interaction parameter on the phase diagram. As shown, the LCST moves to higher temperatures and the miscibi-

bility window (the area outside the binodal) widens as the interaction energy decreases.

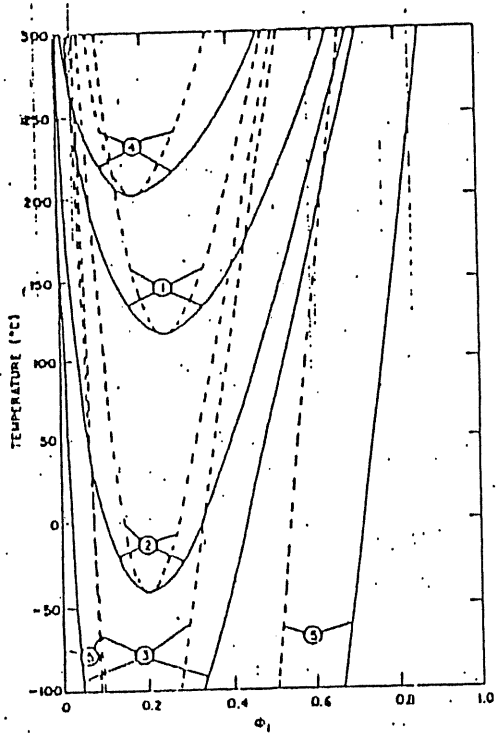

Figure 7.5. Effect of molecular weight of polymer 1 (curve 1, 30,000 molecular weight; curve 2, 50,000 molecular weight; and curve 3, 80,000 molecular weight) and polymer 2 (curve 4, 3000 molecular weight; curve 5, 6000 molecular weight) on the binodal (solid line) and spinodal (broken line) predicted by a modified version of the Flory equation-of-state theory. (Adapted with permission from ref. 5. Copyright 1977 American Chemical Society.)

Recently, there has been interest in blends containing three-component polymers. The phase behavior of these ternary blends is difficult to determine experimentally as well as difficult to theoretically predict and to visualize. One way of representing their phase behavior is through the use of the triangular diagrams familiar to chemical engineers who have studied liquid–liquid equilibrium. The experimentally determined phase diagram[6] for ternary blends of PMMA, poly(ethyl methacrylate) (PEMA), and poly(styrene-*co*-acrylonitrile) (SAN) is shown in Figure 7.7. In this example, SAN (30 wt % acrylonitrile) is compatible (miscible) with PMMA and PEMA; however, PMMA and PEMA, themselves, are immiscible. In other words, two of the three polymer pairs are immiscible. As illustrated, there is a moderately wide range of compositions (represented by the open circles lying outside the phase envelope) for which the three polymers can exist as homogeneous mixtures even though one polymer pair (PMMA/PEMA) is immiscible. In this study, evidence for phase homogeneity was deduced from detection of a single T_g (DSC measurements) for the blend.

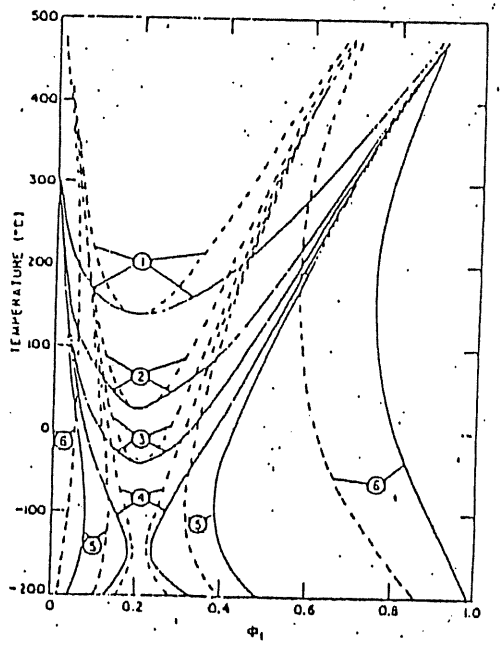

Figure 7.6. Effect of the value of the interaction energy on the binodal (solid line) and spinodal (broken line) predicted by a modified version of the Flory equation of state theory. Values of X_{12} (cal cm^{-3}): curve 1, -0.050; curve 2, -0.100; curve 3, 0; curve 4, 0.005; curve 5, 0.010; and curve 6, 0.100). (Adapted with permission from ref. 5. Copyright 1973 American Chemical Society).

Commercial Polymer Blends. Well-documented examples of miscible polymer blends are given in Table 7.5. Of these, the blends of poly(2,6-dimethyl-1,4-phenylene oxide)/PS and PVC/nitrile rubber (a copolymer of butadiene and acrylonitrile) are important commercially. Blends of poly(methyl vinyl ether)/PS and tetramethylbisphenol-A polycarbonate/PS, as mentioned earlier, have

been reported to exhibit LCST at melt temperatures and have been widely used to study polymer-blend behavior. All these blends consist of only amorphous polymers, with the exception of PVC, which has a small degree of crystallinity (see Section 8.1.2).

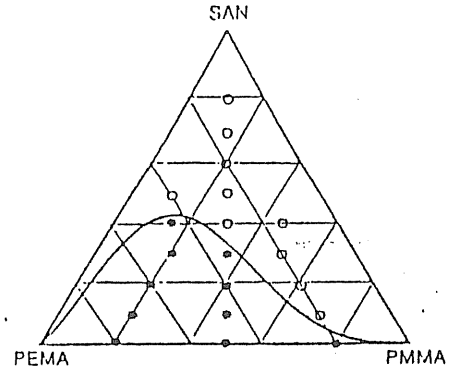

Figure 7.7. Triangular phase diagram for ternary blends of poly(methyl methacrylate) (PMMA), poly(ethyl methacrylate) (PEMA), and poly(styrene-*co*-acrylonitrile (SAN). Filled circles (●) represent blend compositions that are phase separated as indicated by the detection of multiple T_g's. Open circles (○) represent homogeneous compositions. (Adapted from ref. 6 with permission of the publisher).

TABLE 7.5 EXAMPLES OF MISCIBLE POLYMER BLENDS

Polymer 1	Polymer 2
Polystyrene	Poly(2,6-dimethyl-1,4-phenylene oxide) Poly(methyl vinyl ether) Tetramethylbisphenol-A polycarbonate
Poly(vinyl chloride)	Polycaprolactone Nitrile rubber[a]
Poly(vinylidene fluoride)	Poly(ethyl methacrylate) Poly(methyl methacrylate)

[a] For limited acrylonitrile content of the copolymer.

In the case of poly(vinylidene fluoride) (PVDF) blends, PVDF can thermally crystallize depending upon blend composition and crystallization temperature. The second (amorphous) polymer in the blend (i.e., PEMA or PMMA) serves as a diluent, which lowers the crystalline-melting temperature, T_m, of the blend. From this information, the Flory interaction parameter can be obtained as discussed in Chapter 4 (eq. 4.4). A plot of the T_g of the miscible amorphous phase and T_m of the crystalline (i.e., PVDF) phase of PVDF/PMMA blends[7] is shown in Figure 7.8.

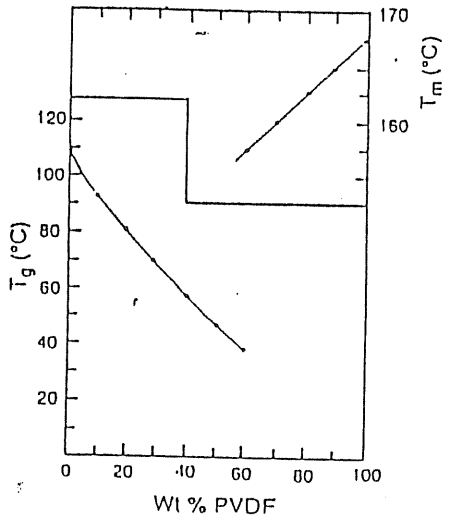

Figure 7.8. Experimental (differential thermal analysis) values of T_g and T_m as a function of wt % of poly(vinylidene fluoride) (PVDF) in blends of PVDF and poly(methyl methacrylate). (Adapted with permission from ref. 7. Copyright 1975 American Chemical Society.)

Properties of Blends. Properties of miscible polymer blends may be intermediate between those of the individual components (i.e., additive behavior), as is typically the case for T_g (see Figure 7.2). In other cases, blend properties may exhibit either positive or negative deviation from additivity, as illustrated by Figure 7.9. For example, both modulus and tensile strength of miscible polymer blends exhibit a small maximum at some intermediate blend composition, while impact strength and permeability (see Chapter 12) will normally go through a broad minimum. This latter behavior has been attributed to a loss in free volume correspond-

ing to a negative volume change of mixing (ΔV_m^1) due to favorable interactions between blend polymers.

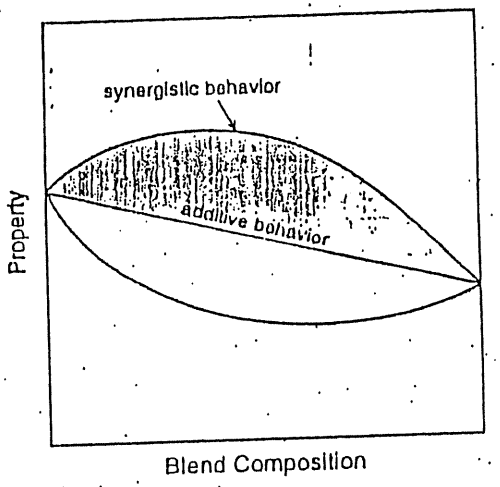

Figure 7.9. Illustration of three types of behavior for the dependence of miscible blend properties on composition.

7.2.2 Toughened Plastics and Phase-Separated Blends

The impact strength of brittle plastics such as PS can be significantly improved by incorporating a rubbery phase (e.g., polybutadiene) in the form of small (< 0.01-μm diameter) dispersed particles. Provided that adhesion between the dispersed phase and matrix polymer is good, the rubber particles can provide an energy-absorbing capability through a change in the mechanical-deformation process either through promotion of extensive shear yielding or craze formation (see Section 4.4.1) or through a combination of both. In the case of high-impact polystyrene (HIPS), interfacial adhesion is promoted by graft polymerization of butadiene with the polystyrene matrix.

Figure 7.10 shows the complex morphology and extensive craze structure of a typical sample of HIPS that has undergone tensile deformation. The phase structure is clearly seen in Figure 7.10A which is a transmission electron micrograph of a sample that had been deformed, microtomed, and stained with osmium tetroxide.†

† Osmium tetroxide (OsO_4) is a stain widely used to provide electron contrast for transmission electron microscopy of unsaturated polymers. This stain reacts with carbon double bonds as shown below and, in addition to providing increased electron density, serves to harden the rubbery component (e.g., polybutadiene in HIPS and ABS) and, therefore, facilitates sectioning by use of a cryogenic microtome.

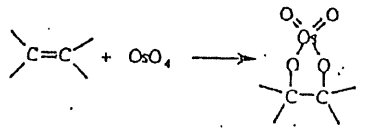

The light-colored areas contain the unstained polystyrene component of HIPS while the stained polybutadiene (PBD) regions appear as the darkened areas. It is noted that the dispersed PBD particles, which range in size from approximately 0.1 to 1.0 μm in diameter, contain significant amounts of occluded PS. These particles also appear to have become spheroidal as a result of the deformation process. The thin dark lines are the crazes, oriented perpendicular to the tensile direction, that have survived the microtoming and staining procedures. As a result of the removal of strain prior to sample preparation, the crazes have had an opportunity to relax or "heal" and therefore appear as thin, rather featureless structures. Extensive crazing is more clearly seen in Figure 7.10B which shows a micrograph of the same sample that was obtained by deforming an unstained thin (0.1 μm) section that had been bonded to a copper cartridge inside the electron micrograph. In this case, the dispersed phase is less distinct due to the absence of staining; however, the craze microstructure is fully developed with the crazes interconnecting the dispersed PBD particles. As before, the crazes are oriented perpendicular to the tensile direction but the fibrils within the unrelaxed crazes are now clearly seen to be aligned in the tensile direction. This type of craze proliferation and bifurcation provides a means of energy dissipation (i.e., toughening) in the otherwise brittle PS matrix.

A higher heat-distortion version of HIPS is ABS, which is an impact-modified styrene–acrylonitrile copolymer. Both HIPS and ABS are blended with other polymers to improve impact strength, as in the case of some commercial resins of polycarbonate (ABS-modified), PVC (ABS-modified), and poly(2,6-dimethyl-1,4-phenylene oxide) (HIPS-modified). Other polymeric impact modifiers include chlorinated polyethylene (CPE) and a variety of important copolymers including ethylene–vinyl acetate (EVA), methyl methacrylate–butadiene–styrene (MBS), and methyl methacrylate–acrylonitrile–butadiene–styrene (MABS).

Heat-distortion temperature (HDT) of a given polymer can sometimes be improved by blending with a high-HDT polymer. An example is the blend of PVC ($T_g \approx 85°C$) and copolymers of styrene and maleic anhydride ($T_g \approx 116$–$123°C$). Additional applications for heterogeneous (i.e., phase separated) polymer blends include coextruded textile polymers for the purpose of modifying some fiber property such as dyeability, self-crimping behavior, or antistatic character. In all these instances, acceptable mechanical properties of the blend require good interfacial adhesion between the continuous and dispersed phase. In the extreme case of macrophase-separated blends, mechanical properties as well as film clarity (i.e., transpar-

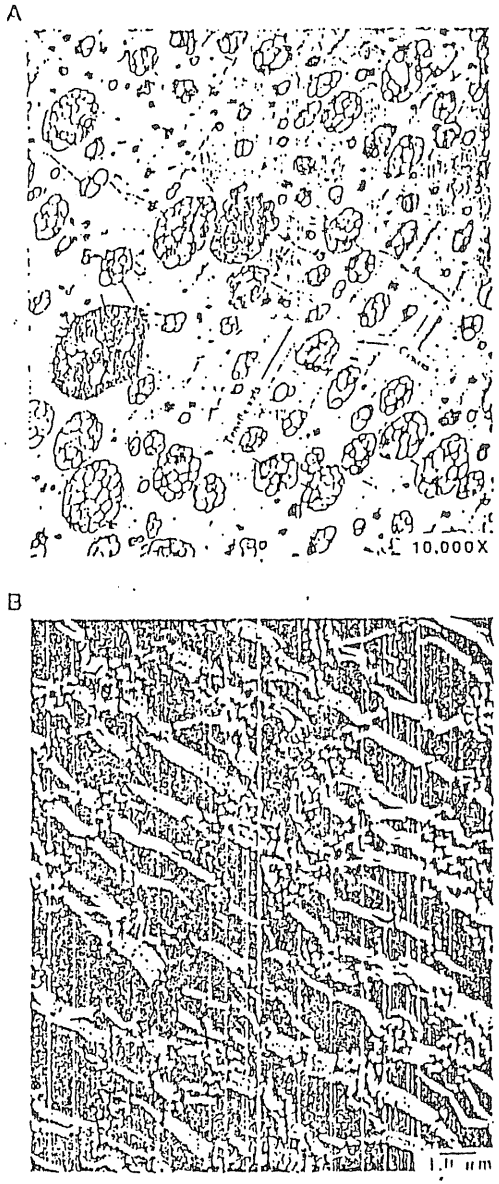

Figure 7.10. Transmission electron micrographs of high-impact polystyrene (HIPS). A. Stained microtomed section. B. In situ crazing using specimen deformation cartridge. (Courtesy of R. C. Cieslinski, The Dow Chemical Company.)

ency) may be unacceptable. In such cases, *compatibilizing agents* such as block copolymers containing one or two of the blend polymers may be useful to improve interfacial coupling.

7.2.3 Interpenetrating Networks

Interpenetrating polymer networks or IPNs are combinations of two or more polymers in network form. At least one of the polymers is synthesized and/or crosslinked in the presence of the other. As such, IPNs share some of the advantages of both polymer blends and network polymers. If the two polymers in an IPN are thermodynamically immiscible, phase separation will occur as the monomer or monomers polymerize, but the size of the dispersed phase will be much smaller (only 10 to 100 nm) than for a physically mixed blend or for a block copolymer or graft of the two components as a consequence of the crosslinking process restricting phase separation. A wide range of morphologies is possible, depending upon the volume fraction of components, the viscosity of the phases, and the relative rates of crosslinking and phase separation.

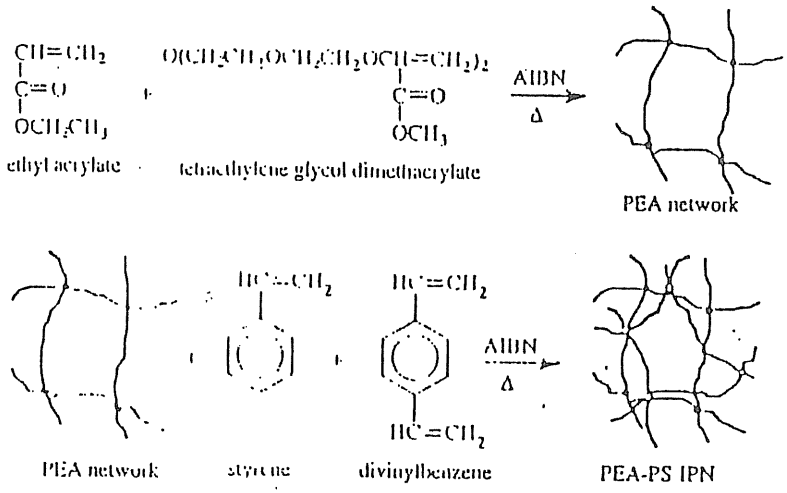

Figure 7.11. Illustration of the preparation of a sequential interpenetrating network (IPN) formed by first forming a poly(ethyl acrylate) (PEA) network by free-radical polymerization of ethyl acrylate with a difunctional monomer, tetraethylene glycol dimethacrylate, using AIBN as an initiator. The PEA network is then swollen with styrene and with the difunctional monomer, divinylbenzene, which are then polymerized to form an interpenetrating polystyrene network. The resulting IPN may be termed *cross*-poly(ethyl acrylate)-*inter-cross*-polystyrene, where the connectives *cross* and *inter* indicate crosslinked and interpenetrating, respectively. [Adapted from L. W. Barrett and L. H. Sperling, *Trends in Polymer Science*, 1, 45 (1993) with permission of the publisher.]

Polymers that can be used in the preparation of IPNs include polyurethanes, polystyrene, poly(ethyl acrylate), and poly(methyl methacrylate). One of the earliest commercialized IPNs, used in many automotive applications, consists of polypropylene and ethylene–propylene–diene terpolymer (EPDM). If the ethylene segments of EPDM are sufficiently long to crystallize, the components are held together by crystalline domains of both polymers without the need of crosslinking (i.e., a thermoplastic IPN).

There are several ways by which IPNs can be prepared. For example, a *sequential IPN* is formed by first crosslinking one polymer. The crosslinked network is then swollen with a mixture of a monomer of the second polymer and a suitable crosslinking agent. The swollen film is then heated to initiate the polymerization and to crosslink the second (interpenetrating) network. An example of an IPN of poly(ethyl acrylate) and polystyrene prepared in this way is shown in Figure 7.11.

If no crosslinking agent is used for the second polymer in the formation of a sequential IPN, only a single network of the initial polymer will result. In this case, the interpenetrating network is called a *semi-IPN*. *Gradient IPNs* are prepared by polymerizing the second monomer before equilibrium sorption occurs. *Simultaneous interpenetrating networks* (SIN) are formed when both polymers are synthesized and crosslinked simultaneously. Normally, SINs utilize polymers with different polymerization mechanisms (i.e., step and chain growth) to eliminate the possibility of copolymerization of the two monomers. Potential applications of IPNs include toughened plastics, ion-exchange resins, pressure-sensitive adhesives, soft contact lenses, controlled release of drugs, and the preparation of novel membrane systems and sound- and vibration-damping material.

7.3 INTRODUCTION TO POLYMER COMPOSITES

The first composite materials may have been bricks fashioned by the ancient Egyptians from mud and straw. Commercialization of composites can be traced to early in this century when cellulose fibers were used to reinforce phenolic and later urea and melamine resins. Probably the most familiar composite material is Fiberglas®, which is widely used to form large lightweight reinforced structures, such as the body of a Corvette, or the hull of a cabin cruiser, or as alternatives to heavy porcelain in the manufacture of bathtubs and shower stalls. Fiberglas, introduced in the 1940s, is the tradename for a composite consisting of glass-fiber reinforcement of an unsaturated-polyester matrix.

As shown by the data given in Table 7.6, composites are used in a wide range of applications, wherever high strength-to-weight ratios are important. Principal uses are found in the automotive, marine, and construction industries. In the majority of cases, especially those requiring high performance in the automotive and aerospace industries, the discontinuous phase or filler is in the form of a fiber. Typical fibers for composite applications include carbon or graphite, glass, aromatic polyamide (e.g., Kevlar), and others that were listed in Table 7.3. In some cases, the filler may be particulate — in the form of microspheres or flakes.

TABLE 7.6 APPLICATIONS FOR POLYMER COMPOSITES[a]

Industry	Millions of lb	Wt %
Aerospace and military	41.1	1.54
Appliances and business	153.3	5.75
Construction	495.4	18.6
Consumer products	170.9	6.41
Corrosion-resistant equipment	350.8	13.2
Electrical and electronics	234.8	8.81
Marine	432.8	16.2
Transportation	703.6	26.4
Other	82.2	3.09
Total	2664.9	100

[a] 1989 statistics; *Chemical and Engineering News*, September 25, 1989, p. 29.

In most cases, composite matrices are thermosets, although there has been recent interest in composites made from thermoplastics and composites having carbon, ceramic, or metallic matrices for high-temperature and other demanding applications. The most important class of thermosets for composite use is the epoxy resins (see Section 9.2.1). Although epoxies are inexpensive and easy to process, they are brittle and have relatively high moisture absorption, which can affect the strength of the filler–matrix interface. As discussed in the following sections, interfacial strength can be improved by the use of coupling agents, which are low-molecular-weight organic–inorganic compounds that serve to promote adhesion between the filler and matrix. In general, thermoplastics such as polysulfone offer higher impact strength than thermosets but are more susceptible to solvent attack and have higher creep compliance, which results in a loss of dimensional stability under load. Recently, some high-impact semicrystalline thermoplastics, such as polyetheretherketone (PEEK) have been evaluated for composite use due to their good solvent resistance and impact strength. Polyimides, which can be either thermoset or thermoplastic, are widely used in aerospace applications. Thermosetting polyimides provide easier processing and higher heat resistance, while thermoplastic polyimides offer greater toughness. Typical properties of some thermoset and thermoplastic matrices are compared in Table 7.7.

TABLE 7.7 PROPERTIES OF COMPOSITE MATRICES

Property	Thermosets		Thermoplastics	
	Epoxy	PI[a]	PSF[b]	PEEK[c]
Modulus, GPa	2.8–4.2	3.2	2.5	3.9
Tensile strength, MPa	55–130	56	70	91
Compressive strength, MPa	140	187	96	—
Density, g cm^{-3}	1.15–1.2	1.43	1.24	1.32
Thermal expansion coefficient, 10^{-6} per °C	45–65	50	—	47
Thermal conductivity, W (m K)$^{-1}$	0.17–0.21	0.36	—	0.25
T_g, °C	130–250	370	185	143

[a] PI, thermosetting polyimide.
[b] PSF, bisphenol-A polysulfone (Udel P1700).
[c] PEEK, polyetheretherketone; ca. 35% crystalline with T_m of 334°C.

Composites are processed by a variety of methods, including compression and resin-transfer molding, which will be described in Chapter 11. Specialized processing operations for composite fabrication are filament winding and pultrusion, which will be described in Section 7.3.2. These are used to prepare continuous fiber-reinforced composites with controlled fiber orientation.

The mechanical properties of composites are strongly influenced by the size, type, concentration, and dispersion of filler, as well as the extent of interfacial adhesion between the filler and matrix (i.e., continuous phase) and the properties of the matrix. The interrelationships between these variables are complex and only basic principles relating these parameters to the mechanical properties and ultimate performance of particulate and fiber-reinforced composites are developed in the following section.

7.3.1 Mechanical Properties

Modulus. The principal function of reinforcing fillers is to increase the modulus of the composite. This is typically accompanied by an increase in the heat-distortion temperature. The modulus of a glassy–polymer composite containing a rigid *particulate* filler may be estimated by use of the modified *Halpin–Tsai equation* given as

$$\frac{M}{M_m} = \frac{1 + AB\phi_f}{1 - B\psi\phi_f} \tag{7.7}$$

where M is the modulus (tensile, shear, or bulk) of the composite, M_m is the corresponding modulus of the unreinforced matrix polymer, A is a constant that depends on the filler geometry and the Poisson's ratio of the matrix, ϕ_f is the volume fraction of filler, ψ depends upon the maximum *packing* volume fraction of the filler (0.601 for random loose packing of spheres), and B is a function of A and the relative moduli of the filler (M_f) and matrix as

$$B = \frac{(M_f/M_m) - 1}{(M_f/M_m) + A}. \tag{7.8}$$

If the particulate filler is uniformly dispersed, the mechanical properties of a particulate-filled composite are independent of the testing direction (i.e., isotropic). By comparison, the properties of fiber-reinforced composites are dependent upon the direction of measurement — they are *anisotropic*. This is because fibers are usually uniaxially oriented or oriented randomly in a plane during the fabrication of the composite. The maximum modulus of the composite is obtained in the orientation direction. For uniaxially oriented fibers, the tensile (Young's) modulus measured in the orientation direction (the longitudinal modulus, E_L) is given by a simple rule of mixtures as

$$E_L = (1 - \phi_f)E_m + \phi_f E_f \tag{7.9}$$

where E_m is the tensile modulus of the matrix and E_f is the tensile modulus of the fiber (see Table 7.5).

The modulus measured in the direction perpendicular to orientation (i.e., the transverse modulus, E_T) is typically much smaller than E_L. It can be expressed in the form of the modified Halpin–Tsai equation (eq. 7.7) as

$$\frac{E_T}{E_m} = \frac{1 + AB\phi_f}{1 - B\psi\phi_f} \tag{7.10}$$

where A is equal to twice the aspect ratio (L/D) for uniaxially oriented fibers.

Strength. In general, composite strength, an ultimate property, depends upon many factors, such as the adhesive strength of the matrix–filler interphase and, therefore, is not as easily modeled as is modulus. Interfacial strength may be reduced by the presence of water adsorbed on the filler surface or by thermal stresses resulting from a mismatch between the thermal coefficients of linear expansion for the filler and matrix polymer. Polymers have relatively high linear-expansion coef-

ficients (60 to 80 × 10^{-6} per °C for PS) compared to fillers such as silica glass (0.6 × 10^{-6} per °C) or graphite (7.8 × 10^{-6} per °C).

Several relationships have been proposed to relate the ultimate strength of a *particulate-filled composite* (σ_u) to the ultimate strength of the unfilled matrix (σ_m). One such equation proposed by Schrager[9] is given as

$$\sigma_u = \sigma_m \exp(-r\phi_f) \tag{7.11}$$

where r is an interfacial factor (typically 2.66 for many composites). This provides a maximum value for strength (up to 35 to 40 vol % filler) and assumes good adhesion between the dispersed filler and matrix. Strength of the composite will decrease with decreasing interfacial strength.

In the case of *fiber-reinforced composites*, strength, like modulus, depends on the orientation of the fiber with respect to the stress direction. The maximum strength is obtained for uniaxially oriented fibers when the fibers are oriented in the tensile (or longitudinal) direction, σ_L. In this case, the strength is given by the simple rule of mixtures in the same form as for modulus (eq. 7.9):

$$\sigma_L = (1-\phi_f)\sigma_m + \phi_f\sigma_f. \tag{7.12}$$

In contrast, the strength of the uniaxially oriented fiber composite is minimal when the strength is measured transverse to the fiber orientation, σ_T. This strength is strongly influenced by the strength of the interfacial bond and will be much lower than the longitudinal strength. As an approximation, σ_T may be approximated as one-half of the matrix strength, σ_m.

TABLE 7.8 PROPERTIES OF PEEK COMPOSITES

Property	PEEK	30% Carbon Fiber	30% Glass Fiber
Heat-deflection temperature °C at 1.82 MPa (264 psi)	148	300	300
Tensile strength (MPa) at 23°C	91.0	146.0	140.0
Flexural modulus (GPa) at 23°C	3.89	15.5	8.0

As an illustration of the effect of fiber reinforcement on composite properties, heat-distortion temperature and some mechanical properties of carbon- and glass-fiber composites of polyetheretherketone (PEEK), an engineering thermoplastic (see Section 10.2.3), are given in Table 7.8. As illustrated, reinforcement increases the heat-distortion temperature of PEEK from 148° to 300°C at 30% fiber loading. In addition, tensile strength and especially (flexural) modulus are increased considerably over corresponding values for the unfilled or "neat" resin due to the high modulus and strength of carbon and glass fibers (see Table 7.8). The modulus of the carbon-fiber composite is higher than that of the glass-fiber composite since the modulus of carbon and graphite fibers is greater than that of glass fibers up to a factor of nearly 5.

Interfacial Adhesion and Coupling Agents. In practice, interfacial strength is improved by the use of low-molecular-weight organofunctional silanes (or titanates) such as those listed in Table 7.9, which act as a *coupling agent* bridging the matrix–filler boundary. Typically, these inorganic–organic additives have one or more hydrolyzable groups (e.g., hydroxyl or alkoxy) capable of silanol-group formation for bonding with mineral surfaces and a matrix-specific organofunctional group such as an epoxy functionality, which can react with, or promote adhesion to, the matrix resin. The most important of the coupling agents are the silanes which are widely used in the form of aqueous dispersions to treat fiber glass and coarse particulate fillers.

TABLE 7.9 COMMON COUPLING AGENTS

Type	Representative Structure
Vinyl silane	$CH_2{=}CH{-}Si(OCH_3)_3$
Epoxy silane	$H_2C\overset{O}{\diagup\diagdown}CHCH_2OCH_2CH_2CH_2CH_2{-}Si(OCH_3)_3$
Primary amine silane	$H_2NCH_2CH_2CH_2{-}Si(OC_2H_5)_3$
Methacrylate	$H_2C{=}\underset{\displaystyle CH_3}{\underset{\displaystyle |}{C}}{-}\overset{\displaystyle O}{\overset{\displaystyle \|}{C}}{-}O{-}CH_2CH_2CH_2{-}Si(OCH_3)_3$
Titanate	$\left(H_2C{=}\underset{\displaystyle CH_3}{\underset{\displaystyle |}{C}}{-}\overset{\displaystyle O}{\overset{\displaystyle \|}{C}}{-}O\right)_3TiOCH(CH_3)_2$

The effect of coupling agents on the dry and wet flexural strength of glass fiber-reinforced polyester is illustrated in Table 7.10. In this example, a silane-

functional coupling agent is shown to greatly improve the flexural strength of the polyester composite, both in the dry state and after immersion in boiling water.

Improved interfacial adhesion may also be achieved by modification or functionalization of the fiber surface. For example, the interfacial adhesion of ultrahigh-molecular-weight polyethylene may be improved by plasma treatment in pure oxygen.

TABLE 7.10 FLEXURAL STRENGTH OF A GLASS-REINFORCED POLYESTER

Coupling Agent	Flexural Strength, GPa[a]	
	Dry	2-Hour Boil
None	0.38	0.23
Vinyl silane	0.46	0.41
Methacrylate silane	0.62	0.59

[a] To convert GPa to psi, multiply by 145,000.

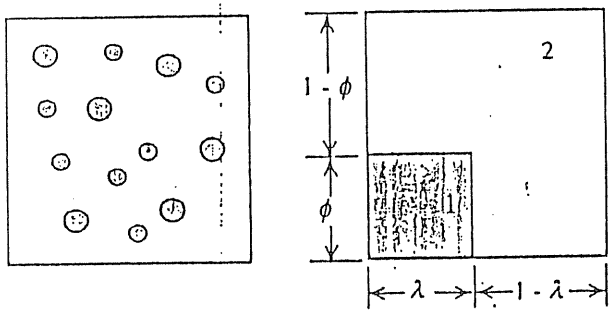

Figure 7.12. Equivalent model of Takayanagi.[10] An idealized two-phase system consisting of a dispersed phase (shaded regions) dispersed in a matrix of component 1 is shown at the left. This composite structure can be modeled as a unit cube (1 × 1 × 1) (pictured at right) with the dispersed phase (component 1) having dimensions of $\phi \times \lambda \times 1$ (i.e., the volume fraction is $\phi\lambda$).

Dynamic-Mechanical Properties. Dynamic-mechanical measurements (see Section 5.1.1) can be used to investigate the morphology of composites and phase-separated polymer blends through the "equivalent model" originally proposed by Takayanagi.[10] As illustrated in Figure 7.12, the dynamic-mechanical properties of any two-phase morphology, such as an immiscible blend, composite, laminate, or semicrystalline polymer, can be modeled as a series and parallel combination of contributions from the individual components — the matrix and dispersed phase.

The dynamic modulus of the composite can be modeled by resolving the equivalent model pictured at the right of Figure 7.12 as contributions from elements in series and parallel, as illustrated in Figure 7.13. Since elements A and B are in series, strains on these elements, or equivalently their weighted compliances, are additive and, therefore, we can write

$$D^* = \frac{1}{E^*} = (1-\phi)D_A^* + \phi D_B^* \tag{7.13}$$

Since element A is pure component 2 (the matrix component),

$$D_A^* = \frac{1}{E_A^*} = \frac{1}{E_2^*} \tag{7.14}$$

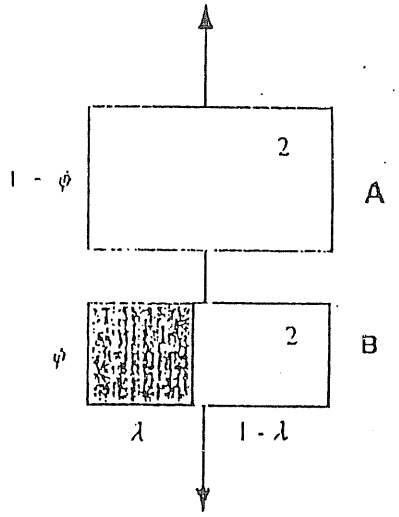

Figure 7.13. Parallel and series elements of equivalent model illustrated in Figure 7.12. Elements A and B are in series combination to the applied strain (arrows). Element B is composed of two elements (dispersed phase and matrix) in parallel.

Element B is a parallel combination of components 1 (dispersed component) and 2 (matrix) and, therefore, stresses or equivalently moduli are additive:

$$E_B^* = \frac{1}{D_B^*} = \lambda E_1^* + (1-\lambda)E_2^* \qquad (7.15)$$

Substituting eqs. 7.14 and 7.15 into eq. 7.13 gives the final relationship for the dynamic compliance or modulus of the equivalent model as

$$D^* = \frac{1}{E^*} = \frac{1-\phi}{E_2^*} + \frac{\phi}{\lambda E_1^* + (1-\lambda)E_2^*}. \qquad (7.16)$$

In eq. 7.16, ϕ and λ have the significance of fitting parameters, although the product ($\phi\lambda$) is equal to the *volume fraction* of the dispersed phase. The values of these fitting parameters obtained by fitting actual dynamic-mechanical data give a qualitative understanding of the morphology of the composite. For example, $\lambda = \phi$ indicates a uniformly dispersed phase, while $\lambda < \phi$ indicates agglomeration of dispersed phases.

7.3.2 Composite Fabrication

As previously indicated, composites can be fabricated by a variety of techniques, including compression and resin-transfer molding, which are discussed in Chapter 11. Composites used for nonstructural (i.e., nonload-bearing) applications are produced by using sheet-molding compound (SMC), bulk-molding compound (BMC), preform molding, injection molding, and spray-up. For the manufacture of composites for structural applications, two important processing methods are filament winding and pultrusion, which are reviewed in the following sections.

In general, BMC consists of styrenated unsaturated-polyester resin (unsaturated polyester containing styrene monomer, which is polymerized during the final cure process), a low-profile thermoplastic polymer, an inert filler such as calcium carbonate, glass fibers, a polymerization initiator, and other additives such as a lubricant (e.g., zinc stearate), and a maturation agent (e.g., MgO). BMC has the consistency of a putty, which can be applied with a trowel. A related composite formulation is SMC, which is formed by combining styrenated polyester resin thickened by 1% of calcium or magnesium oxide, fillers, peroxides, and chopped glass fibers. The SMC is contained between layers of polyethylene film, which are removed at the time of molding. In spray-up, glass fibers and a resin are simultaneously deposited in a mold. In this process, a roving (8 to 120 strands of glass fiber) is fed through a chopper and ejected into a resin stream. A preform refers to a preshaped composite formed by distribution of chopped fibers by air, water flotation, or vacuum over the surface of a preformed screen. A preform may also refer to a mat or cloth preformed to a specific shape on a mandrel or mock-up.

Filament Winding. A simple filament-winding operation is illustrated in Figure 7.14. Fibers are pulled from bobbins through a bath containing the composite resin, such as an epoxy or (unsaturated) polyester formulation, and then the impregnated fibers are wound onto a form (the mandrel) in some predetermined arrangement. Usually, fibers are E--or S-glass (see Table 7.3). Once the mandrel is uniformly covered to the desired thickness and fiber orientation, the composite is cured at elevated temperature and the mandrel may be removed or left as an integral part of the composite. Filament winding may be used to prepare corrosion-resistant (fiber glass) tanks and pipes. Employing advanced resin materials, filament winding is also being used to prepare high-performance composites for structural and other applications in the automotive and aerospace industries. The continuous reinforcement and controlled fiber orientation that can be achieved by filament winding provide a higher level of reinforcement than possible by discontinuous reinforcement using individual fibers.

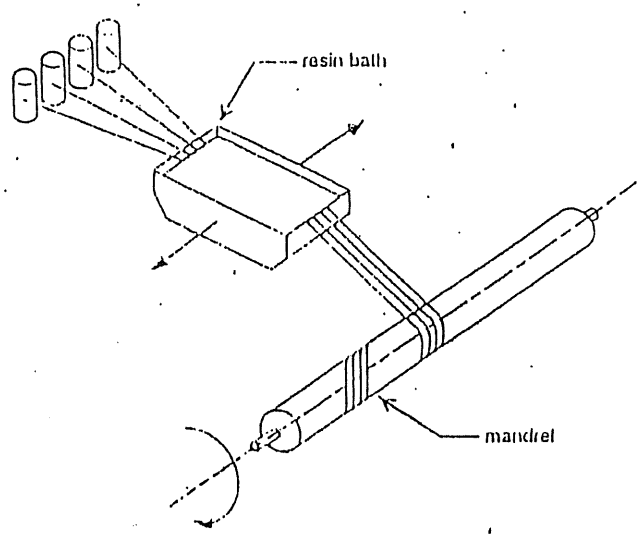

Figure 7.14. Filament-winding operation. (Adapted from R. C. Hayes, in the *Concise Encyclopedia of Polymer Science and Engineering*, J. I. Kroschwitz, ed. Copyright ©1990 by John Wiley & Sons. Reprinted by permission of John Wiley & Sons, Inc.)

Pultrusion. A simplified diagram of a pultrusion operation is illustrated in Figure 7.15. Compared to filament winding, pultrusion is a completely continuous process operation since the cure step is on-line. This makes pultrusion a suitable process for commercial production lines producing of a variety of composite

shapes or profiles. A roving[1] of continuous fibers (e.g., E-glass) and a continuous-strand mat (typically glass/polyester) are combined and immersed in a resin bath before passing through a forming guide and the curing oven. The majority of composites that are pultruded are the fiber-glass variety prepared from unsaturated polyester resin and E-glass. Fiber loadings in pultrusion may range from 20% to 80%.

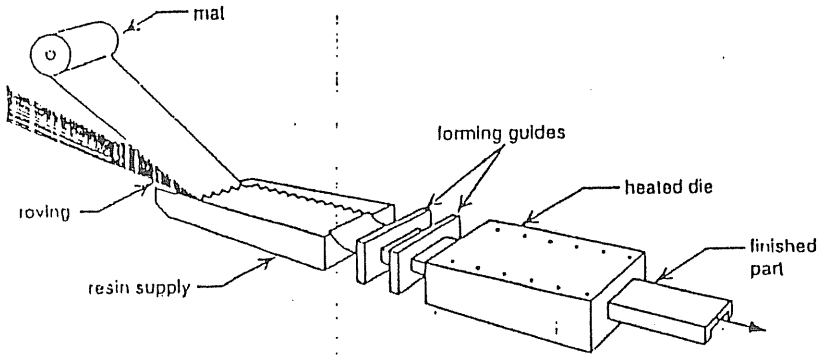

Figure 7.15. Pultrusion line. (Adapted from D. Evans, in the *Concise Encyclopedia of Polymer Science and Engineering*, J. I. Kroschwitz, ed. Copyright ©1990 by John Wiley & Sons. Reprinted by permission of John Wiley & Sons, Inc.)

REFERENCES

1. L. A. Wood, *J. Polym. Sci.*, 28, 319 (1958).
2. J. R. Fried, G. A. Hanna, and H. Kalkanoglu, in *Polymer Compatibility and Incompatibility — Principles and Practice*, K. Solc, ed., Harwood Academic Publishers, New York, Vol. 3 in the MMI Press Symposium Series, Midland, MI, 1982, pp. 237–248.
3. K.-H. Illers, W. Heckmann, and J. Hembrecht, *Colloid & Polymer Sci.*, 262, 557 (1984).
4. R. L. Scott, *J. Chem. Phys.*, 17, 279 (1949).
5. L. P. McMaster, *Macromolecules*, 6, 760 (1973).
6. S. H. Goh and K. S. Siow, *Thermochim. Acta*, 105, 191 (1986).
7. D. R. Paul and J. O. Altamirano, in *Copolymers, Polyblends, and Composites*, N. A. J. Platzer, ed, *Advances in Chemistry Series* No. 142, American Chemical Society, Washington, DC, 1975, pp. 371–385.
8. R. C. Cieslinski, *J. Mater. Sci. Lett.*, 11, 813 (1992).
9. M. Schrager, *J. Appl. Polym. Sci.*, 22, 2379 (1978).
10. M. Takayanagi, H. Harima, and Y. Iwata, *Mem. Faculty Eng., Kyushu Univ.* 23, 1 (1963).

[1] When graphite or boron fibers are used in place of glass fibers, the term *tow* is used rather than roving.

GENERAL READING

L. W. Barrett and L. H. Sperling, "Today's Interpenetrating Polymer Networks," *Trends Polym. Res.*, 1(1), 45–49 (1993).

R. J. Diefendorf and E. Tokarsky, "High-Performance Carbon Fibers," *Polym. Eng. Sci.*, 15, 150 (1975).

L. Nicolais, "Mechanics of Composites," *Polym. Eng. Sci.*, 15, 137 (1975).

L. E. Nielsen, *Mechanical Properties of Polymers and Composites*, Marcel Dekker, Inc., New York, 1977.

O. Olabisi, "Interpretations of Polymer-Polymer Miscibility," *J. Chem. Ed.*, 58, 944–950 (1981).

L. H. Sperling, "Interpenetrating Polymer Networks: An Overview," in *Interpenetrating Polymer Networks*, D. Klempner, L. H. Sperling, and L. A. Utracki, eds., *Adv. Chem. Ser.*, 239, American Chemical Society, Washington, DC, 1994, pp. 3–38.

ADVANCED READING

C. B. Bucknall, *Toughened Plastics*, Applied Science Publishers Ltd., London, 1977.

J. Delmonte, *Technology of Carbon and Graphite Fiber Composites*, Van Nostrand, New York, 1981.

G. Lubin, ed., *Handbook of Composites*, Van Nostrand Reinhold, New York, 1982.

O. Olabisi, L. M. Robeson, and M. T. Shaw, *Polymer–Polymer Miscibility*, Academic Press, New York, 1979.

D. R. Paul and S. Newman, *Polymer Blends*, Academic Press, New York, 1978.

L. H. Sperling, *Interpenetrating Polymer Networks and Related Materials*, Plenum Press, New York, 1981.

S. W. Tsai and H. T. Hahn, *Introduction to Composite Materials*, Technomic Publishing Company, Westport, CT, 1980.

Problems

7–1. For a blend of poly(2,6-dimethyl-1,4-phenylene oxide) (PPO) (T_g = 216°C) and polystyrene (T_g = 105°C), compare the predictions of the inverse rule of mixtures and the logarithmic rule of mixtures (see Section 4.3.4) by plotting the calculated T_g of the blend against the weight fraction of PS. Experimental T_g values for this blend that were obtained by DSC measurements are as follows:

Wt % PPO	T_g (°C)
20	121
40	140
60	158
80	185

7–2. For a graphite-fiber composite of polysulfone containing 40 vol % filler, what is the *maximum* modulus and maximum strength that can be expected?

7–3. Draw the chemical structures for the following plasticizers:
(a) TCP
(b) TOTM
(c) DOA
(d) DIOP

7–4. Give your best estimate for the T_g of PVC that has been plasticized with 30 phr of TOTM (T_g = -72°C).

8

Commodity Thermoplastics and Fibers

As discussed in Chapter 1, polymers may be classified as either thermoplastics, thermosets, or fibers. Of these, thermoplastics constitute the largest share of the U.S. market. In 1993, thermoplastics accounted for about 69%, fibers for 14%, and thermosets for only 10% of the total polymer production of 67 billion pounds.

Thermoplastics are polymers that can be melt processed by a variety of methods, including extrusion and molding. These include polyethylene, polypropylene, polystyrene, and poly(vinyl chloride). Thermoplastics are used for a wide range of applications, such as film for packaging, photographic and magnetic tape, beverage and trash containers, and a variety of automotive parts and upholstery. Fibers are typically semicrystalline polymers that can be spun into long strands that have high strength-to-weight ratios for textile as well as composite applications (see Section 7.3). They are prepared by the melt or solution spinning of both synthetic polymers (e.g., polyesters, nylons, polyolefins, and acrylic polymers such as polyacrylonitrile) and naturally occurring polymers, principally cellulose in the form of rayon (regenerated cellulose) and cellulose acetate. The synthesis and properties of important commercial thermoplastics and textile fibers are presented in this chapter.

Compared to thermoplastics and fibers, thermosets such as phenol–formaldehyde resins are network polymers that result from the chemical crosslinking of individual polymer chains. Once formed, thermosets are infusible and insoluble materials that, therefore, cannot be normally refabricated or recycled. Elastomers are typ-

ically low-T_g polymers that are often *lightly* crosslinked through the vulcanization process to produce commercial rubbers with high resilience, such as polybutadiene. The synthesis and properties of both networklike polymers, thermosets and elastomers, are reviewed in Chapter 9.

8.1 THERMOPLASTICS

As shown by the data given in Table 8.1, the largest sales volume thermoplastics include the polyolefins (principally polyethylene and polypropylene), styrene-based polymers (polystyrene and impact-modified polystyrene), and poly(vinyl chloride). Other important thermoplastics include poly(ethylene terephthalate), which is used for packaging applications — particularly plastic bottles — and as an important fiber (i.e., polyester fiber), as discussed later in Section 8.2.3. Engineering-grade polyesters that reach a specialty market are reviewed in Chapter 10. The synthesis and properties of these important commercial thermoplastics are given in the following sections.

TABLE 8.1 U.S. PRODUCTION OF THERMOPLASTICS IN 1993

Thermoplastic	Billions of Pounds	Total Thermoplastic Market (%)
Low-density polyethylene	12.0	26.0
PVC and copolymers	10.3	22.3
High-density polyethylene	9.9	21.4
Polypropylene	8.6	18.6
Polystyrene	5.4	11.7
TOTAL	46.2	

Source: *Chemical and Engineering News*, April 11, 1994.

8.1.1 Polyolefins

The polyolefins include various grades of polyethylene, differentiated on the basis of their crystallinity (i.e., density), and polypropylene. A comparison of the properties of polypropylene and the two most important polyethylenes — low-density (LDPE) and high-density polyethylene (HDPE) —are given in Table 8.2.

Polyethylene. Ethylene, one of the most important petrochemicals, may be polymerized by a variety of techniques to produce products as diverse as low-molecular-weight waxes to highly crystalline, high-molecular-weight polyethylene (HDPE). The first commercialized polyolefin (1939) was a low-crystallinity, low-density polyethylene (LDPE) produced in 1939 by ICI in England. Today, LDPE is the largest sales volume thermoplastic produced in the United States, as shown by the data given in Table 8.1. The majority (65%) of LDPE produced in the United States is used as thin film for packaging, while the remaining production finds use in wire and cable insulation, coatings, and injection-molded products.

TABLE 8.2 PROPERTIES OF COMMODITY POLYOLEFINS

Property	ASTM	LDPE	HDPE	PP
Specific gravity	D792	0.91–0.93	0.94–0.97	0.90–0.91
Crystallinity, %	---	50–70	80–95	82
Melt temperature, °C	---	98–120	127–135	165–171
Tensile strength, MPa[a]	D638	4.1–16	21–38	31–41
Tensile modulus, GPa[b]	D638	0.10–0.26	0.41–1.24	1.10–1.55
Elongation-to-break, %	D638	90–800	20–130	100–600
Impact strength, notched Izod, J m^{-1} [c]	D256	No break	27–1068	21–53
Heat-deflection temperature, °C, at 455 kPa (66 psi)	D648	38–49	60–88	225–250

[a] To convert MPa to psi, multiply by 145.
[b] To convert GPa to psi, multiply by 1.45×10^5.
[c] To convert J m^{-1} to lb$_f$ in.$^{-1}$, divide by 53.38.

Low-density polyethylene is produced by free-radical bulk polymerization using traces of oxygen or peroxide as the initiator. Polymerization is conducted either in high-pressure autoclaves or in continuous tubular reactors operating at temperatures near 250°C and pressures as high as 3000 atm. Since the heat of ethylene polymerization is high (105 kJ mol^{-1}), the exotherm needs to be carefully controlled. For this reason, the polymerization may be conducted in stages of low conversion.

Small amounts of polar comonomers such as acrylates, vinyl esters, and vinyl ethers may be added during the polymerization process to modify product properties, particularly to impart low-temperature flexibility through the reduction of crystallinity. For example, low molecular-weight copolymers of ethylene and vinyl acetate (EVA) have been used as polymeric plasticizers for PVC (see Section 7.1.1). The incorporation of small amounts (<7%) of vinyl acetate results in polyethylene films (modified LDPE) having better toughness, clarity, and gloss. Copolymers of ethylene and vinyl alcohol (EVOH) provide better processability,

moisture resistance, and high gas-barrier properties for packaging applications. Films made from copolymers of ethylene and ethyl acrylate have outstanding tensile strength, elongation-to-break, clarity, resistance to stress cracking, and flexibility at low temperatures. Copolymers of ethylene and methacrylic acid, particularly neutralized in the form of sodium or zinc salts, are known as ionomers that exhibit extreme toughness and abrasion resistance (see Section 10.2.2).

Molecular weights of LDPE typically fall in the range between 6000 and 40,000. Molecular-weight grades are sold on the basis of their *melt index* (ASTM D1238), which is the weight (in grams) of polymer extruded through a standard capillary at 190°C in 10 min. Typical melt indices of LDPE range from 0.1 to 109. In an oxygen-initiated polymerization, molecular weight can be reduced by increasing the oxygen concentration.

The free-radical polymerization of ethylene produces a highly branched molecule. The number of these branches may be as high as 30 per 500 monomer units. Most of these are short-chain alkyl groups such as ethyl and butyl, which are produced by an intramolecular "back-biting" mechanism illustrated in Figure 8.1A. At higher conversions and at lower pressures, long-chain branches (i.e., hexyl or longer) may be produced through a chain-transfer mechanism as shown in Figure 8.1B. Branching acts as defects that reduce crystallinity, as evidenced by the low density and low crystalline-melting temperature (T_m) of LDPE compared to HDPE (see Table 8.2). Branching can be reduced by increasing the pressure of the polymerization. For example, nearly linear polyethylene can be produced by free-radical polymerization at pressures approaching 5000 atm.

Alternately, polyethylene with reduced branching can be obtained by polymerizing ethylene in the presence of some coordination catalysts (see Section 2.2.3). The production of linear or *high-density polyethylene* (HDPE) by this route dates back to 1956. The first catalysts (Philips type) consisted of chromium oxide (CrO_3) supported on aluminum oxide (Al_2O_3) or a silica-alumina base (as still widely used in the United States). Polymerization is conducted at 100 atm and 200°C in hydrocarbon solvents in which the catalysts are insoluble (i.e., heterogeneous solution polymerization). Alternate schemes employ Ziegler-type catalysts, which typically are complexes of aluminum trialkyls and titanium or other transition-metal halides, originally triethyl aluminum and titanium tetrachloride. Compared to the Philips-type supported catalysts, Ziegler catalysts generally require lower temperatures and pressures, (i.e., 60° to 75°C and 1 to 10 atm) to obtain high-molecular-weight linear polymers. Typical properties of HDPE are given in Table 8.2. The principal commercial applications for HDPE include blow-molded containers, crates, pails, drums, gas tanks, and blown film. Polyethylene with molecular weights as high as 5 million have been used for specialty applications, particularly for medical use such as artificial hip replacements (see Section 10.2.2).

Approximately 30 years ago, another low-pressure process (Unipol) was developed for the polymerization of ethylene. This process produces what may be considered a third-generation hybrid polyethylene — a low-pressure, low-density polyethylene (LLDPE). This new grade of polyethylene is low to medium density. Branches are linear alkanes that are shorter than those of LDPE. One advantage of LLDPE over LDPE is a faster cycling time during the molding of containers and lids. LLDPE is frequently blended with LDPE for film and sheet production. Today, LLDPEs represent approximately one-third of the total world production of LDPE and LLDPE. In addition to LDPE, LLDPE, and HDPE, other commercial grades may include medium-density polyethylene or MDPE and very low density polyethylene or VLDPE ($\rho < 0.915$ g cm^{-3})

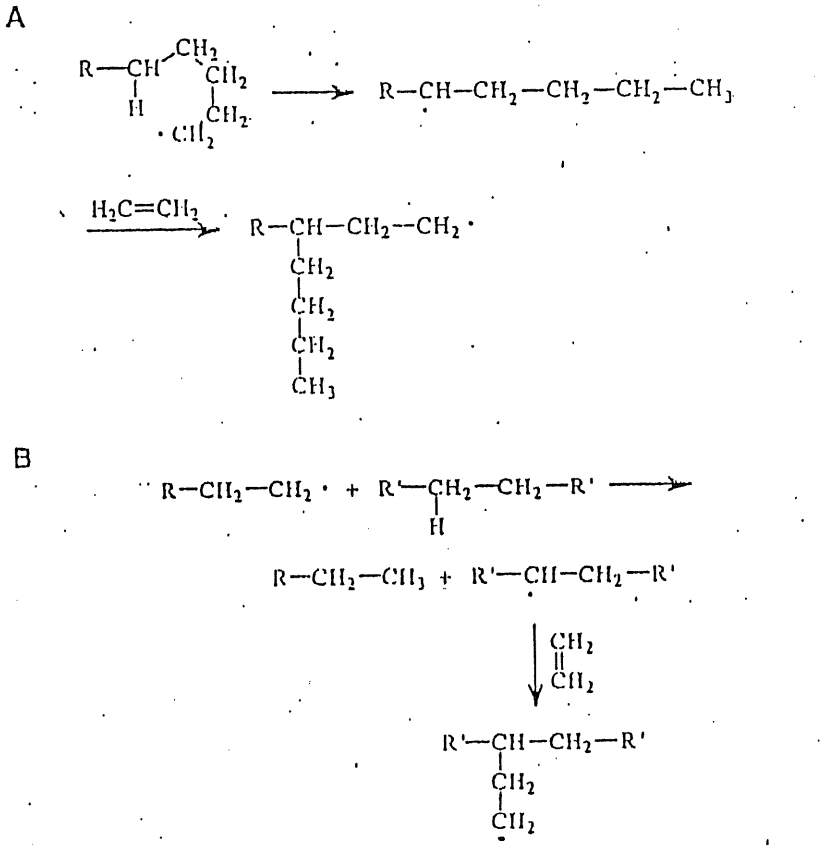

Figure 8.1. Mechanisms of branching during the free-radical polymerization of low-density polyethylene. A. Formation of a *n*-butyl (C_4H_7) branch by an intramolecular "back-biting" mechanism. B. Formation of long-chain branches via an intermolecular chain-transfer mechanism. Long alkyl end chains are represented by R and R'.

Polypropylene. The third largest sales volume polyolefin is polypropylene (PP), properties of which are included in Table 8.2. Polypropylene is a lightweight, moderately high T_m plastic that finds use in the manufacture of pipe, sheet, blow-molded containers, and as a textile fiber (i.e., olefin fiber). In general, α-olefins such as PP cannot be polymerized by either radical or ionic catalysts. While atactic PP can be produced by use of a Lewis acid or organometallic compound, the product is a branched, rubbery polymer (T_g = -20°C) at ambient temperature with no important commercial applications. In the 1950s, Natta showed that Ziegler-type catalysts could be used to produce stereoregular PP with high crystallinity; however, in contrast to the polymerization of HDPE, the coordination polymerization of α-olefins is slower and more critically dependent on the nature of the catalyst. The commercial plastic, first introduced in 1957, is highly isotactic (i.e., *i*-PP). High-molecular-weight (150,000 to 1,500,000) *i*-PP can be obtained by using a heterogeneous catalyst of a violet crystalline modified titanium (III) chloride with a cocatalyst or activator, usually an organoaluminum compound such as diethylaluminum chloride. Catalysts are slurried in a hydrocarbon mixture, which helps to facilitate heat transfer in batch or continuous reactors operating at temperatures of 50° to 80°C and pressures of 5 to 25 atm. Hydrogen, which acts as a chain-transfer agent, may be used to moderate molecular weight. Syndiotactic PP (*s*-PP) can be produced by using homogeneous Ziegler–Natta catalysts at lower temperatures. Compared to its isotactic counterpart, *s*-PP has a slightly lower T_m and is more susceptible to solvent attack.

In comparison to HDPE, commercial grades of *i*-PP have a higher T_m, slightly lower crystallinity, and better crack resistance. Unlike polyethylene, whose lowest-energy conformation is the extended planar zigzag (see Chapter 1), the pendant methyl groups of PP require a more complicated conformation whereby three monomer units constitute a single turn in a helix. Its higher T_m allows PP to be used in products that must be steam sterilized. One disadvantage of PP is the susceptibility of its methyl groups to thermooxidative degradation.

8.1.2 Vinyl Polymers

Styrenics. Polystyrene (PS) was first produced in quantity by Dow in 1938. Today, styrenic polymers, principally general-purpose (GP) and impact grades of polystyrene (PS), comprise about 12% of the total thermoplastic market (see Table 8.1). Properties of different grades of PS are given in Table 8.3. Commercial (atactic) PS is produced by free-radical polymerization in bulk or suspension with peroxides or trace oxygen as initiators. Exotherm control in bulk polymerization can be achieved by using multiple-step polymerizations — an initial low-conversion in a stirred-tank reactor followed by high conversion in a tubular reactor operating with an increasing temperature gradient.

The principal use for PS has been packaging, where it is receiving increasing competition from PP. An especially important application for styrenic polymers is the manufacture of foam and bead for insulation and packaging materials. The first expandable PS (EPS) was produced in England in 1943. Today, the worldwide consumption of EPS is estimated at 1.6 million tons. EPS is a closed-cell structure made from PS beads and a hydrocarbon propellant or blowing agent such as isopentane and butane (see Section 7.1.3). For construction use, flame-retardant grades of EPS can be produced by adding <1% of brominated aliphatic compounds such as hexabromocyclododecane (HBCD).

TABLE 8.3 PROPERTIES OF STYRENIC POLYMERS

Property	ASTM	GP-PS	HIPS	ABS
Specific gravity	D792	1.04–1.05	1.03–1.06	1.03–1.58
Tensile strength, MPa[a]	D638	36.6–54.5	22.1–33.8	41.4–51.7
Tensile modulus, GPA[b]	D638	2.41–3.38	1.79–3.24	2.07–2.76
Elongation-to-break, %	D638	1–2	13–50	5–25
Impact strength, notched Izod, J m^{-1} [c]	D256	13.3–21.4	26.7–587	160–320
Heat-deflection temperature, °C at 455 kPa (66 psi)	D648	75–100	75–95	102–107

[a] To convert MPa to psi, multiply by 145.
[b] To convert GPa to psi, multiply by 1.45×10^5.
[c] To convert J m^{-1} to lb$_f$ in.$^{-1}$, divide by 53.38.

Polystyrene can be crosslinked by copolymerizing styrene with limited amounts of divinylbenzene. Applications of crosslinked PS beads include gel-permeation chromatography (see Section 3.3.4) and ion-exchange resins (see Section 2.4.1).

Disadvantages of GP-PS include its high brittleness and low T_g. To some extent, these limitations can be addressed through copolymerization. For example, copolymerization of styrene with maleic anhydride

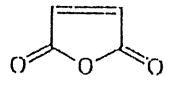

provides slightly higher heat-distortion temperature, while copolymerization of styrene with acrylonitrile (i.e., SAN copolymer) provides higher strength and chemical resistance. Impact modification of PS can be obtained through the incorporation of polybutadiene. For example, high-impact PS (HIPS) is produced by the emulsion polymerization of styrene in a polybutadiene or styrene–butadiene (SBR) latex. The resulting toughened PS consists of a glassy matrix of PS in which are dispersed small domains (~0.005-cm diameter) of polybutadiene. High interfacial

adhesion, important for high strength, is achieved through graft polymerization of styrene, which occurs during the preparation of HIPS. ABS resins (see Section 10.1.2) are produced by blending emulsion latexes of SAN and NBR (acrylonitrile–butadiene rubber) or by grafting styrene and acrylonitrile onto polybutadiene in latex form. Properties of SBR and NBR elastomers are reviewed in Chapter 9.

Recently, a zeolite process has been used to synthesis *p*-methylstyrene (PMS)

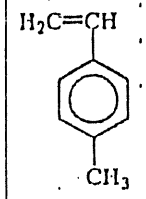

from toluene and ethylene in high yield. This monomer can be polymerized by techniques similar to those used for PS to give poly(*p*-methylstyrene), which has a lower density, a slightly higher heat-distortion temperature, better flame retardancy, and faster molding cycles than conventional GP-PS.

Polystyrene is especially susceptible to photooxidative degradation (see Chapter 6), which results in brittleness and yellowing. Degradation is initiated by the phenyl groups, which absorb UV radiation from sunlight. This energy is transfered to other sites along the polymer chain, resulting in bond cleavage, radical formation, and reaction with oxygen to form hydroperoxide units and carbonyl groups.

One advantage of PS for packaging and related applications is that it can be reprocessed fairly easily. For example, the use of 30% to 50% of clean scrap is common practice in the manufacture of thermofoamed packaging, and used coffee cups can be recycled as regrind for use in the core of three-layer sheet for new cup production.

Poly(vinyl chloride). Poly(vinyl chloride) (PVC) is available in two general grades, rigid and flexible. Rigid-grade PVC is used as sheet, pipe, window profiles, and for other molded parts. Flexible-grade PVC is obtained by blending PVC with low T_g plasticizers as discussed in Section 7.1.1. Applications of plasticized PVC include wire coating, upholstery, floor coverings, film, and tubing. Commercial PVC is a clear, moderately tough, low-crystallinity (T_g = 87°C; T_m = 212°C) material with low to moderate molecular weight (25,000 to 150,000). Properties of rigid- and flexible-grade PVC are summarized in Table 8.4.

Polymerization of commercial-grade PVC is conducted by free-radical polymerization principally by suspension-polymerization techniques, although emulsion- and, more recently, bulk-polymerization methods are also used. PVC is insoluble in its own monomer and, therefore, the polymer precipitates during bulk polymerization or within the monomer droplets in the case of suspension polymerization. If the suspension polymerization is performed under moderate pressure and then vented at the stage of high monomer conversion, a porous "dry-blend" resin is produced. Such resins are able to absorb large amounts of a plasticizer before becoming sticky and are, therefore, used in preparing flexible-grade PVC formulations.

TABLE 8.4 REPRESENTATIVE PROPERTIES OF COMMERCIAL GRADES OF PVC

Property	ASTM	Rigid	Flexible
Specific gravity	D792	1.03–1.58	1.16–1.35
Tensile strength, MPa[a]	D638	41.4–51.7	22.1–33.8
Tensile modulus, GPA[b]	D638	2.41–4.14	1.79–3.24
Elongation-to-break, %	D638	2–80	13–50
Impact strength, notched Izod, J m^{-1} [c]	D256	21.4–1068	26.7–587
Heat-deflection temperature, °C at 455 kPa (66 psi)	D648	57–82	75–95

[a] To convert MPa to psi, multiply by 145.
[b] To convert GPa to psi, multiply by 1.45 x 10^5.
[c] To convert J m^{-1} to lb$_f$ in.$^{-1}$, divide by 53.38.

The polymerization temperature is typically around 50°C for commercial PVC resins since higher temperatures can lead to minor branching and excessive formation of hydrochloric acid through dehydrohalogenation, while lower temperatures result in polymers of high syndiotactic content. Dehydrohalogenation is also a serious problem when unstabilized PVC is heated above its T_g, as during melt processing (see Section 6.1.1). The thermally initiated dehydrohalogenation reaction produces hydrochloric acid, which further accelerates dehydrohalogenation, leading to intense color formation and eventual deterioration of polymer properties. In practice, thermal stability is improved by adding organo-tin and other compounds.

Properties of PVC can be modified through chemical modification, copolymerization, or blending. For example, PVC may be chlorinated (i.e., CPVC) to increase its heat-distortion temperature for applications such as hot-water pipe. A flexible film can be obtained by copolymerizing vinyl chloride with vinylidene chloride (Saran) or vinyl acetate. Vinyl acetate may also be grafted onto the PVC chain. The toughness of PVC can be improved by blending with high-impact resins such as ABS (acrylonitrile–butadiene–styrene) and MBS (methyl methacrylate–butadiene–styrene) (see Section 7.2.2).

Poly(methyl methacrylate). Among other commercially important vinyl polymers are poly(methyl methacrylate) (PMMA) and to a lesser extent poly(vinyl acetate) and its derivatives. Commercial-grade PMMA

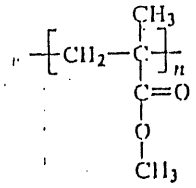

is an amorphous polymer of moderate T_g (105°C), high light transparency, and good resistance to acid and environmental deterioration. It is commercially polymerized by free-radical initiators such as peroxides and azo compounds in suspension or in bulk (e.g., cast polymerization) for sheet and molding compounds or for more specialized applications such as for hard contact lenses. PMMA may also be polymerized anionically (see Section 2.2.2) at low temperatures to give highly isotactic (T_g = 45°C; T_m = 160°C) or highly syndiotactic (T_g = 115°C; T_m = 200°C) polymers. PMMA finds major applications in the automotive industry (e.g., rear lamps, profiles, and light fixtures), as acrylic sheet for bathtubs, advertisement signs, and lighting fixtures, and as composite materials for kitchen sinks, basins, and bathroom fixtures.

Poly(vinyl acetate). Poly(vinyl acetate) (PVAC) (T_g = 29°C), which may be polymerized by free-radical emulsion or suspension polymerization, finds limited applications in adhesives and also as the starting material for the production of poly(vinyl alcohol) (PVAL) and poly(vinyl butyral) (PVB), as discussed in Section 2.4.2. PVAL, which is used as a stabilizing agent in emulsion polymerization and as a thickening and gelling agent, cannot be directly polymerized because its monomer is isomeric with acetaldehyde, as shown:

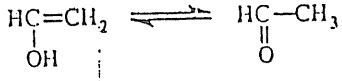

Commercially, PVAL is produced by the hydrolysis of PVAC in concentrated methanol. PVAL can be partially reacted with butyraldehyde to give PVB, which in its plasticized form is used as the inner layer of safety windshield glass. About 25% of the PVAL repeating units are left unreacted to provide strong adhesion to the glass.

Poly(*N*-vinyl-2-pyrrolidinone). Another interesting group of vinyl polymers are the polyvinylamides. As a class, they are highly polar, amphoteric polymers of which poly(*N*-vinyl-2-pyrrolidinone) (PVP)

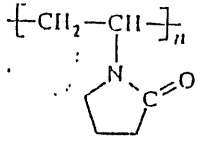

is the most commercially important polymer. Poly(*N*-vinyl-2-pyrrolidinone) is an amorphous polymer with a glass-transition temperature ranging from 126° to 174°C for commercial grades. It has several very useful properties including very low toxicity, good film-forming and adhesive properties, and solubility in a broad range of solvents, including water, alcohols, and a number of other organic solvents. In addition, PVP is able to form complexes with a wide range of compounds through hydrogen-bond formation between its carbonyl group and the hydroxyl groups of water, alcohols, and hydroxyl-containing polymers like poly(vinyl alcohol). During World War II, PVP was used as a plasma extender, and copolymers of vinyl pyrrolidinone and hydroxyethyl methacrylate are used to manufacture soft contact lenses.

Applications for PVP are diverse, including adhesives, coatings, controlled release of drugs, and the clarification of beer and wine in the food industry. PVP also is used as a protective colloid in emulsion and suspension polymerizations and for improving the dyeability of textile material. Vinyl pyrrolidinone is usually bulk polymerized by a free-radical mechanism employing peroxides or azo compounds as initiators and may be grafted or copolymerized with a number of different monomers, such as maleic anhydride, methyl methacrylate, acrylic acid, and acrylonitrile. PVP can be crosslinked in strong alkali, inorganic persulfates (e.g., potassium persulfate), and peroxides or can be crosslinked by irradiation with UV- or γ-radiation.

8.1.3 Thermoplastic Polyesters

The most industrially important polyester is poly(ethylene terephthalate) (PET)

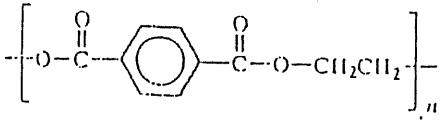

which is principally recognized for its use as a consumer fiber dating back to 1953. Attempts to injection mold PET in the mid 1960s were unsuccessful due to its slow crystallization rate, which translated into unacceptably low molding rates. At

that time, a promising alternative to PET for molding applications appeared to be poly(butylene terephthalate) (PBT)

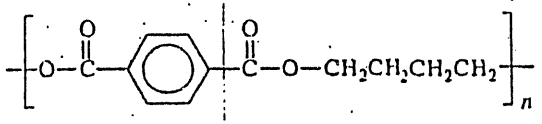

which had the attractive feature that it would crystallized faster than the available grades of PET. Although much interest was directed toward developing PBT for molding (as well as fiber) use during the 1970s, the market for moldable PBT did not develop to the extent originally envisioned due to several issues, including problems with postmolding warpage. In the late 1970s, interest was directed toward the development of faster crystallizing grades of PET suitable for molding applications such as packaging (soft-drink and custom bottles and thermoformed trays). The current usage of PBT has been as an engineering thermoplastic along with several other polyesters, such as polyarylates (see Section 10.1.8) and liquid-crystal polyesters (Section 10.2.6), for specialized applications.

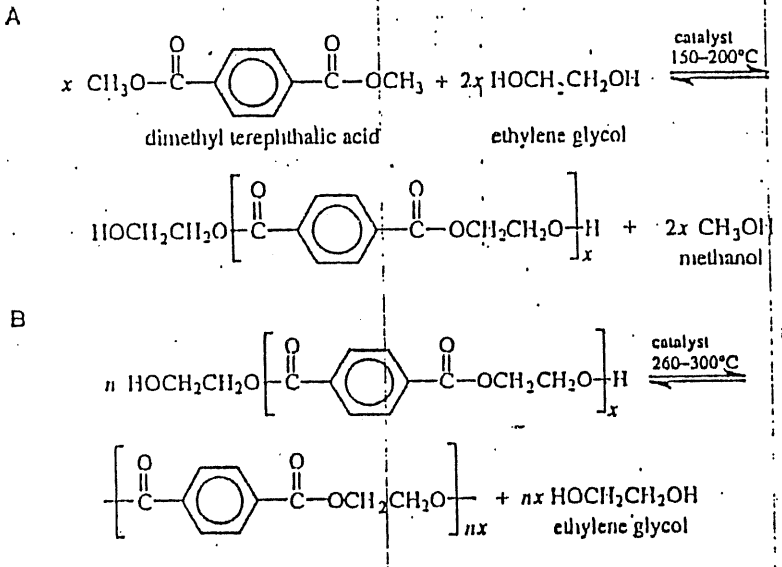

Figure 8.2. Two steps in the polymerization of poly(ethylene terephthalate). A. Ester interchange of dimethyl terephthalate and ethylene glycol. B. High-temperature esterification to yield high-molecular-weight polymer and ethylene glycol as a by-product.

The traditional route to the production of commercial PET is through two successive ester interchange reactions, as shown in Figure 8.2. The first step in the polymerization process (Figure 8.2A) involves an ester interchange of dimethyl terephthalate (DMT) and ethylene glycol at temperatures near 200°C during which methanol is removed and an oligomeric product ($n = 1 - 4$) is obtained. In the second stage (Figure 8.2B), increased temperature results in the formation of high-molecular-weight PET during which ethylene glycol is distilled off.

The total U.S. consumption of PET was approximately 6.0 billion pounds in 1993, of which 3.6 billion pounds were used for fiber applications, 1.58 billion pounds for bottles, and 0.87 billion for films (magnetic recording tape and photographic film). The market for molding grades of PET is growing at a rate of 11.5% as a result of the relative ease with which PET can be recycled. More than 38% of all soft-drink bottles and 28% of all PET containers were recycled in 1992. Although recycled PET cannot be used for beverage bottles, it can be used in the manufacture of other products such as insulation boards or can be thermally or chemically decomposed to its monomers, which can be used for the polymerization of virgin resin (see Section 6.2.1).

8.2 FIBERS

8.2.1 Natural and Synthetic Fibers

Naturally Occurring Fibers. Fibers obtained from natural resources were used for textile applications long before the first polymer was synthesized in the laboratory. These fibers include those derived from vegetables or plants, such as cotton and jute, and those obtained as animal products, especially wool and silk. The principal component of vegetable or plant fibers is cellulose or poly(β-1→4-D-anhydroglucopyranose), whose structure is shown in Figure 8.3. Cellulose is the most abundant of all natural polymers. In its purified form, cotton is nearly pure cellulose (94%) with only small amounts of related products (e.g., hemicellulose and pectin). With the exception of silk, the principal component of animal fibers is *keratin* — a natural cellular system of fibrous proteins that serves as the protective outer barrier (e.g., skin, hair, and scales) for high vertebrates. The protein of a silk filament, which is produced by the silkworm (the caterpillar of a small moth belonging to the species *Bombyx mori*), is *fibroin*, which has a simpler structure than keratin.

Representative properties of some important natural fibers are given in Table 8.5. The tensile strength of a fiber is usually expressed in terms of *tenacity*, which is grams (force) per denier. A *denier* is a measure of fiber thickness given as the fiber weight in grams per 9000 m. The corresponding SI unit is the tex (g per 1000 m). Tenacity is then expressed as mN/tex.

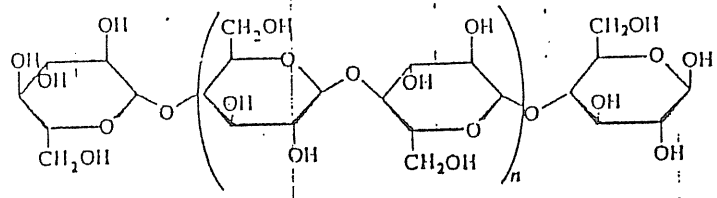

Figure 8.3. Structure of cellulose of $2n+2$ degree of polymerization.

TABLE 8.5 REPRESENTATIVE PROPERTIES OF SOME NATURAL AND SYNTHETIC FIBERS (at 65% relative humidity)

Fiber	Tenacity at Break, N/tex[a]	Extension at Break, %	Elastic Modulus, N/tex[a]	Specific Gravity
Natural Fibers				
Wool	0.09–0.15	25–35	2.2–3.1	1.30
Cotton	0.26–0.44	4–10	9–30	1.54
Cellulosics				
Cellulose[b]	0.12–0.33	10–30	3.7–5.8	1.50–1.54
Cellulose acetate[c]	0.09–0.13	25–40	2.2–3.5	1.30–1.35
Noncellulosics				
Polyester[d]	0.35–0.53	15–30	7.9	1.38
Nylon[d]	0.40–0.71	15–30	3.5	1.14
Acrylic[d]	0.40–0.44	15–20	5.3–6.2	1.17
Olefin (PP)	0.44–0.79	15–30	2.6–4.0	0.90

[a] To convert N/tex to g/den, multiply by 11.3.
[b] From viscose process.
[c] Secondary acetate (DS less than 2.4).
[d] Continuous filament.

Synthetic Fibers. Synthetic fibers are generally semicrystalline polymers that are capable of being spun into filaments of length-to-diameter ratios in excess of 100. Usually, fibers are uniaxially oriented during the spinning process (melt, dry, or wet) to give materials of high tenacity. Fibers may be spun from the melt or from concentrated solution (i.e., wet or dry spinning) as described in Section 8.2.4. Textile *yarns* of synthetic polymers are produced by twisting several

continuous fibers together to form a uniform structure with all filaments aligned parallel to the yarn axis.

Commercially processed fibers may be classified as cellulosic or noncellulosic. *Cellulosics*, regenerated cellulose (rayon) and cellulose acetate (acetate), are derived from naturally occurring cellulose through chemical reaction and modification. The *noncellulosics* (polyester, nylon, polyolefin, and acrylic) are all synthetic polymers. They easily constitute the largest part of the commercial market, as shown by the production data given in Table 8.6. The methods of synthesis and the spinning techniques used to prepare synthetic fibers are presented in the following sections.

TABLE 8.6 U.S. PRODUCTION OF SYNTHETIC FIBERS IN 1993

Fiber	Billions of Pounds	% of Total
Cellulosics		
Rayon	0.28	3.0
Acetate	0.23	2.5
Noncellulosics		
Polyester	3.56	38.3
Nylon	2.66	28.6
Olefin	2.14	23.0
Acrylic	0.43	4.6
TOTAL	9.30	

Source: *Chemical and Engineering News*, April 11, 1994.

8.2.2 Cellulosics

Cellulose. Cellulose obtained from wood pulp and short fibers left from cotton recovery is one of nature's most abundant biopolymers. A typical chain is composed of 200 to 6000 anhydroglucose units (molecular weight 300,000 to 1,000,000), each of which contain three hydroxyl groups and are linked by an acetal bridge (see Figure 8.3). The rigid chain of cellulose is strongly hydrogen bonded and highly crystalline. For these reasons, cellulose is essentially insoluble and infusible (i.e., degrades before melting) and, therefore, fibers and films can be obtained only by chemically modifying cellulose, as discussed next.

Cellulose in fiber (rayon) or film (cellophane) form is usually obtained by the viscose process, which dates to the 1920s. The approach is to regenerate cellulose from an intermediate soluble form, which is called *cellulose xanthate*. In this

highly capital and energy intensive process, cellulose pulp (wood pulp or cotton linters) is treated with a concentrated (18%) aqueous sodium hydroxide solution at room temperature. During treatment, cellulose is oxidatively degraded to lower molecular weight and is partially solubilized. After an aging period, the slurry is reacted with carbon disulfide (CS_2) to produce cellulose xanthate, whose structure is shown in Figure 8.4. Typically, about one in every six hydroxyls groups is reacted during this process. The yellow colloidal dispersion (viscose) of cellulose xanthate is spun into an aqueous bath of an acid (sulfuric) and a salt ($NaHSO_4$), which convert the xanthate back to cellulose, now in fiber form. During spinning, the fiber can be stretched to impart greater strength for textiles and tire-cord applications. Fibers obtained from regenerated cellulose are hydrophilic and have less developed crystalline structure than natural cellulose. Typical properties of cellulose fibers were given in Table 8.5.

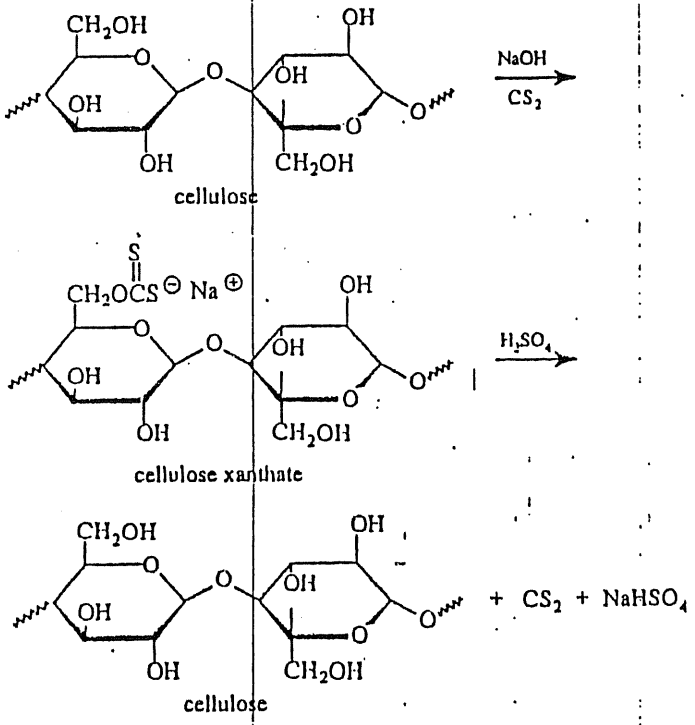

Figure 8.4. Viscose process for the production of regenerated cellulose.

Cellulose Derivatives. As shown in Figure 8.5, a cellulose derivative of important fiber and film properties, cellulose triacetate, is obtained by reacting cellulose with glacial acetic acid in the presence of acetic anhydride and traces of sulfuric acid in refluxing methylene chloride. Although CTA is still moderately crystalline, it has higher solubility than native cellulose and can be wet spun from a methylene chloride–alcohol mixture into toluene. This derivative can be partially hydrolyzed to give cellulose diacetate (CA), which conveniently can be dry spun from acetone. The secondary acetate groups of CTA are the least stable and, therefore, will hydrolyze first. About 65% to 75% of the acetate groups are left unhydrolyzed in commercial cellulose acetate. Cellulose acetate was first produced in 1865 and rapidly replaced its more volatile relative, cellulose nitrate. Large-scale production of cellulose acetate began during World War I.

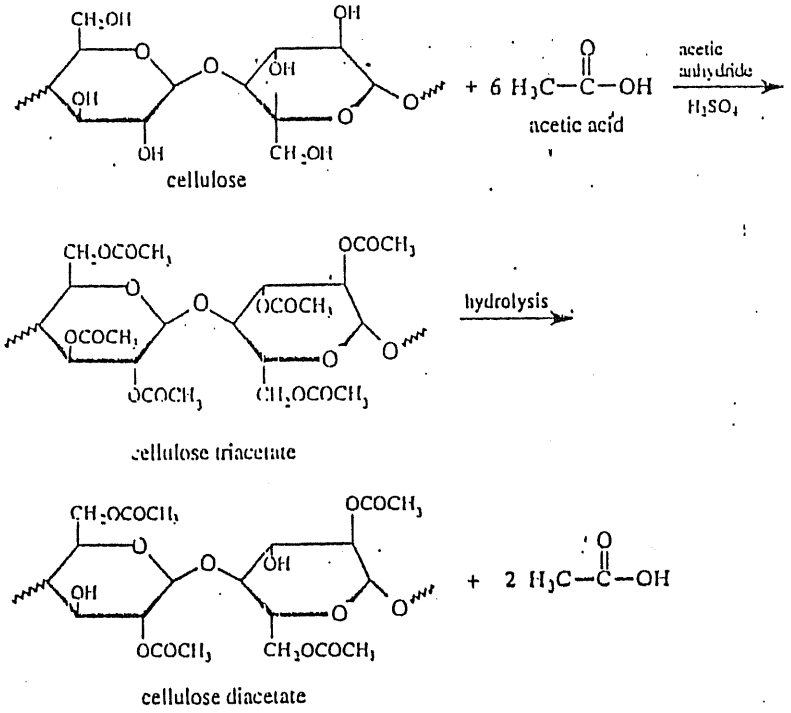

Figure 8.5. Acetylation of cellulose and partial hydrolysis of cellulose triacetate to yield cellulose dinceiate.

8.2.3 Noncellulosics

Polyesters. A polyester fiber is defined as one composed of at least 85 wt % of an ester of a dihydric alcohol (HOROH) and terephthalic acid whose structure is

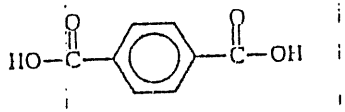

Of all possible polyester combinations, poly(ethylene terephthalate) (PET) is by far the most important and is the largest-volume synthetic fiber (see Table 8.6) although film (Mylar™) and bottle applications are important, as discussed in Section 8.1.3. The first polyester fibers became commercially available in the United States. in 1953 (Du Pont Dacron). About 61% of PET produced for fiber application is used for apparel. Staple blends of polyester and cotton are used for permanent-press garments. The remaining production finds applications in tire cord and home furnishing.

Poly(ethylene terephthalate) has a relatively low T_g (ca. 69°C) but a high T_m (ca. 265°C) with moderate crystallinity. Mechanical properties of polyester fiber are compared with other commercial fibers in Table 8.5. For fiber applications, typical molecular weights range from 10,000 to 15,000. Higher molecular weights provide high-strength fibers for industrial applications. Polyester is resistant to many solvents and to weak mineral acid. In addition, polyester fibers are abrasion and oxidation resistant and display good lightfastness.

Properties of polyester fibers can be modified by copolymerization or by blending with a variety of additives. For example, dyeability can be improved by copolymerization with small amounts of comonomers such as adipic acid and isophthalic acid, which increase the amorphous content available for penetration by disperse dyes. Additives are widely used to enhance properties such as fire retardancy (e.g., bromine or phosphorous compounds) and antistatic properties (e.g., carbon and PEG).

Polyamides. The next largest sales volume fibers are the polyamides, which find a major use in carpets, apparel, tire reinforcement, and various industrial applications. These are either A–A/B–B condensation polymers prepared from diamines and dicarboxylic acids or A–B condensation polymers prepared from lactams (see Chapter 2). The common linkage unit of polyamides is the amide group

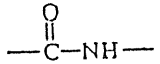

Aliphatic polyamides are called *nylons*. When at least 85% of the amide groups are attached to aromatic groups, the polyamides are generically called *aramids*. Aramids

(e.g., Nomex™ and Kevlar™) are expensive, high-performance fibers that are not used for consumer textile applications. Instead, they find important use as reinforcing fibers for composites, substitutes for asbestos, and material for tire cords (see Chapters 7 and 10). In addition to fiber applications, nylons are available as engineering thermoplastics that can be injection molded into a wide variety of products such as gear wheels, electrical switches and connectors, ski shoes, and automotive coolant tanks, as discussed in Section 10.1.1.

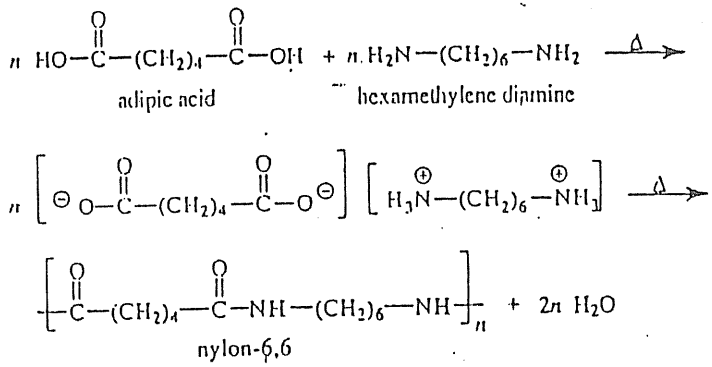

Figure 8.6. Synthesis of nylon-6.6 by means of the A–A/B–B step-growth polycondensation of adipic acid and hexamethylene diamine following an intermediate salt formation.

Principal among the A–A/B–B aliphatic polyamides is nylon-6,6 (or PA 66),[1] more descriptively called poly(hexamethylene adipamide). Nylon-6,6 is synthesized by the step-growth polymerization of hexamethylene diamine and adipic acid. An exact stoichiometric equivalence of functional groups is achieved by formation of an intermediate hexamethylene diammonium adipate salt, as shown in Figure 8.6. A slurry of 60% to 80% of recrystallized salt is heated rapidly, thereby releasing steam, which is air purged from the reaction vessel. Temperature is then raised to 220°C and finally to 270° to 280°C near the end of monomer conversion (80% to 90%). The pressure of steam generated during the polymerization is maintained at 1.38 to 1.72 MPa (200 to 250 psi). At this point, pressure is reduced to atmospheric and heating is continued until the polymerization is complete. Small concentrations of monofunctional acids, such as 0.5 mol % of aluric or acetic acid, may

[1] Nylons are designated by the number of carbons in the chain. The first and second numbers in the name of A–A/B–B polyamides such as nylon-6,6 refer to the number of carbons in the diamine and dicarboxylic acid, respectively. For example, a nylon prepared from hexamethylene diamine (6 carbons) and adipic acid (10 carbons) would be designated as nylon-6,10.

be added to the polymerization mixture to control molecular weight. Other nylons of less commercial importance may be made by using difunctional acids of longer or shorter chains.

Other important polyamides are obtained by the ring-opening polymerization of lactams. Poly(ε-caprolactam), or nylon-6 (PA 6), represents about 25% of total nylon production. High-molecular-weight nylon-6 may be obtained from the anionic polymerization of ε-caprolactam using strong bases such as sodium hydride or commercially by the hydrolytic polymerization of ε-caprolactam, as shown in Figure 8.7. Although the actual mechanism of the latter scheme is not fully understood, it is believed to involve a mixed chain- and step-growth mechanism involving the intermediate formation of the amino acid obtained from the ring opening of caprolactam.

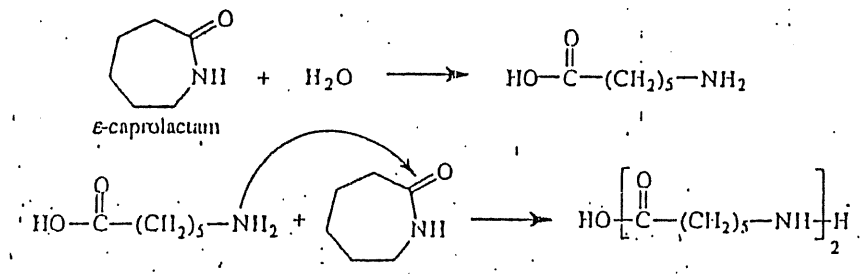

Figure 8.7. Hydrolytic polymerization of ε-caprolactam to the dimer. High-molecular-weight nylon-6 is obtained by the subsequent addition of caprolactam.

Acrylics. Acrylic fibers, primarily used for apparel (70%) and home furnishings (30%), are copolymers of principally acrylonitrile (AN). Polyacrylonitrile (PAN) alone cannot be used for thermoplastic applications because it undergoes cyclization at processing temperatures, as discussed in Chapter 6. The resulting "ladder" polymer can be used as a starting material for the preparation of graphite filaments, which are obtained by further heat treatment at elevated temperatures (see Section 7.1.2). Acrylonitrile (AN) finds use in thermoplastic and elastomeric applications only as a copolymer with other monomers such as styrene (e.g., ABS, SAN, and NBR). Like PVC, PAN is insoluble in its own monomer, which means that the polymer will precipitate during bulk polymerization. It can also be solution polymerized by free-radical mechanism in water or dimethyl formamide (DMF) with ammonium persulfate as initiator. The homopolymer can be dry spun from DMF directly from the polymerization reactor (or wet spun from DMF into water). Fibers are also made from copolymers with styrene, vinyl acetate, vinyl chloride, vinylpyridine, acrylic esters, and acrylamide. Fibers with greater than 85% AN content are termed *acrylic*, while those with lower AN composition (35% to 85%) are called *modacrylic*. The presence of the nitrile group (—C≡N) in acrylic fibers results in strong intermolecular hydrogen-bonding, allowing for high fiber strength.

Olefinics. Olefinic fibers as those that contain at least 85% of any olefin such as ethylene or propylene, the latter being the more common. Olefin fibers are used for home furnishings such as carpet and upholstery as well as some industrial applications, such as rope and geotextiles (used in soil engineering for separation, drainage, reinforcement, and filtration). Mechanical properties of polypropylene fibers are compared with other commodity fibers in Table 8.5. Generally, the advantages of olefin fibers include low cost and light weight, while disadvantages include susceptibility to compressive creep and UV degradation. Olefin fibers are hydrophobic and are resistant to most solvents. Unfortunately, these same properties impede dyeing. Acid-dyeable olefin fibers can be prepared by blending the polyolefin with a copolymer which provides suitable dye sites such as poly(vinyltoluene-*co*-α-methylstyrene), which greatly adds to the cost. Usually, olefin fibers are colored by blending the polyolefin with pigments prior to spinning.

8.2.4 Fiber-Spinning Operations

Three processes are commonly used to form polymeric fibers. These include spinning of a polymer melt, called melt spinning, and two processes that are used to spin fibers from a concentrated polymer solution — dry and wet spinning. Polyamide, polyester, and polyolefin fibers are typically obtained by the melt-spinning process. Solution spinning is used for cellulosic and acrylic fibers.

Melt Spinning. What may be viewed as the most direct process is called melt spinning, which was developed in the late 1930s. During a melt-spinning operation illustrated in Figure 8.8, a polymer is melted or extruded, clarified by a filter, and pumped by means of a gear pump through a die having one or more small holes. This die is called a *spinneret*. The extruded fiber leaving the spinneret is then cooled and may be uniaxially stretched by take-up rollers called *godets* rotating at different speeds. Fiber stretching orients the fiber chains or crystallites and, therefore, serves to increase modulus and strength in the longitudinal direction. Finally, the cooled oriented fiber is wound onto a spin bobbin for subsequent fiber treatment, such as texturing† and dyeing, before being woven into fabric. The most important classes of polymers that are melt spun includes the polyolefins (e.g., polyethylene and polypropylene), polyamides (e.g., nylon-6 and nylon-6,6), and polyester (PET). The relatively high melt-viscosity of the polyolefins requires the use of an extruder rather than a gear pump, such as may be used for nylons.

† In a texturing operation, straight fiber filaments are twisted or kinked to impart a property called *crimp*, which results in fabrics that have a more pleasing touch similar to those prepared from naturally produced fibers such as wool.

Typically, PET is melt spun at 286°C through a spinneret containing 24 orifices having 0.5-mm diameters. The average extrusion velocity is 1 to 20 m min^{-1}.

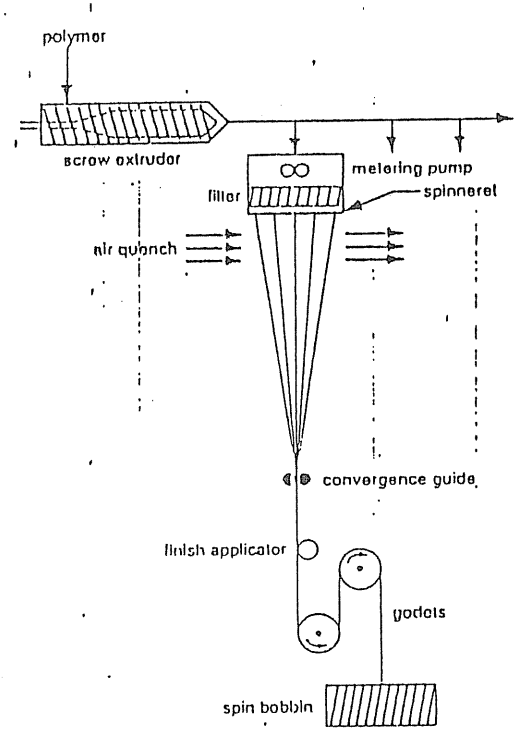

Figure 8.8. Melt spinning of synthetic polymers. (Adapted from J. E. McIntyre and M. J. Denton, in the *Concise Encyclopedia of Polymer Science and Engineering*, J. I. Kroschwitz, ed., John Wiley & Sons, New York, 1990. Copyright © 1990 John Wiley & Sons. Reprinted by permission of John Wiley & Sons, Inc.)

Dry and Wet Spinning. Polymer concentrations in solutions used for dry or wet spinning are typically in the range of 20 to 40 wt %. During a *dry-spinning* process, illustrated in Figure 8.9, the solution is filtered and pumped through a spinneret into a spinning cabinet (up to 25 ft in length) through which heated air is passed. Solvent from the fiber rapidly evaporates into the airstream and is then carried out of the spinning cabinet for future solvent recovery. For this purpose, volatile solvents such as acetone and carbon disulfide are sometimes used. Water has been used as a solvent for the dry spinning of fibers from poly(vinyl alcohol) (PVA). The dried fiber is then oriented and wound onto a bobbin. The

speed of a dry-spinning line can be very high compared to melt- or wet-spinning operations — up to 1000 m min^{-1}. Commodity fibers that are dry spun include cellulose acetate and acrylics.

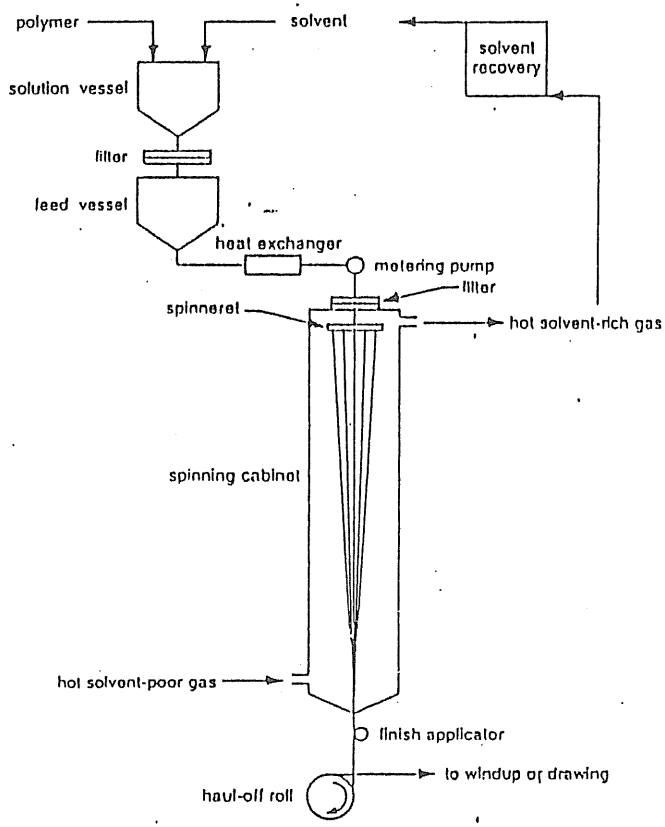

Figure 8.9. Typical process for the dry spinning of synthetic fibers. (Adapted from J. E. McIntyre and M. J. Denton, in the *Concise Encyclopedia of Polymer Science and Engineering*, J. I. Kroschwitz, ed., John Wiley & Sons, New York, 1990. Copyright © 1990 John Wiley & Sons. Reprinted by permission of John Wiley & Sons, Inc.)

Wet spinning, one of the oldest fiber-production methods, differs from dry spinning in that fiber formation results from the coagulation of the polymer solution by immersion in a nonsolvent such as water. As illustrated in Figure 8.10, the spinneret is directly immersed in the nonsolvent bath. Since the coagulation

process is slow, the linear velocity of a wet-spinning line is much slower than either melt- or dry-spinning operations; however, high productivity can be obtained by spinning multiple fibers from a single spinneret. The viscose process used to prepare regenerated cellulose (rayon) fiber (see Section 8.2.2) is a wet-spinning process that employs chemical modification of the side groups of cellulose in both the solution and coagulation step to control solubility properties. Wet spinning has been used to obtain fibers of PVA, poly(vinyl chloride), and polyacrylonitrile (PAN). In the case of PAN, fibers can be wet spun from dimethylformamide (DMF) solution into dimethylacetamide (DMAC) or from 50% sodium thiocyanate into aqueous 10% sodium thiocyanate. Polyurethane elastomers such as Spandex™ (see Section 9.1.2) can be wet-spun from DMF solution into water.

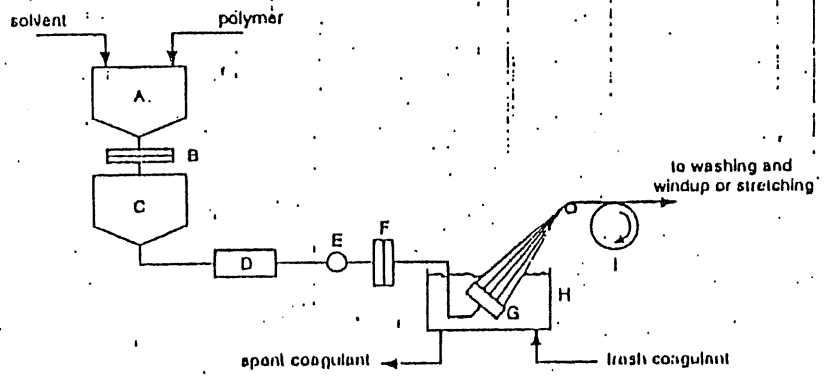

Figure 8.10. Wet-spinning process. A, solution vessel; B and F, filters; C, feed vessel; D, heat exchanger; E, metering pump; G, spinneret; H, spin bath containing coagulant; I, haul-off roll. (Adapted from J. E. McIntyre and M. J. Denton, in the *Concise Encyclopedia of Polymer Science and Engineering*, J. I. Kroschwitz, ed., John Wiley & Sons, New York, 1990. Copyright © 1990 John Wiley & Sons. Reprinted by permission of John Wiley & Sons, Inc.)

For some specialized applications, such as the spinning of hollow-fiber membranes for gas or liquid separation (see Section 12.1.3), the extruded fiber may first pass through air before entering the bath. If the parameters of the spinning process, such as the concentration of the spinning solution, temperature, and extent of air-drying are properly chosen, it is possible to spin asymmetric fibers having a dense thin skin on top of a thick microporous support layer. The thin top layer provides high flux and good selectivity.

BIBLIOGRAPHY

E. Doelker, "Cellulose Derivatives," *Adv. Polym. Sci.*, 107, 199–265 (1993).

M. Grayson, ed., *Encyclopedia of Textiles, Fibers and Nonwoven Fabrics*, Wiley-Interscience, New York, 1984.

M. Lewin and E. M. Pearce, eds., *Handbook of Fiber Science and Technology, Vol. IV: Fiber Chemistry*, Marcel Dekker, New York, 1985.

L. I. Nass and C. A. Heiberger, eds., *Encyclopedia of PVC*, 2nd ed., Marcel Dekker, New York, 1986.

T. Xie, K. B. McAuley, J. C. C. Hsu, and D. W. Bacon, "Gas Phase Ethylene Polymerization: Production Processes, Polymer Properties, and Reactor Modeling," *Ind. Eng. Chem. Res.*, 33, 449–479 (1994).

9

Network Polymers: Elastomers and Thermosets

Of the total synthetic polymer production of 67.35 billion pounds in the United States during 1993, the major synthetic elastomers accounted for about 7.4% and thermosetting resins about 10%. The principal feature of both thermosets and conventional elastomers that distinguishes them from thermoplastic materials is the formation of a network structure upon fabrication. This network may be formed by covalent, or sometimes physical links that connect individual molecules. If only a few such links are formed, the material can be deformed but will return to its original form upon release of the applied force, provided the force is not so great as to rupture the bonds. Polymers that have limited or no crystallinity, have low softening temperatures (glass-transition temperatures in the range from -50° to -70°C), and can be crosslinked in the above manner are candidates for synthetic-elastomer applications. Polymeric materials that have a high density of crosslinks and are therefore infusible, insoluble, and dimensionally stable under load are called *thermosets*.

9.1 ELASTOMERS

Elastomers can be broadly classified as belonging to one of three groups: diene elastomers, nondiene elastomers, and thermoplastic elastomers. Diene elas-

tomers such as polybutadiene, polyisoprene, and polychloroprene are polymerized from monomers containing two sequential double bonds (a diene) having the structure

where R represents a substituent group such as a hydrogen atom (in the case of polybutadiene synthesis), a chlorine atom (in polychloroprene synthesis), or a methyl group (in polyisoprene synthesis). As discussed in Section 9.1.1, polymerization results in a repeating unit containing a single double bond that can provide a site for subsequent crosslinking (i.e., vulcanization). Diene elastomers, including diene copolymers such as styrene–butadiene elastomers (SBR) and nitrile rubber (a copolymer of butadiene and acrylonitrile), represent the largest fraction of the U.S. synthetic-rubber production, as shown by the data given in Table 9.1.

TABLE 9.1 U.S. PRODUCTION OF SYNTHETIC RUBBER IN 1993

Synthetic Rubber	Billions of lb	% Total Rubber Production
SBR rubber	1.89	37.8
Polybutadiene	1.03	20.6
EP rubber	0.58	11.6
Nitrile rubber	0.14	2.8
Other (neoprene, butyl rubber, polyisoprene)	1.37	27.4
TOTAL	5.00	

Source: *Chemical and Engineering News*, April 11, 1994.

Nondiene elastomers includes polyisobutylene, polysiloxanes (silicone rubber), and a number of specialty elastomers, such as polyurethane (Spandex™), and fluoroelastomers, such as Viton™. Nondiene elastomers have no unsaturated sites and, therefore, crosslinking requires alternative methods to vulcanization, such as the use of trifunctional monomers in the case of condensation polymerizations (e.g., polysiloxanes), by the use of free-radical initiators, or by copolymerization with a small amount of a diene monomer (e.g., polybutadiene).

Thermoplastic elastomers such as SBS terpolymer are thermoplastics that contain rigid ("glassy") and soft ("rubbery") segments that can be thermally processed, unlike chemically crosslinked elastomers. Upon cooling, the soft and rigid segments phase separate into physically distinct domains whereby the rigid domains serve as physical anchors for the rubbery segments and, thereby, provide a restoring force when the thermoplastic elastomer is stretched. The methods of synthesis and the properties of these three classes of elastomers are reviewed in the following sections. The principles of rubber elasticity were developed in Section 5.2.

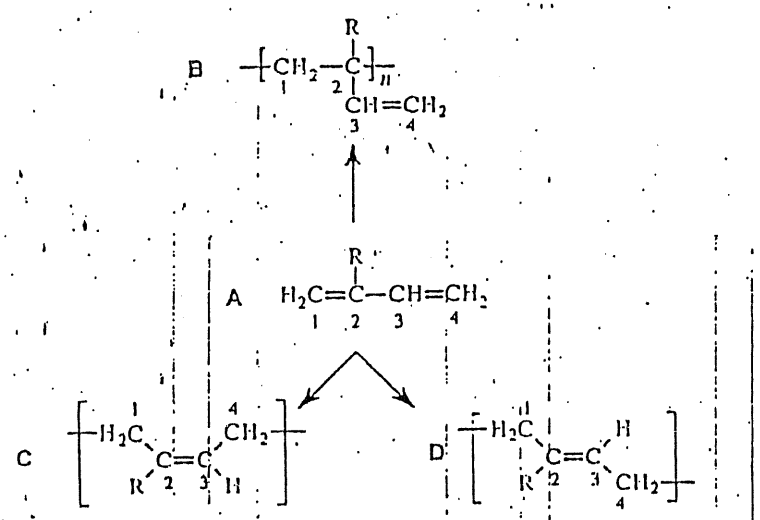

Substituent, R	Monomer	Elastomer
H	1,3-Butadiene	Polybutadiene
Cl	2-Chloro-1,3-butadiene	Polychloroprene
CH_3	2-Methyl-1,3-butadiene	Polyisoprene

Figure 9.1. Polymerization of diene monomer (A) to yield a 1,2- (B), *cis*-1,4- (C), and *trans*-1,4-structures (D). Different elastomers are obtained depending upon the substituent group, R.

9.1.1 Diene Elastomers

One way to form an elastomeric network is by the chemical bonding of two unsaturated carbons located on adjacent polymer molecules. Elastomers containing unsaturated sites include some of the most important synthetic rubbers, such as polybutadiene, polyisoprene, and polychloroprene. As shown in Figure 9.1, conjugated dienes such as isoprene and chloroprene can be polymerized to give either a

1,2-, 3,4-, or 1,4-polymer. In the case of 1,4-polymers, both *cis* and *trans* configurations are possible. In the case of the polymerization of 1,3-butadiene, for which there is no asymmetric substitute group, the 1,2- and 3,4- structures are identical. The proportion of each type of structure incorporated into the polymer chain influences both thermal and physical properties and is controlled by the conditions and method of polymerization. For example, butadiene can be polymerized by free-radical addition (see Chapter 2) at low temperature to give a polymer that is mostly *trans*-1,4 with only about 20% 1,2-structure. As the polymerization temperature is increased, the amount of *cis*-1,4 structure increases, while the proportion of 1,2-structure remains about the same.

Dienes can also be prepared by anionic polymerization using lithium or organolithium initiators like *n*-butyllithium in nonpolar solvents like pentane or hexane to yield polymers with high *cis*-1,4 content. The proportion of *cis*-1,4 structure decreases when higher alkali-metal initiators or more polar solvents are employed. Stereoregularity can also be controlled by use of selective coordination catalysts like Ziegler–Natta (see Chapter 2) or heterogeneous Alfin catalysts, which are combinations of alkenyl sodium compounds, alkali metal halides, and an alkoxide. Use of the latter system gives high-molecular-weight, high *trans*-1,4 content polymers.

Butadiene-Based Elastomers. Of all synthetic elastomers, polybutadiene and butadiene copolymers enjoy the largest sales share. As shown by the data given in Table 9.1, sales of polybutadiene (BR) in 1993 accounted for over 1 billion pounds, which makes it the second largest volume synthetic rubber, next only to styrene–butadiene copolymers (SBR). SBR accounted for 1.89 billion pounds or 38% of the total 1993 synthetic-rubber production. The principal use of both BR and SBR is in the production of tires and tire products, which are typically blends of both natural and synthetic rubbers. BR exhibits properties of good resilience, abrasion resistance, and low heat-buildup. These are important properties for tire applications.

SBR is a highly random copolymer of butadiene and 10% to 25% styrene. The addition of styrene results in a lower price and contributes to the good wearing and bonding characteristics of SBR. In addition, strength, abrasion resistance, and blend compatibility are improved over BR alone. Like BR, SBR can be polymerized by a free-radical mechanism in emulsion either at 30° to 60°C (hot rubber) or near 0°C (cold rubber). A typical composition of the butadiene portion of SBR is approximately 70% of *trans*-1,4-polybutadiene, 15% to 20% of *cis*-1,4-polybutadiene, and 15% to 20% of 1,2-polybutadiene. Coordination copolymerization in solution yields a SBR product (stereo SBR) that has a higher molecular weight, narrower molecular-weight distribution, and higher *cis*-1,4-content than emulsion-polymerized SBR.

Butadiene can also be copolymerized with 15% to 40% acrylonitrile in either hot or cold free-radical emulsion polymerization. The resulting elastomer, NBR or *nitrile rubber*, has improved oil and aromatic solvent resistance and, therefore, can

be used as material for gaskets, tubing, O-rings, and gasoline hose. NBR, whose production was 140 million pounds in the United States during 1993, can also be used as a blend component in tire manufacture.

Polyisoprene. Polyisoprene occurs in nature but can also be produced synthetically. Natural rubber (NR) used in tire manufacture is nearly all *cis*-1,4 polyisoprene, which is obtained from the tree *Hevea brasiliensis* (Hevea rubber) as a latex containing about 35% rubber and 5% solids (e.g., proteins, sugars, resins, and salts). The rubber is obtained by coagulation of the latex. Another source of NR is the shrub guayule, which occurs in parts of the United States and Mexico. The *trans*-isomer of polyisoprene is also obtained from tree products (e.g., gutta percha and balata) but has only limited commercial use in nonelastomeric applications (originally as covers for golf balls and, more recently, as material for orthopedic splints). The synthetic equivalent of *cis*-1,4-polyisoprene (IR) can be obtained by polymerizing 2-methyl-1,3-butadiene (Figure 9.1) with Ziegler–Natta and Alfin catalysts. High *trans*-content polyisoprene may also be obtained by appropriate catalyst selection. IR has many of the good properties of its naturally occurring counterpart including high resilience, strength, and abrasion resistance. As in the case of most other diene-based elastomers, IR has poor resistance to attack by ozone, gasoline, oil, and organic solvents.

Polychloroprene. Another important diene-based elastomer is polychloroprene (neoprene), or CR. Compared to the other elastomers in this class, CR exhibits good resistance to attack by oxygen, ozone, oil, and gas. For these reasons, CR is used primarily as material for gaskets, tubing, O-rings, seals, and gasoline hose. The commercial material is mostly *trans*-1,4-polychloroprene produced by free-radical emulsion-polymerization of 2-chloro-1,3-butadiene (Figure 9.1).

Metathesis Elastomers. At present, polynorbornene and polyoctenamer are two commercial elastomers produced by ring-opening metathesis polymerization, which was discussed in Section 2.5.1. These specialty elastomers offer high oil absorptivity (polynorbornene) and high strength (polyoctenamer). Recent advances have shown that other elastomers, including polybutadiene as well as block and graft copolymers, can be made by metathesis.[1]

Vulcanization. Uncrosslinked rubber products such as natural rubber obtained from the latex of the *Hevea brasiliensis* tree are tacky, gummy materials, much like chewing gum, having none of the resiliency and permanent set we normally associate with commercial rubber products such as rubber bands, rubber hose, and tires. To obtain a network structure, diene elastomers are crosslinked by use of peroxides, ionizing radiation, and especially sulfur or sulfur-containing compounds. An illustration of a crosslinked elastomeric network is shown in Figure 9.2.

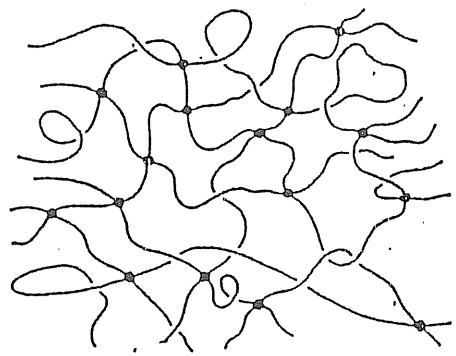

Figure 9.2. Idealized representation of a crosslinked elastomeric network. Filled circles indicate crosslink points (e.g., polysulfide bridges). (J. E. Mark and B. Erman, *Rubberlike Elasticity — A Molecular Primer*)

In the traditional method of vulcanization, which dates back to 1839, the rubber compound is heated with elemental sulfur. Sulfur bridges between individual elastomer molecules are formed by what is believed to be an ionic mechanism involving addition to the double bond. Concentration of sulfur in the vulcanized product is typically 3 parts per hundred (pph) parts of elastomer compared to about 30 pph in highly crosslinked, hard rubber such as ebonite. The traditional vulcanization process is slow and inefficient as long sulfur bridges and cyclic sulfur structures can form. The process is improved by addition of accelerators such as thiuram disulfides, dithiocarbamates, and benzothiazoles. Activators such as zinc oxide and stearic acid serve to reduce the concentration of cyclic sulfide units and promote the formation of shorter-chain sulfide bridges. In addition to these additives, typical formulations for commercial rubber may include antioxidants and reinforcing fillers (see Chapter 7).

A typical formulation for the vulcanization of a diene elastomer includes the following:

Component	phr
Sulfur	0.5–4
Fatty acid	1–4
Zinc oxide	2–10
Accelerator	0.5–2

In this formulation, the fatty acid (e.g., stearic acid) and zinc oxide serve as the vulcanization activators. It is believed that the activators form a salt that complexes with the accelerator. Through this process, the accelerator forms a monomeric

polysulfide as illustrated in Figure 9.3. The Ac group indicated in Figure 9.3 is an organic radical derived from the accelerator. An example is the benzothiazolyl group

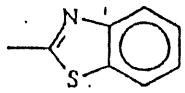

This monomeric polysulfide then reacts with an unsaturated site of an elastomer chain to produce a rubber polysulfide and finally with another chain to form a polysulfide bridge. Typical molecular weight between crosslink points ranges from approximately 4000 to 10,000 where the molecular weight of individual chains is on the order of 100,000 to 500,000.

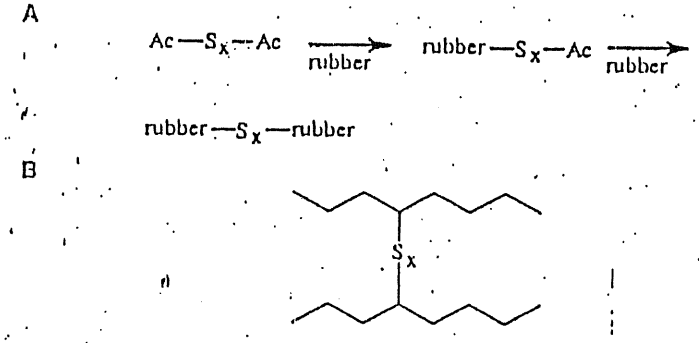

Figure 9.3. A. Illustration of steps in a vulcanization process where monomeric polysulfides formed by reaction of elemental sulfur with an accelerator reacts with individual polymer chains to form a polysulfide bridge. B. Illustration of a polysulfide bridge forming a crosslink between two chains.

9.1.2 Nondiene Elastomers

A number of important elastomers do not have the unsaturated chain structure characteristic of the diene elastomer. These nondiene elastomers include polyisobutylene (butyl rubber), polysiloxane (silicone rubber), fluoroelastomers such as Viton, polyurethane elastomers such as Spandex, and elastomers derived from ethylene and propylene (EP and EPDM elastomers). When included with the diene-elastomer polyisoprene (IR), these represent approximately 27% of the total U.S. synthetic rubber production in 1993 (Table 9.1). In two cases — butyl rubber and EPDM — a small amount of diene monomer that provides a site for vulcanization is included by means of copolymerization. For the other nondiene elastomers, free-radical initiators or polyfunctional monomers are used for network formation.

The absence or low concentrations of double bonds in the main chain of these elastomers results in high resistance to attack by oxygen and ozone and superior chemical resistance of these specialty rubbers compared to diene elastomers.

Polyisobutylene. Polyisobutylene or butyl rubber is marketed as a copolymer (IIR rubber) containing about 0.5% to 2% of isoprene, which provides the necessary unsaturation sites for vulcanization. Butyl rubber exhibits outstanding resistance to attack by oxygen and ozone and exhibits low gas permeability. For these reasons, it finds principal usage in weather stripping and inner tubes. High-molecular-weight butyl rubber may be prepared by low-temperature cationic polymerization using Lewis acids like aluminum chloride in chlorocarbon solvents such as chloromethane.

Polysiloxanes. Silicone elastomers have high-temperature and oxidative stability, low-temperature flexibility, good electrical properties, and resistance to weathering and oil. Typical applications include wire and cable insulation, surgical implants, gasket material and seals, and aircraft tubing. Polysiloxanes can be prepared by the hydrolysis of dichlorosilanes such as dimethyldichlorosilane, as shown in Figure 9.4. This process is unsatisfactory to obtain high-molecular-weight polymer because of a tendency to form cyclic siloxanes, typically trimers and tetramers. High-molecular-weight polymer suitable for elastomer applications can be obtained by subsequent base-catalyzed ring-opening polymerization of the cyclic products. Crosslinked siloxane elastomers may be obtained by cohydrolysis of dichlorosilanes with alkyl-trichlorosilanes, which provide an additional functional group for polymerization. Alternately, polydimethylsiloxane can be crosslinked by the use of peroxides. The efficiency of the vulcanization step is greatly enhanced by incorporation of unsaturated sites through copolymerization with vinyl-group-containing siloxanes such as vinylmethylsilanol.

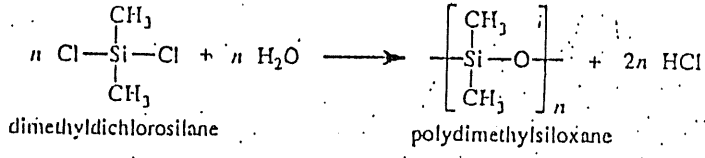

Figure 9.4. Polymerization of polydimethylsiloxane by the hydrolysis of dimethyldichlorosilane.

Fluoroelastomers. Most fluoroelastomers are obtained by high-pressure, free-radical emulsion polymerizations using organic or inorganic initiators. Most are copolymers of fluorinated polyolefins (tetrafluoroethylene and hexafluoropropylene) with vinylidene fluoride. Examples of common fluoroelastomers are

given in Table 9.2. Fluorocarbon elastomers are capable of meeting demanding service applications, including operation over a broad temperature range and exposure to a wide range of chemicals and petroleum products. Uses include hose, tubing, O-rings, and gaskets in automotive, petrochemical, petroleum, and hydraulic applications.

TABLE 9.2 EXAMPLES OF FLUOROELASTOMERS

Fluoroelastomer	Common Trademarks
Poly(vinylidene fluoride-*co*-hexafluoropropylene)	Viton, Fluorel
Poly(vinylidene fluoride-*co*-hexafluoropropylene-*co*-tetrafluoroethylene)	Viton, Fluorel
Poly[vinylidene fluoride-*co*-tetrafluoroethylene-*co*-perfluoro(methyl vinyl ether)]	Viton
Poly[tetrafluoroethylene-*co*-perfluoro(methyl vinyl ether)]	Kalrez
Poly(tetrafluoroethylene-*co*-propylene)	Aflas
Poly(vinylidene fluoride-*co*-chlorotrifluoroethylene)	Kel-F

Fluoroelastomers are compounded with various fillers, processing aids, accelerators, and curatives and then extruded into the desired form such as tubing or O-ring cord. The extrudate is then postcured at 200° to 260°C for up to 24 h to achieve maximum mechanical properties.

Polyurethanes. Polyurethanes (PUR) were developed by Otto Bayer and co-workers in 1937. These polymers have high strength, good resistance to gas, oil, and aromatic hydrocarbons, high abrasion resistance, and excellent resistance to oxygen and ozone, but are susceptible to microbial attack. Applications include shoe soles, solid tires, and impellers. Although the majority of polyurethane usage is for rigid and flexible foams first produced in the 1950s (see Section 7.1.3), about 15% of polyurethane production is for elastomers applications. The preparation of polyurethane elastomers is discussed in this section.

In general, polyurethanes can be prepared either by the step-growth polymerization of diisocyanates with dihydroxyl compounds or, less commonly, by the reaction of bischloroformates with diamines, as illustrated in Figure 9.5. Isocyanates, esters of isocyanic acid (HNCO), can be aliphatic, cycloaliphatic, or polycyclic. Typical diisocyanates include methylene-4,4'-diphenyldiisocyanate (MDI), toluene-2,4-diisocyanate (TDI),[1] and hexamethylene diisocyanate (HMI), as shown in Table 9.3. Dihydroxyl compounds are typically low-molecular-weight hydroxyl-terminated polyesters or polyethers such as poly(tetrahydrofuran) (PTHF). Isocyanates or hydroxyl compounds with functionalities greater than two can be used to introduce branched groups or crosslinks. Characteristic of polyurethanes is the presence of a carbamate group

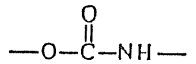

in the chain backbone. Depending upon the reactants, other chain groups can include ester, ether, ether, amide, or urea.

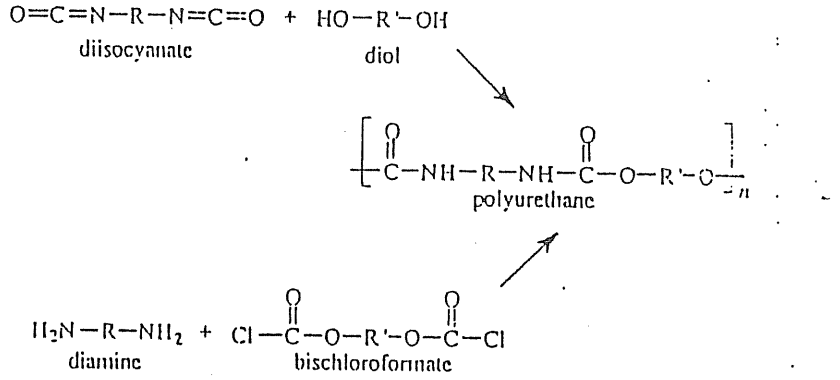

Figure 9.5. Two routes to the synthesis of polyurethanes.

Polyurethane elastomers can be obtained by the formation of $(AB)_n$-block copolymers consisting of alternating "soft" and "hard" segments. Typically, polyurethane elastomers are prepared by reacting an excess of an aromatic diisocyanate (e.g., MDI or TDI) with a hydroxy-terminated polyether or polyester (2000 to 3000 molecular weight) to yield an isocyanate-terminated prepolymer. A typical polyether is poly(propylene glycol)

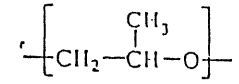

[1] Often used as a mixture with its 2,6-isomer.

while a typical polyester is poly(diethyleneglycol adipate)

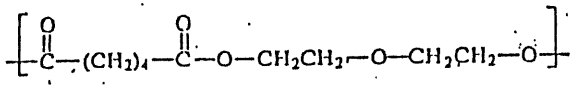

TABLE 9.3 EXAMPLES OF TYPICAL DIISOCYANATES

Diisocyanate	Abbreviation	Structure
Methylene-4,4'-diphenyldiisocyanate	MDI	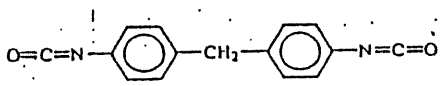
4,4'-Methylene-bis(cyclohexylisocyanate)	H_{12}MDI	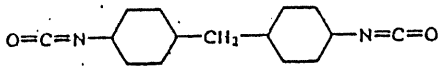
Toluene-2,4-diisocyanate[1]	TDI	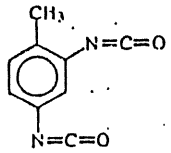
Hexamethylene diisocyanate	HMI	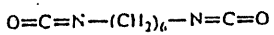
Naphthalene-1,5-diisocyanate	NDI	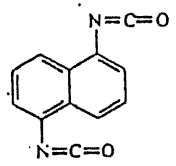

As illustrated in Figure 9.6, the prepolymer can then be reacted with a diamine chain extender, such as ethylenediamine, to give the high-molecular-weight elastomer through a uren linkage

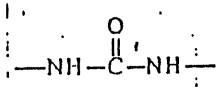

As indicated in Figure 9.6, the soft blocks of the copolymer are the flexible polyether/polyester segments, which constitute the bulk of the elastomer and form an amorphous continuous phase whose T_g is above normal-use temperature. The hard segments ($T_g < T$) segregate into crystalline microdomains, which serve as physical anchor sites or crosslinks. When the polyurethane elastomer is stretched, the soft segments elongate and crystallize until tension is released.

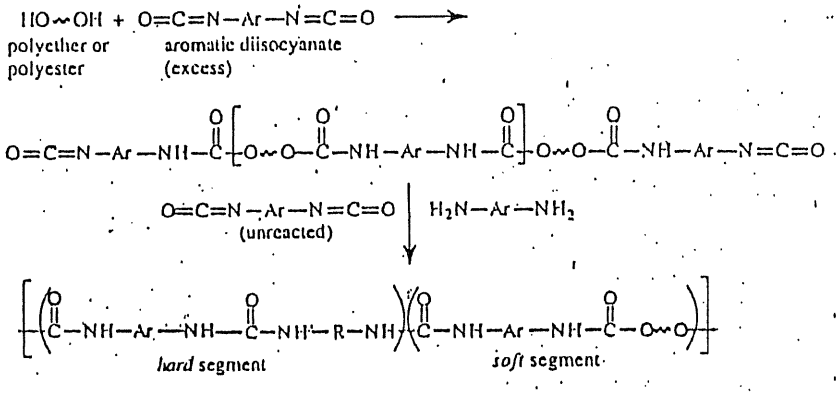

Figure 9.6. Synthesis of an elastomeric polyurethane for fiber applications.

Applications for polyurethane elastomers include use in the manufacture of foundation garments, surgical hose, and swimsuits. These elastomers are easily dyed and have high strength, chemical resistance, and elastic recovery.

Elastomers from Polyolefins. Random copolymers of ethylene and propylene (EPM rubber) can be prepared by use of soluble Ziegler–Natta catalysts (see Section 2.2.3) at controlled ethylene–propylene monomer concentration. The random placement of monomer units limits crystallinity and results in a rubbery material that can be crosslinked with peroxides through hydrogen abstraction and subsequent radical combination. Alternately, an unsaturated terpolymer (EPDM rubber) can be prepared from ethylene, propylene, and unconjugated dienes like dicyclopentadiene, cyclooctadiene, and 1,4-hexadiene. These unsaturated terpolymer may be vulcanized by traditional means. EPM and EPDM have good resistance to acids, good weatherability and color stability, and good electrical stability and may be used as substitutes for SBR and neoprene in automotive applications such as in tires, radiator hose, gaskets, and seals. EPM and EPDM are also used in wire and cable insulation, weather stripping, and in footwear. Blends of polypropylene and EPDM are used as material in the manufacture of car bumpers.

9.1.3 Thermoplastic Elastomers

Commercial elastomers can be made without the formation of the permanent crosslinks that are normally created through vulcanization. In place of covalent bonds, rigid-domain structures are used to create a network structure, as illustrated in Figure 9.7. These are typically the crystalline or glassy phases associated with the crystalline or glassy blocks of block copolymers or result from associations formed through the creation of secondary bonds such as hydrogen bonding between chemical groups in different molecules. Since these domains are physical in nature, they are normally reversible and therefore elastomers belonging to this class are thermoplastic and can be fabricated by conventional molding techniques. Thermoplastic elastomers can be made from polyurethanes, polyesters, polyolefins, and styrenic block copolymers. The absence of a separate vulcanization step and easy recycling of these materials have led to the rapid commercialization of thermoplastic elastomers over the last 20 years.

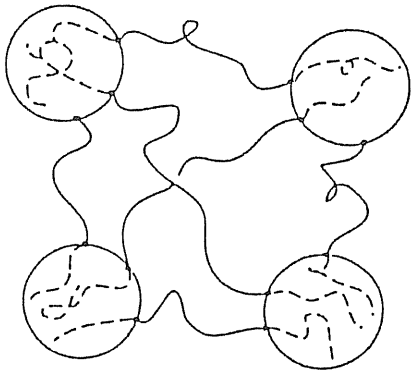

Figure 9.7. Representation of glassy domains in a thermoplastic elastomer such as SBS, polystyrene-*block*-polybutadiene-*block*-polystyrene. Circles represent physically separated domains of high glassy-polymer (e.g., polystyrene) content that serve as physical crosslinks. Glassy domains are interconnected by the elastomeric (e.g., polybutadiene) segments. (Adapted from L. H. Sperling, *Introduction to Physical Polymer Science*., Copyright ©1986. Reprinted by permission of John Wiley & Sons, Inc.)

SBS Elastomers. The most commercially important thermoplastic elastomers are ABA block copolymers composed of a high-molecular-weight (50 to 100,000) polystyrene end block and a central block of low-molecular-weight (10 to 20,000) polybutadiene (YSBR) or other olefins such as isoprene and ethylene-butylene. When cooled from the melt to below their glass-transition temperature, the PS-blocks phase separate to form rigid glassy domains that act as physical

crosslinks for the elastomeric olefin blocks. These block copolymers are prepared by anionic "living" polymerization as discussed in Section 2.2.2. As a class, they have higher tensile strength then SBR rubber but have limited heat resistance. YSBR can be hydrogenated to improve weather and temperature resistance. Blends of styrenic thermoplastic elastomers are used in rubber bands, toy products, shoe soles, and gasket material. YSBR containing 30% polybutadiene content may be blended with PS to produce a resin suitable for thermoforming plastic drinking cups. PS alone is too brittle to withstand the high extension resulting from thermoforming (see Section 11.1.2).

Olefinic Elastomers. Olefinic thermoplastic elastomers, prepared by use of Ziegler–Natta catalysts (see Section 2.2.3), include *polyallomers*, which are block copolymers of polypropylene (the hard, crystalline block) and a second olefinic block, usually ethylene or ethylene and a diene (EPDM). EPDM block copolymers are attractive replacements for neoprene in oil-resistant wire and cable insulation as a result of their better processability and coloration properties.

Urethane Elastomers. Thermoplastic polyurethanes contain "soft" or flexible (low T_g) blocks of a long-chain aliphatic polyester or polyether and "hard" blocks formed by reacting isocyanates and short-chain diols. Intermolecular hydrogen bonding between urethane groups results in domain association of hard blocks, which provides a restorative force when these elastomers are stretched. Thermoplastic polyurethanes exhibit good abrasion and mar resistance and are stable to attack by hydrocarbons and oxygen, although they are susceptible to strong acids and oxygenated solvents like ketones. Applications include coatings, adhesives, footwear, and automotive parts. Polyester-based polyurethanes are less expensive and have better oxidative and high-temperature stability than do polyether-based polyurethanes, which have better hydrolytic stability and lower temperature flexibility.

Copolyesters. Thermoplastic copolyesters consist of a hard (crystalline) polyester block, such as formed by the reaction of terephthalic acid and butanediol, and an amorphous long-chain polyester (e.g., polytetramethylene ether glycol) soft block. Like thermoplastic polyurethanes, they have good hydrocarbon and abrasion resistance. Applications include wire and cable insulation, gaskets, seals, hose, and automotive parts.

9.2 THERMOSETS

Principal commercial thermosets include epoxies, polyesters, and formaldehyde-based resins (i.e., urea–formaldehyde and melamine–formaldehyde). As a group, these thermosets represented approximately 12% of the synthetic polymer production in the United States during 1993 as shown by the data given in

Table 9.4. Synthesis and properties of the principal thermoset resins are given in this section.

TABLE 9.4 U.S. THERMOSET PRODUCTION
(billions of pounds)

	1993	1992
Thermosetting Resins		
Phenol resins	3.08	2.92
Urea resins	1.74	1.55
Polyesters (unsaturated)	1.26	1.18
Epoxies	0.51	0.46
Melamine resins	0.27	0.23
TOTAL	6.87	6.34

Source: *Chemical and Engineering News*, April 11, 1994.

9.2.1 Epoxies

Epoxies are complex network polymers usually formed in a two-stage process. Initially, a low-molecular-weight prepolymer is prepared by a base-catalyzed step-growth reaction of a dihydroxy compound such as bisphenol-A with an epoxide, typically epichlorohydrin, as illustrated in Figure 9.8.

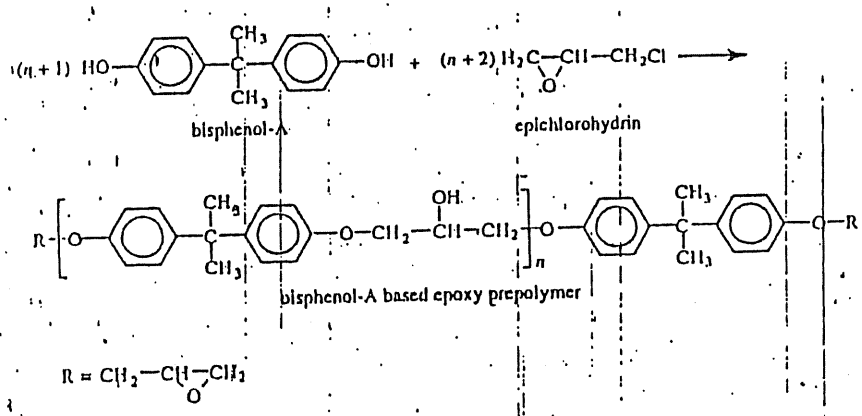

Figure 9.8. Formation of an epoxy prepolymer by reaction of bisphenol-A and epichlorohydrin.

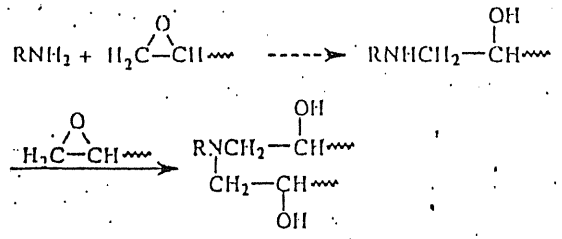

Figure 9.9. Cure of an epoxy resin by reaction of the prepolymer with an amine.

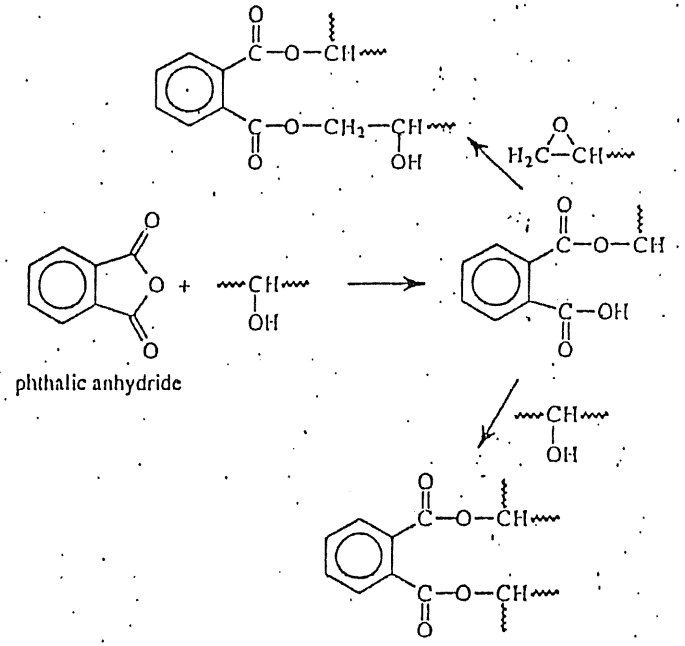

Figure 9.10. Cure of an epoxy resin by reaction of the prepolymer with an anhydride.

The prepolymer molecular weight is increased and the network is formed during a separate cure step, as shown in Figures 9.9 and 9.10. Amines, usually aromatic, may be used to cause ring opening of the end epoxide groups through nucleophilic addition (Figure 9.9). Carboxylic acid anhydrides such as phthalic acid anhydride can react with pendant hydroxyl to give ester acids, which can then react

with epoxide or other hydroxyl groups to create additional ester groups (Figure 9.10).

Major used for epoxies (510 million pounds of a total 6.87 billion pounds thermoset production in 1993) include coatings, laminates, and composites. Epoxy resins have high chemical and corrosion resistance, outstanding adhesion properties, low shrinkage upon cure, and good electrical properties. Principal applications for these resins include protective coatings, composite matrices, and adhesives.

9.2.2 Unsaturated Polyesters

Polyester resins (1.26 billion pounds produced in 1993) are widely used in construction and marine applications. Network formation distinguishes polyester resins from linear (thermoplastic) polyesters such as PET. Crosslinking is achieved either by use of polyols such as glycerol, as in the case of saturated polyesters (glyptal), or by the use of unsaturated dicarboxylic acids, such as maleic anhydride in the case of unsaturated polyester resins. Glyptal, which is used mainly as an adhesive or modified with natural or synthetic oils (oil-modified alkyds) for coatings, is formed by the reaction of glycerol and phthalic anhydride, as shown in Figure 9.11. The reaction is allowed to continue until a viscous liquid is obtained. The liquid can then be transferred to a mold for further network development (hardening).

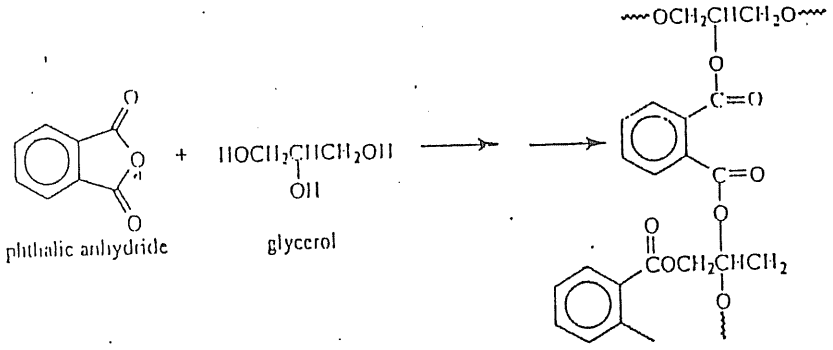

Figure 9.11. Formation of glyptal resin by the reaction of phthalic anhydride and glycerol.

Unsaturated-polyester resins, which are used as the matrix component of glass-fiber composites, may be obtained by copolymerization of both saturated acids (e.g., phthalic anhydride) and unsaturated acids (e.g., maleic anhydride) with a diol such as propylene glycol or diethylene glycol, as shown in Figure 9.12. Incorporation of the saturated acid serves to decrease crosslink density and consequently resin brittleness. Fumaric acid may be used in place of maleic acid to increase impact resistance. The low-molecular-weight product is soluble in styrene, which can then participate in a crosslinking step with the double bonds of the prepolymer during initiation by peroxides.

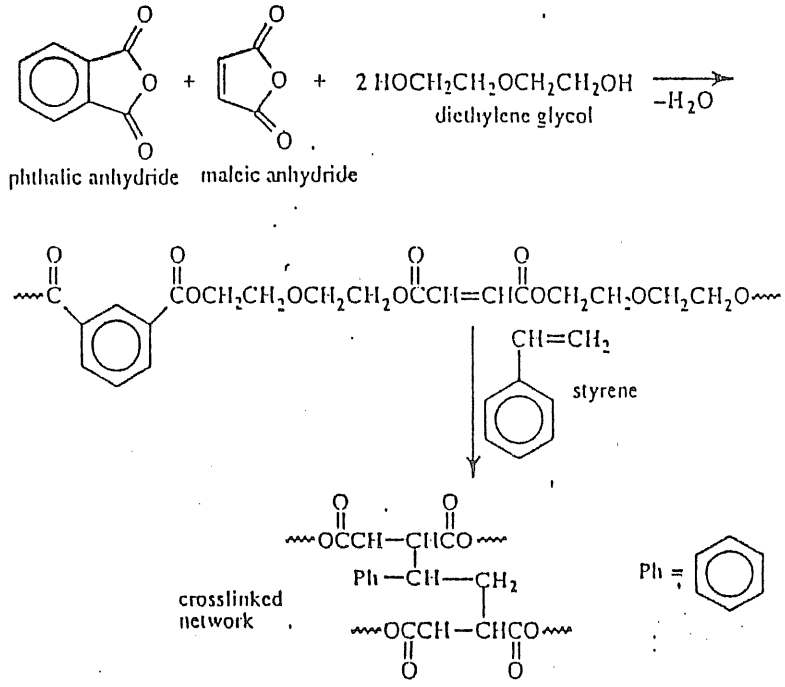

Figure 9.12. Formation of an unsaturated polyester resin.

9.2.3 Formaldehyde Resins

Formaldehyde is used in the production of two different but related classes of thermosets — phenoplasts and aminoplasts. *Phenoplasts*, or phenolic (PF) resins (3.08 billion pounds produced in 1993), are produced from the condensation products of phenol (or resorcinol) and formaldehyde and were the first synthetic thermoset. About 41% of PF resins are used in plywood manufacture and about 14% in insulation. Other applications include lacquers and varnishes, molding compounds, and laminates (e.g., wall panels and table tops).

Aminoplasts are prepared from the condensation products of either urea (UF resins) or melamine (MF resins) with formaldehyde. Applications of aminoplasts

are similar to those of phenoplasts and also include the treatment of textile fibers for improving their shrink and crease resistance and use to increase the wet strength of paper. In terms of sales volume, UF resins (1.74 billion pounds in 1993) are the most important. Like phenolic resins, they can be used in molding, laminating, and adhesive applications, especially where the darker color of phenolics may be objectionable, such as in interior-grade plywood. They also find use in the manufacture of electrical switches and plugs and insulating foam. MF resins (270 million pounds in 1993) are harder and more chemical, temperature, and moisture resistant than UF resins but are more expensive. Typical applications for MF resins include decorative plastic dinnerware, laminated worktops, and electrical fittings. Formaldehyde-based resins may be used as unmodified compounds or may be compounded with additives such as wood flour or glass fibers that serve as reinforcing fillers.

Phenoplasts. Phenolic resin was the first totally synthetic coating material. It was commercialized in 1909 as a replacement for cellulose nitrate. Phenolic resins may be prepared by either a base-catalyzed addition of formaldehyde to phenol (resole formation) or by an acid-catalyzed reaction (novolac formation), as described next.

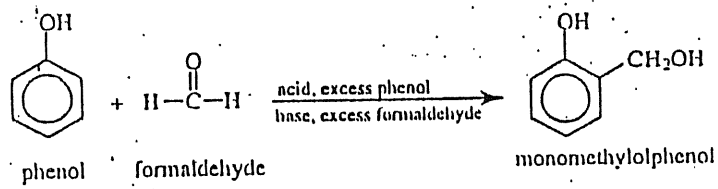

Figure 9.13. Example of the reaction of phenol and formaldehyde to yield a monomethylolphenol. Formation of dimethylolphenols and trimethylolphenols also is possible. Either acidic or basic conditions can be used.

The first step in resole formation is the reaction of phenol and excess formaldehyde under basic conditions to form mono-, di-, and trimethylolphenols. The formation of monoethylolphenol is illustrated in Figure 9.13. Under these conditions, phenol is present as a resonance-stabilized anion, and substitution is exclusively *ortho* and *para*. Upon heating, the methylolphenols condense to give a low-molecular-weight prepolymer called a resole (see Figure 9.14), which contains a large number of free methylol groups and is soluble in base. Further heating of the resole at elevated temperatures and under basic, neutral, or slightly acidic conditions yields the final high-molecular-weight network called the *resite*.

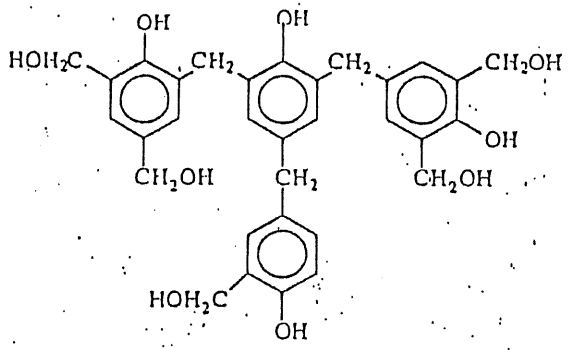

Figure 9.14. Representative structure of a resole.

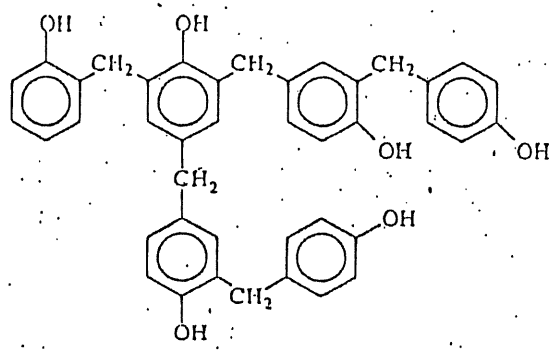

Figure 9.15. Representative structure of a novolac.

Resole formation can also be obtained by an initial acid-catalyzed reaction of formaldehyde with excess phenol. The mechanism involves protonation of the carbonyl group of formaldehyde, followed by electrophilic aromatic substitution at the *ortho* and *para* positions of phenol. Under acidic conditions, further reaction yields a low-molecular-weight, fusible but insoluble prepolymer called a *novolac* whose structure is illustrated in Figure 9.15. Unlike resole (Figure 9.14), novolac contains no residual hydroxymethyl groups. The high-molecular-weight network, the resite, is obtained from the novolac by heating with additional formaldehyde, paraformaldehyde, or hexamethylenetetramine.

Aminoplasts. The first step in the production of UF resins is the nucleophilic addition of urea to formaldehyde to give methylol derivatives, as illus-

trated in Figure 9.16, in a manner similar to the initial stages of phenolic-resin production. Subsequent condensation of these derivatives gives the final high-molecular-weight resin, whose structure is still controversial. The UF resin may be a true network structure, such as shown in Figure 9.17A, or a colloidal dispersion of UF condensates (Figure 9.17B), which are stabilized by association with excess formaldehyde.

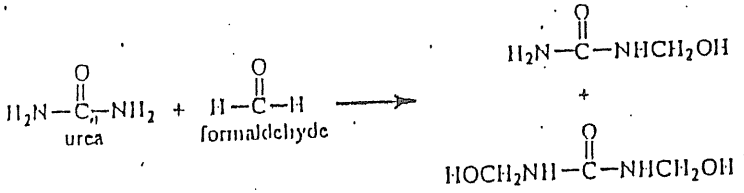

Figure 9.16. Reaction of urea and formaldehyde to yield methylol derivatives as the first step in the production of urea-formaldehyde resins.

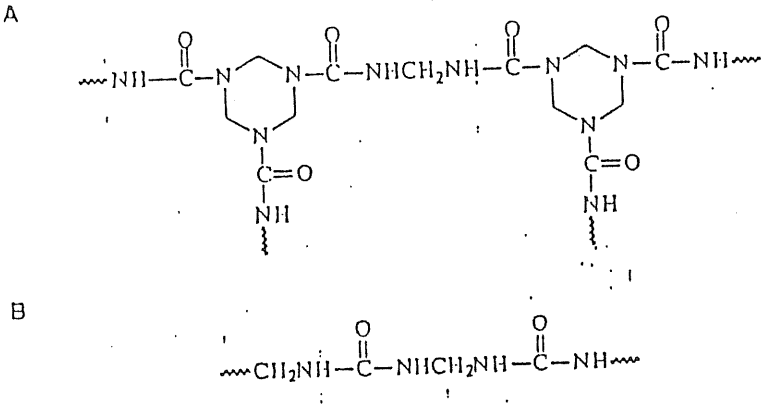

Figure. 9.17. Proposed structures of a fully cured UF resin formed by the condensation of methylol derivatives. A. Network model. B. Oligomeric UF condensates in the colloidal dispersion mode.

As illustrated in Figure 9.18, the initial step in the preparation of MF resin is a condensation of formaldehyde and melamine similar to that of urea and formaldehyde (Figure 9.15). A difference is that the majority of amino groups of melamine form *dimethylol* derivatives rather than monomethylol derivatives, as in the case of UF resins. In the final stage of resin production, methylol groups

condense with amino groups to form methylene bridges, which link the prepolymer chains in a rigid network structure, as illustrated in Figure 9.19.

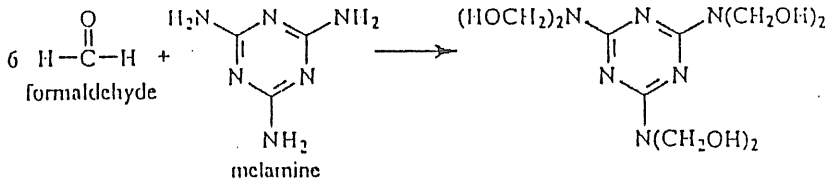

Figure 9.18. Condensation of melamine and formaldehyde to yield the dimethylol derivative of melamine.

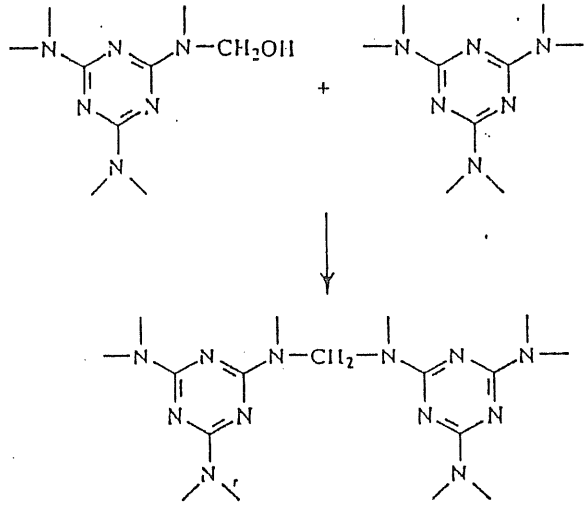

Figure 9.19. Formation of MF-resin network.

REFERENCES

1. S. C. Stinson, *Chem. Eng. News*, April 27, 1987, pp. 41–43.

BIBLIOGRAPHY

S. J. Clarson and J. A. Semlyen, eds., *Siloxane Polymers*, Prentice Hall, Englewood Cliffs, NJ, 1993.

Z. Wirpsza, *Polyurethanes: Chemistry, Technology and Applications*, Ellis Horwood, London, 1993.

10

Engineering and Specialty Polymers

Engineering and specialty thermoplastics provide one or more outstanding properties when compared with the commodity thermoplastics such as polystyrene and the polyolefins (Chapter 8). Advantages may include high thermal stability or excellent chemical resistance, low creep compliance, and high tensile, flexural, and impact strength. Not unexpectantly, these properties come at a premium in price, typically above $1 per pound for high-sales-volume engineering thermoplastics like nylons and $20 or more per pound for specialty polymers like polyimides and polyetheretherketone. In many cases, these polymers can be used as replacements for metals, particularly where a high strength-to-weight ratio is an important consideration, such as in automotive and aerospace applications.

The classification between engineering and specialty plastics is a somewhat arbitrary one. For purposes of discussion, the term *engineering plastics* is used to refer to those polymers that are used in the manufacture of premium plastics products where high temperature resistance, high impact strength, chemical resistance, or other special properties are required. The price range for these plastics is from $1 to $5 per pound compared to prices below $1 for the commodity plastics. The important engineering plastics are normally considered to include aliphatic polyamides (nylon-6 and -6,6), ABS resin, acetal, polycarbonate, polysulfones, poly(phenylene oxide) resins; poly(*p*-phenylene sulfide), and fluoroplastics such as Teflon™, and engineering polyesters. Properties of some of these engineering

thermoplastics are given in Table 10.1. By comparison, *specialty plastics*, which can cost $50 per pound or more, achieve very high performance in one or more areas and find limited but critical use in aerospace composites, as membranes for gas and liquid separations (see Section 12.1), as fire-retardant textile fabrics for fire fighters and race-car drivers, and as sutures and surgical implants. The most important class of specialty plastics are the polyimides. Other specialty polymers include polyetherimide, poly(amide-imide), polybismaleimides, ionic polymers, polyphosphazenes, poly(aryl ether ketones), polyarylates and related aromatic polyesters, and ultrahigh-molecular-weight polyethylene.

10.1 ENGINEERING PLASTICS

10.1.1 Polyamides

Polyamides can have either all aliphatic- or aromatic-chain backbones. The aliphatic polyamides, particularly nylon-6 and nylon-6,6, are the most widely used engineering thermoplastics. In addition to their important fiber applications (see Section 8.2.3), aliphatic polyamides may be used as molded parts for automotive and other applications. Commercial nylon resins for molding applications may be modified for improved flame retardancy and impact strength, or reinforced with minerals or glass fibers to increase modulus as well as to lower cost. Fibers made from aromatic polyamides, such as Nomex™ and Kevlar™, provide outstanding high-temperature resistance and high tensile strength for use as fire-retardant fabric and for tire cord. As a class, polyamides exhibit excellent resistance to wear and abrasion, low coefficient of friction, good resilience, and high impact strength. The chemical structures of the repeating units of the most important aliphatic and aromatic polyamides and the monomers from which they are polymerized are given in Table 10.2. Properties of nylon-6 and nylon-6,6 are given in Table 10.1.

All nylons are water sensitive due to the hydrogen-bonding character of the amide groups. For example, nylon-6,6 absorbs about 9% water during equilibrium at ambient temperature and 100% relative humidity. Water absorption decreases with decreasing amide-group concentration in the polymer backbone as in the case of nylon-11 (1.9% water absorption) obtained by the ring-opening polymerization of 11-aminoundecanoic acid. Water acts as a plasticizer, which reduces tensile strength and modulus (and, therefore, dimensional stability), while increasing elongation-to-break and consequently toughness. Care must be taken to reduce water content of nylon resins to below 0.3% before melt processing to avoid embrittlement due to hydrolytic degradation.

Of the nonfiber polyamide market of 1 million metric tons worldwide in 1992, nylon-6,6 and nylon-6 represent nearly 90% of the total market volume. Nylon-6,6 has higher rigidity, but nylon-6 is more weather and thermally resistant. Due to its good barrier properties, nylon-6 film is used for packaging of some oxygen-sensitive foods. Other aliphatic nylons having more specialized markets in-

TABLE 10.1 REPRESENTATIVE PROPERTIES OF IMPORTANT ENGINEERING THERMOPLASTICS

Property	ASTM	Nylon-6[a]	Nylon-6,6[a]	ABS[b]	PC	PPO	Acetal	PSF	PES
Specific gravity	D792	1.12–1.14	1.13–1.15	1.03–1.06	1.20	1.06	1.42	1.24	1.37
Tensile strength, MPa[c]	D638	62	76	41–52	66	66	68–83	70	84
Tensile modulus, GPa[d]	D638	1.65	—	2.1–2.8	2.4	2.6	3.6	2.6	2.8
Elongation-to-break, %	D638	300	300	5–25	110	20–60	25–75	50–100	7
Flexural strength MPa[d]	D790	34	42	76–90	93	93	97	106	138
Flexural modulus GPa[d]	D790	0.7	12–28	26–28	23	25–28	26–30	27	41
Impact strength notched Izod, J m^{-1}[e]	D265	160	112	160–320	854	96–267	69–125	160–320	11
Heat-deflection temperature, °C at 455 kPa (66 psi)	D648	150–185	180–240	102–107	138	137	124	150–175	137

[a] Moisture conditioned.
[b] Medium-impact grade.
[c] To convert MPa to psi, multiply by 145.
[d] To convert GPa to psi, multiply by 1.45×10^5.
[e] To convert J m^{-1} to lb in.$^{-1}$, divide by 53.38.

TABLE 10.2 CHEMICAL STRUCTURES OF IMPORTANT POLYAMIDES

Monomer(s)	Polymer	Structure
Caprolactam	Poly(ε-caprolactam) (nylon-6)	
Hexamethylene diamine adipic acid	Poly(hexamethylene adipamide) (nylon-6,6)	
Hexamethylene diamine sebacic acid	Poly(hexamethylene sebacamide) (nylon-6,10)	
Isophthaloyl chloride *m*-phenylenediamine	Poly(*m*-phenylene isophthalamide) (Nomex™)	
Terephthaloyl chloride *p*-phenylenedianine	Poly(*p*-phenylene terephthalamide) (Kevlar™)	

include nylon-11, nylon-12, and nylon [illegible]
have been used in the manufacture of fuel lines and compressed-air brake tubing.

Aromatic Polyamides. In the 1960s, aromatic polyamides, often called *aramids*, were developed to improve the heat and flammability resistance of nylons. Poly(*m*-phenylene isophthalamide) (Nomex™) is a highly heat resistant nylon (decomposes about 370°C) obtained by the solution or interfacial polymerization of a *meta*-substituted aromatic diacid chloride and diamine, as illustrated in Figure 10.1. Nomex may be used as a substitute for asbestos in many applications, such as flame-resistant protective clothing and hot-gas filtration equipment. Nomex in the form of thin pads was used to isolate the fragile sintered silica-fiber mats of the space shuttle from stress and vibration during flight.

Figure 10.1. Synthesis of an aromatic polyamide, poly(*m*-phenylene isophthalamide) (Nomex™).

The corresponding linear aromatic polyamide, poly(*p*-phenylene terephthalamide) (PPT) (Kevlar™) (see Table 10.2), decomposes only above 500°C. Fibers of Kevlar have higher strength and modulus than steel on an equal-weight basis. It has been used as a substitute for steel in belted radial tires (i.e., aramid fiber) and in the manufacture of mooring lines, as well as bullet-resistant vests and other protective clothing. Kevlar fiber is also used in the manufacture of fiber-reinforced plastics (see Chapter 7). Fabric made from Kevlar has been used as the skin covering for the first human-powered aircraft, the *Gossamer Albatross*, which was flown across the English Channel.

10.1.2 ABS

Another important thermoplastic with a major market share is ABS, which represents a resin containing acrylonitrile, butadiene, and styrene. ABS is a high-impact, high-HDT grade of polystyrene (see Table 10.1) that, together with the thermoplastic nylons, marks the boundary in price and performance between commodity and engineering thermoplastics. Worldwide sales of ABS in 1992 are estimated at 2.3 million tons. Applications for ABS include automotive applications (18% of the total market), consumer products including small and large appliances (22%), and business machines and telecommunications where good impact strength at moderate cost is required.

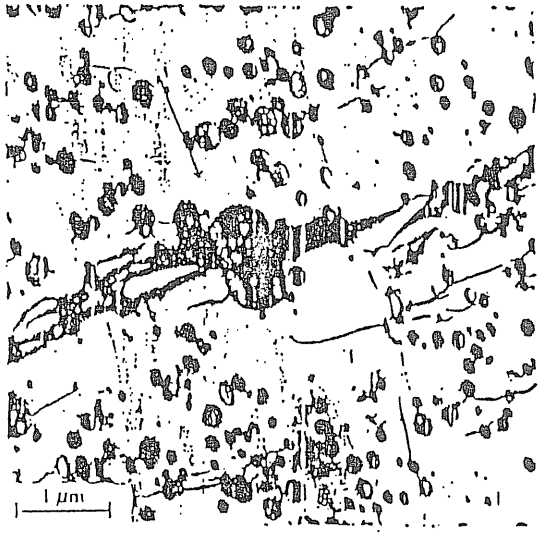

Figure 10.2. Electron micrograph of a section cut parallel to the surface of a deformed sample of ABS. The arrow shows the direction of applied strain. The dispersed phase (dark regions) are PBD particles. Crazes appear as dark lines running across the photograph. These craze structures are oriented perpendicular to the strain direction and pass through a number of PBD particles. [Reproduced from M. Matsuo, *Polym. Eng. Sci.*, 9, 206:(1969), with permission of the publisher.]

ABS was first developed in the 1950s by grafting styrene–acrylonitrile copolymer (SAN) onto semicrosslinked particles of polybutadiene (PBD). The PBD component of ABS increases impact strength over that of SAN alone. Developments during the 1960s led to a variety of methods to obtain ABS, including bulk, emulsion, and suspension polymerizations, although emulsion processes (free-radical polymerization of styrene and acrylonitrile in the presence of PBD or

butadiene copolymers) are still the most widely used. A typical ABS formulation contains ≤15% butadiene and ≤20% acrylonitrile. The morphology of an ABS resin as can be seen by scanning electron microscopy aided by staining the unsaturated sites of the butadiene component, varies with the production process. In general, immiscibility of PBD with SAN results in phase separation whereby PBD is dispersed in the form of small PBD particles contained within a matrix of SAN, as shown in Figure 10.2. Rubber particles produced by bulk or suspension processes are larger (0.5 to 5 μm) than those produced by emulsion methods (0.1 to 1 μm). Graft polymerization of SAN and PBD provides good interfacial adhesion between the dispersed and matrix phases. When ABS is mechanically deformed, the PBD particles act to modify the deformation process by either promoting craze formation (see Figure 10.2) or shear yielding (see Section 7.2.2). As a result, the total energy-to-fail (i.e., impact strength) of ABS is increased over that of unmodified PS or SAN.

10.1.3 Polycarbonates

The polycarbonate obtained from bisphenol-A is the second largest sales volume engineering thermoplastic. Polycarbonate (PC) is an amorphous polymer with attractive engineering properties (see Table 10.1), including high impact strength, low moisture absorption, low combustibility, good dimensional stability, and high light transmittance (up to 88%). The latter property has resulted in the application of PC as an impact resistant substitute (e.g., Lexan®) for window glass. Other important applications for PC include its use for molding compact disks. Worldwide consumption of PC in 1992 was estimated to be 660,000 tons. Among the disadvantages of PC are limited chemical and scratch resistance and a tendency to yellow with long-term ultraviolet exposure. These problems have been addressed by the introduction of silicone-coated and free-radical stabilized polycarbonate resins.

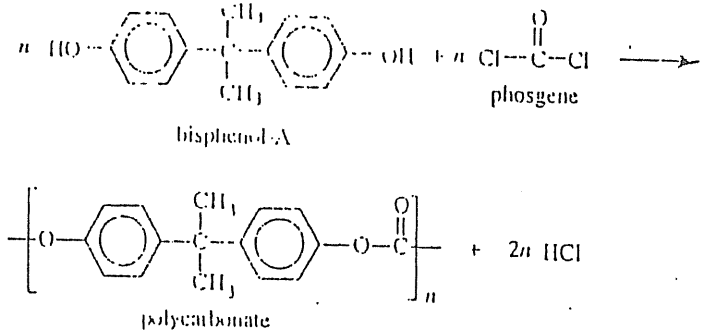

Figure 10.3. Synthesis of bisphenol-A polycarbonate by the polycondensation of bisphenol-A and phosgene.

Polycarbonate can be synthesized by the polycondensation of bisphenol-A and phosgene, as shown by Figure 10.3. For each repeating unit that is formed, two molecules of hydrogen chloride are liberated. Alternately, if the *sodium salt* of bisphenol-A is used in the polymerization, the by-product becomes sodium chloride rather than hydrogen chloride. This is an obvious advantage because the salt will precipitate out of the organic solvent used in the polymerization and, therefore, can be easily and safely removed. In contrast, the production of strongly acidic hydrogen chloride requires special consideration for disposal and in the selection of construction material used in the polymerization reactor.

Other polycarbonates can be polymerized by modified interfacial condensation or by melt transesterification of tetrasubstituted bisphenols. These polycarbonates have the general structure

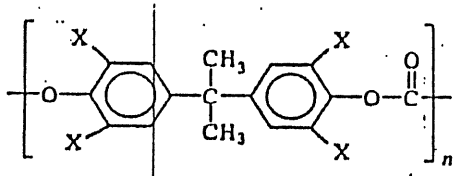

where X represents a halogen, especially bromine, or a methyl group. One example is tetramethylbisphenol-A polycarbonate (TMPC), X = CH_3, which has a higher heat-distortion temperature (HDT) and better hydrolytic stability than PC. The HDT or T_g is a result of the greater rigidity of the TMPC chain due to the steric hindrance of the substituent methyl groups. One disadvantage of TMPC is its low impact resistance; however, this may be improved through blending with impact-resistant resins such as HIPS, ABS, and MBS (see Section 7.2.2). The styrene component of these impact modifiers forms a homogeneous phase with TMPC. Impact-modified grades of TMPC can also be used to increase the HDT of PVC. Tetrabromobisphenol-A polycarbonate (TMBPC), X = Br, can be blended with PC to increase HDT. Copolymers of bisphenol-A and tetrabromobisphenol-A or tetrachlorobisphenol-A provide better flame retardancy. The polycarbonate obtained from cyclohexanonebisphenol can be blended with PC to increase the HDT from 160° to 205°C.

10.1.4 Modified Poly(phenylene oxide)

Another large sales volume engineering thermoplastic, having substantially higher HDT than PC, is poly(2,6-dimethyl-1,4-phenylene oxide) or PPO™, which is obtained from the free-radical, step-growth, oxidative-coupling polymerization of 2,6-xylenol[1] as shown in Figure 10.4.

A related polymer, poly(2,6-diphenyl-1,4-phenylene oxide) (Tenax™), originally considered for fiber applications, has limited commercial use as a packing for GC columns. A good review of oxidative-coupling polymerization and the commercialization of PPO has been given by Hay.[2] PPO has many attractive properties (see Table 10.1), including high impact strength, chemical stability to mineral and organic acids, and low water absorption. A limitation that had restricted its commercialization is its high glass-transition temperature (T_g = 214°C) in relation to the susceptibility of its methyl groups to thermal oxidation, which poses problems for melt processing. For these reasons, commercial resins (Noryl™) are made by blending PPO with high-impact polystyrene (HIPS), which serves to reduce processing temperature, although heat-distortion temperature is reduced as well. Like impact-modified grades of TMPC, the styrene component of HIPS forms a homogeneous phase with PPO. Noryl resins are also available in flame-retardant and filled grades and are used in many electrical and automotive applications.

In addition to PPO/HIPS blends, commercial resins of PPO and polyamides (PA) are available for improved thermal stability required for certain electrical and electronic applications. In this case, a compatibilizer (see Section 7.2.1) such as PA-grafted styrene–maleic anhydride copolymer serves to improve blend properties. Blends of PPO with polyesters and polyolefins offer better dimensional stability than PPO/PA resins at the expense of lower thermal stability. Worldwide consumption of all PPO resins is estimated at greater than 200,000 tons per year.

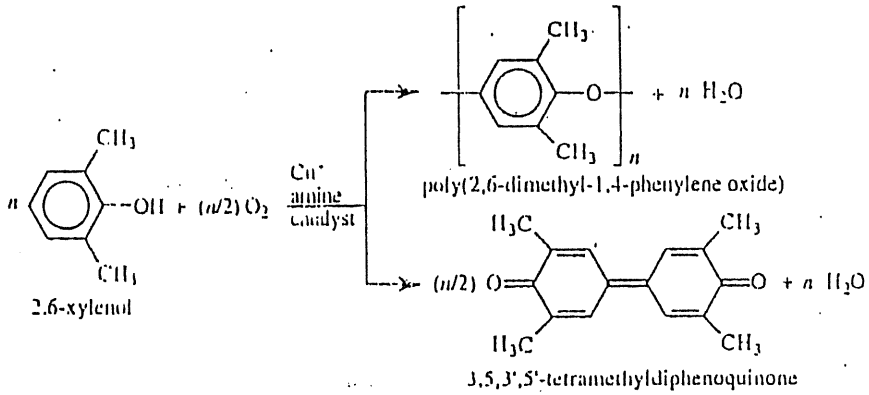

Figure 10.4. Oxidative-coupling polymerization of 2,6-xylenol. 3,5,3',5'-Tetramethyldiphenoquinone (DPQ) is a by-product of this polymerization. The concentration of DPQ impurity depends upon the choice of catalyst and conditions of the polymerization. For example, the yield of DPQ is about 3 wt % using a cupric formate and pyridine catalyst.

10.1.5 Acetal

Polyacetal, sometimes known simply as acetal or as polyformaldehyde and polyoxymethylene (POM), may be the first universal polymer. In 1987, mass spectral data revealed the presence of POM in the gas cloud of Halley's comet. On earth, POM may be obtained by the anionic or cationic polymerization of

formaldehyde or by the cationic ring-opening polymerization of trioxane, as shown in Figure 10.5. The highly regular chain structure of polyacetal contributes to its high crystallinity and excellent chemical resistance. Properties of a typical acetal resin are given in Table 10.1.

Acetal is degraded by UV radiation, leading to color change and loss of toughness and tensile strength; however, acetal can be stabilized against UV degradation by the usual UV absorbers and hindered-amine light stabilizers (HALS). Carbon black and titanium dioxide fillers are also effective for light and UV screening. A particularly attractive property of acetal is its high dimensional stability (creep resistance), which allows acetal to be used as a replacement for metals in gears and machine parts. Rubber-toughened grades of polyacetals are available for applications where higher impact strength, flexural strength, and tensile-fracture resistance are desired. Worldwide consumption of acetal was approximately 380,000 tons in 1992. Automotive and electrical/electronic use accounted for approximately two-thirds of this production. Another important consideration for the continued growth of acetal resins is that acetal can be chemically recycled to monomers.

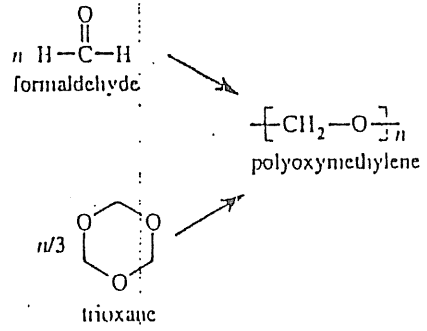

Figure 10.5. Two routes for the synthesis of polyoxymethylene.

10.1.6 Polysulfones

Polysulfones comprise a class of engineering thermoplastics with high thermal, oxidative, and hydrolytic stability and good resistance to aqueous mineral acids, alkali, salt solutions, oils, and greases. Their high biocompatibility and ability to be sterilized by a variety of techniques make them highly suitable for medical applications.[3] Polysulfones also have high permeability and permselectivity that make them attractive as membrane polymers in gas separations (see Section 12.1.1). Chemical structures and representative properties of three commercial aromatic polysulfones are given in Tables 10.3 and 10.4, respectively.

TABLE 10.3 CHEMICAL STRUCTURES OF COMMERCIAL POLYSULFONES

Polysulfone	Structure of Repeating Unit
Polysulfone (Udel™, Ultrason S™)	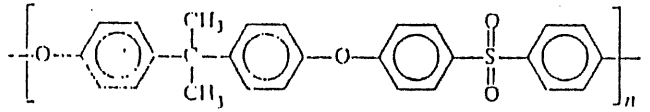
Polyethersulfone (Ultrason E™, Victrex™)	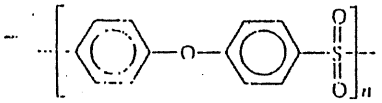
Polyphenylsulfone (Radel R™)	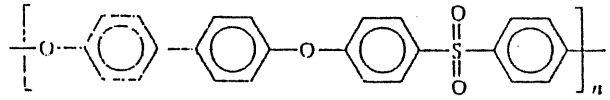

TABLE 10.4 REPRESENTATIVE PROPERTIES OF COMMERCIAL POLYSULFONES

Property	ASTM	PSF	PES	PPS
Specific gravity	D 1505	1.25	1.37	1.29
Tensile strength at yield, MPa[a]	D 638	70.3	84.1	71.7
Tensile modulus, GPa[b]	D 638	2.48	2.70	2.14
Elongation to break, %	D 638	50–100	40–80	60
Flexural strength, MPa[a]	D 790	106	129	85.5
Flexural modulus, GPa[b]	D 790	2.69	2.57	2.30
Impact strength (Notched Izod), J m^{-1}[c]	D 256	69	85	641
Heat-deflection temperature, °C at 455 kPa (66 psi)	D 648	174	203[d]	200–204

[a] To convert MPa to psi, multiply by 145.
[b] To convert GPa to psi, multiply by 1.45×10^5.
[c] To convert J m^{-1} to lb$_f$ in^{-1}, divide by 53.38.
[d] Reported at 1.82 MPa (264 psi).

Polysulfones can be synthesized by condensation polymerizations involving nucleophilic substitution of alkali salts of bisphenates with activated aromatic dihalides. The synthesis of bisphenol-A polysulfone (PSF) is shown in Figure 10.6. In addition, polysulfones can be synthesized by electrophilic substitution (Friedel-Crafts) of sulfonyl chlorides by use of Lewis-acid catalysts, as in the polymerization of polyethersulfone (PES), as shown in Figure 10.7. Polysulfones are widely used in the automotive, aerospace, and medical industries for such applications as quartz–iodine headlamp reflectors for cars, sterilizable medical devices, and overhead passenger-service modules on aircraft.

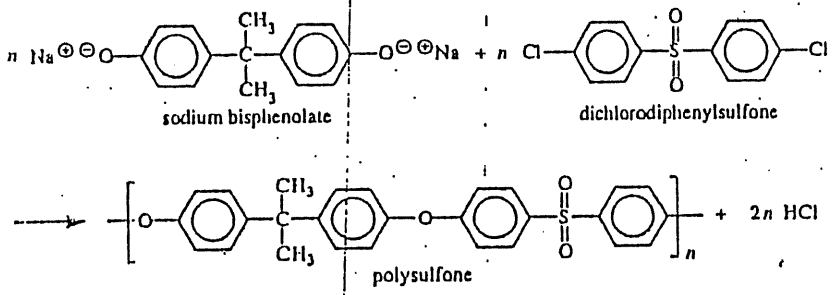

Figure 10.6. Polycondensation of bisphenol-A polysulfone.

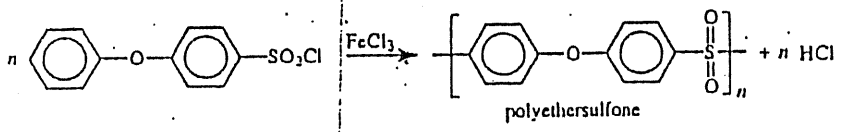

Figure 10.7. Polycondensation of a polyethersulfone.

10.1.7 Poly(phenylene sulfide)

Poly(*p*-phenylene sulfide) (PPS), or poly(thio-1,4-phenylene), is another important engineering thermoplastic with many attractive properties (Table 10.1), such as outstanding chemical resistance, good electrical properties, excellent flame retardance, low coefficient of friction, and high transparency to microwave radiation. As illustrated in Figure 10.8, PPS can be prepared by the polycondensation of *p*-dichlorobenzene and sodium sulfide.

PPS is highly crystalline with a relative high melting temperature (285°C) and is insoluble in organic solvents below 200°C. This means that special processing techniques must be used to manufacture products from this engineering resin. For example, PPS coatings are obtained by spraying an aqueous *slurry* of PPS particles and heating the coated object to temperatures above 370°C. PPS can be injection and compression molded at high temperatures (300° to 370°C) at which PPS particles soften and undergo an apparent crosslinking reaction to yield a totally insoluble product. Principal applications of PPS include cookware, bearings, and pump parts for service in various corrosive environments. PPS is frequently produced as reinforced grades (typically filled with glass fiber and mixtures of minerals such as talc and chalk), which have higher strength and HDT. The worldwide market for PPS compounds was 20,000 tons in 1992.

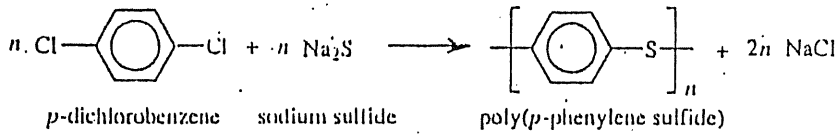

Figure 10.8. Synthesis of poly(*p*-phenylene sulfide).

10.1.8 Engineering Polyesters

The slow rate of crystallization of poly(ethylene terephthalate) (PET), which is widely used as a textile fiber (see Section 8.2.3), normally results in poor surface quality and release properties of molded parts. Modified grades of PET have enabled penetration of this polyester into the beverage-bottle market (1.58 billion pounds in the United States alone) and use in other molding applications (see Section 8.1.3). In the nonbottle market, PET is in competition with a related engineering polyester, poly(butylene terephthalate) (PBT)

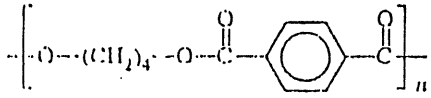

which was introduced by several companies in the early 1970s. Worldwide production of PBT in 1992 was 52,000 tons. Principal applications for PBT include injection-molded parts for electrical and electronic use and for automotive markets. Both polyesters, like polycarbonates, are moisture sensitive (hydrolytic instability), but have high strength, rigidity and toughness, excellent dimensional stability, low coefficient of friction, abrasion resistance, and good resistance to chemicals and grease.

In the late 1970s, an all-aromatic polyester (polyarylate, PAR), produced by the condensation polymerization of bisphenol-A and mixed phthalic acids

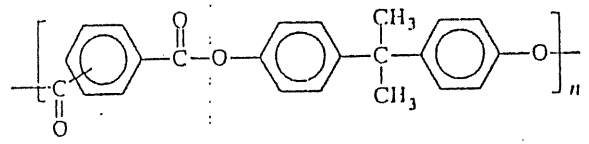

was marketed in the United States. Unlike PET and PBT, polyarylate is amorphous and has high clarity, as well as high heat-distortion temperature (T_g in the range of 150° to 200°C), UV stability, inherent flame retardance, and good electrical properties. Typical outdoor applications for polyarylate include solar collectors, safety devices, construction, and transportation. Other uses include the manufacture of plastic parts for electronic and electrical hardware such as lighting fixtures. Unfortunately, a variety of factors, including competition with polysulfone and polycarbonate and poor processability, has virtually eliminated the market for PAR.

Another engineering polyester having recent interest is poly(dimethylene cyclohexane terephthalate) (PCT)

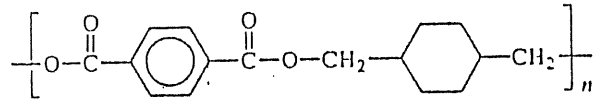

which has high thermal stability and finds applications in some electronic components. Like PET, PCT crystallizes slowly and, therefore, nucleating agents and "hot" oil-cooled molds must be used in order to process PCT in a reasonable time scale.

Very recently, interest has focused on the monomer, naphthalene dicarboxylate (NDC)

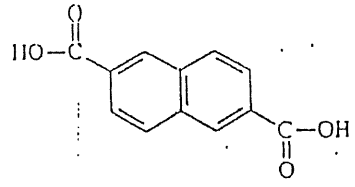

which can be copolymerized with DMT to yield a copolyester with better barrier and heat resistance for bottle and packaging applications or can be polymerized (with ethylene glycol) to yield poly(ethylene naphthalate) (PEN)

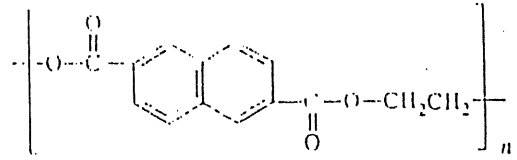

which can be blended with PET to improve properties. PEN can be extruded and blow molded and has better mechanical strength, higher heat and chemical resistance, better dimensional, thermal, UV, and hydrolytic stability, and improved barrier properties compared to PET. The higher thermal resistance of PEN (T_g of 120°C compared to approximately 78°C for PET) expands the potential market for polyester bottles to those such as baby food jars that need to be steam-sterilized. Current applications for PEN include industrial fiber cord for rubber reinforcement, blood evacuation tubing, and electronic film, such as long-lasting video-recording tape. Other potential markets include electrical and electronic parts (e.g., motor insulation, magnetic tapes, and capacitors) and microwaveable packaging for medical and other applications. Further commercial development of PEN will require the large-scale production of NDC (now underway by a number of producers) to reduce the price of PEN from its 1992 high of $18 per pound.

10.1.9 Fluoropolymers

Among the most important fluoropolymers is polytetrafluoroethylene (PTFE or Teflon™), which is obtained by the emulsion free-radical polymerization of tetrafluoroethylene. Polytetrafluoroethylene is highly dense (2.1 to 2.3 g cm^{-3}) with high temperature stability, low temperature flexibility, extremely low coefficient of friction, low dielectric constant and dissipation factor, and chemical inertness. Many of these properties are similar to those of PPS described earlier. Also like PPS, PTFE is extremely difficult to process by conventional techniques. Limited processability is attributed to its extremely high crystallinity and high crystalline melting temperature (T_m = 327°C), resulting from its highly regular structure and unusually high molecular weight. For coatings applications, PTFE is sintered at high temperature and pressure. Improvement in melt processability is obtained by incorporating a small concentration of a comonomer such as hexafluoropropylene (Teflon FEP), ethylene (ETFE), or more recently perfluoroalkoxy (PFA) fluorocarbon resins. In these cases, copolymerization serves to reduce crystallinity.

In addition to PTFE, several other partially fluorinated polymers listed in Table 10.5 have achieved commercial importance. These include polychlorotrifluoroethylene (CTFE or Kel-F™), which is also available as a copolymer with ethylene or vinylidene fluoride. Applications include electrical insulators, gaskets and seals, and pump parts. Poly(vinylidene fluoride) (PVDF or Kynar™), also available as a copolymer with hexafluoroisobutylene (HFIB), is a crystalline poly-

mer (T_m = 170°C) which finds primary applications in coatings, gasket material, wire and cable insulation and in the extrusion of vinyl siding for houses. Poly(vinyl fluoride) (PVF or Tedlar™) is another highly crystalline polymer (T_m = 197°C) that can provide tough, flexible films with excellent outdoor weatherability and good abrasion and stain resistance. Applications include protective coatings for materials that are used in the building industry.

TABLE 10.5 CHEMICAL STRUCTURES OF SOME IMPORTANT FLUOROPOLYMERS

Fluoropolymer	Repeating Unit
Polytetrafluoroethylene	$-[CF_2-CF_2]-$
Fluorinated ethylene–propylene copolymer (FEP)	$-[CF_2-CF_2]_m-[CF_2-CF(CF_3)]_n-$
Polychlorotrifluoroethylene (CTFE)	$-[CF_2-CCl(F)]-$
Poly(vinylidene fluoride) (PVDF)	$-[CH_2-CF_2]-$
Poly(vinyl fluoride) (PVF)	$-[CH_2-CH(F)]-$

Fluorinated polymers also find significant applications as highly thermally and chemically resistant elastomers, as discussed in Section 9.1.2. These include amorphous copolymers of vinylidene fluoride and hexafluoropropylene, which can be crosslinked in the presence of diamines and basic oxides through dehydrofluorination followed by amine addition. Elastomers can also be made from copolymers of tetrafluoroethylene and perfluoroalkyl vinyl ethers, such as perfluoromethyl vinyl ether, and copolymers of vinylidene fluoride and hexafluoroisobutylene. Network formation can be achieved by incorporation of comonomers containing nitrile pendant groups, which when heated can form triazine structures.

10.2 SPECIALTY POLYMERS

Specialty polymers have small but important commercial markets in the aerospace and electronics industries and as materials for biomedical applications. The most important of these include polyimides, ionomers, polyaryletherketones, polyorganophosphazenes, certain aromatic polyesters and high-performance fibers, and polyacetylenes and other electrically-conductive polymers.

10.2.1 Polyimides and Related Specialty Polymers

Polyimides represent an important class of high-temperature, solvent-resistant polymers. Typical uses for polyimides include electronics, sleeve bearings, and valve seatings and as the matrix component of graphite composites for compressor vanes in jet engines and other aerospace applications. Often, polyimides are formed by a two-stage process. The first step involves the polycondensation of an aromatic dianhydride and aromatic diamine to form an intermediate poly(amic acid). Dehydration of the poly(amic acid) at elevated temperatures yields the polyimide (PI) structure. A representative polymerization of a polyimide is shown in Figure 10.9. Unlike the intermediate poly(amic acid), the cured (i.e., fully imidized) PI is insoluble and infusible and has high-temperature and oxidative stability and good electrical-insulation properties and radiation resistance.

Almost an infinite number of PI structures are possible limited only by the number of available dianhydrides and diamines. An example of a commercially important PI is a polypyromellitimide that is available as film is Kapton® (Du Pont), whose imidized structure is:

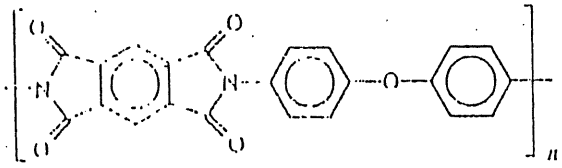

Kapton is obtained by the condensation polymerization of pyromellitic anhydride

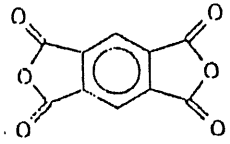

and 4,4-diamino diphenyl ether

† Simple stock shapes in the form of rods and tubes for subsequent machining to the required product are available under the trade name Vespel™.

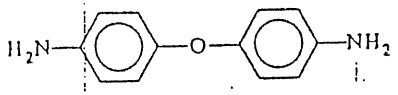

Properties of Kapton are given in Table 10.6.

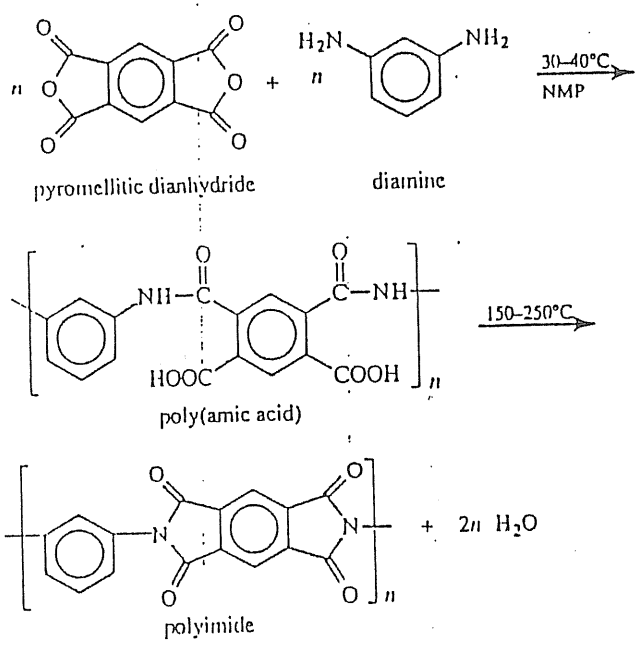

Figure 10.9. Polymerization of a polyimide.

Some disadvantages of these "imidizable" polyimides are the limited shelf life of the precursor poly(amic acids) and possible structural weakness of the fully imidized product due to void formation as a result of water release in the curing process. More recently, some thermoplastic polyimides have become available. These polyimides are fully imidized but can be melt processed at high temperatures or can be solution cast. Solubility in relatively nonpolar liquids is achieved by incorporation of aromatic polyether linkages in the backbone or pendant phenyl and alkyl groups introduced through appropriate selection of the aromatic diamine.

Another approach to PI synthesis particularly suited for structural composites is the use of thermoset PIs. A thermoset PI is one prepared by heating a fully imidized PI-prepolymer having a reactive functional group at each end that can react with another prepolymer. An example of a thermoset PI is Thermid® resin which

uses acetylene-terminated prepolymers for network formation. The structure of Thermid is given as

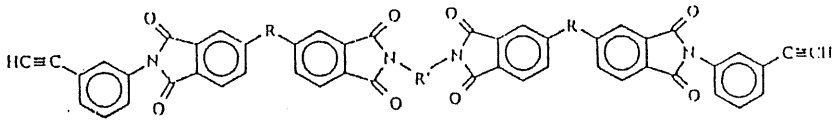

where R represents a carbonyl group (C=O) or a hexafluoropropane (6F) functionality, $C(CF_3)_2$, and R' represents the aromatic group

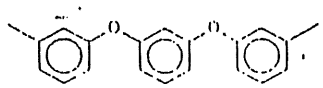

TABLE 10.6 PROPERTIES OF A POLYIMIDE, POLYETHERIMIDE, AND POLY(AMIDE-IMIDE)

Property	Polyimide[a]	PEI[b]	PAI[c]
T_g (°C)	385	217	—
Heat-deflection temperature, °C at 1.82 MPa (264 psi)	—	200	278
Density (g cm^{-3})	1.42	1.27	1.42
Water absorption, % over 24 h and RT and 40% RH	2.9	0.25	0.33
Tensile modulus (GPa), 1% secant	3.0	3.0	4.8
Tensile strength (MPa) at 23°C at yield	17.2	105	192
% Elongation at 23°C			15
at yield		7–8	
at break	70	60	
Flexural modulus (GPa), tangent at 23°C		3.31	5.0
Flexible strength (MPa)	—	—	241
Impact strength, Izod (J m^{-1})			
notched	—	53.4	144
unnotched	—	1,335	1,068

[a] Kapton H.
[b] Ultem 1000.
[c] Torlon 4203L; contains 3% TiO_2 and 0.5% fluorocarbon.

Another important example of a thermoset PI is PMR-15, which has been widely used as the matrix for graphite composites for aerospace applications. PMR-15 uses a norbornene end functionality for network formation

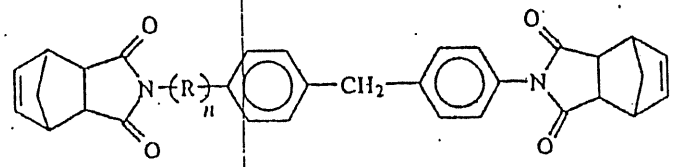

where R (n = 2) has the aromatic structure

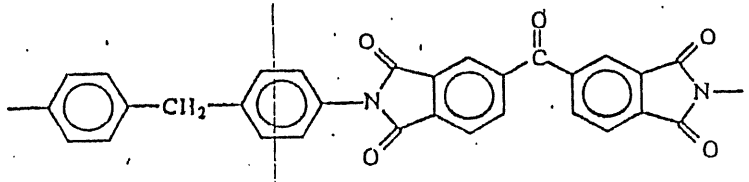

In general, polyimides having excellent thermal and thermooxidative stability (although at much higher cost) can be obtained from fluorinated dianhydrides, especially 6FDA

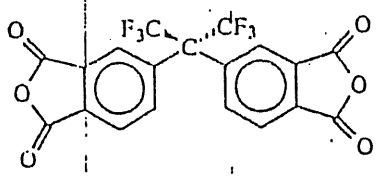

or fluorinated diamines such as 2,2-bis[(4-aminophenoxy)phenyl]hexafluoropropane

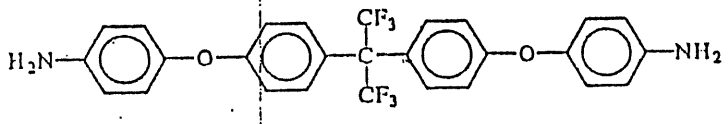

Poly(amide-imide) and Polyetherimide. To improve the melt processability of polyimides, the basic imide structure can be combined with more flexible aromatic groups, such as aromatic ethers and amides. For example, poly(amide-imide) (PAIs) (e.g., Torlon™)

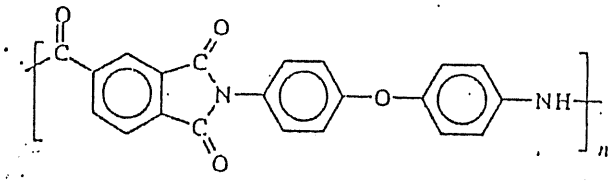

is obtained from the polycondensation of trimellitic anhydride (TMA) and an aromatic diamine (e.g., 4,4'-oxydianiline). Another imide-type engineering thermoplastic is polyetherimides (PEI, Ultem™), which is obtained by a nitro-displacement reaction[4] involving bisphenol-A, 4,4'-methylene-dianiline and 3-nitrophthalic anhydride.

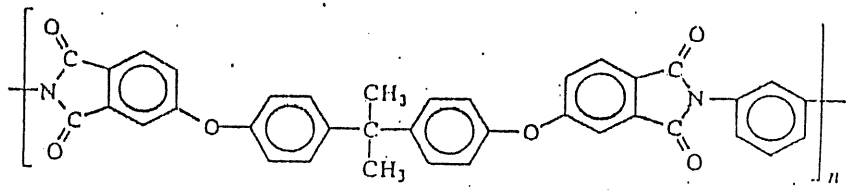

Both PAI and PEI have high heat-distortion temperature, tensile strength, and modulus. Properties of a representative polyimide (Kapton H) and two representative grades of PEI and PAI are compared in Table 10.6. Once imidized, Kapton is no longer melt-processable, unlike PAI and PEI, which are compromised by lower softening temperatures (T_g or HDT). Kapton has a HDT of 357°C and a continuous-use temperature of ca. 270°C. One advantage of PAI and PEI over Kapton are their lower water absorption, which is especially important for composite applications. Applications for PAI and PEI include high-performance electrical and electronic parts, microwave appliances, and under-the-hood automotive parts.

Polybismaleimides. A related imide-type polymer is the polybismaleimides (Kerimid™, Kinel™), whose repeating unit may be represented as

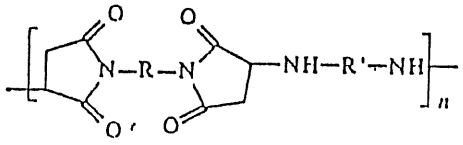

where R and R' represent a variety of possible aromatic groups. Polybismaleimide is obtained by (Michael) *addition* of diamine to the unsaturated sites at the ends of a bismaleimide having a structure similar to

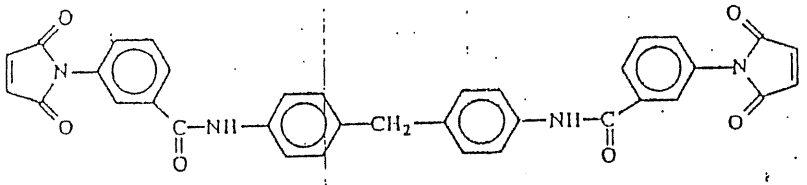

Applications for polybismaleimides include use as composite resin for filament winding and laminates (see Chapter 7), friction pads, gears, and bearings.

Ladder Polymers. At the extreme in high-temperature stability are polymers that incorporate highly fused ring backbones such as polyimidazopyrrolones. They are obtained by a two-step cure process involving the initial condensation of an aromatic tetracarboxylic acid and aromatic tetramine (Figure 10.10). Such materials, which are sometimes known as *ladder polymers* because their fused ring structure resembles the rungs of a ladder, are capable of withstanding temperatures in excess of 500°C (see also Section 6.1.1).

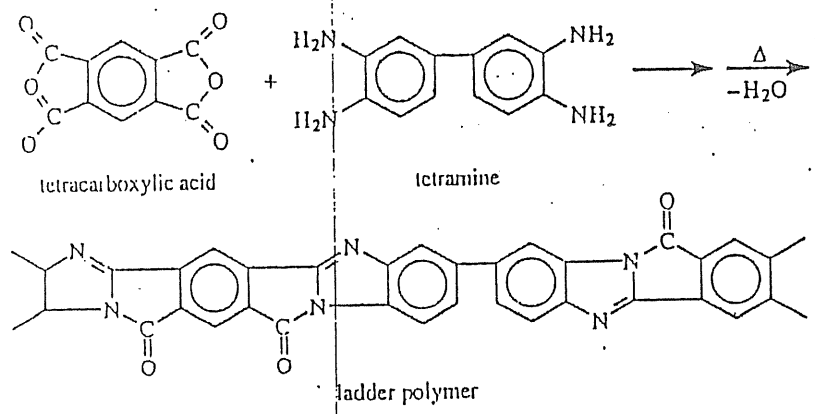

Figure 10.10. Polymerization of a ladder polymer, polyimidazopyrrolane.

10.2.2 Ionic Polymers

Ionic sites may be introduced into polymers through chemical modification or copolymerization. Ionic polymers derived from synthetic organic polymers and containing up to 10 to 15 mol % ionic content are called *ionomers*. Those with higher ionic content are called *polyelectrolytes*. Polyelectrolytes are soluble in water but insoluble in common organic solvents. Typical applications for ionomers include ion-exchange resins, membranes for liquid and facilitated gas separations, superacid catalysts, and most importantly as separators in chloralkaline electrolytes.

Ionic sites are typically pendant carboxylic or sulfonic acid groups that are partially or completely neutralized to form the polymeric salt. Counterions may be sodium, zinc, ammonium, or a halide. Typical nonionic polymer backbones includes polyethylene, polystyrene, and copolymers of fluorocarbons such as tetrafluoroethylene. Due to the general incompatibility of ionic and nonionic segments, microphase separation of the ionic groups is typical of ionic polymers. Small aggregates consisting of only ionic material are termed *multiplets*, while larger aggregates that also include nonionic material are called *clusters*. Multiplets, consisting of only of a few ions or ion pairs, act as moderately strong, temporary, ionic crosslinks. The larger clusters also act as mechanical reinforcement.

The introduction of ionic groups can have significant effects on the properties of polymers. For example, ionic sites can increase T_g, modulus, and melt viscosity. The extent of property modification depends upon the dielectric constant of the backbone, the position and type of ionic group, the type of counterion, ionic concentration, and the degree of neutralization. The concentration of ionic groups and the strength of interaction between the anion and cation determine the increase in T_g with a relationship given as

$$T_g = \frac{cq}{a} \tag{10.1}$$

where c is the concentration of ionic repeat units in the backbone, q is the charge of the counterion, and a is the distance of closest approach between the centers of charge of anion and cation. Generally, T_g is observed to increase 2° to 10°C per mole % of ionic repeat units.

Ionomers. A common commercial ionomer is Surlyn A™, a copolymer of ethylene and about 15% of methacrylic acid. About 33% of the methacrylic acid comonomers are neutralized with sodium hydroxide to produce the sodium salt, as illustrated in Figure 10.11. Ionic bonding provides a tough material, often used for covering golf balls as a replacement for gutta percha (see Section 9.1.1), in packaging applications such as a coating for safety bottles to store hazardous chemicals, and in the manufacture of automotive bumper strips and guards.

Another important class of ionomers are *perfluorosulfonate ionomers* (PFSI), which are copolymers of tetrafluoroethylene and a perfluorinated vinyl ether containing a terminal sulfonyl fluoride (SO_2F) group, as shown in Figure 10.12. The most important commercial PFSI product is Nafion™ ($y = 1$ in Figure 10.12) manufactured by Du Pont, while a related PFSI (designated as XUS; $y = 0$) has been developed by Dow Chemical Company. Commercial PFSI films are melt extruded but can also be solution-cast under special conditions. After film formation, the sulfonyl fluoride groups are converted to sulfonate groups by reaction with

sodium or potassium hydroxide, with further conversion to the commercial sulfonic acid (SO_3H) form (Nafion-H). Other ionic forms (e.g., Na^+, Li^+, K^+, Ag^+, Ca^{2+}, and Al^{3+} salts) can be obtained by ion exchange with the appropriate salts. Nafion has selective permeability to ions and can therefore be used in the production of chlorine and caustic by electrolysis of salt solutions; it also has been evaluated for use in many other applications, such as a membrane for gas separations, organic electrosynthesis, fuel cells, electrodes, separation of amino acids, controlled drug release, and biosensors (see Section 12.1.1).

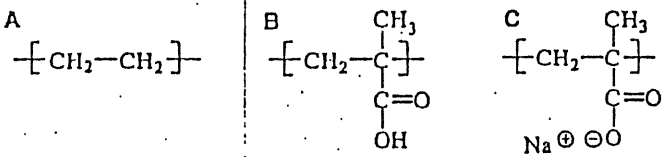

Figure 10.11. Comonomer units in Surlyn A. A. Ethylene. B. Methacrylic acid. C. Sodium salt of methacrylic acid.

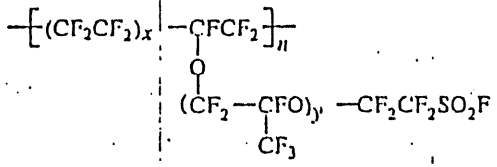

Figure 10.12. Structure of Nafion perfluorinated ionomer

10.2.3 Polyaryletherketones

A important entry into the engineering thermoplastic market are the polyaryletherketones (PAEK), of which polyetheretherketone (PEEK, Victrex®)

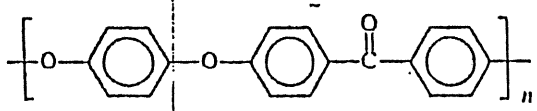

is the most important.[5] As indicated by the data given in Table 10.7, PEEK is partially (20% to 30%) crystalline, but can be melt processed at elevated temperatures. Attractive properties include good abrasion resistance, low flammability and emission of smoke and toxic gases, low water absorption, and resistance to hydrolysis, wear, radiation, and high-temperature steam. The high solvent resistance, good impact-strength, and good thermal stability (maximum continuous working temperature of 260°C) of PEEK make it a good candidate as a thermoplastic matrix for graphite composites (see Section 7.3). Other applications include, solvent-resistant tubing for chromatography, wire and cable insulation for hostile environments, and as magnet-wire coating.

TABLE 10.7 TYPICAL PROPERTIES OF PEEK

Property	Value
T_g (°C)	143
Heat-deflection temperature, °C at 1.82 MPa (264 psi)	148
T_m (°C)	334
Crystallinity, %	
typical	20–35
maximum	48
Heat of fusion, ΔH_f (J g^{-1})	130–161
Density (g cm^{-3})	
amorphous	1.263
crystalline	1.400
Water absorption, % over 24 h and 40% RH	0.15
Solubility parameter (cal/cm^3)$^{1/2}$	9.5
Tensile strength (MPa) at 23°C	91.0
Elongation at 23°C, %	150
Flexural modulus at 23°C, GPa	3.89
Impact strength, Charpy (J m^{-1})	1388

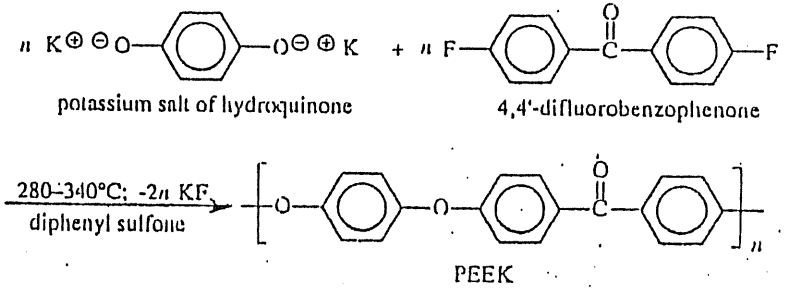

Figure 10.13. Condensation polymerization of polyetheretherketone (PEEK).

High-molecular-weight PEEK can be synthesized by the solution polycondensation of alkali bisphenates with activated aromatic dihalides (typically difluoride) at high temperatures, as shown in Figure 10.13. A wide variety of other arylene ether homopolymers and copolymers with T_gs ranging from 114° to 310°C can be prepared by the nucleophilic displacement of aromatic dihalides and potassium bisphenates.[6]

10.2.4 Specialty Polyolefins

Polyethylene, having molecular weight in the range of 1 to 5 million, has exceptional impact and tensile strength, tear and puncture resistance, high-abrasion resistance, low coefficient of friction, chemical inertness, and good fatigue resistance. Worldwide production of this ultrahigh-molecular-weight polyethylene (UHMWPE) was 40,000 tons in 1992. Applications for UHMWPE include orthopedic implants, battery separators, grocery sacks, and as additives for improving the sliding and wear behavior of other thermoplastics. Melt processability of this high-viscosity polymer can be improved by limiting branching during its polymerization or by incorporating a controlled amount of low-molecular-weight polyethylene, which results in a distinctive bimodal molecular-weight distribution. UHMWPE is processed mainly by compression sintering and ram extrusion into sheet and rod. Recently, there has been moderate interest in the gel spinning of UHMWPE fibers, which combine high tensile strength with low density.

Another entry in the specialty polyolefin market is poly(4-methylpentene-1) or PMP, whose structure is

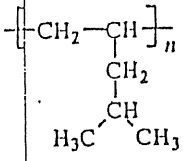

Isotactic PMP, having moderate (40% to 65%) crystallinity, may be polymerized by use of homogeneous Ziegler catalysts like those used in the preparation of *i*-PP (see Chapter 2). Compared to *i*-PP, PMP has a higher T_g (18°C compared to -20°C), much higher T_m (300°C compared to 165°C), lower density (0.83 compared to 0.90), and better transparency. The commercial material (TPX) is a copolymer containing a small amount of linear olefins for improved impact resistance and transparency.

10.2.5 Inorganic Polymers

In addition to the polysiloxanes (Section 9.1.2), there are several other polymers having an all inorganic backbone that have commercial potential for some specialized applications. These include poly(organophosphazenes) and polysilastyrene.

Poly(organophosphazenes). The structure of a basic poly(organophosphazene) repeat unit, having substituent groups, R' and R"

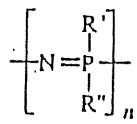

Symmetric substitution (i.e., R' = R") yields crystalline polymers while asymmetric substitution (R' ≠ R') yields noncrystalline rubbery materials suitable for elastomer application. Properties range from highly solvent resistant, low-temperature flexible elastomers to glassy materials that can be fabricated in film and fiber form. Potential applications of poly(organophosphazenes) include elastomers, coatings, and biomedical uses.

Poly(organophosphazenes) may be prepared by substitution of poly(dichlorophosphazene), which is obtained from the radiation or plasma polymerization of hexachlorocyclotriphosphazene. The intermediate polymer, poly(dichlorophosphazene), is unstable due to high susceptibility to hydrolysis. In the presence of atmospheric moisture, poly(dichlorophosphazene) decomposes to ammonium phosphates and phosphoric acids. Fortunately, the active chlorine sites can be readily substituted by nucleophiles such as alkoxides, aryloxides, and amines to yield a wide variety of high-molecular-weight polymers that are chemically and thermally stable. Various synthesis routes to prepare poly(organophosphazenes) were discussed in Section 2.4.1.

Polysilastyrene. Polysilastyrene can be prepared from the solution copolycondensation of dimethyldichlorosilane and phenylmethyldichlorosilane. It is highly soluble and can be spun into fibers, which when heated in an inert atmosphere at very high temperature are converted to a variety of gaseous by-products and β-silicon carbide filaments, as shown in Figure 10.14. Silicon-carbide fibers have extreme strength, as well as exceptional chemical and heat resistance, that makes them suitable for many aerospace applications.

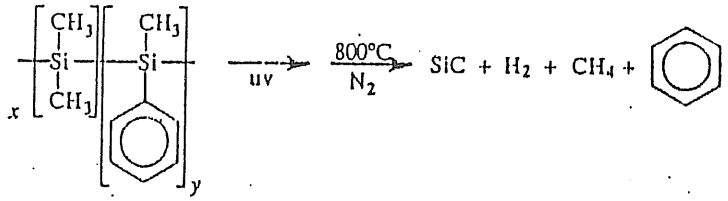

Figure 10.14. Pyrolysis of polysilastyrene to give silicon carbide.

10.2.6 Liquid-Crystal Polymers

Low-molecular-weight liquid crystals have been known since 1888 when it was shown that heating could cause certain cholesteryl esters to change their optical state from colored and opaque to clear. Flory suggested in 1956 that polymers containing long rigid units could form anisotropic ordered solutions above some minimum concentration depending upon temperature and the axial (length/diameter) ratio, x, of the polymer chain. According to Flory's lattice theory, the threshold volume fraction, ϕ, is given as

$$\phi = \frac{8}{x}\left[1 - \frac{2}{x}\right] \approx \frac{8}{x}$$

for high values of x. Above the critical threshold volume fraction, a stable anisotropic phase is formed from solutions and melts of rodlike polymers.

In 1974, liquid-crystal behavior for a polymeric system was first observed in a concentrated solution of poly(benzyl L-glutamate)

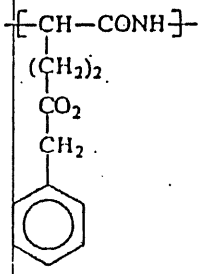

which forms a rodlike α-helical conformation in a variety of organic solvents.

The rigid units or *mesogens* of a liquid-crystal polymer (LCP) can lie along the polymer backbone or be attached to the backbone as a substituent group (i.e., side-chain liquid-crystal polymer). Polymers that form liquid-crystal organization in solution are termed *lyotropic*, while those that form from the melt are called *thermotropic*. There are three recognized forms of liquid-crystal structures. As illustrated in Figure 10.15, the most ordered structure, the *smectic state*, is observed when all the mesogens are arranged in a parallel and lateral order. The smectic state is rare and has been observed only for thermotropic polymers. More common for polymers is the *nematic* state in which there is parallel but not lateral order. Aromatic polyamides (aramid) form a nematic liquid-crystal state in concentrated solution. If mesogens are oriented parallel to one another but the directions vary from one layer to another, the liquid crystal structure is termed *cholesteric*.

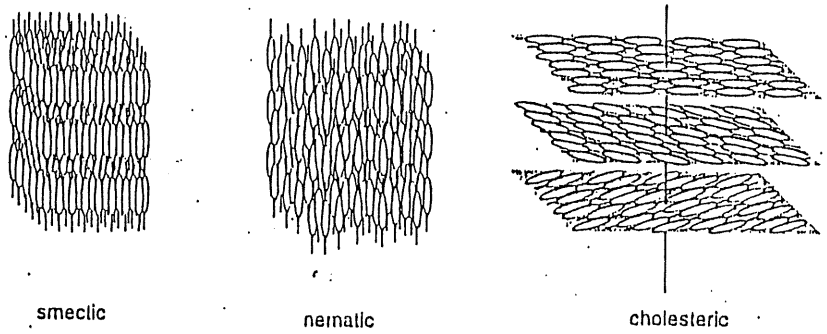

Figure 10.15. Representation of three principal liquid-crystal structures: smectic, nematic, and cholesteric. [Adapted from R. W. Lenz and J.-I. Jin, *Polymer News*, 11, 200 (1986), with permission of the publisher.]

Liquid-crystal polyesters and copolyesters may have been recognized as early as 1965. Liquid-crystal polyesters have highly aromatic structures such as Vectra (Hoechst Celanese)

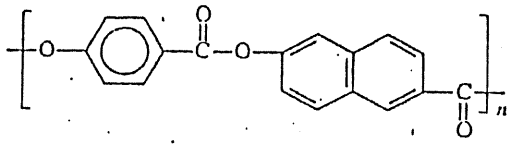

and the thermotropic polyester Xydar (Amoco)

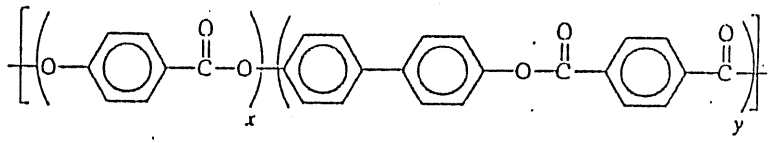

which is made from the polycondensation of *p*-hydroxybenzoic acid (HBA), *p,p'*-biphenol, and terephthalic acid. Such stiff-chain structures lead to ordering of the chains of liquid-crystal polymers (LCPs) in a manner similar to low-molecular-weight liquid crystals.

In general, LCPs are manufactured in a stepwise polycondensation by either a batch or continuous process. The LCP is then mixed with various additives and extruded. Approximately, 60% to 70% of the LCPs sold are reinforced with 30% to 40% glass filler having polymeric sizing to provide a strong interface between the

fiber and matrix. Unreinforced grades are injection molded for specialty applications.

Properties of a part molded from a LCP are highly dependent upon the morphology of the part, which is determined by the conditions of processing. Injection-molded parts exhibit highly oriented skins, with rigid chains oriented in the direction of flow. The core zone beneath this skin is less ordered. This morphology results in very good properties (particularly in the direction of flow) and very high dimensional stability. Other attractive properties of LCPs include exceptional oxygen and barrier properties (100 times that of PETP), very high thermal stability, high modulus and strength, good dimensional stability, and high chemical and solvent resistance. Properties of Xydar are compared to those of a molding-grade PETP in Table 10.8.

TABLE 10.8 COMPARISON OF PROPERTIES OF PET WITH A LIQUID-CRYSTAL POLYESTER

Property	PET[a]	LC Polyester[b]
Tensile strength, MPa	81	126
Tensile modulus, GPa	2.8	8.3
Elongation, %	4–70	5
Flexural strength, MPa		131
Flexural modulus, MPa	3.0	13.1
Izod impact strength, J m^{-1}		
notched		208
unnotched		454
Density, g cm^{-3}		1.35
T_m, °C (or Vicat softening point)	235	358
Heat-deflection temperature at 1.8 MPa, °C	80	337

[a] Arnite
[b] Xydar

At the moment, the high cost of liquid-crystal polyesters (up to $44 per pound for film) has limited these resins to specialty applications such as electronic components (e.g., computer memory modules), housings for light-wave conductors, a variety of aerospace applications, and filaments to compete with aramid fibers. Total worldwide production of LCPs of all kinds is small, estimated at 3000 tons in 1992. This situation may change as monomer costs are reduced through increasing production and supply.

10.2.7 Conductive Polymers

As will be discussed in Section 12.3.1, a number of polymers are electrically conductive or can be made to be conductive by doping with an electron donor or acceptor. Applications include polymeric electrodes for lightweight batteries, variable-transmission windows, electrochromic displays, sensors, and nonlinear optical materials. The first of these electrically conductive polymers was polyacetylene. Other specialty polymers in this class that have been extensively studied include polyaniline, polythiophene, poly(*p*-phenylene), and polypyrrole.

Polyacetylene with molecular weight up to 1 million can be prepared through a complicated process involving a metathesis polymerization (Durham process), as shown in Figure 10.16. The *cis* isomer of polyacetylene can be transformed to the more stable *trans* isomer by heating, as follows:

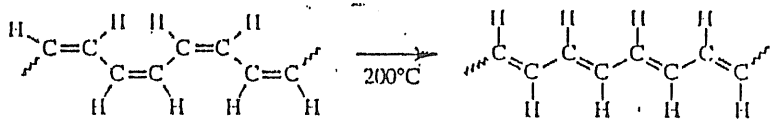

cis-polyacetylene *trans*-polyacetylene

The *trans*-isomer has higher conductivity (4.4×10^{-5} S cm^{-1}) than the *cis*-isomer (1.7×10^{-9}). Conductivity is greatly increased by doping. For example, addition of AsF_5 increases conductivity to 400 S cm^{-1}. Polyacetylene has a T_g in the range from -40° to 0°C and good thermal stability (decomposition temperature above 420°C); however, polyacetylene is easily oxidized. Applications include solar cells and batteries.

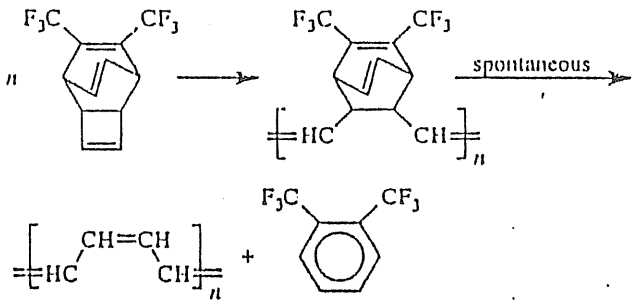

Figure 10.16. Synthesis of *cis*-polyacetylene by metathesis polymerization.

Polyaniline can be obtained by the electrochemical or chemical oxidation of aniline in aqueous acidic media using common oxidants such as ammonium peroxydisulfate. Polyaniline can exist in several oxidation states with vastly different conductivities (ranging from 10^{-11} to 10^{2} S cm^{-1}). Only the emeraldine salt of polyaniline

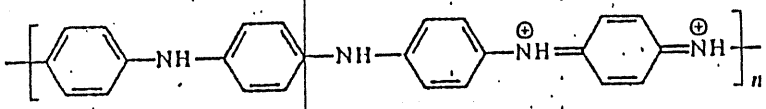

is electrically conductive.

Poly(*p*-phenylene) (PPP) can be prepared by the Friedel-Crafts polymerization of benzene

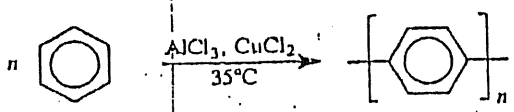

Polypyrrole

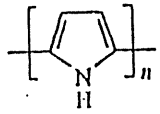

and polythiophene

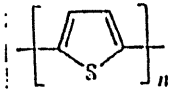

are related in structure and properties. Polypyrrole is obtained by the electropolymerization of pyrrole as a highly colored, dense conducting film while polythiophene can be polymerized by the anodic oxidation of thiophene. Unlike polyacetylene, polypyrrole and polythiophene can be synthesized in the doped form and are very stable in air. Unfortunately, their conductivities are lower (see Section 12.3.1).

Photoconductive Polymers. Some polymers become conductive when illuminated. The ability to become photoconductive has great importance for the xerographic-copier, laser-printer, and duplicator industries. The most important example of a photoconductive polymer is poly(*N*-vinylcarbazole) (PVK)

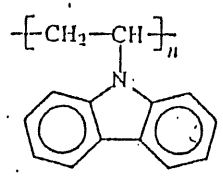

which can be polymerized by free-radical and cationic mechanisms. Both amorphous (free radical) and tactic PVK can be prepared. Amorphous PVK has a T_g of 227°C and a density of 1.184 g cm^{-3}. In the dark, PVK is an insulator; however, it becomes conductive when exposed to UV radiation. Incorporation of sensitizing dyes or electron acceptors extends the photoconductive response to the visible and near IR region. In general, photoconductivity can be attributed to the ability to generate free-charge carriers (electron hole) by the absorption of radiation and the subsequent transport of these carriers to the electrodes.

10.2.8 High-Performance Fibers

In addition to the aramids, Kevlar and Nomex (see Section 10.1.1), there are several other aromatic-chain polymers that can be spun into fibers for high-temperature composite and related applications. These include the polybenzimidazoles, poly(*p*-phenylene benzobisthiazole) (PPBT), and polybenzoxazole (PBO).

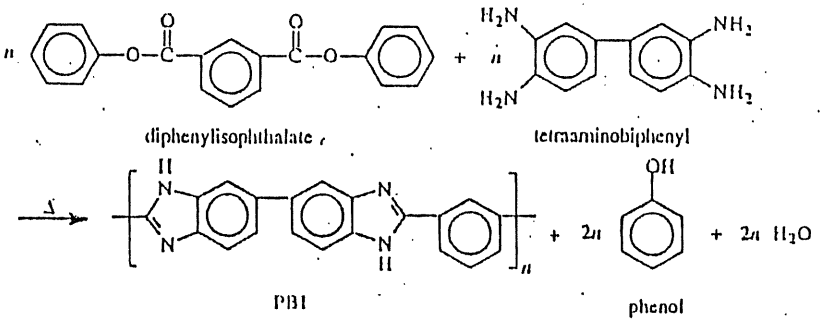

Figure 10.17. Synthesis of a polybenzimidazole, PBI.

The most important of the polybenzimidazoles is poly[2,2'-(*m*-phenylene)-5,5'-bibenzimidazole], which is more commonly known by the acronym PBI. This polymer is obtained from the condensation of an aromatic tetramine, tetraaminobiphenyl, and diphenylisophthalate with the loss of phenol, as illustrated in Figure 10.17. It may be dry spun from solution in dimethylacetamide and drawn under high temperature to obtain a very high tensile-strength fiber. PBI is an amorphous polymer with high temperature stability (in excess of 400°C) and excellent chemical resistance. PBI will burn only in a high-oxygen-content atmosphere (>48%

oxygen). Applications include many of those for which Kevlar may be used, including flue-gas filtration, and generally as a substitute for asbestos.

Poly(*p*-phenylene benzobisthiazole) (PPBT) is synthesized by the step-growth polycondensation of terephthalic acid and 1,4-dimercapto-2,5-diaminobenzene dihydrochloride, as illustrated in Figure 10.18. PPBT fibers, which can be spun from anisotropic acid solutions, have very high modulus (ca. 250 GPa), tenacity of 2.4 GPa, elongation % of 1.4, and undergo a weight loss of only 2% at 316°C after 200 h. One disadvantage is that the compressive strength of composites made from PPBT fibers is poor because of fiber buckling qand interlaminar shear failure as it is for Kevlar-fiber composites.

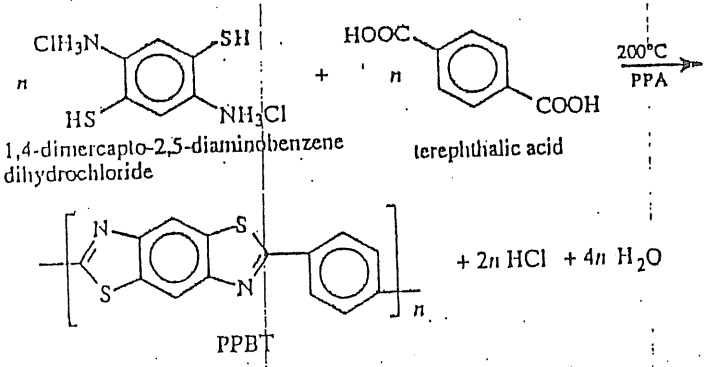

Figure 10.18. Synthesis of poly(*p*-phenylene benzobisthiazole) (PPBT).

A related polymer is polybenzoxazole (PBO) which can be prepared by polycondensation of 4,6-diaminoresorcinol dihydrochloride and terephthaloyl chloride. Fiber properties include a modulus of 84.6 GPa and tenacity of 570 MPa.

10.2.9 Other Specialty Polymers

In addition to the specialty polymers described in the previous sections, new ones are continuously being developed. These include polyphthalamide (Amodel), which, like PEEK, is a semicrystalline thermoplastic having high rigidity and tensile strength, good thermal properties (HDT of 310°C), and excellent chemical resistance and dimensional stability. There is also continued development in the area of poly(aryl ether ketones) such as PEKEKK (Ultrapek), which offers a higher HDT (170°C) than PEEK (138°C) and superior creep resistance.

REFERENCES

1. A. S. Hay, *J. Polym. Sci.*, 58, 581 (1962).
2. A. S. Hay, *Polym. Eng. Sci.*, 16, 1 (1976).
3. B. L. Dickinson, *Eng. Plast.*, 4, 297 (1991).
4. T. Takekoshi, *Polym. J.*, 19, 191 (1987).
5. H. X. Nguyen and H. Ishida, *Polym. Compos.*, 8, 57 (1987).
6. P. M. Hergenrother, B. J. Jensen, and S. J. Havens, *Polymer*, 29, 358 (1988).

Bibliography

H. R. Allcock, "Polyphosphazenes," *J. Inorg. Organometallic Polym.*, 2, 197–211 (1992).

C. G. Baziun and A. Eisenberg, "Ion-Containing Polymers: Ionomers," *J. Chem. Ed.*, 58. 938–943 (1981).

W. Brostow, "Properties of Polymer Liquid Crystals: Choosing Molecular Structures and Blending," *Polymer*, 31, 979–995 (1990).

S. J. Clarson and J. A. Semlyen, *Siloxane Polymers*, Prentice Hall, Englewood Cliffs, NJ, 1993.

R. W. Dyson, ed., *Specialty Polymers*; Chapman and Hall, New York, 1987.

E. M. Genies, A. Boyle, M. Lapkowski, and C. Tsintavis, "Polyaniline: A Historical Survey," *Synthetic Metals*, 36, 139–182 (1990).

K. Hodd, "Trends in High Performance Polymers. Part I — Linear High Performance Polymers," *Trends Polym. Sci.*, 1(5), 129–137 (1993).

R. W. Lenz and J.-I. Jin, "Liquid Crystal Polymers: A New State of Matter," *Polym. News*, 11, 200–204 (1986).

L. C. Lopez and G. L. Wilkes, "Poly(*p*-Phenylene Sulfide) — An Overview of an Important Engineering Thermoplastic," *J. Macromol. Chem. — Rev. Macromol. Chem. Phys.*, C29, 83–151 (1989).

V. A. Lopyrev, G. F. Myachina, O. I. Shevaleyevskii, and M. L. Khodekel, "Polyacetylene Review," *Polym. Sci. USSR*, 10, 2151–2173 (1988).

J. Masamoto, "Modern Polyacetals," *Prog. Polym. Sci.*, 18, 1–84 (1993).

K. L. Mittal, ed., *Polyimides: Synthesis, Characterization, and Applications*, Plenum Press, New York, 1984, Volumes 1 and 2.

G. M. Moelter, R. F. Tetrenult, and M. J. Hefferon, "Polybenzimidazole Fiber," *Polym. News*, 9, 134–138 (1983).

R. B. Rigby, "Polyetheretherketone PEEK," *Polym. News*, 9, 325–328 (1984).

C. E. Sroog, "Polyimides," *Prog. Polym. Sci.*, 16, 561–694 (1991).

11

Polymer Processing and Rheology

Polymer melts and concentrated solutions exhibit both viscous and elastic properties — they are said to be *viscoelastic*. The viscoelastic properties of polymeric solids were the principal topic of discussion in Chapter 5. In this chapter, we are more concerned with the viscoelastic properties of polymer melts and concentrated solutions, particularly in relation to polymer-processing operations. The viscous properties determine such processing issues as the form of the velocity profile, the magnitude of the pressure drop, and the amount of heat generation (i.e., viscous heating) during extrusion through a die. Elastic behavior is responsible for such extrusion phenomena as die swell, melt fracture, and nonzero exit pressure. The fundamentals of polymer-processing operations and the basics of polymer rheology are presented in this chapter.

11.1 BASIC PROCESSING OPERATIONS

Polymer-processing operations may be classified in five broad categories — extrusion, molding, spinning, calendering, and coating. Of these, extrusion is perhaps the most widely used. Applications of extrusion include the continuous production of plastic pipe, sheet, and rods. Molding is normally a batch process, principally in the form of injection- and compression-molding operations used to make

plastic parts as diverse as the cap to a ball-point pen to a fiber-reinforced bathtub. Other important processing methods include the fiber spinning of textiles (discussed in Section 8.2.4), the calendering of plastic sheet, and the deposition of organic coatings on plastic sheet. Two specialized methods of preparing fiber-reinforced composites — filament winding and pultrusion — were discussed in Chapter 7.

11.1.1 Extrusion

A form of extrusion was probably first used in England at the end of the eighteenth century to produce seamless lead pipe. In 1845, a ram-driven device was used to extrude threads of gutta percha (see Section 9.1.1) and to produce pipe from shellac and gutta percha. The first submerged cable laid across the English channel in 1851 was an insulated copper conductor produced by what may be the first application of a commercial wire-coating operation. Screw-driven extruders were developed in the second half of the nineteenth century, and twin-screw extruders appeared in the late 1930s.

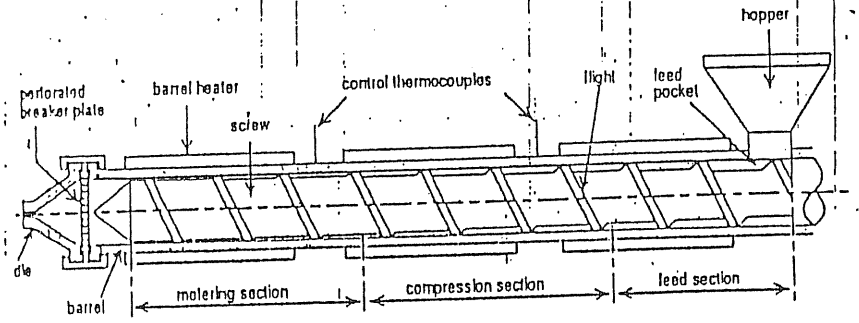

Figure 11.1. Illustration of a single-screw extruder. (Adapted from N. G. McCrum, C. P. Buckley, and C. B. Bucknall, *Principles of Polymer Engineering*, Oxford University Press, Oxford, 1988, by permission of Oxford University Press.)

The two principal components of an extrusion operation are the extruder and the die. As illustrated in Figure 11.1, the extruder consists of a hopper that holds the resin stock (usually in the form of small pellets or powder) and the extruder barrel which can be conceptually divided into three sections on the basis of function. These are called the *feed*, *compression*, and *metering* sections. In the feed section, the solid feed is conveyed by the rotating screw from the hopper to the compression zone where the resin begins to melt due to the action of electrical heaters attached to the barrel wall. By the time the resin reaches the metering zone, all the resin has melted, and the shearing action of the screw rotating against the inner wall of the extruder barrel forces the melt out of the extruder and through a die. The die shapes the extrudate to the desired form. For example, a die with an opening in the for of an annulus (i.e., two concentric cylinders) is used to extrude pipe; a capillary d is used to extrude rods; and a slit die having a rectangular opening is used to extru sheet. A specially designed capillary die is used to coat wire with a layer of plas insulation.

After the extrudate leaves the die, it is cooled and chopped to the desir length. In commercial polymer production, powder from a polymerization react may be feed directly to an extruder that has an opening for venting volatiles — process called *devolatilization*. Examples of volatile contaminants include residu monomer and solvent that may be used during the polymerization process. The e truded melt is then passed through a capillary die, cooled, and chopped to for small pellets. These pellets are easier and safer to handle than the powder and c be shipped, stored, dried, and finally fed into the hopper of another extruder or inje tion-molding machine to produce the final product.

The extruder illustrated in Figure 11.1 has a single screw that is tapered that the distance between the bottom of the screw channel and the wall of the bar decreases as the metering section is reached. This provides increasing shear rate (s Section 11.5) as the melt is forced toward the exit of the extruder. This is adva tageous since the viscosity of polymer melts and concentrated polymer solutio decreases with increasing shear rate, as discussed in Section 11.2.1. Extrude equipped with twin screws that rotate in opposite directions are used when ev higher shear rates are needed, as in the case of temperature-sensitive, high-viscos polymer melts.

11.1.2 Molding

Compression Molding. In many ways, compression molding is t least expensive and simplest of all polymer-processing operations. An early for of compression molding was used by the ancient Chinese to form articles from p per maché. During the early nineteenth century, compression molding was used the United States and other countries to mold rubber parts and cases made from composite of gum shellac and woody fibers. In 1907, Leo Backeland employed compression-molding process to produce phenol–formaldehyde (i.e., phenol resins.

Today, compression molding and a related technique, transfer molding, are t principal methods of molding thermosets such as phenolic resins, alkyds, and uns urated polyesters (see Section 9.2). Injection molding, described in the next se tion, is the preferred method for molding thermoplastics, except in the case of mo ing large parts where the cost of transfer molding or injection molding may be e cessive compared to compression molding. The compression-molding process fairly simple. First, the resin is placed in the bottom half of an open, heated mo Next, the top half of the mold is placed over the bottom half and pressure is appli to cause the molten resin to completely fill the mold cavity, while the excess re is forced out of the mold as *flash*. Presses with clamping capacities from 5 to 40

tons are available for manual and semiautomatic operation. A illustration of a compression-molding operation is shown in Figure 11.2.

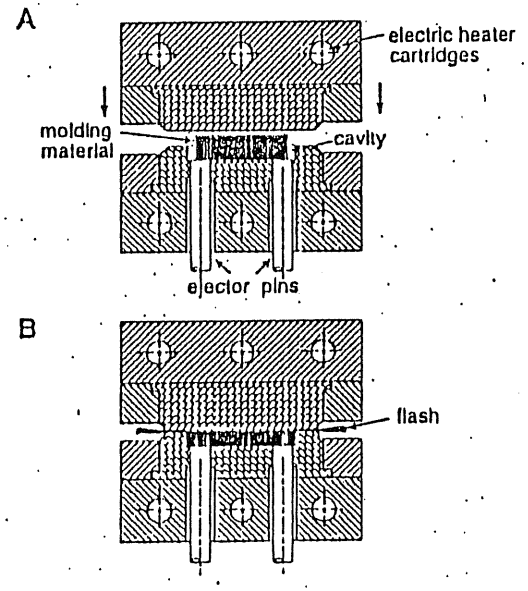

Figure 11.2. Compression-molding process. A. View of an open mold with molding material in place. B. Closed mold showing formed part and flash formed from excess resin. (Adapted from J. L. Hull, in the *Concise Encyclopedia of Polymer Science and Engineering*, J. I. Kroschwitz, ed. Copyright © 1990 by John Wiley & Sons. Reprinted by permission of John Wiley & Sons, Inc.)

Transfer Molding. In the case of *transfer* (or *plunger*) *molding*, the mold is closed prior to resin entry. A simplified diagram of a transfer-molding process is shown in Figure 11.3. A plunger is used to force a predetermined amount of molten resin from an open *transfer pot* through a small opening in the mold. After the mold is opened (Figure 11.3C), ejector pins are used to push the molded part out of the mold. Residual (i.e., uninjected molding resin) is called the *cull*. Molding cycles tend to be shorter than for compression molding because mold temperatures can be higher and the premelted polymer flows more easily through the mold, typically under lower pressure. For these reasons, transfer molding is used to mold parts with intricate geometries and to mold fragile parts or when an insert is used in the mold and the flow of granular molding material during compression molding would, otherwise, damage or displace the insert.

In the case of molding thermoset resins, the molding compound is first placed in the cavity of the compression mold or the transfer pot of a transfer-molding process and heated (ca. 150°C) to provide sufficient flow for mold filling. Pressure (e.g., 2000 psi or 13.4 MPa) is then applied over sufficient time to allow the resin to cure (i.e., crosslink).

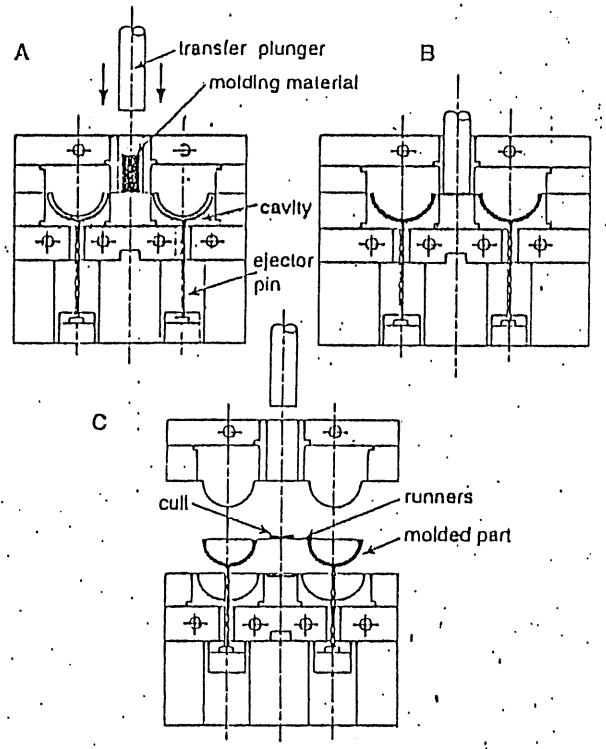

Figure 11.3. Transfer-molding operation. A. Transfer pot is loaded while mold is in closed position. B. Plunger pushes molding material into mold form. C. Mold opens and ejector pins push out molded part. (Adapted from J. L. Hull, in the *Concise Encyclopedia of Polymer Science and Engineering*, J. I. Kroschwitz, ed. Copyright © 1990 by John Wiley & Sons. Reprinted by permission of John Wiley & Sons, Inc.)

Injection Molding. Another important polymer-processing operation is injection molding. The principle behind injection molding dates back to 1856 when E. Pelouze of the United States developed a die-casting machine for forcing molten metal into a die by mechanical or hydraulic means. The development of the

first injection-molding machine for thermoplastics was a result of ivory shortages during the Civil War. In 1868, the Phelan and Collender Co., a producer of billiard balls, offered an impressive award of $10,000 to anyone who could produce a satisfactory substitute for ivory. In 1869, John Wesley Hyatt, a printer from Boston, invented the material celluloid (cellulose nitrate) to replace ivory. Celluloid was the world's first commercial synthetic resin and was used to produce a wide variety of products as diverse as billiard balls and dentures. In 1872, John and his brother Isaiah patented a simple extrusion device consisting of a steam-heated cylinder, hydraulic plunger, and discharge nozzle to extrude rods and tubes from cellulose nitrate.

As illustrated in Figure 11.4, one type of a modern injection-molding operation uses a reciprocating screw to melt a measured volume of feed introduced through the hopper. After a sufficient time has elapsed to form a homogeneous melt, the rotation of the screw ceases, and the melt is rammed into a mold under high pressure by a hydraulically driven thrust of the screw. The amount of resin that can be molded may vary with a particular machine from a few grams to a few kilograms, with clamping forces up to 5000 tons.

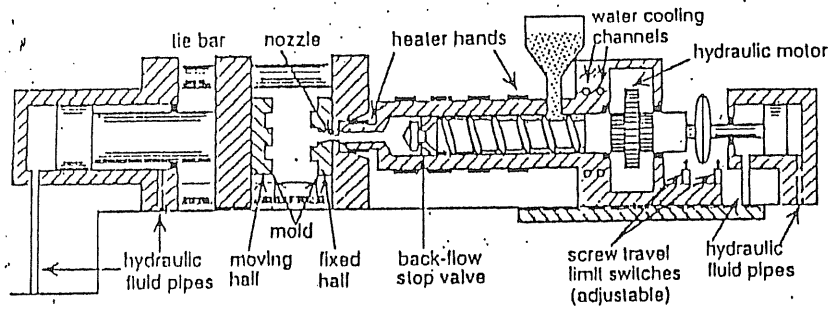

Figure 11.4. Illustration of a reciprocating-screw injection-molding machine and mold. (Adapted from N. G. McCrum, C. P. Buckley, and C. B. Bucknall, *Principles of Polymer Engineering*, Oxford University Press, Oxford, 1988, by permission of Oxford University Press).

A mold may be used to produce a single part such as a computer keyboard or several smaller parts simultaneously (i.e., multiimpression molds). As an illustration, the cross section of a multiimpression mold to produce plastic boxes is shown in Figure 11.5A. The resulting molded assembly after removal from the mold is illustrated in Figure 11.5B. Anyone who has ever built a plastic model airplane is already familiar, albeit unknowingly, with the features of an injection-molded assembly. The thick section through which the molten resin is forced from the nozzle of the injection-molding machine and first enters the mold is called the *sprue*. From the sprue, the melt is pushed through *runners*, which evenly distribute the melt to each mold cavity. The narrow point of attachment of the runner to the mold cavity is called the *gate*. After the mold is totally filled, it is cooled and opened to release the molded assembly. The molded parts are then broken from their attachment at the gates and scrapped sprues, runners, and gates may be recycled to the molding operation. Molds must be able to withstand significant pressures and high temperatures and produce parts with close tolerances after numerous and rapid operations. For these reasons, great care must be exercised in mold design and manufacture. This usually represents a significant expenditure of capital, which contributes significantly to the total price of the molded part.

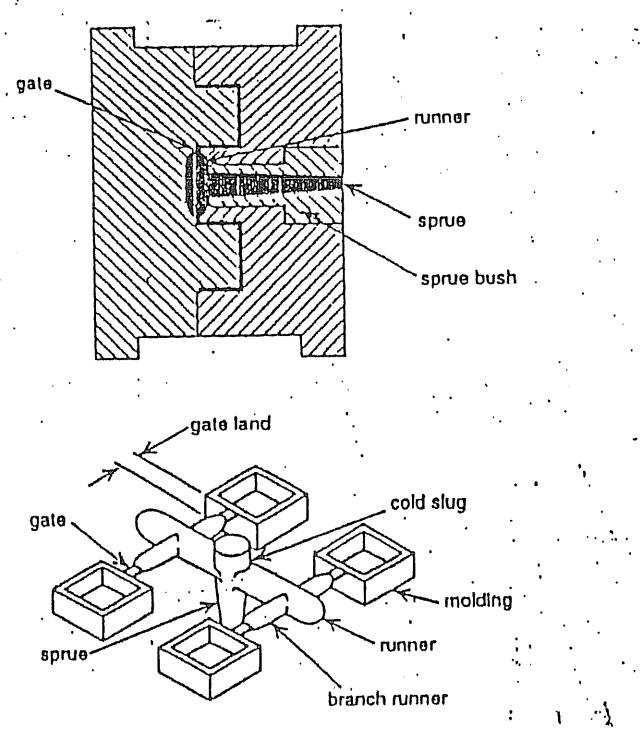

Figure 11.5. A. Typical mold design used in a multiimpression injection molding process for the production of plastic boxes in this example. B. Removed mold assembly showing boxes and plastic scrap (i.e., sprue and runners). (Adapted from N. G. McCrum, C. P. Buckley, and C. B. Bucknall, *Principles of Polymer Engineering*, Oxford University Press, Oxford, 1988, by permission of Oxford University Press.)

There are several variations of the basic design of the reciprocating-screw in-ion-molding machine illustrated in Figure 11.4. For example, a less common ign often used for thermoplastics is called the screw pot or *two-stage* screw. In variation of the injection-molding process, the operations of the extruder screw injection plunger are separated. A fixed (i.e., nonreciprocating) screw is used to lt the resin, which flows into a separate injection chamber and plunger assembly. reciprocating-screw design is preferred for molding thermosets and elastomers for heat-sensitive thermoplastics.

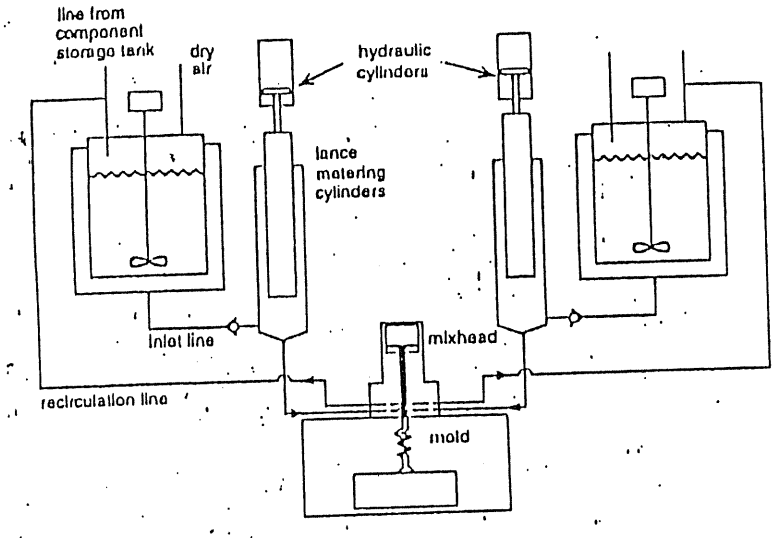

Figure 11.6. Illustration of a reaction injection-molding process showing separate tanks for polymerization reagents. (Adapted from L. T. Manzione, in the *Concise Encyclopedia of Polymer Science and Engineering*, J. I. Kroschwitz, ed. Copyright © 1990 by John Wiley & Sons. Reprinted by permission of John Wiley & Sons, Inc.)

Reaction Injection Molding. Reaction injection molding or RIM is relatively new process (developed in Germany during the late 1960s) whereby the polymer is simultaneously synthesized and molded into the finished product. An illustration of a RIM process is shown in Figure 11.6. At the start of the process, exact quantities of monomers (including catalyst and other additives) are metered into a mixing unit and rapidly forced into the mold, where most of the polymerization occurs. In contrast to injection molding, temperatures and clamping pressures in a RIM process are relatively low, allowing the use of inexpensive aluminum tooling. Other advantages of RIM include low energy consumption, rapid start-up time, and its suitability for the manufacture of large articles such as automotive bumpers. Disadvantages include the risk of worker exposure to noxious, high vapor-pressure reagents such as diisocyanates, which are used in the RIM production of polyurethane.

Due to the need for a controlled and rapid polymerization process, RIM is suited only for condensation-type polymers with favorable polymerization kinetics. Examples of polymers that can be processed in this way include polyamides, epoxies, and especially polyurethanes, which represent more than 95% of total RIM production. Polyurethanes are prepared by reacting diisocyanates with diols and chain extenders as illustrated next and discussed in Section 9.1.2.

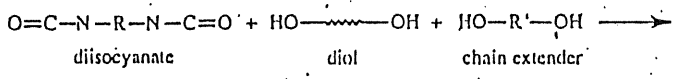

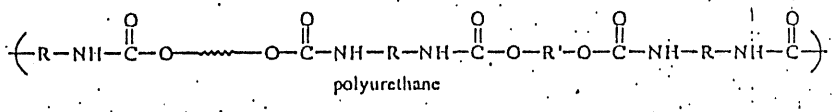

The majority of the RIM-produced polyurethane is used for elastomer applications (e.g., automotive bumpers and fascia), with the remainder used for structural foam. In addition, milled glass and short glass fibers can be added during RIM to provide reinforcement to the molded part. This process, called reinforced RIM or RRIM, was developed in the 1970s.

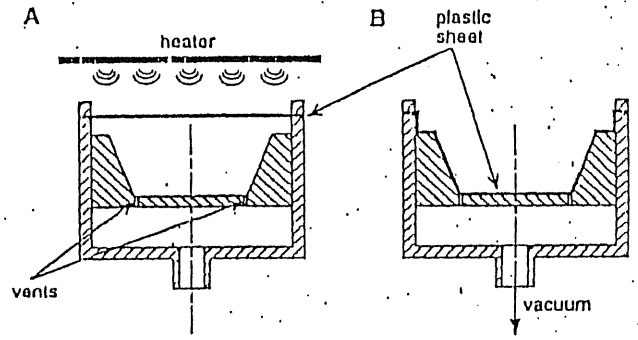

Figure 11.7. Illustration of a simple vacuum-forming operation. A. Flat sheet is heated, B. Softened sheet is forced to fit the mold contour by evacuating the space between the sheet and the mold. (Adapted from R. J. Crawford, *Plastics Engineering*, Copyright 1981, Page No. 200, with kind permission from Elsevier Sciences Ltd, The Boulevard, Langford Lane, Kidlington OX5 1GB, U.K.)

Thermoforming. Thermoforming is an operation borrowed from metallurgy. In thermoforming, a plastic sheet is heated until it softens and then is formed to the shape of a mold preform by application of external air pressure or by pulling vacuum (i.e., vacuum forming) between the sheet and the mold, as illustrated in Figure 11.7. Ancient Egyptian craftsmen who softened tortoise shells to form a variety of shapes may have been the first thermoformers, but it was not until 1938 with the production of blister packaging from cellulose acetate sheet that the modern thermoforming industry began. Applications for thermoforming in today's plastics industry range from the high-volume production of plastic drinking cups to the production of plastic bed liners of half-ton pickup trucks.

Blow Molding. Blow molding uses a gas (e.g., air or sometimes nitrogen) to expand a hot preform, or *parison*, against the form of a mold cavity to produce a hollow object. Blow molding may date back to 1880 when John Wesley Hyatt used this technique to produce baby rattles. Plastic bottles, automotive fuel tanks, toy tricycles, and other consumer products are made in this way. The first plastic bottle was blow molded from polyethylene in 1943. Two types of processes are used for blow molding — injection and extrusion.

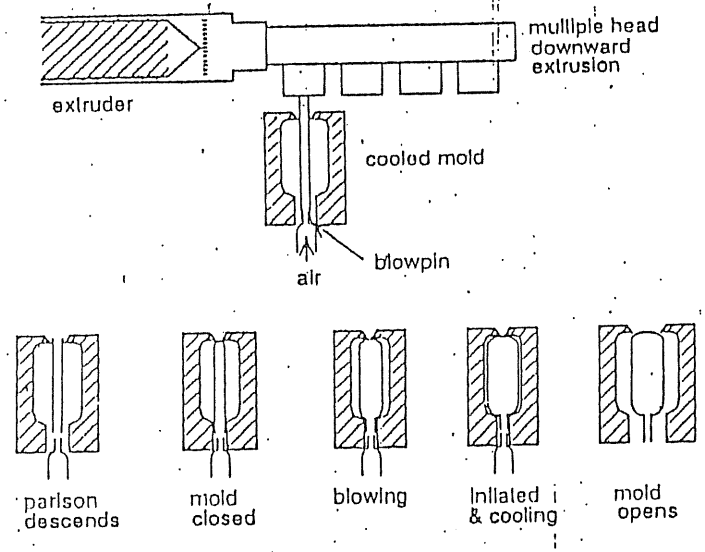

Figure 11.8. Extrusion blow-molding process in the production of plastic bottles. (Adapted from D. H. Morton-Jones, *Polymer Processing*, Chapman and Hall, London, 1989, with permission of the publisher.)

Injection blow molding is used primarily to produce small bottles and other parts. In this process, a parison is first injection molded around a core rod in a preform mold and then transferred to a bottle blow-mold cavity. In the cavity, air expands the parison to the shape of the bottle.

For larger bottles and plastic tanks, an extrusion blow-molding process is used as illustrated in Figure 11.8. In this process, the plastic resin is first extruded as a tube (i.e., the parison) and is then captured by two halves of a mold in a continuous process. A blowpin is inserted, the mold is closed, and air is forced into the parison through the blow pin to expand the parison to the form of the mold cavity.

Rotational Molding. Rotational molding, or rotomolding, uses centrifugal force to force coat the inside of a mold with molten resin. The process is relatively simple, inexpensive to operate, and particularly suited for molding very large objects — the largest reported is a 85-m^3 tank. The forerunner of the modern rotational-molding process was called slush molding, developed by the rubber industry to produce gloves, boots, and other items from plastisols. In slush molding, the liquid was first poured into a hot mold. Once the layer of plastic solidified, excess liquid was poured off.

In a typical rotational-molding operation, the mold cavity is first charged with a predetermined amount of resin powder or liquid. It is then closed and biaxially rotated in an oven. Finally, the mold is removed and cooled. Rotational molding produces little or no flash, thereby eliminating trimming operations and wasted resin. In addition, rotational molding produces very uniform wall thickness as well as strong corner sections, which may be difficult to obtain by other methods.

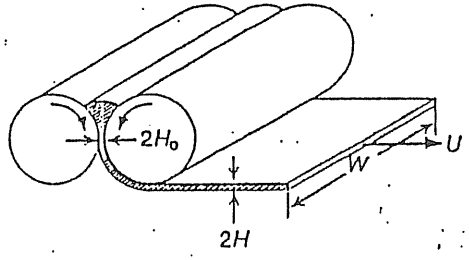

Figure 11.9. Simplified representation of a calendering process. (Adapted from J. M. McKelvey, *Polymer Processing*, John Wiley and Sons, New York, 1962. Courtesy of J. M. McKelvey.)

11.1.3 Calendering

Calendering is another method, in addition to extrusion, that can be used to produce plastic sheet. As illustrated in Figure 11.9, molten polymer is compressed

the small gap (the nip region) between two heated cylinders rotating in opposite directions. Sheets with widths up to 6 ft and thicknesses as small as 0.002 inch can be produced at speeds up to 300 ft min^{-1}. The bulk of U.S. calendering output is poly(vinyl chloride) (PVC), including flexible sheet and film and blends and copolymers of PVC. Calenders can also be used to impart a finish (e.g., gloss or roughness) to a preformed plastic sheet or to laminate two sheets.

11.1.4 Coating

Many different types of processes can be used to coat a thin layer of liquid (e.g., polymer melt or solution) onto a moving sheet, called the *web*. Examples of coatings include the deposition of a

- photographic emulsion on a cellulosic web
- magnetic surface on poly(ethylene terephthalate) for recording and computer tape
- polymer layer on a metal foil for capacitor applications and
- finishes and backings on textile fibers and fabrics.

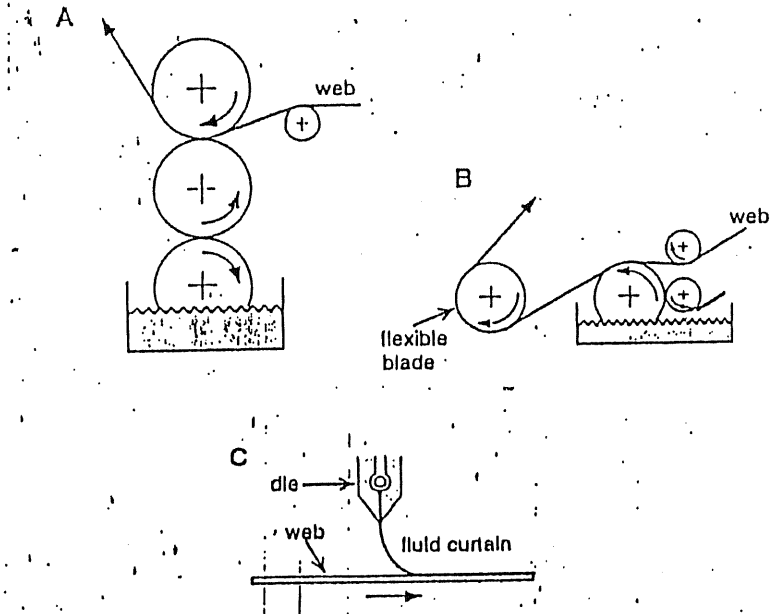

Figure 11.10. Examples of coating process. A. Roll coating. B. Blade coating. C. Curtain coating. (After S. Middleman, *Fundamentals of Polymer Processing*, McGraw-Hill, New York, 1977. Reproduced with permission of McGraw-Hill, Inc.)

Examples of different coating operations are illustrated in Figure 11.10. In *roll coating* (Figure 11.10A), the lower roll picks up liquid from a bath and delivers it to a second roll or directly to the moving web. The thickness of the coating depends upon properties of the liquid (i.e., viscosity, etc.) and the spacing between the rolls through which the web moves. This spacing may be controlled directly or indirectly by controlling pressure between the two rolls.

Another important type of coating operation is called *blade coating*. In this process, a flexible blade is used either to directly meter the coating liquid onto a moving web from the fluid reservoir or the blade can be combined with a roll-coating operation, as shown in Figure 11.10B. The blade is flexible and pressure developed under the blade determines the coating thickness.

The most direct method to apply a coating is by direct extrusion onto the moving web, as shown in Figure 11.10C. This process is sometimes called *curtain coating* and is often used in conjunction with UV curing. The thickness of the coating is determined by the speed of the web and the volumetric output of the extruder.

11.2 INTRODUCTION TO POLYMER RHEOLOGY

The viscous flow of a Newtonian fluid is described by *Newton's law of viscosity* given for shear flow as

$$\boxed{\tau = \mu \frac{d\gamma}{dt}} \tag{11.1}$$

where τ is shear stress, μ is the Newtonian viscosity coefficient, and γ is the shear strain. The time dependence of shear strain is called the *shear strain rate* or simply shear rate:

$$\dot{\gamma} \equiv \frac{d\gamma}{dt}$$

A *simple flow* is defined as one in which *only one* of the three components of the velocity vector

$$\mathbf{u} = (u_1, u_2, u_3)$$

is nonzero. The subscripts 1, 2, and 3 identifying the three components of the velocity vector, u_i, refer to the axes of the particular coordinate system used to analyze the flow process (i.e., x, y, and z in rectangular coordinates; r, θ, and z in cylindrical coordinates; and r, θ, and ϕ in spherical coordinates).

An example of a simple shear flow is Couette shear flow between two infinitely wide parallel plates, as illustrated in Figure 11.11. To analyze this simple flow, it is convenient to establish a rectangular-coordinate system having its x-axis fixed in the bottom plate and oriented along the shear direction, with the y-axis perpendicular to the plate surface. In this case, the shear strain, γ, is defined as the ratio of the deformation of a differential element in the x-direction (dx) to that in the y-direction (dy) during shear. It is easily shown that the shear *rate* in plane Couette flow is equal to the velocity gradient as

$$\dot{\gamma} \equiv \frac{d\gamma}{dt} = \frac{d}{dt}\left(\frac{dx}{dy}\right) = \frac{d}{dy}\left(\frac{dx}{dt}\right) = \frac{du_x}{dy} \tag{11.2}$$

where u_x is the velocity of the fluid in the x-direction. The *maximum* shear rate occurs at the moving plate surface and is given as U/H, where U is the constant (maximum) velocity of the upper plate moving in the x-direction and H is the distance of separation between the two plates. The *minimum* shear rate is zero which occurs at the bottom (stationary) plate (i.e., $y = 0$) assuming there is *no slip* of the fluid layer at the plate surface; therefore, $u_x(0) = 0$. As illustrated in Figure 11.11 and later discussed in Section 11.3.2, the velocity, u_x, is a linear function of the y-coordinate.

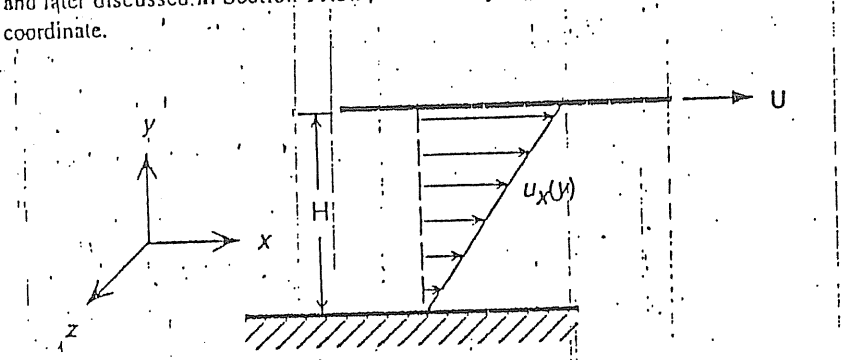

Figure 11.11. Representation of simple shear-flow (plane Couette flow) between parallel plates whereby the upper plate is moving at a constant velocity (U).

In the case of Newtonian fluids such as water and mineral oil, the viscosity, μ, is a function of temperature and pressure but is *independent* of $\dot{\gamma}$. In contrast, the viscosity of non-Newtonian fluids such as concentrated polymer solutions and polymer melts is a function of temperature, pressure, *and* $\dot{\gamma}$. In addition, the viscosity of polymer solutions and melts exhibits a strong dependence on molecular weight. These unique aspects of polymer rheology are discussed in the following section.

11.2.1 Non-Newtonian Flow

Shear-Rate Dependence. A non-Newtonian or *apparent viscosity*,† η, of polymer solutions and melts is defined following Newton's law of viscosity (eq. 11.1) as

$$\boxed{\tau = \eta(\dot{\gamma})\dot{\gamma}} \tag{11.3}$$

Equation 11.3 is called the *generalized Newtonian fluid* (GNF) model. The actual analytical relationship between τ and $\dot{\gamma}$ and, therefore, the dependence of η on $\dot{\gamma}$ are given by the *constitutive* equation of the material. Melts of high-molecular-weight polymers and their concentrated solutions display three characteristic regions, as illustrated in Figure 11.12. At low shear rates, η is nearly independent of $\dot{\gamma}$ (i.e., Newtonian behavior) and approaches a limiting zero shear rate value of η_0. At higher $\dot{\gamma}$, η decreases with increasing $\dot{\gamma}$. Fluids that display this behavior are termed *shear thinning*. Finally, η once again approaches a limiting Newtonian plateau, η_∞, at very high $\dot{\gamma}$.

The molecular basis for shear-thinning behavior is the effect of shear on entanglements, as illustrated in Figure 11.13. At low shear rates, the entanglements impede shear flow and, therefore, viscosity is high. As the shear rate increases, chains begin to orient in the flow direction and disentangle from one another — the viscosity begins to drop. Finally, the molecules become fully oriented in the flow direction at very high shear rates. At this point, stable entanglements are no longer possible and the viscosity reaches a low level that is again independent of shear strain rate. This second Newtonian plateau region is observed in the case of polymer solutions but is rarely observed for polymer melts, because the shear rates required for chain orientation in the melt are so high that the chains actually can be broken (i.e., shear-induced degradation or mechanodegradation; see Section 6.1.5).

---

† Since τ and $\dot{\gamma}$ are the shear stress and shear rate, respectively, the viscosity defined by eq. 11.3

$$\eta = \frac{\tau}{\dot{\gamma}}$$

is the *shear* viscosity. An extensional or Trouton viscosity is defined by the corresponding expression for tensile stress and strain as

$$\eta_T = \frac{\sigma}{\dot{\varepsilon}}.$$

The extensional viscosity and its dependence upon the tensile strain rate are important in modeling processing operations where significant extensional flow occurs, such as converging flow in a runner during injection molding and during calendering and blow-molding operations. Extensional viscosity may also have significant importance to the drag-reduction properties of dilute polymer solutions (see Section 12.5).

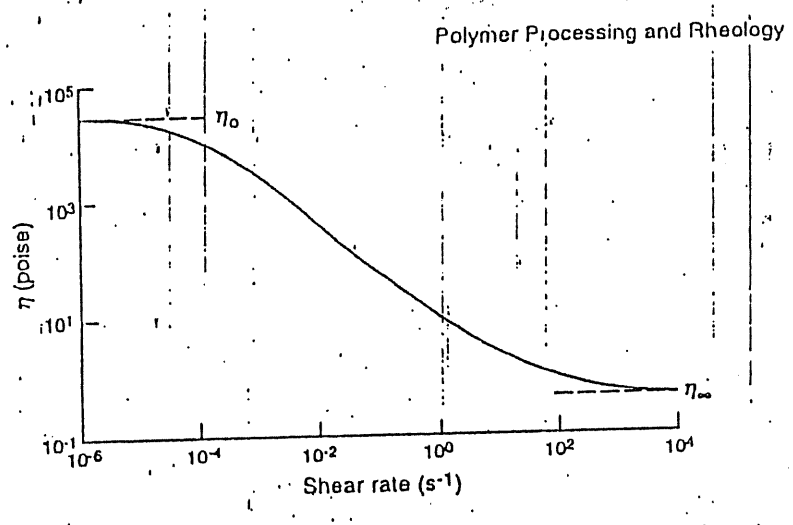

Figure 11.12. Typical dependence of apparent viscosity, η, of a polymeric melt on shear rate, $\dot{\gamma}$, showing the zero-shear viscosity, η_o, plateau. (Adapted from H. A. Barnes, J. F. Hutton, and K. Walters, *An Introduction to Rheology*, Elsevier, Amsterdam, 1989, with permission of the publisher.)

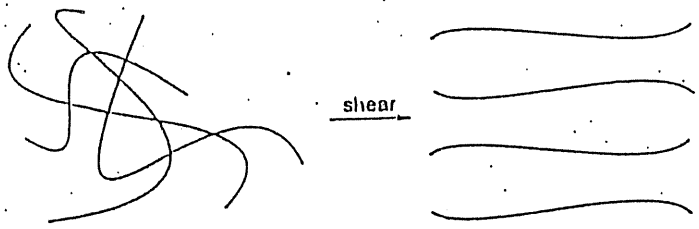

Figure 11.13. Idealized view of the effect of shear on the entanglements of concentrated polymer solutions and polymer melts.

In rare cases, the viscosity may *increase* with increasing shear rate. Fluids that exhibit this behavior are called shear thickening (or dilatant). Examples of shear-thickening behavior are generally limited to concentrated suspensions such as PVC pastes and polymer melts that undergo shear-induced crystallization.

Molecular-Weight Dependence. The significance of entanglements to shear-thinning flow suggests that molecular weight and the critical molecular weight for entanglements, M_c (see Section 4.1.1), should significantly influence the rheological properties of polymers. It has been shown that the zero-shear viscosity, η_o, is directly related to the weight-average molecular weight, $\overline{M}_w$, when $\overline{M}_w < M_c$, but follows a 3.4 power dependence on $\overline{M}_w$ when $\overline{M}_w \geq M_c$. In addition, the onset of shear-thinning behavior occurs at progressively lower $\dot{\gamma}$ as molecular weight increases, as shown by viscosity data for polystyrene given in Figure 11.14.

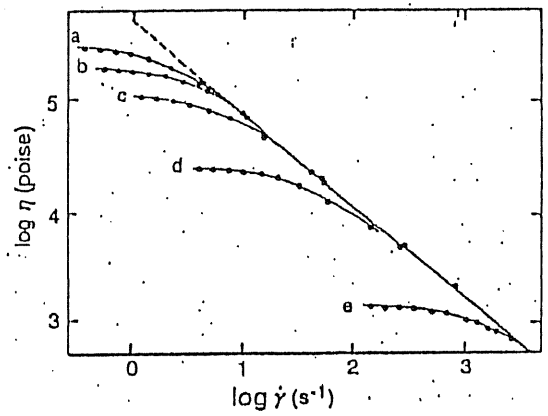

Figure 11.14. Effect of increasing molecular weight on the dependence of polymer viscosity on $\dot{\gamma}$ for polystyrene (M_c = 31,200) at 183°C. Molecular weights are (a) 242,000; (b) 217,000; (c) 179,000; (d) 117,000; and (e) 48,500. [Adapted from R. A. Stratton, *J. Colloid Interface Sci.*, 22, 517 (1966), with permission of the publisher.]

Temperature Dependence. The temperature dependence of the apparent viscosity of a polymer melt follows a typical *Arrhenius relationship* at high temperatures, ca. 100°C above T_g, as given by

$$\eta = \eta_r \exp\left[\frac{E}{R}\left(\frac{1}{T} - \frac{1}{T_r}\right)\right] \qquad (11.4)$$

where η_r is the viscosity at some reference temperature, T_r, E is the activation energy (typically 21 to 210 kJ mol^{-1}), and R is the ideal gas constant. At lower temperatures, in the vicinity of the glass-transition temperature, approximately $T_g < T < T_g + 100°C$, viscosity increases much more rapidly with decreasing temperature than given by the Arrhenius expression. In this case, the temperature dependence of melt viscosity can be obtained by the WLF equation (see Section 5.1.5) as

$$\log\left[\frac{\eta(T)}{\eta(T_g)}\right] = \log a_T = \frac{-C_1(T-T_g)}{C_2+T-T_g} \qquad (11.5)$$

where $\eta(T_g)$ is the viscosity at T_g. Figure 11.15 shows the fit of experimental data for polycarbonate, for which excellent agreement between experimental viscosities and those predicted by the WLF equation is observed over the temperature range from T_g + 55°C to T_g + 185°C.[1]

As discussed in Chapter 4, one view of the glass transition is that it is an isoviscous state where the viscosity at T_g, $\eta(T_g)$, is approximately 10^{12} Pa-s (10^{13} poise). Use of eq. 11.5 provides a means of relating the WLF parameters, C_1 and C_2, to the free volume, V_f, and the thermal-expansion coefficient, α, of the polymer as shown in Appendix 1 of this chapter.

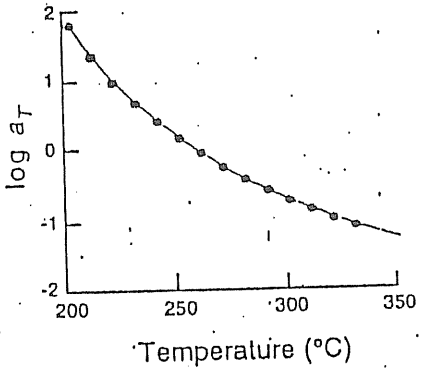

Figure 11.15. WLF fit (curve) of the shift factor, $a_T = \eta(T)/\eta(260°C)$, for polycarbonate at a reference temperature of 260°C. (Adapted from ref. 1 with permission of the publisher.)

Pressure Dependence. Unlike the case for the glass-transition temperature, viscosity can be significantly affected by pressure. This pressure dependence may be an important consideration in the design of some processing operations, such as injection molding for which pressures of several thousand psi are routinely experienced. At constant temperature, the effect of pressure on viscosity can be approximated by the relation

$$\ln\left(\frac{\eta}{\eta_r}\right) = \beta(p-p_r) \qquad (11.6)$$

where η_r is a reference viscosity corresponding to some reference pressure, p_r, and β is a pressure coefficient in the range of 0.87 to 4.93 × 10^{-8} Pa^{-1} (0.6 to 3.4 × 10^{-4} $psia^{-1}$). As an example, the viscosity of a polystyrene melt at 250°C will nearly double with an increase in pressure from 13.8 to 27.6 MPa (2000 to 4000 psi). Often, in the modeling of processing operations, it is necessary to neglect the effect of pressure in order to obtain analytical or even numerical solutions that are manageable, as discussed in Section 11.3.

Time Dependence. Shear-thinning (and shear-thickening) behavior is considered to be reversible providing no thermal or mechanical degradation has occurred. In some cases, the subsequent flow behavior of a previously sheared fluid may depend upon the prior shear history and the time allowed for recovery. A fluid whose viscosity is reduced by prior deformation or decreases with time under conditions of constant stress or shear rate is called *thixotropic*.[2] Eventually, the viscosity will recover (increase) once the stress is removed. An example of a thixotropic fluid is nondrip latex paint. Similarly, a fluid whose viscosity has increased as a result of prior deformation history or increases in time under application of constant stress or strain is called antithixotropic. As will be shown shortly, the successful modeling of polymer-processing operations is difficult enough without introducing time-dependent viscosity terms, and no attempt to do so will be made here.

11.2.2 Viscosity of Polymer Solutions and Suspensions

Solution Viscosity. For very dilute solutions, polymer coils are widely separated and do not overlap, as illustrated in Figure 11.16. At a critical concentration, c^{**}, marking the transition from the extremely dilute to dilute regions, the hydrodynamic volumes of individual coils start to touch. As concentration is further increased ($c > c^*$), coils begin to overlap and finally entanglements are formed that increase viscosity.

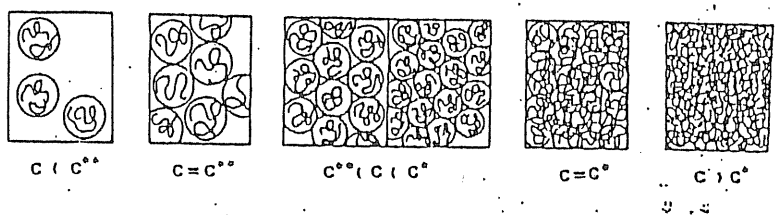

Figure 11.16. Critical concentration regions showing transition from the extremely dilute region ($c < c^{**}$) where polymer coils are isolated to the dilute region ($c > c^*$) where coils become entangled. [Reproduced from A. Dondos and C. Tsitsilianis, *Polym. Int.*, 28, 151 (1992), with permission of the publisher.]

The critical concentration, c^*, may be marked by an abrupt increase in the relative viscosity increment (or specific viscosity, eq. 3.120). This transition is shown for cellulose acetate (CA) in dimethyl sulfoxide (DMSO) in Figure 11.17. The critical transition concentration was found to be 3.7 g dL^{-1} and approximately independent of the solvent,[3] although a dependence of c^* on the molecular weight of CA would be expected.

Below c^*, viscosity is proportional to concentration, but above c^*, viscosity is approximately proportional to the *fifth power* of concentration. In general, the effect of molecular weight and solution concentration of viscosity can be modeled as[4]

$$\eta = K(c\rho)^{\alpha} M^{\beta} \tag{11.7}$$

where K is a constant and α and β are parameters; the ratio β/α is usually in the range from 0.54 to 0.74.

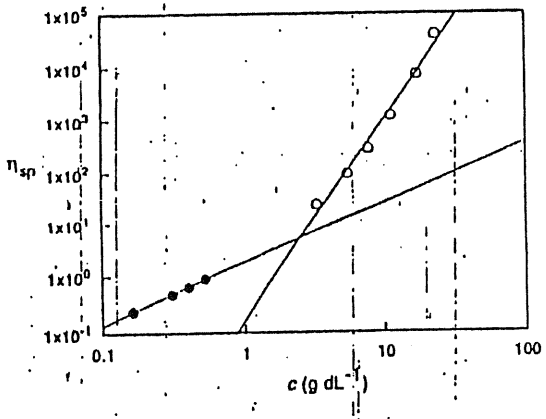

Figure 11.17. Concentration dependence of the specific viscosity of dilute and moderately concentrated solutions of cellulose acetate in dimethyl sulfoxide.[3] The intersection of straight lines that are drawn through the dilute-solution (●) and concentrated-solution (○) data marks the critical concentration, c^* (ca. 3.7 g dL^{-1} in this case).

The presence of a solvent (or plasticizer) has two effects on polymer viscosity in the concentrated solution region: the solvent (1) lowers the T_g and (2) increases the molecular weight between entanglements, M_e (see Section 4.1.1), as

$$M_e = \frac{M_e^{\circ}}{\phi} \tag{11.8}$$

where M_e° is the molecular weight between entanglements for the undiluted polymer and ϕ is the volume fraction of solvent. As polymer concentration increases, polymer solutions become more non-Newtonian as the number of entanglements increases, as illustrated for concentrated solutions of polystyrene in *n*-butyl benzene in Figure 11.18. The data show that viscosity of a concentrated polymer solution rapidly increases with increasing polymer concentration. In addition, the onset of shear-thinning behavior occurs at lower shear rate with increasing concentration.

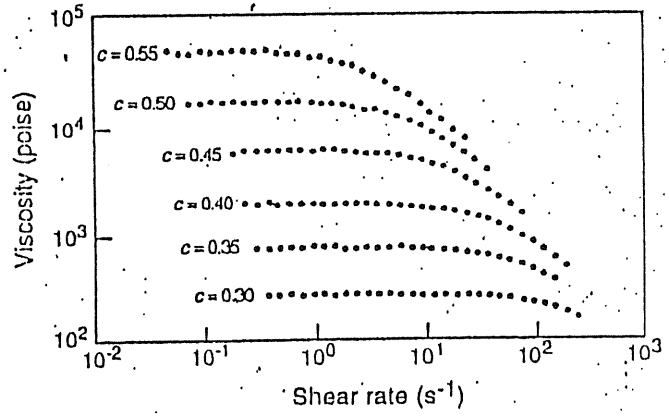

Figure 11.18. Viscosity of polystyrene (411,000 molecular weight) in *n*-butyl benzene at different concentrations (c, units of g cm^{-3}) as a function of shear strain-rate ($\dot{\gamma}$) at 30°C. [Adapted from W. W. Graessley, R. L. Hazelton, and L. R. Lindeman, *Trans. Soc. Rheol.*, 11, 267 (1967), with permission of the publisher.]

Viscosity of Suspensions. In many cases, concentrated polymer solutions and melts may contain particulate or fiber fillers. For example, commercial rubber formulations usually contain carbon black. Poly(vinyl chloride) for floor tile or wire insulation applications typically contains rigid fillers such as calcium carbonate. A *plastisol* is a suspension of polymer particles in a liquid plasticizer, while a *latex* is a suspension of polymer particles in water. In all these cases, suspended particles affect the rheological properties of the suspension.

In 1906, Einstein theorized that the viscosity of dilute suspensions in a Newtonian liquid can be expressed as

$$\eta = \eta^{\circ}(1 + k_E\phi) \tag{11.9}$$

where η° is the viscosity of the suspending liquid, k_E is called the Einstein coefficient, and ϕ is the volume fraction of suspended particles. The Einstein coefficient

depends upon the geometry of the dispersed phase as well as the orientation of fibers and other nonspherical fillers. In the case of spherical fillers, such as calcium carbonate, k_E is 2.5. Equation 11.9 indicates that the relative viscosity, η/η°, depends only upon the concentration of filler and is independent of the size and nature of the particles. Over the years, many other equations have been proposed with various degrees of success. One of the best was proposed by Mooney, given as

$$\ln\left(\eta/\eta^\circ\right) = \frac{k_E \phi}{1 - \phi/\phi_m} \tag{11.10}$$

where ϕ_m is the maximum packing (volume) fraction, which varies from 0.065 for rod-shaped particles to 0.7405 for hexagonal close-packed spheres. It may be noted that even Newtonian fluids such as water become non-Newtonian at moderate concentrations of suspended particles. Some suspensions such as lattices and plastisols exhibit yield (Bingham) behavior, as discussed in the following section.

11.2.3 Constitutive Equations

In order to model a simple-flow geometry as a prelude to handling more complicated processes such as extrusion, it is necessary to begin with some reasonable model for the relation between shear stress and shear rate (eq. 11.3). The most widely used relationship is the *power-law* (or Ostwald–de Waele–Nutting) model given as

$$\boxed{\tau = m\dot{\gamma}^n} \tag{11.11}$$

where m is called the *consistency* and n is the *power-law index*. For a given polymer, m is a decreasing function while n is an increasing function of increasing temperature, which means that the melt becomes more Newtonian (i.e., less shear thinning) with an increase in temperature. It follows from the GNF model given by eq. 11.3 that the dependence of apparent viscosity, η, on $\dot{\gamma}$ for a power-law fluid (PLF) is

$$\boxed{\eta = m\dot{\gamma}^{n-1}} \tag{11.12}$$

Equation 11.12 indicates that, when $n = 1$, η is independent of $\dot{\gamma}$. This means that Newton's law of viscosity may be considered to be a special case (i.e., $n = 1$ and $m = \mu$) of the more general PLF model. For shear-thinning behavior, $n < 1$. Representative values of the power-law parameters, m and n, and the $\dot{\gamma}$ range for which they are applicable are given for several commercially important polymers in Table 11.1.

Some non-Newtonian fluids require an application of a threshold (or yield) stress, τ_y, before flow will begin. Such fluids are termed *Bingham* fluids and may be viewed as having some internal structure that collapses at τ_y. Examples include some suspensions, slurries, pulps, and ketchup. If the viscous response is Newtonian once the yield stress has been reached, the constitutive equation for a Bingham fluid can be written as

$$\tau = \tau_y + \mu\dot{\gamma}. \tag{11.13}$$

TABLE 11.1 POWER-LAW PARAMETERS FOR SOME REPRESENTATIVE POLYMERS

Polymer	Temp. °C	$\dot{\gamma}$ Range s^{-1}	m N s^n m^{-2}	n
Polystyrene	190	100–4500	4.47×10^4	0.22
	210	100–4500	2.38×10^4	0.25
	225	100–5000	1.56×10^4	0.28
Polypropylene	180	100–400	6.79×10^3	0.37
	190	100–3500	4.89×10^3	0.41
	200	100–4000	4.35×10^3	0.41
Polycarbonate	180	100–1000	8.39×10^3	0.64
	200	100–1000	4.31×10^3	0.67
	220	100–1000	1.08×10^3	0.80

TABLE 11.2 TYPICAL $\dot{\gamma}$ RANGE FOR POLYMER PROCESSING OPERATIONS

Operation	$\dot{\gamma}$ Range (s^{-1})
Compression molding	1–10
Calendering	10–10^2
Extrusion	10^2–10^3
Injection molding	10^3–10^4

It is clear that eq. 11.12 is suitable for representing the dependence of viscosity on shear rate only in the shear-thinning region where a plot of $\log \eta$ versus $\log \dot{\gamma}$ is linear. Since this is normally the $\dot{\gamma}$ range for most important processing operations, particularly extrusion and injection molding (see Table 11.2), this restriction is seldom significant considering the simplicity of the model. Other constitutive equations, such as the Carreau model,[5] are available to fit data over a more extensive $\dot{\gamma}$ range but, typically, make the solution to processing problems more difficult.

11.2.4 Elastic Properties of Polymeric Fluids

A unique and important characteristic of polymer melts and concentrated solutions is their elastic recovery after shear deformation. When polymer chains are oriented in the flow direction, there is an entropic driving force for the chains to recover their random coil conformation upon cessation of the stress. For example, chains undergoing shear deformation during flow in a capillary will recover their original equilibrium conformations at the exit of a capillary where stress goes to zero. This gives rise to *die swell* whereby the diameter of the extruded fiber is larger than the diameter of the capillary. As an illustration, the die swell of polyethylene extruded through a capillary die is shown in Figure 11.19.

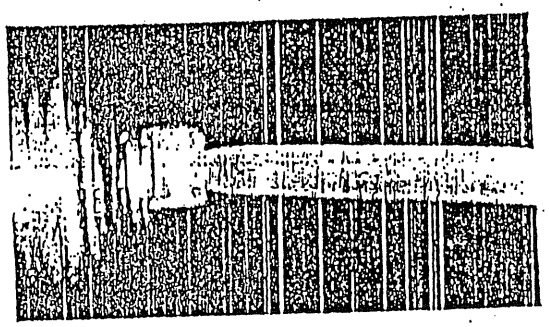

Figure 11.19. Die swell of high-density polyethylene exiting a circular tube at 180°C. (Reproduced with permission of the publisher from C. D. Han, *Rheology in Polymer Processing*, Academic Press, New York, 1976.)

Quantitatively, elastic response is expressed in terms of *normal stresses*. Both stress and strain are second-order tensors and can be represented by a 3×3 matrix having nine components. For example, the stress tensor, τ, in an arbitrary coordinate system with axes 1, 2, and 3 (equivalent to x, y, and z in a rectangular coordinates; r, z, and θ in a cylindrical coordinates; or r, θ, ϕ in a spherical coordinates) is given as

$$\tau = \begin{pmatrix} \tau_{11} & \tau_{12} & \tau_{13} \\ \tau_{21} & \tau_{22} & \tau_{23} \\ \tau_{31} & \tau_{32} & \tau_{33} \end{pmatrix} \tag{11.14}$$

The first and second subscripts of each stress component, τ_{ij}, in the matrix identify the row (the direction of the force vector) and the column (the normal to the plane on which the component of force acts), respectively. The stress tensor (as well as the strain tensor,† which can be written in an analogous fashion) is symmetrical. This means that $\tau_{ij} \equiv \tau_{ji}$ and, therefore, only six of the total of nine stress components are independent. The normal stress components are those lying along the diagonal of the matrix where $i \equiv j$ (i.e., τ_{11}, τ_{22}, τ_{33}). The orientation of normal stresses for a cubical fluid element in simple plane shear is illustrated in Figure 11.20.

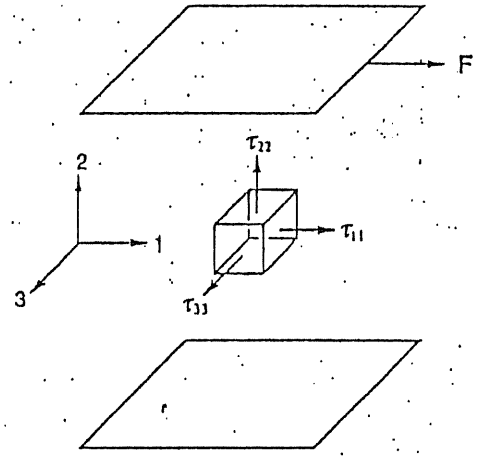

Figure 11.20. Normal stresses generated at the faces of a cubical element of fluid undergoing simple shear (shear stress τ_{12}).

† The rate-of-deformation tensor is given as

$$\Delta = \begin{pmatrix} \Delta_{11} & \Delta_{12} & \Delta_{13} \\ \Delta_{21} & \Delta_{22} & \Delta_{23} \\ \Delta_{31} & \Delta_{32} & \Delta_{33} \end{pmatrix}$$

for which the components of the tensor are symmetric, $\Delta_{ij} = \Delta_{ji}$.

When considering normal stresses, it is convenient to define two *normal-stress differences* that, like apparent viscosity, have a dependence on $\dot{\gamma}$. These are the *first* (or primary) *normal-stress difference*

$$\tau_{11} - \tau_{22} = \Psi'_1(\dot{\gamma})\dot{\gamma}^2 \tag{11.15}$$

and the *second normal-stress difference*

$$\tau_{22} - \tau_{33} = \Psi'_2(\dot{\gamma})\dot{\gamma}^2 \tag{11.16}$$

where Ψ'_1 and Ψ'_2 are called the first and second normal-stress coefficients, respectively, which are also functions of $\dot{\gamma}$. The apparent viscosity, η, and the two normal-stress coefficients are the three *material functions* that describe the complete shear response (viscous and elastic) of polymeric fluids.

In terms of their importance to polymer processing, the first normal-stress difference is the more significant of the two. It is responsible for the swelling of extrudate exiting a die (called *die swell*, the Barus effect, or puffup) and for a non-zero pressure drop that has been observed to occur at the die exit (see Section 11.4.1). By comparison, the second normal-stress difference is small (only 10% to 15% of the magnitude of the first normal-stress difference) and has a negative sign. Both normal-stress differences can be measured directly at low $\dot{\gamma}$ by modern rheological instruments such as cone-and-plate and parallel-plate rheometers, which have sensitive force-transducers mounted in the three directions orthogonal to the plane of shear. Basic concepts of rheometry are covered in Section 11.4. For evaluation of normal-stress effects at higher $\dot{\gamma}$ typical of actual processing operations, on-line rheometers such as a slit die (rectangular die) attached to an extruder may be used. By reading pressures along the length of the die using flush-mounted pressure transducers, the exit pressure may be determined by extrapolation of a plot of pressure versus die length. Correlations may then be used to relate die swell to exit pressure for given operating conditions.

11.3 ANALYSIS OF SIMPLE FLOWS

Polymer-processing operations like extrusion, injection molding, pultrusion, roll coating, blow molding, and others are too complicated to model rigorously. Fortunately, most processing operations can be broken down into a set of simpler flow processes for which analytical or numerical solutions can be obtained using various simplifying approximations and constraints. In this way, it is possible to understand how process variables such as screw speed and temperature in an extruder affect performance variables such as volumetric output. A complete discussion of the modeling of polymer processes is well beyond the scope of this chapter and the reader is encouraged to consult the excellent texts by Han, McKelvey, Middleman, and Tadmor and Gogos that are cited in the bibliography at the end of this chapter. In the next sections, a general development of this subject is given along with some important results to serve as an introduction to the subject.

All polymer-processing operations involve the flow of polymer solutions or melts under a pressure gradient, shear deformation, or both. Since concentrated polymer solutions and polymer melts are non-Newtonian fluids, it is necessary to know the exact relationship between stress and strain — the constitutive equation — in order to analyze flow through even the simplest geometry. As mentioned earlier, the power-law fluid (PLF) model is the one most frequently used. The simplest geometries to model are those for which (1) edge effects can be neglected, (2) flow is isothermal, and (3) a coordinate system (rectangular, cylindrical, or spherical) can be selected such that there is only one nonzero component of the velocity vector (i.e., flow is viscometric). Examples include pressure flow through long capillaries and between infinitely wide parallel plates. Simple *shear* flows† include those created by long concentric cylinders of which one cylinder is rotating or moving along the axial direction and between infinitely wide parallel plates of which one is moving at a constant velocity and parallel to the other.

The solution to a simple-flow model is usually in the form of an expression for velocity as a function of the coordinate parameter(s) of the system. For example, the velocity in the axial (z) direction (i.e., along the length of a capillary) is a function of the radial distance from the center line, $u_z(r)$, as discussed in the following section. In cases where the flow is directed out of the system, as it is in pressure flow through a capillary, the velocity profile can be used to obtain an expression for the volumetric flow rate.

In general, any solution to a flow problem must satisfy the conservation of momentum (i.e., the dynamic equations), conservation of mass (i.e., the continuity equations), and conservation of energy (i.e., the energy equations). The solutions given in the following examples of pressure and shear flow are obtained with the assumptions that the flow is isothermal, laminar, fully developed, steady, and incompressible. In addition, it is assumed that all body forces such as gravity can be neglected. The imposition of isothermal conditions is an especially major con-

† A simple shear flow is formerly defined as one for which a coordinate system can be chosen such that there is a nonzero component of velocity in only one direction

$$\mathbf{u} = \begin{pmatrix} u_1 & 0 & 0 \end{pmatrix}$$

and the rate-of-deformation tensor is given as

$$\Delta = \dot{\gamma}\begin{pmatrix} 0 & 1 & 0 \\ 1 & 0 & 0 \\ 0 & 0 & 0 \end{pmatrix}$$

where $\dot{\gamma}$ is the shear rate (a scalar).

straint, especially since processing operations are seldom isothermal and the flow of viscous polymer melts results in the generation of heat (i.e., viscous dissipation). The advantage of the restraint of isothermal flow is that it removes the energy equations from consideration in the solution and, therefore, greatly simplifies the task.† Taken together, these assumptions mean that only *one* dynamic equation usually needs to be solved for a particular problem.

The dynamic equations for an *incompressible* fluid of density ρ subject to an external force field f are written in Cartesian coordinate as

$$\boxed{\rho\left(\frac{\partial u_i}{\partial t}+u_j\frac{\partial u_i}{\partial x_i}\right)=\frac{\partial T_{ij}}{\partial x_j}+\rho f_i} \tag{11.17}$$

where u is velocity, t is time, f is a body force (e.g., gravity), and the summation is over all j — the coordinate parameters x, y, and z. This means that there are three dynamic equations for each coordinate system. The parameter T_{ij} appearing in eq. 11.17 is a component of the *total* stress tensor and is defined as

$$T_{ij}=\tau_{ij}-p\delta_{ij} \tag{11.18}$$

where τ_{ij} is the component of the shear-stress tensor (see eq. 11.14) corresponding to T_{ij} and sometimes called the dynamic (or deviatoric) stress tensor; p is (hydrostatic) pressure; and δ_{ij} is called the Kronecker delta, a component of a unity tensor‡ (where $\delta_{ij}=1$ for $i=j$ and $\delta_{ij}=0$ for $i\neq j$).

The continuity equation for an incompressible fluid is written in Cartesian coordinates as

$$\frac{\partial u_i}{\partial x_i}=0. \tag{11.19}$$

The complete expressions for the dynamic and continuity equations in Cartesian and cylindrical coordinates are given in Appendices 2A and B at the end of this chapter.

Velocity is introduced into the solution of a process-flow problem through its relationship to strain (e.g., eq. 11.2) and the constitutive equation (eq. 11.3) which relates the stress, τ, and shear-strain rate.† For simple isothermal flows, where there is only one non-zero component of the velocity vector, the problem reduces to the solution of a single differential-equation provided by the dynamic equations.

The terms within parentheses on the left-hand side of eq 11.17 are called the *inertial* terms and usually can be neglected.† This is particularly fortunate since the second of the inertial terms introduces nonlinearity to the set of partial differential equations. Since we are also neglecting body forces, what remains of eq. 11.17 is a much simpler relationship

$$\frac{\partial T_{ij}}{\partial x_{ij}}=0. \tag{11.20}$$

Another assumption, and one that is a very good, is that there is *no slip* between the fluid and the surface of the flow geometry. This no-slip assumption provides one or two boundary conditions for the solution of the differential equation. The example of pressure flow through a capillary given in the next section serves to illustrate this general approach for solving a fluid-flow problem.

11.3.1 PRESSURE (POISEUILLE) FLOW

Flow through a Capillary. Analysis of simple pressure flow through a tube or capillary is important in the modeling of extrusion through a capillary die and in the measurement of melt viscosity by means of a capillary rheometer, as discussed in Section 11.4.1. As discussed in the previous section, it is helpful to assume that flow is isothermal, fully developed, incompressible, laminar, and steady. For an infinitely long, horizontal tube for which undeveloped flow in the entrance region and gravitational forces can be ignored, the dynamic equations are reduced to the single differential equation (see Problem 11–8)

---

† The energy equation for an incompressible fluid is written in Cartesian coordinates as

$$\rho\hat{C}_p\left(\frac{\partial T}{\partial t}+u_j\frac{\partial T}{\partial x_j}\right)=\frac{\partial}{\partial x_j}\left(k\frac{\partial T}{\partial x_j}\right)+\tau_{ij}\frac{\partial u_i}{\partial x_j}$$

where $\hat{C}_p$ is the heat capacity per unit mass and k is the thermal conductivity. The dynamic and energy equations are usually coupled through the velocity terms, making the solution of differential equations especially difficult. Numerical solutions are available for adiabatic conditions, but, in general, temperature effects are very difficult to handle for non-Newtonian flow.

‡ The unity tensor is formally given as

$$\delta=\begin{pmatrix}1&0&0\\0&1&0\\0&0&1\end{pmatrix}.$$

† It should be noted that the well-known Navier–Stokes equations are just a special case of the more general dynamic equations — one for which the incompressible fluid is Newtonian and, therefore, $\tau_{ij}=\mu\dot{\gamma}_{ij}$.

† Note that all derivatives with respect to time (e.g., the first of the inertial terms) become zero when the flow is assumed to be steady in time.

$$\frac{\partial p}{\partial z} = \frac{1}{r}\left[\frac{\partial}{\partial r}(r\tau_{rz})\right] \tag{11.21}$$

where z is chosen to be the direction of flow (the axial direction). Substitution of the PLF constitutive equation (eq. 11.11) in the form

$$\tau_{rz} = m\dot{\gamma}_{rz}^{\ n} = m\left(\frac{du_z}{dr}\right)^n \tag{11.22}$$

into eq. 11.21 and integration twice gives the velocity of a PLF as

$$u_z(r) = \left(\frac{nR}{1+n}\right)\left(\frac{R\Delta p}{2mL}\right)^{1/n}\left[1-\left(\frac{r}{R}\right)^{(1+n)/n}\right] \tag{11.23}$$

where R is the tube radius, $\Delta p/L$ is the pressure drop across the capillary per unit length, and r is the radial distance from the center line (see Problem 11–9). Boundary conditions are obtained by realizing that the velocity at the surface (i.e., at $r = R$) of the capillary wall is zero, given a condition of no-slip and the maximum velocity

$$u_z^{\max} = \left(\frac{nR}{1+n}\right)\left(\frac{R\Delta p}{2mL}\right)^{1/n} \tag{11.24}$$

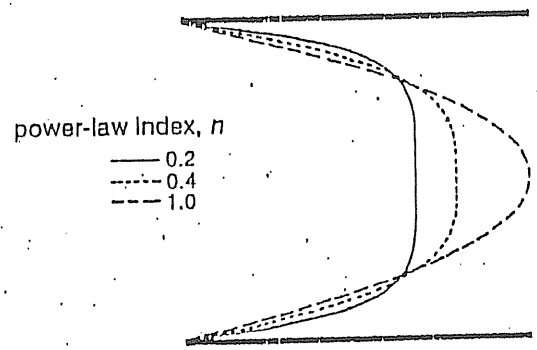

Figure 11.21. Velocity profile of a power-law fluid during isothermal pressure flow through a capillary as a function of the power-law index (n). (Adapted from H. A. Barnes, J. F. Hutton, and K. Walters, *An Introduction to Rheology*, Elsevier, Amsterdam, 1989, with permission from the publisher.)

occurs at the center line ($r = 0$) and, therefore, $du_z/dr = 0$ (i.e., $\dot{\gamma} = 0$ at the center line of the capillary). Division of eq. 11.23 by eq. 11.24 gives the velocity profile in dimensionless form as

$$\frac{u_z}{u_z^{\max}} = 1-\left(\frac{r}{R}\right)^{(1+n)/n} \tag{11.25}$$

As shown in Figure 11.21, the velocity profile of a PLF becomes flatter (i.e., more *plug flow*) with decreasing n (i.e., with increasing shear-thinning behavior).

The volumetric flow rate, Q, through the capillary can be obtained by integrating the velocity function (eq. 11.23) as

$$Q = \int_{r=0}^{R} \pi r u_z(r)dr = \left(\frac{n\pi R^3}{1+3n}\right)\left(\frac{R\Delta p}{2mL}\right)^{1/n} \tag{11.26}$$

TABLE 11.3 DIE CHARACTERISTICS FOR A POWER-LAW FLUID IN PRESSURE FLOW

Geometry	Die Characteristic
Capillary	$Q = \left(\frac{n\pi R^3}{1+3n}\right)\left(\frac{R\Delta p}{2mL}\right)^{1/n}$
Annulus[a]	$Q = \left(\frac{n\pi R_o}{1+2n}\right)(R_o - R_i)^{2+1/n}\left(\frac{\Delta p}{2mL}\right)^{1/n} F(n,\kappa)$
Parallel plates[b]	$\frac{Q}{W} = \left[\frac{nH^2}{2(1+2n)}\right]\left(\frac{H\Delta p}{2mL}\right)^{1/n}$
Rectangular duct[c]	$Q = WH^2\left(\frac{W\Delta p}{2mL}\right)^{1/n} S_p$

[a] R_i, inner radius; R_o, outer radius; F is a function of n and the aspect ratio of the annulus, $\kappa = R_i/R_o$.
[b] Infinitely wide parallel plates where H represents the separation of plates and W is unit width.
[c] This is an example of a nonsimple flow geometry; S_p is a shape factor that is a function of n and the aspect ratio, W/H.

For the special case of a Newtonian fluid for which $m = \mu$ and $n = 1$, eq. 11.26 reduces to the familiar *Hagen–Poiseuille equation*

$$\boxed{Q = \frac{\pi R^4 \Delta p}{8 \mu L}} \tag{11.27}$$

Similar models can be developed for isothermal pressure flow through other simple-flow geometries such as an annulus or infinitely wide parallel plates. Respectively, these approximate the flow through tubing (i.e., annular die) and sheet (i.e., slit) dies used in extrusion. The exact form of the relationship between Q and the pressure drop, Δp, is called the *die characteristic*. As will be discussed in Section 11.5, a *screw characteristic*, which relates the volumetric output of an extruder as a function of different variables such as the extruder screw speed and geometry, may be obtained by modeling extruder operation as combined pressure and shear flow in a rectangular duct. Simultaneous solution of the die and screw characteristics gives the operating conditions of pressure and flow rate for the coupled operation of the extruder and die. For completeness, the die characteristics for a PLF in different die geometries are summarized in Table 11.3.

11.3.2 DRAG FLOW

Plane Couette Flow. An example of a simple shear flow is plane (Couette) flow between two infinitely wide parallel plates as used as an example in Section 11.2 and illustrated in Figure 11.11. In this case, the top plate is driven at a constant velocity, U, in the x-direction while the bottom plate is fixed. Since the plates are infinitely wide, there are no edge effects and, therefore, the only nonzero component of the velocity vector is the x-component. This is an example of a *viscometric flow* as were the previous cases for simple pressure flows. Assuming that there is *no slip* of the fluid at the surface of the two plates and the vertical distance between the two plates is given as H, the velocity of the fluid element, u_x, at the top surface (i.e., $y = H$) is U, while the velocity at the bottom plate (i.e., $y = 0$) is zero. With these boundaries conditions, the velocity profile is linear and *independent of the fluid* type (or constitutive equation). Specifically, the solution of the (x-component) dynamic equation gives the velocity of each fluid element as

$$u_x = \left(\frac{y}{H}\right) U. \tag{11.28}$$

The volumetric flow rate, Q, per unit width is then obtained from the velocity equation as

$$\frac{Q}{W} = \int_0^H u_x \, dy = \frac{UH}{2}. \tag{11.29}$$

As was the case for the velocity profile, the volumetric flow rate is independent of the fluid constitutive relationship — it is the same whether the fluid is Newtonian or a PLF.

Axial Annular Couette Flow. An important geometry that can be used as a model of a processing operation (e.g., wire coating) consists of two concentric cylinders of which the inner cylinder (e.g., the wire) is pulled at a constant linear velocity, U, as illustrated in Figure 11.22.

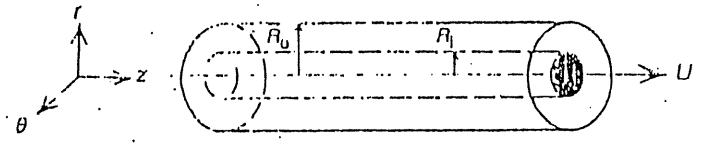

Figure 11.22. Representation of axial annular Couette flow. The inner cylinder is pulled at a velocity, U.

A solution of this problem for a Newtonian fluid is easily obtained and gives

$$\frac{u_z}{U} = \frac{\ln(r/R_0)}{\ln \kappa} \tag{11.30}$$

where $\kappa = R_i / R_0$. The solution for a PLF is given as†

$$\frac{u_z}{U} = \frac{1}{\kappa^q - 1}\left[\left(\frac{r}{R_0}\right)^q - 1\right] \tag{11.31}$$

where

$$q = 1 - \frac{1}{n}. \tag{11.32}$$

The volumetric flow rate is then obtained as

† In the case of axial annular Couette flow, the solutions for u_z and Q for a Newtonian fluid cannot be obtained from the PLF results by letting $n = 1$ ($q = 0$) and must be obtained independently.

$$Q = 2\pi \int_{R_i}^{R_o} r u_z(r)\, dr. \tag{11.33}$$

Using eq. 11.31 and performing the integration gives the following relationship for Q (in dimensionless form) of a power-law fluid in axial annular Couette flow:

$$\frac{Q}{2\pi R_o (R_o - R_i) U} = \frac{1}{q+2} \frac{1-\kappa^{q+2}}{(1-\kappa)(\kappa^q - 1)} - \frac{1+\kappa}{2(\kappa^q - 1)}. \tag{11.34}$$

In this case, Q has the general significance of the volume of coating extruded on the wire per unit time. The complete analysis of an actual wire-coating operation is more complicated than indicated above because it involves the superposition of a pressure flow on the drag flow. The pressure flow is introduced as a result of the attachment of an extruder to the wire-coating die (see Section 11.5).

11.4 RHEOMETRY

The relationship between stress and shear rate, and therefore the dependence of apparent viscosity upon shear rate, can be determined over a wide temperature range by a variety of techniques that utilize some of the simple pressure or shear geometries discussed in the previous section. These include capillary and Couette rheometry, which are based upon simple pressure flow through a capillary and simple shear flow through two rotating, concentric cylinders, respectively. Other common methods include cone-and-plate and parallel-plate rheometry, which can also give information concerning normal stresses through measurements by force transducers mounted in the direction normal to the plane of shear. Slit rheometers, which can be used to measure exit pressures in pressure flow through a rectangular channel, can be used to measure normal stress under typical processing conditions. The basics of capillary, Couette, and cone-and-plate rheometry are presented in this section. A complete discussion of rheometry can be found in a number of excellent texts such as those by Nielsen, Middleman, and Walters cited in the bibliography at the end of this chapter.

11.4.1 Capillary Rheometer

In addition to providing a model for flow of a non-Newtonian fluid through a capillary die, an understanding of pressure flow through a tube may be used to determine the apparent viscosity of a polymer melt as a function of $\dot{\gamma}$. This method is called *capillary rheometry* and can be used over the $\dot{\gamma}$ range from 1 to 10^5 s^{-1}, which includes most polymer-processing operations (see Table 11.2). As can be shown by a simple force balance on a fluid element in the capillary, the shear stress $(\tau_{rz} \equiv \tau_{zr})$ given as

$$\tau = \frac{r \Delta p}{2L} \tag{11.35}$$

depends only upon the pressure drop and distance from the center line — it is totally independent of whether the fluid is Newtonian or non-Newtonian (see Problem 11-6).

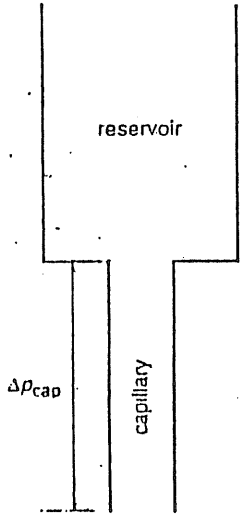

Figure 11.23. Pressure reservoir and capillary showing the overall pressure drop across the capillary (Δp_{cap}).

The experimental procedure requires the measurement of Q as a function of Δp through a capillary of known dimensions. The capillary is attached to a reservoir containing the polymer solution or melt, as illustrated in Figure 11.23. Pressurization of the reservoir forces the fluid through the capillary. From the value of Δp, the shear stress at the tube wall, τ_w (the maximum stress in capillary flow), is calculated as

$$\tau_w = \frac{R \Delta p}{2L}. \tag{11.36}$$

A second parameter used in the analysis of capillary-rheometry data is the *apparent shear rate*, $\dot{\gamma}_a$, which is calculated from the experimentally measured volumetric flow rate, Q, as

$$\phi = \frac{4Q}{\pi R^3}. \tag{11.37}$$

As in the case for τ_w, ϕ is independent of the constitutive relation of the fluid; however, the exact form of the relationship between ϕ and $\dot{\gamma}$ *is* dependent upon the fluid model. For example, $\dot{\gamma}_w \equiv \phi$ for a Newtonian fluid. In the case of a PLF, it may be shown that the shear rate at the wall is given as

$$\dot{\gamma}_w = \frac{3n+1}{4n}\phi. \tag{11.38}$$

The apparent viscosity for any non-Newtonian fluid is then calculated from values of the model-independent expression for τ_w (eq. 11.36) and the model-dependent expression for $\dot{\gamma}$ (e.g., eq. 11.38) through the GNF model (eq. 11.3) as

$$\eta = \frac{\tau_w}{\dot{\gamma}_w}. \tag{11.39}$$

If the fluid behavior is power law over the entire experimental range of $\dot{\gamma}$, a plot of $\log \tau_w$ versus $\log \phi$ will be linear with slope equal to the power-law index, n, and an intercept of $\log m'$, which is related to the consistency, m, as[†]

$$m = m'\left(\frac{4n}{3n+1}\right)^n. \tag{11.40}$$

Values of $\dot{\gamma}$ for each ϕ can then be calculated from knowledge of n and use of eq. 11.38.

One problem with the use of capillary rheometry is that the equations given above were obtained by assuming the usual model conditions that the flow in the capillary is isothermal, fully developed, incompressible, laminar, and steady. The most difficult assumption to realize (and the one most easy to accommodate) is that the flow is fully developed over the entire length of the capillary. As shown in Figure 11.24, a significant pressure drop can occur at the entrance region of the capillary due to the extra stress needed to support the nonaxial components of the velocity profile that result from the flow of the fluid from the large-diameter reservoir into the narrow capillary. For this reason, the pressure drop is not linear over the entire length of the capillary. Entrance effects can usually be neglected if the capillary is sufficiently long (e.g., $L/D > 200$); however, capillaries used in

[†] It follows from eq. 11.22 in the form $\tau_w = m\dot{\gamma}_w^n$ and from eq. 11.38 that

$$\log \tau_w = n \log \phi + \log m'.$$

melt rheometry are typically short and, therefore, the experimental data need to be corrected for any entrance effects.

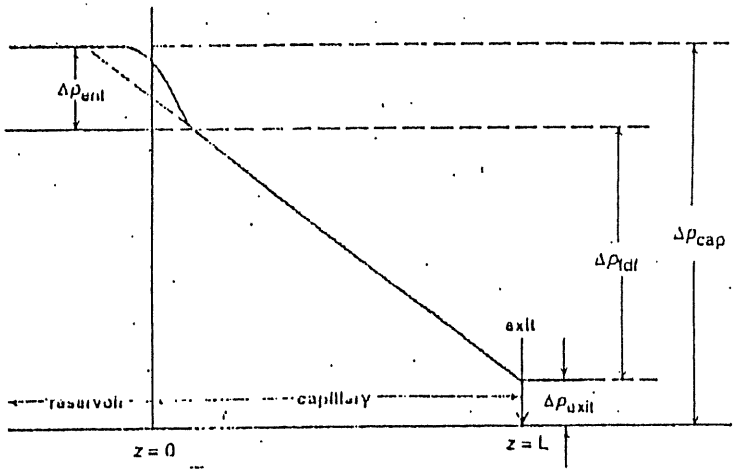

Figure 11.24. Pressure profile in reservoir and capillary (see Figure 11.23) showing the pressure drop in the entrance region between the reservoir and capillary, Δp_{ent}, the pressure drop across the capillary, and the exit pressure, p_{exit}.

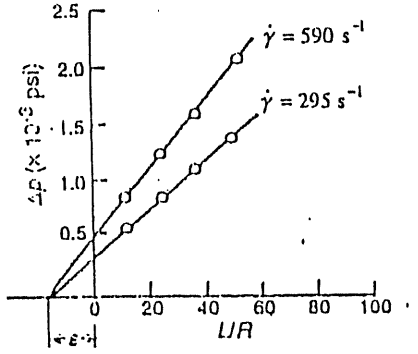

Figure 11.25. Bagley plot of pressure drop along a capillary versus capillary aspect ratio, l/R, at two different values of $\dot{\gamma}$. (Adapted from M. H. Wohl, *Chemical Engineering*, March 25, 1968, pp. 99–104.)

Bagley[6] has suggested that entrance effects can be handled by assuming that the *effective* length of the capillary is greater than the actual length and, therefore, the shear stress at the wall can be corrected as

$$\tau_w{}^c = \frac{R\Delta p}{2(L+\varepsilon R)} \tag{11.41}$$

where ε is an empirical parameter obtained by extrapolating a plot of Δp versus the capillary aspect ratio, L/R, to zero pressure drop at constant $\dot{\gamma}$ for capillaries of different lengths as shown in Figure 11.25. Procedures for incorporating the effects of viscous heating and pressure on capillary flow have been proposed[7] but are not usually made.

11.4.2 Couette Rheometer

Another example of a simple shear flow is circular Couette flow whereby a cylinder of radius, R_i, is driven at a constant angular velocity of Ω (usual units of rad s^{-1}) within an outer concentric cylinder of radius, R_o, as illustrated in Figure 11.26.

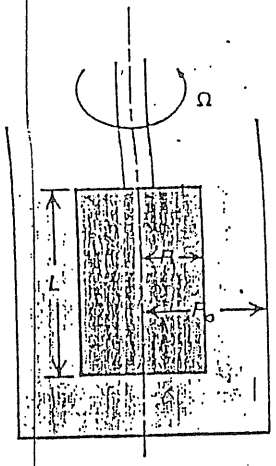

Figure 11.26. Couette rheometer.

The solution to this flow problem is simplified by using cylindrical coordinates and assuming that the cylinders have infinite length so that edge effects can be

neglected.† Using the assumption of no-slip of the fluid at the surface of the two cylinders, the boundary conditions are

$$u_\theta(r = R_i) = R_i\Omega$$

and

$$u_\theta(r = R_o) = 0.$$

Unlike the case for plane Couette flow, the velocity profile is dependent upon the rheological properties of the fluid. The general solution for the θ component of the velocity vector for a PLF (eq. 11.11) is

$$\frac{u_\theta}{R_i\Omega} = \left(\frac{r}{R_i}\right)\frac{1-(R_o/r)^{1/n}}{1-\kappa^{1/n}} \tag{11.42}$$

where $\kappa = R_i/R_o$ is the aspect ratio. Again this is an example of a viscometric flow where the remaining components of the velocity vector (i.e., u_r and u_z) are zero. For a Newtonian fluid ($n = 1$) such as water or mineral oil, eq. 11.42 reduces to

$$u_\theta = \frac{\Omega R_i{}^2}{R_i{}^2 - R_o{}^2}\left(r - \frac{R_o{}^2}{r}\right). \tag{11.43}$$

The expressions for shear stress and shear rate are

$$\tau = \frac{M}{2\pi r^2 L} \tag{11.44}$$

and

$$\dot{\gamma} = \frac{2\Omega R_i{}^2 R_o{}^2}{r^2\left(R_i{}^2 - R_o{}^2\right)} \tag{11.45}$$

where M is the measured torque and L is the (submerged) length of the inner cylinder.

† Corrections can be made for edge effects by taking data for cylinders of different lengths in a manner similar to the Bagley correction for capillary data.

11.4.3 Cone-and-Plate Rheometer

Another important method of measuring the rheological properties of polymer solutions and melts is the cone-and-plate rheometer, which is illustrated in Figure 11.27. Either steady-shear or dynamic-viscosity data (see Section 5.1.3) can be obtained by this method.

The cone angle, β, is typically very small (1 to 3 radians) — much smaller than suggested by Figure 11.27. At these low angles, the shear rate is given as

$$\dot{\gamma} = \frac{\Omega}{\beta} \tag{11.46}$$

where Ω is the angular velocity of the cone. Dynamic viscosity can be obtained by applying an oscillatory shear on the cone. The shear stress, τ, is determined as

$$\tau = \frac{3M}{2\pi R_c^3} \tag{11.47}$$

where M is the measured torque on the cone having radius R_c. The apparent viscosity is then obtained from steady-shear measurements as

$$\eta = \frac{\tau}{\dot{\gamma}} \tag{11.48}$$

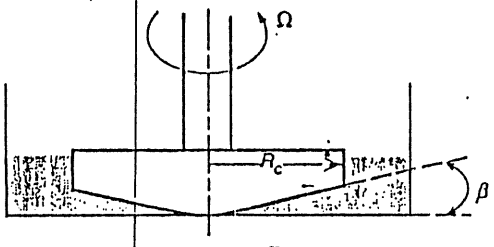

Figure 11.27. Idealized illustration of a cone-and-plate rheometer.

11.4.4 Rheometric Characterization of Polymer Solutions and Melts

Cone-and-plate, Couette cylinder, and also parallel-plate and eccentric rotating-plate rheometers can measure apparent viscosity over a low to moderate range of shear rates (e.g., 10^{-4} to 10^{3} s^{-1}). Slit and capillary rheometers operate at high shear rates typical of many processing operations such as extrusion (see Table 11.2). Measurements using a variety of rheometers (e.g., cone-and-plate, slit, and capillary rheometers) can be used to cover the entire range of shear rates, as illustrated in Figure 11.28.

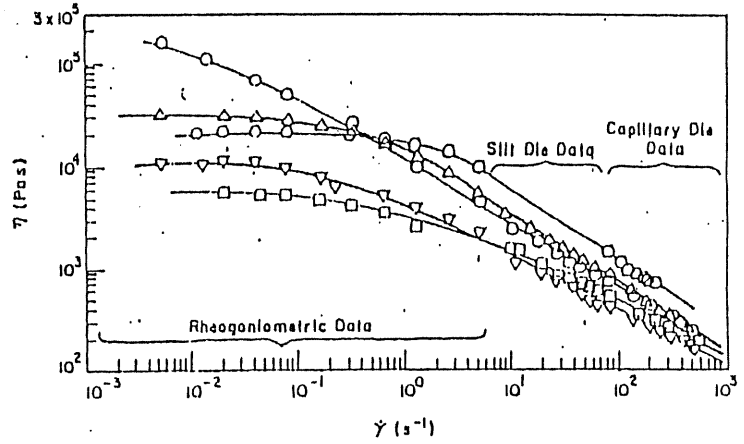

Figure 11.28. Viscosity versus shear rate for polymer melts at 200°C showing ranges of shear rate over which rheogoniometric (cone-and-plate), slit die, and capillary rheometric measurements apply. Data for (○) high-density polyethylene; (△) polystyrene; (◯) poly(methyl methacrylate); (▽) low-density polyethylene; and (□) polypropylene. (Reproduced from C. D. Han, *Rheology in Polymer Processing*, Academic Press, New York, 1976, with permission of the publisher.)

11.5 INTRODUCTION TO THE MODELING OF POLYMER-PROCESSING OPERATIONS: EXTRUSION

Most complex polymer-processing operations can be reduced to a number of simple-flow operations (see Section 11.3), which can be more easily solved. This is true for processing operations such as wire coating, blow molding, calendering, extrusion, and others. A full discussion of the modeling of polymer-processing operations is beyond the scope of this chapter and the reader is encouraged to consult any of a number of excellent texts, such as those by Middleman and by McKelvey cited in the bibliography at the end of this chapter. As an illustration the basics of the modeling of extrusion are given in this section.

As discussed in Section 11.1.1, an extruder has three zones — feed, compression, and metering. In the modeling of extrusion, the metering section is the easiest to analyze because the screw is conveying a homogeneous melt compared to solid pellets in the feed zone and a complex mixture of pellets and molten polyme-

in the compression zone. Clearly, a complete modeling of the extrusion process requires a coupled analysis of all three zones; however, the simpler treatment required to model the metering zone serves to illustrate how basic rheological principles developed in Sections 11.2 and 11.3 can be applied to tackle more complex processing problems.

To analyze flow in the metering zone, an approximation that is made (i.e., the lubrication approximation) is that rotation of the screw in the extruder shears the melt along the screw channel in a manner similar to plane Couette flow (Section 11.3.2) as described below. When no die is attached to the extruder, shear flow is the only consideration and the modeling is particularly easy. This is called a condition of *open discharge*. When a die (e.g., capillary, slit, or annular) is attached to the extruder, a pressure drop is produced across the die (pressure flow) and flow through the extruder is a combination of shear flow along the screw channel and pressure flow (back flow) against the extrusion direction. The volumetric flow, Q, therefore can be expressed as a simple combination of drag (shear) and pressure flows as[†]

$$Q = Q_d - Q_p. \tag{11.49}$$

From eq. 11.49, it is clear that the case of open discharge (i.e., $Q_p = 0$) results in the maximum extruder output. Simple pressure flow through various die geometries has been discussed in Section 11.3.1. Expressions were given for isothermal flow of both Newtonian and power-law fluids. In these cases, Q was given as some function of the pressure drop across the die (see Table 11.3). These relationships were called the *die characteristics*.

In order to obtain an expression for a *screw characteristic* (Q versus Δp), it is necessary to make some assumptions about the extruder screw geometry that allow the flow to be modeled as plane Couette flow. An illustration of a simple screw geometry is shown in Figure 11.29. If the diameter of the screw, D, is much greater than the channel depth, B,[‡] and the screw is assumed to have constant depth along the extruder barrel, the screw channel can be visually unwrapped from the screw barrel to give a long rectangular channel, as illustrated in Figure 11.30. Drag flow along the screw channel can then be modeled as plane shear flow with the barrel wall shearing fluid in the channel. Due to the presence of the channel walls, the flow is not a simple flow such as plane Couette flow between two infinitely wide parallel plates as discussed in Section 11.3.2; however, if the width of the channel, W, is much greater than the channel height, B, the simpler case of plane Couette flow may be a reasonable assumption.

[†] Back flow due to leakage between the top of the screw flight and barrel wall is usually neglected. This expression is strictly true for Newtonian fluids for which the two flows are not coupled as they would be in the case of non-Newtonian flow.

[‡] The flight clearance, δ, is usually considered to be negligible with respect to B.

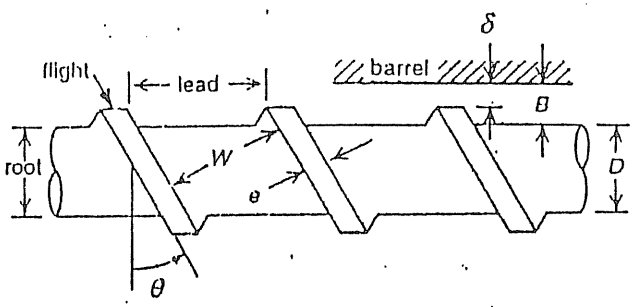

Figure 11.29. Illustration of extruder-screw geometry. (Adapted from S. Middleman, *Fundamentals of Polymer Processing*, McGraw-Hill Book Company, New York, 1977. Reproduced with permission of McGraw-Hill, Inc.)

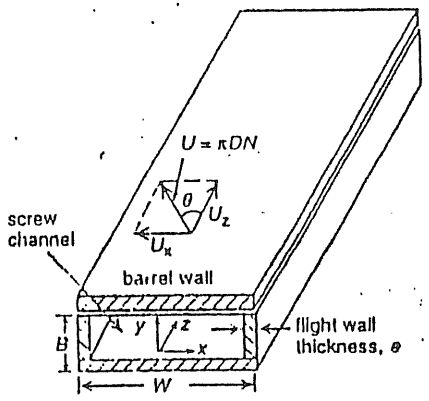

Figure 11.30. Geometry of unwrapped screw channel.

In order to simplify the analysis of the extrusion process, the flow can be assumed to be isothermal and the fluid to be Newtonian. Under these conditions and using the geometric approximations that $W>>B$ and $D>>B$, the screw characteristic, a combination of both drag and pressure flows along the screw channel, is given as

$$Q = AN - C\frac{\Delta p}{\mu} \tag{11.50}$$

where N is the screw speed (in rpm) and μ is the Newtonian viscosity. The parameters A and C are determined by the geometry of the screw (see Figure 11.29) as

$$A = \frac{1}{2}\pi DWB\cos\theta \tag{11.51}$$

and

$$C = \frac{WB^3}{12Z} \tag{11.52}$$

where Z is the screw channel length, which is related to the overall length of the extruder, L, and angle of the flight, θ, as

$$Z = \frac{L}{\sin\theta}. \tag{11.53}$$

For Newtonian fluids, the die characteristic can be put in the form

$$Q = \frac{k}{\mu}\Delta p \tag{11.54}$$

where k is a function of the geometry for a given die (e.g., capillary, annulus, or slit), as given in Table 11.4. For Newtonian fluids, the die characteristic is a linear function of Δp, as was the screw characteristic. A plot of Q versus Δp for the screw (eq. 11.50) and for the die (eq. 11.54) will intersect at the point of intersection defining the *operating parameters* of Q and Δp for the combined operation of the extruder and die. Alternately, Δp can be obtained analytically for extrusion of a Newtonian fluid since a mass balance dictates that

$$Q_{\text{extruder}} \equiv Q_{\text{die}}. \tag{11.55}$$

Substitution of eqs. 11.50 and 11.54 into eq. 11.55 gives the operating pressure-drop as

$$\Delta p = \frac{\mu AN}{k + C}. \tag{11.56}$$

Once Δp is obtained from eq. 11.56, Q can then be calculated from eq. 11.50 or 11.54.

The *power* consumption for extrusion of a Newtonian fluid under isothermal conditions is given as

$$P = E\mu N^2 Z + AN\Delta p \tag{11.57}$$

where Δp is the operating pressure and E is a parameter determined from the screw geometry as

$$E = \left(\frac{\pi^2 D^2}{B}\right)\sin\theta\left(1 + 3\sin^2\theta\right). \tag{11.58}$$

TABLE 11.4 DIE PARAMETERS, k

Die	Expression for k
Capillary	$\pi R^4/8L$
Annulus	$\left(\pi R_o^4/8L\right)\left[1 - \kappa^4 - \frac{\left(1-\kappa^2\right)^2}{\ln(1/\kappa)}\right]$
Slit[a]	$WH^3F_p/12L$

[a] F_p is a shape factor that is an infinite series as a function of the aspect ratio, W/H; F_p goes to unity in the limit as W/H goes to zero (equivalent to pressure flow through infinitely wide parallel plates).

Alternately, the screw characteristic may be expressed in a dimensionless form by defining the variables

$$\Pi_Q = \frac{Q}{U_Z BW} \tag{11.59}$$

and

$$\Pi_p = \frac{\Delta pB^2}{\mu U_Z Z} \tag{11.60}$$

where U_Z is the linear velocity of the screw barrel along the screw channel (the z-direction), given as

$$U_Z = \pi DN\cos\theta. \tag{11.61}$$

For a Newtonian fluid in isothermal flow, a plot of Π_Q versus Π_p is linear, as shown in Figure 11.31. The limiting case of open discharge, which provides the maximum extruder output, is given by $\Pi_p = 0$ for which $\Pi_Q = 1/2$, as shown by

the plot of Figure 11.31. This means that Q for open discharge in Newtonian flow is

$$Q = \frac{1}{2} U_z B W \tag{11.62}$$

which is the equivalent expression for drag Couette flow of a Newtonian fluid between two infinitely wide, parallel plates (eq. 11.29). In the case of the extruder, the two parallel plates are taken to be the bottom of the screw channel and the inner surface of the extruder barrel (where the "lubrication" approximation has been made that $W >> B$ and $D >> B$).

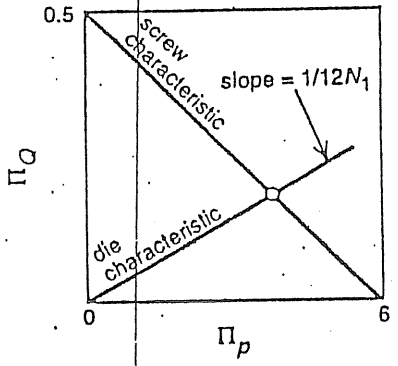

Figure 11.31. Plot of dimensionless screw and die characteristics for isothermal, Newtonian flow. (Adapted from S. Middleman, *Fundamentals of Polymer Processing*, McGraw-Hill Book Company, New York, 1977. Reproduced with permission of McGraw-Hill, Inc.)

The die characteristic for isothermal Newtonian flow can be also put in dimensionless form as

$$\Pi_Q = \frac{\Pi_p}{12 N_1} \tag{11.63}$$

where N_1 is given as

$$N_1 = \frac{C}{k} \tag{11.64}$$

In the above equation, C is a function of screw geometry (eq. 11.52) and k is a function of the die geometry, as given in Table 11.4. The dimensionless die characteristic is included in the plot of the screw characteristic shown in Figure 11.31. For given die and screw geometries, Newtonian viscosity, and screw speed, the intersection of the dimensionless screw and die characteristics define the operating parameters of volumetric screw output, Q, and pressure drop, Δp. This information can then be used to determine the power requirement for the extruder given by eq. 11.57.

The assumptions of isothermal, Newtonian flow may be viewed as rather extreme assumptions for the modeling of extrusion of a non-Newtonian fluid; however, they form a basis for further refinements. As was given in Table 11.3, die characteristics are available for the isothermal flow of power-law fluids. Numerical solutions are also available for combined pressure and drag flow of a power-law fluid in a channel. From this information, the screw characteristics for PLF flow can be obtained as shown in dimensionless form in Figure 11.32.

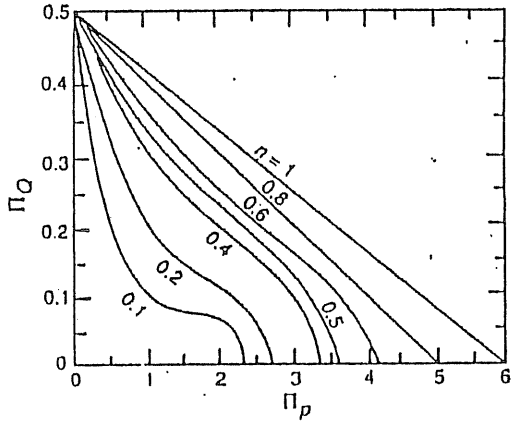

Figure 11.32. Dimensionless screw characteristics for isothermal power-law flow. (Adapted from S. Middleman, *Fundamentals of Polymer Processing*, McGraw-Hill Book Company, New York, 1977. Reproduced with permission of McGraw-Hill, Inc.)

As shown, the relationship between Π_Q and Π_p is no longer linear except in the case when the power-law index, n, is unity; this is the limiting case for isothermal Newtonian flow, as illustrated in Figure 11.31. Similar nonlinearity would follow for the die characteristics and, therefore, an analytical solution for Δp as given in eq. 11.56 for a Newtonian fluid is not possible. In the graphical solu-

tion, the intersection of the dimensionless die and screw characteristics defines the operating parameters, Q and Δp, for the combination of extruder and die, as illustrated for Newtonian fluid flow in Figure 11.31. Further refinements to include adiabatic flow of a power-law fluid in the screw channel have also been made and give a better picture of actual extrusion operation.

APPENDICES

1. Relationship between the WLF Parameters and Free Volume

The Doolittle equation[8] relates viscosity to the fractional free volume, f, which is defined as

$$f = \frac{V_f}{V} \tag{A.1}$$

where V is the actual volume of the polymer at some temperature, T. The Doolittle equation is given as

$$\ln \eta(T) = \ln A + B\left(\frac{1}{f} - 1\right) \tag{A.2}$$

where A and B are constants. The corresponding equation for $T = T_g$ is then

$$\ln \eta\left(T_g\right) = \ln A + B\left(\frac{1}{f_g} - 1\right) \tag{A.3}$$

where f_g is the fractional free volume at T_g. The fractional free volume, f, at a given temperature, T, is related to f_g as

$$f = f_g + \alpha_f\left(T - T_g\right) \tag{A.4}$$

where α_f is the thermal-expansion coefficient of the free volume

$$\alpha_f = \left(\frac{\partial V_f}{\partial T}\right)_p. \tag{A.5}$$

Substitution of eqs. A.2 to A.4 into eq. 11.5 gives

$$\log a_T = \log \frac{\eta(T)}{\eta\left(T_g\right)} = -\left(\frac{B}{2.303 f_g}\right)\left[\frac{T - T_g}{\left(f_g / \alpha_f\right) + T - T_g}\right]. \tag{A.6}$$

Comparison of the form of eq. A.6 with the WLF expression (eq. 5.115) for $\log a_T$ gives the following relationships for the WLF parameters:

$$C_1 = \frac{B}{2.303 f_g} \tag{A.7}$$

and

$$C_2 = \frac{f_g}{\alpha_f}. \tag{A.8}$$

Since it is not possible to actually measure the thermal-expansion coefficient of free volume, the thermal-expansion coefficient of the melt, which is easily determined by dilatometry (Section 4.3.2), may be used.

2. Dynamic and Continuity Equations

A. Cartesian Coordinates

x-component:

$$\rho\left(\frac{\partial u_x}{\partial t} + u_x\frac{\partial u_x}{\partial x} + u_y\frac{\partial u_x}{\partial y} + u_z\frac{\partial u_x}{\partial z}\right) = -\frac{\partial p}{\partial x} + \left(\frac{\partial \tau_{xx}}{\partial x} + \frac{\partial \tau_{yx}}{\partial y} + \frac{\partial \tau_{zx}}{\partial z}\right) + \rho g_x \tag{A.9}$$

y-component:

$$\rho\left(\frac{\partial u_y}{\partial t} + u_x\frac{\partial u_y}{\partial x} + u_y\frac{\partial u_y}{\partial y} + u_z\frac{\partial u_y}{\partial z}\right) = -\frac{\partial p}{\partial y} + \left(\frac{\partial \tau_{xy}}{\partial x} + \frac{\partial \tau_{yy}}{\partial y} + \frac{\partial \tau_{zy}}{\partial z}\right) + \rho g_y \tag{A.10}$$

z-component:

$$\rho\left(\frac{\partial u_z}{\partial t} + u_x\frac{\partial u_z}{\partial x} + u_y\frac{\partial u_z}{\partial y} + u_z\frac{\partial u_z}{\partial z}\right) = -\frac{\partial p}{\partial z} + \left(\frac{\partial \tau_{xz}}{\partial x} + \frac{\partial \tau_{yz}}{\partial y} + \frac{\partial \tau_{zz}}{\partial z}\right) + \rho g_z \tag{A.11}$$

continuity equation:

$$\frac{\partial u_x}{\partial x} + \frac{\partial u_y}{\partial y} + \frac{\partial u_z}{\partial z} = 0 \tag{A.12}$$

B. Cylindrical Coordinates

r-component:

$$\rho\left(\frac{\partial u_r}{\partial t} + u_r\frac{\partial u_r}{\partial r} + \frac{u_\theta}{r}\frac{\partial u_r}{\partial \theta} - \frac{{u_\theta}^2}{r} + u_z\frac{\partial u_r}{\partial z}\right) = -\frac{\partial p}{\partial r}$$

$$+\left[\frac{1}{r}\frac{\partial}{\partial r}\left(r\tau_{rr}\right) + \frac{1}{r}\frac{\partial \tau_{rq}}{\partial q} - \frac{\tau_{qq}}{r} + \frac{\partial \tau_{rz}}{\partial z}\right] + \rho g_r \tag{A.13}$$

θ-component:

$$\rho\left(\frac{\partial u_\theta}{\partial t}+u_r\frac{\partial u_\theta}{\partial r}+\frac{u_\theta}{r}\frac{\partial \theta}{\partial u_\theta}-\frac{u_r u_\theta}{r}+u_z\frac{\partial u_\theta}{\partial z}\right)=-\frac{1}{r}\frac{\partial p}{\partial \theta}$$

$$+\left[\frac{1}{r^2}\frac{\partial}{\partial r}\left(r^2\tau_{r\theta}\right)+\frac{1}{r}\frac{\partial \tau_{\theta\theta}}{\partial \theta}+\frac{\partial \tau_{\theta z}}{\partial z}\right]+\rho g_\theta \qquad \text{(A.14)}$$

z-component:

$$\rho\left(\frac{\partial u_z}{\partial t}+u_r\frac{\partial u_z}{\partial r}+\frac{u_\theta}{r}\frac{\partial u_z}{\partial \theta}+u_z\frac{\partial u_z}{\partial z}\right)=-\frac{\partial p}{\partial z}$$

$$+\left[\frac{1}{r}\frac{\partial}{\partial r}\left(r\tau_{rz}\right)+\frac{1}{r}\frac{\partial \tau_{\theta z}}{\partial \theta}+\frac{\partial \tau_{zz}}{\partial z}\right]+\rho g_z \qquad \text{(A.15)}$$

continuity equation:

$$\frac{1}{r}\frac{\partial}{\partial r}\left(ru_r\right)+\frac{1}{r}\frac{\partial u_\theta}{\partial \theta}+\frac{\partial u_z}{\partial z}=0 \qquad \text{(A.16)}$$

REFERENCES

1. P. Lomellini, *Makromol. Chem.*, 193, 69 (1992).
2. J. Mewis, *J. Non-Newtonian Fluid Mech.*, 6, 1 (1979).
3. C. S. Wang and J. R. Fried, *J. Rheol.*, 36, 929 (1992).
4. S. Onogi, S. Kimura, T. Kato, T. Masuda, and N. Miyanaga, *J. Polym. Sci., Polym. Symp.*, 15, 381 (1966).
5. P. J. Carreau, Ph.D. Dissertation, University of Wisconsin, 1968.
6. E. B. Bagley, *J. Appl. Phys.*, 28, 624 (1957).
7. M. R. Kamal and H. Nyun, *Polym. Eng. Sci.*, 20, 109 (1980).
8. A. K. Doolittle, *J. Appl. Phys.*, 22, 1471 (1951); 23, 236 (1952).

BIBLIOGRAPHY

S. M. Aharoni, "Critical Concentration for Intermolecular Interpenetration and Entanglements," *J. Macromol. Sci. — Phys.*, B15, 347–3790 (1978).

L. M. Alberino, "Reaction Injection Molding: Review and Overview," *Polymer News*, 11, 135–142 (1985).

H. A. Barnes, J. F. Hutton, and K. Walters, *An Introduction to Rheology*, Elsevier, Amsterdam, 1989.

C. D. Han, *Rheology in Polymer Processing*, Academic Press, New York, 1976.

N. G. McCrum, C. P. Buckley, and C. B. Bucknall, *Principles of Polymer Engineering*, Oxford University Press, New York, 1988.

J. M. McKelvey, *Polymer Processing*, John Wiley & Sons, Inc., New York, 1962.

S. Middleman, *The Flow of High Polymers*, Interscience Publishers, New York, 1968.

S. Middleman, *Fundamentals of Polymer Processing*, McGraw-Hill Book Company, New York, 1977.

D. H. Morton-Jones, *Polymer Processing*, Chapman and Hall, London, 1989.

L. E. Nielsen, *Polymer Rheology*, Marcel Dekker, Inc., New York, 1977.

Z. Tadmor and C. G. Gogos, *Principles of Polymer Processing*, John Wiley & Sons, New York, 1979.

K. Walters, *Rheometry*, Chapman and Hall, London, 1975.

G. L. Wilkes, "An Overview of the Basic Rheological Behavior of Polymer Fluids," *J. Chem. Ed.*, 58, 880–892 (1981).

Problems

11–1. Poly(vinyl acetate) (PVAc) is extruded at 180°C at constant temperature through a capillary rheometer having a ram (reservoir) diameter of 0.375 in. and a capillary with an inside diameter of 0.041 in. and length of 0.622 in. The data provided give the efflux time to extrude 0.0737 in.^{3} at different ram loads. Using only these data:

Ram Load (lb_f)	Efflux Time (min)
97.5	5.32
145	1.58
217	0.31
250	0.17

(a) Determine the power-law parameters n and m for PVAc and state all assumptions used to obtain your results.

(b) Plot the apparent viscosity, η, in units of Pa-s versus the nominal shear rate at the wall, $\dot{\gamma}_w$ (s^{-1}), on log–log paper.

11–2. Plot the dimensionless velocity profile for polystyrene flowing in a capillary at 483 K.

11–3. As illustrated, two capillaries of identical length are connected to the same liquid reservoir in which a power-law fluid is held. The tubes differ in radii by a factor of 2. When a pressure is applied to the reservoir, the volumetric flow rates from the two tubes differ by a factor of 40. What is the value of n? How different are the nominal shear rates in the two cases?

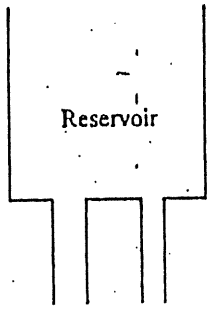

11–4. Molten polystyrene flows through a circular tube at 210°C under a pressure drop of 1000 psi. Given that the inside diameter of the tube is 0.25 in. and that the tube is 3 in. in length, calculate the following:

(a) The (nominal) shear stress at the wall in units of $N\,m^{-2}$
(b) The (nominal) shear rate at the wall in s^{-1}
(c) The volumetric flow rate in $cm^3\ s^{-1}$

Assume that flow is isothermal, steady, and fully developed.

11–5. (a) Given that tensile (Trouton's) viscosity is defined as

$$\eta_T = \frac{\sigma}{\dot{\varepsilon}}$$

where σ and ε are the *true* tensile stress and *true* strain, respectively, show that

$$\ln L = \left(\frac{1}{\eta_T}\right)\sigma t + \ln L_o$$

when viscosity is independent of $\dot{\varepsilon}$ and L_o is the *initial* length of the sample.

(b) A strip of polyisobutylene (800,000 molecular weight) is subjected to a fixed tensile load at ambient conditions. Initially, the sample is 0.699 cm wide, 6.0 cm long, and 0.155 cm thick. The strip is hung vertically and a mass of 75 g is attached to the bottom of the strip. The sample length is then recorded as a function of time with the following measurements:

Time (min)	Length (cm)
1	6.90
2	7.00
3	7.10
6	7.25
12	7.48
15	7.60
18	7.69
21	7.79
24	7.90

Plot the data given in the form of $\ln L$ versus σt and determine the value of η_T in SI units. Comment on the probable phenomenological significance of the actual intercept of the plot obtained by extrapolating the linear portion of the data.

11–6. Show that eq. 11.35, which defines shear stress in pressure flow through a capillary is correct by balancing pressure force and shear force in a cylindrical element.

11–7. A 2-in. melt extruder is pumping a *Newtonian fluid* through a slit die for which the form factor, F_p, is 0.5. The dimensions of the slit die are 1 in. in width, 0.8 in. in height, and 3 in. in length. The geometric parameters for the extruder are given in the following table. The viscosity, μ, of the fluid at operating conditions is 0.2 lb_f-s $in.^{-2}$. If the extruder is rotating at 60 rpm under isothermal conditions, determine the following:

(a) Pressure drop, Δp, in psi
(b) Volumetric flow rate, Q, in units of $in.^3\ min^{-1}$
(c) Power, P, required to operate the extruder in hp (1 hp = 500 ft-lb_f s^{-1})

Extruder Geometry	
Extruder length, L_{extr}	14.75 in.
Diameter of the screw, D	1.982 in.
Channel depth, B	0.166 in.
Flight angle, θ	30°
Channel width, W	3.11 in.

11–8. Using the dynamic equations for cylindrical coordinates given in Appendix 2B of this chapter, show how eq. 11.21 can be obtained making the usual assumptions of isothermal, steady, fully developed, laminar flow through a capillary. State any additional assumptions necessary to obtain eq. 11.21.

11–9. Obtain eq. 11.23 for the velocity profile of a power-law fluid.

12

Applications for Polymers in Separations, Biotechnology, and Electronics

As discussed in earlier chapters, plastics are important materials for use in commodity products such as textiles, tires, and packaging (e.g., film and containers). Polymers, particularly thermosets, also have widespread use as composite materials for applications in transportation, including automotive, marine, and aerospace materials. Most of these markets are now mature and future growth is expected to be small; however, there are many more applications for polymers that may be less obvious but have great potential and offer challenges for new technology and growth into the twenty-first century. Some of these uses include polymeric membranes for purification of air and water and for important separations in the chemical and biotech industries. Polymers also have important applications in medicine, including uses in controlled drug delivery, artificial organs, and protein synthesis. Some polymers can be made to be electrically conductive and offer potential for the semiconductor industry and as lightweight electrodes and electrolytes for batteries for automotive and aerospace applications. Newly developed polymers exhibit unusual optical properties that have attracted significant interest from the defense industries. This chapter seeks to present a picture of these emerging areas in polymer science and engineering.

12.1 MEMBRANE SEPARATIONS

Although the major uses of membranes are in the production of potable water by reverse osmosis and the separation of industrial gases membranes, they can be used for many other important applications. These include the filtration of particulate matter from liquid suspensions, air, and industrial flue-gas and the separation of liquid mixtures, such as the dehydration of ethanol azeotropes. More specialized applications include ion separation in electrochemical processes, membrane dialysis of blood and urine, artificial lungs and skin, the controlled release of therapeutic drugs, the affinity separation of biological molecules, membrane-based sensors for gas and ion detection, and membrane reactors. Although membranes can be prepared from metals, ceramics, and microporous carbon, polymeric membranes have great versatility and are widely used. The applications and mechanisms of transport in polymeric membranes are outlined in this section.

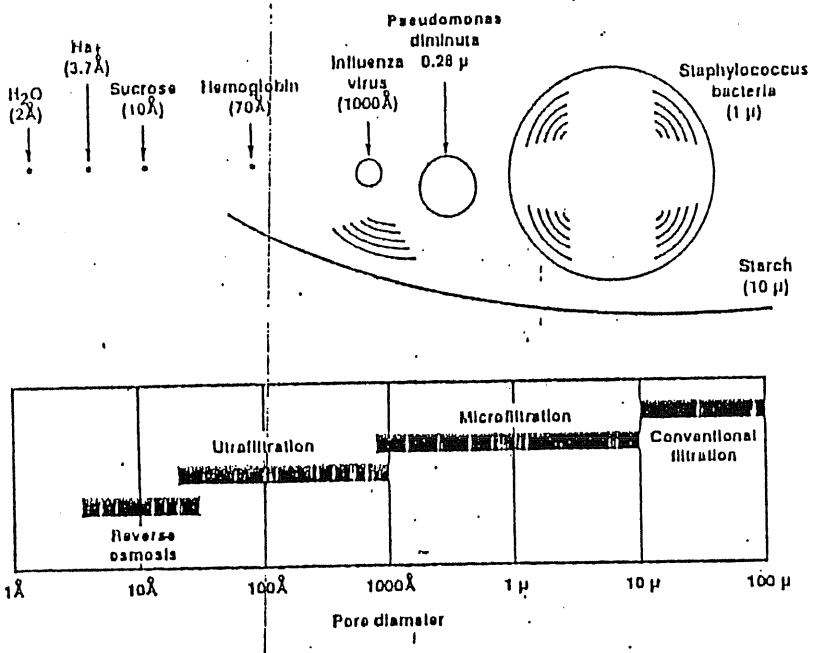

Figure 12.1. Pore sizes and terminology used in filtration. (Courtesy of Membrane Technology and Research, Inc.; Menlo Park, CA).

12.1.1 Membrane Applications for Polymeric Materials

Filtration. The most obvious use of membranes is in the filtration of solid particles such as dust, salts, bacteria, and some large viruses from liquids or airstreams. As illustrated by Figure 12.1, large organic molecules such as starch and large-diameter bacteria such as *Staphylococcus* can be filtered by membranes having pore diameters in the range from ca. 1 to 10 μm. Membranes having pore diameters in the range of 0.01 to 10 μm are called *microfilters*, while those with smaller pore diameters in the range of 10 Å to 1000 Å are called *ultrafilters*. Ultrafilters are suitable for filtering smaller particles, including some bacteria and viruses, as well as some moderately sized organic molecules like sugars. For example, heat-sensitive medical serums can be *cold sterilized* by microfiltration or ultrafiltration to remove bacterial contamination. Microporous membranes of polypropylene are being evaluated for the removal of SO_2 from flue gas and for the removal of suspended solids and clarification of industrial sewage. Examples of other industrial applications for microfiltration and ultrafiltration are given in Table 12.1.

TABLE 12.1 INDUSTRIAL APPLICATIONS FOR MICROFILTRATION AND ULTRAFILTRATION MEMBRANES

Industry	Examples
Food	Clarification of apple juice and egg-white concentration
Biotechnology	Product separation from fermentation broths and blood/plasma filtration
Semiconductor/electronic	Production of 18 megohm or ultrapure water
Pharmaceutical	Cold sterilization by removal of microorganisms such as bacteria and yeast cells from aqueous solutions
Electrocoating	Electrocoat paint filtration
Waste management	Oil–water separation and metals recovery

At the extreme limit of filtration is a process called *reverse osmosis* (or hyperfiltration), which is used to obtain potable water from brackish water or salt water. The process is termed "reverse" osmosis since water would be expected to diffuse from the side of low salt concentration to that of high concentration in normal osmosis. In reverse osmosis, a pressure drop up to several thousand psi is used to offset the osmotic pressure differential between fresh and salt water. In order for successful reverse-osmosis (RO) operation, the diameter of any pores that may be present in the dense separating layer of a RO membrane must be no larger than ca. 5 to 20 Å in order to retain dissolved microsolutes such as salt ions while allowing water to freely transport through the membrane. A polymer frequently used for preparing RO membranes is cellulose triacetate, although some other polymers such as aromatic polyamides and sulfonated polysulfone are also used.

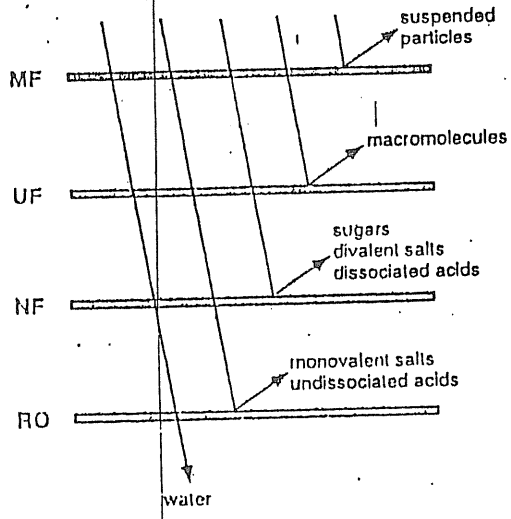

Figure 12.2. Comparison of the rejection performance of microfiltration (MF), ultrafiltration (UF), nanofiltration (NF), and reverse-osmosis (RO) membranes to solutes of different sizes and charge. (Adapted from L. P. Raman, M. Cheryan, and N. Rajagopalan, *Chemical Engineering and Progress*, March, 1994, with permission of the American Institute of Chemical Engineers.)

Another growing area in membrane filtration is nanofiltration (NF). The performance of NF membranes falls between RO and UF membrane with pore sizes in the area of 10 Å and nominal molecular-weight cutoffs in the range from 100 to 200. Nanofilters are usually prepared as thin-film composite membranes consisting of a thin separating layer containing negatively charged hydrophilic groups attached to a UF-membrane support. Polymers suitable for the separating layer include cellulose acetate, polyamides, poly(vinyl alcohol), and sulfonated polysulfone and polyethersulfone. As illustrated by Figure 12.2, NF membranes retain sugars and some multivalent salts (e.g., $MgSO_4$) but pass many monovalent salts (e.g., NaCl) and undissociated acids. Salt rejection is due to electrostatic interactions between ions and the separating layer. Applications for NF membranes include the demineralization of water, the removal of heavy metals, and the removal of lignin and related impurities from wood-pulp streams. Advantages of NF membranes over RO membranes are higher water flux and improved fouling resistance against hydrophobic colloids, proteins, and oils.

Gas Separations. The potential of using polymeric membranes to separate mixtures of gases may have been realized as early as 1866 when Thomas Graham reported that the oxygen content of atmospheric air could be enriched from 21% to 41% by permeation through a membrane of natural rubber. The first commercial membrane for the large-scale separation of gas mixtures was introduced in 1979. As indicated by Table 12.2, there are several important industrial applications where membrane operations can be competitive with more traditional methods of gas separations, such as cryogenic separation and pressure-swing adsorption (PSA). These include oxygen enrichment of air, hydrogen separation from carbon monoxide and other gases, removal of carbon dioxide from natural gas, and the reduction of organic vapor concentration in air. Other, smaller-scale applications include the preservation of food such as apples and bananas during transport by blanketing with low-oxygen-content air, the generation of inert gases for safety purposes, and the dehydration of gases.

Although ultraporous (i.e., molecular sieve) carbon and certain metallic (e.g., palladium, palladium–silver alloys, and microporous aluminum) as well as ceramic membranes have been used for gas separation, polymers have particularly high selectivity for many important gas mixtures and are easily fabricated into a variety of membrane configurations, such as flat film, hollow fiber, and composite membranes consisting of a thin polymer film on a macroporous support. For example, hollow-fiber membranes of polysulfone are used commercially to adjust the H_2/CO ratio in process syn gas for methanol synthesis and the H_2/N_2 ratio in ammonia purge gas.

The selection of a polymer for a particular gas-separation application is guided by the permeability (P_A) and its permselectivity (α_{AB}) for that gas as defined next. The driving force for transport of the gas through the membrane is the pressure drop (Δp) between the high-pressure upside and low-pressure downside of the membrane. Pressure drops may be as high as 2000 psi (13.8 MPa) in certain circumstances.

The *permeability* is defined as the ratio of flux (J_A) to pressure drop as

$$P_A \equiv \frac{J_A \ell}{\Delta p} \tag{12.1}$$

where ℓ is membrane thickness. The most commonly used unit of gas permeability is the *barrer*, which is 10^{-10} cm^3 (STP)-cm/(cm^2-s-cm Hg).

TABLE 12.2 APPLICATIONS FOR POLYMERIC MEMBRANES IN GAS SEPARATIONS

Separation	Suitable Polymers
Oxygen/nitrogen	Silicone rubber Polysiloxane-*block*-polycarbonate Polysulfone Ethylcellulose Poly[(1-trimethylsilyl)-1-propyne] Polypyrrolone Polytriazole Polyaniline
Hydrogen from carbon monoxide, methane, nitrogen	Polysulfone
Acid gases (CO_2 and H_2S) from hydrocarbons (e.g., natural gas and enhanced oil-recovery)	Cellulose acetate Poly(vinyl chloride) Polysulfone Polyetherimide
Hydrocarbon vapors from air	Silicone rubber

The *permselectivity* of a polymeric membrane for one gas (A) over another gas (B) is given by the ratio of their permeabilities

$$\alpha_{AB} = \frac{P_A}{P_B} \tag{12.2}$$

When the permeabilities are measured for pure gases, the permeability ratio is called the *ideal* permselectivity. Since gas mixtures are usually nonideal, especially under high pressure, the actual permselectivity expressed as the ratio of permeabilities for each gas in the mixture may be quite different from the ideal value. Nonetheless, permselectivities are usually reported as ideal values because pure-gas permeabilities are more frequently available.

TABLE 12.3 GAS PERMEABILITY AND PERMSELECTIVITY OF REPRESENTATIVE POLYMERS (at 25° to 35°C)

Polymer	$P(O_2)$[a]	$\frac{P(O_2)}{P(N_2)}$	$P(CO_2)$	$\frac{P(CO_2)}{P(CH_4)}$
Rubbery Polymers				
High-density polyethylene (ρ = 0.964)	0.4	2.9	1.7	4.4
Butyl rubber	1.3	3.9	5.8	6.6
Low-density polyethylene (ρ = 0.914)	2.9	3.0	12.6	4.3
Natural rubber	24	3.0	134	4.7
Silicone rubber	610	2.2	4,553	3.4
Polyphosphazene[b]	13,600	0.7	—	—
Glassy Polymers				
Poly(ethylene terephthalate) (50% crystallinity)	0.06	4.5	0.30	—
Cellulose acetate	0.68	3.4	5.5	28
Polysulfone	1.3	5.2	4.9	23
Polycarbonate	1.5	5.2	6.0	23
Polystyrene	2.6	3.3	10.5	—
Poly(2,6-dimethyl-1,4-phenylene oxide)	18	5.0	59	15
Poly(4-methylpentene-1)	29	4.4	93	—
Poly[1-(trimethylsilyl)-1-propyne]	7,200	1.7	19,000	4.4

[a] Permeability in barrer [10^{-10} cm^3 (STP)-cm/(cm^2-s-cm Hg)].
[b] *n*-Propylamine-disubstituted polyphosphazene.

In general, permeability of a polymer for a gas increases with decreasing size and increasing solubility (or condensibility) of the gas. The relative permeability of a gas is usually independent of polymer structure and is given in the order of decreasing gas permeability as

$$H_2 > He > H_2S > CO_2 > O_2 > Ar > CO > CH_4 > N_2$$

As shown by values given in Table 12.3, the actual magnitude of the permeability coefficient and, to a lesser extent, the permselectivity varies widely with polymer structure and the physical state (i.e., rubber, glass, or crystalline) of the polymer. Generally, permeability is higher while permselectivity is lower for rubbery polymers than for glassy polymers, although a few exceptions exist. One interesting exception is poly[1-(trimethylsilyl)-1-propyne]

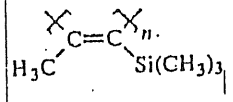

which is a glassy polymer having higher gas permeability than polysiloxane and almost all other rubbery polymers (see data in Table 12.3). The unusually high permeability of this polymer has been attributed to its especially low density and correspondingly high free volume, which results in high gas diffusivity. Unfortunately, this high free volume leads to an inability of the polymer to differentiate gas molecules on the basis of size and, as a result, permselectivity is low. This inverse relationship between permeability and permselectivity — highly permeable polymers are not selective and vice versa — is a general one for all polymers. Particularly attractive membrane polymers for a specific gas separation are those whose values of permeability and permselectivity fall above the general trend.

As shown by the data given in Table 12.3, polymers such as polyethylene and poly(ethylene terephthalate) have very low gas (and water-vapor) permeabilities due to high crystallinity. Such polymers are unsuitable for gas separations but find important applications as *barrier* films in food packaging, where low permeability to water vapor, O_2, and CO_2 may be required. For example, low-density polyethylene film is used as cereal-box liners (O_2 and moisture barrier) and poly(ethylene terephthalate) is used as the material in the manufacture of plastic bottles for carbonated beverages (barrier to CO_2 and water).

Liquid Separations. Membranes can be used effectively to separate liquid mixtures (e.g., water–organic and organic–organic) in competition with traditional chemical processes such as distillation, adsorption, liquid–liquid extraction, and fractional crystallization. One important membrane operation termed *pervaporation* uses a pressure drop (reduced pressure on the downside) to separate components from a liquid mixture on the basis of preferential solubility and diffusivity in a manner fundamentally similar to gas separation.

In pervaporation, the (liquid) feed mixture is pumped *across* the membrane surface, as is the case in many other membrane processes. As illustrated by Figure 12.3, crossflow operation reduces the potential for fouling and concentration polarization by providing a rapid flow at the membrane surface to sweep away contaminating particles and to encourage mixing at the membrane–liquid interface.

A representative process flow chart for pervaporation is illustrated in Figure 12.4. Vacuum (i.e., vacuum pervaporation) or reduced pressure (i.e., sweep-gas pervaporation) is applied at the downside of the membrane. Separation occurs by selective solution–diffusion (see Section 12.1.2) and subsequent evaporation at the downside and is driven by the partial-pressure gradient between the liquid feed and the permeate vapor. The permeate vapor phase is condensed and recovered as the product stream. The portion of the feed that is not permeated is called the *retentate*.

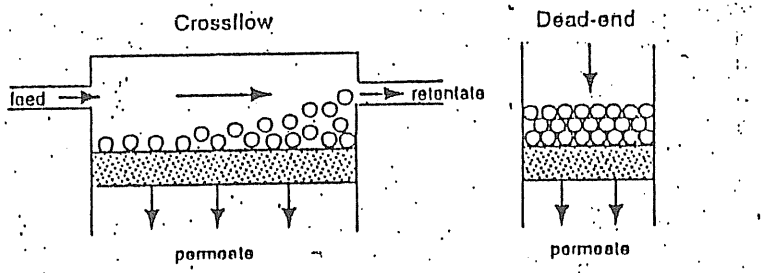

Figure 12.3. Illustration of a crossflow membrane process (left) compared to dead-end filtration (right).

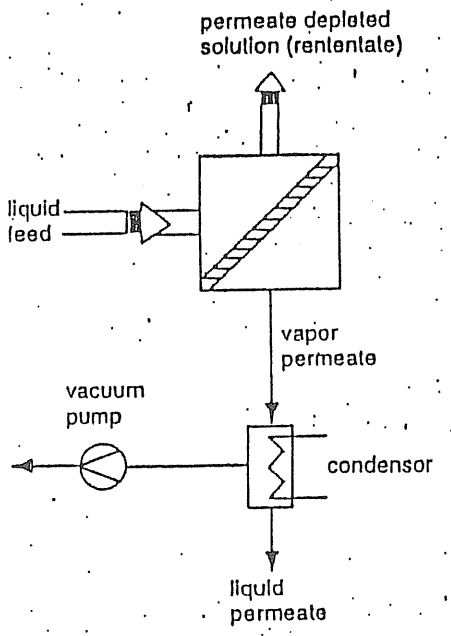

Figure 12.4. Schematic of membrane-pervaporation process. A binary liquid mixture passes crossflow over a polymeric membrane and the permeate, enriched in the more permeable component, is vaporized on the downside (low-pressure) side, condensed, and collected. (Courtesy of Membrane Technology and Research, Inc., Menlo Park.)

Related processes include *pertraction* by which the permeate is dissolved in a circulating carrier fluid rather than being vaporized and vapor permeation or *evapomeation*, where the feed stream is a vapor or vapor–gas mixture and, therefore, no phase change occurs during the process. Pervaporation has been used to dehydrate or concentrate ethanol produced by the fermentation of biomass (e.g., starch, sugar, and cellulose), to remove trace organics from water supplies, and to separate mixtures of organic compounds. Vapor permeation (evapomeation) may be used to remove trace organics from air or in hybrid distillation processes whereby a separate membrane stage may be used. The choice between pervaporation and more traditional processes such as distillation is largely controlled by the economics of energy consumption. In pervaporation, the principal form of energy utilization is the heat of vaporization of the permeate. Economics are particularly favorable for pervaporization in the separation of azeotropic mixtures such as 5% water in ethanol–water.

Membranes for pervaporation may be dense (homogeneous) membranes, asymmetric membranes, or composite membranes consisting of a thin permselective polymeric layer covering a microporous support. For alcohol–water separation, cellulose derivatives have high permeability with moderate selectivity. Poly(vinyl alcohol) (PVA), used as a graft copolymer or as the separating layer in a composite membrane, has preferential permeability to water over alcohols or other organic molecules, while silicone rubber is more permeable to alcohols (also aldehydes and ketones) than to water.

Flux in pervaporation is a function of a diffusion term (D_o), the concentration of the penetrant (C_i), and the strength of penetrant–membrane (polymer) interaction (γ) and is inversely dependent on membrane thickness (ℓ) as

$$J_i = \frac{D_o}{\gamma \ell}\left[\exp(\gamma C_i) - 1\right]. \tag{12.3}$$

The selectivity for component A over B in a binary liquid mixture may be expressed by the *separation factor* (α_{AB})

$$\alpha_{AB} = \frac{y_A / y_B}{x_A / x_B} \tag{12.4}$$

or by the *enrichment factor* (β_A), the ratio of concentrations (typically in mass units) of the preferentially pervaporating species (A) in the permeate and feed:

$$\beta_A = \frac{y_A}{x_A} \tag{12.5}$$

where x_A and y_A represent the concentration in the feed (i.e., liquid phase) and permeate (i.e., vapor phase), respectively.

Other Separations. In addition to the major membrane processes — filtration, gas separation, and pervaporation — several other fundamental membrane operations are important to the chemical and biomedical industries, such as those listed in Table 12.4. Processes like electrodialysis which can be used to desalt ionic solution use ion-exchange membranes, which are swollen gels or microporous membranes carrying a fixed positive or negative charge. For example, anion-exchange membranes have fixed positive charges (typical charge density of 2 to 4 milliequivalents per gram of membrane) that bind anions from solution. Separation is based upon exclusion of co-ions (same charge as fixed ions of the membrane).

TABLE 12.4 OTHER MEMBRANE PROCESSES

Process	Applications	Driving Force	Membrane Type	Applications
Dialysis	Separation of colloids and other large particles from inorganic ions and other small particles	Concentration gradient	Hydrophilic ultrafilters	Artificial kidney Plasma purification Caustic recovery in the viscose process
Electro-dialysis	Separation of ions having opposite charges	Electrical potential	Ion exchange	Concentration of electrolyte solutions Desalting
Electro-osmosis	Treatment of coloidal suspensions and sludges in effluent and waste streams	Electrical potential	Ion exchange	Dewatering

An important application for membranes is in electrochemical processes such as the production of caustic, as shown in Figure 12.5. In this process, water enters at the cathode compartment while saturated brine (NaCl) is fed to the anode compartment. Electrodes are separated by a perfluorosulfonate ionomer membrane such as Nafion™ (see Section 10.2.2), which has a low diffusion coefficient for Cl^- and a high diffusion coefficient for Na^+. Water is decomposed at the cathode to produce concentrated sodium hydroxide and hydrogen. At the anode, chloride ions are reduced to chlorine, while the sodium ions are able to permeate the membrane to the cathode compartment, and the anions (Cl^- and OH^-) are excluded. The mechanism

of transport through perfluorosulfonate ionomer membranes is briefly discussed in Section 12.1.2.

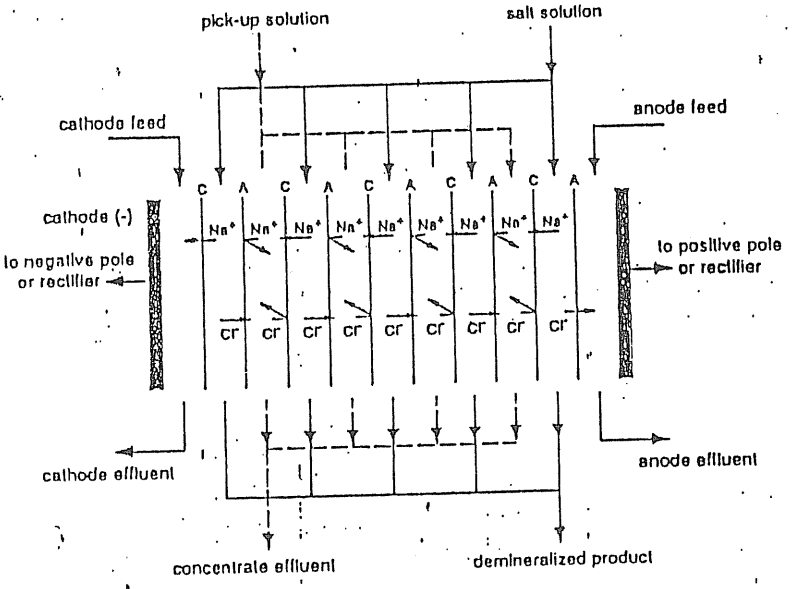

Figure 12.5. Typical chlor-alkali cell used in the production of caustic. (Courtesy of Membrane Technology and Research, Inc., Menlo Park, CA.)

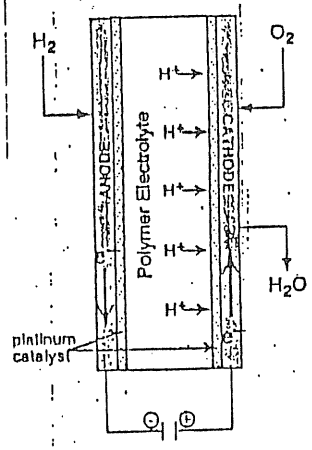

Figure 12.6. Typical fuel-cell configuration.

Polymeric membranes also have important potential in the development of efficient and inexpensive fuel cells that could be used to power electric cars and have other important aerospace and military applications. An illustration of a proton-exchange fuel cell is shown in Figure 12.6. At the anode, hydrogen is ionized, and electrons produced by the ionization travel through the external circuit (i.e., the electric motor) and return to the cathode, where they combine with oxygen to form oxygen ions. These reactions are accelerated by the platinum catalyst. The hydrogen ions travel through a polymer membrane to the cathode, where they combine with the oxygen ions to form water. As in the case of the chlor-alkali process, perfluorosulfonate ionomers such as Nafion are effective membrane polymers for fuel-cell applications.

12.1.2 Mechanisms of Transport

The two principal modes of transport that can occur in membrane separations are *size exclusion* in the case of porous membranes and *solution–diffusion* in the case of nonporous or dense membranes. Size exclusion is determined by the diameter of the pore in relation to the penetrant size and diffusional path (i.e., mean-free path in the case of gases). Size exclusion may be used to separate particles as large as 10 μm or as small as a couple of angstroms in the case of gas molecules. The size and (Lennard-Jones)† collision parameters for several industrially important gas molecules are given in Table 12.5.

† The potential energy, U, is the work required to bring two gas molecules from infinite distance to some separation distance, r, as illustrated:

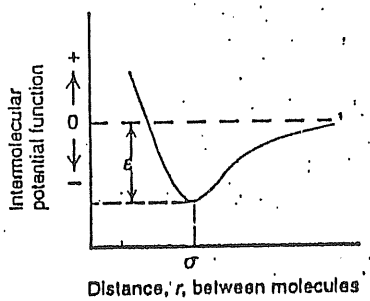

The Lennard-Jones or 6–12 potential function is given as

$$U = 4\varepsilon\left[\left(\frac{\sigma}{r}\right)^{12} - \left(\frac{\sigma}{r}\right)^{6}\right]$$

where ε is the depth of the potential well and σ is the distance of separation at which the potential energy is minimum.

TABLE 12.5 KINETIC DIAMETERS AND LENNARD-JONES POTENTIAL WELL DEPTH[a] OF IMPORTANT GASES

Gas:	He	H_2	CO_2	O_2	N_2	CO	CH_4
Kinetic diameter (Å)	2.6	2.89	3.3	3.46	3.64	3.76	3.80
ε/k (K)	10.2	59.7	195	107	71.4	91.7	149
σ (Å)	2.55	2.83	3.94	3.47	3.80	3.69	3.76

[a] See text footnote.

Transport through nonporous membranes is controlled by the solubility and diffusivity of the penetrant in the polymer matrix. In this regard, the transport of gases through a glassy polymer differs from that in a rubbery polymer. This is a result of an additional mode of sorption that is available in glassy polymers — the filling of Langmuir-type microvoids or regions of localized high free-volume present in the glassy state.[1] A discussion of diffusion through porous media and the solution–diffusion model is presented in the following sections, as are two other more specialized membrane-transport processes — facilitated and coupled transport and transport through perfluorosulfonate ionomers.

Transport through Porous Media. As illustrated in Figure 12.7, the mechanism of flow of gas molecules through porous membranes depends upon the size of the pores in relation to the *mean free-path* of the gas molecules. The mean free path can be defined as the average distance traversed by gas molecules between collisions. The Knudsen number (N_k) is defined as the ratio of the mean free path to the mean pore diameter. When the Knudsen number is small, flow is inversely proportional to the viscosity of the fluid (gas). This is called *viscous flow*. In contrast, *Knudsen flow* occurs when the Knudsen number is large (i.e., for small pore sizes). In this case, flow is inversely proportional to the *square root* of the molecular mass of diffusing species. Although some separation can be achieved by selective Knudsen flow of gas molecules, permselectivity is small unless the molecules are very different in size. For example, the ideal separation factor for O_2/N_2 for Knudsen flow is only

$$\alpha^{O_2}_{N_2} = \frac{\sqrt{MW\,(O_2)}}{\sqrt{MW\,(N_2)}} = \frac{\sqrt{31.999}}{\sqrt{28.013}} = 1.069.$$

This compares with a value of 5.2 (Table 12.3) for permeation through a dense membrane of polysulfone by the solution–diffusion mechanism described in the following section.

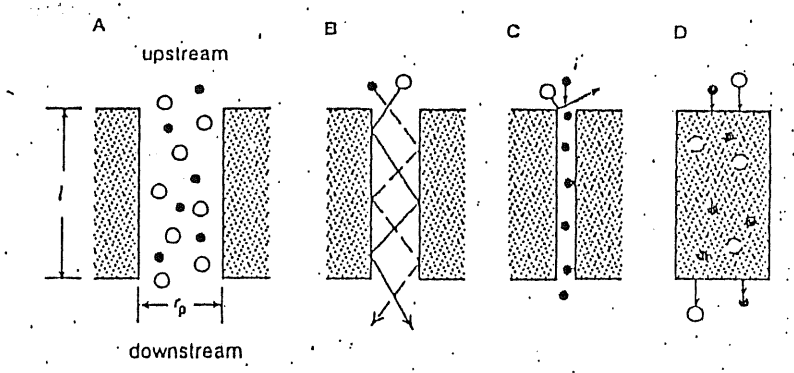

Figure 12.7. Illustration of the membrane transport of two differently sized molecules by various mechanisms. From left to right, A *viscous flow* through large pores of radii, r_p (no separation); B *Knudsen flow* (separation based upon difference in molecular weights); C *molecular sieving* (separation due to relative diffusive rates and surface sorption on pore walls); and D *solution–diffusion* through a dense membrane (separation based upon relative solubility and diffusivity).

Solution–Diffusion Transport. The predominant mechanism of transport for industrial gas- and liquid-separating membranes involves the dissolution and subsequent diffusion of molecules in a nonporous or dense membrane. In general, the permeability can be represented as a product of the solubility, S, and diffusivity, D, coefficients of the penetrant in the polymer membrane as

$$\boxed{P = SD} \qquad (12.6)$$

The mechanism of penetrant *solubility* in a polymeric membrane depends upon the activity of the penetrant and whether the polymer is in the rubbery or glassy state. The solubility of organic vapors at very low activities and gases at low to moderate pressures in liquids and rubbery polymers is given by *Henry's law* expressed as

$$\boxed{C = Sp} \qquad (12.7)$$

where C is the concentration of sorbed penetrant (typically units of cc of gas at STP per cc of polymer) and p is the pressure. In general, the solubility of a gas increases with its condensability. More condensable gases are those with higher boiling points or critical temperatures, such as CO_2. At higher penetrant activities, as is the case for organic vapors and highly condensable gases like CO_2 at moderate to high pressures, Henry's law no longer applies. In this case, the Flory–Huggins

lattice model (see Section 3.2.1) may be used to represent the observed increase in solubility with increasing pressure in rubbery polymers (i.e., $T > T_g$). An illustration of this behavior is shown in Figure 12.8, which plots the sorbed concentration of CO_2 in a silicone elastomer against pressure. Below approximately 400 psia, sorption is adequately represented by the linear relationship given by Henry's law. At higher pressures, the sorbed concentration increases at an increasing rate as modeled by the Flory–Huggins theory.

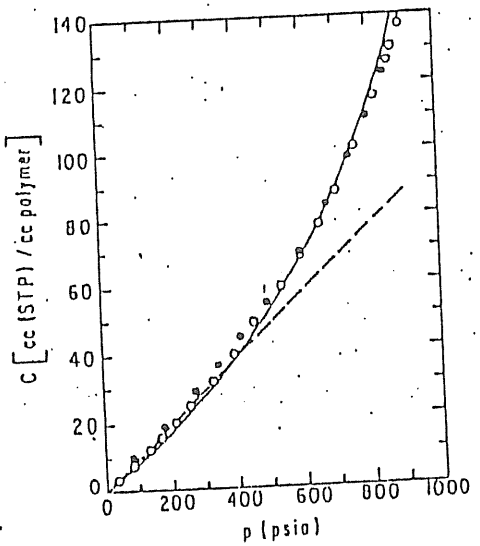

Figure 12.8. Sorption isotherm of CO_2 in silicone rubber at 35°C. Data points give CO_2 concentrations measured at different pressures during sorption (○) and desorption (●). The solid line represents the fit by the Flory–Huggins equation; the broken line represents Henry's law behavior. [Reprinted with permission from G. K. Fleming and W. J. Koros, *Macromolecules*, 19, 2285 (1986). Copyright 1986 American Chemical Society.]

Below T_g and at low to moderate gas pressures, the sorption isotherm curves *downward* with increasing pressure, as illustrated by the data for polysulfone in Figure 12.9. The most successful model for sorption in glassy polymers is given by the *dual-mode* model, which postulates that an additional (Langmuir) mode of sorption is possible by the filling of microvoids in the glassy state. The total sorbed concentration is then a summation of Henry's-law dissolution (C_D) and Langmuir-type hole-filling (C_H) contributions as

$$C = C_D + C_H = k_D p + \frac{C_H' bp}{1 + bp} \tag{12.8}$$

The parameters characterizing dual-mode sorption are the Henry's-law coefficient, k_D, the Langmuir or hole-filling capacity of the glass, C_H' and the hole-affinity parameter, b. Dual-mode parameters for representative polymers are given in Table 12.6.

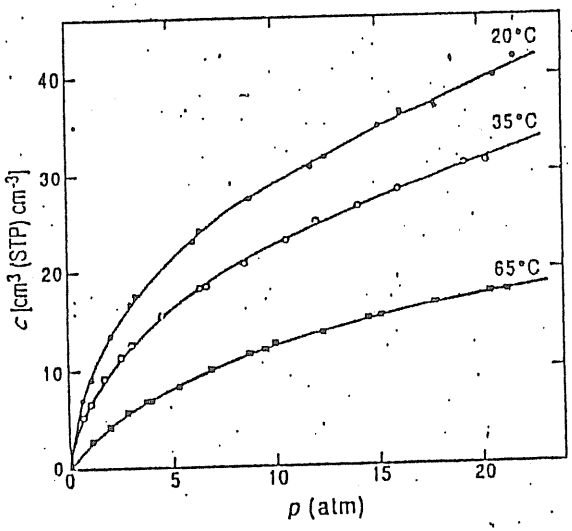

Figure 12.9. Sorption isotherm of CO_2 in a glassy polymer, polysulfone (T_g = 186°C), showing dual-mode behavior. As temperature is decreased from 65° to 20°C, the isotherm becomes increasingly more nonlinear as the Langmuir capacity increases with increasing $T-T_g$. [Adapted from Y. Maeda and D. R. Paul, *J. Polym. Sci.: Part B: Polym. Phys.*, 25, 957 (1987), with permission of the publisher.]

As discussed earlier, the Henry's law coefficient, k_D, is strongly influenced by the condensability of the gas. For example, k_D is particularly high for CO_2 (see Table 12.6) which is a very condensable gas. In turn, the condensability of a gas can be related to ε/k, the well depth of the Lennard-Jones potential-energy plot for a gas. Values of ε/k were given for some gases in Table 12.5. For a given polymer, k_D is exponentially related to ε/k as

$$\ln k_D = \ln k_D^{\circ} + m\frac{\varepsilon}{k} \tag{12.9}$$

where k_D^0 is a constant for a given polymer and temperature and m is the slope (~0.01 K^{-1}) of a plot of $\ln k_D$ versus ε/k. The second contribution to solubility for glassy polymers — the Langmuir capacity, C_H' — depends upon the size and distribution of microvoids and, therefore, can be related to the free volume of the glass. Free volume is determined by the stiffness and molecular dimensions of the polymer chain and the extent of undercooling of the glass.

TABLE 12.6. REPRESENTATIVE DUAL-MODE PARAMETERS FOR SORPTION OF NITROGEN, METHANE, AND CARBON DIOXIDE IN IMPORTANT GAS-SEPARATING POLYMERS AT 35°C

Polymer	k_D $cm^3(STP)/cm^3$ atm	C_H' $cm^3(STP)/cm^3$	b atm^{-1}
Poly(vinyl chloride)			
N_2	0.0169	0.451	0.0448
CO_2	0.587	8.939	0.2094
Cellulose acetate[a]			
CO_2	1.43	34.2	0.197
Polystyrene			
N_2	0.65	7.7	0.37
Poly(methyl methacrylate)			
N_2	0.020	1.902	0.043
CH_4	0.102	8.507	0.046
CO_2	0.944	19.680	0.158
Polycarbonate			
N_2	0.0909	2.11	0.0564
CO_2	0.685	18.81	0.262
Polysulfone			
N_2	0.0753	9.98	0.0156
CO_2	0.664	17.8	0.326
Poly(2,6-dimethyl-1,4-phenylene oxide)	0.33	18.1	0.11
CH_4	0.95	27.5	0.25
CO_2			

[a] Data obtained at 30°C.

The fundamental law for transport through a flat membrane is given by *Fick's first law* as

$$\boxed{J = -D\frac{dC}{dx}} \tag{12.10}$$

where J is the flux (units of mass per unit time), D is the diffusion coefficient, and dC/dx is the concentration gradient of penetrant across the membrane. Integration of eq. 12.10 from $x = 0$ to $x = \ell$, using Henry's law for C (eq. 12.7), and assuming that D is independent of concentration, gives

$$J = \frac{SD}{\ell}(p_2 - p_1) \tag{12.11a}$$

where p_1 and p_2 are the pressure at the low-and high-pressure sides of the membrane, respectively. Substitution of $P = SD$ (eq. 12.6) into eq. 12.11a gives

$$J = \frac{P}{\ell}\Delta p \tag{12.11b}$$

which is equivalent to eq. 12.1.

Equations 12.10 and 12.11 are appropriate expressions for the diffusion of gases at low to moderate pressures through rubbery polymers where Henry's law applies and the diffusion coefficient is independent of concentration. For glassy polymers, the concentration of gases at low to moderate pressures is no longer given by Henry's law but by the dual-mode model (eq. 12.8). The most successful approach to predict gas permeability in glassy polymers, the *partial immobilization* theory,[2] is based upon the dual-mode model, which postulates that there are two populations of sorbed gas — the Henry's-law dissolution component and the Langmuir sites. In the partial immobilization theory, each population is assigned separate diffusion coefficients, which allows Fick's first law to be given as

$$J = -D_D\left(\frac{dC_D}{dx}\right) - D_H\left(\frac{dC_H}{dx}\right) \tag{12.12}$$

where D_D and D_H are the diffusion coefficients for the Henry's-law dissolution and hole populations, respectively. Generally, the diffusion coefficient for gas molecules contained in the Langmuir sites is smaller than that for the Henry's-law regions. For example, $D_D = 5.15 \times 10^{-8}$ cm^2 s^{-1} and $D_H = 5.83 \times 10^{-9}$ cm^2 s^{-1} for polycarbonate at 35°C. Integration of eq. 12.12 and using the dual-mode model for C_D nd C_H (eq. 12.8) gives the expression for permeability as

$$P = k_D D_D \left(1 + \frac{FK}{1 + bp_2}\right) \tag{12.13}$$

where

$$F = \frac{D_H}{D_D} \tag{12.14}$$

and

$$K = \frac{C_H' b}{k_D} \tag{12.15}$$

Equation 12.13 was obtained by assuming a pressure of p_2 at the high-pressure side of the membrane and zero pressure at the downside. For the example of polycarbonate cited above, the ratio of the diffusion coefficients, F, given by eq 12.14, is 0.113. It is noted that as temperature increases to above T_g the polymer passes from the glassy to the rubbery state (see Section 4.3) and the Langmuir-capacity term, C_H', and, therefore, K, goes to zero, and $P = k_D D \equiv SD$ (eq. 12.6).

Both the permeability and diffusion coefficients can be determined by measuring the amount, Q_t, of permeant passing through a membrane at some time, t, as illustrated in Figure 12.10. From the steady-state transport rate, $(dQ_t/dt)_{ss}$, the permeability is determined as

$$P = \left(\frac{\ell}{p_2 A}\right)\left(\frac{dQ_t}{dt}\right)_{ss} \tag{12.16}$$

where A is the surface area of the membrane of thickness ℓ. The diffusion coefficient, which influences the initial or transient permeation behavior of the membrane, is obtained from measurement of the *time lag* (θ), which is the extrapolated value of Q_t, as shown in Figure 12.10. In the partial-immobilization model, the diffusion coefficient is related to the time lag as

$$\theta = \frac{\ell^2}{6D}\left[1 + f(K, F, bp_2)\right] \tag{12.17}$$

where $f(K, F, bp_2)$ is a function of the dual-mode parameters and pressure. For a rubbery polymers where $C_H' = 0$, this term is zero and, therefore, the diffusion coefficient is simply obtained as

$$\boxed{D = \frac{\ell^2}{6\theta}} \tag{12.18}$$

at some high temperature (e.g., 220°C) but a nonsolvent at lower temperature. Examples of latent solvents include *N*-tallowdiethanolamine (TDEA), menthol, and sulfolane. The polymer and latent solvent are melt-blended, cast into a film or extruded as a fiber, and then cooled to induce phase separation. As shown in Figure 12.15, phase separation occurs when the temperature is lowered to below the upper critical solution temperature (UCST). After phase inversion, the latent solvent (the pore former) is then extracted by another solvent (a nonsolvent for the polymer). Membrane morphology is determined by many parameters, such as the polymer concentration, solution temperature, and rate of cooling. Phase separation within the spinodal results in phase separation by a mechanism called *spinodal decomposition*. Spinodal decomposition results in a "lacy" membrane structure. Phase separation within the metastable region located between the spinodal and binodal occurs by nucleation and growth and leads to an open pore structure. Microporous membranes of high-density polyethylene, polypropylene, polystyrene, and poly(2,6-dimethyl-1,4-phenylene oxide) can be prepared by this procedure.

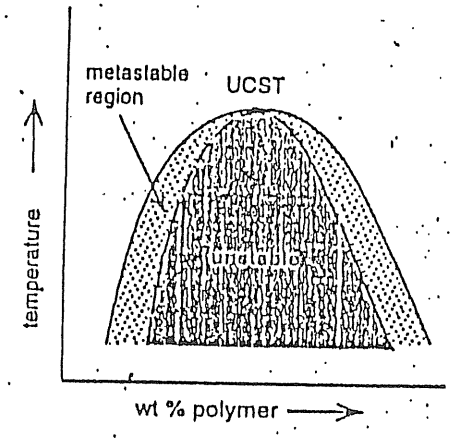

Figure 12.15. Phase diagram of a polymer solution illustrating phase separation as temperature decreases below the upper critical solution temperature (UCST). The binodal is indicated by the solid curve; the spinodal is represented by the broken curve.

The polymer-assisted method of membrane formation utilizes a mixture of *two* physically compatible but immiscible polymers dissolved in a common solvent. This means that the two polymers form a homogeneous solution with the solvent at low to moderately high polymer content, but do not form a homogeneous mixture in the solid state. When the solution is cast and the solvent evaporated, phase separation of the two polymers results. The polymer with lower con-

Facilitated and Coupled Transport. As described in the previous sections, the basis of separation by filtration is particle size, while gas separation and pervaporation use differences in solute solubility and diffusivity to separate components from a mixture. In contrast, transport in two related processes — facilitated and coupled transport — is by means of a carrier mechanism. In both processes, a macroporous membrane (e.g., Celgard™ macroporous polypropylene) containing a free mobile carrier separates two liquid phases. The carrier, which is insoluble in the liquid phase, is contained in the membrane pores by capillary attraction. In facilitated transport, the carrier interacts with the permeant at the membrane–liquid interface. The permeant–carrier complex diffuses through the membrane and the permeant is released at the opposite membrane–liquid interface. An example of facilitated transport is the transport of oxygen by hemoglobin, as illustrated in Figure 12.11A. In the case of coupled transport, a chemical reaction occurs at the interface of the membrane and liquid phases, and mass flux occurs in both directions, as illustrated for Cu^{2+}/H^{+} transport in Figure 12.11B. One practical problem with facilitated and coupled transport is the instability of the membrane, as the carrier may diffuse out of the pores of the macroporous membrane with time.

Transport through Perfluorosulfonate Ionomers As mentioned earlier, a class of polymers frequently used for a number of membrane-separation processes, including the chlor-alkali process, fuel cells, facilitated gas transport, and liquid separations, are the perfluorosulfonate ionomers (PFSI). As discussed in Section 10.2.2, PFSIs are copolymers of tetrafluoroethylene and a perfluorinated vinyl ether containing a terminal sulfonyl fluoride (SO_2F) group as follows:

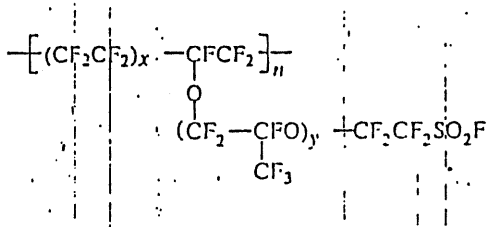

The most important commercial PFSI product is Nafion™ ($y = 1$), which is produced as film by melt extrusion. After film formation, the sulfonyl fluoride groups are converted to sulfonate groups by reaction with sodium or potassium hydroxide, with further conversion to the commercial sulfonic acid (SO_3H) form (Nafion-H). Other ionic forms (e.g., Na^+, Li^+, K^+, Ag^+, Ca^{2+}, Al^{3+} salts) can be obtained by ion exchange with the appropriate salts. The importance of Nafion to chlor-alkali production is its selective permeability to ions. The morphology of Nafion membranes has been extensively studied to understand its transport properties. A widely accepted theory is the cluster–network model[3] illustrated in Figure 12.12. According to this model, the ionic sites (SO_3^-) of the pendant groups phase

$$R_p = \left(\frac{\ell}{P_i}\right)A. \tag{12.21}$$

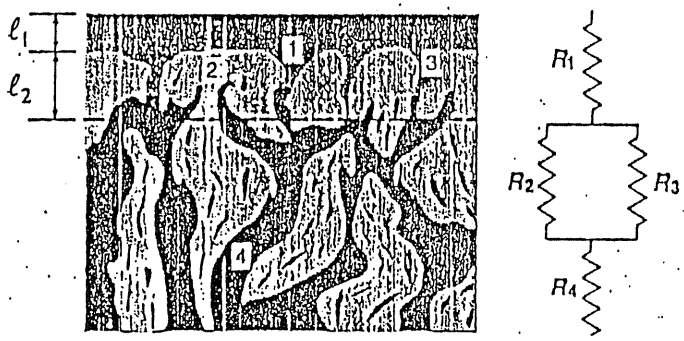

Figure 12.16. Illustration of the resistance model of coated asymmetric membranes showing the coating (1), dense layer (2), pore (3), and substrate (4) regions. [Adapted from J. M. S. Henis and M. K. Tripodi, *J. Membr. Sci.*, 8, 233 (1981), with permission of the publisher.]

The coated membrane illustrated in Figure 12.16 is equivalent to a resistor (dense coating layer, 1) in series with two parallel resistors (i.e., the dense layer, 2, and the pore region, 3, of the skin) and with the porous substrate (4). The total resistance of the network is then given as

$$R_T = R_1 + \frac{R_2 R_3}{R_2 + R_3} + R_4. \tag{12.22}$$

The substrate is typically sufficiently porous to pose no significant resistance to permeation (i.e., P_4/ℓ_4 is very large), and therefore R_4 may be safely neglected. To simplify the analysis, it may be assumed that the smaller pores in the skin are filled completely with the coating material to the depth of the skin (ℓ_2) although it can be shown that, in usual circumstances, complete filling is not required for the coating to be effective. Furthermore, the pore area, A_3, is typically only a small fraction of the total surface area of the fiber (i.e., $A_2 >> A_3$) and, therefore, $A_2 \simeq A_1$. Using these assumptions, the resulting equation for total membrane flux becomes[4]

$$\frac{Q_i}{A_2 \Delta p} = \left(\frac{P}{\ell}\right)_i = \left[\frac{\ell_1}{P_{1,i}} + \frac{\ell_2}{P_{2,i} + P_{1,i}(A_3/A_2)}\right]^{-1}. \tag{12.23}$$

size of approximately 40 Å and a 40% void volume can be obtained by this procedure.

TABLE 12.7 METHODS USED TO PREPARE MICROPOROUS AND ULTRAPOROUS MEMBRANES

Method	Description
Phase Inversion	Phase separation of a ternary mixture of polymer, solvent, and nonsolvent
Sintering	Melting of a semicrystalline polymer powder
Track etching	Irradiation of polymer films resulting in the production of fission fragments followed by caustic etching
Stretching	Combined stretching and annealing of extruded semicrystalline film
Leaching	Extraction of solid pore formers
Thermally induced phase separation	Cooling a mixture of a polymer with a latent solvent to a point of thermal separation of the mixture followed by extraction of the latent-solvent phase

Microporous membranes can be prepared from a wide variety of thermoplastics by irradiation. This process is called nucleation track etching. When radioactive elements decay, fission fragments including heavy positive ions are produced. These can penetrate polymers to significant depths. For example, fission fragments from ^{252}Cf can penetrate polycarbonate to a depth of 20 μm while those from ^{235}U will penetrate to a depth of 10 to 12 μm. Collision of the fragments with polymer chains results in chain scission along the penetration path (see Chapter 6). These radiation-degraded polymer molecules are then etched from the film by treatment with acid or base. If the films are sufficiently thin compared to the depth of penetration, the combination of track formation and etching results in the creation of cylindrical pores that pass completely through the film and have a narrow pore-size distribution. Typical pore diameters are in the range of 0.02 to 20 μm. In addition to polycarbonate, other polymers that can be track etched include poly(ethylene terephthalate), cellulose acetate, cellulose nitrate, and poly(methyl methacrylate).

Asymmetric-Membrane Formation. In order to ensure favorable economics for membrane separations compared to other, more traditional separation techniques, it is necessary to achieve both high selectivity *and* high flux. While permeability and selectivity of dense membranes are intrinsic properties of the membrane material, flux can be increased by decreasing the membrane thickness (eq. 12.11). Since membranes must be sufficiently strong to withstand significant pressure drops (e.g., potentially as high as 2000 psi in some applications), there is a limit to how thin a membrane can be and still provide the necessary strength under operating conditions. A major technological advance that has addressed this problem was the development of asymmetric membranes by Loeb and Sourirajan (1960) for reverse-osmosis applications. As described next, these membranes are prepared by a phase-inversion process that produces a thin, dense surface layer or *skin* and a thick, macroporous substrate. The skin, which may be only 0.1 to 1 μm in thickness, provides the separating function while the substrate provides the mechanical strength. An electron micrograph of a typical asymmetric fiber is shown in Figure 12.13.

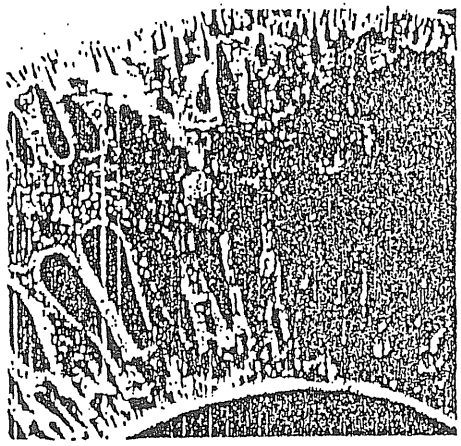

Figure 12.13. Photomicrograph of a cross section of an asymmetric hollow-fiber membrane showing large macrovoids in a porous substructure and a thin, dense skin on the outer and inner surface of the fiber. [Reprinted with permission from J. M. S. Henis and M. K. Tripodi, *Science*, 220, 11 (1983). Copyright 1983 American Association for the Advancement of Science.]

There are four techniques by which asymmetric membranes can be prepared — dry, wet, thermal, and polymer-assisted. All involve the phase separation of a moderately concentrated polymer solution to form a gel in which the polymer becomes the continuous phase and solvent molecules coalesce to form pockets. Removal of the solvent from these pockets leaves voids, which constitute the macroporous structure of the asymmetric membrane. Phase inversion can be induced either by the action of a nonsolvent such as water (i.e., chemically induced) or by a change in temperature (i.e., thermally induced), which causes the membrane solution to become thermodynamically unstable and consequently to phase separate (see Chapter 3).

In the dry process of membrane formation, a polymer, solvent, and nonsolvent are mixed to give a composition within the miscible or single-phase region of the triangular diagram, as shown in Figure 12.14. The solution is then evaporated to dryness. As the volatile components (i.e., solvent and nonsolvent) are lost, the overall composition moves into the miscibility gap and phase separation occurs. In the wet process, a polymer solution is partially evaporated and then coagulated in a nonsolvent, typically water.

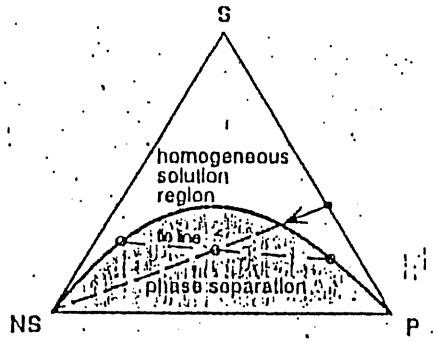

Figure 12.14. Phase diagram of a ternary mixture containing polymer (P), solvent (S), and nonsolvent (NS) at constant temperature. When a nonsolvent is added to a concentrated polymer solution whose composition is indicated by the filled circle along the S–P side, the overall composition of the mixture follows the line connecting this point and the NS vertex. When the composition reaches the phase envelope, phase separation (coagulation) begins. The composition of the two equilibrium phases is given by a tie line through the point on the phase diagram representing the overall composition of the ternary mixture, as shown.

The thermal process or thermally induced phase separation (TIPS) utilizes a "latent" solvent and a decrease in temperature to cause phase separation. A latent solvent is one that is a high-boiling, low-molecular-weight solvent for the polymer

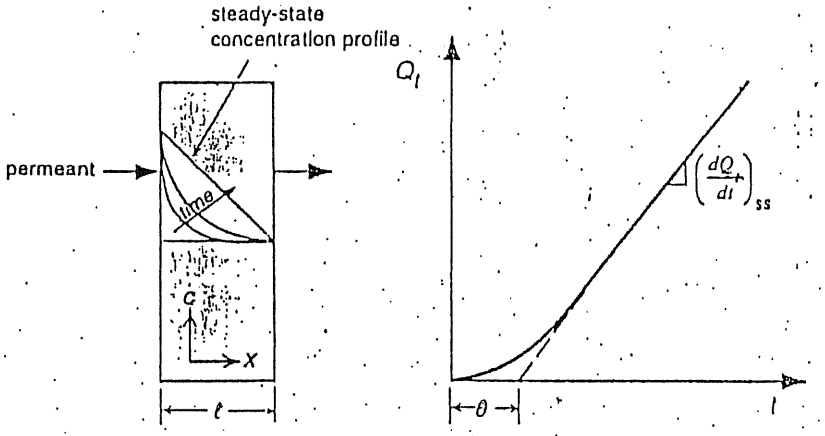

Figure 12.10. Plot of the amount of permeant versus time for a flat film illustrated at the left. The slope of the linear portion of the curve gives the steady-state permeability, while the intercept with the time axis yields the time lag, θ, from which the apparent diffusion coefficient can be obtained (eq. 12.18). The increase in permeant concentration in the film up to the attainment of steady state is illustrated at the left.

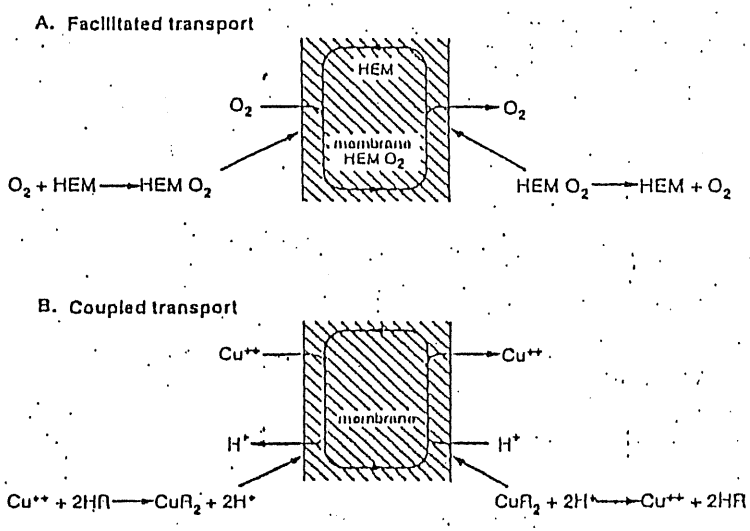

Figure 12.11. A. Facilitated transport of oxygen. B. Coupled transport of cupric and hydrogen ions. (Courtesy of Membrane Technology and Research, Inc., Menlo Park, CA).

centration in the blend will form the dispersed phase in a continuous phase of the polymer present in higher concentration. The art is to select the dispersed phase polymer to be soluble in some convenient solvent (usually water) that is not a solvent for the polymer forming the continuous phase. An example of a water-soluble polymer that is used for this purpose is poly(*N*-vinylpyrrolidone) (PVP). After casting and drying, the dispersed phase is extracted out of the membrane by the solvent. The resulting membrane will have a skinless, microporous structure suitable as a substrate for the preparation of composite membranes.

Coated Asymmetric and Composite Membranes. Although asymmetric membranes have great potential as highly efficient membranes for gas separations, small defects or pores can develop in the skin layer during their preparation. These pinholes permit the free passage of gas molecules through the membrane, resulting in reduced separation. Such pores need only to be approximately 10 Å or more in diameter to cause a significant decrease in selectivity. The problem of achieving defect-free skinned membranes was solved by Henis and Tripodi,[4] who showed that coating an asymmetric fiber with a thin layer of a highly permeable polymer such as silicone rubber plugged the open pores and forced separation to occur through the dense, separating region of the skin.

Membranes with attractive flux and permselectivity can also be prepared by using a microporous membrane (e.g., a skinned asymmetric membrane) as a support for casting a thin film of another polymer with the desired separation properties. A composite membrane with a very thin separating layer can be obtained by this procedure. Alternately, lamination and plasma polymerization can be used to prepare the surface layer. The membrane flux and permselectivity of a coated asymmetric or composite membrane can be related to membrane morphology and the individual transport properties of the components by analogy to an electrical-resistance network, as illustrated by Figure 12.16.

In the resistance model, the permeation flux

$$Q_i = \left(\frac{P_i}{l}\right) A \Delta p \qquad (12.19)$$

is equated with electrical current, I, and the driving force or pressure drop, Δp, across the membrane with the electrical potential, E. In an electrical network, the resistance, R_e, is related to I and E by Ohm's law

$$R_e = \frac{E}{I} \qquad (12.20)$$

It follows that the analogous resistance to permeation, R_p, is given as

separate from the polytetrafluoroethylene backbone to form clusters approximately 4 nm (40 Å) in diameter and connected by short, narrow channels. The ionic channels provide a relatively free diffusional path for cations such as Na^+, for which it is highly selective. By the same reasoning, small polar molecules such as water and aliphatic alcohols easily pass through the ionic channels, while the diffusion of larger nonpolar molecules is restricted.

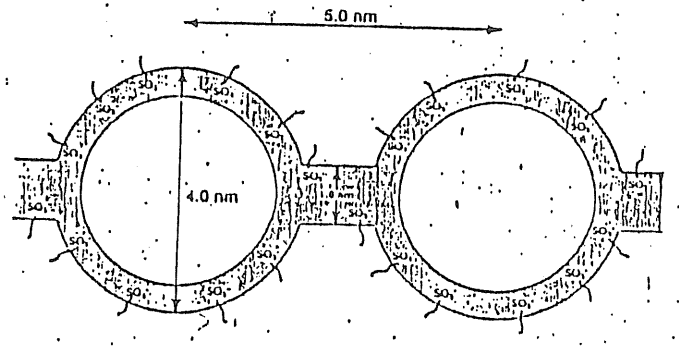

Figure 12.12. Illustration of the cluster-network model of perfluorosulfonate membranes.[3]

12.1.3 Membrane Preparation

Dense membranes may be formed by any of the methods normally used to prepare films. These include melt extrusion, compression molding, and solution casting (see Chapter 11). As described next, procedures to prepare microporous and asymmetric membranes that consist of an integral dense skin covering a microporous substrate require significant art, as well as a basic understanding of polymer morphology and solution thermodynamics.

Microporous Membranes. Techniques that can be used to prepare microporous and ultraporous membranes are summarized in Table 12.7. Some microporous membranes suitable for ultrafiltration and microfiltration applications can are prepared by stretching a semicrystalline polymer film such as a polyolefin (e.g., Celgard™ polypropylene) or polytetrafluorethylene (e.g., Gore-Tex®) in the solid state. Stretching forces a separation of crystalline lamella (see Section 4.2.1) and results in the creation of slitlike pores that are typically 0.2 μm in length and 0.02 μm in width. Total porosity may be 40%.

Pore structure can also be obtained by leaching solids dispersed in a solid material by use of a suitable extraction solvent. For example, porous ("thirsty") glass (e.g., Vicor glass) can be prepared by extracting boron-containing compounds and alkali metal oxides from hollow glass fibers with dilute hydrochloric acid. A pore

Values of P/ℓ for the coating and substrate polymers may be easily obtained from steady-state permeability measurements of dense films of the two materials and the fiber morphology (e.g., λ_1/λ_2, ℓ_1, and ℓ_2) can be determined by electron microscopy.

Module Fabrication. For commercial separations of liquids and gases and for purification and desalination of seawater, membranes with very large surface areas (10^3 to 10^7 m^2) and high area-to-volume ratios (packing density) are needed to meet flux requirements. A hollow-fiber membrane module illustrated in Figure 12.17 gives the highest packing densities (10^4 to 10^5 $m^2 \cdot m^{-3}$). Other configurations include spiral-wound, plate-and-frame, tubular, and capillary. Typical module designs used for reverse osmosis (RO), pervaporation (PV), gas permeation (GP), ultrafiltration (UF), electrodialysis (ED), and microfiltration (MF) are given in Table 12.8.

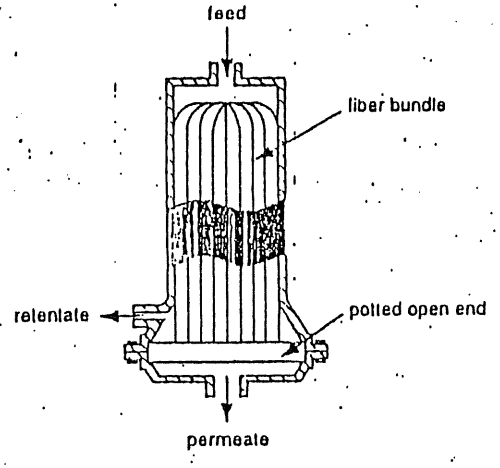

Figure 12.17. Cutaway view of a typical hollow-fiber membrane module. (Adapted from K. Scott, *Membrane Separation Technology*, STI, Oxford, 1990.)

Hollow-fiber modules are frequently used for commercial RO and gas separations. The typical o.d. of hollow fiber ranges from 80 to 200 μm with wall thicknesses of 20 μm or greater. These fibers are made (melt or wet spinning) from polyamide, cellulose triacetate, and sulfonated polysulfone for RO applications and usually polysulfone for gas separations. Seals for membrane bundles are usually made from epoxy. Modules containing fibers of larger diameters are sometimes called *capillary modules* and are used for UF (and MF) applications. Typical polymers used for UF capillary modules include polysulfone, polyacrylonitrile, and chlorinated polyolefins. In all cases, process streams must be pretreated to remove large particles that can plug pores or chemicals that can dissolve or craze the polymeric fibers or lead to swelling or leakage of the seal materials.

TABLE 12.8 PREFERRED MODULE DESIGNS FOR MAJOR MEMBRANE SEPARATIONS

Module Type	Separation
Hollow fiber	RO, GP, PV,
Spiral wound	RO, PV, GP
Plate and frame	PV, UF, ED
Tubular	UF, MF
Capillary	UF, MF

[a] Code: RO, reverse osmosis; GP, gas permeation; PV, pervaporation; UF, ultrafiltration; ED, electrodialysis; MF, microfiltration.

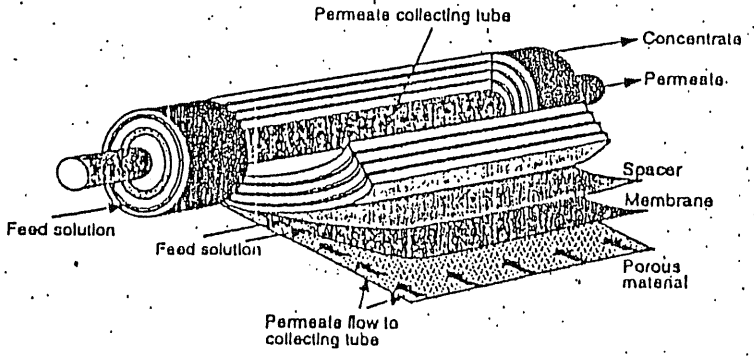

Figure 12.18. Spiral-wound membrane modules. (Adapted from K. Scott, *Membrane Separation Technology*, STI, Oxford, 1990.)

The principal application for *spiral-wound membranes* has been reverse osmosis. As illustrated in Figure 12.18, spiral-wound modules are prepared by sandwiching alternate layers of flat sheet membranes, spacers, and porous material around an inner porous permeate-collection tube. The feed flows axially along the sandwich in the channels, approximately 1.0 mm in depth, formed by the spacers,

while the permeate flows radially to the collection tube. Spiral-wound membrane modules designed for RO separations are typically about 1 m in length and 0.2 m in diameter and can accommodate flow rates up to 28 m^3 per day and pressures up to 40 bars.

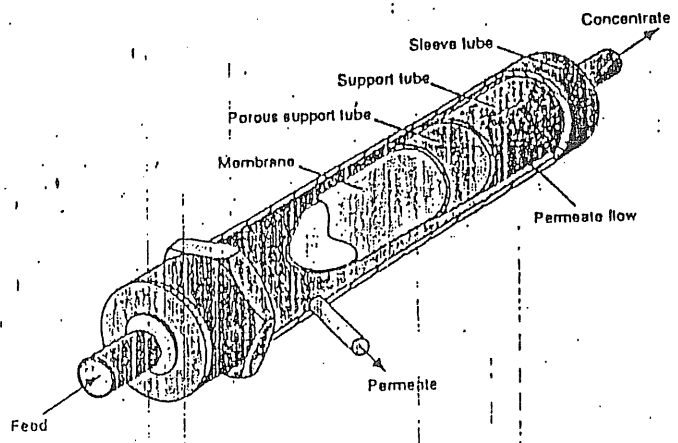

Figure 12.19. Tubular-membrane module. (Adapted from K. Scott, *Membrane Separation Technology*, STI, Oxford, 1990.)

In cases where feeds cannot be pretreated to remove potential fouling contaminants or where the module must be steam sterilized, a tubular-membrane module, as illustrated in Figure 12.19, is sometimes used. The module, which looks much like a shell-and-tube heat exchanger, consists of an inner membrane tube surrounded by porous supporting tubes. In some cases, the membrane may be inorganic (e.g., ceramic) rather that organic to meet the more aggressive environments for which such modules are used. Such units can be easily cleaned and can be steam-sterilized; however, pressure losses are high and productivity is low compared to hollow-fiber and spiral-wound units. Principal applications for tubular-membrane modules are UF and MF.

12.2 BIOMEDICAL APPLICATIONS

Polymers are widely used in medicine as materials for sutures, artificial organs such as kidney and heart, orthopedic implants, and devices for the controlled release of drugs. Depending upon the application, polymers used in the biomedical field, must have one or more specific properties such as biocompatibility, selective permeability, the ability to biodegrade, and high strength or modulus. A few examples of the biomedical uses of polymers are given in this section.

12.2.1 Artificial Organs

One of the important medical application of polymeric membranes is kidney dialysis, which is used to remove toxins of low to moderate molecular weight from blood. These include sodium chloride, potassium chloride, urea, creatinine, and uric acid. At the same time, larger molecules necessary for life, such as cellular particles and plasma proteins, must be retained. The driving force for dialysis is a concentration gradient. Polymers suitable for kidney dialysis include cellophane (regenerated cellulose), which can be prepared in the form of small-diameter (ca. 200-μm) hollow fibers approximately 17 cm in length. As many as 10,000 of these fibers may be used in a typical-dialysis module. Practical problems that are encountered in operation include concentration polarization and clogged pores due to plasma proteins that limit performance.

12.2.2 Controlled Drug Delivery

Medical drugs have a specific therapeutic range of concentration within which these are effective. Below this range, they are ineffective in the treatment of infection and disease and they can be toxic to healthy cells at higher concentrations. Obviously, it is desirable to maintain a constant level of drug concentration that is within the therapeutic range for an extended period of time. It is also important for effective drug therapy that the drug be able to target the specific area of disease in the body, especially in the administration of antitumor agents in the treatment of cancer. In these respects, conventional methods of drug administration, including pills and injections, are not satisfactory, and novel techniques for controlled drug delivery are being sought.

Controlled drug delivery provides two important potential applications for the use of polymers in the effective management of medical drugs in the body. The first of these is *controlled release* whereby a steady therapeutic concentration of the drug is maintained. Current examples of the use of controlled drug release include the delivery of contraceptives and the treatment of glaucoma. The other application is *site-directed* drug delivery whereby a polymer serves as a carrier to bring a drug to a specific site in the body, such as a site of infection, diseased organ, or collection of malignant cells.

The rate of drug release can be controlled by diffusion, reaction, or solvent. In *diffusion control*, the driving force for diffusion is the concentration gradient across the delivery device, which can be a reservoir or matrix system. In the former case, the reservoir containing the drug is encapsulated by a polymeric membrane, which can be either microporous or nonporous. Delivery is constant in time if the drug core is maintained at a saturated level. In the case of a matrix system, the drug is dissolved or dispersed in a polymer. In contrast to the reservoir system, the release rate in a matrix device will decrease with time as the distance the drug has to travel from within the matrix increases due to depletion of drug concentration at the

surface of the device. Polymers that have been used for diffusion-controlled devices include polydimethylsiloxane and poly(ethylene-*co*-vinyl acetate).

Reaction-controlled systems utilize biodegradable polymers as a means of delivery. The drug can be physically dispersed in the polymer, which gradually degrades in the body as a result of hydrolysis or enzymatic attack. Alternately, the drug can be chemically linked to a polymer chain by a suitable spacer group that provides a biodegradable link. For reaction-controlled delivery, poly(lactide-*co*-glycolide) is particularly attractive because its breakdown products, lactic and glycolic acids, are biologically safe.

In *solvent-controlled* delivery, drug release is regulated by the permeation of water through the polymer. This may be achieved by the use of a simple osmotic pump, as illustrated in Figure 12.20. In this example, the drug core is enclosed by a semipermeable membrane that allows water to penetrate into the device due to osmotic pressure. The drug solution is dispersed through the orifice of the device at a rate equal to the rate of water uptake.

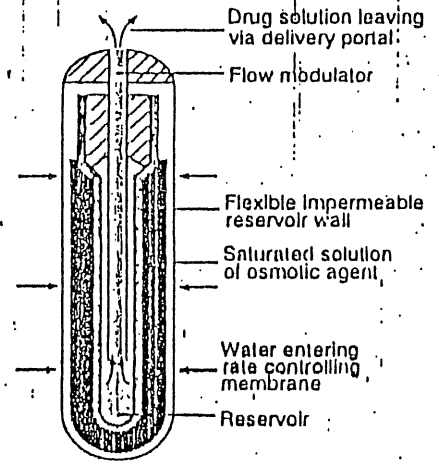

Figure 12.20. Illustration of an osmotic pump used in controlled drug delivery. (Copyright ASTM, reprinted with permission from *ASTM Standardization News*, October, 1986.)

Another type of solvent-activated system for controlled release uses polymeric *hydrogels*, which are water-swollen crosslinked polymer networks. The drug is incorporated in hydrogel polymer in the dry (glassy) state. When introduced in an aqueous environment, the polymer swells. The resulting gel provides a medium favorable for drug diffusion. A commonly used hydrogel is prepared from poly(2-hydroxyethyl methacrylate) (PHEMA)

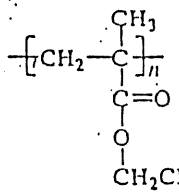

crosslinked by copolymerization with a difunctional polymer. Since PHEMA is water soluble, the crosslinked network will swell to form a gel containing about 35% water in an aqueous environment. In addition to controlled-release applications, PHEMA is used in the manufacture of soft contact lenses.

Although the technology for *site-directed drug delivery* is still in its infancy, some examples illustrate its potential. One application uses a block copolymer of poly(ethylene glycol) (PEG) and poly(aspartic acid) as the drug carrier. PEG provides the carrier solubility, while the poly(amino acid) is used to attach an anticancer drug (e.g., adriamycin).

12.2.3 Hemodialysis and Hemofiltration

An important application for membrane separations (Section 12.1) is hemodialysis by which low-molecular-weight (up to 6000 molecular weight) metabolic, toxic wastes such as urea and creatine are removed from the blood of uremia patients. Separation is based upon size under a concentration gradient. For the removal of larger solutes (up to 20,000 molecular weight), hemodialysis is combined with hemofiltration, which employs a UF membrane and a pressure drop to achieve separation.

12.3 APPLICATIONS IN ELECTRONICS

12.3.1 Electrically-Conductive Polymers

In general, polymers have very poor electrical conductivity. In fact, some polymers such as polytetrafluoroethylene find applications as electrical insulators. In the 1800s, it was observed that the conductivity of natural rubber — normally an excellent insulator — could be significantly increased by adding carbon black which has natural conductivity. In the 1930s, natural rubber filled with acetylene black was used as an antistatic device in hospitals and other facilities where it was necessary to control the danger of sparks due to the buildup of static electricity.

Before 1973, only one polymer — polysulfurnitride $(SN)_x$ — was known to have any appreciable conductivity ($\sim 10^3$ S cm^{-1}).† As in the case of natural rubber,

† The basic unit of conductivity (the inverse of resistivity) is the siemen (S) per cm. A sieman is a reciprocal ohm (i.e., 1 $S = \Omega^{-1}$) For comparisons, the conductivity of polytetrafluoroethylene, an excellent insulator, is approximately 10^{-18} S cm^{-1}.

it was found that this conductivity could be increased by doping with an electron acceptor such as bromine (~10^4 S cm^{-1}).[‡] Unfortunately, interest in this polymer was less than it would otherwise be because of the explosive nature of its precursor monomer, S_2N_2.

By the late 1970s, researchers in Japan and the United States had shown that the electrical conductivity of an organic polymer — polyacetylene — could also be increased by a factor of 10^{12} (to ~10^3 S cm^{-1}) when it was doped with an electron donor such as an alkali-metal ion or an electron acceptor such as arsenic pentafluoride (AsF_5) or iodine. The conductivity of doped polyacetylene is comparable to that of copper on an *equal weight basis*. A comparison of the electrical conductivities and specific gravities of several polymers, common metals, and carbon is made in Table 12.9.

TABLE 12.9 CONDUCTIVITIES OF POLYMERS AND METALS

Material	Conductivity[a] S cm^{-1}	Specific Gravity
Silver	10^6	10.5
Copper	6×10^5	8.9
Aluminum	4×10^5	2.7
Polyacetylene (doped)	1.5×10^5	1
Platinum	10^5	21.4
Polythiophene (doped)	10^1	1
Mercury	10^4	13.5
Carbon fiber	500	1.7–2
Carbon-black-filled polyethylene	10	1
H_2SO_4 electrolyte	10^{-1}	2
Polymer electrolyte	10^{-4}	1
Polytetrafluoroethylene (Teflon)	10^{-18}	2.1–2.3
Polyethylene	10^{-22}	0.9–0.97

[a] Units of siemans (S) per cm.

More recently, conductivity has been demonstrated for doped versions of poly(*p*-phenylene), polypyrrole, polythiophene, and polyaniline. The synthesis and properties of conductive polymers were discussed in Section 10.2.7. Although the electrical conductivities of these polymers are lower than polyacetylene, these

[‡] Polysulfurnitride has been observed to become superconductive (~10^8 S cm^{-1}) at temperatures approaching absolute zero (~0.3 K).

TABLE 12.10 CHEMICAL STRUCTURES AND CONDUCTIVITIES OF SOME ELECTRICALLY CONDUCTIVE POLYMERS

Conductive Polymer	Repeating Unit	Dopants	Conductivity[a] (S cm^{-1})
Polyaniline[b]	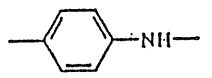	HCl	200
trans-polyacetylene		I_2, Br_2, Li, Na, AsF_5	10^4
Polypyrrole	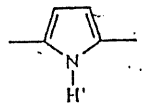	BF_4^-, ClO_4^-, tosylate[c]	500–7500
Polyisothinnaphthalene	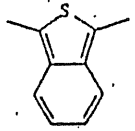	BF_4^-, ClO_4^-	50
Poly(*p*-phenylene)	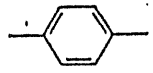	AsF_5, Li, K	10^3
Poly(*p*-phenylene-vinylene)	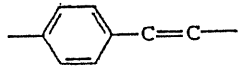	AsF_5	10^4
Polythiophene	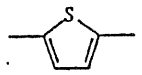	BF_4^-, ClO_4^-, tosylate,[c] $FeCl_4^-$	10^3
Poly(3-alkylthiophene)	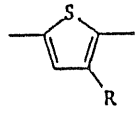	BF_4^-, ClO_4^-, $FeCl_4^-$	$10^3 - 10^4$

[a] Approximate maximum conductivity of doped polymer.
[b] Polyaniline exists in four oxidation states, of which only the emeraldine salt

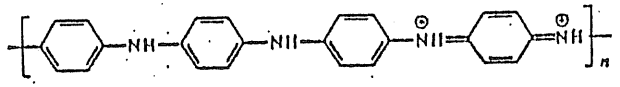

is a good conductor requiring only protonic doping of the imine nitrogen as shown.
[c] *p*-Methylphenylsulfonate.

polymers are more stable to effects of oxygen and moisture. As shown by the chemical structure of the repeating units of these polymers in Table 12.10, a common feature that makes these polymers capable of transporting electrical charge is a conjugated π-electron consisting of alternating single and double bonds along the polymer chain backbone or ring structure. It is believed that doping results in an electron imbalance, and the extended π-conjugated structure of the conductive polymer allows the new electron population to move along the backbone when an electric potential is applied.

In general, conductivity increases with decreasing *band gap* which is the amount of energy needed to promote an electron from the highest occupied energy level or valence band to the empty band immediately above it. The empty band is the conduction band. Metals have zero band gaps, while insulators like many polymers have large band-gaps (1.5 to 4 eV) which impede electron flow. By careful design of the chemical structure of the polymer backbone, it may be possible to obtain band gaps as low as 0.5 to 1 eV. Currently, the lowest band gap observed for a polymer is ~1 eV reported for polyisothianaphthalene (see Table 12.10).

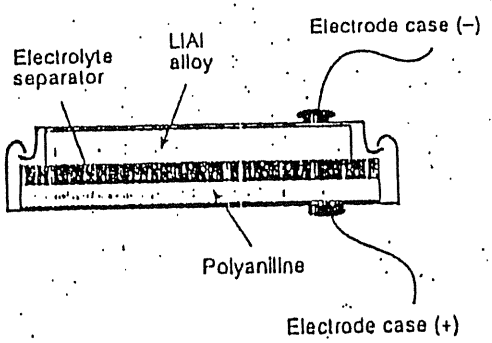

Figure 12.21. Illustration of a rechargeable battery using a polymeric cathode (polyaniline). The anode is a lithium–aluminum alloy, while the electrolyte can be a solution (e.g., propylene carbonate) of an appropriate salt or a solid polymer electrolyte (e.g., Li–PEO). (Courtesy of M. G. Kanatzidis.)

Potential applications of conductive polymers are significant since they are generally lighter, more flexible, and easier to fabricate than many of the materials they seek to replace. Current examples include the use of polymers as both cathodes and solid electrolytes in batteries for automotive and other applications as alternatives to lead–acid batteries in automotive and other applications. A diagram of a typical lithium–polymer battery is shown in Figure 12.21. Potential advantages of polymeric batteries include high reliability, light weight, nonleakage of electrolyte solution, ultrathin-film form, flexibility, and high energy density (up can be used as the cathode material, while lithium dissolved in aluminum foil serves as the anode. Lithium–poly(*p*-phenylene) batteries can deliver current densities as high as 50 mA cm^{-2} have efficiencies of 91% in charging and discharging, and have theoretical energy densities of 320 W-h kg^{-1}. Examples of polymers used in the formulation of solid electrolytes include poly(alkyl sulfide)s, polyphosphazene (see Section 10.2.5) having oligo(oxyethylene) side groups, and especially poly(ethylene oxide). Salts that are added to form the electrolyte include a number of lithium salts having low crystal lattice energies, such as lithium tetrafluoroborate ($LiBF_4$), lithium hexafluoroarsenate ($LiAsF_6$), lithium perchlorate ($LiClO_4$), and lithium trifluoromethanesulfonate sometimes called lithium triflate ($LiCF_3SO_3$).

Other possible uses of conductive polymers include variable-transmission ("smart") windows, electrochromic displays, fuel cells, sensors, conductive paints, semiconductor circuits, low-current wires, electromechanical actuators, electromagnetic shielding, light-emitting diodes, and nonlinear-optical material. Wider commercial utilization awaits further increases in intrinsic conductivity and improvements in the mechanical properties and processability of these interesting polymers.

12.3.2 Electronic Shielding

Undesirable signals in the radio-frequency (rf) range emitted by many electrical devices such as computers can interfere with normal rf reception. This behavior is called electromagnetic interference (EMI). Recent regulations from the Federal Communications Commission (FCC) have placed restrictions on rf transmissions by computers and other electrical devices. Unfilled polymers provide very little EMI shielding capability. Generally, carbon- and metal-filled composites such as PVC filled with aluminum flakes provide suitable housings for low-emission electronic devices.

12.3.3 Encapsulation

Polymers are used to provide integrated-circuit devices with a protective seal against moisture, radiation, and ion contamination. Thermosets, thermoplastics, and elastomers are all used as encapsulants. Included among thermosets are thermosetting polyimides, epoxies, unsaturated polyesters, and alkyd resins, as reviewed in Section 9.2. Candidates among thermoplastic encapsulants are poly(vinyl chloride), polystyrene, polyethylene, fluoropolymers, and acrylics. Elastomers can include silicone rubber and polyurethanes. For the most critical applications, epoxies and polyimides have been the most favored.

12.4 PHOTONIC POLYMERS

The next technological revolution may be the widespread use of optical rather than electronic devices for the storage and processing of data. Optical technology has the advantages of both speed and compactness of storage space. Optical storage of computer data is already common (i.e., CD-ROM and WORM drives), and ways to use optical devices for processing data are being explored. Among materials that are suitable for optical technology are polymers that exhibit *nonlinear-optical* properties. This means that their optical properties vary with the intensity of the light compared to ordinary glass, which is linear in its optical properties. Photoresponsive sunglasses that change tint with the intensity of sunlight are examples of nonlinear-optical materials.

In general, molecules with π-electron structures can exhibit nonlinear-optical effects when these electrons are optically excited. In the case of polymers, these π-electron structures can be part of the main-chain backbone, as for example in the case of the 6F-polyimide (see Section 10.2.1)

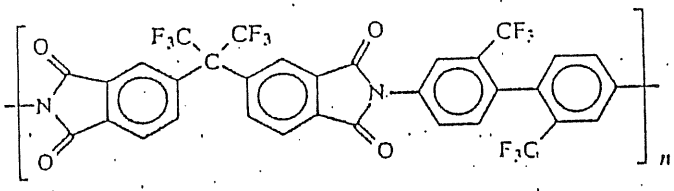

The nonlinear-optical functionality can also be incorporated as a side chain, as in the case of an acrylate polymer

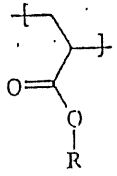

having a substituent group (R) that contains a 4-methoxy-4'-nitrostilbene moiety connected by a six-carbon spacer

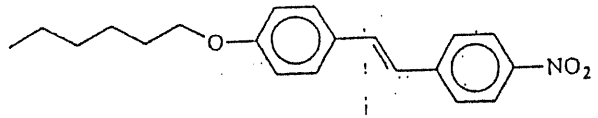

12.5 DRAG REDUCTION

It has been observed that dilute solutions (1 to 100 ppm) of many high-molecular-weight (>100,000), linear polymers can reduce turbulent friction in fluid flow by as much as 70% to 80%. Examples of synthetic water-soluble polymers that are very effective as drag-reducing agents include poly(ethylene oxide) and polyacrylamide. An example of a commonly used *oil-soluble* polymer is polyisobutylene. Some naturally occurring polymers such as guar (from *Cyamopsis tetragonologus*) and xanthan (*Xanthamonas* exudate) are also effective drag reducers. It has also been observed that suspensions of some fibers, including nylons, can impart good drag reduction in turbulent flow.

Although the exact mechanism of drag reduction is still unclear, it is believed that drag reduction may be related to extensional flow. During flow, the long polymer chains become disentangled and oriented in the direction of flow. Extensional viscosity (see Chapter 11) significantly increases and a form of strain-rate hardening occurs, which imposes a maximum limit on the strain rate. The high extensional viscosity reduces turbulent fluctuations (probably through the suppression of the roll-wave motion and vortex stretching in the sublayer) and, thereby, reduces friction.

Applications for drag reduction include any where reduced friction in fluid flow is desired. For example, a small amount of a water-soluble polymer can be injected into sewers during periods of heavy rain to upgrade flow and, thereby, prevent flooding. Also a drag-reducing polymer can be injected at the bow of a ship to decrease friction and increase speed or be used to decrease pressure drop in water lines for fire fighting.

REFERENCES

1. W. R. Vieth, J. M. Howell, and J. H. Hsieh, *J. Membr. Sci.*, 1, 177 (1976).
2. D. R. Paul and W. J. Koros, *J. Polym. Sci., Polym. Phys. Ed.*, 14, 675 (1976).
3. T. D. Gierke and W. Y. Hsu, *ACS Symp. Ser.*, 180, 283 (1982).
4. J. M. S. Henis and M. K. Tripodi, *J. Membr. Sci.*, 8, 233 (1981).

BIBLIOGRAPHY

G. Belfort, *Synthetic Membrane Processes*, Academic Press, Orlando, FL, 1984.

J. Comyn, *Polymer Permeability*, Elsevier Applied Science Publishers, London, 1985.

J. Crank, *The Mathematics of Diffusion*, Oxford University Press, New York, 1975.

J. Crank and G. S. Park, *Diffusion in Polymers*, Academic Press, London, 1968.

J. M. S. Henis and M. K. Tripodi, "The Developing Technology of Gas Separating Membranes," *Science*, 220, 11–17 (1983).

W. S. Ho and K. K. Sirkar, eds., *Membrane Handbook*, Van Nostrand Reinhold, New York, 1992.

R. Y. M. Huang, *Pervaporation Membrane Separation Processes*, Elsevier, Amsterdam, 1991.

R. B. Kaner and A. G. MacDiarmid, "Plastics That Conduct Electricity," *Sci. Am.*, Feb. 1988, pp. 106–111.

R. E. Kesting, *Synthetic Polymeric Membranes*, John Wiley & Sons, New York, 1985.

R. E. Kesting and A. K. Fritzsche, *Polymeric Gas Separation Membranes*, John Wiley & Sons, Inc., New York, 1993.

W. J. Koros and G. K. Fleming, "Membrane-based Gas Separation," *J. Membr. Sci.*, 83, 1–80 (1993).

C. C. Ku and R. Liepins, *Electrical Properties of Polymers*, Hanser Publications, Munich, 1987.

J. M. Margolis, ed., *Conductive Polymers and Plastics*, Chapman and Hall, New York, 1989.

T. Matsuura, *Synthetic Membranes and Membrane Separation Processes*, CRC Press, Boca Raton, FL, 1994.

M. Mulder, *Basic Principles of Membrane Technology*, Kluwer Academic Publishers, Dordrecht, The Netherlands, 1991.

D. R. Paul, "Gas Sorption and Transport in Glassy Polymers," *Ber. Bunsenges. Phys. Chem.*, 83, 294–302 (1979).

Problem

12–1. An asymmetric hollow fiber of polysulfone has a surface pore area, A_3/A_2, of 1.9×10^{-6} and an effective skin thickness of 1000 Å. If the fiber is coated with a 1-μm layer of silicone rubber, calculate the effective P/ℓ for the coated membrane for CO_2 and the permselectivity for CO_2/CH_4.

Appendix A

Polymer Abbreviations

ABS	acrylonitrile/butadiene/styrene rubber
CA	cellulose acetate
CAB	cellulose acetate butyrate
CAP	cellulose acetate propionate
CF	cresol–formaldehyde
CMC	carboxymethylcellulose
CN	cellulose nitrate
CP	cellulose propionate
CPE	chlorinated polyethylene
CTA	cellulose triacetate
CTFE	poly(chlorotrifluoroethylene)
EC	ethylcellulose
EP	epoxy resin
E/P	ethylene/propylene copolymer
EPDM	elastomeric terpolymer of ethylene, propylene, and a nonconjugated diene
EPS	expanded polystyrene (foam)
ETFE	ethylene/tetrafluoroethylene copolymer
EVA	ethylene/vinyl acetate copolymer
FEP	elastomeric copolymer of tetrafluoroethylene and hexafluoroethylene
FF	furan–formaldehyde resin
GP	gutta percha
HDPE	high-density polyethylene
HEC	hydroxyethylcellulose
HIPS	high-impact polystyrene
HMWPE	high-molecular-weight polyethylene
LDPE	low-density polyethylene
LLDPE	linear low-density polyethylene
MBS	methyl methacrylate/butadiene/styrene copolymer
MC	methylcellulose
MDPE	medium-density polyethylene
MF	melamine–formaldehyde resin
MPF	melamine/phenol–formaldehyde resin
NBR	nitrile rubber (elastomeric copolymer of butadiene and acrylonitrile)
NR	natural rubber
PA	polyamide
PAA	poly(acrylic acid)
PAI	polyamide-imide
PAMS	poly(α-methylstyrene)
PAN	polyacrylonitrile
PB	polybutene-1
PBA	poly(butyl acrylate)
PBI	poly(benzimidazole)
PBTP	poly(butylene terephthalate)
PC	polycarbonate
PCTFE	poly(chlorotrifluoroethylene)
PDAP	poly(diallyl phthalate)
PDMS	polydimethylsiloxane
PE	polyethylene
PEO	poly(ethylene oxide)
PES	polyethersulfone
PETP	poly(ethylene terephthalate)
PF	phenol–formaldehyde resin
PHEMA	poly(2-hydroxyethyl methacrylate)
PI	polyimide
PIB	polyisobutylene
PMMA	poly(methyl methacrylate)
PMP	poly(4-methyl-1-pentene)
POM	poly(oxymethylene); polyformaldehyde
POP	poly(phenylene oxide)
PP	polypropylene
PPS	poly(phenylene sulfide)
PPSU	poly(phenylene sulfone)
PS	polystyrene
PSF	polysulfone
PTFE	polytetrafluoroethylene
PUR	polyurethane
PVAC	poly(vinyl acetate)
PVAL	poly(vinyl alcohol)
PVB	poly(vinyl butyral)
PVC	poly(vinyl chloride)
PVF	poly(vinyl fluoride)
PVDC	poly(vinylidene dichloride)

PVDF	poly(vinylidene difluoride)
PVFM	poly(vinyl formal)
PVK	poly(*N*-vinylcarbazole)
PVP	poly(*N*-vinylpyrrolidone)
S/B	styrene/butadiene copolymer
SIN	simultaneous interpenetrating network
SMC	sheet molding compound
UF	urea-formaldehyde resin
UHMW-PE	ultrahigh-molecular-weight PE
UP	unsaturated polyester

Appendix B

Representative Properties of Some Important Commercial Polymers

1. Physical and Thermal Properties[a]

Polymer	ρ[b] g cm^{-3}	T_g °C	T_m[b] °C
Cellulose acetate	1.27–1.34	(49)	—
Nylon-6	1.08–1.23	46–60	223
Nylon-6,6	1.07–1.24	45–57	265
Polycarbonate	1.20–1.31	141–150	227
Polyethylene (all grades)	0.91–1.00	(-120)	98–135
Poly(ethylene terephthalate)	1.33–1.48	69–77	267
Poly(methyl methacrylate)	1.17–1.23	105–126	160
Polyoxymethylene	1.43–1.54	-85 to -30	187
Polypropylene	0.9–0.95	-10 to -18	177
Polysulfone	1.24	190	—
Polystyrene	1.05–1.13	100	240
Polytetrafluoroethylene	2.1–2.35	-73	327–332
Poly(vinyl acetate)	1.19–1.34	28–31	—
Poly(vinyl chloride)	1.39–1.52	81	273
Silicone rubber	1.07	-123	-43

[a] Numbers typically indicate a range of reported values for samples with different crystallinity, water content, molecular weight, and thermal histories. Uncertain or controversial values are given within parentheses.
[b] In most cases, values indicate the range of densities between that of the glassy amorphous state to that of the fully crystalline polymer as calculated from X-ray data of crystalline domains.

2. Mechanical Properties

Polymer	E [a] GPa	σ_b (σ_y) [b] MPa	ϵ_b (ϵ_y) [c] %	Izod Impact Strength, J/m [d]
Cellulose acetate	2	30 (60)	30 (6)	6–133
Nylon-6	1.9	75 (50)	300 (30)	(25)
Nylon-6,6	2.0	80 (57)	200 (25)	110
Polycarbonate	2.5	60 (65)	125 (30)	800
Polyethylene (all grades)	0.2–1	10–30 (8–30)	600–800 (9–20)	130–700
Poly(ethylene terephthalate)	3.0	54	275 (6)	70
Poly(methyl methacrylate)	3.2	65	10	27
Polyoxymethylene	2.7	65	40	80
Polypropylene	1.4	33 (32)	400 (12)	80
Polystyrene	3.4	50	2.5	28
Polysulfone	2.5	65	75	85
Polytetrafluoroethylene	0.5	25 (13)	200 (63)	160
Poly(vinyl acetate)	0.6	29–49	10–20	160
Poly(vinyl chloride)	2.6	50 (48)	30 (3)	43
Silicone rubber	—	4.8–7.0	100–400	—

[a] Tensile modulus; to convert GPa to psi, multiply by 1.45×10^5.
[b] Stress at break (yield); to convert MPa to psi, multiply by 145.
[c] Elongation at break (yield).
[d] To convert J m^{-1} to ft-lb$_f$ in.$^{-1}$ divide by 53.38.

Appendix C

MAJOR ASTM[†] STANDARDS FOR PLASTICS AND RUBBER

1. Plastics (Vols. 8.01, 8.02, and 8.03)

ASTM	Standard
D 256	Impact resistance of plastics and electrical insulating materials
D 412	Rubber properties in tension
D 542	Index of refraction of transparent organic plastics
D 543	Resistance of plastics to chemical reagents
D 568	Rate of burning and/or extent and time of burning of flexible plastics in a vertical position
D 569	Measuring the flow properties of thermoplastic molding materials
D 570	Water absorption of plastics
D 618	Conditioning plastics and electrical insulating materials for testing
D 621	Deformation of plastics under load
D 635	Rate of burning and/or extent and time of burning of self-supporting plastics in a horizontal position
D 638	Tensile properties of plastics
D 647	Design of molds for test specimens of plastic molding compounds
D 648	Deflection temperature of plastics under flexural load
D 671	Flexural fatigue of plastics by constant-amplitude-of-force
D 695	Compressive properties of rigid plastics
D 696	Coefficient of linear thermal expansion of plastics
D 746	Brittleness temperature of plastics and elastomers by impact
D 785	Rockwell hardness of plastics and electrical insulating materials
D 790	Flexural properties of unreinforced and reinforced plastics and electrical insulating materials
D 792	Specific gravity and density of plastics by displacement
D 882	Tensile properties of thin plastic sheeting
D 1238	Flow rates of thermoplastics by extrusion plastometer

[†] ASTM, American Society for Testing and Materials, 1916 Race Street, Philadelphia, PA 19103.

ASTM	Standard
D 1434	Determining gas permeability characteristics of plastic film and sheeting
D 1435	Outdoor weathering of plastics
D 1505	Density of plastics by the density-gradient technique
D 1525	Vicat softening temperature of plastics
D 1637	Tensile heat distortion temperature of plastic sheeting
D 1708	Tensile properties of plastics by use of microtensile specimens
D 1746	Transparency of plastic sheeting
D 1790	Brittleness temperature of plastic sheeting by impact
D 1822	Tensile-impact energy to break plastics and electrical insulating materials
D 1870	Elevated temperature aging using a tubular oven
D 1894	Static and kinetic coefficients of friction of plastic film and sheeting
D 1895	Apparent density, bulk factor, and pourability of plastic materials
D 1896	Transfer molding test specimens of thermosetting compounds
D 1897	Injection molding test specimens of thermoplastic molding and extrusion materials
D 1898	Sampling of plastics
D 1925	Yellowness index of plastics
D 1929	Ignition properties of plastics
D 1938	Tear propagation resistance of plastic film and thin sheeting by a single-tear method
D 2117	Melting point of semicrystalline polymers by the hot stage microscopy method
D 2126	Response of rigid cellular plastics to thermal and humid aging
D 2134	Softening of organic coatings by plastic compositions
D 2236	Dynamic mechanical properties of plastics by means of a torsional pendulum
D 2240	Rubber property — durometer hardness
D 2288	Weight loss of plasticizers on heating
D 2471	Gel time and peak exothermic temperature of reacting thermosetting resins
D 2566	Linear shrinkage of cured thermosetting casting resins during cure
D 2582	Puncture–propagation tear resistance of plastic film and thin sheeting
D 2684	Determining permeability of thermoplastic containers
D 2732	Unrestrained linear thermal shrinkage of plastic film and sheeting
D 2734	Void content of reinforced plastics
D 2843	Density of smoke from the burning or decomposition of plastics
D 2856	Open cell content of rigid cellular plastics by the air pycnometer
D 2857	Dilute solution viscosity of polymers
D 2863	Measuring the minimum oxygen concentration to support candlelike combustion of plastics (oxygen index)
D 2990	Tensile, compressive, and flexural creep and creep rupture of plastics
D 3029	Impact resistance of rigid plastic sheeting or parts by means of a tub (falling weight)
D 3420	Test method for dynamic ball burst (pendulum) impact resistance of plastic films
D 3593	Test method for molecular weight averages and molecular weight distribution of certain polymers by liquid size-exclusion chromatography (gel permeation chromatography, GPC) using universal calibration
D 3750	Practice for determination of number-average molecular weight of polymers by membrane osmometry
D 3763	Test method for high-speed puncture properties of plastics using load and displacement sensors
D 3795	Test method for thermal flow and cure properties of thermosetting resins by torque rheometer
D 3845	Test method for the rheological properties of thermoplastics with a capillary rheometer
D 3846	Test method for in-plane shear strength of reinforced plastics
D 4000	Specifying plastic material
D 4001	Practice for determination of weight-average molecular weight of polymers by light scattering
D 4065	Practice for determining and reporting dynamic mechanical properties of plastics
D 4093	Test method for photoelastic measurements of birefringence and residual strains in transparent or translucent plastic materials
D 4272	Test method for impact resistance of plastic film by instrumented dart drop
D 4440	Practice for rheological measurement of polymer melts using dynamic mechanical procedures
D 4473	Practice for measuring the cure behavior of thermosetting resins using dynamic mechanical procedures
D 4526	Determination of volatiles in polymers by headspace chromatography

2. Rubber (Vols. 9.01 and 9.02)

ASTM	Standard
D 297	Methods for rubber products — chemical analysis
D 395	Test methods for rubber property — compression set
D 412	Test methods for rubber properties in tension
D 471	Test methods for rubber property — effect of liquids
D 624	Test methods for rubber property — tear resistance
D 797	Test methods for rubber property — Young's modulus at normal and subnormal temperatures
D 814	Test methods for rubber property — vapor transmission of volatile liquids

ASTM	Standard
D 1349	Recommended practice for rubber — standard temperatures and atmospheres for testing and conditioning
D 1630	Test method for rubber property — abrasion resistance (NBS abrader)
D 2084	Test method for rubber property — vulcanization characteristics using oscillating disk curemeter
D 2228	Test method for rubber property — abrasion resistance (Pico abrader)
D 2240	Test method for rubber property — Durometer hardness
D 3137	Test method for rubber property — hydrolytic stability
D 3452	Practice for rubber — identification by pyrolysis-gas chromatography
D 3677	Test methods for rubber — identification by infrared spectrophotometry

Appendix D

SI Units[a] and Physical Constants

Units and Symbols

Quantity	Name	Symbol	CGS Equiv.
Capacity	liter	L	10^{-3} m^3
Electric current	ampere	A	ampere
Electric capacitance	farad	F	A s V^{-1}
Energy, work, heat	joule	J	N m
Force	newton	N	m kg s^{-2}
Frequency	hertz	Hz	s^{-1}
Mass	kilogram	kg	kg
Plane angle	radian	rad	rad
Power	watt	W	J s^{-1}
Pressure, stress	pascal	Pa	N m^{-2}
Viscosity (dynamic)	pascal second	Pa s	N s m^{-2}

Conversion Factors

Energy: 1 J = 0.2387 cal

Force: 1 N = 10^5 dynes = 0.102 kg_f = 0.2248 lb_f

Pressure, stress: 1 Pa = 10 dyne cm^{-2} = 7.5 × 10^{-3} mm Hg = 10^{-5} bar
= 1.02 × 10^{-5} kg cm^{-2} = 1.45 × 10^{-4} psi = 9.869 × 10^{-6} atm

Viscosity: 1 Pa s = 10 poise

Density: 1 g cm^{-3} = 0.0361 lb in.$^{-3}$

Temperature: °R = (5/9)K
°C = (5/9)(°F - 32) = K + 273.15

[a] International System of Units.

SI Prefixes

Prefix	Symbol	Equivalent
pico	p	10^{-12}
nano	n	10^{-9}
micro	μ	10^{-6}
milli	m	10^{-3}
centi	c	10^{-2}
deci	d	10^{-1}
kilo	k	10^{3}
mega	M	10^{6}
giga	G	10^{9}

Fundamental Physical Constants

	Symbol	Unit	Value
Avogadro constant	N_A	mol^{-1}	6.0220×10^{23}
Boltzmann constant, R/N_A	k	$J\ K^{-1}$	1.3807×10^{-23}
Gas law constant	R	$J\ (mol\ K)^{-1}$	8.3144
		$bar\ cm^3\ (mol\ K)^{-1}$	83.144
		$psia\ ft^3\ (lb\ mol\ °R)^{-1}$	10.732
		$atm\ cm^3\ (mol\ K)^{-1}$	82.057
Gravitational acceleration	g_o	$m\ s^{-2}$	9.80665
Planck constant	h	$J\ s$	6.6262×10^{-34}
Permeability of vacuum	μ_o	$N\ A^{-2}$	12.566×10^{-7}
Permittivity of vacuum, $1/\mu_o c^2$	ε_o	$F\ m^{-1}$	8.85419×10^{-12}
Speed of light in vacuum	c	$m\ s^{-1}$	2.9979×10^{8}

Appendix E

Mathematical Relationships

Trigonometric Functions

$$\sin^2\theta = \frac{1}{2} - \frac{1}{2}\cos 2\theta$$

$$\sin^2\theta + \cos^2\theta = 1$$

$$\sin(\theta \pm \phi) = \sin\theta\cos\phi \pm \cos\theta\sin\phi$$

$$\sin 2\theta = 2\sin\theta\cos\theta$$

$$\cos 2\theta = \cos^2\theta - \sin^2\theta$$

Exponential and Logarithmic Functions

Euler's Identities

$$e^{i\theta} = \cos\theta + i\sin\theta$$

$$e^{-i\theta} = \cos\theta - i\sin\theta$$

Solution of Algebraic Equations

Quadratic Equation $(ax^2 + bx + c = 0)$

$$x = \frac{-b \pm \sqrt{b^2 - 4ac}}{2a}$$

Derivatives

$$\frac{d}{dx}(u^n) = nu^{n-1}\frac{du}{dx}$$

$$\frac{d}{dx}(uv) = u\frac{dv}{dx} + v\frac{du}{dx}$$

$$\frac{d}{dx}\left(\frac{u}{v}\right) = \frac{v(du/dx) - u(dv/dx)}{v^2}$$

$$\frac{d}{dx}\sin\theta = \cos\theta\frac{d\theta}{dx}$$

$$\frac{d}{dx}\cos\theta = -\sin\theta\frac{d\theta}{dx}$$

$$\frac{d}{dx}\ln u = \frac{1}{u}\frac{du}{dx}$$

$$\frac{d}{dx}e^u = e^u\frac{du}{dx}$$

Integrals

Indefinite

$$\int u^n du = \frac{u^{n+1}}{n+1} \qquad (n \neq -1)$$

$$\int a^u du = \frac{a^u}{\ln a}$$

$$\int u dv = uv - \int v du \qquad \text{(integration by parts)}$$

$$\int e^u du = e^u$$

$$\int \frac{du}{u} = \ln u$$

$$\int \ln x dx = x \ln x - x$$

$$\int \sin u du = -\cos u$$

$$\int \cos u du = \sin u$$

$$\int \sin ax \cos ax dx = \frac{\sin^2 ax}{2a}$$

$$\int \cos^2 u du = \frac{u}{2} + \frac{\sin 2u}{4} = \frac{1}{2}(u + \sin u \cos u)$$

Definite

$$\int_0^{\pi} \sin mx \cos nx dx = \begin{cases} 0 & m \text{ and } n, \text{ integers} \quad m+n, \text{ odd} \\ 2m/(m^2 - n^2) & m \text{ and } n, \text{ integers} \quad m+n, \text{ even} \end{cases}$$

Series of Constants

Geometric Series

$$a + ar + ar^2 + ar^3 + \cdots + ar^{n-1} = \frac{a(1-rn)}{1-r} = \frac{a-rl}{1-r}$$

where $l = ar^{n-1}$ is the last term and $r \neq 1$

$$a + ar + ar^2 + ar^3 + \cdots = \frac{a}{1-r} \qquad (-1 < r < 1)$$

Taylor Series

$$e^x = 1 + x + \frac{x^2}{2!} + \frac{x^3}{3!} + \cdots \qquad (-\infty < x < \infty)$$

$$\ln(1+x) = x - \frac{x^2}{2!} + \frac{x^3}{3!} + \cdots \qquad (-1 < x \leq 1)$$

$$\ln x = 2\left\{\left(\frac{x-1}{x+1}\right) + \frac{1}{3}\left(\frac{x-1}{x+1}\right)^3 + \frac{1}{5}\left(\frac{x-1}{x+1}\right)^5 + \cdots\right\} \qquad (x > 0)$$

$$\ln x = \left(\frac{x-1}{x}\right) + \frac{1}{2}\left(\frac{x-1}{x}\right)^2 + \frac{1}{3}\left(\frac{x-1}{x}\right)^3 + \cdots \qquad \left(x \geq \frac{1}{2}\right)$$

$$\sin x = x - \frac{x^3}{3!} + \frac{x^5}{5!} - \frac{x^7}{7!} + \cdots \qquad (-\infty < x < \infty)$$

$$\cos x = 1 - \frac{x^2}{2!} + \frac{x^4}{4!} - \frac{x^6}{6!} + \cdots \qquad (-\infty < x < \infty)$$

Laplace Transforms

$$L[F(t)] = \int_0^{\infty} e^{-pt} F(t) dt = f(p)$$

$$F(t) = L^{-1}[f(p)] \quad \text{(inverse Laplace transform)}$$

$F(t)$	$f(p)$
a	$\frac{a}{p}$
t	$\frac{1}{p^2}$
at	$\frac{a}{p^2}$
e^{at}	$\frac{1}{p-a}$
e^{-at}	$\frac{1}{p+a}$
$\cos at$	$\frac{p}{p^2+a^2}$
$\frac{\sin at}{a}$	$\frac{1}{s^2+a^2}$
$F(t-a)$	$e^{-ap}L[F(t)]$
$F'(t)$	$pf(p) - F(0)$
$F''(t)$	$p^2 f(p) - pF(0) - F'(0)$
$\int_0^t F(u)G(t-u)du$	$f(p)g(p)$

Fourier Transforms

Fourier Sine Transforms

$$F_S(\alpha) = \int_0^\infty f(x) \sin \alpha x \, dx$$

$f(x)$	$F_S(\alpha)$
$\begin{cases} 1, & 0 < x < b \\ 0, & x > b \end{cases}$	$\dfrac{1-\cos b\alpha}{\alpha}$
x^{-1}	$\dfrac{\pi}{2}$
$\dfrac{x}{x^2+b^2}$	$\dfrac{\pi}{2}\exp(-b\alpha)$
$\exp(-bx)$	$\dfrac{\alpha}{\alpha^2+b^2}$

Fourier Cosine Transforms

$$F_C(\alpha) = \int_0^\infty f(x) \cos \alpha x \, dx$$

$f(x)$	$F_C(\alpha)$
$\begin{cases} 1, & 0 < x < b \\ 0, & x > b \end{cases}$	$\dfrac{\sin b\alpha}{\alpha}$
$\dfrac{1}{x^2+b^2}$	$\dfrac{\pi \exp(-b\alpha)}{2b}$
$\exp(-bx)$	$\dfrac{b}{\alpha^2+b^2}$

Appendix F

Table of the Major Elements

Name	Symbol	Atomic Number	Atomic Weight
Aluminum	Al	13	26.98154
Argon	Ar	18	39.948
Arsenic	As	33	74.9216
Barium	Bs	56	137.33
Boron	B	5	10.81
Bromine	Br	35	79.904
Calcium	Ca	20	40.08
Carbon	C	6	12.011
Chlorine	Cl	17	35.453
Chromium	Cr	24	51.996
Cobalt	Co	27	51.9332
Copper	Cu	29	63.546
Fluorine	F	9	18.998404
Germanium	Ge	32	72.59
Gold	Au	79	196.9665
Helium	He	2	4.00260
Hydrogen	H	1	1.00794
Iodine	I	53	126.9045
Iron	Fe	26	55.847
Lead	Pb	82	207.2
Lithium	Li	3	6.941
Magnesium	Mg	12	24.305
Mercury	Hg	80	200.59
Neon	Ne	10	20.1179
Nickel	Ni	28	58.69
Nitrogen	N	7	14.0067
Osmium	Os	76	190.2
Oxygen	O	8	15.9994
Palladium	Pd	46	106.42
Phosphorus	P	15	30.97376
Platinum	Pt	78	195.08

Name	Symbol	Atomic Number	Atomic Weight
Potassium	K	19	39.0983
Radon	Rn	86	(222)
Rhodium	Rh	45	102.9055
Silicon	Si	14	28.0855
Silver	AG	47	107.8682
Sodium	Na	11	22.98977
Sulfur	S	16	32.06
Tin	Sn	50	118.69
Titanium	Ti	22	47.88
Tungsten	W	74	183.85
Vanadium	V	23	50.9415
Zinc	Zn	30	65.38

Index

F

G

Q,R

S

Chemical Engineering

POLYMER SCIENCE & TECHNOLOGY

second edition

The definitive guide to polymer principles, properties, synthesis, and applications

Polymer Science and Technology, Second Edition systematically reviews both the current state of polymer science and technology and emerging advances in the field. Leading polymer specialist Joel R. Fried offers thoroughly updated coverage of both polymer processing principles and the latest polymer applications in a wide range of industries—including medicine, biotechnology, chemicals, and electronics.

In addition to synthetic polymer chemistry, Fried covers polymer properties in solution and in melt, rubber, and solid states, and surveys all important categories of plastics. This Second Edition also adds many new example calculations, homework problems, and bibliographic references. In-depth coverage includes:

- Polymer synthesis, including metallocene catalysis, atom-transfer radical and plasma polymerization, the use of supercritical fluids, and genetic engineering
- Amorphous and crystalline states, transitions, and mechanical properties
- Characterization techniques, including new coverage of temperature-modulated DSC
- Polymer engineering, from rheology to modeling of polymer processing operations
- Fundamental principles of polymer blends and composites—including up-to-the-minute discussions of nanocomposites
- Commodity thermoplastics and fibers, with new coverage of syndiotactic polystyrene, biopolymers, and naturally occurring polymers
- Elastomers and thermosets
- Engineering and specialty polymers, including dendrimers and hyperbranched polymers, amorphous Teflon, and new electrical/optical applications
- Membrane separations and new coverage of barrier polymers

ABOUT THE AUTHOR

JOEL R. FRIED is Professor of Chemical Engineering and Past Director of the Polymer Research Center, and Head of the Department of Chemical and Materials Engineering at the University of Cincinnati. He has authored over 125 journal articles and several patents and book chapters and serves as Editor of *Polymer Contents* and a member of the Editorial Boards of *Polymer* and the *Journal of Polymer Engineering*. His research interests include computational polymer science and membrane science and technology. He holds a B.S. degree in biology from RPI, B.S. and M.E. degrees in chemical engineering from RPI, and M.S. and Ph.D. degrees in polymer science and engineering from the University of Massachusetts (Amherst).

PRENTICE HALL
Professional Technical Reference
Upper Saddle River, NJ 07458
www.phptr.com